Rapport quadriennal 2007 - 2011

Jérôme Dyment

Comité National Français de Géodésie et Géophysique

French National Committee of Geodesy and Geophysics

RAPPORT QUADRIENNAL

QUADRENNIAL REPORT

2007 - 2011

FRANCE

Comité National Français de Géodésie et Géophysique

French National Committee of Geodesy and Geophysics

RAPPORT QUADRIENNAL DU CNFGG A l'UGGI

QUADRENNIAL REPORT OF CNFGG TO IUGG

PREFACE

FOREWORDS

PREFACE

Le CNFGG (Comité National Français de Géodésie et de Géophysique), organisme correspondant français de l'Union Géodésique et Géophysique Internationale (UGGI), a le plaisir de publier son rapport quadriennal pour la période 2007-2010, préparé à l'intention de l'UGGI et des autres organismes correspondants nationaux.

Cette année, les huit sections du CNFGG – calquées sur les huit associations constitutives de l'UGGI – ont eu toute liberté de décider de la forme et du fond de leur contribution à ce rapport. Certaines sections ont bâti leur rapport sur les activités françaises de leur domaine, telles les sections 1 (Géodésie) ou 3 (Volcanologie et Chimie de l'Intérieur de la Terre). D'autres l'ont centré sur quelques contributions importantes dans leur domaine, collectées dans la communauté, telles les sections 4 (Géomagnétisme et Aéronomie) ou 7 (Sciences Physiques de l'Océan). D'autres encore ont compilé la liste des publications de leur domaine auxquelles des auteurs français ont contribué, rassemblées par thèmes, telle la section 8 (Sciences de la Cryosphère), ou pas, telle la section 2 (Sismologie et Physique de l'Intérieur de la Terre). Les sections 5 (Météorologie et Sciences de l'Atmosphère) et 6 (Sciences Hydrologiques) n'ont malheureusement pas fourni de contribution à ce jour.

Je profite de l'opportunité de ce rapport pour décrire rapidement le CNFGG et ses activités. Le CNFGG joue deux rôles. Il est le correspondent français de UGGI et, *per se*, échange avec l'Union et aussi avec l'Académie des Sciences de Paris sur tous sujets qui relèvent de la Géodésie et de la Géophysique. Il est aussi une société savante, association d'environ 300 membres, qui acquittent une cotisation annuelle de 30 € et participent aux activités de l'association, principalement des réunions scientifiques organisées par le Comité ou les sections.

Outre ses assemblées générales annuelles, dont la partie scientifique porte sur un thème multidisciplinaire (multi-section), le Comité a récemment lancé un colloque biennal sur des sujets spécifiques et s'adressant en priorité aux jeunes scientifiques. Deux colloques ont déjà eu lieu, le premier intitulé "L'eau dans tous ses états" dans les locaux prestigieux de l'UNESCO à Paris en 2008, et le second intitulé "Topographie et déformations multi-échelles, reflet d'une Terre dynamique" à l'ESGT (Ecole Supérieure des Géomètres et Topographes" au Mans en 2010. Le CNFGG participe occasionnellement à l'organisation d'événements conduits par d'autres sociétés (par exemple le C2I, "Colloque Interdisciplinaire en Instrumentation", organisé par l'Université du Mans en 2010). Au delà des réunions scientifiques, le CNFGG a été très actif au sein du Comité National Français pour l'Année Internationale de la Planète Terre (AIPT) qui a coordonné les nombreux événements organisés localement, régionalement, et nationalement entre 2008 et 2010.

Le CNFGG distribue aussi des subventions de voyage pour permettre à des scientifiques français de participer à des réunions internationales ; cet effort est plus particulièrement dirigé vers les jeunes scientifiques et les réunions organisées par les Associations de la famille UGGI. Enfin, le CNFGG remet annuellement son Prix de Thèse, de renommée nationale, à la meilleure thèse de doctorat soutenue dans l'année et soumise à son appréciation.

La liste des membres du Bureau et du Conseil du CNFGG à la date de la XXV Assemblée Générale de l'UGGI est donnée en Annexe de ce rapport. A tous ceux qui ont préparé ce rapport, et à tous ceux qui ont contribué et contribuent aux activités du CNFGG, j'adresse mes plus sincères remerciements.

Jérôme Dyment, President du CNFGG, Melbourne 2011.

FOREWORDS

CNFGG (*Comité National Français de Géodésie et de Géophysique*), the French corresponding organization to the International Union of Geodesy and Geophysics (IUGG), is glad to release its 2007-2010 quadrennial report to the IUGG and other corresponding bodies.

This year, the eight sections of CNFGG – mimicking the eight constitutive associations of the IUGG – have been given complete freedom to decide what their contribution should be. Some sections have built a report of the French activities in their field, as Section 1 (Geodesy) or Section 3 (Volcanology and Chemistry of the Earth Interior). Some others have focused on some important contributions in their field, collected in the community, as Section 4 (Geomagnetism and Aeronomy) or Section 7 (Physical Sciences of the Ocean). Others have listed the important publications to which French authors have contributed, gathered by topics, as Section 8 (Cryospheric Sciences), or not, as Section 2 (Seismology and Physics of the Earth Interior). Section 5 (Meteorology and Sciences of the Atmosphere) and Section 6 (Hydrological Sciences) have not provided a contribution so far.

I use the opportunity of this report to say a few words on CNFGG and its activities. CNFGG plays two roles. It is the French correspondent to the IUGG and, *per se*, exchanges with the Union and with the French National Academy of Sciences as well on all topics which are relevant to Geodesy and Geophysics. It is also a non-profit organisation with about 300 members, who pay an annual fee of 30 € and can participate the activities of the Society, mostly scientific meetings organized either by the Committee or by the Sections.

In addition to its annual General Assembly, which scientific part focuses on a multidisciplinary (multi-section) topic, the Committee has recently started a biennial topical meeting addressed to young scientists. Two such meetings have already taken place, the first one entitled "*L'eau dans tous ses états*" in the prestigious location of UNESCO in Paris in 2008, and the second entitled "*Topographie et déformations multi-échelles, reflet d'une Terre dynamique*" in ESGT (*Ecole Supérieure des Géomètres et Topographes*" in Le Mans in 2010. CNFGG occasionally participates in the organisation of events led by other societies (e.g. C2I, the "*Colloque Interdisciplinaire en Instrumentation*" organized by the University of Le Mans in 2010). Beyond meetings, CNFGG has been very active in the French National Committee for the International Year of Planet Earth (IYPE) which has coordinated the many events organized locally, regionally, and nationally between 2008 and 2010.

CNFGG also distribute travel grants for French scientists to attend international meeting; this effort is particularly aimed toward young scientists and the meetings gathered by the IUGG family of Associations. Last but not least, CNFGG awards annually its nationally renowned "Thesis Prize" to the best Ph.D. thesis produced in the year and submitted to its appreciation.

The list of the members of the Bureau and Council of CNFGG at the date of the XXV UGGI General Assembly is given in the Annex. To all who have been active to prepare this report, and to all who contributed and contribute in CNFGG activities, I address my most sincere thanks.

Jérôme Dyment, President of CNFGG, Melbourne 2011.

Comité National Français de Géodésie et Géophysique

French National Committee of Geodesy and Geophysics

RAPPORT QUADRIENNAL DU CNFGG A l'UGGI

QUADRENNIAL REPORT OF CNFGG TO IUGG

SECTION I - GEODESIE

SECTION I - GEODESY

CNFGG quadriennal report 2007-2010
Section of Geodesy

Trough its members the section 1 of the CNFGG gathers French competences in terms of research and realization aspects in geodesy. They pertain to national organisms such as BDL, BRGM, CNES, CNRS, EOST, ESGT, IGN, OCA, OMP, OP, SHOM, UPF involved in different geodetic activities.
This quadriennal report of the geodesy section cannot evidently claim being exhaustive. It includes a selection of reports delivered from eigth organisms: Bureau des longitudes, Centre National d'Etudes Spatiales, Ecole Supérieure des Géomètres et Topographes, Institut Géographique National, Observatoire de la Côte d'Azur, Observatoire de Paris Service Hydrographique et Océanographique de la Marine, and Université de la Rochelle. It includes moreover in appendix a list of publications from these organisms.

1) Bureau des longitudes (Nicole Capitaine)

Missions

The *Bureau des longitudes*, established in 1795, devotes its activities to scientific areas which come from its history (astronomy, geodesy, geophysics, etc.), constantly adapting to developments and projects in these areas. It functions as a scientific academy, with one session per month, plus meetings of working groups on specific topics for the preparation of books, documents, or colloquiums.

The *Bureau des longitudes* has been given the mission of publication and provision of public French astronomical ephemeris (*Connaissance des temps*, *Annuaire du Bureau des longitudes*), both having an annual publication. It has the scientific responsibility of these ephemeredes, whose implementation is entrusted, since 1998, to the *Institut de mécanique céleste et de calcul des éphémérides* (IMCCE), a division of Paris Observatory. The *Bureau des longitudes* "*Commission des éphémérides*" has been in charge of defining, in coordination with IMCCE, the content and evolution of these publications, with a special care to comply with the IAU and IUGG resolutions. This was especially the case for the IAU 2006/IUGG 2007 resolutions. As a member of the Research Group of Space Geodesy (GRGS), the *Bureau des longitudes* has a representative in its Directing Board, its Executive Committee and Scientific Council and gives advice on the GRGS organization, work and projects.

As part of its mission to disseminate scientific information, the *Bureau des longitudes* organizes each year a series of monthly lectures related to its areas, as well as one scientific colloquium, each year on a specific theme. These lectures and colloquiums have brought together a wide audience during the period 2007-2011. The *Bureau des longitudes* also participates in the organization and scientific sponsorship of colloquiums at national, European or international level, especially in the field of celestial and space navigation. It gives advice and recommendations on scientific issues related to its areas, in particular as published documents, with the participation of outside experts and in cooperation with other institutions.

Organization

The *Bureau des longitudes* is composed of 13 members, ex-officio representatives and additional corresponding members as described below:

Members (as of March 2011, provided in chronological order of the year of election): J.-F. Denisse, J. Kovalevsky, B. Guinot, P. Giacomo, R. Cayrel, N. Capitaine, J.-L. Le Mouël, S. Débarbat, J.-P. Poirier, C. Audoin, F. Barlier, A. Lebeau, P. Bauër. (NB: C. Fehrenbach passed away on January 9, 2008.)

Ex-officio representatives (as of March 2011): P. Delécluse (MétéoFrance), B. Frachon (SHOM, D. Hestroffer (Paris Observatory), J.-Ph. Lagrange (IGN).

NB: G. Bessero served as SHOM representative until 2010, while W. Thuillot served as IMCCE representative until February 2011.

Corresponding members (as of March 2011, provided in chronological order of the year of election): M. Golay, J.-C. Pecker, P. Merlin, R. Michard, G. Amat, M. Lefebvre, C. Boucher, J. Chapront, J.-C. Duplessy, J.-E. Arlot, F. Mignard, V. Brumberg, J.-C. Husson, J.-L. Simon, G. Balmino, M. Crépon, P. Willis, S. Ferraz-Mello, E.F. Arias, C. Turon, C. Sotin, J. Achache, C. de Bergh, Y. Desnoës, F. Rémy, C. Balkovski, A. Cazenave, V. Déhant, N. Dimarcq, M. Diament, A. Souriau, A. Morbidelli. (NB: B. Saint-Guily passed away on December 1, 2007).

The Bureau is elected and appointed for a 1-year period; its composition for 2007-2011, was:
2007: President: François Barlier, Vice-President: André Lebeau, Secretary: Pierre Bauër,
2008-2009: President: André Lebeau, Vice-President: Nicole Capitaine, Secretary: Pierre Bauër,
2010-2011: President: Nicole Capitaine, Vice-President: Pierre Bauër, Secretary: Pascal Willis.

Meetings 2007-2011

Monthly meetings and scientific colloquiums

Besides its regular monthly meetings open to a large public (see above), the scientific colloquiums (including 4 to 5 presentations each), organized on a yearly basis by the *Bureau des longitudes* have been as follows:

2008 (June 18): *Les glaces de la Terre*
2009 (June 17): *La quête Galiléenne*
2010 (June 16): *Terre en mouvement*
2011 (June 15): *La nouvelle géographie*

Scientific colloquiums with the scientific sponsorship of the Bureau des longitudes

The *Bureau des longitudes* was involved in the organization of the 1st and 2nd Colloquium on "Scientific and Fundamental Aspects of the Galileo System", organized by the European Space Agency, in Toulouse (France) from 1 to 4 October 2007, and in Padova (Italy) from 14 to 16 October 2009, respectively. It was also involved in the "Journées Lalande and Lœwy", from 13 to 14 June 2007, and in a scientific meeting on the "Nautical Ephemerides", on 19 June 2007, both organized at Paris Observatory. More details as well as past scientific conferences can be found at (http://www.bureau-des-longitudes.fr/conferences.htm#).

Publications 2007-2011

Besides its responsibility of yearly publications of the French astronomical ephemeredes (see above), the Bureau des longitudes publishes books, written by its members or corresponding members, with the participation of outside experts and in cooperation with other institutions on selected scientific topics related to its mission.

In the last 4 years, the following books were published. More details can be found at http://www.bureau-des-longitudes.fr/publications.htm.

The book on *Galileo* (2003, 2005: English version and 2008: 2d edition) includes recommendations on Galileo development, its civil use, technical applications, scientific applications, security and defence and industrial issues.

The book "*Les Observatoires: Observer la Terre*" (2009), includes general recommendations on the importance of observations, on the sustainability, continuity and accuracy of these observations, archival and accessibility, interoperability, governance and services; it also includes specific recommendations in the fields of geodesy, geodynamics, solid Earth, oceanography, glaciology and hydrology, atmospheric environment and climate.

2) Centre National d'Etudes Spatiales (Richard Biancale)

Les activités du CNES en géodésie, et notamment en géodésie spatiale, sont multiples. Elles vont de la conception d'instruments de géodésie spatiale, tel DORIS, à la programmation de missions spatiales de métrologie (par exemple MICROSCOPE), aux études de faisabilité de nouvelles missions (par exemple MICROMEGA), aux activités de traitement et de recherche qui sont essentiellement conduites par l'équipe de Géodésie Spatiale du CNES.

Ce rapport présente de façon succincte des réalisations de cette équipe, membre du Groupe de Recherche de Géodésie Spatiale (GRGS), et notamment celles relevant de la thématique champ de gravité dans trois chapitres : *modélisation par méthodes spatiales, réalisation de cartes d'anomalies de gravité corrigées de la topographie, champs planétaires.*

Cette équipe est également impliquée dans les traitements des mesures GNSS et DORIS – elle est centre d'analyse de l'IGS et de l'IDS -, dans des projets de modélisation de la thermosphère, dans les activités relevant du Bureau Gravimétrique International (BGI)… De plus et dans un cadre coopératif, elle met à disposition d'autres équipes de recherche son logiciel de géodésie spatiale, GINS-PC, pour lequel elle assure la formation d'utilisation.

La bibliographie des années 2007-2010 est à retrouver dans celle du GRGS donnée en annexe.

- *Modélisation du champ de gravité par méthodes spatiales*

La mission GRACE (Gravity Recovery and Climat Experiment) a révolutionné notre appréhension de la gravité depuis l'espace. Cette mission NASA/DLR composée de deux satellites jumeaux en orbites polaires vers 460 km d'altitude a continué à délivrer des mesures inter-satellites de précision micrométrique. Ces mesures acquises sur une distance moyenne de 220 km donnent une information relative sur les perturbations gravitationnelles entre les deux satellites, les accélérations non-gravitationnelles étant mesurées directement à bord par des accéléromètres électrostatiques (à 10^{-10} m/s^2 près)

A côté des centres de traitements officiels du projet GRACE, l'équipe CNES s'est investi dans le traitement des données de niveau 1b (mesures GPS, laser, Kbr, accélérométriques, quaternions) pour modéliser le champ de gravité terrestre par périodes décadaires à la résolution spatiale de 400 km. Ces modèles, disponibles à travers le site internet du GRGS (http://grgs.obs-mip.fr), servent notamment à l'interprétation des variations hydrologiques et à quantifier la déglaciation des zones polaires (par exemple, l'estimation obtenue de la déglaciation du Groendland est de l'ordre de 150Gt/an). La série décadaire RL02 a servi à produire le premier modèle statique en 2008 (EIGEN-GRGS.RL02.MEAN_FIELD) qui incorpore des termes temporels, à savoir les dérives linéaires, et des termes périodiques de périodes annuelle et semi-annuelle pour tous le coefficients harmoniques sphériques du degré 2 au degré 50. Ce modèle, comme le modèle suivant, EIGEN-5S, produit en coopération avec l'institut allemand GFZ, est développé jusqu'au degré harmonique sphérique 160, correspondant à la résolution spatiale de 125 km.

En 2009, la mission GOCE (Gravity field and Ocean Circulation Explorer) est venue compléter la constellation de satellites dédiés à la gravimétrie spatiale. Le satellite est maintenu sur une orbite héliocentrique à 255 km d'altitude grâce une propulsion ionique qui compense la traînée atmosphérique. La gravité est mesurée de façon relative par six accéléromètres (de précision 10^{-12} m/s^2 près) qui produisent par différentiation le tenseur des gradients gravitationnels.

L'équipe CNES fait partie du consortium européen EGG qui participe aux traitements des données gradiométriques GOCE. En coopération avec le GFZ-Potsdam, l'équipe a produit le premier modèle GOCE de référence en 2010. Ce modèle améliore et homogénéise notre connaissance du géoïde aux longueurs d'onde de 200 à 80 km, soit bien en complément de GRACE. La précision atteinte dorénavant est de 2 mGal (10^{-5} m/s^2) en anomalie de gravité et de 5 cm en hauteur de géoïde à la

résolution de 100 km. Elle permet de déterminer à cette échelle la topographie dynamique moyenne des océans (différence entre la surface altimétrique moyenne et le géoïde) et de quantifier ainsi, à quelques cm/s près, la circulation océanique générale.

En parallèle, de nouveaux concepts de missions de gravimétrie spatiale ont été étudiés, tels les formations en roue inclinée (3 satellites en mouvement relatif circulaire) ou pendulaire (2 satellites en oscillation relative dans la direction normale au plan orbital). Cette dernière version a d'ailleurs été proposée en réponse à un appel d'offre de l'ESA (Earth Explorer 8 Opportunity Mission) à travers un partenariat européen. Ce projet, dénommé e.motion, qui vise à mesurer les transferts de masse à l'intérieur du système Terre avec une précision d'environ 10 cm de hauteur d'eau équivalente à 250 km de résolution spatiale et avec une résolution temporelle d'environ 10 jours, n'a finalement pas été retenue par l'ESA. Cependant, ce travail a permis de réunir de nombreux scientifiques européens pour réfléchir à la suite de la mission GRACE à moyen terme.

- *Réalisation de la carte d'anomalies gravimétriques mondiales*

A l'initiative du BGI et de la Commission de la Carte Géologique du Monde (CCGM), un projet de réalisation d'une carte globale des anomalies de pesanteur a été initié en 2007 avec le soutien de l'IAG, de l'IGFS et de l'UNESCO. Ce projet « WGM » (World Gravity Map) vise à mettre à disposition de la communauté internationale une carte des anomalies (ou perturbations) gravimétriques, corrigée de la topographie, et divers produits dérivés (grilles numériques d'anomalie, livret en différentes langues…), pour des applications de recherche et d'éducation. Ce projet doit venir compléter une série de cartes géologiques et géophysiques globales produites par la CCGM (http://ccgm.free.fr), à l'instar de la carte magnétique mondiale publiée et également disponible sous forme numérique à une résolution spatiale de 3'x 3'.

Pour les besoins de cette carte, de nouveaux développements ont été réalisés au BGI, dans le but d'effectuer le calcul global des corrections topographiques en symétrie sphérique. En 2010, de nouveaux développements théoriques ont été mis au point par G. Balmino (CNES) en vue de la modélisation haute résolution du champ de gravité en harmoniques sphériques. Ces développements originaux ont été appliqués spécifiquement à ce projet de cartographie globale. Un calcul global des corrections de terrain à 1' de résolution (sur la base de ETOPO1), prenant en compte l'effet des masses liées aux irrégularités topographiques (reliefs terrestres et sous-marins) ainsi qu'aux océans, grands lacs et calottes polaires a été réalisé pour la première fois. Ces corrections ont été appliquées au modèle de référence global EGM08, produit en 2008 par la NGA (National Geospatial-intelligence Agency, USA) et qui intègre l'information la plus actualisée et complète à ce jour sur le champ de pesanteur terrestre (ensemble des observations issues de mesures sol, aéroportées ou spatiales).

- *Modélisation des champs de gravité planétaires*

Les études planétaires ont principalement concerné la planète Mars et la comète Churyumov-Gerasimenko (67P), objectif de la sonde ROSETTA de l'ESA en 2014.

Les travaux sur le champ de gravité martien ont utilisé les observations de trajectographie des missions américaines Mars Global Surveyor (MGS), Mars Odyssey (MODY) ainsi que Mars Reconnaissance Orbiter (MRO), collectées par les stations du réseau DSN de NASA-JPL. Un nouveau champ de gravite de Mars développé au degré 95 (MGGM08A) a été produit en coopération avec l'Observatoire Royal de Belgique (ORB). Les variations saisonnières des termes C20 et C30 (amplitude : $2\ 10^{-9}$) dues aux transferts de masse (sublimation/condensation du CO2) entre les calottes polaires et l'atmosphère ont pu être déterminées ainsi que le nombre de Love k_2 dont la valeur (0,12) laisse penser que le noyau de Mars aurait un rayon de quelque 1500 km.

L'objectif des études sur la comète Churyumov-Gerasimenko est d'analyser les possibilités de restitution du champ de gravité par l'analyse des perturbations d'orbite de la sonde ROSETTA (à l'aide des données de radio-science). Des simulations ont donc été menées à partir d'un modèle de

forme en tenant compte de plusieurs hypothèses de densité (de 0,3 à 1g/cm^3), et par différentes modélisations : en harmoniques sphériques et sous forme polyédrique. Ce travail est réalisé en étroite collaboration avec l'équipe du CNES en charge de la trajectoire de descente de l'atterrisseur Philae car il doit servir à analyser les scénarii d'atterrissage de Philae sur la comète.

3) Ecole Supérieure des Géomètres et Topographes – ESGT (Stéphane Durand)

L'Ecole Supérieure des Géomètres et Topographes est un institut du Cnam (Conservatoire National des Arts et Métiers) destiné à la formation initiale d'ingénieurs dans le domaine des sciences topographiques et l'aménagement du territoire. L'ESGT qui apporte une double compétence technique et juridique est la principale voie d'accès à la profession de géomètre-expert.

L'ESGT héberge deux équipes de recherche en son sein, l'ADéGeF (Administration, Délimitation et Gestion du Foncier) liée aux activités juridiques et foncières de l'école, et le Laboratoire de Géodésie et Géomatique (L2G), orienté vers les domaines de la géomatique. Ce dernier est par ailleurs reconnu depuis 2007 comme Jeune Equipe (JE 2508) du Ministère.

Le présent rapport ne fait état que de l'activité de recherche de l'ESGT dans les domaines liés aux activités de la section 1 du CNFGG, à savoir la géodésie, la gravimétrie et l'interférométrie radar différentielle (DInsar). Dans ces domaines, l'ESGT s'intéresse essentiellement à l'utilisation de la géodésie pour la mesure de déformation géophysique ou géotechniques.

L'ESGT utilise principalement la géodésie pour mesurer les déformations de l'écorce terrestre, à toutes les échelles et qu'elles soient d'origine naturelle ou anthropique. Trois techniques sont maîtrisées au sein du laboratoire L2G de l'ESGT:

- la topométrie de précision, qui consiste à mesurer des distances et des angles entre les points d'un réseau,
- le GPS différentiel qui fournit des mesures ponctuelles
- l'interférométrie radar qui exploite les interférences obtenues entre les images radar acquises par un satellite à deux différentes pour mettre en évidence des déformations de surface .

L'étude de ces techniques, l'évaluation et les tentatives d'amélioration de leurs performance, leur mise en oeuvre dans des projets de recherche en géophysique, sont abordés dans un esprit comparatif qui permet avec l'expérience, dans une situation donnée, de recommander la technique la plus adaptée. Parallèlement au développement de cette expertise, le L2G s'était notamment fixé comme objectifs :

- la modélisation des effets atmosphériques sur ces techniques et notamment sur le GPS (travaux sur la ionosphère dans le cadre de l'accueil d'un thésard australien P.Grgich, et sur la troposphère dans le cadre de la thèse de F.Fund).
- la tentative de combinaison des 3 techniques (pour l'instant limitée à deux techniques – topométrie de précision et GPS – dans le cadre de la thèse de B. Legru, mais la fusion avec l'interférométrie radar reste un objectif réaliste à moyen terme).

La thèse de François Fund, réalisée en collaboration avec le laboratoire de Planétologie et Géodynamique de Nantes, cofinancée par l'Ordre des Géomètres-Experts français et la Région des Pays de la Loire, a été soutenue en décembre 2009. Cette thèse a conduit à deux études spécifiques , d'une part l'évaluation des produits troposphériques issus des données météo dans le cadre du réseau européen GPS, et d'autre part l'étude du phénomène de surcharge océanique dans le Grand Ouest avec une plus forte densité de stations, une période de données plus conséquente que celle des études antérieures ainsi qu'une optimisation du traitement tenant compte des dernières évolutions.

La thèse de Benoit Legru, débutée fin 2007 et financée par le Cnam, devrait être achevée courant 2011. Cette thèse vise essentiellement à exploiter la complémentarité des différentes techniques et aura permis entre autre de clarifier les conditions théoriques de cette complémentarité et de les tester avec le GPS et la topométrie sur la base de simulations numériques (amélioration des précisions formelles par combinaison) et d'expérimentations sur le terrain dans des conditions contrôlées.

Concernant l'interférométrie radar différentielle (DInsar), le laboratoire a essentiellement durant le quadriennal 2007-2011 élaborer sa chaîne de traitement. Les méthodes ont été mises en place à partir d'outils gratuits (compilation et écriture de scripts) : DORIS, STAMPS. Les développements entrepris dans le cadre d'un stage de M2 puis d'un post-doctorat d'un an (M. Chendeb) terminé en

décembre 2009, permettent à la fois de disposer d'outils de traitement opérationnels et d'une bonne connaissance du potentiel et des limites des logiciels existants (libres et commerciaux). Les outils de mesure de déformation du sol ont été appliqués en contexte urbain. Des données des satellites ERS sont actuellement utilisées, et d'autres capteurs seront utilisés par la suite. La confrontation de l'interférométrie radar avec les autres techniques de mesure de déformation devrait se concrétiser au cours du prochain quadriennal.

En matière de gravimétrie, l'ESGT est devenue membre du Bureau Gravimétrique International pour l'élaboration et la validation de données gravimétriques. Le L2G contribue dans ce cadre à la validation de l'automatisation du calcul du géoïde sur un jeu de données du BGI (travaux en cours). Les travaux en matière de gravimétrie mobile constituent le prolongement de travaux antérieurs, avec le développement d'un système inertiel à composants discrets liés (strapdown) permettant d'estimer les composantes du champs de pesanteur avec une exactitude de l'ordre du mGal et une résolution spatiale de quelques kilomètres, en collaboration avec le Laboratoire de Recherche en Géodése de l'IGN. Ces travaux ont aboutis à la soutenance en juin 2008 de la thèse de bertrand de Saint Jean intitulée « Etude et développement d'un système de gravimétrie mobile » (thèse de l'Observatoire de Paris avec co-encadrement LAREG et L2G). Le système actuel, appelé LiMOG, permet de fonctionner en gravimétrie scalaire avec une précision du mGal mais d'autres développements instrumentaux sont nécessaires pour restituer les trois composantes du champ de pesanteur avec une précision du même ordre de grandeur.

4) Institut Géographique National (David Coulot, Françoise Duquenne, Pascal Willis)

The geodetic activity of IGN is divided in two parts: operational and research respectively managed by the SGN (Service de la Géodésie et du Nivellement) and the LAREG (Laboratoire de Recherche en Géodésie)
The SGN is in charge of the realization and maintenance of the national geodetic and height references in France, and has also a significant activity on International networks and services.
The RGP is the French GNSS permanent network. The constitution of this network is based on a wide partnership between the IGN, public institutions (universities, research laboratories, urban communities, etc..) and private companies, especially RTK networks managers. The increase of the number of stations, from 75 in 2006 to 241 in 2010 is mainly due to these private partners. The present repartition of stations is IGN (9,5%), public institutions(25%), private companies (65,5%). Since 2008 the GPS network is becoming a GNSS one by installing GPS and GLONASS receivers (174 at the end of 2010). SGN collects data, checks data quality, delivers data on the internet, process hourly, daily and weekly solution and manages two operational centers. SGN contributes to E-GVAP by sending every hour atmospheric behavior parameters (ZTD) which are introduced by Météo-France in the atmospheric prediction models.

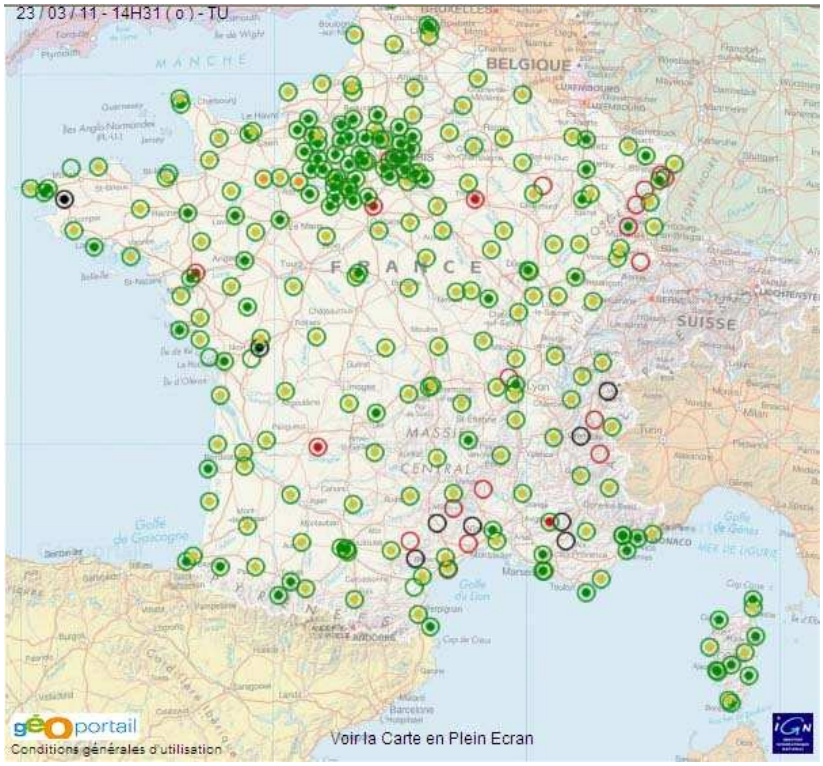

All the observations of the RGP measured between 1998 and 2009 have been reprocessed and a new set of coordinates has been obtained in the ETRS89 (European geodetic system) with a millimetric accuracy.
The RBF (Réseau de Base Français) , geodetic network of about 1000 points, created in 1995 was observed again with GPS between 2000 and 2009. A new set of coordinates was obtained with the new RGP coordinates. In June 2010, these new coordinates were published with a new altimetric conversion grids (RAF09, RAC09).

The RBF is now a combined network.The link with the vertical network was made with spirit levelling and since 2000 IGN has measured gravimetry on every point of the RBF, in relative gravimetry and for about 200 points of them in absolute gravimetry with a A10 gravimeter in collaboration with the “Institut de Géophysique du Globe de Paris” and the “Institut de Recherche pour le Développement”. Every point of the RBF has a geometrical position (λ, φ, h), an altitude (H) and a gravity value (g).

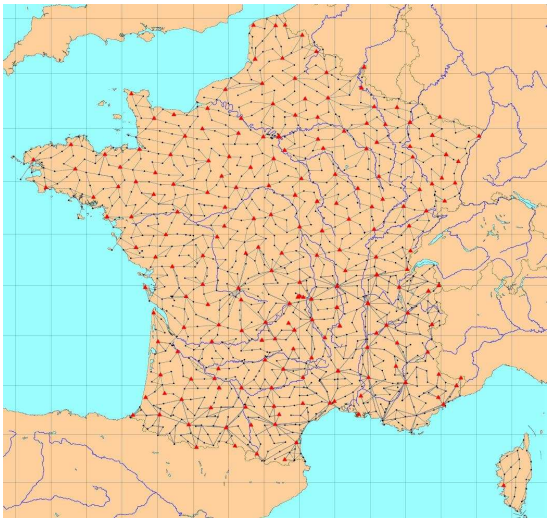

Concerning the French Vertical Reference (IGN69), IGN has deployed a new process for the network maintenance. The French territory is covered with 13200 “triplets” which are composed of at least three benchmarks, far away one another at the most one kilometre. Anywhere in France, some body is at five kilometers far from a “triplet”. During the period 2000-2007 a visit was performed on the entire leveling network (about 350000 benchmarks) and the aeras without triplets were completed. Since 2009 about 1100 triplets/year are observed with spirit levelling to control the inside stability and with GPS which provides the ellipsoid height on each triplet and give the absolute stability in connection with the RGP stations. This will allow the monitoring of the vertical deformations.

The observations of the Reference Levelling Network started in 2001, were carried on between 2007-2010 with 717 kilometers. New vehicules and levels were purchased for the motorized levelling. This network will be the French component of EVRS. The first processing shows that this levelling has a very good agreement with tide gauges and European Geoid (EGG2008). It confirms that IGN69 is biased.

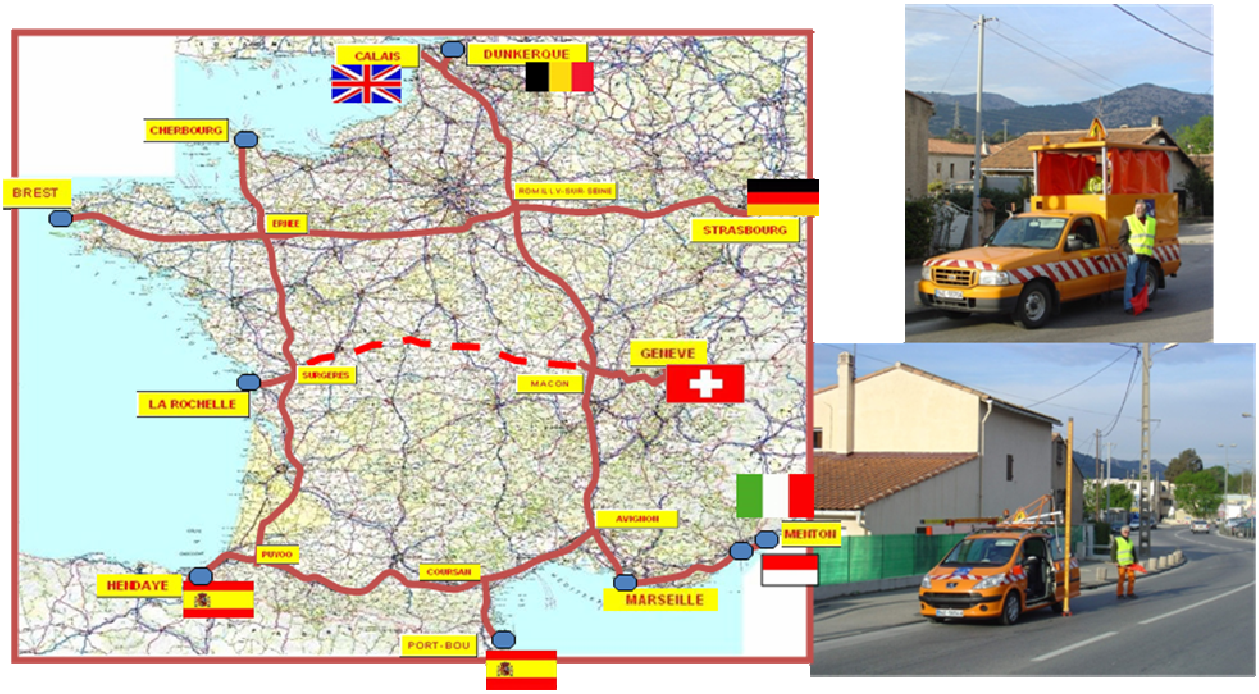

IGN has also activities in the international services and networks : DORIS in collaboration with CNES and IGS (International GNSS Service) in the frame of IAG.
DORIS activity at IGN includes 4 different aspects and are handled by SGN or in conjunction with Institut de Physique du Globe de Paris (IPGP):

1) DORIS network installation and maintenance
2) DORIS/IGN analysis center activity
3) Research activity related to DORIS (geodetic positioning and precise orbit determination
4) Geophysical research activity based on DORIS results

The first 2 points are already addressed in the IDS Report to the IAG Travaux (Willis, 2011). In the last 4 years, the DORIS permanent tracking network has been very stable and a major renovation was undergone leading to an almost complete network based on Starec 3.0 antennas with improved geodetic stability. The latest DORIS/IGN weekly solution provided is ignwd08 (Willis et al., 2010), also available as expressed in ITRF2005 and named ignwd09. This solution was used to create the IDS combined solution used for ITRF2008. Both weekly solutions can be downloaded at: ftp://cddis.gsfc.nasa.gov/pub/doris/products/sinex_series/ignwd. They include early data since 1993 and are updated about once a week with a couple of days of delay after DORIS data are released by CNES.
Major research activities at IGN in the last 4 years and linked with Marie-Line Gobinddass' doctoral dissertation presented on October 1, 2010 and addressed issues related to solar radiation pressure estimation as well as atmospheric drag corrections (Gobinddass et al., 2009, 2010a, 2010b). Other research activities are linked to tropospheric estimation using the DORIS system (Bock et al., 2010, Willis et al., in press) or inter-comparisons with other space technique (Teke et al., in press). All these research are mostly dependant on precise orbit determination (Cerri et al., 2010, Lemoine et al., 2010, Zelensky et al., 2010). A DORIS-specific reference, including all DORIS stations, based on ITRF2005 was also produced (DPOD2005, Willis et al., 2009) for precise orbit applications. Aspects related to DORIS phase center location were also addressed (Doornbos and Willis, 2007, Willis et al., 2007).
Time series of precise geodetic coordinates of all DORIS stations can be found at http://ids-doris.org/network/ids-station-series.html. A few stations were analyzed in more details for geophysical purposes in cooperation with other scientists over the world: global plate tectonic (Argus et al., 2010), post-glacial rebound (King et al., 2010) Socorro island (volcanic activity, Briole et al., 2009), Everest station (Himalaya, Flouzat et al., 2009), Syowa (Antarctica, Amalvict et al., 2007), Ny-Alesund (post-glacial rebound, Kierulf et al., 2009), Tahiti station (vertical monitoring for altimetry calibration, Fadil et al., in press).

IGN is one of the IGS data center. Between 2007 and 2010 a big effort was done in the modernization and optimization of this data center. Since February 2010, IGN has replaced Natural Resources Canada as the terrestrial frame coordinator of IGS.
The activities of the LAREG aims to reach two main objectives:

- to improve the quality of geodetic references, namely the International terrestrial reference frame (ITRF) and the height references (geoid) ;
- to improve the modeling of the atmosphere delay (and, in particular, the troposphere delay) for the space-geodetic data processing, to reach a better precision for the height component of the station positions.

The researches are organized in four themes: reference systems, gravity field, geodesy and atmosphere and space geodesy.

Reference systems

In the field of reference systems, the research activities are mainly related to the determination of the ITRF (LAREG is the ITRS center) and the assessment of its quality, which is of primary importance for the measurement of sea-level rise, for instance.
The computation of the first realization of ITRF based on time series of station positions and EOP (ITRF2005) has been a step towards the consistency between IERS products. Indeed, since its computation, a new process has been developed and maintained at the IERS EOP Product Center (SYRTE, Observatoire de Paris), which ensures the long-term consistency between reference EOP time series and ITRF. A specific study, based on the interpolation of velocity fields, has showed that there was a rotation between ITRF2005 and a NNR frame (PhD thesis of J. Legrand, March 2007). We took the opportunity of ITRF2005 computation to also develop a methodology of comparison of the station position time series of different techniques at colocation sites. We also searched for the best way of referencing times series to improve the determination of the geocenter by SLR (PhD thesis of X. Collilieux, June 2008).

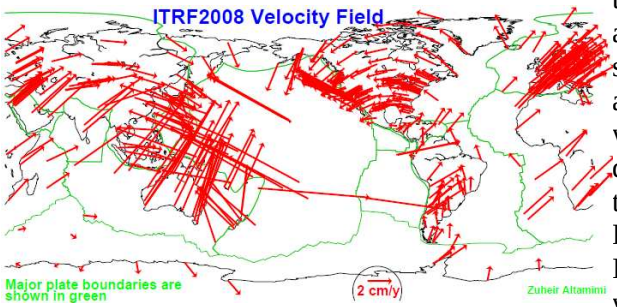

During the time period, a new realization of the ITRS (ITRF2008, cf. figure) has been computed with significant improvements with respect to the past realizations, especially regarding scale. All the results are available on the ITRF Website[1]. Since 2008, collaborations with geophysics laboratories (especially at the Institut de physique du Globe de Paris – IPGP – France, and at the European Centre for Geodynamics and Seismology – ECGS – Luxembourg) have been intensified. They aim at confronting the kinematic model of Earth provided by space geodesy to the geodynamical models of the phenomena at hand, to validate reference frames. For instance, we have established a link between the loading effects and the stability of the origin and the scale of the SLR terrestrial frame and we currently compare the secular origin of ITRF to the secular motion of the geocenter predicted by geophysical models.
A PhD thesis (P. Rebischung) on the improvement of the contribution of GNSS to ITRF began in October 2010.

Gravity field

The activities related to the determination of the gravity field are conducted in two main directions: (i) the computation of multiscale determinations of the gravity field (based on spherical wavelet decompositions) and (ii) the methodologies for processing mobile measurements of gravity (vectorial accelerometry). The methodologies developed at LAREG aims to merge, into a unique modeling, measurements of heterogeneous resolutions: large wavelengths with space gravimetry, medium wavelenghts with mobile gravimetry and short wavelengths with ground measurements.

1 http://itrf.ign.fr/ITRF_solutions/2008/ITRF2008.php

Regarding the first axis, the interest of the representation of the gravity field by decompositions over wavelets for interpreting gravity data has been demonstrated. The exploitation of the GRACE-derived monthly gravity field models with this methodology has provided an interpretation of the seisms of Sumatra in december 2004 and march 2005. This approach has also been applied to compute a high-resolution (10-15 km) model over Japan (cf. figure), in collaboration with the Geospatial Information Authority (GSI) of Japan. The time period has seen the launch of the ESA GOCE satellite (17.03.2009). Since this launch, LAREG has been involved, in collaboration with IPGP, in the SEEGOCE project (exploration of solid Earth with GOCE).

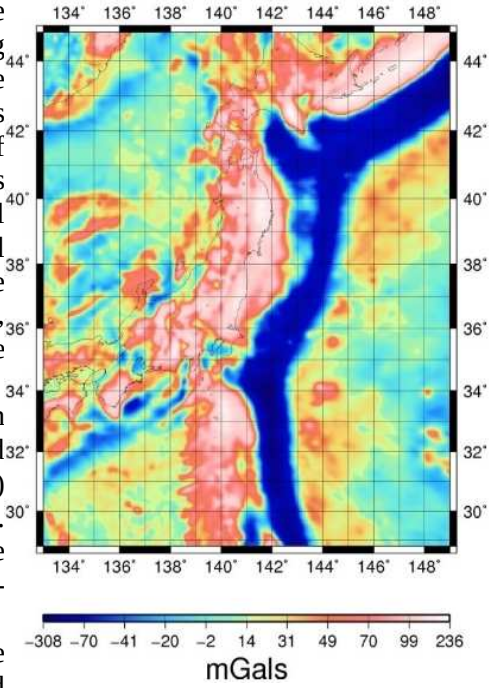

The second axis has given rise to two PhD theses, in collaboration with L2G (Laboratoire Géodésie et Géomatique) de l'ESGT[2] and IPGP. The first one was defended in June 2008 (B. de Saint-Jean) and the second one (Q. Li) will be defended at the end of 2011. Both theses are related to the validation and the exploitation of the measurements provided by the mobile gravimetric system Limo-G[3].

A PhD thesis (P. Valty) on the study of the climatic change in the Mediterranean, based on GRACE data, GPS data and geodynamical models, began in October 2009.

Geodesy and atmosphere

Ground-based GNSS networks are increasingly used in geodesy, meteorology and environmental research (climatology, hydrology). Our research in this fields are both at a methodological level (study and mitigation of errors sources in GNSS measurements) and at the application-level.

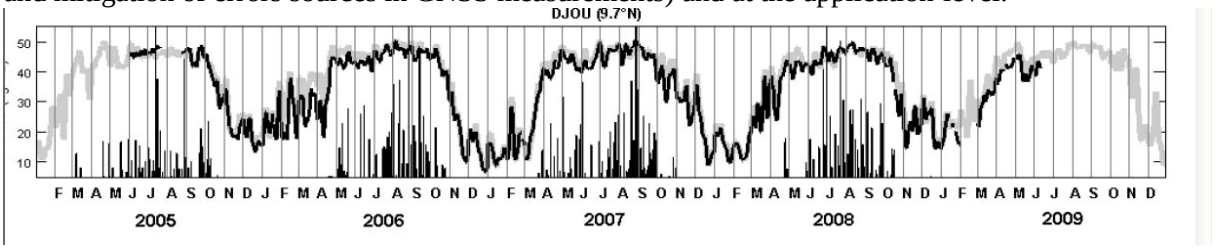

We have been involved in several international scientific projects for studying the atmospheric water cycle like AMMA (African Monsoon Multidisciplinary Analyses, http://www.amma-international.org) and HYMEX (http://www.hymex.org). With AMMA, we have installed six GPS stations in West Africa. We investigated the multiscale nature of the water cycle with the help of precipitable water vapour estimates retrieved from the GPS data in addition to other observational data and numerical models (PhD thesis of R. Meynadier, March 2010) – cf. figure. We have also detected biases in the measurements from radiosondes and have provided useful diagnostics for the evaluation of meteorological models.

In the framework of the GHYRAF project (gravity and hydrology in Africa, coordinated by the EOST[4]), the time series of positions of the African GPS stations have also revealed a signature of regional surface loadings from the atmosphere and hydrology. They have been confronted to geodynamical models and GRACE loading estimates (PhD thesis of S. Nahmani which will be defended during 2011).

LAREG is also participating to the development of a Raman lidar devoted to the measurements of water vapour profiles in the troposphere and the correction of wet tropospheric delay in GPS signals. The use of lidar measurements has been shown to improve the positioning precision for short-time measurement sessions (6h). It is considered as an efficient tool for studying the error sources in GNSS data and achieving a high level of positioning accuracy (~2mm) from short sessions (whereas GNSS

2 École supérieure des géomètres et topographes.
3 Light moving gravimetry system.
4 École et observatoire des sciences de la Terre.

data usually need be averaged over days to months). This research activity has been conducted in collaboration with the Laboratoire d'opto-électronique et de micro-informatique (LOEMI) of IGN since 2001.

Space geodesy

The IGN carries out methodological researches on the GNSS, DORIS (see above), SLR and VLBI data processing. Since September 2007, the LAREG has contributed, in collaboration with IMCCE[5] and OCA[6], to the ILRS GRGS[7] analysis center. In this framework, during the debate on the scale bias between VLBI and SLR techniques evidenced by the ITRF2005 computation, we demonstrated the great impact of range biases on the scale derived by SLR. The LAREG also participated, in collaboration with the University of la Rochelle (ULR), to an analysis center of the IGS TIGA pilot project with, as a result, a new improved GPS velocity field to correct the measurements of tide gauges of ground motions (PhD thesis of A. Santamaría-Gómez, October 2010).

We also study the direct combination of space-geodetic measurements (cf. figure) for the determination of terrestrial frames and EOP. We proved the feasibility of such a computation, showed its interest for EOP determination and quantified the impact of local ties, common zenithal tropospheric delays and measurements of satellites embarking several geodetic instruments (PhD thesis of A. Pollet, January 2011).

During the period, some new research topics also emerged: researches on the benefit of modern global optimization methods for space-geodetic issues and on the modeling of the drag force in the framework of the kinetic theory of gas, in collaboration with the Centre de Mathématiques Laurent Schwartz (CMLS, École Polytechnique).

IAG REFAG 2010 symposium

Since 2007, Z. Altamimi has been chair of the first commission (reference systems) of IAG. In this context, IGN organized, with the support of NASA, CNES, the Leica society and the University of Marne la Vallée, the symposium of this commission in October 2010. This symposium gathered about 150 scientists, coming from 30 countries, who presented and discussed issues related to the definition, realization and use of geodetic references for Earth's sciences.

5 Institut de mécanique céleste et de calcul des éphémérides.
6 Observatoire de la Côte d'Azur.
7 Groupe de recherche en géodésie spatiale.

5) Observatoire de la Côte d'Azur (Pierre Exertier)

Le site géodésique et métrologique du plateau de Calern

Le site accueille les équipements propres à la télémétrie laser (instrument fixe MeO, basé sur un télescope de 154cm et laboratoire de la station mobile) ainsi qu'au transfert de temps (T2L2, GPS et Two-Way ou TWSTFT). En outre, le système de temps de référence est fourni par l'horloge Cesium de l'Observatoire accompagnée, en 2010, d'un nouveau Maser-hydrogène (modèle TS-4), en remplacement du Maser de l'ex LHA (Paris).

S'ajoute aux équipements laser, les installations liées aux systèmes de positionnement GPS et DORIS (balise re-installée fin 2008 dans le cadre de T2L2), ce qui fait de Calern un site multi-techniques, aspect fortement recommandé par le GGOS.

L'ILRS a noté la reprise d'activités du Laser Lune français en 2008, et les tirs laser effectués régulièrement sur les satellites géodynamiques LAGEOS, se sont ajoutés à la la nouvelle solution ITRF2008 du repère de référence terrestre international.

Développements des stations Laser, Mobile (FTLRS) et Fixe (MEO)

FTLRS

Evolutions technologiques

Suite à la campagne probatoire menée à l'Observatoire de Paris en Octobre 2009, une faiblesse dans le bilan de liaison laser avait été mise en évidence menant à des observations peu nombreuses en raison aussi de la forte atténuation atmosphérique du ciel parisien.

Un important travail de remise en état, avec des améliorations conceptuelles sur le système laser, a été entrepris au cours du premier semestre 2010. Le but de ces travaux a été d'obtenir une répartition spatiale de la tâche laser proche d'un profil gaussien et surtout sans « points chauds » de façon à éviter l'endommagement récurrent des éléments optiques (barreaux laser, lentilles, miroirs, lames de phase, ...). Les résultats sont satisfaisants avec une divergence du faisceau réduite à quelques secondes d'arc et, par conséquent, un bilan de liaison très nettement amélioré (confirmé par la suite lors de la campagne T2L2 à Paris).

Campagne Laser Mobile à Paris pour le projet T2L2 (Juin-Octobre 2010) :

Afin d'observer dans de meilleures conditions et de sécuriser l'accès des personnels aux installations d'observation Laser, le projet T2L2 a fait développer, en 2008/2009, et installer une plateforme métallique sur la toiture terrasse de l'Observatoire de Paris.

La campagnes T2L2 de 2010 proprement dite s'est déroulée du 1er juin au 6 octobre avec une interruption de deux semaines au mois d'août impliquant la présence continue d'équipes du groupe laser pour maintenir les équipements et effectuer les tâches d'observations opérationnelles 24h/24, à la fois à Grase et à Paris.

Les résultats ont été tout à fais satisfaisants avec 140 passages télémétrés depuis l'Observatoire de Paris sur Jason2 dont 88 simultanément avec la station Meo de Grasse.

Les données scientifiques ont été traitées par le Centre de Mission Scientifique (CMS) de T2L2, installé à l'OCA, et la stabilité du lien atteinte dans ce transfert de temps entre les Masers (OP et OCA), eux-mêmes suivis par des fontaines atomiques de part et d'autre, se situe aujourd'hui aux alentours de quelques dizaines de picosecondes.

Prospective pour une station mobile de nouvelle génération :

Un projet de station de télémétrie Laser Ultra mobile de nouvelle génération couplée au développement d'un système pour équiper l'observatoire géodésique de Tahiti est en cours d'élaboration depuis début 2009, avec une participation budgétaire à répartir entre le CNES et le projet RESIF proposé dans le cadre d'Equipex et soutenu par l'INSU.

Ce projet ambitieux pourra permettre à la communauté géodésique Française d'envisager à la fois la pérennité de cette activité alliée à des évolutions technologiques et opérationnelles très intéressantes dans le contexte scientifique international. L'INSU a mis en place un CDD de 3 ans, avec un personnel (Ing de Recherche, C. Courde) qui commencera un travail d'analyse dès le début de 2011.

Station MeO

Instrumentation

Le développement de la station MeO suit son cours avec, notamment, le développement des logiciels, l'organisation du coudé optique, le développement de la nouvelle détection et le démarrage d'un programme de détection des débris spatiaux (notamment avec l'IMCCE).

Plusieurs travaux ont été entrepris en 2010, sur MeO, dont schématiquement, l'intégration d'une optique guide grand champ (1°) en parallèle sur l'optique primaire du télescope, le développement d'une chaine de détection faible bruit et grand champ adapté à la détection des débris spatiaux (compromis bruit – performance), enfin l'intégration de l'infrastructure pour un projet d'optique adaptative d'imagerie satellitaire (en collaboration avec l'ONERA) ;

Observations

La station MeO est opérationnelle depuis juin 2009. Elle observe régulièrement des cibles LEO (Jason2) et MEO (dont Lageos, GIOVE et GNSS), les réflecteurs de la Lune ainsi que la sonde LRO en orbite autour de la Lune. Nombre de passage acquis depuis juillet 2008 :

Cibles	Nombre de passages
Lageos 1&2	608
Glonass, Etalon GPS	758
LEO	1749
Apollo XV	43
Apollo XI	3
Apollo XIV	1
LRO	25 (6 h d'observation)
Total	3187

Analyses

IERS-ITRF

L'OCA est devenu Centre d'Analyse ILRS (Internat. Laser Ranging Service, de l'AIG) depuis 2007, suite aux travaux de thèse de D.Coulot (IGN/Lareg) et à l'investissement de F.Deleflie (aujourd'hui à l'OP/IMCCE).

Ce centre s'est développé autour de l'assimilation des données de poursuite de télémétrie laser sur les satellites Lageos (à 6000 Km, d'altitude), et de la réduction en terme d'orbitographie précise puis en termes de positionnement géocentrique absolu, incluant les paramètres de rotation de la Terre et les coordonnées des stations (ITRF).

CMS-T2L2

Le CMS a été créé à l'occasion du lancement du satellite Jason2, porteur de l'instrument T2L2, de transfert de temps par lien laser. Ce centre s'est développé autour de l'assimilation des données bord (dates bord des pulses laser reçus) et des données sol (dates sol et temps de vol des pulses laser).

Plusieurs cmapagnes ont été analysées, en plus des données courantes, afin de valider l'expérience en vol, établir le bilan des performances instrumentales, et ouvrir aux applications scientifiques, notamment en temps-fréquence, géodésie spatiale et physique fondamental.

Altimétrie Spatiale

L'Observatoire de la Côte d'Azur est un des rares centres à développer les expériences d'étalonnage absolu des altimètres spatiaux, grâce à la télémétrie laser et à des équipements spécifiques au sol (bouées, GPS, marégraphes, stations météo, ...). Le site de Corse est ainsi maintenu depuis 1998, permettant de créer une base de données, sol et spatiales, liée à l'étude du niveau moyen de la Méditerranée et de façon corrélative au suivi des missions d'altimétrie satellitaire.

Depuis 2007, l'OCA a participé a l'étalonnage de Jason2 (campagne en 2008), en colocation avec Jason1, ainsi qu'aux développements liés au suivi de la mission EnviSat dans le cadre d'EumetSAT. Une groupe, le groupe FOAM, s'est créé autour de P.Bonnefond, incluant IFREMER, l'OMP/Legos et d'autres partenaires. Le but de ce groupe de recherche est d'appliquer le savoir-faire du site de Corse à d'autres sites (mers intérieurs, grands fleuves et grands lacs). D'où des relations avec l'hydrologie continentale.

6) Observatoire de Paris (Daniel Gambis)

I - Activités de recherches

Elles concernent les aspects conceptuels liés aux divers systèmes de référence et à la rotation de la Terre: définition de ces systèmes de référence, modèles et paramètres propres aux études géodynamiques (précession, nutation, mouvement du pôle, variations de la rotation de la Terre). L'équipe a un rôle important dans le cadre des travaux de l'Union Astronomique Internationale notamment dans l'édification du modèle de référence de la Précession adopté par l'UAI en 2006. Celle-ci a largement contribué à la préparation et l'adoption de Résolutions UAI sur la nomenclature des Systèmes de référence ainsi qu'à une redéfinition rigoureuse du Temps dynamique barycentrique, TDB (http://syrte.obspm.fr/iauWGnfa).

Citons également d'autres recherches concernant des comparaisons entre divers modèles de précession-nutation et les modèles semi-analytiques UAI 2000/2006 et pour la première fois le développement des équations de la rotation de la Terre en fonction des coordonnées célestes du pôle céleste intermédiaire, qui expriment le plus directement possible cette orientation sans utiliser l'écliptique auquel ces observations ne sont pas sensibles.

Parallèlement à ces travaux qui s'inscrivent dans la continuité de ceux développés à l'Observatoire de Paris depuis sa création dans le domaine de l'Astronomie fondamentale, l'équipe poursuit également ses recherches sur des sujets scientifiques liés à l'Astronomie, la Géodésie spatiale, la Géodynamique et la Géophysique et qui sont aujourd'hui en plein essor grâce à la précision croissante des observations modernes. D'une part, les aspects métrologiques concernant les relations entre systèmes de référence terrestres et systèmes de référence célestes, et d'autre part, l'analyse des phénomènes géophysiques externes (atmosphère, océans) ou internes (noyau, manteau) affectant la rotation de la Terre.

La connaissance de l'orientation de la Terre dans l'espace est fondamentale. Les applications principales concernent la navigation spatiale, l'astrométrie, la géodésie et la géophysique. La rotation de la Terre est irrégulière sous l'action, en premier lieu, des marées gravitationnelles induites par le Soleil et la Lune, et, en second lieu, des couches externes (atmosphère, océans, hydrosphère, glaces continentales) et internes (manteau, noyau, graine) difficilement prévisibles. Les thématiques de recherche concernent plusieurs axes , citons notamment :

- Les effets atmosphériques, océaniques et hydrologiques sur la rotation terrestre
- L'influence de l'activité solaire sur la durée du jour
- Relations entre champ magnétique de la Terre et rotation terrestre
- Effets des séismes sur la rotation Terrestre notamment estimation de l'effet des séismes de Sumatra, du Chili et du japon en 2011 sur la variabilité de la rotation de la Terre (Durée du jour, mouvement du pôle)
- L'exploration de la structure interne de la Terre par VLBI
- La détermination des coordonnées célestes du pôle à partir de la télémétrie laser Lune
- La détermination astro-géodésique de la rotation terrestre (réduction des observations VLBI, réduction des observations LLR, combinaisons multi techniques (projet DYNAMO).

I I- Activités de services

Plusieurs composantes de services internationaux : centres de produits IERS, centres d'analyses des techniques VLBI et télémétrie laser Lune sont hébergés par le département du SYRTE à l'Observatoire de Paris.

- **Service international de la rotation de la Terre et des systèmes de référence (IERS)**

  - Le Centre de produits de la rotation de la Terre (EOP-PC)

Il a pour mission de collecter les données sous forme de séries temporelles concernant les variations de l'orientation terrestre (Earth Orientation Parameters ou EOP) afin de les combiner de manière optimale et de mettre les résultats à disposition ades utilisateurs travaillant dans les domaines liés à la navigation, l'astronomie, la géodésie et les sciences spatiales, la géophysique, et le temps. Une base de données sous ORACLE contient l'ensemble des informations historiques de référence concernant les variations de la rotation de la Terre.

- Le Centre de produits des Systèmes de référence célestes (ICRS-PC)

Il a été chargé par l'UAI du suivi du Repère International de Référence Céleste (ICRF) et d'en estimer les rattachements avec d'autres repères célestes (optique, GAIA,..). Il poursuit en parallèle plusieurs thématiques de recherche associées à la géodésie spatiale et aux systèmes de référence célestes : il s'agit du suivi au sol de satellites géostationnaires, de la construction d'une base de données des quasars par le biais du catalogue LQAC et de l'astrométrie grand champ.

- Le Groupe de travail sur les combinaisons au niveau des observations

Actuellement les séries de variations de la rotation terrestre sont calculées séparément des systèmes de référence terrestre et céleste. Cependant la cohérence entre les produits dérivés par chaque technique n'est pas pleinement assurée. L'approche de combinaison inter-technique globale devrait résoudre cette problématique. La tâche principale de ce groupe crée en 2009 est d'étudier les avantages de ces méthodes de combinaison par rapport aux méthodes courantes de combinaison de séries temporelles.

- **Centres d'analyse et de données du Service international VLBI pour la géodésie et l'astrométrie (IVS/OPAR)**

Les développements récents du centre d'analyse concernent la mise en place des solutions opérationnelles trimestrielles et rapides, ces dernières devant être lancées deux à trois fois par semaine. La solution trimestrielle donne des séries temporelles d'EOP et des catalogues de positions/vitesses des stations d'observation et de coordonnées de radiosources extragalactiques. Les EOP sont disséminés à l'IVS via les centres de données primaires de ce service et au centre de produits de l'IERS (IERS/EOP-PC). La solution rapide, générée dans les 48 heures après la corrélation des observations, donne uniquement les paramètres de rotation de la Terre (EOP) et les positions des stations d'observation. Les produits du centre d'analyse sont compatibles avec le format de l'Observatoire Virtuel (OV).

- **Centre d'analyse des données Laser Lune**

Le centre d'analyse POLAC (Paris Observatory Lunar Analysis Centre) est intégré à l'ILRS (International Laser Ranging Service). Il travaille en étroite collaboration avec l'équipe Laser Lune de l'Observatoire de la Côte d'Azur. Il collabore aussi avec les deux centres de produits de l'IERS implantés au SYRTE. Les analyses faites au SYRTE sur les données de télémétrie Laser Lune ont pour but principal d'améliorer la connaissance de la dynamique du système Terre-Lune et d'évaluer les paramètres des mouvements de circulation et de libration de la Lune qui sont mesurables grâce à l'observation.

7) Service Hydrographique et Océanographique de la Marine : SHOM (Marie Françoise Lalancette)

Parmi les activités du SHOM depuis 2007 on peut cité deux projets relatifs à l'amélioration des références géodésiques (GRAL et BATHYELLI).

Projet GRAL : Gravimétrie par altimétrie haute résolution

Le projet GRAL est piloté par le SHOM/GRGS et regroupe des chercheurs de l'IFREMER et de l'Université de Bretagne Occidentale (IUEM/UMR 6538 Domaines Océaniques

Ce projet se situe en amont des prochaines missions altimétriques. Il s'agit de réaliser un bilan des modèles gravimétriques actuellement disponibles et après avoir identifié les besoins précis en terme de couverture spatiale et de précision, de spécifier une future mission altimétrique. Les apports des missions déjà programmées ainsi que les possibilités induites par des constellations de micro satellites seront évalués. Quatre étapes ont été définies :

1) Analyser les données actuelles, faire une évaluation systématique à partir des données marines disponibles des zones sous échantillonnée et/ou de mauvaise qualité.
2) Spécifier les besoins en terme de couverture spatiale et de résolution. Définir les spécifications d'une nouvelle mission altimétrique géodésique en analysant les contraintes liées à l'échantillonnage spatiale en terme de stratégie de mesures et de technologie de l'altimètre.
3) Evaluer les potentialités des missions altimétriques futures (Altika, cryosat, SWOT..) et des possibilités induites par une constellation de micro satellites.

Ce projet est en cours et à démarrer en 2007 par une journée scientifique réunissant les acteurs en gravimétrie/altimétrie de la communauté française (réunion juin 2007 – CNES Paris). Ensuite les thématiques 1 et 2 ont été étudiées et ont fait l'objet de présentation en colloque et de publications (voir publications).

Quelques références :

a – Journée scientifique 'altimétrie pour un champ de gravité haute résolution : quel avenir ? ». http://ganymede.ipgp.jussieu.fr/frog/actualites.htm

b - Groupe de projet : GRAL : Projet 'gravimétrie par altimétrie haute résolution" proposé au séminaire de prospective du CNES en avril 2008 ? en cours d'examen pour le séminaire prévu en mars 2009.

c - Projet ˝gravimétrie par altimétrie haute résolution" soumis en 2008 pour le séminaire de prospective du CNES; non retenue par le CNES mais bien évalué par le groupe PASO.

Projet BATHYELLI

Ce projet a en particulier pour but la détermination du zéro hydrographique à partir de l'altimétrie spatiale et du GPS. Il a pour objectifs :

- Produire un modele de zero hydrographique par rapport à l'ITRS
- Produire des surfaces de references en hydrographie (CD, MSL, LAT, IGN69, geoid, ITRS ellipsoid)

- Permettre de changer de système de référence verticale (passage d'un système marin à un système terrestre)

- Permettre de réaliser des measures bathymétriques avec le GPS sans corrections de mare ou météorologiques

- Permettre de mesurer la bathymétrie par rapport à un ellipsoide de référence (BATHYELLI)

Les résultats sont très importants pour les références d'altitudes et de profondeur en mer ainsi que pour la réalisation de cartes Terre-Mer.

8) Université de la Rochelle (Guy Wöppelmann, M. Gravelle, M. Guichard, P. Tiphaneau)

Introduction: Les activités géodésiques de l'université de la Rochelle portent sur l'observation du niveau de la mer et ses variations long terme à la côte par marégraphes co-localisés à des stations GPS permanentes. Elles se placent dans le cadre de l'infrastructure de recherche basée sur l'observation SONEL, développée en partenariat avec le SHOM et le laboratoire LEGOS (http://www.sonel.org). Les grandeurs enregistrées sont le niveau de la mer par rapport au socle sur lequel repose un marégraphe à la côte et la position du marégraphe déterminée dans un repère géocentrique le plus stable et précis possible, en l'occurrence la dernière réalisation de l'ITRS.

Dans ce rapport nous mettons l'accent sur la composante GPS de SONEL car elle a connu un développement notable et remarqué au niveau international depuis les premiers résultats publiés en 2007 à l'échelle globale dans une application du GPS exigeante en termes de métrologie [1]. Les résultats sont encourageants mais l'objectif constitue encore un défi pour la Géodésie, car les contributions climatiques aux tendances du niveau de la mer enregistrées par les marégraphes sont de l'ordre de 1 à 3 mm/an. Pour être utiles, les vitesses GPS aux marégraphes doivent donc être déterminées à quelques dixièmes de millimètres par an sur la composante verticale dans un repère géocentrique. La meilleure réalisation d'un repère géocentrique, l'ITRF, reste encore le facteur limitant dans cette application exigeante [2].

Infrastructure d'observation: La composante GPS de SONEL comprend un centre de données et un centre d'analyses. Le centre de données rassemble aujourd'hui les mesures GPS de quelque 480 stations permanentes réparties dans le monde. Il s'agit de stations en co-localisation avec un marégraphe ou de stations dites '*reference frame*' par le service international IGS (http://igs.org). Certaines remontent au début des années 1990 et le nombre de fichiers journaliers de mesures disponibles au format RINEX totalise plus de 1,5 millions. Le système informatique de collecte, gestion, archivage et diffusion des observations s'est considérablement développé depuis 2007, doté d'une base de données relationnelle de plus de 90 tables. L'accès aux données se fait par serveurs FTP et Web (http://www.sonel.org/-GPS-.html). De nombreux outils sont développés en relation avec la base de données pour la meilleure gestion possible de l'information et sa diffusion aux utilisateurs. Le centre de données GPS de SONEL contribue au projet TIGA du service international IGS et en constitue le centre de données prinicipal.

Le centre d'analyses GPS contribue également à ce projet TIGA. Il est connu sous le nom de 'consortium ULR', car l'initiative vient de l'université de la Rochelle et l'infrastructure informatique matérielle et logicielle sur laquelle il s'appuie y est implantée. La puissance de calcul a considérablement évolué avec l'acquisition d'un cluster qui comprend aujourd'hui 392 cœurs de calcul. Il a permis de réduire de un an à deux semaines le traitement de dix ans de mesures d'un réseau global de 220 stations GPS, ouvrant ainsi des possibilités d'expérimentation considérables.

Consortium ULR et solutions GPS: Le consortium ULR réunit aujourd'hui des chercheurs de l'IGN France (LAREG), de l'IGN Espagne et de l'UMR LIENSs (CNRS – Université de la Rochelle). Quatre générations de solutions se sont succédées. Chacune est caractérisée par le réseau de stations analysé (nombre de stations, géométrie), par la période des mesures couverte (de plus en plus longue), par le repère terrestre dans lequel elle est exprimée (réalisation de l'ITRF), et par le choix des modèles, des corrections, de la paramétrisation et de la stratégie d'ajustement. Une stratégie en réseau global avec des contraintes très lâches sur les positions des stations et sur les orbites, qui sont également ajustées, a prévalu dès l'origine du centre d'analyses ULR. Le principe sous-jacent est la réanalyse complète des mesures dès lors qu'un élément de la stratégie est changé. Les logiciels utilisés sont GAMIT/GLOBK du MIT et CATREF du LAREG (IGN) pour le traitement des mesures GPS, d'une part, et la combinaison des solutions journalières, hébdomadaires et long terme, d'autre part. Les détails sont dans les publications associées, par ordre de solution, qui n'est pas celui de parution des articles en raison des délais des journaux : [3] ; [1] ; [4] et [5]. Les deux dernières solutions (ULR3 [4] et ULR4 [5]) examinent la nature du bruit dans les séries de position avec le logiciel CATS pour estimer avec rigueur les erreurs sur les vitesses GPS selon le type de bruit et son niveau. L'étude

détaillée [5] confirme la dominante de bruit de scintillation observée par ailleurs et explore différentes sources possibles du bruit.

Quelques resultats marquants: Le centre d'analyses ULR fait figure de précurseur en France dans le traitement des mesures GPS en réseau global de plusieurs centaines de stations, et au niveau international dans la publication des premiers résultats à l'échelle globale de prise en compte des mouvements verticaux du sol aux marégraphes [1]. Nous avons montré que nous étions capables de mettre en place un centre d'analyses GPS aux dimensions globales et, par la suite, de concourir honorablement avec le club assez restreint des équipes internationales à la pointe de ce domaine du spatial réunies dans la campagne *reprocessing* du service international IGS (http://acc.igs.org/reprocess.html). Les retombées de cette campagne sont riches. La figure suivante montre le niveau de qualité des résultats ULR en terme de positionnement des stations sur les trois composantes (vert clair ou UL1 dans la légende). Cette évaluation géodésique nous situe parmi les meilleurs groupes. Elle complète l'évaluation géophysique que nous avions menée sur la solution précédente [6] et donne confiance dans l'application de nos solutions pour corriger les mouvements verticaux des marégraphes.

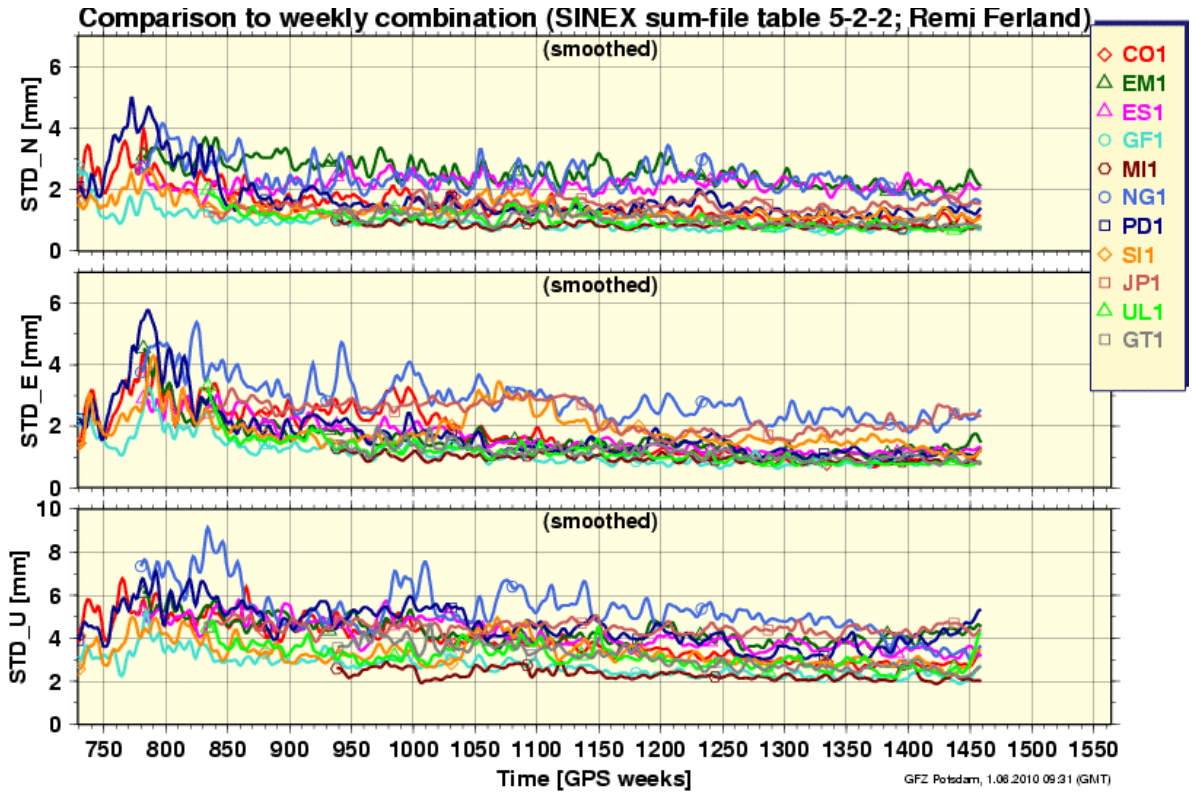

Ecarts moyens quadratiques hebdomadaires sur les composantes Nord (haut), Est (milieu) et Verticale (bas) par rapport aux solutions combinées IGS. Résultats du consortium ULR : UL1, en vert clair.

Autres activités et perspectives: Des progrès sont encore nécessaires dans l'application visée. Les retours d'expérience de la campagne *reprocessing* de l'IGS permettront de progresser dans la maîtrise fine des analyses GPS, aussi bien pour la correction des mouvements verticaux des marégraphes que dans les autres exploitations géodésiques ou géodynamiques que nous envisageons (e.g., [6] ; [7] ; [8]).

Outre les centres de données et d'analyses GPS, l'université de la Rochelle a installé plusieurs stations GPS aux marégraphes avec le concours du SHOM et du GRGS, et en assure la gestion. Il s'agit de La Rochelle (2001), Sète (2007), Roscoff (2009) et Saint-Malo (2010). Notre concours est par ailleurs apporté pour le contrôle géodésique de la référence d'autres marégraphes, mais aussi dans la métrologie des technologies modernes des marégraphes et l'évaluation de leurs performances ([9] et [10]).

Un travail original sur des nivellements historiques a été mené dans le cas de Brest pour établir la continuité de la référence de la série de mesures remise en question par la destruction du marégraphe

en 1944 [11]. Un travail analogue a été réalisé sur l'île de Saint-Paul dans l'océan Indien où des observations historiques de niveau de la mer effectuées lors du passage de Vénus devant le Soleil en 1874 ont été retrouvées et rattachées aux modernes [12].

Remerciements: à nos collègues partenaires dans cette aventure : M-N. Bouin, Z. Altamimi, A. Santamaria-Gomez et X. Collilieux.

Appendix: list of publications over 2007-2010 from the organisms contributing to the report of the section of Geodesy

2011

Bureau des longitudes (éphémérides astronomiques): *Connaissance des Temps*; *Annuaire du Bureau des longitudes*, EDP Sciences (Ed), and *Ephémérides nautiques* (in cooperation with the SHOM) , Edinautic (Ed), for each year year of the period 2008-2011 (in French).

Bureau des longitudes, *Temps et calendriers*, 2011 (Internet publication).

Collilieux X. and Wöppelmann G. (2011). Global sea level rise and its relation to the terrestrial reference frame definition. *J. Geodesy, 85*, 9-22.

Santamaria-Gomez A., Bouin M-N., Collilieux X. and Wöppelmann G. (2011). Correlated errors in GPS position time series: Implications for velocity estimates. *J. Geophys. Res., 116*, B01405

2010

Argus D.F., Gordon R.G., Heflin M.B., Ma C., Eanes R., Willis P., Peltier W.R., Owen S. (2010), The angular velocities of the plates and the velocity of Earth's Center from Space Geodesy, Geophysical Journal International, 180(3):916-960. DOI: 10.1111/j.1365-246X.2009.04463.x

Altamimi, Z. and X. Collilieux (2010) Quality assessment of the IDS contribution to ITRF2008, *Advances in Space Research*, **45**(12), DOI:10.1016/j.asr.2010.03.010

Argus D.F., Gordon R.G., Heflin M.B., Ma C., Eanes R., Willis P., Peltier W.R., Owen S., The angular velocities of the plates and the velocity of Earth's Center from Space Geodesy, Geophys. J. Int., DOI: 10.1111/j.1365-246X.2009.04463.x, 2010.

Ballu, V., M.-N. Bouin, S. Calmant, J. Ammann, E. Folcher, J.M. Boré, M. Diament, B. Pelletier and O. Pot (2010) Absolute seafloor vertical positioning using combined pressure gauge and kinematic GPS data, *Journal of Geodesy*, **84**(1), p. 65-77, DOI:10.1007/s00190-009-0345-y

Bernard, E., E. Caglioti and F. Golse (2010) Homogenization of the Linear BoltzmannEquation in a Domain with a Periodic Distribution of Holes, *Siam Journal on Mathematical Analysis*, **42**(5), p. 2082-2113

Bernard, E., F. Golse and F. Salvarani (2010a) Homogenization of transport problems and semigroups, *Mathematical Methods in the Applied Sciences*, **33**(10), p. 1228-1234

Blewitt, G., Z. Altamimi, J.L. Davis, R.S. Gross, C. Kuo, F.G. Lemoine, A. Moore, R.E. Neilan, H.P. Plag, M. Rothacher, C.K. Shum, M.G. Sideris, T. Schöne, P. Tregoning and S. Zerbini (2010) *Geodetic Observations and Global Reference Frame Contributions to Understanding Sea-Level Rise and Variability*, chap. 9, p. 256-284, Wiley-Blackwell

Bock O., Willis P., Lacarra M., Bosser P. (2010), An intercomparison of DORIS tropospheric delays estimated from DORIS and GPS data, Advances in Space Research, 46(12):1648-1660, DOI: 10.1016/j.asr.2010.05.018.

Bonnefond, P., P. Exertier, O. Laurain, and G. Jan, Absolute Calibration of Jason-1 and Jason-2 Altimeters in Corsica during the Formation Flight Phase, Special Issue on Jason-2

Calibration/Validation, Part 1, Mar. Geod., 33(S1) :80-90, DOI: 10.1080/01490419.2010.487790, 2010.

Bosser P., Bock O., Thom C., Pelon J., Willis P. (2010), Improvement of GPS tropospheric and height estimates using Raman lidar measurements, Journal of Geodesy, 84(4):251-265, DOI: 10.1007/s00190-009-0362-x..

Bouin, M.-N. and G. Wöppelmann (2010) Land motion estimates from GPS at tide gauges: a geophysical evaluation, *Geophysical Journal International*, **180**, DOI:10.1111/j.1365-246X.2009.04411.x

Bruinsma S., Lemoine J.-M., Biancale R., Valès N., CNES/GRGS 10-day gravity field models (release 2) and their evaluation, FEB 15 2010, Advances in Space Research, Volume: 45 Issue: 4, Pages: 587-601, 2010.

Bruinsma, S.L., and J.M. Forbes, Anomalous behavior of the thermosphere during solar minimum observed by CHAMP and GRACE, J. Geophys. Res., doi:10.1029/2010JA015605, 2010.

Bruinsma, S.L., and J.M. Forbes, Large-Scale Traveling Atmospheric Disturbances (LSTADs) in the Thermosphere Inferred from CHAMP, GRACE and SETA Accelerometer Data, Journal of Atmospheric and Solar-Terrestrial Physics, doi: 10.1016/j.jastp.2010.06.010, 2010.

Bruyninx, C., Z. Altamimi, M. Becker, M. Craymer, L. Combrinck, A. Combrink, R. Dietrich, R.M.S. Fernandes, R. Govind, T.A. Herring, A. Kenyeres, R.W. King, C. Kreemer, D. Lavallée, J. Legrand, L. Sanchez, G. Sella, Z. Shen, A. Santamaría, G. Wöppelmann and J. Dawson (2010) A dense global velocity field based on GNSS observations : preliminary results, *Proceedings of the IAG 2009 General Assembly, Buenos Aires*, IAG

Cerri L., Berthias J.P., Bertiger W.I., Haines B.J., Lemoine F.G., Mercier F., Ries J.C., Willis P., Zelensky N.P., Ziebart M. (2010), Precision Orbit Determination Standards for the Jason Series of altimeter missions, Marine Geodesy, 33(S1):379-418, DOI: 10.1080/01490419.2010.488966..

Collilieux, X., L. Métivier, Z. Altamimi, T. van Dam and J. Ray (2010) Quality assessment of GPS reprocessed Terrestrial Reference Frame, *GPS Solutions*, DOI:10.1007/s10291-010-0184-6

Collilieux, X., Z. Altamimi, D. Coulot, T. van Dam and J. Ray (2010a) Impact of loading effects on determination of the International Terrestrial Reference Frame, *Advances in Space Research*, **45**, p. 144-154, DOI:10.1016/j.asr.2009.08.024

Collilieux, X. and G. Wöppelmann, Global sea-level rise and its relation to the terrestrial reference frame, Journal of Geodesy, doi:10.1007/s00190-010-0412-4, 2010.

Coulot, D., A. Pollet, X. Collilieux and P. Berio (2010) Genetically Modified Networks: A Genetic Algorithm Contribution to Space Geodesy. Application to the referencing of the SLR Earth Orientation Parameters with respect to ITRF., *Journal of Geodesy*, **84**(1), p. 31-53, DOI:10.1007/s00190-009-0342-1

Coulot, D., F. Deleflie, P. Bonnefond, P. Exertier, O. Laurain and B. de Saint-Jean (2010a) Satellite Laser Ranging, *Solid Earth Geophysics Encyclopedia (2nd edition) 'Gravity'*, in press, Springer

Couvreux, F., F. Guichard, O. Bock, B. Campistron, J.-P. Lafore and J.L. Redelsperger (2010) Synoptic variability of the monsoon flux over West Africa prior to the onset, *Quarterly Journal of the Royal Meteorological Society*, DOI:10.1002/qj.473

Deleflie, F. and D. Coulot (2010) GRGS evaluation of the ITRF2008P solution, from SLR data, *Actes des Journées de la Société Française d'Astronomie et d'Astrophysique (SF2A'10), Marseille, France, 21-24 juin 2010*, in press, SF2A

Deleflie, F., A. Rossi, C. Portmann, G. Métris, F. Barlier, Semi-analytical investigations of the long term evolution of the eccentricity of Galileo and GPS-like orbits, J. Adv. Space Res. (2010), doi:10.1016/j.asr.2010.11.038.

P. Exertier, P. Bonnefond, et al., Status of T2L2 Experiment, Adv. Space Res., 2010

P. Exertier, P. Bonnefond, et al., T2L2 and DORIS, OSTST, Lisbonne, octobre 2010

Frappart F., Ramillien G., Maisongrande P., Bonnet M-P., Denoising satellite gravity signals by Independent Component Analysis, IEEE Geosciences and Remote Sensing Letters, 7(3), 421-425, doi:10.1109/LGRS.2009.2037837, 2010.

Gendt, G., Z. Altamimi, R. Dach, W. Söhne and T. Springer (2010) GGSP: Realisation and maintenance of the Galileo Terrestrial Reference Frame, *Advances in Space Research*,DOI:10.1016/j.asr.2010.02.001

Gobinddass M.L., Willis P., Menvielle M., Diament M. (2010), Refining DORIS atmospheric drag estimation in preparation of ITRF2008, Advances in Space Research, 46(12):1566-1577, DOI: 10.1016/j.asr.2010.04.004.

Greff-Lefftz, M., L. Métivier and J. Besse (2010) Dynamic Mantle Density Heterogeneities and global geodetic observables, *Geophysical Journal International*, **180**(3), p. 1080-1094, DOI:10.1111/j.1365-246X.2009.04490.x

P. Guillemot, P.Exertier, E. Samain, The T2L2 Experiment, PTTI, 2009, 2010

P. Guillemot, P.Exertier, E. Samain, T2L2, EFTF, 2009, 2010

Harmel A. (2010) La rénovation du RGF93, *XYZ n°124, septembre 2010*, p.

Horwath, M., Lemoine, J.-M., Biancale, R., Bourgogne, S., Improved GRACE science results after adjustment of geometric biases in the Level-1B K-band ranging data, Journal of Geodesy, 2010/10/06, doi: 10.1007/s00190-010-0414-2, 2010.

Jamet, O., D. Tsoulis, J. Verdun and N. Gonindard (2010) Assessment of a numerical method for computing the spherical harmonic coefficients of the gravitational potential of a constant density polyhedron, *Proceedings IAG International Symposium GGEO2008, Chania, Crête, Greece, 23-27 June 2008*, International Association of Geodesy Symposia, Vol.135, p. 437-444, Springer

Kalarus M., Schuh, Kosek W., Akyilmaz O., Bizouard Ch., Gambis D., Gross R., Jovanovic B., Kumakshev S., Kutterer H., Ma L., Mendes Cerveira P.J., Pasynok S, Zotov L., Achievements

of the Earth Orientation Parameters Prediction Comparison Campaign, JoG, Vol 84, number 10, pp 587-596, 2010.

Karbou, F., F. Rabier, J.-P. Lafore, J.L. Redelsperger and O. Bock (2010) Global 4D-Var assimilation and forecast experiments using land surface emissivities from AMSU-A and AMSU-B. Part-II: Impact of adding surface channels on the African Monsoon during AMMA, *Weather and Forecasting*, DOI:10.1175/2009WAF2222244.1

Karbou, F., F. Rabier, J.-P. Lafore, J.L. Redelsperger and O. Bock (2010a) The impact of assimilating microwave surface sensitive observations over land on the representation of humidity in the ARPEGE 4D-VAR system, *EMS Annual Meeting Abstracts*, Vol.EMS2009-298, n°6

King M.A., Altamimi Z., Boehm J., Bos M., Dach R., Elosegui P., Fund F., Hernandez-Pajares M., Lavallee D., Cerveira P.J.M., Riva R.E.M., Steigenberger P., van Dam T., Vittuari L., Williams S., Willis P. (2010), Improved constraints on models of glacial isostatic adjustment, A review of the contribution of ground-based geodetic observations, Surveys in Geophysics, 31(5):465-507, DOI: 10.1007/s10712-010-9100-4.

Legrand, J., N. Bergeot, C. Bruyninx, G. Wöppelmann, A. Santamaría, M.-N. Bouin and Z. Altamimi (2010) Comparison of regional and global GNSS positions, velocities and residual times series, *Proceedings of the IAG 2009 General Assembly, Buenos Aires*, IAG .

Lemoine F.G., Zelensky N., Chinn D., Pavlis D., Beckley B., Luthcke S.B., Willis P., Ziebart M., Sibthorpe A., Boy J.P., Luceri V. (2010), Towards development of a consistent orbit determination, TOPEX/Poseidon, Jason-1 and Jason-2, Advances in Space Research, 46(12):1513-1540, DOI: 10.1016/j.asr.2010.05.007.

Letetrel C., M. Marcos, B. Martin Miguez and G. Woppelmann Sea level extremes in Marseille (NW Mediterranean) during 1885-2008, Continental Shelf Research, Volume 30, Issue 12, 1 July 2010, Pages 1267-1274, ISSN 0278-4343, DOI : 10.1016/j.csr.2010.04.003, 2010.

Llovel W., M. Becker, Cazenave A. and Crétaux J.F., Contribution of land water storage change to global mean sea level from GRACE and satellite altimetry, C.R. Geosciences, 342, 179-188, 2010a.

Llovel W., Guinehut S. and Cazenave A., Regional variability in sea level over 2002 – 2009 based on satellite altimetry, Argo float data and GRACE ocean mass, Ocean Dynamics, 60, 1193-1204, DOI 10.1007/s10236-010-0324-0, 2010b.

Louis G, Lequentrec-Lalancette M-F, Royer J-Y, Rouxel D, Gely L, Maïa M, Ocean Gravity Models from future satellite missions, EOS, Vol 91, No3, 2010.

Métivier, L., M. Greff-Lefftz and Z. Altamimi (2010) On secular geocenter motion: the impact of climate changes, *Earth and Planetary Science Letters*, **296**(3-4), p. 360-366, DOI:10.1016/j.epsl.2010.05.021

Milly P.C.D., Cazenave A., Famiglietti J., Gornitz V., Laval K., Lettenmaier D., Sahagian D., Wahr J. and Wilson C., Terrestrial water storage contributions to sea level rise and variability, Proceedings of the WCRP workshop 'Understanding sea level rise and variability', eds. J. Church, P. Woodworth, T. Aarup and S. Wilson et al., Blackwell Publishing, Inc., 2010.

Nicholls R. and Cazenave A., Sea level change and the impacts in coastal zones, Science, 328, 1517-1520, 2010.

Oberheide, J., J.M. Forbes, X. Zhang, S.L. Bruinsma, Wave-driven variability in the ionosphere-thermosphere-mesosphere system from TIMED observations: What contributes to the "wave 4"? J. Geophys. Res., doi:10.1029/2010JA015911, 2010.

Panet, I., V. Mikhailov, F. Pollitz, M. Diament, P. Banerjee and K. Grijalva (2010) Upper mantle rheology from GRACE and GPS post-seismic deformations after the 2004 Sumatra-Andaman earthquake, *Geochemistry Geophysics Geosystems*, **11**(6), DOI:10.1029/2009GC002905

Panet, I., Y. Kuroishi and M. Holschneider (2010a) Flexible dataset combination and modelling by domain decomposition approaches, *Proceeding of the Hotine-Marussi Symposium, 6-10 juillet 2009, Rome, Italie*, Springer

Panet, I., G. Ramillien, B. Legrésy, W. Llovel, M. Diament and R. Biancale (2010b) *Space gravimetry*

Patzold M., T.P. Andert, B. Hausler, S. Tellmann, J.D. Anderson, S.W. Asmar, J.-P. Barriot, and M.K. Bird, Pre-flyby estimates of the precision of the mass determination of asteroid (21) Lutetia from Rosetta radio tracking, accepted Astronomy & Astrophysics, June 29, 2010.

Patzold M., Andert, T., Häusler, B., Tellmann, S., Anderson, J. D., Asmar, S. W., Barriot, J., Bird, M. K., The Mass and Density of (21) Lutetia from Radio Tracking During the Rosetta Flyby, American Astronomical Society, DPS meeting #42, #43.07; Bulletin of the American Astronomical Society, Vol. 42, p.1044, Oct. 2010.

Pollet, A., D. Coulot and N. Capitaine (2010) Combination of space-geodetic Techniques at the Measurement Level, *Proceedings of the IAG Symposium on Geodesy for Planet Earth. Buenos Aires (Argentine)*, International Association of Geodesy Symposia, in press, IAG proceedings

L. Pineau-Guillou, 2008 □ BATHYELLI Project : set-up of Chart Datum using spatial altimetry and kinematic GPS □, NSHC TWG (North Sea Hydrographic Commission Tidal Working Group), 29-30 octobre 2008, La Haye, Pays-Bas

L. Pineau-Guillou, MF Le Quentrec-Lalancette, 2008 □ Determination des surfaces de references en hydrographie a partir du GPS et de l'altimetrie spatiale , Colloque du CNFG2 (Comite National Francais de Geodesie et Geophysique), L'eau dans tous ses etats, visions spatiales □, Session References Geodesiques, 17-19 novembre 2008, Paris

Lucia Pineau-Guillou , Proceedings of the European navigation conference/GNSS2008, 23-25 avril 2008, Toulouse, France.

L.Pineau-Guillou, 2008, □ BATHYELLI Project: Set-up of Chart Datum (CD) using altimetry and GPS □, European Navigation Conference/GNSS 2008, 23-25 avril 2008, Toulouse

Pospichal, B., D. Bou Karam, S. Crewell, C. Flamant, A. Hünerbein, O. Bock and F. Saïd (2010) Diurnal cycle of the inter-tropical discontinuity over West Africa analysed by remote sensing and mesoscale modelling, *Quarterly Journal of the Royal Meteorological Society*, in press, DOI:200910.1002/qj.435

P.Rebischung, B.Garayt (2010) Recent result from IGS terrestrial frame combinations- *in proceedings IAG commission 1, REFAG, Marne-La-Vallée(France) october 4-8, 2010* ,in press

Taris F., J. Souchay, C. Barache, S.Bouquillon et al., " Astro-photometric variability of CFHTLS Deep-2 QSO's ", A&A 526A, 25T, 2010.

Testut L., Martin Miguez, B., Wöppelmann, G., Tiphaneau, P., Pouvreau, N., Karpytchev, M., The sea level at Saint-Paul, Southern Indian Ocean, from 1874 to the present. Journal of Geophysical Research, 115, C12028, doi:10.1029/2010JC006404, 2010.

van Camp, M., L. Métivier, O. de Viron, B. Meurers and S. Williams (2010) Characterizing long-time scale hydrological effects on gravity for improved distinction of tectonic signals, *Journal of Geophysical Research*, **115**(B07407), DOI:10.1029/2009JB006615

Valette J.J., Lemoine F.G., Ferrage P., Yaya P., Altamimi Z., Willis P., Soudarin L. (2010), IDS contribution to ITRF2008, Advances in Space Research, 46(12):1614-1632, DOI: 10.1016/j.asr.2010.05.029.

Valette J.J., Lemoine F.G., Ferrage P., Yaya P., Altamimi Z., Willis P., Soudarin L. (2010), IDS contribution to ITRF2008, Advances in Space Research, 46(12):1614-1632, DOI: 10.1016/j.asr.2010.05.029.

Willis P. (2010), Preface, in DORIS: scientific applications in geodesy and geodynamics, P. Willis (Ed.), Advances in Space Research, 45(12):1407, DOI: 10.1016/j.asr.2010.04.013

Willis, P. (2010), Preface, DORIS, Precise orbit determination and applications to Earth Sciences, P. Willis (Ed.), Advances in Space Research, 46(12):1483, DOI: 10.1016/j.asr.2010.07.013

Willis P., Fagard H., Ferrage P., Lemoine F.G., Noll C.E., Noomen R., Otten M., Ries J.C., Rothacher M., Soudarin L., Tavernier G., Valette J.J. (2010), The International DORIS Service, Toward maturity, Advances in Space Research, 45(12):1408-1420, DOI: 10.1016/j.asr.2009.11.018

Willis P., Boucher C., Fagard H., Garayt B., Gobinddass M.L. (2010), Contributions of the French Institut Géographique National (IGN) to the International DORIS Service, Advances in Space Research, 45(12):1470-1480, DOI: 10.1016/j.asr.2009.09.019

Wöppelmann G., Pouvreau N., Coulomb A., Simon B. and Woodworth P.L. (2008). Tide gauge datum continuity at Brest since 1711: France's longest sea-level record. *Geophys. Res. Lett., 35*, L22605.

Wöppelmann G., Bouin M-N. and Altamimi Z. (2008). Terrestrial reference frame implementation in global GPS analysis at TIGA ULR consortium. *Physics and Chemistry of the Earth, 33*, 217-224.

Zelensky N., Lemoine F.G., Chinn D., Rowlands D., Luthcke S., Beckley B., Pavlis D., Klosko S., Ziebart M., Sibthorpe A.J., Willis P., Luceri V. (2010), DORIS/SLR POD modeling improvements for Jason-1 and Jason-2, Advances in Space Research, 46(12):1541-1558, DOI: 10.1016/j.asr.2010.05.008.

2009

Ablain M., Cazenave A., DoMinh K, Guinehut S., Llovel W., Lombard A. and Valladeau G., A new assessment of global mean sea level from altimeters highlights a reduction of global slope from 2005 to 2008 in agreement with in-situ measurements, Ocean Sciences, 5, 193-201, 2009.

Amalvict M., Willis P., Wöppelmann G., Ivins E., Bouin M.N., Testut L. and Hinderer J. (2009). Stability of the East Antarctic station Dumont d'Urville from long-term time series of geodetic and geophysical observations. *Polar Research, 28,* 193-202.

Abbondanza, C., Z. Altamimi, P. Sarti, M. Negusini and L. Vittuari (2009) Local effects of redundant terrestrial and GPS-based tie vectors in ITRF-like combinations, *Journal of Geodesy*, **83**(11), p. 1031-1040, DOI:10.1007/s00190-009-0321-6

Agusti-Panareda, A., D. Vasiljevic, A. Beljaars, O. Bock, F. Guichard, M. Nuret, J.-P. Lafore, E. Andersson, P. Bechtold, A. Fink, H. Hersbach, A. Garcia Mendez, J.-B. Ngamini, D.J. Parker, J.L. Redelsperger and A. Tompkins (2009) Radiosonde humidity bias correction over the West African region for the special AMMA reanalysis at ECMWF, *Quarterly Journal of the Royal Meteorological Society*, **135**(640), p. 595-617, DOI:10.1002/qj.396

Altamimi, Z. (2009) Importance of local ties for the ITRF, *Proceedings of the 4th IAG Symposium on Geodesy for Geotechnical and Structural Engineering, Lisbon, Portugal*

Altamimi, Z., X. Collilieux and L. Métivier (2009) *Institut Géographique National (IGN) Combination Centre*, chapter 3.6.1.2, IERS annual report 2008

Altamimi, Z. and X. Collilieux (2009) Strengths and limitations of the ITRF : ITRF2005 and beyond, *Geodetic Reference Frames, IAG Symposium Munich, Germany, 9-14 October 2006*, International Association of Geodesy Symposia, Vol.134, p. 73-79, Springer, DOI:10.1007/978-3-642-00860-3_11

Altamimi, Z., X. Collilieux, B. Garayt and L. Métivier (2009a) *ITRS Centre*, chapter 3.5.5., IERS annual report 2008

Altamimi, Z., D. Coulot and X. Collilieux (2009b) Status of the ITRF development and SLR contribution, *Proceedings of the 16th International Laser Ranging Workshop, Poznan, Poland, oct 2008*, StanisÅ‚aw Schillak Ed., Vol.2, p. 35-42, Space Research Centre, Polish Academy of Sciences

Altamimi, Z. and X. Collilieux (2009a) IGS contribution to ITRF, *Journal of Geodesy*, **83**(3-4), p. 375-383, DOI:10.1007/s00190-008-0294-x

Altamimi Z., ETRS89 realization: current status, ETRF2005 and future development, Bulletin of Geodesy and Geomatics, 2009.

Amory-Mazaudier, C., S. Basu, O. Bock, A. Combrink, K. Groves, T. Fuller Rowell, P. Lassudrie-Duchesne, M. Petitdidier and E. Yizengaw (2009) International Heliophysical Year: GPS Network in Africa, *Earth, Moon and Planets*, **104**(1-4), DOI:10.1007/s11038-008-9273-8

Argus D.F., Gordon R.G., Heflin M.B., Ma C., Eanes R., Willis P., Peltier W.R., Owen S., The angular velocities of the plates and the velocity of Earth's Center from Space Geodesy, Geophysical Journal International. doi:10.1111/j.1365-246X.2009.04463.x, 2009.

Asmar S.W., K. Aksnes, R. Ambrosini, A. Anabtawi, J. D. Anderson, J. W. Armstrong, D. Atkinson, JP Barriot, B. Bertotti, B. G. Bills, M. Bird, Dehant, V., P. Edenhofer, F. Michael Flasar, W. Folkner, R. G. French, H. Hanada, B. Häusler, D. P. Hinson, L. Iess, Ö. Karatekin, A. J. Kliore, A. S. Konopliv, F. Lemoine, I. Linscott, E. Marouf, JC Marty, K. Matsumoto, H. Noda, K. Oudrhiri, M. Paik, R. S. Park, M. Pätzold, R. Preston, N. Rappaport, P. Rosenblatt, R. A. Simpson, D. E. Smith, S. Smrekar, P. G. Steffes, S. Tellmann, P. Tortora, G. L. Tyler, T. van Hoolst, M. Watkins, J. G. Williams, P. Withers, X. Wu, D. Yeomans, DN Yuan, M. T. Zuber, Planetary Radio Science: Investigations of Interiors, Surfaces, Atmospheres, Rings, and Environments, Planetary Sciences Decadal Survey, The National Academies White Papers Report, 2009.

Ballu, V., J. Ammann, O. Pot, O. de Viron, G. Sasagawa, G. Reverdin, M.-N. Bouin, M. Cannat, C. Deplus, S. Deroussi, M. Maia and M. Diament (2009) A seafloor experiment to monitor vertical deformation at the Lucky Strike volcano, Mid-Atlantic Ridge, *Journal of Geodesy*, **83**(2), p. 147-159, DOI:10.1007/s00190-008-0248-3

Ballu V, Bouin MN, Calmant S, Folcher E, Bore JM, Ammann J, Pot O, Diament M, Pelletier B., Absolute seafloor vertical positioning using combined pressure gauge and kinematic GPS data Journal of Geodesy, doi: 10.1007/s00190-009-0345-y, 2009.

Becker M., W. Llowel, A. Cazenave, A. Güntner, J-F Crétaux, Recent hydrological behaviour of the East African Great Lakes region inferred from GRACE, satellite altimetry and rainfall observations, in press to C.R Geosciences, 2009.

Bergeot, N., M.-N. Bouin, M. Diament, B. Pelletier, M. Régnier, S. Calmant and V. Ballu (2009) Horizontal and vertical interseismic velocity fields in the Vanuatu subduction zone from GPS measurements: Evidence for a central Vanuatu locked zone, *Journal of Geophysical Research*, **114**(B06405), DOI:10.1029/2007JB005249

Bhawar, R., P. Di Girolamo, D. Summa, C. Flamant, D. Althausen, A. Behrendt, A. Blyth, O. Bock, P. Bosser, B.J. Brooks, M. Cacciani, S. Crewell, C. Champollion, F. Davies, T. Di Iorio, G. Ehret, R. Engelmann, C. Kiemle, C. Herold, S. Mobbs, D. Mueller, S. Pal, M. Radlach, A. Riede, P. Seifert, M. Shiler, M. Wirth and V. Wulfmeyer (2009) Water vapour intercomparison effort in the frame of the convective and orographically-induced precipitation study, *CURRENT PROBLEMS IN ATMOSPHERIC RADIATION (IRS 2008): Proceedings of the International Radiation Symposium (IRC/IAMAS)*, AIP Conference Proceedings, Vol.1100 issue 1, p. 215-218, DOI:10.1063/1.3116952

Bizouard C., F. Rémus, L. Seoane and D. Gambis, Variable atmospheric and oceanic forcing of the Chandler wobble, subm. to Journal of Geophys, 2009.

Bizouard C. and D. Gambis, The combined solution C04 for Earth Orientation Parameters, recent improvements, Springer Verlag series, Series International Association of Geodesy Symposia , Vol. 134 Drewes, Hermann (Ed.), pp 265-270., DOI 10.1007/978-3-642-00860-3, 2009.

Bizouard C., Gambis D. , Richard J.Y. , Becker O., Combination of earth orientation parameters from different techniques, Proc. Journées Systèmes de Référence 2008, M. Soffel and N. Capitaine (eds.), p153, 2009.

Brzezinski A., Capitaine N., ‘’Semidiurnal signal in UT1 due to the influence of tidal gravitation on the triaxial structure of the Earth”, in Highlights of Astronomy, Volume 14, XXVIIth IAU General Assembly, August 2009, Ian F. Corbett ed, 2009.

Bock, O. and M. Nuret (2009) Verification of NWP model analyses and radiosonde humidity data with GPS precipitable water vapor estimates during AMMA, *Weather and Forecasting*, **24**(4), p. 1085-1101, DOI:10.1175/2009WAF2222239.1

Bouin, M.-N., V. Ballu, S. Calmant, J.M. Boré, E. Folcher and J. Ammann (2009) A kinematic GPS methodology for sea surface mapping, Vanuatu, *Journal of Geodesy*, **83**(12), p. 1203-1217, DOI:10.1007/s00190-009-0338-x

Briole P., Willis P., Dubois J., Charade O. (2009), Potential volcanic applications of the DORIS system, A geodetic study of the Socorro Island (Mexico) coordinate time series, Geophysical Journal International, 178(1):581-590. DOI: 10.1111/j.1365-246X.2009.04087.x

Brown S., A Novel Near-Land Radiometer Wet Path Delay Retrieval Algorithm: Application to the Jason-2/OSTM Advanced Microwave Radiometer, IEEE Trans. Geosci. Rems. Sens., in press, 2009.

Bruyninx, C., Z. Altamimi, C. Boucher, E. Brockmann, A. Caporali, W. Gürtner, H. Habrich, H. Hornik, J. Ihde, A. Kenyeres, J. Mäkinen, G. Stangl, H. van der Marel, J. Simek, W. Söhne, J.A. Torres and G. Weber (2009) The European Reference Frame: Maintenance and Products, *Geodetic Reference Frames, IAG Symposium Munich, Germany, 9-14 October 2006*, International Association of Geodesy Symposia, Vol.134, p. 131-136, Springer, DOI:10.1007/978-3-642-00860-3_20

Bureau des longitudes, *Les Observatoires, observer la Terre*, Hermann (Ed.), 309 pages, 2009 (in French).

Champollion, C., P. Drobinski, M. Haeffelin, O. Bock, J. Tarniewicz, M.-N. Bouin and R. Vautard (2009) Water vapour variability induced by urban surface heterogeneities during convective conditions, *Quarterly Journal of the Royal Meteorological Society*, **135**(642), p. 1266-1276, DOI:10.1002/qj.446

Capitaine N., “Models and nomenclature in Earth rotation”, in “Relativity in Fundamental Astronomy”, invited paper, Proceedings IAU Symposium No. 261, 2009, Virginia Beach, 27-30 April 2009, pp. 69-78, 2009.

Capitaine N., “Recent progress in modeling precession-nutation and prospects for future improvements”, invited paper, in IAU Transactions, Vol XXVIIB, Proc. 27th IAU General Assembly, August 2009, Ian F. Corbett, ed., in press, 2009.

Capitaine N., “Nomenclature and numerical standards for IAU models and IERS Conventions for Earth rotation”, in Proc. Journées Systèmes de Référence 2008, M. Soffel and N. Capitaine (ed.), Observatoire de Paris, pp. 46-49, 2009.

Capitaine N. et al., On the IAU 2000/2006 precession-nutation and comparison with other models and VLBI observations, Celest. Mech. Dyn. Astr., 103, 179, 2009.

Capitaine N., Mathews P.M., Dehant V., Wallace P.T., Lambert S.B., "On the IAU 2000/2006 precession-nutation and comparison with other models and VLBI observations", Celest. Mech. & Dynamical Astronomy 103, 2, 179-190, 2009.

Cazenave A., "Hausse du niveau de la mer et changement climatique", Revue Questions Internationales, 2009.

Cazenave A., 'Sea level rise', in Encyclopedia for ice and snow, 2009.

Cazenave A., Guinehut S., Ramillien G., Llovel W., DoMinh K., Ablain M., Larnicol G. and Lombard A., Sea level budget over 2003-2008; a reevalution from satellite altimetry, GRACE and Argo data, Global and Planetary Change, 65, 83-88, doi:10.1016/j/gloplacha.2008.10.004, 2009.

Chapanov Y. and D. Gambis, Solar-terrestrial energy transfer during sunspot cycles and mechanism of Earth rotation excitation Solar and Stellar Variability Impact on Earth and Planet Proceedings IAU Symposium No. 264, A. Kosovichev, J.-P. Rozelot and A. Andrei (eds), 2009.

Chapanov Y. and D. Gambis, Change of the earth moment of inertia as the observed response to the 11 year solar variation, Proc. Journées Systèmes de Référence 2008, M. Soffel and N. Capitaine (eds.), p131, 2009.

Champollion, C., O. Bock, C. Flamant, F. Masson, D. Turner and T. Weckwerth (2009a) Mesoscale GPS tomography applied to the 12 June 2002 convective initiation event of IHOP_2002, *Quarterly Journal of the Royal Meteorological Society*, **135**(640), p. 645-662, DOI:10.1002/qj.386

Cheng K., S. Calmant, C. K. Shum, C-Y Kuo, F. Seyler, J. Santos da Silva, Accurate Data Collection of River stage gradient and hydrological geospatial information in the Branco River, the Amazon, A Pilot Mission, Marine Geodesy, 32, (3), 267-283, DOI 10.1080/01490410903094460, 2009.

Christophe B. et al., GAP, Odyssey: a solar system mission. Experimental Astronomy, 23(2), pages 529-547, 2009.

Collilieux, X., Z. Altamimi, D. Coulot, A. Pollet and L. Métivier (2009) *Institut Géographique National (IGN) Combination Research Centre*, chapter 3.6.2.8, IERS annual report 2008

Collilieux, X., Z. Altamimi, J. Ray, T. van Dam and X. Wu (2009a) Effect of the satellite laser ranging network distribution on geocenter motion estimation, *Journal of Geophysical Research*, **114**(B04402), DOI:10.1029/2008JB005727

Collilieux, X. and Wöppelmann, G., Global sea-level rise and its relation to the terrestrial reference frame definition. AGU Fall Meeting, San Francisco, 14-18 December 2009, Session G11C "Terrestrial Reference Systems: Theory, Realizations, and Applications".

Coulomb A. (2009) Entretien du réseau de nivellement par les triplets *revue XYZ n°119*, p.39-42, june 2009

Coulomb A. (2009) Le marégraphe de Marseille : patrimoine et modernité, *revue XYZ n°118*, PP 17-24, march 2009

Coulot, D., Ph. Bério, P. Bonnefond, P. Exertier, D. Féraudy, O. Laurain and F. Deleflie (2009) Satellite Laser Ranging biases and Terrestrial Reference Frame scale factor, *Observing our Changing Earth, Proceedings of the 2007 IAG General Assembly, Perugia, Italy, July 2 - 13, 2007*, Vol.133, p. 39-46, Springer

Coulot D., Pollet A., Collilieux X., Deleflie F., Gobinddass M.L., Soudarin L., Willis P., Genetically Modified Networks: A Genetic Algorithm contribution to Space Geodesy. Application to the transformation of SLR and DORIS EOP time series into ITRF2005, IAG 2009.

Crétaux J-F., V. Jelinski, S. Calmant, A. Kouraev, V. Vuglinski, M. Bergé-Nguyen, M-C Gennero, F. Nino, R. Abarco Del Rio, A. Cazenave, P. Maisongrande, SOLS, a lake database to monitor in Near real time water level storage variations from remote sensing data, Advanced Space research, submitted, 2009a.

Crétaux J-F., R. Letolle, A.V. Kouraev, Aral Sea level variability, Handbook of environmental chemistry, Vol 5 Water pollution, Ed A.G. Kostianoy, A.N. Kosarev, (invited papers) in press, 2009b.

Crétaux J-F, M. Leblanc, S. Tweed, S. Calmant, and G. Ramillien, Combination of radar and laser altimetry, MODIS and GPS for the monitoring of flood events : application to the Diamantina river, submitted, Remote Sensing of Environment, 2009c.

Crétaux J-F, S. Calmant, R. Abarca Del Rio, A. Kouraev, and M. Bergé-Nguyen, Lakes studies from satellite altimetry, invited papers, in press, Handbook on Coastal altimetry, Springer ed., chap. 19, 2009d.

Dehant, V., Folkner, W., Renotte, E., Orban, D., Asmar, S., Balmino, G., Barriot, J.-P., Benoist, R. Biancale, J. Biele, F. Budnik, S. Burger, O. de Viron, B. Häusler, Ö. Karatekin, S. Le Maistre, P. Lognonné, M. Menvielle, M. Mitrovic, M. Pätzold, A. Rivoldini, P. Rosenblatt, G. Schubert, T. Spohn, P. Tortora, T. van Hoolst, O. Witasse and M. Yseboodt, Lander radioscience for obtaining the rotation and orientation of Mars, Planetary and Space Science, Volume 57, Issues 8-9, Pages 1050-1067, July 2009.

Deleflie, F., S. Lambert, X. Collilieux, C. Barache, J. Berthier, O. Laurain, D. Coulot, P. Exertier and A.-M. Gontier (2009) The Virtual Observatory in Geodesy and Earthâ€™s Sciences: The French activities, *Proceedings of the 16th International Laser Ranging Workshop, Poznan, Poland, oct 2008*, StanisÅ‚aw Schillak Ed., Vol.2, p. 193-198, Space Research Centre, Polish Academy of Sciences

S. Durand et L. Morel. Evaluation ponctuelle des performances du réseau TERIA. *Revue XYZ,* n°118, 1er trimestre 2009.

Drobinski, P., S. Bastin, S. Janicot, O. Bock, A. Dabas, P. Delville and O. Reitebuch (2009) On the late northward propagation of the West African monsoon in summer 2006 in the region of Niger/Mali, *Journal of Geophysical Research*, **114**(D09108), DOI:10.1029/2008JD011159

Eissa, L. and M. Kasser (2009) Vers une nouvelle représentation des déformations horizontales de la croûte terrestre et de leurs erreurs avec un champ régulier de tenseurs, *XYZ*, **4e trimestre 2009**(121), p. 27-32

Faccani, C., F. Rabier, N. Fourrié, A. Agusti-Panareda, F. Karbou, P. Moll, J.-P. Lafore, M. Nuret, F. Hdidou and O. Bock (2009) The impact of the AMMA radiosonde data on the French global assimilation and forecast system, *Weather and Forecasting*, **24**(5), p. 1268-1286, DOI:10.1175/2009WAF2222237.1

Fadil A., Barriot J.-P., Ortéga P., and Sichoix L., Seasonal Atmospheric Water Vapor Monitoring over Tahiti Using GPS measurements, Proceedings of the 11-th Pacific Science Inter-Congress, March 2nd - 6th 2009, Tahiti, French Polynesia, ISBN 978-2-11-098964-2, 2009.

Flouzat M., Bettinelli P., Willis P., Avouac J.P., Heritier T., Gautam U. (2009), Investigating tropospheric effects and seasonal position variations in GPS and DORIS time series from the Nepal Himalaya, Geophysical Journal International, 178(3):1246-1259. DOI: 10.1111/j.1365-246X.2009.04252.x

Fontdecaba J., Métris G., Exertier P., An alternative representation of the relative motion: the local orbital elements, Volume 45, Issue 3, 1 February 2010, Pages 410-420, doi:10.1016/j.asr.2009.09.008, 2009.

F. Fund, L. Morel, J. Boehm, A. Mocquet (2009). Assessment of ECMWF derived tropospheric delay models within the EUREF Permanent Network. *GPS Solutions*.

Gobinddass M.L., Willis P., de Viron O., Sibthorpe A.J., Zelensky N.P., Ries J.C., Ferland R., Bar-Sever Y.E., Diament M. (2009), Systematic biases in DORIS-derived geocenter time series related to solar radiation pressure mis-modeling, Journal of Geodesy, 83(9):849-858. DOI: 10.1007/s00190-009-0303-8

Gambis D., C. Bizouard, Monitoring UT1 using VLBI and GPS estimates, Proc. 19th European VLBI for Geodesy and Astrometry and EVGA, Bourda, Charlot and Collioud (eds), p107, 2009.

Gambis D., Monitoring Earth Orientation variations; State of the art and prospective, in Transactions IAU, Volume XXVIIB, Proc. XXVII IAU General Assembly, August 2009, Ian F. Corbett (ed.), p.126, 2009.

Gambis D., Biancale R., Carlucci T., Lemoine J.M., Marty J.C, Bourda G., Charlot P., Loyer S., Lalanne L., Soudarin L., Combination of Earth Orientation Parameters and terrestrial frame at the observation level, Springer Verlag series, Series International Association of Geodesy Symposia ,Vol. 134, Drewes (ed.), pp 3-9., DOI 10.1007/978-3-642-00860-3, 2009.

Gegout P., Boy J.-P., Hinderer J. & Ferhat G., Modeling and Observation of Loading Contribution to Time-Variable GPS Sites Positions, Proceedings of the International Symposium of Gravity, Geoid and Earth Observation GGEO 2008, IAG, Chania, Crete, Greece, accepté en 2009, 2009.

Getirana A-C-V, M-P Bonnet, E. Roux, S. Calmant, F. Seyler, O. C. Rotunno Filho, W. J. Mansur, Hydrological Monitoring of Poorly Gauged Basins Based on Rainfall-Runoff Modeling and Spatial Altimetry, J. Hydrology, in press, 2009.

Gobinddass M.L., Willis P., Sibthorpe A., Zelensky N.P., Lemoine F.G., Ries J.C., Ferland R., Bar-Sever Y.E., de Viron O., Diament M. (2009), Improving DORIS geocenter time series using an empirical rescaling of solar radiation pressure models, Advances in Space Research, 44(11):1279-1287. DOI: 10.1016/j.asr.2009.08.004, COSPAR Outstanding Paper Award for Young Scientist

Gontier A.-M. et al. VLBI at OPAR: analysis service and research, In: G. Bourda et al. (Eds.), 19th European VLBI for Geodesy and Astrometry (EVGA) Working Meeting Proc., 177, 2009.

Hinderer, J., C. de Linage, J.-P. Boy, P. Gegout, F. Masson, Y. Rogister, M. Amalvict, J. Pfeffer, F. Little, B. Luck, R. Bayer, C. Champollion, P. Collard, N. Le Moigne, M. Diament, S. Deroussi, O. de Viron, R. Biancale, J.M. Lemoine, S. Bonvalot, G. Gabalda, O. Bock, P. Genthon, M. Boucher, G. Favreau, L. Seguis, F. Delclaux, B. Cappelaere, M. Oi, M. Descloitres, S. Galle, J.-P. Laurent, A. Legchenko and M.-N. Bouin (2009) The GHYRAF (Gravity and Hydrology in Africa) experiment: Description and first results, *Journal of Geodynamics*, **48**(3-5), p. 172-181, DOI:10.1016/j.jog.2009.09.014

Jiang, Z., M. Becker, O. Francis, A. Germak, V. Palinkas, P. Jousset, J. Kostelecky, T. Dupont, C. Lee, C.-L. Tsai, R. Falk, H. Wilmes, A. Kopaev, D. Ruess, C. Ullrich, B. Meurers, J. Mrlina, S. Deroussi, L. Métivier, G. Pajot, F. Pereira Dos Santos, M. van Ruymbeke, S. Naslin and M. Ferry (2009) Relative Gravity Measurement Campaign during the 7th International Comparison of Absolute Gravimeters (2005), *Metrologia*(46), p. 214-226, DOI:10.1088/0026-1394/46/3/008

Kierulf H.P., Pettersen B., McMillan D.S., Willis P. (2009), The kinematics of Ny-Alesund from space geodetic data, Journal of Geodynamics, 48(1):37-46. DOI: 10.1016/j.jog.2009.05.002

Kouraev A. and J-F Crétaux, Aral Sea Ice conditions from historical and satellite observations, Handbook of environmental chemistry, Vol 5 Water pollution, Ed A.G. Kostianoy, A.N. Kosarev, (invited papers) in press, 2009a.

Kouraev A.V., J-F Crétaux, S.A. Lebedev, A.G. Kostianoy, A.I. Ginzburg, N.A. Sheremet, R. Mamedov, E.A. Zhakharova, L. Roblou, F. Lyard, S. Calmant, M. Bergé-Nguyen, The Caspian Sea, invited papers, in press, Handbook on Coastal altimetry, Springer ed., chap. 19, 2009b.

Lambert S., Gontier A.-M., On radio source selection to define a stable celestial frame, A&A, 493, 317, 2009.

Lambert S.B. , Gontier A.-M., On radio source selection and frame stability, In: G. Bourda et al. (Eds.), 19th European VLBI for Geodesy and Astrometry (EVGA) Working Meeting Proc., 27, 2009.

Lambert S., Le Poncin-Lafitte C., Determining the relativistic parameter g using very long baseline interferometry, A&A, 499, 331, 2009.

Legrand, J., N. Bergeot, C. Bruyninx, G. Wöppelmann, M.-N. Bouin and Z. Altamimi (2009) Impact of Regional Reference Frame Definition on Geodynamic Interpretations, *Journal of Geodynamics*, **49**, DOI:10.1016/j.jog.2009.10.002

Lequentrec-Lalancette MF, Rouxel D, Pineau-Guillou L, 2009, Comparison of GPS and gravity data on french coastal zones, paper presented at the IAG Meeting "Geodesy for Planet Earth", Buenos-Aires, Argentina, 30 august-4sept

Levy A., B. Christophe, P. Berio, G. Métris, J.-M. Courty, and S. Reynaud, Pioneer 10 Doppler data analysis: disentangling periodic and secular anomalies, Advance in Space Research 43, pages 1538-1544, 2009

Llovel W., Cazenave A., Berge-Nguyen M. and Rogel P., Past sea level reconstruction (1950-2000) using the OPA/NEMO global ocean circulation model, tide gauge and satellite altimetry data, Climate of the Past, 5, 1-11, 2009.

Llovel W., K. DoMinh K., A. Cazenave, Crétaux J.F., M.C. Gennero and M. Becker, Contribution of land water storage change to global mean sea level from GRACE and satellite altimetry, in press to C.R. Geosciences, 2009.

Louis G., Lequentrec-Lalancette M.-F., Rouxel D., Geli L., Royer J.-Y., Maia M., Faillot M., Toward a high resolution geoid from altimetry: requirement for a new mission, EOS accepted, 2009.

Marty J.C., G. Balmino, J. Duron, P. Rosenblatt, S. Le Maistre, A. Rivoldini, V. Dehant, T. Van Hoolst, Martian gravity field model and its time variations from MGS and Odyssey data, Planetary and Space Science,doi: 10.1016/j.pss.2009.01, 2009.

Métivier, L., O. de Viron, C.P. Conrad, S. Renault, M. Diament and G. Patau (2009) Evidence of earthquakes triggering by the solid Earth tides, *Earth and Planetary Science Letters*, **278**, p. 370-375, DOI:10.1016/j.epsl.2008.12.024

Merrifield M., Aarup T., Aman A., Caldwell P., Fernandes R. M. S., Hayashibara H., Kilonsky B., Martin Miguez B., Mitchum G., Perez Gomez B., Rickards L., Rosen D., Schöne T., Testut L., Woodworth P., Wöppelmann G., The Global Sea Level Observing System (GLOSS). In OceanObs'09, Ocean Information for society: sustaining the benefits, organizing the potential, Community White Papers, 21-25 Sept. 2009, Venice, Italy, 2009.

Métivier, L. and C.P. Conrad (2009) Body tides of a convecting, laterally heterogeneous, and aspherical Earth, *CIG-related one-pagers*

Minchev, B., A. Chambodut, M. Holschneider, I. Panet, E. Schöll and M. Mandea (2009) Local multipolar expansions in potential fields modelling, *Earth, Planets and Space*, **61**, p. 1127-1141

Panet, I., Y. Kuroishi and M. Holschneider (2009) Wavelet modeling of the gravity field over Japan, *Bulletin of the Geographical Survey Institute (Japan)*(57)

Pineau-Guillou, L., 2009, □ Projet BATHYELLI : determination du zero hydrographique à partir de l'altimetrie spatiale et du GPS, Navigation, Vol.57, n°226

Prandi P., Cazenave A. and Becker M. , Is coastal mean sea level rising faster than the global mean? A comparison between tide gauges and satellite altimetry over 1993-2007, Geophys. Res. Lett., 36, doi:10.1029/2008GL036564, 2009.

Rebischung P., Duquenne H. (2009)- the French zero-order leveling network – first global results and possible consequences for UELN – *Proceedings of the Symposium of IAG subcommission for Europe (EUREF), Brussels, Belgium, June 18-21, 2008*

Richard, E., C. Flamant, F. Bouttier, J. van Baelen, C. Champollion, S. Argence, J. Arnault, C. Barthlott, A. Behrendt, P. Bosser, P. Brousseau, J.-P. Chaboureau, U. Corsmeier, J. Cuesta, P. Di Girolamo, M. Hagen, C. Kottmeier, P. Limnaios, F. Masson, G. Pigeon, Y. Pointin, Y. Seity and V. Wulfmeyer (2009) La campagne COPS : Initiation et cycle de vie de la convection en région montagneuse, *La Météorologie*(64)

Rignot E. and A. Cazenave, Ice and sea level, in Arctic Climate feedbacks: global implications, WWF International, 2009.

Rosat S., Lambert S., FCN resonance parameters from VLBI and superconducting gravimeter data, A&A, 503, 287, 2009.

Seoane L., Nastula J, Bizouard C. and D. Gambis, The use of gravimetric data from GRACE mission in the understanding polar motion variations, Geophys. J. Int., 178, p614?622, DOI 10.1111/j.1365-246X.2009.04181.x, 2009.

Seoane L., J. Nastula, C. Bizouard, D. Gambis, Hydrological excitation of polar motion, Proc. Journées Systèmes de Référence 2008, M. Soffel and N. Capitaine (eds.), p149, 2009.

Seyler, F, S. Calmant, J. da Silva, N. Filizola, G. Cochonneau, M-P Bonnet, A-C Zoppas Costi, Inundation risk in large tropical basins and potential survey from radar altimetry: example in the Amazon basin, Marine Geodesy, 32 (3), 303-319, DOI 10.1080/01490410903094809, 2009.

E. Simonetto, J.M. Follin (2009), An overview on interferometric SAR software and a comparison between DORIS and SARSCAPE processing, *Springer series: Lecture Notes in Geoinformation and Cartography (LNG&C)* series, accepté.

Tsoulis, D., O. Jamet, J. Verdun and N. Gonindard (2009) Recursive algorithms for the computation of the potential harmonic coefficients of a constant density polyhedron, *Journal of Geodesy*, **83**(10), p. 925-942, DOI:10.1007/s00190-009-0310-9

Uribe C.,Li J., Daillet S., Xiaoling C., Bergé-Nguyen M., Li X., Crétaux J-F., Hubert C., Lai X., Marie T., Huang S., Andreaoli R., and Yesou H., Monitoring of the largest Chinese inland lakes within the ESA-MOST DRAGON project using conjointly ENVISAT image time series and altimetric data: case of Dongting and Poyang lakes, proceeding of ILEC conference, Wuhan, in press, 2009.

Valk S., Lemaitre A., Deleflie F., Semi-analytical theory of mean orbital motion for geosynchronous space debris under gravitational influence, Advances in space research, vol. 43, no7, pp. 1070-1082, 2009.

Wolf P. et al., Quantum Physics Exploring Gravity in the Outer Solar System: The Sagas Pro ject, Experimental Astronomy, 23(2), pages 651–687, 2009.

Wöppelmann, G., C. Letetrel, A. Santamaría, M.-N. Bouin, X. Collilieux, Z. Altamimi, S. Williams and B. Martín Míguez (2009) Rates of sea-level change over the past century in a geocentric reference frame, *Geophysical Research Letters*, **36**(L12607), DOI:10.1029/2009GL038720

Woodworth, P. L., L. J. Rickards et B. Pérez, A survey of European sea level infrastructure, Nat. Hazards Earth Syst. Sci., 9, pp. 927–934, 2009a.

Woodworth, P. L., N. Pouvreau et G. Wöppelmann, The gyre-scale circulation of the North Atlantic and sea level at Brest, Ocean Sci. Discuss., 6, pp. 2327-2339, 2009b.

Willis P., Boucher C., Fagard H., Garayt B., Gobinddass M.L., Contributions of the French Institut Géographique National (IGN) to the International DORIS Service, Advances in Space Research. doi:10.1016/j.asr.2009.09.019, 2009.

Willis P., Ries J.C., Zelensky N.P., Soudarin L., Fagard H., Pavlis E.C., Lemoine F.G. (2009), DPOD2005 : Realization of a DORIS terrestrial reference frame for precise orbit determination, Advances in Space Research, 44(5):535-544. DOI: 10.1016/j.asr.2009.04.018

Wilmes, H., Wziontek, H., Falk, R., Bonvalot, S., AGrav – the New International Absolute Gravity Database and a Proposed Cooperation with the Global Geodynamics Project (GGP). Journal of Geodynamics, 48, pp. 305-309. doi:10.1016/j.jog.2009.09.035.

Yésou H., J. Li, S. Daillet, X. Lai, M. Bergé-Nguyen, X. Chen, S. Huang, J-F Crétaux, C. Hubert, T. Marie, J. Li, R. Andreoli, C. Uribe, Large Inland lakes monitoring exploiting conjointly Envisat low and medium resolution image time series and altimetric data: Case of Poyang and Dongting lakes (P.R. China) from 2000 to 2008 within Dragon project, submitted to proceedings of “Earth observation and the water cycle”, Frascati, 2009.

Zambrano G ., R. Abarca Del Rio, J-F. Crétaux, B. Reid, First Insights on Lake General Carrera /Buenos Aires/ Chelenko water balance, in press in Advance in geoscience, 2009.

Zerhouni W., Capitaine N., “Celestial pole offsets from lunar laser ranging and comparison with VLBI”, A&A 507, 3, 1687-1695 , DOI: 10.1051/0004-6361/200912644, 2009.

Zerhouni Z., Capitaine N., Francou G., What could bring LLR observations in determining the position of the celestial pole, Proceedings of the "Journées 2008 Systèmes de référence spatio-temporels", M. Soffel and N. Capitaine (eds.), Lohrmann-Observatorium and Observatoire de Paris., pp. 186-189, 2009.

Zerhouni Z., Capitaine N., Francou G., Determination of the corrections to the celestial pole coordinates using LLR observations, SF2A-2008: Proceedings of the Annual meeting of the French Society of Astronomy and Astrophysics Eds.: C. Charbonnel, F. Combes and R. Samadi. Available online at http://proc.sf2a.asso.fr, p.153, 2009.

2008

Altamimi Z., X. Collilieux, IGS contribution to ITRF, Journal of Geodesy, vol. 83, n. 3-4, pp. 375-383, doi:10.1007/s00190-008-0294-x, 2008.

Altamimi, Z. and X. Collilieux (2008) *Institut Géographique National (IGN) Combination Centre*, chapter 3.6.1.2, IERS annual report 2007

Altamimi, Z., X. Collilieux and C. Boucher (2008) Accuracy Assessment of the ITRF Datum Definition, *VI Hotine-Marussi Symposium on Theoretical and Computational Geodesy IAG Symposium Wuhan, China 29 May - 2 June, 2006*, Xu,P. and Liu, J. and Dermanis, A. Ed., International Association of Geodesy Symposia, Vol.132, p. 101-110, Springer, DOI: 10.1007/978-3-540-74584-6_16

Altamimi, Z., X. Collilieux and B. Garayt (2008a) *ITRS Centre*, chapter 3.5.5., IERS annual report 2007

Altamimi, Z., D. Gambis and C. Bizouard (2008b) Rigorous combination to ensure ITRF and EOP consistency, *Actes des Journées Systèmes de Référence Spatio-Temporels 2007*

Amalvict M., P. Willis, G. Woppelmann, E.R. Ivins, L. Testud, J. Hinderer, M.N. Bouin , Stability of the East Antarctic station Dumont d'Urville from long-term geodetic and geophysical observations, Polar Res., doi: 10.1111/j.1751-8369.2008.00091.x., 2008.

Anthony, E. J., Dolique, F., Gardel, A., Gratiot, L. Polidori, N., Proisy, C. (2008) "Nearshore intertidal topography and topographic-forcing mechanisms of an Amazon-derived mud bank in French Guiana". *Continental Shelf Research*. 28(6): 813-822. DOI:10.1016/j.csr.2008.01.003.

Barlier F., (Ed.), Académie de marine, Bureau des Longitudes, Académie nationale de l'air et de l'espace, ouvrage collectif, Galileo. Un enjeu stratégique, scientifique, technique. Fondation pour la Recherche Scientifique, l'Harmattan, février 2008, 255 pages.

Berge-Nguyen M., Cazenave A., Lombard A., Llovel W. and Cretaux J.F., Reconstruction of past decades sea level using tide gauge, altimetry and in situ hydrographic data, Global and Planetary Change, 62, 1-13, 2008.

Biancamaria S., P. Bates, A. Boone., N.M. Mognard, J.-F. Crétaux, Modelling the Ob River in Western Siberia, using Remotely Sensed Digital Elevation Models Proceedings of the "2nd Space for Hydrology Workshop" WMO, Geneva, November 11-14, 2007, ESA Special Publication SP-xxx, 2008.

Bizouard C. and D. Gambis, The combined solution C04 for Earth Orientation Parameters, recent improvements, Springer Verlag series, sous presse, 2008.

Bruinsma S.L., and J.M Forbes, Properties of Traveling Atmospheric Disturbances (TADs) inferred from CHAMP accelerometer observations, Adv. Sp. Res., doi:10.1016/j.asr.2008.10.031, 2008.

Bruinsma S.L. and J.M Forbes, Medium to Large-Scale Density Variability as Observed by CHAMP, Space Weather, Vol. 6, S08002, doi:10.1029/2008SW000411, 2008.

Bock, O., R. Meynadier, F. Guichard, P. Roucou, A. Boone, J.L. Redelsperger and S. Janicot (2008) Assessment of water budgets computed from NWP models and observational datasets during AMMA-EOP, *Proceedings of the 28th Conference on Hurricanes and Tropical Meteorology, Orlando, Florida, United States, 28 April-2 May 2008*

Bock, O., M.-N. Bouin, E. Doerflinger, P. Collard, F. Masson, R. Meynadier, S. Nahmani, M. Koité, K. Gaptia Lawan Balawan, F. Didé, D. Ouedraogo, S. Pokperlaar, J.-B. Ngamini, J.-P. Lafore, S. Janicot, F. Guichard and M. Nuret (2008a) The West African Monsoon observed with ground-based GPS receivers during AMMA, *Journal of Geophysical Research,* **113**(D21105), DOI:10.1029/2008JD010327

Bosser, P., O. Bock, C. Thom and J. Pelon (2008) Processing of Raman lidar measurements for water vapor mixing ratio retrieval, *24th International Laser Radar Conference*

Bureau des longitudes, Académie de l'Air et de l'Espace, Académie de Marine, *Galileo, un enjeu stratégique, scientifique et technique*, L'Harmattan (Ed.), Fondation pour la Recherche Stratégique, 2nd Edition, 254 pages, 2008 (in French).

Calmant S., Seyler F. and Cretaux J.F., Monitoring Continental Surface Waters by Satellite Altimetry, Survey in Geophysics, special issue on 'Hydrology from Space', in press, 2008.

Capitaine N., Wallace P.T., Concise CIO based precession-nutation formulations, Astron. Astrophys. 478, 277-284 doi:10.1051/0004-6361:20078811, 2008.

Capitaine N., Recent progress in concepts, nomenclature and models in fundamental astronomy, "Journées Systèmes de référence spatiotemporels", Dresden, Germany, M. Soffel, N. Capitaine (eds.), pp 61-64, 2008.

Capitaine N., Wallace P.T., "The transformation between the Terrestrial and Celestial Reference Systems: Needs and potential of GPS and Galileo", Proceedings of the ESA 1st Colloquium Scientific and Fundamental Aspects of the Galileo Programme, ESA (ed), 2008.

Capitaine N., J. Vondrak, and Hilton. J.L., Joint Discussion 16 Nomenclature, precession and new models in fundamental astronomy. Highlights of Astronomy, 14:457-458, 2008a.

Capitaine N., Mathews, P.M., Dehant, V., Wallace, P.T., & Lambert, S.B., Comparisons of precession-nutation models, In: D. Behrend and K.D. Baver (Eds.), in Measuring the Future, A.Finkelstein and D. Behrend (eds.), Saint Petersburg, Nauka, pp. 221-230, 2008.

Cazenave A., A. Lombard and W. Llovel., Present-day sea level rise: a synthesis, C.R. Geosciences, doi:10.1016/j-crte-2008.07.008, 2008.

Cazenave A., Guinehut S., Ramillien G., Llovel W., DoMinh K., Ablain M., Larnicol G. and Lombard A., Sea level budget over 2003-2008; a reevalution from satellite altimetry, GRACE and Argo data, Global and Planetary Change, doi:10.1016/j/gloplacha.2008.10.004, 2008.

Chapanov Y. and D. Gambis, Correlation between the solar activity cycles and the Earth rotation, "Journées Systèmes de référence spatiotemporels", Dresden, Germany, M. Soffel, N. Capitaine (eds.), 2008.

Chapanov Y. and D. Gambis, Influence of atmospheric and oceanic angular momemtum excitation on the variations of Universal Time, Exploring the solar system and Universe, Mioc et al. (eds), American Institute of Physics, AIP Conference Proceedings, pp 218-219, 2008.

Chaumillon E., X. Bertin, H. Falchetto, J. Allard, N. Weber, P. Walker, N. Pouvreau, G. Woppelmann, Multi-time scale evolution of a wide estuary linear sandbank, the Longe de Boyard, Atlantic coast of France, Marine Geology, 251, 209-223, 2008.

Collilieux, X. and Z. Altamimi (2008) Impact of the network effect on the origin and scale : Case study of Satellite Laser Ranging, *Observing our Changing Earth, Proceedings of the 2007 IAG General Assembly, Perugia, Italy, July 2 - 13, 2007*, International Association of Geodesy Symposia, Vol.133, p. 31-37, Springer, DOI:10.1007/978-3-540-85426-5_4

Collilieux, X., Z. Altamimi, D. Coulot and A. Pollet (2008) *Institut Géographique National (IGN) Combination Research Centre*, chapter 3.6.2.8, IERS annual report 2007

Coulot D., P. Berio, P. Bonnefond, P. Exertier, D. Féraudy, O. Laurain & F. Deleflie, Satellite Laser Ranging biases and Terrestrial Reference Frame scale factor, Observing our Changing Earth, International Association of Geodesy Symposia, Vol. 133, Part 1, pp. 39-46, M. G. Sideris (Ed.), Springer Verlag Berlin Heidelberg, doi: 10.1007/978-3-540-85426-5, 2008.

Cretaux J.F., S. Calmant, V. Romanovski, Pr, A. Shabunin, F. Lyard, M. Bergé-Nguyen, A. Cazenave, F. Perosanz, An absolute calibration site for radar altimeters in the continental domain: Lake Issykkul in Central Asia, Journal of Geodesy, 2008.

Cretaux J.F., Calmant S., Romanovski V., Shibuyin A., Lyard F., Berge-Nguyen M., Cazenave A., Hernandez F., and F. Perosanz, Implementation of a new absolute calibration site for radar altimeter in the continental area: lake Issykkul in Central Asia, Journal of Geodesy, doi:10.1007/s00190-008-0289-7, 2008.

Cretaux J-F, R. Letolle, and S. Calmant, Investigations on Aral Sea regressions from Mirabilite deposits and remote sensing, aquatic geochemistry, doi: 10.1007/s10498-008-9051-2, 2008.

Dehant V., de Viron, O. and Capitaine, N., "The 3D representation of the new transformation from the terrestrial to the celestial system", Highlights of Astronomy, 14:486–486, 2008.

de Viron, O., I. Panet, V. Mikhailov, M. van Camp and M. Diament (2008) Retrieving earthquake signature in Grace gravity solutions, *Geophysical Journal International*, **174**(1), p. 14-20, DOI:10.1111/j.1365-246X.2008.03807.x

Diament, M. and I. Panet (2008) Signatures gravimétriques des séismes de Sumatra, *E-Space & Science*(24)

Duquenne, H., P. Rebischung, F. Duquenne, A. Harmel and A. Coulomb (2008) Status of the zero-order levelling network of France and consequences for UELN, *Proceedings of EUREF Symposium 2007*

Duquenne, H. and P. Valty (2008) *Calcul du quasi-géoïde de Nouvelle-Calédonie QGNC08 et de la grille de référence altimétrique RANC08*, rapport technique, publication LAREG n° R11

Duquenne, F., A. Harmel, H. Duquenne and B. Garayt (2008a) National report of France, *Report of the symposium of the IAG subcommission for Europe (EUREF)*, EUREF publications

Forbes J.M., S.L. Bruinsma, Y. Miyoshi, H. Fujiwara, A Solar Terminator Wave in Thermosphere Neutral Densities Measured by the CHAMP Satellite, Geophys. Res. Lett., doi:10.1029/2008GL034075, 2008.

Forbes J.M., Lemoine, F.G., Bruinsma, S.L., Smith, M.D., Zhang, X., Solar Flux Variability of Mars'Exosphere Densities and Temperatures, Geophys. Res. Lett., vol. 35, L01201, doi:10.1029/2007GL031904, 2008.

Folgueira M., Capitaine, N., Souchay, J., New expressions for the celestial coordinates of the CIP, Highlights of Astronomy, 14, 49, 2008.

Gambis D., J.Y. Richard, D. Salstein, Use of Atmospheric Angular Momentum forecasts for UT1 prediction, "Journées Systèmes de référence spatiotemporels", Dresden, Germany, M. Soffel, N. Capitaine (eds.), pp 210-212, 2008.

Gambis D., Richard, J.Y., Salstein, D., Using various sets of Atmospheric Angular Momentum forecasts for UT1 predictions, Series of the Research Institute of Geodesy, Topography and Cartography, Volume 54, 45, Zdiby, Prague East, P. Holota (ed.), 2008.

Gontier A.-M., & Lambert, S.B., Stable radio sources and reference frame, In: N. Capitaine (Ed.), "Journées Systèmes de référence spatiotemporels", Dresden, Germany, M. Soffel, N. Capitaine (eds.), ISBN 978-2-901057-59-8, 42, 2008.

Gourine B., S. Kahlouche, P. Exertier, P. Berio, D. Coulot & P. Bonnefond, Corsica SLR Positioning Campaigns (2002 and 2005) for Satellite Altimeter Calibration Missions, Marine Geodesy, 31 : 103-116, 2008.

Gouriou T., N. Pouvreau, G. Woppelmann, Mesures du niveau de la mer en France : un patrimoine historique à fort potentiel scientifique. L'exemple du littoral charentais, Géologues, 158, Spécial Littoral, pp. 83-88, 2008.

Guo J., W. Wan, J. M. Forbes, E. Sutton, R S. Nerem, S. Bruinsma, Inter-annual and Latitudinal Variability of the Thermosphere Annual Harmonics, J. Geophys. Res., 113, A08301,doi:10.1029/2008JA013056, 2008.

Janicot, S., A. Ali, N. Asencio, G. Berry, O. Bock, B. Bourles, G. Caniaux, F. Chauvin, A. Deme, L. Kergoat, J.-P. Lafore, C. Lavaysse, T. Lebel, B. Marticorena, F. Mounier, J.L. Redelsperger, R. Roca, P. de Rosnay, B. Sultan, C.D. Thorncroft, M. Tomasini and ACMAD forecasters team (2008) Large-scale overview of the summer monsoon over West and Central Africa during AMMA field experiment in 2006, *Annales Geophysicae*, **26**(9), p. 2569-2595, DOI:10.5194/angeo-26-2569-2008

Lambert S.B., Dehant, V., & Gontier, A.-M., Earth's interior with VLBI… and the celestial reference frame? In: N. Capitaine (Ed.), "Journées Systèmes de référence spatiotemporels", Dresden, Germany, M. Soffel, N. Capitaine (eds.), ISBN 978-2-901057-59-8, 103, 2008.

Lambert S.B., & Gontier, A.-M., Earth's interior with VLBI: pushing the limits, In: C. Charbonnel et al. (Eds.), Proc. Semaine de l'Astrophysique Française - Journées SF2A 2008, 123, 2008.

Lambert S.B., & Le Poncin-Lafitte, C., An estimate of the relativistic parameter using VLBI, In: C. Charbonnel et al. (Eds.), Proc. Semaine de l'Astrophysique Française – Journées SF2A 2008, 127.

Lambert S.B., & Le Poncin-Lafitte, C., Measuring the relativistic parameter using the current geodetic VLBI data set, In: A. Finkelstein and D. Behrend (Eds.), International VLBI 78, Service for Geodesy and Astrometry (IVS) 2008 General Meeting Proceedings, ISBN 978-5-02-025332-2, 341, 2008.

Lambert S. et al., Celestial frame instability in VLBI analysis and impact on geophysics, A&A, 481, 535, 2008.

Lambert S., F. Deleflie, A.-M. Gontier, P. Bério, C. Barache, The astronomical Virtual Observatory and application to Earth's sciences, In: A. Finkelstein and D. Behrend (Eds.), International VLBI Service for Geodesy and Astrometry (IVS) 2008 General Meeting Proceedings, ISBN 978-5-02-025332-2, 203, 2008.

Lathuillère C., M. Menvielle, A. Marchaudon, S.Bruinsma, A statistical study of the observed and modelled global thermosphere response to magnetic activity at mid and low latitudes, J. Geophys. Res., 113, A07311, doi:10.1029/2007JA012991, 2008.

Llubes, M., N. Florsch, J.-P. Boy, M. Amalvict, P. Bonnefond, M.-N. Bouin, S. Durand, M.F. Esnoult, P. Exertier, J. Hinderer, M.F. Lalancette, F. Masson, L. Morel, J. Nicolas, M. Vergnolle and G. Wöppelmann (2008) Multi-technique monitoring of ocean tide loading in northern France, *Comptes-rendus Géosciences*, **340**(6), p. 379-389, DOI:10.1016/j.crte.2008.03.005

M.F. Lequentrec-Lalancette, D. Rouxel, M Maïa, J.Y. Royer, L. Géli. *Modeling the gravity field: constraints and limitations*, EGU2008 Meeting, Vienna, April 14-18, 2008

Manche H., J. Laskar, A. Fienga, N. Capitaine, S. Bouquillon, G. Francou, M. Gastineau , "The geodesic precession in the INPOP ephemerides", "Journées Systèmes de référence spatiotemporels", Dresden, Germany, M. Soffel, N. Capitaine (eds.), 2008.

Martin Miguez B., R. Le Roy, G. Woppelmann, The use of radar gauges to measure variations in sea level along the French coast, Journal of Coastal Research, 24, pp. 61-68, 2008a.

Martin Miguez B., L. Testut, G. Woppelmann, The van de Casteele test revisited: an efficient approach to tide gauge error characterization, Journal of Atmospheric and Oceanic Technologies, Vol. 25, Nr. 7, pp. 1238–1244, 2008b.

Melachroïnos, S.A., R. Biancale, M. Llubes, F. Perosanz, F. Lyard, M. Vergnolle, M.-N. Bouin, F. Masson, J. Nicolas, L. Morel and S. Durand (2008) Ocean tide loading (OTL) displacements from global and local grids : comparisons to GPS estimates over the shelf of Brittany, France, *Journal of Geodesy*, **82**(6), p. 357-371, DOI:10.1007/s00190-007-0185-6

Métivier, L. and C.P. Conrad (2008) Body tides of a convecting, laterally heterogeneous, and aspherical Earth, *Journal of Geophysical Research*, **113**(B11405), DOI:10.1029/2007JB005448

Métivier, L., Ö. Karatekin and V. Dehant (2008) The effect of the internal structure of Mars on its seasonal loading deformations, *Icarus*, **194**, p. 476-486, DOI:10.1016/j.icarus.2007.12.001

L. Morel et S. Durand. Comparaison du positionnement temps réel classique RTK et du positionnement GPS temps réel réseau : Mise en œuvre dans le réseau Orphéon. *Revue XYZ*, n°115, 2ème trimestre 2008.

Nuret, M., J.-P. Lafore, O. Bock, A. Agusti-Panareda, J.-B. Ngamini and J.L. Redelsperger (2008) Correction of humidity bias for Vaïsala RS80 sondes during AMMA 2006 Observing Period, *Journal of Atmospheric and Oceanic Technology*, **25**(11), p. 2152-2158, DOI:10.1175/2008JTECHA1103.1

Pajot G., O de Viron, M Diament, M-F Lequentrec-Lalancette, V Mikhailov, Noise reduction through joint processing of gravity and gravity gradient data, Geophysics, VO73, 3, pp123-134, 2008.

Ramillien G., Bouhours S., Lombard A., Cazenave A., Flechtner F. and Schmidt R., Land water contributions from GRACE to sea level rise over 2002-2006, Global and Planetary Change, 60, 381-392, 2008.

Ray, J., Z. Altamimi, X. Collilieux and T. van Dam (2008) Anomalous harmonics in the spectra of GPS position estimates, *GPS Solutions*, **12**(1), DOI:10.1007/s10291-007-0067-7

Rebischung, P., R. Hipkin, C. Calvert, M. Greaves, C. Fane, H. Duquenne, A. Harmel, F. Duquenne and A. Coulomb (2008) Connection of French and British levelling networks, application to UELN, *Proceedings of EUREF Symposium 2007*

Richard J.Y. , D. Gambis, J.M. Lemoine, C. Bizouard, R. Biancale, Global combination of station coordinates and Earth rotation parameters, Series of the Research Institute of Geodesy, Topography and Cartography, Volume 54, 45, Zdiby, Prague East, P. Holota (ed.), 2008.

Rosat S., & Lambert, S.B., Outer and inner core parameters from joint analysis of superconducting gravimeter and VLBI data, In: A. Finkelstein and D. Behrend (Eds.), International VLBI Service for Geodesy and Astrometry (IVS) 2008 General Meeting Proceedings, ISBN 978-5-02-025332-2, 246, 2008.

Rothacher M., G. Beutler, W. Bosch, A. Donnellan, R. Gross, J. Hinderer, C. Ma, M. Pearlman, H.-P. Plag, B. Richter, J. Ries, H. Schuh, F. Seitz, C.K. Shum, D. Smith, M. Thomas, I. Velicogna, J. Wah, P. Willis, P. Woodworth, The future Global Geodetic Observing System (GGOS), in GGOS 2020, Chapter 9, pp. 142-159, 2008.

Roux E, M. Cauhopé, M-P. Bonnet, S. Calmant, F. Seyler, Daily water stage estimated from satellite altimetric data for large river basin monitoring, Hydrological Sciences Journal - Journal des Sciences Hydrologiques,Vol 53-1, 81-99, 2008.

Roux, E., J. Santos da Silva, A. Cesar Vieira Getirana, M-P Bonnet, S. Calmant et F. Seyler, Producing time-series of river water height by means of satellite radar altimetry – Comparison of methods; Produire des séries temporelles de hauteur d'eau grâce à l'altimétrie radar satellitaire – Comparaison de méthodes, Hydrological sciences Journal, in revision, 2008.

Sarzeau O., M-F Lequentrec-Lalancette, D Rouxel, Optimal Interpolation of gravity maps using a modified neural network, 2008, Mathematical geosciences, V41, 4, pp 379-395, 2008.

Seoane L., J. Nastula, C. Bizouard, D. Gambis, Effets hydrologiques sur la rotation terrestre, proc. SF2A, Paris, juillet 2008.

Seoane L., C. Bizouard, D. Gambis, Polar motion interpretation using gravimetric date, "Journées Systèmes de référence spatiotemporels", Dresden, Germany, M. Soffel, N. Capitaine (eds.), pp 196-200, 2008.

Souchay S.B. Lambert, A.H. Andrei, S. Bouquillon, C. Barache, C. Le Poncin-Lafitte, "Astrometric comparisons of quasars catalogues, Astronomy and Astrophysics, 485,299-302, 2008.

Stefka V., Folgueira, M., Lambert, S., Capitaine, N., The Descartes project: “Solving the rotational Earth’s equations in rectangular coordinates for a non-rigid Earth”, "Journées Systèmes de référence spatiotemporels", Dresden, Germany, M. Soffel, N. Capitaine (eds.), 2008.

Valty P. and H. Duquenne, Quasi-geoid of New Caledonia : computation, results and analysis, Proceedings IAG International Symposium GGEO2008, Chania, Crête, Greece, 23-27 June 2008, Springer.

Vergnolle, M., M.-N. Bouin, L. Morel, F. Masson, S. Durand, J. Nicolas and S.A. Melachroïnos (2008) GPS estimates of ocean tide loading in NW-France : Determination of ocean tide loading constituents and comparison with a recent ocean tide model, *Geophysical Journal International*, **173**(2), p. 444-458, DOI:10.1111/j.1365-246X.2008.03734.x

Wallace P.T., Capitaine, N., Using the P03 precession model, Highlights of Astronomy, 14:466-466, 2008.

Willis P., Book review, Statistical orbit determination, B.D. Tapley, B.E. Schutz, G.H. Born, Adv. Sp. Res, 41(10), 1710-1711, 2008, doi: 10.1016/j.asr.2007.08.036, 2008.

Willis P., Book review, Modern astrodynamics, P. Gurfil, Adv. Space Res, 41(1), 230-231, doi: 10.1016/j.asr.2007.07.047, 2008.

Woppelmann G., Bouin, M.N., Altamimi, Z., Terrestrial reference frame implementation in global GPS analysis at TIGA ULR consortium, Physics and Chemistry of the Earth, Parts A/B/C, 33 (3-4): 217-224, doi:10.1016/j.pce.2006.11.001, 2008.

Wöppelmann, G., N. Pouvreau, A. Coulomb, B. Simon and P.L. Woodworth (2008a) Tide gauge datum continuity at Brest since 1711: France's longest sea-level record, *Geophysical Research Letters*, **35**, p. 22605, DOI:10.1029/2008GL035783

Zerhouni W., Capitaine, N., Francou, G., The use of LLR observations (1969-2006) for the determination of the celestial coordinates of the pole, "Journées Systèmes de référence spatiotemporels", Dresden, Germany, M. Soffel, N. Capitaine (eds.), pp 123-124, 2008.

Zerhouni W., Capitaine, N., Francou, G., Determination of the corrections to the IAU 2000A-2006 X, Y coordinates using LLR observations, Proceedings. Semaine de l'Astrophysique Française - Journées SF2A 2008.

2007

Abbasi, M., J.-P. Barriot and J. Verdun (2007) Airborne LaCoste & Romberg gravimetry: a space domain approach, *Journal of Geodesy*, **81**(4), p. 269-284, DOI:10.1007/s00190-006-0107-z

Alsdorf D., L.L. Fu, N. Mognard, A. Cazenave, E. Rodriguez, D. Chelton and D. Lettemaier, Measuring global oceans and terrestrial fresh water from space, EOS, Transactions, AGU, v88, n24, p253, 2007.

Altamimi, Z., X. Collilieux and C. Boucher (2007) Preliminary analysis in view of the ITRF2005, *Dynamic Planet: Monitoring and Understanding a Dynamic Planet with Geodetic and Oceanographic Tools*, Tregoning, P. and Rizos, C. Ed., International Association of Geodesy Symposia, Vol.130, p. 685,691, Springer

Altamimi, Z., X. Collilieux and B. Garayt (2007a) *ITRS Centre*, chapter 3.5.5 of the IERS annual report 2006

Altamimi, Z., X. Collilieux, J. Legrand, B. Garayt and C. Boucher (2007b) *Institut Géographique National (IGN) Combination Centre*, chapter 3.6.1.2 of the IERS annual report 2006

Altamimi, Z., X. Collilieux, J. Legrand, B. Garayt and C. Boucher (2007c) ITRF2005: A new release of the International Terrestrial Reference Frame based on time series of station positions and Earth Orientation Parameters, *Journal of Geophysical Research*, **112**(B09401), DOI:10.1029/2007JB004949

Altamimi Z., Gambis D., Bizouard Ch., Rigorous combination to ensure ITRF and EOP consistency, Proc. Journées Systèmes de Référence 2007, N. Capitaine (ed.), 2007.

Amalvict M., Willis P., Shibuya K. (2007), Status of DORIS stations in Antarctica from precise geodesy, in Dynamic Planet - Monitoring and Understanding a Dynamic Planet with Geodetic and Oceanographic Tools, P. Tregoning, C. Rizos, (Eds.), IAG Symposium, 130:94-102. DOI: 10.1007/978-3-540-49350-1_17

Amalvict, M., R. Bayer, S. Bonvalot, N. Debeglia, M. Diament, F. Duquenne, H. Duquenne, G. Gabalda, J. Hinderer, M.F. Lalancette, N. Lemoigne, B. Luck, G. Martelet, D. Rémy, M. Sarrailh and G. Wöppelmann (2007) *French Activities in Ground Gravimetry During the Period 2003-2006*

Arioli M., Duff I., Gratton S., Pralet. S., Note on GMRES Preconditionned by a Perturbed LDLt Decomposition with Static Pivoting, SIAM Journal on Scientific Computing., 25 5:2024-2044, 2007.

Arioli M., Baboulin M., Gratton S., A partial condition number for linear least-squares problems, SIAM J. Matrix Analysis and Applications. 29(2):413-433, 2007.

Baboulin M., Giraud L., Gratton S., Langou J., A distributed packed storage for large dense incore parallel calculations, Concurrency and Computation: Practice and Experience. 19(04), 483-502, 2007.

Bastin, S., C. Champollion, O. Bock, P. Drobinski and F. Masson (2007) Diurnal cycle of water vapor as documented by a dense GPS network in a coastal area during ESCOMPTE-IOP2, *Journal of Applied Meteorology and Climatology*, **46**, p. 167-182, DOI:10.1175/JAM2450.1

Barache, C., Ph. Bério, C. Bizouard, S. Bouquillon, X. Collilieux, D. Coulot, F. Deleflie, P. Exertier, D. Féraudy, A.-M. Gontier, S. Lambert and Y. Vanderschueren (2007) A first step for the French geodetic VO, *Actes des Journées de la Société Française d'Astronomie et d'Astrophysique (SF2A'06), Paris, France, 26-30 juin 2006*

Biancale R., Gambis D., and A. Pollet, Toward a new strategy for multi-technique combined series of EOP and TRF, Eos Trans. AGU, 88(23), Jt. Assem. Suppl., Abs. G42A-08, 2007.

Bindoff N., Willebrand J., Artale V. , Cazenave A., Gregory J., Gulev S., Hanawa K., Le Quéré C., Levitus S., Nojiri Y., Shum C.K., Talley L., Unnikrishnan A., Observations: oceanic climate and sea level. In: Climate change 2007: The physical Science Basis. Contribution of Working Group I to the Fourth Assessment report of the Intergouvernmental Panel on Climate Change [Solomon S., D. Qin, M. Manning, Z. Chen, M. Marquis, K.B. Averyt, M. Tignor and H.L. Miller (eds.)]. Cambridge University Press, Cambridge, UK, and New York, USA., 2007.

Bonnefond P., P. Exertier, O. Laurain, Y. Menard, A. Orsoni, G. Jan, and E. Jeansou, Absolute Calibration of Jason-1 and TOPEX/Poseidon Altimeters in Corsica, Special Issue on Jason-1 Calibration/Validation, Part 1, Marine Geodesy, Vol. 26, No. 3-4, 261-284, 2007.

Bonnefond P., P. Exertier, O. Laurain, Y. Menard, A. Orsoni, E. Jeansou, B. Haines, D. Kubitschek, and G. Born, Leveling Sea Surface using a GPS catamaran, Special Issue on Jason-1 Calibration/Validation, Part 1, Marine Geodesy, Vol. 26, No. 3-4, pages 319-334, 2007.

Bock, O., M.-N. Bouin, A. Walpersdorf, J.-P. Lafore, S. Janicot, F. Guichard and A. Agusti-Panareda (2007) Comparison of ground-based GPS precipitable water vapor to independent observations and Numerical Weather Prediction model reanalyses over Africa, *Quarterly Journal of the Royal Meteorological Society*, **133**, p. 2011-2027, DOI:10.1002/qj.185

Bock, O., F. Guichard, S. Janicot, J.-P. Lafore, M.-N. Bouin and B. Sultan (2007a) Multiscale analysis of precipitable water vapor over Africa from GPS data and ECMWF analyses, *Geophysical Research Letters*, **34**(L09705), DOI:10.1029/2006GL028039

Bosser, P., O. Bock, C. Thom and J. Pelon (2007) Study of the statistics of water vapor mixing ratio determined from Raman lidar measurements, *Applied Optics*, **46**(33), p. 8170-8180, DOI:10.1364/AO.46.008170

Bosser, P., O. Bock, C. Thom and J. Pelon (2007a) An improved mean-gravity model for GPS hydrostatic delay calibration, *IEEE Geoscience and Remote Sensing Letters*, **4**, p. 3-7, DOI:10.1109/LGRS.2006.881725

Boucher, C., Z. Altamimi, X. Collilieux, F. Duquenne, B. Garayt and J. Legrand (2007) *Geodetic Reference Frames in France : Highlights 2004-2007*

Briole P., P. Willis, J. Dubois, Volcanic activity at Socorro Island (Mexico) derived from DORIS absolute positioning, Geophysical Journal International, in press.

Bruinsma S., Forbes J.M., Global Observation of Traveling Atmospheric Disturbances (TADs) in the Thermosphere, Geophysical Research Letters, 34, L14103, doi :10.1029/2007GL030243, 2007.

Bruinsma S., Forbes J.M., Storm-time Equatorial Density Enhancements Observed by CHAMP and GRACE, Journal of Spacecraft and Rockets, vol 44, 6, p.1154-1159, 2007.

Bruinsma S., Forbes J.M., Observations of Traveling Atmospheric Disturbances (TADs) in thermosphere density using the CHAMP and GRACE accelerometers, International CAWSES Symposium, Kyoto (Japon), 23-27 Octobre 2007.

Cali, J., B. de Saint-Jean, J. Verdun and H. Duquenne (2007) Kalman smoothing filter algorithm design for moving vector gravimetry using a low-cost integrated GPS/Inertial system LIMOG, *Proceedings of International Symposium 'Terrestrial Gravimetry : Static and Mobile Measurements', Elektropribor TG-SMM 2007*, p. 54-59

Capitaine N., Andrei A.H., Calabretta M. et al., "Proposed terminology in fundamental astronomy based on IAU 2000 Resolutions", Highlights of Astronomy, 14:474-475, 2007.

Capitaine N., "Definition and realization of the celestial intermediate reference system", Proc. IAU Symp. 248, Shanghai, Octobre 2007, Cambridge University Press, in press.

Carpentieri B., Giraud L., Gratton S., Additive and multiplicative two-level spectral preconditioning for general linear systems, SIAM J. Scientific Computing., 29(4):1593-1612, 2007.

Cazenave A., Lombard A., Dominh K., Llovel W., Bouhours S., Ramillien G. and Nerem R.S., Recent advances in measuring and understanding sea level change during the satellite altimetry era, OST publication, in press, 2007.

Collilieux, X., Z. Altamimi, D. Coulot and J. Legrand (2007) *Institut Géographique National (IGN) Combination Research Centre*, chapter 3.6.2.8, IERS annual report 2006

Collilieux, X., Z. Altamimi, D. Coulot, J. Ray and P. Sillard (2007a) Comparison of very long baseline interferometry, GPS, and satellite laser ranging height residuals from ITRF2005 using spectral and correlation methods, *Journal of Geophysical Research*, **112**(B12403), DOI:10.1029/2007JB004933

Coulot, D., Ph. Bério, R. Biancale, S. Loyer, L. Soudarin and A.-M. Gontier (2007) Towards a direct combination of space-geodetic techniques at the measurement level : methodology and main issues, *Journal of Geophysical Research*, **112**(B05410), DOI:DOI:10.1029/2006JB004336

Coulot, D., Ph. Bério and A. Pollet (2007a) Least-square mean effect : Application to the analysis of SLR time series, *Proceedings of the 15th International Laser Ranging Workshop, Canberra, Australia, 2006*

Coulot D., P. Berio, P. Bonnefond, P. Exertier, D. Féraudy, O. Laurain & F. Deleflie, Satellite Laser Ranging biases and Terrestrial Reference Frame scale factor, Proceedings IAG IUGG XXIV General Assembly, Perugia, Italy, 2-13 July 2007, submitted.

Coulot, D., Ph. Bério, O. Laurain, D. Féraudy and P. Exertier (2007b) An original approach to compute SLR ranging biases, *Proceedings of the 15th International Laser Ranging Workshop, Canberra, Australia, 2006*

Coulot, D., Ph. Bério, O. Laurain, D. Féraudy, P. Exertier and F. Deleflie (2007c) Analysis of 13 years of SLR data on the two LAGEOS satellites for Terrestrial Reference Frames and Earth Orientation Parameters, *Proceedings of the 15th International Laser Ranging Workshop, Canberra, Australia, 2006*

Dehant V. et al., Recent advances in modeling precession-nutation, In: N. Capitaine (Ed.), Proc. Journées 2007 systèmes de référence spatio-temporels, Observatoire de Paris, sous presse, 2007.

Deleflie F., Valk S., Guzzo M., Exertier P., Portmann C., Investigating the stability of the Galileo constellation in the framework of celestial mechanics, submitted to Celestial Mechanics, special issue in the honour of Claude Froeschlé, 2007.

Deleflie F., Exertier P., Valk S., Guzzo M., Portmann C., Stability of the Galileo Constellation, and Long Term Evolution of Disposal Orbit,Proceedings of the 1st workshop on Scientific and Fundamental Aspects of the Galileo Programme, 2007.

de Saint-Jean, B., J. Verdun, H. Duquenne, J.-P. Barriot, S.A. Melachroïnos and J. Cali (2007) Fine analysis of lever arm effects in moving gravimetry, *Dynamic Planet: Monitoring and Understanding a Dynamic Planet with Geodetic and Oceanographic Tools*, Tregoning, Paul and Rizos, Chris Ed., International Association of Geodesy Symposia, Vol.130, p. 809-816, Springer

Doornbos E., Willis P. (2007), Analysis of DORIS range-rate residuals for TOPEX/Poseidon, Jason, ENVISAT and SPOT, Acta Astronautica, 60(8-9):611-621. DOI : 10.1016/j.actaastro.2006.07.012

Duff I., Gratton S., Pinel X., Vasseur X., Multigrid based preconditioners for the numerical solution of two-dimensional heterogeneous problems in geophysics, International Journal of Computer Mathematics . 84 (8):1167-1181, 2007.

Duquenne, H. (2007) Modelling the vertical gravity gradient for gravity measurements reduction, *Harita Dergisi (Turkish Journal of Mapping)*(18), p. 377-381

Duquenne, H. (2007a) A data set to test geoid computation methods, *Harita Dergisi (Turkish Journal of Mapping)*(18), p. 61-65

Exertier P., J. Nicolas, P. Berio, D. Coulot, P. Bonnefond, and O. Laurain, The Role of Laser Ranging for Calibrating Jason-1: The Corsica Tracking Campaign, Mar. Geod., Special Issue on Jason-1 Calibration/Validation, Part 2, Vol. 27, No. 1-2, 2007.

Feissel-Vernier, M., O. de Viron and K. Le Bail (2007) Stability of VLBI, SLR, DORIS and GPS positioning, *Earth, Planets and Space*, **59**, p. 475-497

Flamant, C., J.-P. Chaboureau, D.J. Parker, C.M. Taylor, J.-P. Cammas, O. Bock, F. Timouk and J. Pelon (2007) Airborne observations of the impact of a convective system on the planetary boundary layer thermodynamics and aerosol distribution in the inter-tropical discontinuity region of the West African Monsoon, *Quarterly Journal of the Royal Meteorological Society*, **133**(626), p. 1175-1189, DOI:10.1002/qj.97

Folgueira M., Dehant V., Lambert S. B., Rambaux N., Impact of tidal Poisson terms on nonrigid Earth rotation, Astronomy and Astrophysics 469, 1197, 2007.

Follin, J.-M. et A. Bouju, 2007. Cartographie multi-résolution dans un contexte mobile. *Revue Internationale de Géomatique*, numéro special "Dynamiques urbaines et mobilités". 17 (2), pp. 227-245.

Fontdecaba J., G. Métris, P. Exertier , Topology of the relative motion : circular and eccentric reference orbit cases, Proceedings of the 20th ISSFD, Annapolis, Septembre 2007.

Fontdecaba J., G. Métris, P. Exertier, F. Deleflie, Perturbations of the gravity field on a flight formation for an eccentric reference frame. Proceedings of the AAS/AIAA 2007 summer meeting, Mackinack Island, August 2007.

Fontdecaba J., G. Métris, P. Exertier, The local orbital elements ; an alternative representation of relative motion. Proceedings of SF2A 2007, Grenoble, Juillet 2007.

Forbes J.M., Bruinsma S., Lemoine F.G., Bowman B.R., Konopliv A., Variability of the Satellite Drag Environments of Earth, Mars and Venus due to Rotation of the Sun, Journal of Spacecraft and Rockets, vol 44, 6, p.1160-1164, 2007.

Forste Ch., Schmidt R., Stubenvoll, Flechtner F., Meyer Ul., Konig R., H. Neumayer, Biancale R., Lemoine J.M., Bruinsma S., Loyer S., **Barthelmes F. and Esselborn S.**, The GeoForschungsZentrum Potsdam/Groupe de Recherches de Géodésie Spatiale Satellite-Only and Combined Gravity Field Models : EIGEN-GL04S1 and EIGEN-GL04C, Journal of Geodesy, Springer Berlin/Heidelberg, ISSN 0949-7714, doi: 10.1007/s00190-007-0183-S, 2007.

Gambis D. , **Altamimi Z. and J. Ray**, Maintenance of the IERS EOP and ITRF2005 Consistency, Geophysical Research Abstracts, Vol. 9, 08366, 2007, SRef-ID: 1607-7962/gra/EGU2007-A-08366, 2007.

Gambis D., Biancale R., Bourda G., Loyer S., Soudarin L., Deleflie F., Comparison of GRGS EOP+TRF combined solution to intra-technique combinations, Geophysical Research Abstracts, Vol. 9, 08658, 2007, SRef-ID: 1607-7962/gra/EGU2007-A-08658, 2007.

Gambis D., Biancale R. and A. Pollet, Toward consistent weekly determinations of Earth Orientation Parameters and station coordinates, IUGG XXIV General Assembly, Perugia, Italy, 2-13 September 2007.

Garcia D., A. Lombard, G. Ramillien and A. Cazenave , Steric sea level variations inferred from combined Topex/Poseidon altimetry and GRACE gravimetry, PAGEOPH, 164, 721-731, doi:10.1007/s00024-007-0182y., 2007.

Giraud L., Gratton S., Martin E., Incremental spectral preconditioners for sequences of linear systems, Applied Numerical Mathematics., 57 11-12:1164-1180, 2007.

Giraud L., Gratton S., Langou J., Convergence in backward error of relaxed GMRES, SIAM J. Scientific Computing, 29 (2):710-728, 2007.

Gontier A.-M., et al., Paris Observatory Analysis Center OPAR: Report on Activities, January - December 2007, in: International VLBI Service for Geodesy and Astrometry 2007 Annual Report, edited by D. Behrend and K. D. Baver, NASA/TP-2008-, sous presse, 2007.

Gratton S., Lawless A., Nichols N., Approximate Gauss-Newton methods for nonlinear least squares problems, SIAM J. on Optimization ., 18 :106-132, 2007.

Grippa, M., N. M. Mognard, T. Le Toan and S. Biancamaria, Observations of changes in surface water over the western Siberia lowland. Geophys. Res. Lett. 34, L15403 10.1029/2007GL030165, 2007.

Guo J., Wan W., Forbes J.M., Sutton E., Nerem R.S., Woods T.N., Bruinsma S., Liu L., Effects of solar variability on thermosphere density from CHAMP accelerometer data, Journal of Geophysical Research, 112, A10308, doi:10.1029/2007JA012409, 2007.

Jan G., Y. Menard, M. Faillot, F. Lyard, E. Jeansou, and P. Bonnefond, Offshore Absolute Calibration of Space Borne Radar Altimeters, Marine Geodesy, Special Issue on Jason-1 Calibration/Validation, Part 3, Vol. 27, No. 3-4, 615-629, 2007.

Kouraev A. V. , Semovski S. V., Shimaraev M. N., Mognard N. M., Legrésy B., Rémy F., « The ice regime of Lake Baikal from historical and satellite data: Relationship to air temperature, dynamical, and other factors", Limnol. Oceanogr., 52, 1268-1286, 2007.

Kouraev A. V., Semovski S. V., Shimaraev M. N., Mognard N. M., Legresy B., Remy F., «Observations of lake Baikal ice from satellite altimetry and radiometry» Remote Sensing of Environment, 108, 240-253, 2007.

Lambert S.B., et al., Some issues about the Earth's core and inner core through VLBI, In: J. Boehm et al. (Eds.), Proc. 18th European VLBI for Geodesy and Astrometry (EVGA) Working Meeting, Geowissenschaftliche Mitteilungen, Heft Nr. 79, Schriftenreihe der Studienrichtung Vermessung und Geoinformation, Technische Universitaet Wien, 206, 2007.

Lambert S. B., Dehant V., The Earth's core parameters as seen by the VLBI, Astronomy and Astrophysics, 469, p. 777, 2007.

Lemoine J.M., Bruinsma S., Loyer S., Biancale R., Marty J.C., Perosanz F., Balmino G., Temporal Gravity Field Models Inferred from GRACE Data, Advances in Space Research 39 p. 1620–1629,doi:10.1016/j.asr.2007.03.062, 2007.

Lemoine J.M., Bruinsma S., Loyer S., Biancale R., Marty J.C., Perosanz F., Balmino G., Temporal gravity field models inferred from GRACE data, Advances in Space Research, 39, p.1620-1629, 2007.

Levy A., Christophe B., Reynaud S., Courty J.M., Bério P. and Métris G., The Pioneer Anomaly : Data Analysis and Mission Proposal. Comptes rendus des journées scientifiques de la SF2A 2007, J. Bouvier, A. Chalabaev, éditeurs, 2007.

Llubes M., Lemoine J.M., Remy F., Antarctica seasonal mass variations detected by GRACE, Earth and Planetary Science Letters 260, p. 127–136 doi:10.1016 /j.epsl.2007.05.022, 2007.

Lombard A., Garcia D., Ramillien G., Cazenave A., Biancale R., Lemoine J.M., Flechtner F., Schmidt R., Ishii M., Estimation of Steric Sea Level Variations from Combined GRACE and Jason-1 Data, Earth and Planetary Science Letters 254 194–202 doi:10.1016/j.epsl.2006.11.035, 2007.

Lombard A., Garric G., Penduff T. and Molines J.M., Regional variability of sea level change using a global ocean at model1/4° resolution, Submitted to Ocean Dyn. 2007.

Manche H., S. Bouquillon, A. Fienga, J. Laskar, G. Francou, M. Gastineau, Towards INPOP07, adjustments to LLR data, Journées 2007 - Systèmes de références spatio-temporels, Eds. N. Capitaine et al., Paris, (Septembre 2007).

Maraldi C., B. Galton-Fenzi, F. Lyard, L. Testut, R. Coleman, Barotropic tides of the Southern Indian Ocean and the Amery Ice Shelf cavity. Geophys. Res. Lett., 34, L18602, doi:10.1029/2007GL030900, 2007.

Marcos M., G. Wöppelmann, W. Bosch, R. Savcenko, Decadal sea level trends in the Bay of Biscay from tide gauges, GPS and TOPEX, Journal of Marine Systems, 68, 529-536, doi:10.1016/j.jmarsys.2007.02.006, 2007.

Martin Miguez B., R. Le Roy, G. Wöppelmann, The use of radar gauges to measure variations in sea level along the French coast, Journal of Coastal Research, on-line June 2007, doi:10.2112/06-0787, 2007.

Martin Miguez B., L. Testut, G. Wöppelmann, The van de Casteele test revisited: an efficient approach to tide gauge error characterization, Journal of Atmospheric and Oceanic Technologies, accepted December 2007.

Mariano-Goulart D., Maréchal P., Gratton S., Giraud L., A priori selection of the regularization parameters in emission tomography by Fourier synthesis, Computerized Medical Imaging and Graphics,. 31 7:502-509, 2007.

Mathews P. M., Capitaine N., Dehant V., "Comments on the ERA-2005 numerical theory of Earth rotation", 2007arXiv0710.0166M, 2007.

Menvielle, M., Lathuillère C., Bruinsma S., Viereck R., A new method for studying the thermospheric density variability derived from CHAMP/STAR accelerometer data for magnetically active conditions, Annales Geophysicae, 25, p.1-10, 2007.

Le Bail, K., J.J. Valette, W. Zerhouni and M. Feissel-Vernier (2007) Long-term consistency of multitechnique terrestrial reference frames, a spectral approach, *Dynamic Planet: Monitoring and Understanding a Dynamic Planet with Geodetic and Oceanographic Tools*, P. Tregoning and C. Rizos Ed., International Association of Geodesy Symposia, Vol.130, Springer

Melachroinos S. A., Deleflie F., Perosanz F., Biancale R., Laurain O., Exertier P., Galileo In Orbit Validation Element-A and GPS-35/36 satellite orbits: analysis of dynamical properties based on SLR-only tracking data, 15th International Laser Ranging Workshop proceedings, Canberra, Australia, 2007.

Métivier, L., M. Greff-Lefftz and M. Diament (2007) Mantle lateral variations and elasto-gravitational deformations - II. Possible effects of a superplume on body tides, *Geophysical Journal International*, **168**, p. 897-903, DOI:10.1111/j.1365-246X.2006.03309.x

Minghelli-Roman A., Laurent Polidori, Sandrine Mathieu, Lionel Loubersac, and François Cauneau (2007) Bathymetric Estimation Using MERIS Images in Coastal Sea Waters. *IEEE Geoscience and Remote Sensing Letters*, vol. 4, N°2, pp. 274-277.

Milly P.C.D., Cazenave A., Famiglietti J., Gornitz V., Laval K., Lettenmaier D., Sahagian D., Wahr J. and Wilson C., Terrestrial water storage contributions to sea level rise and variability, Proceedings of the WCRP workshop 'Understanding sea level rise and variability', eds. J., 2007.

Nerem R.S., A. Cazenave, D.P. Chambers, L.L. Fu, E.W. Leuliette and G.T. Mitchum, Comment on 'Estimating future sea level change from past records' by Nils-Axel Morner, Global and Planetary Change, 55, 358-360, 2007.

Ngo-Duc T., Laval. K., Polcher J., Ramillien G. and A. Cazenave, Validation of the land water storage simulated by Organising Carbon and Hydrology in Dynamic Ecosystems (ORCHIDEE) with Gravity Recovery and Climate Experiment (GRACE) data, Water Res. Res, 43, W04427, doi:10.1029/2006WR004941, 2007.

Nuret, M., J.-P. Lafore, N. Asencio, H. Bénichou, O. Bock, F. Favot, T. Montmerle and Y. Seity (2007) Evaluation of METEO-FRANCE Numerical Weather Prediction models during AMMA 2006-SOP, *ALADIN Newsletter*, **32**

Panet, I., V. Mikhailov, M. Diament, F. Pollitz, G. King, O. de Viron, M. Holschneider, R.Biancale and J.M. Lemoine (2007) Co-seismic and post-seismic signatures of the Sumatra December 2004 and March 2005 earthquakes in GRACE satellite gravity, *Geophysical Journal International*, **171**(1), p. 177-190, DOI:10.1111/j.1365-246X.2007.03525.x

Pearlman M., Altamimi Z., Beck N., Forsberg R., Gurtner W., Kenyon S., Behrend D., Lemoine F.G., Ma C., Noll C.E., Pavlis E.C., Malkin Z., Moore A., Webb F.H., Neilan R.E., Ries J.C., Rothacher M., Willis P. (2007), GGOS Working Group on Ground Networks Communications, in Dynamic Planet - Monitoring and Understanding a Dynamic Planet with Geodetic and Oceanographic Tools, P. Tregoning, C. Rizos, (Eds.), IAG Symposium, 130:719-726. DOI: 10.1007/978-3-540-49350-1_103

Pearlman, M., Z. Altamimi, N. Beck, F.G. Lemoine, A. Moore and J.C. Ries (2007a) GGOS and its users requirements, linkage and outreach, *Dynamic Planet: Monitoring and Understanding a Dynamic Planet with Geodetic and Oceanographic Tools*, P. Tregoning and C. Rizos Ed., International Association of Geodesy Symposia, Vol.130, Springer

Pierron, F., B. Gourine, P. Exertier, Ph. Bério, P. Bonnefond and D. Coulot (2007) FTLRS Ajaccio campaigns: operations and positionning analysis over 2002/2005, *Proceedings of the 15th International Laser Ranging Workshop, Canberra, Australia, 2006*

Polidori L. (2007) Les origines et les principes de la géomatique. Texte de la leçon inaugurale de la Chaire de Géomatique du CNAM, *Revue XYZ*, N°114, pp. 12-19.

Pollet A., Cumul de mesures de télémétrie laser sur satellites. Contributions aux systèmes de référence terrestres et aux paramètres d'orientation de la Terre, publication LAREG n° MS20, 2007.

Pollet, A., Coulot D., Capitaine N., Nahmani S., Altamimi Z., « Combination of Space Geodetic Techniques at the Measurement Level: Methodological Issues", 2007 AGU FM. G41A.01P, 2007.

Rahmstorf S., Cazenave A., Church J.A., Hansen J., Keeling R., Parker D. and Somerville R. , Recent climate observations compared to projections, Science, vol 316, 709, 10.1126/science.1136843, 2007.

Roemmich D. , J. Willis, J. Gilson, D. Stammer, A. Koehl, T. Yemenis, D. P. Chambers, F. Landerer, J. Marotzke, T. Suzuki, J. Church, A. Cazenave and P. Y Letraon, Global Ocean Warming and Sea Level Rise Proceedings of the WCRP workshop 'Understanding sea level rise and variability', eds. J. Church, P. Woodworth, T. Aarup and S. Wilson et al., Blackwell Publishing, Inc., 2007.

Souchay J., Lambert S. B., Le Poncin-Lafitte C., A comparative study of rigid Earth, non-rigid Earth nutation theories, and observational data, Astronomy and Astrophysics, 472, p.681, 2007.

Souchay J., A. Andrei, C. Leponcin-Lafitte, Close-approaches between Jupiter and quasars during GAIA scheduled mission, Astronomy and Astrophysics, 471, p.335 S, 2007.

Vergnolle M., Bouin M-N., Morel L., Masson F., Durand S., Nicolas J., Melachroinos S., GPS estimates of ocean tide loading constituents and comparison with a recent ocean tide model, in Geophys J Int, doi: 10.1111/j.1365-246X.2008.03734.x, 2007.

Wallace P. T., Capitaine N., « Precession-nutation procedures consistent with IAU 2006 resolutions», Astronomy and Astrophysics, 464, p 793, 2007.

Wallace P. T., Capitaine N., « Using the P03 precession model", in Highlights of Astronomy, Volume 14, Issue 14, p. 466-466, 2007.

Walpersdorf, A., M.-N. Bouin, O. Bock and E. Doerflinger (2007) Assessment of GPS data for meteorological applications over Africa : study of error sources and analysis of positionning accuracy, *Journal of Atmospheric and Solar-Terrestrial Physics*, **69**, p. 1312-1330, DOI:10.1016/j.jastp.2007.04.008

Wöppelmann, G., B. Martín Míguez, M.-N. Bouin and Z. Altamimi (2007) Geocentric sea-level trend estimates from GPS analyses at relevant tide gauges world-wide, *Global and Planetary Change*, **57**(3-4), p. 396-406, DOI:10.1016/j.gloplacha.2007.02.002

Willis P. (2007), Analysis of a possible future degradation in the DORIS geodetic results related to changes in the satellite constellation, Advances in Space Research, 39(10):1582-1588. DOI: 10.1016/j.asr.2006.11.018

Willis P., Haines B.J., Kuang D. (2007), DORIS satellite phase center determination and consequences on the derived scale of the Terrestrial Reference Frame, Advances in Space Research, 39(10):1589-1596. DOI: 10.1016/j.asr.2007.01.007.

Willis P., Lemoine F., Soudarin L. (2007), Looking for systematic errors in scale from terrestrial reference frames derived from DORIS data, in Dynamic Planet - Monitoring and Understanding a Dynamic Planet with Geodetic and Oceanographic Tools, P. Tregoning, C. Rizos, (Eds.), IAG Symposium, 130:143-151. DOI: 10.1007/978-3-540-49350-1_23

Willis P., Soudarin L., Jayles C., Rolland L. (2007), DORIS applications for Solid Earth and Atmospheric Sciences, Applications du système DORIS aux sciences de la Terre solide et aux sciences de l'atmosphère, Comptes Rendus Geoscience, 339(16):949-959. DOI : 10.1016/j.crte.2007.09.015

Wöppelmann G., Martin Miguez B., Bouin M-N. and Altamimi Z. (2007). Geocentric sea-level trend estimates from GPS analyses at relevant tide gauges world-wide. *Global & Planet. Change, 57*, 396-406.

Zerhouni W., N. Capitaine, G. Francou, The use of LLR observations (1969-2006) for the determination of the celestial coordinates of the pole, Journées 2007 - Systèmes de références spatio-temporels, Eds. N. Capitaine et al., Paris, (Septembre 2007).

Comité National Français de Géodésie et Géophysique

French National Committee of Geodesy and Geophysics

RAPPORT QUADRIENNAL DU CNFGG A l'UGGI

QUADRENNIAL REPORT OF CNFGG TO IUGG

SECTION 2 – SISMOLOGIE ET PHYSIQUE DE L'INTÉRIEUR DE LA TERRE

SECTION 2 - SEISMOLOGY AND PHYSICS OF THE EARTH'S INTERIOR

Le bureau de la Section 2, en place depuis 2005 est en cours de renouvellement. La recherche des candidats n'est pas aisée et le bureau continue d'assurer le fonctionnement, mais dans une version très réduite, son Vice-président étant démissionnaire depuis 2 ans, et son Président appelé vers de nouvelles responsabilités scientifiques et administratives prenantes.

Lors du précédant rapport, nous avions réussi à trouver le temps pour organiser et gérer la rédaction de récentes découvertes sous forme de 3 articles, par des collègues de différents laboratoires. Cette fois-ci, nous avons choisi une démarche alternative, à savoir compiler de façon aussi exhaustive que possible toutes les contributions françaises aux publications scientifiques avec comité de lecture des 4 dernières années relevant des disciplines de la section 2. Cela peut paraître fastidieux à première vue, mais nous disposons aujourd'hui de base de données très complètes et d'outils de recherche performants, rendant réalisable une telle compilation, et ce en peu de temps. Nous avons utilisé le moteur de recherche Web of Science disponible sur le Portail d'information scientifique des unités CNRS en Sciences de la Terre et de l'Univers "BiblioPlanets" donnant accès au texte intégral des articles de plus de 4000 publications mises à disposition de ses unités par le CNRS et l'INSU.

Cette liste présentée et qui contient 344 références résulte d'une recherche sur les quatre dernières années (2007-2010) incluant les domaines de Sismologie et de Physique de l'Intérieur de la terre, et où au moins l'un des auteurs a une adresse d'affiliation en France.

Mireille Laigle et Tony Monfret
(Secrétaire et Président de la Section 2)

Abbassi, A., A. Nasrabadi, M. Tatar, F. Yaminifard, M. R. Abbassi, D. Hatzfeld and K. Priestley (2010). "Crustal velocity structure in the southern edge of the Central Alborz (Iran)." Journal of Geodynamics **49**(2): 68-78.

Adda-Bedia, M. and R. Madariaga (2008). "Seismic radiation from a kink on an antiplane fault." Bulletin of the Seismological Society of America **98**(5): 2291-2302.

Afilhado, A., L. Matias, H. Shiobara, A. Hirn, L. Mendes-Victor and H. Shimamura (2008). "From unthinned continent to ocean: The deep structure of the West Iberia passive continental margin at 38 degrees N." Tectonophysics **458**(1-4): 9-50.

Ageron, M., J. A. Aguilar, A. Albert, F. Ameli, M. Anghinolfi, G. Anton, S. Anvar, F. Ardellier-Desages, E. Aslanides, J. J. Aubert, R. Auer, E. Barbarito, S. Basa, M. Battaglieri, M. Bazzotti, Y. Becherini, N. Bethoux, J. Beltramelli, V. Bertin, A. Bigi, M. Billault, R. Blaes, N. de Botton, M. C. Bouwhuis, R. Bruijn, J. Brunner, G. F. Burgio, J. Busto, F. Cafagna, L. Caillat, A. Calzas, A. Capone, L. Caponetto, E. Carmona, J. Carr, D. Castel, E. Castorina, V. Cavasinni, S. Ceechini, A. Ceres, P. Charvis, P. Chauchot, T. Chiarusi, M. Circella, J. Y. Coail, C. Colnard, C. Compere, R. Coniglione, N. Cottini, P. Coyle, S. Cuneo, A. S. Cussatlegras, G. Damy, R. van Dantzig, G. DeBonis, C. De Marzo, R. De Vita, I. Dekeyser, E. Delagnes, D. Denans, A. Deschamps, J. X. Dessa, J. J. Destelle, B. Dinkespieler, C. Distefano, C. Donzaud, J. F. Drogou, F. Druillole, D. Durand, J. P. Ernenwein, S. Escoffier, E. Falchini, S. Favard, F. Fehr, F. Feinstein, C. Florello, V. Flaminio, K. Fratini, J. L. Fuda, S. Galeotti, J. M. Gallone, G. Giacomelli, N. Girard, C. Gojak, P. Goret, K. Graf, F. Guilloux, G. Hallewell, M. N. Harakeh, B. Hartmann, A. Heijboer, E. Heine, Y. Hello, J. J. Hernandez-Rey, J. Hossl, C. Hoffman, J. Hogenbirk, J. R. Hubbard, M. Jaquet, M. Jaspers, M. de Jong, F. Jouvenot, N. Kalantar-Nayestanaki, A. Kappes, T. Karg, U. Katz, P. Keller, J. P. Kneib, E. Kok, H. Kok, P. Kooijman, C. Kopper, A. Kouchner, W. Kretschmer, A. Kruijer, S. Kuch, P. Lagier, R. Lahmann, G. Lamanna, P. Lamare, G. Lambard, J. C. Languillat, H. Laschinsky, J. Lavalle, Y. Le Guen, H. Le Provost, A. L. Van Suu, D. Lefevre, T. Legou, G. Lelaizant, G. Lim, D. Lo Presti, G. Loaec, H. Loehner, S. Loucatos, F. Louis, F. Lucarelli, V. Lyashuk, S. Mangano, M. Marcelin, A. Margiotta, R. Masullo, F. Mazeas, A. Mazure, R. Megna, M. Melissas, E. Migneco, M. Mongelli, T. Montaruli, M. Morganti, L. Moscoso, H. Motz, M. Musumeci, C. Naumann, M. Naumann-Godo, V. Niess, A. Noble, C. Olivetto, R. Ostasch, N. Palanque-Delabrouille, P. Payre, H. Z. Peek, A. Perez, C. Petta, P. Piattelli, R. Pillet, J. P. Pineau, J. Poinsignon, V. Popa, T. Pradier, C. Racca, N. Randazzo, J. van Randwijk, D. Real, M. Regnier, B. van Rens, F. Rethore, P. Rewiersma, G. Riccobene, V. Rigaud, M. Ripani, V. Roca, C. Roda, J. F. Rolin, A. Rostovtsev, J. Roux, M. Ruppi, G. V. Russo, G. Rusydi, F. Salesa, K. Salomon, P. Sapienza, F. Schmitt, J. P. Schuller, R. Shanidze, I. Sokalski, T. Spona, M. Spurio, G. van der Steenhoven, T. Stolarczyk, K. Streeb, L. Sulak, M. Taiuti, C. Tamburini, C. Tao, L. Tasca, G. Terreni, F. Urbano, P. Valdy, V. Valente, B. Vallage, G. Vaudaine, G. Venekamp, B. Verlaat, P. Vernin, R. van Wijk, G. Wijnker, G. Wobbe, E. de Wolf, A. F. Yao, D. Zaborov, H. Zaccone, J. D. Zornoza and J. Zuniga (2007). "Studies of a full-scale mechanical prototype line for the ANTARES neutrino telescope and tests of a prototype instrument for deep-sea acoustic measurements." Nuclear Instruments & Methods in Physics Research Section a-Accelerators Spectrometers Detectors and Associated Equipment **581**: 695-708.

Agudelo, W., A. Ribodetti, J. Y. Collot and S. Operto (2009). "Joint inversion of multichannel seismic reflection and wide-angle seismic data: Improved imaging and refined velocity model of the crustal structure of the north Ecuador-south Colombia convergent margin." Journal of Geophysical Research-Solid Earth **114**.

Aksoy, M. E., M. Meghraoui, M. Vallee and Z. Cakir (2010). "Rupture characteristics of the AD 1912 Murefte (Ganos) earthquake segment of the North Anatolian fault (western Turkey)." Geology **38**(11): 991-994.

Al Atik, L., N. Abrahamson, J. J. Bommer, F. Scherbaum, F. Cotton and N. Kuehn (2010). "The Variability of Ground-Motion Prediction Models and Its Components." Seismological Research Letters **81**(5): 794-801.

Albaric, J., J. Deverchere, C. Petit, J. Perrot and B. Le Gall (2009). "Crustal rheology and depth distribution of earthquakes: Insights from the central and southern East African Rift System." Tectonophysics **468**(1-4): 28-41.

Albaric, J., J. Perrot, J. Deverchere, A. Deschamps, B. Le Gall, R. W. Ferdinand, C. Petit, C. Tiberi, C. Sue and M. Songo (2010). "Contrasted seismogenic and rheological behaviours from shallow and deep earthquake sequences in the North Tanzanian Divergence, East Africa." Journal of African Earth Sciences **58**(5): 799-811.

Amitrano, D., S. Gaffet, J. P. Malet and O. Maquaire (2007). "Understanding mudslides through micro-seismic monitoring: the Super-Sauze (South-East French Alps) case study." Bulletin De La Societe Geologique De France **178**(2): 149-157.

Asada, M., A. Deschamps, T. Fujiwara and Y. Nakamura (2007). "Submarine lava flow emplacement and faulting in the axial valley of two morphologically distinct spreading segments of the Mariana back-arc basin from Wadatsumi side-scan sonar images." Geochemistry Geophysics Geosystems **8**.

Autin, J., S. Leroy, M. O. Beslier, E. d'Acremont, P. Razin, A. Ribodetti, N. Bellahsen, C. Robin and K. Al Toubi (2010). "Continental break-up history of a deep magma-poor margin based on seismic reflection data (northeastern Gulf of Aden margin, offshore Oman)." Geophysical Journal International **180**(2): 501-519.

Baig, A. M., M. Campillo and F. Brenguier (2009). "Denoising seismic noise cross correlations." Journal of Geophysical Research-Solid Earth **114**.

Barruol, G., A. Deschamps, J. Deverchere, V. V. Mordvinova, M. Ulziibat, J. Perrot, A. A. Artemiev, T. Dugarmaa and G. H. R. Bokelmann (2008). "Upper mantle flow beneath and around the Hangay dome, Central Mongolia." Earth and Planetary Science Letters **274**(1-2): 221-233.

Battaglia, J., A. Zollo, J. Virieux and D. Dello Iacono (2008). "Merging active and passive data sets in traveltime tomography: The case study of Campi Flegrei caldera (Southern Italy)." Geophysical Prospecting **56**(4): 555-573.

Bazin, S., N. Feuillet, C. Duclos, W. Crawford, A. Nercessian, M. Bengoubou-Valerius, F. Beauducel and S. C. Singh (2010). "The 2004-2005 Les Saintes (French West Indies) seismic aftershock sequence observed with ocean bottom seismometers." Tectonophysics **489**(1-4): 91-103.

Beauval, C., P. Y. Bard and J. Douglas (2010). "Comment on "Test of Seismic Hazard Map from 500 Years of Recorded Intensity Data in Japan" by Masatoshi Miyazawa and Jim Mori." Bulletin of the Seismological Society of America **100**(6): 3329-3331.

Beauval, C., P. Y. Bard, S. Hainzl and P. Gueguen (2008). "Can strong-motion observations be used to constrain probabilistic seismic-hazard estimates?" Bulletin of the Seismological Society of America **98**(2): 509-520.

Beauval, C., L. Honore and F. Courboulex (2009). "Ground-Motion Variability and Implementation of a Probabilistic-Deterministic Hazard Method." Bulletin of the Seismological Society of America **99**(5): 2992-3002.

Becel, A., M. Laigle, B. de Voogd, A. Hirn, T. Taymaz, A. Galve, H. Shimamura, Y. Murai, J. C. Lepine, M. Sapin and S. Ozalaybey (2009). "Moho, crustal architecture and deep deformation under the North Marmara Trough, from the SEISMARMARA Leg 1 offshore-onshore reflection-refraction survey." Tectonophysics **467**(1-4): 1-21.

Becel, A., M. Laigle, B. de Voogd, A. Hirn, T. Taymaz, S. Yolsal-Cevikbilen and H. Shimamura (2010). "North Marmara Trough architecture of basin infill, basement and faults, from PSDM reflection and OBS refraction seismics." Tectonophysics **490**(1-2): 1-14.

Beck, C., B. Mercier de Lepinay, J. L. Schneider, M. Cremer, N. Cagatay, E. Wendenbaum, S. Boutareaud, G. Menot, S. Schmidt, O. Weber, K. Eris, R. Armijo, B. Meyer, N. Pondard and M. A. Gutscher (2007). "Late Quaternary co-seismic sedimentation in the Sea of Marmara's deep basins." Sedimentary Geology **199**(1-2): 65-89.

Bengouhou-Valerius, M., S. Bazin, D. Bertil, F. Beauducel and A. Bosson (2008). "CDSA: A new seismological data center for the french Leser Antilles." Seismological Research Letters **79**(1): 90-102.

Ben-Hadj-Ali, H., S. Operto and J. Virieux (2008). "Velocity model building by 3D frequency-domain, full-waveform inversion of wide-aperture seismic data." Geophysics **73**(5): 101-117.

Benjemaa, M., N. Glinsky-Olivier, V. M. Cruz-Atienza and J. Virieux (2009). "3-D dynamic rupture simulations by a finite volume method." Geophysical Journal International **178**(1): 541-560.

Benjemaa, M., N. Glinsky-Olivier, V. M. Cruz-Atienza, J. Virieux and S. Piperno (2007). "Dynamic non-planar crack rupture by a finite volume method." Geophysical Journal International **171**: 271-285.

Bergeot, N., M. N. Bouin, M. Diament, B. Pelletier, M. Regnier, S. Calmant and V. Ballu (2009). "Horizontal and vertical interseismic velocity fields in the Vanuatu subduction zone from GPS measurements: Evidence for a central Vanuatu locked zone." Journal of Geophysical Research-Solid Earth **114**.

Berglar, K., C. Gaedicke, D. Franke, S. Ladage, F. Klingelhoefer and Y. S. Djajadihardja (2010). "Structural evolution and strike-slip tectonics off north-western Sumatra." Tectonophysics **480**(1-4): 119-132.

Bethoux, N., C. Sue, A. Paul, J. Virieux, J. Frechet, F. Thouvenot and M. Cattaneo (2007). "Local tomography and focal mechanisms in the south-western Alps: Comparison of methods and tectonic implications." Tectonophysics **432**(1-4): 1-19.

Bethoux, N., E. Tric, J. Chery and M. O. Beslier (2008). "Why is the Ligurian Basin (Mediterranean Sea) seismogenic? Thermomechanical modeling of a reactivated passive margin." Tectonics **27**(5).

Blacic, T. M., D. Latorre, J. Virieux and M. Vassallo (2009). "Converted phases analysis of the Campi Flegrei caldera using active seismic data." Tectonophysics **470**(3-4): 243-256.

Bokelmann, G. and E. Maufroy (2007). "Mantle structure under Gibraltar constrained by dispersion of body waves." Geophysical Research Letters **34**.

Bommer, J. J., J. Douglas, F. Scherbaum, F. Cotton, H. Bungum and D. Fah (2010). "On the Selection of Ground-Motion Prediction Equations for Seismic Hazard Analysis." Seismological Research Letters **81**(5): 783-793.

Bonnardot, M. A., R. Hassani, E. Tric, E. Ruellan and M. Regnier (2008). "Effect of margin curvature on plate deformation in a 3-D numerical model of subduction zones." Geophysical Journal International **173**(3): 1084-1094.

Bonnardot, M. A., M. Regnier, C. Christova, E. Ruellan and E. Tric (2009). "Seismological evidence for a slab detachment in the Tonga subduction zone." Tectonophysics **464**(1-4): 84-99.

Bonnefoy-Claudet, S., A. Kohler, C. Cornou, M. Wathelet and P. Y. Bard (2008). "Effects of Love waves on microtremor H/V ratio." Bulletin of the Seismological Society of America **98**(1): 288-300.

Bordes, C., L. Jouniaux, S. Garambois, M. Dietrich, J. P. Pozzi and S. Gaffet (2008). "Evidence of the theoretically predicted seismo-magnetic conversion." Geophysical Journal International **174**(2): 489-504.

Bouchon, M., H. Karabulut, M. P. Bouin, J. Schmittbuhl, M. Vallee, R. Archuleta, S. Das, F. Renard and D. Marsan (2010). "Faulting characteristics of supershear earthquakes." Tectonophysics **493**(3-4): 244-253.

Bourouis, S. and P. Bernard (2007). "Evidence for coupled seismic and aseismic fault slip during water injection in the geothermal site of Soultz (France), and implications for seismogenic transients." Geophysical Journal International **169**(2): 723-732.

Brenguier, F., M. Campillo, C. Hadziioannou, N. M. Shapiro, R. M. Nadeau and E. Larose (2008). "Postseismic relaxation along the San Andreas fault at Parkfield from continuous seismological observations." Science **321**(5895): 1478-1481.

Brenguier, F., N. M. Shapiro, M. Campillo, V. Ferrazzini, Z. Duputel, O. Coutant and A. Nercessian (2008). "Towards forecasting volcanic eruptions using seismic noise." Nature Geoscience **1**(2): 126-130.

Brenguier, F., N. M. Shapiro, M. Campillo, A. Nercessian and V. Ferrazzini (2007). "3-D surface wave tomography of the Piton de la Fournaise volcano using seismic noise correlations." Geophysical Research Letters **34**(2).

Briais, A., H. Ondreas, F. Klingelhoefer, L. Dosso, C. Hamelin and H. Guillou (2009). "Origin of volcanism on the flanks of the Pacific-Antarctic ridge between 41 degrees 30 ' S and 52 degrees S." Geochemistry Geophysics Geosystems **10**.

Brossier, R., S. Operto and J. Virieux (2009). "Robust elastic frequency-domain full-waveform inversion using the L-1 norm." Geophysical Research Letters **36**.

Brossier, R., S. Operto and J. Virieux (2009). "Seismic imaging of complex onshore structures by 2D elastic frequency-domain full-waveform inversion." Geophysics **74**(6): WCC105-WCC118.

Brossier, R., S. Operto and J. Virieux (2009). "Seismic imaging of complex onshore structures by 2D elastic frequency-domain full-waveform inversion." Geophysics **74**(6): WCC105-WCC118.

Brossier, R., S. Operto and J. Virieux (2010). "Which data residual norm for robust elastic frequency-domain full waveform inversion?" Geophysics **75**(3): R37-R46.

Brossier, R., J. Virieux and S. Operto (2008). "Parsimonious finite-volume frequency-domain method for 2-D P-SV-wave modelling." Geophysical Journal International **175**(2): 541-559.

Bukchin, B., E. Clevede and A. Mostinskiy (2010). "Uncertainty of moment tensor determination from surface wave analysis for shallow earthquakes." Journal of Seismology **14**(3): 601-614.

Burtin, A., L. Bollinger, R. Cattin, J. Vergne and J. L. Nabelek (2009). "Spatiotemporal sequence of Himalayan debris flow from analysis of high-frequency seismic noise." Journal of Geophysical Research-Earth Surface **114**.

Burtin, A., L. Bollinger, J. Vergne, R. Cattin and J. L. Nabelek (2008). "Spectral analysis of seismic noise induced by rivers: A new tool to monitor spatiotemporal changes in stream hydrodynamics." Journal of Geophysical Research-Solid Earth **113**(B5).

Burtin, A., J. Vergne, L. Rivera and P. Dubernet (2010). "Location of river-induced seismic signal from noise correlation functions." Geophysical Journal International **182**(3): 1161-1173.

Buske, S., I. Lecomte, T. Nemeth, S. Operto and V. Sallares (2009). "Imaging and inversion - Introduction." Geophysics **74**(6): WCA1-WCA4.

Buske, S., I. Lecomte, T. Nemeth, S. Operto and V. Sallares (2009). "Imaging and inversion - Introduction." Geophysics **74**(6): WCA1-WCA4.

Bykova, V. V., S. S. Aref'ev and L. Rivera (2010). "Simulation of ground motion in the Moscow region using the empirical Green's function." Izvestiya-Physics of the Solid Earth **46**(1): 19-33.

Cadet, H., P. Y. Bard and A. Rodriguez-Marek (2010). "Defining a Standard Rock Site: Propositions Based on the KiK-net Database." Bulletin of the Seismological Society of America **100**(1): 172-195.

Calahorrano, A., V. Sallares, J. Y. Collot, F. Sage and C. R. Ranero (2008). "Nonlinear variations of the physical properties along the southern Ecuador subduction channel: Results from depth-migrated seismic data." Earth and Planetary Science Letters **267**(3-4): 453-467.

Calais, E., N. d'Oreye, J. Albaric, A. Deschamps, D. Delvaux, J. Deverchere, C. Ebinger, R. W. Ferdinand, F. Kervyn, A. S. Macheyeki, A. Oyen, J. Perrot, E. Saria, B. Smets, D. S. Stamps and C. Wauthier (2008). "Strain accommodation by slow slip and dyking in a youthful continental rift, East Africa." Nature **456**(7223): 783-U767.

Calvet, M. and L. Margerin (2008). "Constraints on grain size and stable iron phases in the uppermost inner core from multiple scattering modeling of seismic velocity and attenuation." Earth and Planetary Science Letters **267**(1-2): 200-212.

Candela, T., F. Renard, M. Bouchon, A. Brouste, D. Marsan, J. Schmittbuhl and C. Voisin (2009). "Characterization of Fault Roughness at Various Scales: Implications of Three-Dimensional High Resolution Topography Measurements." Pure and Applied Geophysics **166**(10-11): 1817-1851.

Capdeville, Y., L. Guillot and J. J. Marigo (2010). "1-D non-periodic homogenization for the seismic wave equation." Geophysical Journal International **181**(2): 897-910.

Capdeville, Y., L. Guillot and J. J. Marigo (2010). "2-D non-periodic homogenization to upscale elastic media for P-SV waves." Geophysical Journal International **182**(2): 903-922.

Capdeville, Y. and J. J. Marigo (2007). "Second order homogenization of the elastic wave equation for non-periodic layered media." Geophysical Journal International **170**(2): 823-838.

Capdeville, Y. and J. J. Marigo (2008). "Shallow layer correction for Spectral Element like methods." Geophysical Journal International **172**(3): 1135-1150.

Cappa, F., Y. Guglielmi and J. Virieux (2007). "Stress and fluid transfer in a fault zone due to overpressures in the seismogenic crust." Geophysical Research Letters **34**(5).

Cara, M., P. J. Alasset and C. Sira (2008). "Magnitude of Historical Earthquakes, from Macroseismic Data to Seismic Waveform Modelling: Application to the Pyrenees and a 1905 Earthquake in the Alps." Historical Seismology: Interdisciplinary Studies of Past and Recent Earthquakes **2**: 369-384.

Carton, H., S. C. Singh, A. Hirn, S. Bazin, B. de Voogd, A. Vigner, A. Ricolleau, S. Cetin, N. Ocakoglu, F. Karakoc and V. Sevilgen (2007). "Seismic imaging of the three-dimensional architecture of the Cinarcik Basin along the North Anatolian Fault." Journal of Geophysical Research-Solid Earth **112**(B6).

Causse, M., E. Chaljub, F. Cotton, C. Cornou and P. Y. Bard (2009). "New approach for coupling k(-2) and empirical Green's functions: application to the blind prediction of broad-band ground motion in the Grenoble basin." Geophysical Journal International **179**(3): 1627-1644.

Causse, M., F. Cotton, C. Cornou and P. Y. Bard (2008). "Calibrating median and uncertainty estimates for a practical use of empirical Green's functions technique." Bulletin of the Seismological Society of America **98**(1): 344-353.

Causse, M., F. Cotton and P. M. Mai (2010). "Constraining the roughness degree of slip heterogeneity." Journal of Geophysical Research-Solid Earth **115**.

Chaljub, E., D. Komatitsch, J. P. Vilotte, Y. Capdeville, B. Valette and G. Festa (2007). "Spectral-element analysis in seismology." Advances in Geophysics, Vol 48 **48**: 365-419.

Chaljub, E., P. Moczo, S. Tsuno, P. Y. Bard, J. Kristek, M. Kaser, M. Stupazzini and M. Kristekova (2010). "Quantitative Comparison of Four Numerical Predictions of 3D Ground Motion in the Grenoble Valley, France." Bulletin of the Seismological Society of America **100**(4): 1427-1455.

Chardon, D., J. A. Austin, G. Cabioch, B. Pelletier, S. Saustrup and F. Sage (2008). "Neogene history of the northeastern New Caledonia continental margin from multichannel reflection seismic profiles." Comptes Rendus Geoscience **340**(1): 68-73.

Chauhan, A. P. S., S. C. Singh, N. D. Hananto, H. Carton, F. Klingelhoefer, J. X. Dessa, H. Permana, N. J. White, D. Graindorge and O. B. S. S. T. Sumatra (2009). "Seismic imaging of forearc backthrusts at northern Sumatra subduction zone." Geophysical Journal International **179**(3): 1772-1780.

Chavez, M., E. Cabrera, R. Madariaga, H. Chen, N. Perea, D. Emerson, A. Salazar, M. Ashworth, C. Moulinec, X. Li, M. Wu and G. Zhao (2010). "Low-Frequency 3D Wave Propagation Modeling of the 12 May 2008 M-w 7.9 Wenchuan Earthquake." Bulletin of the Seismological Society of America **100**(5B): 2561-2573.

Chen, J. H., B. Froment, Q. Y. Liu and M. Campillo (2010). "Distribution of seismic wave speed changes associated with the 12 May 2008 Mw 7.9 Wenchuan earthquake." Geophysical Research Letters **37**.

Chevrot, S. and V. Monteiller (2009). "Principles of vectorial tomography-the effects of model parametrization and regularization in tomographic imaging of seismic anisotropy." Geophysical Journal International **179**(3): 1726-1736.

Chevrot, S., M. Sylvander, S. Benahmed, C. Ponsolles, J. M. Lefevre and D. Paradis (2007). "Source locations of secondary microseisms in western Europe: Evidence for both coastal and pelagic sources." Journal of Geophysical Research-Solid Earth **112**.

Chevrot, S. and L. Zhao (2007). "Multiscale finite-frequency Rayleigh wave tomography of the Kaapvaal craton." Geophysical Journal International **169**(1): 201-215.

Cociani, L., C. J. Bean, H. Lyon-Caen, F. Pacchiani and A. Deschamps (2010). "Coseismic velocity variations caused by static stress changes associated with the 2001 M-w=4.3 Agios Ioanis earthquake in the Gulf of Corinth, Greece." Journal of Geophysical Research-Solid Earth **115**.

Collot, J., L. Geli, Y. Lafoy, R. Vially, D. Cluzel, F. Klingelhoefer and H. Nouze (2008). "Tectonic history of northern New Caledonia Basin from deep offshore seismic reflection: Relation to late Eocene obduction in New Caledonia, southwest Pacific." Tectonics **27**(6).

Cornee, J. J., A. Maillard, G. Conesa, F. Garcia, J. P. Martin, F. Sage and P. Munch (2008). "Onshore to offshore reconstruction of the Messinian erosion surface in Western Sardinia, Italy: Implications for the Messinian salinity crisis." Sedimentary Geology **210**(1-2): 48-60.

Cotton, F., G. Pousse, F. Bonilla and F. Scherbaum (2008). "On the discrepancy of recent European ground-motion observations and predictions from empirical models: Analysis of KiK-net accelerometric data and point-sources stochastic simulations." Bulletin of the Seismological Society of America **98**(5): 2244-2261.

Courboulex, F., J. Converset, J. Balestra and B. Delouis (2010). "Ground-Motion Simulations of the 2004 M-w 6.4 Les Saintes, Guadeloupe, Earthquake Using Ten Smaller Events." Bulletin of the Seismological Society of America **100**(1): 116-130.

Courboulex, F., C. Larroque, A. Deschamps, C. Kohrs-Sansorny, C. Gelis, J. L. Got, J. Charreau, J. F. Stephan, N. Bethoux, J. Virieux, D. Brunel, C. Maron, A. M. Duval, L. Perez and P. Mondielli (2007). "Seismic hazard on the French Riviera: observations, interpretations and simulations." Geophysical Journal International **170**(1): 387-400.

Coutant, O., F. Dore, F. Brenguier, J. F. Fels, D. Brunel, S. Judenherc and M. Dietrich (2008). "The high-resolution imaging (HRI) portable array: A seismic (and internet) network dedicated to kilometric-scale seismic imaging." Seismological Research Letters **79**(1): 47-54.

Cruz-Atienza, V. M., J. Virieux and H. Aochi (2007). "3D finite-difference dynamic-rupture modeling along nonplanar faults." Geophysics **72**: SM123-SM137.

Cupillard, P. and Y. Capdeville (2010). "On the amplitude of surface waves obtained by noise correlation and the capability to recover the attenuation: a numerical approach." Geophysical Journal International **181**(3): 1687-1700.

Dan, G., N. Sultan, B. Savoye, J. Deverchere and K. Yelles (2009). "Quantifying the role of sandy-silty sediments in generating slope failures during earthquakes: example from the Algerian margin." International Journal of Earth Sciences **98**(4): 769-789.

de Linage, C., L. Rivera, J. Hinderer, J. P. Boy, Y. Rogister, S. Lambotte and R. Biancale (2009). "Separation of coseismic and postseismic gravity changes for the 2004 Sumatra-Andaman earthquake from 4.6 yr of GRACE observations and modelling of the coseismic change by normal-modes summation." Geophysical Journal International **176**(3): 695-714.

Deemer, S., J. Hall, K. Solvason, K. W. H. Lau, K. Louden, S. Srivastava and J. C. Sibuet (2009). "Structure and development of the southeast Newfoundland continental passive margin: derived from SCREECH Transect 3." Geophysical Journal International **178**(2): 1004-U1036.

Delost, M., J. Virieux and S. Operto (2008). "First-arrival traveltime tomography using second generation wavelets." Geophysical Prospecting **56**(4): 505-526.

Delouis, B., J. Charlety and M. Vallee (2009). "A Method for Rapid Determination of Moment Magnitude M-w for Moderate to Large Earthquakes from the Near-Field Spectra of Strong-Motion Records (MWSYNTH)." Bulletin of the Seismological Society of America **99**(3): 1827-1840.

Delouis, B. and D. Legrand (2007). "Mw 7.8 Tarapaca intermediate depth earthquake of 13 June 2005 (northern Chile): Fault plane identification and slip distribution by waveform inversion." Geophysical Research Letters **34**(1).

Delouis, B., J. M. Nocquet and M. Vallee (2010). "Slip distribution of the February 27, 2010 Mw=8.8 Maule Earthquake, central Chile, from static and high-rate GPS, InSAR, and broadband teleseismic data." Geophysical Research Letters **37**.

Delouis, B., M. Pardo, D. Legrand and T. Monfret (2009). "The M-w 7.7 Tocopilla Earthquake of 14 November 2007 at the Southern Edge of the Northern Chile Seismic Gap: Rupture in the Deep Part of the Coupled Plate Interface." Bulletin of the Seismological Society of America **99**(1): 87-94.

Deparis, J., D. Jongmans, F. Cotton, L. Baillet, F. Thouvenot and D. Hantz (2008). "Analysis of rock-fall and rock-fall avalanche seismograms in the French Alps." Bulletin of the Seismological Society of America **98**(4): 1781-1796.

Deschamps, A., Y. Hello, P. Charvis, T. Frontera, C. Gojak, C. Antares and Ieee (2008). "A Real Time Seismological Station at 2500 m Depth in Front Toulon." Passive '08: 2008 New Trends for Environmental Monitoring Using Passive Systems: 144-147.

Deschamps, A., R. Shinjo, T. Matsumoto, C. S. Lee, S. E. Lallemand, S. G. Wu and K. R. K. R. C. Sci Party (2008). "Propagators and ridge jumps in a back-arc basin, the West Philippine Basin." Terra Nova **20**(4): 327-332.

Deschamps, A., M. Tivey, R. W. Embley and W. W. Chadwick (2007). "Quantitative study of the deformation at Southern Explorer Ridge using high-resolution bathymetric data." Earth and Planetary Science Letters **259**(1-2): 1-17.

Dessa, J. X., F. Klingelhoefer, D. Graindorge, C. Andre, H. Permana, M. A. Gutscher, A. Chauhan, S. C. Singh and S.-O. S. Team (2009). "Megathrust earthquakes can nucleate in the forearc mantle: Evidence from the 2004 Sumatra event." Geology **37**(7): 659-662.

Deverchere, J., B. M. de Lepinay, A. Cattaneo, P. Strzerzynski, E. Calais, A. Domzig and R. Bracene (2010). "Comment on "Zemmouri earthquake rupture zone (M-w 6.8, Algeria): Aftershocks sequence relocation and 3D velocity model" by A. Ayadi et al." Journal of Geophysical Research-Solid Earth **115**.

Di Carli, S., C. Voisin, F. Cotton and F. Semmane (2008). "The 2000 western Tottori (Japan) earthquake: Triggering of the largest aftershock and constraints on the slip-weakening distance." Journal of Geophysical Research-Solid Earth **113**(B5).

Domzig, A., V. Gaullier, P. Giresse, H. Pauc, J. Deverchere and K. Yelles (2009). "Deposition processes from echo-character mapping along the western Algerian margin (Oran-Tenes), Western Mediterranean." Marine and Petroleum Geology **26**(5): 673-694.

Drouet, S., S. Chevrot, F. Cotton and A. Souriau (2008). "Simultaneous inversion of source spectra, attenuation parameters, and site responses: Application to the data of the french accelerometric network." Bulletin of the

Seismological Society of America **98**(1): 198-219.

Drouet, S., F. Cotton and P. Gueguen (2010). "nu(S30), kappa, regional attenuation and M-w from accelerograms: application to magnitude 3-5 French earthquakes." Geophysical Journal International **182**(2): 880-898.

Drouet, S., F. Scherbaum, F. Cotton and A. Souriau (2007). "Selection and ranking of ground motion models for seismic hazard analysis in the Pyrenees." Journal of Seismology **11**(1): 87-100.

Duputel, Z., M. Cara, L. Rivera and G. Herquel (2010). "Improving the analysis and inversion of multimode Rayleigh-wave dispersion by using group-delay time information observed on arrays of high-frequency sensors." Geophysics **75**(2): R13-R20.

Duputel, Z., V. Ferrazzini, F. Brenguier, N. Shapiro, M. Campillo and A. Nercessian (2009). "Real time monitoring of relative velocity changes using ambient seismic noise at the Piton de la Fournaise volcano (La Reunion) from January 2006 to June 2007." Journal of Volcanology and Geothermal Research **184**(1-2): 164-173.

Durand, V., M. Bouchon, H. Karabulut, D. Marsan, J. Schmittbuhl, M. P. Bouin, M. Aktar and G. Daniel (2010). "Seismic interaction and delayed triggering along the North Anatolian Fault." Geophysical Research Letters **37**.

Dusunur, D., J. Escartin, V. Combier, T. Seher, W. Crawford, M. Cannat, S. C. Singh, L. M. Matias and J. M. Miranda (2009). "Seismological constraints on the thermal structure along the Lucky Strike segment (Mid-Atlantic Ridge) and interaction of tectonic and magmatic processes around the magma chamber." Marine Geophysical Researches **30**(2): 105-120.

Escartin, J., R. Garcia, O. Delaunoy, J. Ferrer, N. Gracias, A. Elibol, X. Cufi, L. Neumann, D. J. Fornari, S. E. Humphris and J. Renard (2008). "Globally aligned photomosaic of the Lucky Strike hydrothermal vent field (Mid-Atlantic Ridge, 37 degrees 18.50 ' N): Release of georeferenced data, mosaic construction, and viewing software." Geochemistry Geophysics Geosystems **9**.

Etienne, V., E. Chaljub, J. Virieux and N. Glinsky (2010). "An hp-adaptive discontinuous Galerkin finite-element method for 3-D elastic wave modelling." Geophysical Journal International **183**(2): 941-962.

Favreau, P., A. Mangeney, A. Lucas, G. Crosta and F. Bouchut (2010). "Numerical modeling of landquakes." Geophysical Research Letters **37**.

Favreau, P. and S. Wolf (2009). "Theoretical and numerical stress analysis at edges of interacting faults: application to quasi-static fault propagation modelling." Geophysical Journal International **179**(2): 733-750.

Feuillet, N., F. Leclerc, P. Tapponnier, F. Beauducel, G. Boudon, A. Le Friant, C. Deplus, J. F. Lebrun, A. Nercessian, J. M. Saurel and V. Clement (2010). "Active faulting induced by slip partitioning in Montserrat and link with volcanic activity: New insights from the 2009 GWADASEIS marine cruise data." Geophysical Research Letters **37**.

Fournier, M., N. Chamot-Rooke, C. Petit, P. Huchon, A. Al-Kathiri, L. Audin, M. O. Beslier, E. d'Acremont, O. Fabbri, J. M. Fleury, K. Khanbari, C. Lepvrier, S. Leroy, B. Maillot and S. Merkouriev (2010). "Arabia-Somalia plate kinematics, evolution of the Aden-Owen-Carlsberg triple junction, and opening of the Gulf of Aden." Journal of Geophysical Research-Solid Earth **115**.

Franco, A., E. Molina, H. Lyon-Caen, J. Vergne, T. Monfret, A. Nercessian, S. Cortez, O. Flores, D. Monterosso and J. Requenna (2009). "Seismicity and Crustal Structure of the Polochic-Motagua Fault System Area (Guatemala)." Seismological Research Letters **80**(6): 977-984.

Froment, B., M. Campillo, P. Roux, P. Gouedard, A. Verdel and R. L. Weaver (2010). "Estimation of the effect of nonisotropically distributed energy on the apparent arrival time in correlations." Geophysics **75**(5): SA85-SA93.

Fry, B., F. Deschamps, E. Kissling, L. Stehly and D. Giardini (2010). "Layered azimuthal anisotropy of Rayleigh

wave phase velocities in the European Alpine lithosphere inferred from ambient noise." Earth and Planetary Science Letters **297**(1-2): 95-102.

Gaffet, S., Y. Guglielmi, F. Cappa, C. Pambrun, T. Monfret and D. Amitrano (2010). "Use of the simultaneous seismic, GPS and meteorological monitoring for the characterization of a large unstable mountain slope in the southern French Alps." Geophysical Journal International **182**(3): 1395-1410.

Gailler, A., P. Charvis and E. R. Flueh (2007). "Segmentation of the Nazca and South American plates along the Ecuador subduction zone from wide angle seismic profiles." Earth and Planetary Science Letters **260**(3-4): 444-464.

Gailler, A., F. Klingelhoefer, J. L. Olivet, D. Aslanian, P. Sardinia Sci and O. B. S. T. Tech (2009). "Crustal structure of a young margin pair: New results across the Liguro-Provencal Basin from wide-angle seismic tomography." Earth and Planetary Science Letters **286**(1-2): 333-345.

Garcia, R. and F. Crespon (2008). "Radio tomography of the ionosphere: Analysis of an underdetermined, ill-posed inverse problem, and regional application." Radio Science **43**(2).

Garcia, R. F., S. Chevrot and M. Calvet (2009). "Statistical study of seismic heterogeneities at the base of the mantle from PKP differential traveltimes." Geophysical Journal International **179**(3): 1607-1616.

Gautier, S., G. Nolet and J. Virieux (2008). "Finite-frequency tomography in a crustal environment: Application to the western part of the Gulf of Corinth." Geophysical Prospecting **56**(4): 493-503.

Geissler, W. H., L. Matias, D. Stich, F. Carrilho, W. Jokat, S. Monna, A. IbenBrahim, F. Mancilla, M. A. Gutscher, V. Sallares and N. Zitellini (2010). "Focal mechanisms for sub-crustal earthquakes in the Gulf of Cadiz from a dense OBS deployment." Geophysical Research Letters **37**.

Gelis, C., J. Virieux and G. Grandjean (2007). "Two-dimensional elastic full waveform inversion using Born and Rytov formulations in the frequency domain." Geophysical Journal International **168**(2): 605-633.

Gesret, A., M. Laigle, J. Diaz, M. Sachpazi and A. Hirn (2010). "The oceanic nature of the African slab subducted under Peloponnesus: thin-layer resolution from multiscale analysis of teleseismic P-to-S converted waves." Geophysical Journal International **183**(2): 833-849.

Godano, M., E. Gaucher, T. Bardainne, M. Regnier, A. Deschamps and M. Valette (2010). "Assessment of focal mechanisms of microseismic events computed from two three-component receivers: application to the Arkema-Vauvert field (France)." Geophysical Prospecting **58**(5): 772-787.

Godano, M., M. Regnier, A. Deschamps, T. Bardainne and E. Gaucher (2009). "Focal Mechanisms from Sparse Observations by Nonlinear Inversion of Amplitudes: Method and Tests on Synthetic and Real Data." Bulletin of the Seismological Society of America **99**(4): 2243-2264.

Got, J. L., V. Monteiller, J. Virieux and S. Operto (2008). "Potential and limits of double-difference tomographic methods." Geophysical Prospecting **56**(4): 477-491.

Gouedard, P., C. Cornou and P. Roux (2008). "Phase-velocity dispersion curves and small-scale geophysics using noise correlation slantstack technique." Geophysical Journal International **172**(3): 971-981.

Gouedard, P., P. Roux and M. Campillo (2008). "Small-scale seismic inversion using surface waves extracted from noise cross correlation." Journal of the Acoustical Society of America **123**(3): EL26-EL31.

Gouedard, P., P. Roux, M. Campillo and A. Verdel (2008). "Convergence of the two-point correlation function toward the Green's function in the context of a seismic-prospecting data set." Geophysics **73**(6): V47-V53.

Gouedard, P., L. Stehly, F. Brenguier, M. Campillo, Y. C. de Verdiere, E. Larose, L. Margerin, P. Roux, F. J. Sanchez-Sesma, N. M. Shapiro and R. L. Weaver (2008). "Cross-correlation of random fields: mathematical

approach and applications." Geophysical Prospecting **56**(3): 375-393.

Graindorge, D., F. Klingelhoefer, J. C. Sibuet, L. McNeill, T. J. Henstock, S. Dean, M. A. Gutscher, J. X. Dessa, H. Permana, S. C. Singh, H. Leau, N. White, H. Carton, J. A. Malod, C. Rangin, K. G. Aryawan, A. K. Chaubey, A. Chauhan, D. R. Galih, C. J. Greenroyd, A. Laesanpura, J. Prihantono, G. Royle and U. Shankar (2008). "Impact of lower plate structure on upper plate deformation at the NW Sumatran convergent margin from seafloor morphology." Earth and Planetary Science Letters **275**(3-4): 201-210.

Granet, M. and F. Chabaux (2007). "U-series isotopes in suspended sediments of the Himalayan rivers." Geochimica Et Cosmochimica Acta **71**(15): A350-A350.

Granet, M., F. Chabaux, P. Stille, A. Dosseto, C. France-Lanord and E. Blaes (2010). "U-series disequilibria in suspended river sediments and implication for sediment transfer time in alluvial plains: The case of the Himalayan rivers." Geochimica Et Cosmochimica Acta **74**(10): 2851-2865.

Granet, M., F. Chabaux, P. Stille, C. France-Lanord and E. Pelt (2007). "Time-scales of sedimentary transfer and weathering processes from U-series nuclides: Clues from the Himalayan rivers." Earth and Planetary Science Letters **261**: 389-406.

Green, D. N., J. Guilbert, A. Le Pichon, O. Sebe and D. Bowers (2009). "Modelling Ground-to-Air Coupling for the Shallow M-L 4.3 Folkestone, United Kingdom, Earthquake of 28 April 2007." Bulletin of the Seismological Society of America **99**(4): 2541-2551.

Grob, M., J. Schmittbuhl, R. Toussaint, L. Rivera, S. Santucci and K. J. Maloy (2009). "Quake Catalogs from an Optical Monitoring of an Interfacial Crack Propagation." Pure and Applied Geophysics **166**(5-7): 777-799.

Gueguen, P., C. Cornou, S. Garambois and J. Banton (2007). "On the limitation of the H/V spectral ratio using seismic noise as an exploration tool: Application to the Grenoble Valley (France), a small apex ratio basin." Pure and Applied Geophysics **164**(1): 115-134.

Gueguen, P., V. Jolivet, C. Michel and A. S. Schveitzer (2010). "Comparison of velocimeter and coherent lidar measurements for building frequency assessment." Bulletin of Earthquake Engineering **8**(2): 327-338.

Gueguen, P., C. Michel and L. LeCorre (2007). "A simplified approach for vulnerability assessment in moderate-to-low seismic hazard regions: application to Grenoble (France)." Bulletin of Earthquake Engineering **5**(3): 467-490.

Guillot, L., Y. Capdeville and J. J. Marigo (2010). "2-D non-periodic homogenization of the elastic wave equation: SH case." Geophysical Journal International **182**(3): 1438-1454.

Gutscher, M. A. (2010). "Reply to Comment by Fernando Marques (on Tectonophysics article "Deep structure, recent deformation and analog modeling of the Gulf of Cadiz accretionary wedge")." Tectonophysics **485**(1-4): 330-331.

Gutscher, M. A., S. Dominguez, G. K. Westbrook, P. Gente, N. Babonneau, T. Mulder, E. Gonthier, R. Bartolome, J. Luis, F. Rosas, P. Terrinha, Delila and T. DelSis Sci (2009). "Tectonic shortening and gravitational spreading in the Gulf of Cadiz accretionary wedge: Observations from multi-beam bathymetry and seismic profiling." Marine and Petroleum Geology **26**(5): 647-659.

Gutscher, M. A., S. Dominguez, G. K. Westbrook and P. Leroy (2009). "Deep structure, recent deformation and analog modeling of the Gulf of Cadiz accretionary wedge: Implications for the 1755 Lisbon earthquake." Tectonophysics **475**(1): 85-97.

Gutscher, M. A. and G. K. Westbrook (2009). "Great Earthquakes in Slow-Subduction, Low-Taper Margins." Subduction Zone Geodynamics: 119-133.

Hadziioannou, C., E. Larose, O. Coutant, P. Roux and M. Campillo (2009). "Stability of monitoring weak changes

in multiply scattering media with ambient noise correlation: Laboratory experiments." Journal of the Acoustical Society of America **125**(6): 3688-3695.

Hallier, S., E. Chaljub, M. Bouchon and H. Sekiguchi (2008). "Revisiting the Basin-edge Effect at Kobe During the 1995 Hyogo-Ken Nanbu Earthquake." Pure and Applied Geophysics **165**(9-10): 1751-1760.

Hatzfeld, D. and P. Molnar (2010). "COMPARISONS OF THE KINEMATICS AND DEEP STRUCTURES OF THE ZAGROS AND HIMALAYA AND OF THE IRANIAN AND TIBETAN PLATEAUS AND GEODYNAMIC IMPLICATIONS." Reviews of Geophysics **48**.

Hayes, G. P., L. Rivera and H. Kanamori (2009). "Source Inversion of the W-Phase: Real-time Implementation and Extension to Low Magnitudes." Seismological Research Letters **80**(5): 817-822.

Hebert, H., D. Reymond, Y. Krien, J. Vergoz, F. Schindele, J. Roger and A. Loevenbruck (2009). "The 15 August 2007 Peru Earthquake and Tsunami: Influence of the Source Characteristics on the Tsunami Heights." Pure and Applied Geophysics **166**(1-2): 211-232.

Hebert, H., A. Sladen and F. Schindele (2007). "Numerical modeling of the great 2004 Indian Ocean tsunami: Focus on the Mascarene Islands." Bulletin of the Seismological Society of America **97**(1): S208-S222.

Hetenyi, G., R. Cattin, F. Brunet, L. Bollinger, J. Vergne, J. Nabelek and M. Diament (2007). "Density distribution of the India plate beneath the Tibetan plateau: Geophysical and petrological constraints on the kinetics of lower-crustal eclogitization." Earth and Planetary Science Letters **264**(1-2): 226-244.

Hobiger, M., P. Y. Bard, C. Cornou and N. Le Bihan (2009). "Single station determination of Rayleigh wave ellipticity by using the random decrement technique (RayDec)." Geophysical Research Letters **36**.

Hofstetter, R., Y. Klinger, A. Q. Amrat, L. Rivera and L. Dorbath (2007). "Stress tensor and focal mechanisms along the Dead Sea fault and related structural elements based on seismological data." Tectonophysics **429**(3-4): 165-181.

Hok, S., M. Campillo, F. Cotton, P. Favreau and I. Ionescu (2010). "Off-fault plasticity favors the arrest of dynamic ruptures on strength heterogeneity: Two-dimensional cases." Geophysical Research Letters **37**.

Houlie, N. and J. P. Montagner (2007). "Hidden dykes detected on ultra long period seismic signals at Piton de la Fournaise volcano?" Earth and Planetary Science Letters **261**: 1-8.

Houlie, N. and J. P. Montagner (2009). "A comment on "Hidden dykes detected on ultra long period seismic signals at Piton de la Fournaise volcano?" by N. Houlie and J.-P. Montagner, EPSL 261, (2007) Discussion Reply." Earth and Planetary Science Letters **287**(1-2): 288-291.

Hsu, Y. J., L. Rivera, Y. M. Wu, C. H. Chang and H. Kanamori (2010). "Spatial heterogeneity of tectonic stress and friction in the crust: new evidence from earthquake focal mechanisms in Taiwan." Geophysical Journal International **182**(1): 329-342.

Husker, A., S. Peyrat, N. Shapiro and V. Kostoglodov (2010). "Automatic non-volcanic tremor detection in the Mexican subduction zone." Geofisica Internacional **49**(1): 17-25.

Iassonov, P. and W. Crawford (2008). "Two-dimensional finite-difference model of seafloor compliance." Geophysical Journal International **174**(2): 525-541.

Ioualalen, M., E. Pelinovsky, J. Asavanant, R. Lipikorn and A. Deschamps (2007). "On the weak impact of the 26 December Indian Ocean tsunami on the Bangladesh coast." Natural Hazards and Earth System Sciences **7**(1): 141-147.

Iturbe, I., P. Roux, B. Nicolas, J. Virieux and J. I. Mars (2009). "Shallow-Water Acoustic Tomography Performed

From a Double-Beamforming Algorithm: Simulation Results." Ieee Journal of Oceanic Engineering **34**(2): 140-149.

Iturbe, I., P. Roux, J. Virieux and B. Nicolas (2009). "Travel-time sensitivity kernels versus diffraction patterns obtained through double beam-forming in shallow water." Journal of the Acoustical Society of America **126**(2): 713-720.

Jaffal, M., F. Klingelhoefer, L. Matias, F. Teixeira and M. Amrhar (2009). "Crustal structure of the NW Moroccan margin from deep seismic data (SISMAR Cruise)." Comptes Rendus Geoscience **341**(6): 495-503.

Jansky, J., V. Plicka, H. Lyon-Caen and O. Novotny (2007). "Estimation of velocity in the uppermost crust in a part of the western Gulf of Corinth, Greece, from the inversion of P and S arrival times using the neighbourhood algorithm." Journal of Seismology **11**(2): 199-204.

Kanamori, H. and L. Rivera (2008). "Source inversion of W phase: speeding up seismic tsunami warning." Geophysical Journal International **175**(1): 222-238.

Kanamori, H., L. Rivera and W. H. K. Lee (2010). "Historical seismograms for unravelling a mysterious earthquake: The 1907 Sumatra Earthquake." Geophysical Journal International **183**(1): 358-374.

Kaviani, A., D. Hatzfeld, A. Paul, M. Tatar and K. Priestley (2009). "Shear-wave splitting, lithospheric anisotropy, and mantle deformation beneath the Arabia-Eurasia collision zone in Iran." Earth and Planetary Science Letters **286**(3-4): 371-378.

Kaviani, A., A. Paul, E. Bourova, D. Hatzfeld, H. Pedersen and M. Mokhtari (2007). "A strong seismic velocity contrast in the shallow mantle across the Zagros collision zone (Iran)." Geophysical Journal International **171**: 399-410.

Kherani, E. A., P. Lognonne, N. Kamath, F. Crespon and R. Garcia (2009). "Response of the ionosphere to the seismic trigerred acoustic waves: electron density and electromagnetic fluctuations." Geophysical Journal International **176**(1): 1-13.

Kherroubi, A., J. Deverchere, A. Yelles, B. Mercier de Lepinay, A. Domzig, A. Cattaneo, R. Bracene, V. Gaullier and D. Graindorge (2009). "Recent and active deformation pattern off the easternmost Algerian margin, Western Mediterranean Sea: New evidence for contractional tectonic reactivation." Marine Geology **261**(1-4): 17-32.

Klingelhoefer, F., M. A. Gutscher, S. Ladage, J. X. Dessa, D. Graindorge, D. Franke, C. Andre, H. Permana, T. Yudistira and A. Chauhan (2010). "Limits of the seismogenic zone in the epicentral region of the 26 December 2004 great Sumatra-Andaman earthquake: Results from seismic refraction and wide-angle reflection surveys and thermal modeling." Journal of Geophysical Research-Solid Earth **115**.

Klingelhoefer, F., C. Labails, E. Cosquer, S. Rouzo, L. Geli, D. Aslanian, J. L. Olivet, M. Sahabi, H. Nouze and P. Unternehr (2009). "Crustal structure of the SW-Moroccan margin from wide-angle and reflection seismic data (the DAKHLA experiment) Part A: Wide-angle seismic models." Tectonophysics **468**(1-4): 63-82.

Klingelhoefer, F., Y. Lafoy, J. Collot, E. Cosquer, L. Geli, H. Nouze and R. Vially (2007). "Crustal structure of the basin and ridge system west of New Caledonia (southwest Pacific) from wide-angle and reflection seismic data." Journal of Geophysical Research-Solid Earth **112**.

Klingelhoefer, F., C. S. Lee, J. Y. Lin and J. C. Sibuet (2009). "Structure of the southernmost Okinawa Trough from reflection and wide-angle seismic data." Tectonophysics **466**(3-4): 281-288.

Kohler, A., M. Ohrnberger, F. Scherbaum, M. Wathelet and C. Cornou (2007). "Assessing the reliability of the modified three-component spatial autocorrelation technique." Geophysical Journal International **168**(2): 779-796.

Komatitsch, D., L. P. Vinnik and S. Chevrot (2010). "SHdiff-SVdiff splitting in an isotropic Earth." Journal of Geophysical Research-Solid Earth **115**.

Kumagai, I., A. Davaille, K. Kurita and E. Stutzmann (2008). "Mantle plumes: Thin, fat, successful, or failing? Constraints to explain hot spot volcanism through time and space." Geophysical Research Letters **35**(16).

Kuo, C. Y., Y. C. Tai, F. Bouchut, A. Mangeney, M. Pelanti, R. F. Chen and K. J. Chang (2009). "Simulation of Tsaoling landslide, Taiwan, based on Saint Venant equations over general topography." Engineering Geology **104**(3-4): 181-189.

Laigle, M., A. Becel, B. de Voogd, A. Hirn, T. Taymaz, S. Ozalaybey and S. L. Team (2008). "A first deep seismic survey in the Sea of Marmara: Deep basins and whole crust architecture and evolution." Earth and Planetary Science Letters **270**(3-4): 168-179.

Lambotte, S., L. Rivera and J. Hinderer (2007). "Constraining the overall kinematics of the 2004 Sumatra and the 2005 Nias earthquakes using the earth's gravest free oscillations." Bulletin of the Seismological Society of America **97**(1): S128-S138.

Landes, M., F. Hubans, N. M. Shapiro, A. Paul and M. Campillo (2010). "Origin of deep ocean microseisms by using teleseismic body waves." Journal of Geophysical Research-Solid Earth **115**.

Larmat, C., J. P. Montagner, Y. Capdeville, W. B. Banerdt, P. Lognonne and J. P. Vilotte (2008). "Numerical assessment of the effects of topography and crustal thickness on martian seismograms using a coupled modal solution-spectral element method." Icarus **196**(1): 78-89.

Larmat, C., J. Tromp, Q. Liu and J. P. Montagner (2008). "Time reversal location of glacial earthquakes." Journal of Geophysical Research-Solid Earth **113**(B9).

Larroque, C., B. Delouis, B. Godel and J. M. Nocquet (2009). "Active deformation at the southwestern Alps-Ligurian basin junction (France-Italy boundary): Evidence for recent change from compression to extension in the Argentera massif." Tectonophysics **467**(1-4): 22-34.

Latorre, D., P. De Gori, C. Chiarabba, A. Amato, J. Virieux and T. Monfret (2008). "Three-dimensional kinematic depth migration of converted waves: application to the 2002 Molise aftershock sequence (southern Italy)." Geophysical Prospecting **56**(4): 587-600.

Lay, T., C. J. Ammon, H. Kanamori, L. Rivera, K. D. Koper and A. R. Hutko (2010). "The 2009 Samoa-Tonga great earthquake triggered doublet." Nature **466**(7309): 964-U985.

Lay, T., H. Kanamori, C. J. Ammon, A. R. Hutko, K. Furlong and L. Rivera (2009). "The 2006-2007 Kuril Islands great earthquake sequence." Journal of Geophysical Research-Solid Earth **114**.

Le Gall, B., P. Nonnotte, J. Rolet, M. Benoit, H. Guillou, M. Mousseau-Nonnotte, J. Albaric and J. Deverchere (2008). "Rift propagation at craton margin. Distribution of faulting and volcanism in the North Tanzanian Divergence (East Africa) during Neogene times." Tectonophysics **448**(1-4): 1-19.

Le Pichon, A., J. Vergoz, E. Blanc, J. Guilbert, L. Ceranna, L. Evers and N. Brachet (2009). "Assessing the performance of the International Monitoring System's infrasound network: Geographical coverage and temporal variabilities." Journal of Geophysical Research-Atmospheres **114**.

Legrand, D., B. Delouis, L. Dorbath, C. David, J. Campos, L. Marquez, J. Thompson and D. Comte (2007). "Source parameters of the M-w=6.3 Aroma crustal earthquake of July 24, 2001 (northern Chile), and its aftershock sequence." Journal of South American Earth Sciences **24**(1): 58-68.

Leroy, S., F. Lucazeau, E. d'Acremont, L. Watremez, J. Autin, S. Rouzo, N. Bellahsen, C. Tiberi, C. Ebinger, M. O. Beslier, J. Perrot, P. Razin, F. Rolandone, H. Sloan, G. Stuart, A. Al Lazki, K. Al-Toubi, F. Bache, A. Bonneville, B. Goutorbe, P. Huchon, P. Unternehr and K. Khanbari (2010). "Contrasted styles of rifting in the eastern Gulf of Aden: A combined wide-angle, multichannel seismic, and heat flow survey." Geochemistry Geophysics Geosystems

Leveque, J. J., A. Maggi and A. Souriau (2010). "Seismological constraints on ice properties at Dome C, Antarctica, from horizontal to vertical spectral ratios." Antarctic Science **22**(5): 572-579.

Lin, J. Y., X. Le Pichon, C. Rangin, J. C. Sibuet and T. Maury (2009). "Spatial aftershock distribution of the 26 December 2004 great Sumatra-Andaman earthquake in the northern Sumatra area." Geochemistry Geophysics Geosystems **10**.

Lin, J. Y., J. C. Sibuet and S. K. Hsu (2008). "Variations of b-values at the western edge of the Ryukyu subduction zone, north-east Taiwan." Terra Nova **20**(2): 150-153.

Lin, J. Y., J. C. Sibuet, S. K. Hsu, C. S. Lee and F. Klingelhoefer (2009). "Seismicity and volcanism in the southwestern Okinawa trough (northeast Taiwan)." Bulletin De La Societe Geologique De France **180**(2): 155-170.

Lin, J. Y., J. C. Sibuet, C. S. Lee, S. K. Hsu and F. Klingelhoefer (2007). "Origin of the southern Okinawa Trough volcanism from detailed seismic tomography." Journal of Geophysical Research-Solid Earth **112**(B8).

Lin, J. Y., J. C. Sibuet, C. S. Lee, S. K. Hsu and F. Klingelhoefer (2007). "Spatial variations in the frequency-magnitude distribution of earthquakes in the southwestern Okinawa Trough." Earth Planets and Space **59**(4): 221-225.

Lin, J. Y., J. C. Sibuet, C. S. Lee, S. K. Hsu, F. Klingelhoefer, Y. Auffret, P. Pelleau, J. Crozon and C. H. Lin (2009). "Microseismicity and faulting in the southwestern Okinawa Trough." Tectonophysics **466**(3-4): 268-280.

Lognonne, P., M. Le Feuvre, C. L. Johnson and R. C. Weber (2009). "Moon meteoritic seismic hum: Steady state prediction." Journal of Geophysical Research-Planets **114**.

Lombard, B., J. Piraux, C. Gelis and J. Virieux (2008). "Free and smooth boundaries in 2-D finite-difference schemes for transient elastic waves." Geophysical Journal International **172**(1): 252-261.

Loris, I., H. Douma, G. Nolet, I. Daubechies and C. Regone (2010). "Nonlinear regularization techniques for seismic tomography." Journal of Computational Physics **229**(3): 890-905.

Maad, N., P. Le Roy, M. Sahabi, M. A. Gutscher, M. Hssain, N. Babonneau, M. Rabineau and B. V. Lanoe (2010). "Seismic stratigraphy of the NW Moroccan Atlantic continental shelf and Quaternary deformation at the offshore termination of the southern Rif front." Comptes Rendus Geoscience **342**(9): 731-740.

Madariaga, R. (2007). "Slippery when hot." Science **316**(5826): 842-843.

Madariaga, R., M. Metois, C. Vigny and J. Campos (2010). "Central Chile Finally Breaks." Science **328**(5975): 181-182.

Malinowski, M. and S. Operto (2008). "Quantitative imaging of the Permo-Mesozoic complex and its basement by frequency domain waveform tomography of wide-aperture seismic data from the Polish Basin." Geophysical Prospecting **56**(6): 805-825.

Mangeney, A., F. Bouchut, N. Thomas, J. P. Vilotte and M. O. Bristeau (2007). "Numerical modeling of self-channeling granular flows and of their levee-channel deposits." Journal of Geophysical Research-Earth Surface **112**(F2).

Mangeney, A., O. Roche, O. Hungr, N. Mangold, G. Faccanoni and A. Lucas (2010). "Erosion and mobility in granular collapse over sloping beds." Journal of Geophysical Research-Earth Surface **115**.

Mangeney, A., L. S. Tsimring, D. Volfson, I. S. Aranson and F. Bouchut (2007). "Avalanche mobility induced by the presence of an erodible bed and associated entrainment." Geophysical Research Letters **34**.

Manighetti, I., M. Campillo, S. Bouley and F. Cotton (2007). "Earthquake scaling, fault segmentation, and structural maturity." Earth and Planetary Science Letters **253**(3-4): 429-438.

Manighetti, I., D. Zigone, M. Campillo and F. Cotton (2009). "Self-similarity of the largest-scale segmentation of the faults: Implications for earthquake behavior." Earth and Planetary Science Letters **288**(3-4): 370-381.

Margerin, L. (2008). "COHERENT BACK-SCATTERING AND WEAK LOCALIZATION OF SEISMIC WAVES." Advances in Geophysics, Vol 50 **50**: 1-19.

Margerin, L., M. Campillo, B. A. Van Tiggelen and R. Hennino (2009). "Energy partition of seismic coda waves in layered media: theory and application to Pinyon Flats Observatory." Geophysical Journal International **177**(2): 571-585.

Meier, U., N. M. Shapiro and F. Brenguier (2010). "Detecting seasonal variations in seismic velocities within Los Angeles basin from correlations of ambient seismic noise." Geophysical Journal International **181**(2): 985-996.

Mercerat, D., L. Guillot and J. P. Vilotte (2009). "Application of the Parareal Algorithm for Acoustic Wave Propagation." Numerical Analysis and Applied Mathematics, Vols 1 and 2 **1168**: 1521-1524.

Mercerat, E. D., L. Driad-Lebeau and P. Bernard (2010). "Induced Seismicity Monitoring of an Underground Salt Cavern Prone to Collapse." Pure and Applied Geophysics **167**(1-2): 5-25.

Meric, O., S. Garambois, J. P. Malet, H. Cadet, P. Gueguen and D. Jongmans (2007). "Seismic noise-based methods for soft-rock landslide characterization." Bulletin De La Societe Geologique De France **178**(2): 137-148.

Merrer, S., M. Cara, L. Rivera and J. Ritsema (2007). "Upper mantle structure beneath continents: New constraints from multi-mode Rayleigh wave data in western North America and southern Africa." Geophysical Research Letters **34**(6).

Michel, C. and P. Gueguen (2010). "Time-Frequency Analysis of Small Frequency Variations in Civil Engineering Structures Under Weak and Strong Motions Using a Reassignment Method." Structural Health Monitoring-an International Journal **9**(2): 159-171.

Michel, C., P. Gueguen and P. Y. Bard (2008). "Dynamic parameters of structures extracted from ambient vibration measurements: An aid for the seismic vulnerability assessment of existing buildings in moderate seismic hazard regions." Soil Dynamics and Earthquake Engineering **28**(8): 593-604.

Michel, C., P. Gueguen, S. El Arem, J. Mazars and P. Kotronis (2010). "Full-scale dynamic response of an RC building under weak seismic motions using earthquake recordings, ambient vibrations and modelling." Earthquake Engineering & Structural Dynamics **39**(4): 419-441.

Michel, C., P. Gueguen, P. Lestuzzi and P. Y. Bard (2010). "Comparison between seismic vulnerability models and experimental dynamic properties of existing buildings in France." Bulletin of Earthquake Engineering **8**(6): 1295-1307.

Mocquet, A. (2007). "Analysis and interpretation of the October 21, 1766 earthquake in the Southeastern Caribbean." Journal of Seismology **11**: 381-403.

Monnereau, M., M. Calvet, L. Margerin and A. Souriau (2010). "Lopsided Growth of Earth's Inner Core." Science **328**(5981): 1014-1017.

Montagner, J. P., V. Clouard, J. Campos, A. Cisternas, M. Gerbault and B. Romanowicz (2009). "Earthquakes in subduction zones: A multidisciplinary approach Introduction." Physics of the Earth and Planetary Interiors **175**(1-2): 1-2.

Montagner, J. P., B. Marty, E. Stutzmann, D. Sicilia, M. Cara, R. Pik, J. J. Leveque, G. Roult, E. Beucler and E. Debayle (2007). "Mantle upwellings and convective instabilities revealed by seismic tomography and helium isotope geochemistry beneath eastern Africa." Geophysical Research Letters **34**(21).

Montagner, J. P. and G. Roult (2008). "Normal modes of the Earth - art. no. 012004." Proceedings of the Second Helas International Conference: Helioseismology, Asteroseismology and Mhd Connections **118**: 12004-12004.

Monteiller, V. and S. Chevrot (2010). "How to make robust splitting measurements for single-station analysis and three-dimensional imaging of seismic anisotropy." Geophysical Journal International **182**(1): 311-328.

Mordvinova, V. V., A. Deschamps, T. Dugarmaa, J. Deverchere, M. Ulziibat, V. A. Sankov, A. A. Artem'ev and J. Perrot (2007). "Velocity structure of the lithosphere on the 2003 Mongolian-Baikal transect from SV waves." Izvestiya-Physics of the Solid Earth **43**(2): 119-129.

Mozziconacci, L., J. Angelier, B. Delouis, R. J. Rau, N. Bethoux and B. S. Huang (2009). "Focal mechanisms and seismotectonic stress in North Central Taiwan in relation with the Chi-Chi earthquake." Tectonophysics **466**(3-4): 409-426.

Mozziconacci, L., B. Delouis, J. Angelier, J. C. Hu and B. S. Huang (2009). "Slip distribution on a thrust fault at a plate boundary: the 2003 Chengkung earthquake, Taiwan." Geophysical Journal International **177**(2): 609-623.

Nabelek, J., G. Hetenyi, J. Vergne, S. Sapkota, B. Kafle, M. Jiang, H. P. Su, J. Chen, B. S. Huang and C. T. Hi (2009). "Underplating in the Himalaya-Tibet Collision Zone Revealed by the Hi-CLIMB Experiment." Science **325**(5946): 1371-1374.

Nishida, K., J. P. Montagner and H. Kawakatsu (2009). "Global Surface Wave Tomography Using Seismic Hum." Science **326**(5949): 112-112.

Nouze, H., E. Cosquer, J. Collot, J. P. Foucher, F. Klingelhoefer, Y. Lafoy and L. Geli (2009). "Geophysical characterization of bottom simulating reflectors in the Fairway Basin (off New Caledonia, Southwest Pacific), based on high resolution seismic profiles and heat flow data." Marine Geology **266**(1-4): 80-90.

Novotny, O., J. Jansky, V. Plicka and H. Lyon-Caen (2008). "A layered model of the upper crust in the Aigion region of Greece, inferred from arrival times of the 2001 earthquake sequence." Studia Geophysica Et Geodaetica **52**(1): 123-131.

Obrebski, M., S. Kiselev, L. Vinnik and J. P. Montagner (2010). "Anisotropic stratification beneath Africa from joint inversion of SKS and P receiver functions." Journal of Geophysical Research-Solid Earth **115**.

Occhipinti, G., P. Dorey, T. Farges and P. Lognonne (2010). "Nostradamus: The radar that wanted to be a seismometer." Geophysical Research Letters **37**.

Operto, S., J. Virieux, P. Amestoy, J. Y. L'Excellent, L. Giraud and H. B. H. Ali (2007). "3D finite-difference frequency-domain modeling of visco-acoustic wave propagation using a massively parallel direct solver: A feasibility study." Geophysics **72**: SM195-SM211.

Operto, S., J. Virieux, A. Ribodetti and J. E. Anderson (2009). "Finite-difference frequency-domain modeling of viscoacoustic wave propagation in 2D tilted transversely isotropic (TTI) media." Geophysics **74**(5): T75-T95.

Pacchiani, F. and H. Lyon-Caen (2010). "Geometry and spatio-temporal evolution of the 2001 Agios Ioanis earthquake swarm (Corinth Rift, Greece)." Geophysical Journal International **180**(1): 59-72.

Pandey, D., S. Singh, M. Sinha and L. MacGregor (2009). "Structural imaging of Mesozoic sediments of Kachchh, India, and their hydrocarbon prospects." Marine and Petroleum Geology **26**(7): 1043-1050.

Panning, M. P., Y. Capdeville and B. A. Romanowicz (2009). "Seismic waveform modelling in a 3-D Earth using

the Born approximation: potential shortcomings and a remedy." Geophysical Journal International **177**(1): 161-178.

Panning, M. P. and G. Nolet (2008). "Surface wave tomography for azimuthal anisotropy in a strongly reduced parameter space." Geophysical Journal International **174**(2): 629-648.

Payero, J. S., V. Kostoglodov, N. Shapiro, T. Mikumo, A. Iglesias, X. Perez-Campos and R. W. Clayton (2008). "Nonvolcanic tremor observed in the Mexican subduction zone." Geophysical Research Letters **35**(7).

Pedersen, H., N. Arndt, D. B. Snyder and D. Francis (2009). "Special Issue: Continental Lithospheric Mantle: The Petro-Geophysical Approach Introduction." Lithos **109**(1-2): VII-VIII.

Pequegnat, C., P. Gueguen, D. Hatzfeld and M. Langlais (2008). "The french accelerometric network (RAP) and national data centre (RAP-NDC)." Seismological Research Letters **79**(1): 79-89.

Petit, C., C. Tiberi, A. Deschamps and J. Deverchere (2008). "Teleseismic traveltimes, topography and the lithospheric structure across central Mongolia." Geophysical Research Letters **35**(11).

Peyrat, S. and P. Favreau (2010). "Kinematic and spontaneous rupture models of the 2005 Tarapaca intermediate depth earthquake." Geophysical Journal International **181**(1): 369-381.

Peyrat, S., R. Madariaga, E. Buforn, J. Campos, G. Asch and J. P. Vilotte (2010). "Kinematic rupture process of the 2007 Tocopilla earthquake and its main aftershocks from teleseismic and strong-motion data." Geophysical Journal International **182**(3): 1411-1430.

Pillet, R., A. Deschamps, D. Legrand, J. Virieux, N. Bethoux and B. Yates (2009). "Interpretation of Broadband Ocean-Bottom Seismometer Horizontal Data Seismic Background Noise." Bulletin of the Seismological Society of America **99**(2B): 1333-1342.

Pillet, R. and J. Virieux (2007). "The effects of seismic rotations on inertial sensors." Geophysical Journal International **171**: 1314-1323.

Pletser, V., P. Lognonne, M. Diament and V. Dehant (2009). "Subsurface water detection on Mars by astronauts using a seismic refraction method: Tests during a manned Mars mission simulation." Acta Astronautica **64**(4): 457-466.

Poupinet, G., J. L. Got and F. Brenguier (2008). "MONITORING TEMPORAL VARIATIONS OF PHYSICAL PROPERTIES IN THE CRUST BY CROSS-CORRELATING THE WAVEFORMS OF SEISMIC DOUBLETS." Advances in Geophysics, Vol 50 **50**: 373-399.

Poupinet, G. and N. M. Shapiro (2009). "Worldwide distribution of ages of the continental lithosphere derived from a global seismic tomographic model." Lithos **109**(1-2): 125-130.

Priestley, K., D. McKenzie, E. Debayle and S. Pilidou (2008). "The African upper mantle and its relationship to tectonics and surface geology." Geophysical Journal International **175**(3): 1108-1126.

Qin, Y. L., Y. Capdeville, V. Maupin, J. P. Montagner, S. Lebedev and E. Beucler (2008). "SPICE benchmark for global tomographic methods." Geophysical Journal International **175**(2): 598-616.

Qin, Y. L., Y. Capdeville, J. P. Montagner, L. Boschi and T. W. Becker (2009). "Reliability of mantle tomography models assessed by spectral element simulation." Geophysical Journal International **177**(1): 125-144.

Quentel, E., X. Carton, M. A. Gutscher and R. Hobbs (2010). "Detecting and characterizing mesoscale and submesoscale structures of Mediterranean water from joint seismic and hydrographic measurements in the Gulf of Cadiz." Geophysical Research Letters **37**.

Rabinowicz, M., M. Bystricky, M. Schmocker, M. J. Toplis, A. Rigo and H. Perfettini (2010). "Development of

Fluid Veins during Deformation of Fluid-rich Rocks close to the Brittle-Ductile Transition: Comparison between Experimental and Physical Models." Journal of Petrology **51**(10): 2047-2066.

Radiguet, M., F. Cotton, I. Manighetti, M. Campillo and J. Douglas (2009). "Dependency of Near-Field Ground Motions on the Structural Maturity of the Ruptured Faults." Bulletin of the Seismological Society of America **99**(4): 2572-2581.

Radjaee, A., D. Rham, M. Mokhtari, M. Tatar, K. Priestley and D. Hatzfeld (2010). "Variation of Moho depth in the central part of the Alborz Mountains, northern Iran." Geophysical Journal International **181**(1): 173-184.

Renalier, F., D. Jongmans, M. Campillo and P. Y. Bard (2010). "Shear wave velocity imaging of the Avignonet landslide (France) using ambient noise cross correlation." Journal of Geophysical Research-Earth Surface **115**.

Ribe, N. M., E. Stutzmann, Y. Ren and R. van der Hilst (2007). "Buckling instabilities of subducted lithosphere beneath the transition zone." Earth and Planetary Science Letters **254**(1-2): 173-179.

Rigo, A. (2010). "Precursors and fluid flows in the case of the 1996, M-L=5.2 Saint-Paul-de-Fenouillet earthquake (Pyrenees, France): A complete pre-, co- and post-seismic scenario." Tectonophysics **480**(1-4): 109-118.

Rigo, A., N. Bethoux, F. Masson and J. F. Ritz (2008). "Seismicity rate and wave-velocity variations as consequences of rainfall: the case of the catastrophic storm of September 2002 in the Nimes Fault region (Gard, France)." Geophysical Journal International **173**(2): 473-482.

Robert, A., M. Pubellier, J. de Sigoyer, J. Vergne, A. Lahfid, R. Cattin, N. Findling and J. Zhu (2010). "Structural and thermal characters of the Longmen Shan (Sichuan, China)." Tectonophysics **491**(1-4): 165-173.

Robert, A., J. Zhu, J. Vergne, R. Cattin, L. S. Chan, G. Wittlinger, G. Herquel, J. de Sigoyer, M. Pubellier and L. D. Zhu (2010). "Crustal structures in the area of the 2008 Sichuan earthquake from seismologic and gravimetric data." Tectonophysics **491**(1-4): 205-210.

Romanowicz, B. A., M. P. Panning, Y. C. Gung and Y. Capdeville (2008). "On the computation of long period seismograms in a 3-D earth using normal mode based approximations." Geophysical Journal International **175**(2): 520-536.

Roult, G., J. P. Montagner, B. Romanowicz, M. Cara, D. Rouland, R. Pillet, J. F. Karczewski, L. Rivera, E. Stutzmann, A. Maggi and G. Team (2010). "The GEOSCOPE Program: Progress and Challenges during the Past 30 Years." Seismological Research Letters **81**(3): 427-452.

Roult, G., J. P. Montagner, B. Romanowicz, M. Cara, D. Rouland, R. Pillet, J. F. Karczewski, J. Trampert, L. Rivera, E. Stutzmann, A. Maggi, J. C. Lepine and G. Team (2010). "The GEOSCOPE Program: Progress and Challenges during the Past 30 Years (vol 81, pg 427, 2010)." Seismological Research Letters **81**(5): 802-802.

Roult, G., J. Roch and E. Clevede (2010). "Observation of split modes from the 26th December 2004 Sumatra-Andaman mega-event." Physics of the Earth and Planetary Interiors **179**(1-2): 45-59.

Sachpazi, M., A. Galve, M. Laigle, A. Him, E. Sokos, A. Serpetsidaki, J. M. Marthelot, J. M. P. Alperin, B. Zelt and B. Taylor (2007). "Moho topography under central Greece and its compensation by Pn time-terms for the accurate location of hypocenters: The example of the Gulf of Corinth 1995 Aigion earthquake." Tectonophysics **440**(1-4): 53-65.

Sahal, A., B. Pelletier, J. Chatelier, F. Lavigne and F. Schindele (2010). "A catalog of tsunamis in New Caledonia from 28 March 1875 to 30 September 2009." Comptes Rendus Geoscience **342**(6): 434-447.

Sahal, A., J. Roger, S. Allgeyer, B. Lemaire, H. Hebert, F. Schindele and F. Lavigne (2009). "The tsunami triggered by the 21 May 2003 Boumerdes-Zemmouri (Algeria) earthquake: field investigations on the French Mediterranean coast and tsunami modelling." Natural Hazards and Earth System Sciences **9**(6): 1823-1834.

Salichon, J., C. Kohrs-Sansorny, E. Bertrand and F. Courboulex (2010). "A Mw 6.3 earthquake scenario in the city of Nice (southeast France): ground motion simulations." Journal of Seismology **14**(3): 523-541.

San'kov, V. A., A. V. Lukhnev, A. I. Miroshnichenko, S. V. Ashurkov, L. M. Byzov, M. G. Dembelov, E. Calais and J. Deverchere (2009). "Extension in the Baikal rift: Present-day kinematics of passive rifting." Doklady Earth Sciences **425**(1): 205-209.

Sauter, D., M. Cannat, C. Meyzen, A. Bezos, P. Patriat, E. Humler and E. Debayle (2009). "Propagation of a melting anomaly along the ultraslow Southwest Indian Ridge between 46 degrees E and 52 degrees 20'E: interaction with the Crozet hotspot ?" Geophysical Journal International **179**(2): 687-699.

Schindele, F., A. Loevenbruck and H. Hebert (2008). "Strategy to design the sea-level monitoring networks for small tsunamigenic oceanic basins: the Western Mediterranean case." Natural Hazards and Earth System Sciences **8**(5): 1019-1027.

Sebai, A. and P. Bernard (2008). "Contribution to the knowledge of the seismicity of the 18th-century at Algiers and its surroundings extracted from French archives." Comptes Rendus Geoscience **340**(8): 495-512.

Semblat, J. F., M. Kham and P. Y. Bard (2008). "Seismic-Wave Propagation in Alluvial Basins and Influence of Site-City Interaction." Bulletin of the Seismological Society of America **98**(6): 2665-2678.

Sens-Schonfelder, C., L. Margerin and M. Campillo (2009). "Laterally heterogeneous scattering explains Lg blockage in the Pyrenees." Journal of Geophysical Research-Solid Earth **114**.

Shabani, E., P. Y. Bard, N. Mirzaei, M. Eskandari-Ghadi, C. Cornou and E. Haghshenas (2010). "An extended MSPAC method in circular arrays." Geophysical Journal International **182**(3): 1431-1437.

Sibuet, J. C., C. Rangin, X. Le Pichon, S. Singh, A. Cattaneo, D. Graindorge, F. Klingelhoefer, J. Y. Lin, J. Malod, T. Maury, J. L. Schneider, N. Sultan, M. Umber, H. Yamaguchi and Sat (2007). "26th December 2004 great Sumatra-Andaman earthquake: Co-seismic and post-seismic motions in northern Sumatra." Earth and Planetary Science Letters **263**(1-2): 88-103.

Sibuet, J. C., S. Srivastava and G. Manatschal (2007). "Exhumed mantle-forming transitional crust in the Newfoundland-Iberia rift and associated magnetic anomalies." Journal of Geophysical Research-Solid Earth **112**(B6).

Sicilia, D., J. P. Montagner, M. Cara, E. Stutzmann, E. Debayle, J. C. Lepine, J. J. Leveque, E. Beucler, A. Sebai, G. Roult, A. Ayele and J. M. Sholan (2008). "Upper mantle structure of shear-waves velocities and stratification of anisotropy in the Afar Hotspot region." Tectonophysics **462**(1-4): 164-177.

Silveira, G., L. Vinnik, E. Stutzmann, V. Farra, S. Kiselev and I. Morais (2010). "Stratification of the Earth beneath the Azores from P and S receiver functions." Earth and Planetary Science Letters **299**(1-2): 91-103.

Sladen, A., H. Hebert, F. Schindele and D. Reymond (2007). "Tsunami hazard in French polynesia: Constraints from numerical modelling." Comptes Rendus Geoscience **339**(5): 303-316.

Song, X. D. and G. Poupinet (2007). "Inner core rotation from event-pair analysis." Earth and Planetary Science Letters **261**: 259-266.

Sourbier, F., S. Operto, J. Virieux, P. Amestoy and J. Y. L'Excellent (2009). "FWT2D: A massively parallel program for frequency-domain full-waveform tomography of wide-aperture seismic data-Part 1 Algorithm." Computers & Geosciences **35**(3): 487-495.

Sourbier, F., S. Operto, J. Virieux, P. Amestoy and J. Y. L'Excellent (2009). "FWT2D: A massively parallel program for frequency-domain full-waveform tomography of wide-aperture seismic data-Part 2 Numerical examples

and scalability analysis." Computers & Geosciences **35**(3): 496-514.

Souriau, A. (2009). "Inner core structure: Constraints from frequency dependent seismic anisotropy." Comptes Rendus Geoscience **341**(6): 439-445.

Souriau, A., S. Chevrot and C. Olivera (2008). "A new tomographic image of the Pyrenean lithosphere from teleseismic data." Tectonophysics **460**(1-4): 206-214.

Souriau, A., A. Roulle and C. Ponsolles (2007). "Site effects in the city of Lourdes, France, from H/V measurements: Implications for seismic-risk evaluation." Bulletin of the Seismological Society of America **97**(6): 2118-2136.

Stehly, L., M. Campillo, B. Froment and R. L. Weaver (2008). "Reconstructing Green's function by correlation of the coda of the correlation (C-3) of ambient seismic noise." Journal of Geophysical Research-Solid Earth **113**(B11).

Stehly, L., M. Campillo and N. M. Shapiro (2007). "Traveltime measurements from noise correlation: stability and detection of instrumental time-shifts." Geophysical Journal International **171**: 223-230.

Stehly, L., B. Fry, M. Campillo, N. M. Shapiro, J. Guilbert, L. Boschi and D. Giardini (2009). "Tomography of the Alpine region from observations of seismic ambient noise." Geophysical Journal International **178**(1): 338-350.

Strzerzynski, P., J. Deverchere, A. Cattaneo, A. Domzig, K. Yelles, B. M. de Lepinay, N. Babonneau and A. Boudiaf (2010). "Tectonic inheritance and Pliocene-Pleistocene inversion of the Algerian margin around Algiers: Insights from multibeam and seismic reflection data." Tectonics **29**.

Stutzmann, E., M. Schimmel, G. Patau and A. Maggi (2009). "Global climate imprint on seismic noise." Geochemistry Geophysics Geosystems **10**.

Sultan, N., A. Cattaneo, J. C. Sibuet and J. L. Schneider (2009). "Deep sea in situ excess pore pressure and sediment deformation off NW Sumatra and its relation with the December 26, 2004 Great Sumatra-Andaman Earthquake." International Journal of Earth Sciences **98**(4): 823-837.

Sylvander, M., B. Monod, A. Souriau and A. Rigo (2007). "Analysis of an earthquake swarm (May 2004) in the French eastern Pyrenees: Towards a new tectonic interpretation of the Saint-Paul-de-Fenouillet earthquake (1996)." Comptes Rendus Geoscience **339**(1): 75-84.

Sylvander, M., C. Ponsolles, S. Benahmed and J. F. Fels (2007). "Seismoacoustic recordings of small earthquakes in the Pyrenees: Experimental results." Bulletin of the Seismological Society of America **97**(1): 294-304.

Sylvander, M., A. Souriau, A. Rigo, A. Tocheport, J. P. Toutain, C. Ponsolles and S. Benahmed (2008). "The 2006 November, M-L=5.0 earthquake near Lourdes (France): new evidence for NS extension across the Pyrenees." Geophysical Journal International **175**(2): 649-664.

Tanimoto, T. and L. Rivera (2008). "The ZH ratio method for long-period seismic data: sensitivity kernels and observational techniques." Geophysical Journal International **172**(1): 187-198.

Tatar, M. and D. Hatzfeld (2009). "Microseismic evidence of slip partitioning for the Rudbar-Tarom earthquake (M-s 7.7) of 1990 June 20 in NW Iran." Geophysical Journal International **176**(2): 529-541.

Tatar, M., J. Jackson, D. Hatzfeld and E. Bergman (2007). "The 2004 May 28 Baladeh earthquake (M-w 6.2) in the Alborz, Iran: overthrusting the South Caspian Basin margin, partitioning of oblique convergence and the seismic hazard of Tehran." Geophysical Journal International **170**(1): 249-261.

Tauzin, B., E. Debayle and G. Wittlinger (2008). "The mantle transition zone as seen by global Pds phases: No clear evidence for a thin transition zone beneath hotspots." Journal of Geophysical Research-Solid Earth **113**(B8).

Tauzin, B., E. Debayle and G. Wittlinger (2010). "Seismic evidence for a global low-velocity layer within the Earth's upper mantle." Nature Geoscience **3**(10): 718-721.

Tavakoli, F., A. Walpersdorf, C. Authemayou, H. R. Nankali, D. Hatzfeld, M. Tatar, Y. Djamour, F. Nilforoushan and N. Cotte (2008). "Distribution of the right-lateral strike-slip motion from the Main Recent Fault to the Kazerun Fault System (Zagros, Iran): Evidence from present-day GPS velocities." Earth and Planetary Science Letters **275**(3-4): 342-347.

Thouvenot, F., A. Paul, J. Frechet, N. Bethoux, L. Jenatton and R. Guiguet (2007). "Are there really superposed Mohos in the southwestern Alps? New seismic data from fan-profiling reflections." Geophysical Journal International **170**: 1180-1194.

Tiberi, C., A. Deschamps, J. Deverchere, C. Petit, J. Perrot, D. Appriou, V. Mordvinova, T. Dugaarma, M. Ulzibaat and A. A. Artemiev (2008). "Asthenospheric imprints on the lithosphere in Central Mongolia and Southern Siberia from a joint inversion of gravity and seismology (MOBAL experiment)." Geophysical Journal International **175**(3): 1283-1297.

Tocheport, A., L. Rivera and S. Chevrot (2007). "A systematic study of source time functions and moment tensors of intermediate and deep earthquakes." Journal of Geophysical Research-Solid Earth **112**(B7).

Vallee, M. (2007). "Rupture properties of the giant Sumatra earthquake imaged by empirical green's function analysis." Bulletin of the Seismological Society of America **97**(1): S103-S114.

Vallee, M., M. Landes, N. M. Shapiro and Y. Klinger (2008). "The 14 November 2001 Kokoxili (Tibet) earthquake: High-frequency seismic radiation originating from the transitions between sub-Rayleigh and supershear rupture velocity regimes." Journal of Geophysical Research-Solid Earth **113**(B7).

Van Camp, M., J. Steim, G. Rapagnani and L. Rivera (2008). "Connecting a Quanterra Data Logger Q330 on the GWR C021 Superconducting Gravimeter." Seismological Research Letters **79**(6): 785-796.

Verhoeven, O., A. Mocquet, P. Vacher, A. Rivoldini, M. Menvielle, P. A. Arrial, G. Choblet, P. Tarits, V. Dehant and T. Van Hoolst (2009). "Constraints on thermal state and composition of the Earth's lower mantle from electromagnetic impedances and seismic data." Journal of Geophysical Research-Solid Earth **114**.

Vinnik, L., Y. Ren, E. Stutzmann, V. Farra and S. Kiselev (2010). "Observations of S410p and S350p phases at seismograph stations in California." Journal of Geophysical Research-Solid Earth **115**.

Virieux, J., P. Y. Bard and H. Modaressi (2007). "Quantitative seismic hazard assessment." Earthquake Early Warning Systems: 153-177.

Virieux, J. and S. Operto (2009). "An overview of full-waveform inversion in exploration geophysics." Geophysics **74**(6): WCC1-WCC26.

Virieux, J. and S. Operto (2009). "An overview of full-waveform inversion in exploration geophysics." Geophysics **74**(6): WCC1-WCC26.

Voisin, C., J. R. Grasso, E. Larose and F. Renard (2008). "Evolution of seismic signals and slip patterns along subduction zones: Insights from a friction lab scale experiment." Geophysical Research Letters **35**(8).

Voisin, C., F. Renard and J. R. Grasso (2007). "Long term friction: From stick-slip to stable sliding." Geophysical Research Letters **34**(13).

Weaver, R., B. Froment and M. Campillo (2009). "On the correlation of non-isotropically distributed ballistic scalar diffuse waves." Journal of the Acoustical Society of America **126**(4): 1817-1826.

Welford, J. K., J. Hall, J. C. Sibuet and S. P. Srivastava (2010). "Structure across the northeastern margin of Flemish

Cap, offshore Newfoundland from Erable multichannel seismic reflection profiles: evidence for a transtensional rifting environment." Geophysical Journal International **183**(2): 572-U551.

Welford, J. K., J. A. Smith, J. Hall, S. Deemer, S. P. Srivastava and J. C. Sibuet (2010). "Structure and rifting evolution of the northern Newfoundland Basin from Erable multichannel seismic reflection profiles across the southeastern margin of Flemish Cap." Geophysical Journal International **180**(3): 976-U974.

Wittlinger, G., V. Farra, G. Hetenyi, J. Vergne and J. Nabelek (2009). "Seismic velocities in Southern Tibet lower crust: a receiver function approach for eclogite detection." Geophysical Journal International **177**(3): 1037-1049.

Wustefeld, A. and G. Bokelmann (2007). "Null detection in shear-wave splitting measurements." Bulletin of the Seismological Society of America **97**(4): 1204-1211.

Wustefeld, A., G. Bokelmann and G. Barruol (2010). "Evidence for ancient lithospheric deformation in the East European Craton based on mantle seismic anisotropy and crustal magnetics." Tectonophysics **481**(1-4): 16-28.

Wustefeld, A., G. Bokelmann, G. Barruol and J. P. Montagner (2009). "Identifying global seismic anisotropy patterns by correlating shear-wave splitting and surface-wave data." Physics of the Earth and Planetary Interiors **176**(3-4): 198-212.

Wustefeld, A., G. Bokelmann, C. Zaroli and G. Barruol (2008). "SplitLab: A shear-wave splitting environment in Matlab." Computers & Geosciences **34**(5): 515-528.

Wyss, M., F. Pacchiani, A. Deschamps and G. Patau (2008). "Mean magnitude variations of earthquakes as a function of depth: Different crustal stress distribution depending on tectonic setting." Geophysical Research Letters **35**(1).

Yamini-Fard, F., D. Hatzfeld, A. M. Farahbod, A. Paul and M. Mokhtari (2007). "The diffuse transition between the Zagros continental collision and the Makran oceanic subduction (Iran): microearthquake seismicity and crustal structure." Geophysical Journal International **170**(1): 182-194.

Yano, T., T. Tanimoto and L. Rivera (2009). "The ZH ratio method for long-period seismic data: inversion for S-wave velocity structure." Geophysical Journal International **179**(1): 413-424.

Yao, H. J., R. D. van der Hilst and J. P. Montagner (2010). "Heterogeneity and anisotropy of the lithosphere of SE Tibet from surface wave array tomography." Journal of Geophysical Research-Solid Earth **115**.

Yedlin, M., A. Cresp, C. Pichot, I. Aliferis, J. Y. Dauvignac, S. Gaffet and G. Senechal (2009). "Ultra-wideband microwave imaging of heterogeneities." Journal of Applied Geophysics **68**(1): 17-25.

Yelles, A., A. Domzig, J. Deverchere, R. Bracene, B. M. de Lepinay, P. Strzerzynski, G. Bertrand, A. Boudiaf, T. Winter, A. Kherroubi, P. Le Roy and H. Djellit (2009). "Plio-Quaternary reactivation of the Neogene margin off NW Algiers, Algeria: The Khayr al Din bank." Tectonophysics **475**(1): 98-116.

Yelles-Chaouche, A., J. Roger, J. Deverchere, R. Bracene, A. Domzig, H. Hebert and A. Kherroubi (2009). "The 1856 Tsunami of Djidjelli (Eastern Algeria): Seismotectonics, Modelling and Hazard Implications for the Algerian Coast." Pure and Applied Geophysics **166**(1-2): 283-300.

Zaroli, C., E. Debayle and M. Sambridge (2010). "Frequency-dependent effects on global S-wave traveltimes: wavefront-healing, scattering and attenuation." Geophysical Journal International **182**(2): 1025-1042.

Zhong, S. J., M. Ritzwoller, N. Shapiro, W. Landuyt, J. S. Huang and P. Wessel (2007). "Bathymetry of the Pacific plate and its implications for thermal evolution of lithosphere and mantle dynamics." Journal of Geophysical Research-Solid Earth **112**(B6).

Zollo, A., N. Maercklin, M. Vassallo, D. Dello Iacono, J. Virieux and P. Gasparini (2008). "Seismic reflections

reveal a massive melt layer feeding Campi Flegrei caldera." Geophysical Research Letters **35**(12).

Comité National Français de Géodésie et Géophysique

French National Committee of Geodesy and Geophysics

RAPPORT QUADRIENNAL DU CNFGG A l'UGGI

QUADRENNIAL REPORT OF CNFGG TO IUGG

SECTION 3 – VOLCANOLOGIE ET CHIMIE DE L'INTÉRIEUR DE LA TERRE

SECTION 3 - VOLCANOLOGY AND CHEMISTRY OF THE EARTH'S INTERIOR

Rapport quadriennal Section 3 du CNFGG 'Volcanologie et Chimie de l'intérieur de la Terre' 2007 - 2010

Activités des équipes de recherche françaises

Ce rapport présente un résumé des principales recherches, principaux résultats et publications des équipes françaises en Volcanologie dans la période 2007-2010. Les recherches ont concerné différents aspects allant de la genèse des magmas, de leur différenciation et transfert, à la dynamique des éruptions volcaniques, aux processus de dégazage magmatique, aux panaches volcaniques, et à la prévision des éruptions et l'évaluation des risques. Des approches méthodologiques variées ont été utilisées, tant sur le terrain qu'en laboratoire. Les résultats, excellents, ont donné lieu à un grand nombre de publications dans des revues internationales à comité de lecture (246 publications de rang A en quatre ans, soit une moyenne de 3.1 publications par an, en auteurs ou co-auteurs pour les membres de la Section 3).

Four years Report of CNFGG's Section 3 'Volcanology and Chemistry of the Earth interior' 2007 - 2010

Summary of activities of French research teams

Here below are summarized the main activities, results and publications of French research groups in the domain of Volcanology during the period 2007-2010. Research activities have dealt with different aspects of magma genesis, differentiation and transfer, eruption dynamics and processes, magma degassing and volcanic plumes, eruption forecasting and volcanic hazard assessment, by using various methodological approaches both in the field and in laboratory. Excellent results have led to a great number of peer-reviewed publications in international journals during that period (co-authoring of 246 A-ranked publications in four years, i.e. an average of 3.1 publications per year, for the Section 3 members).

Equipe de Volcanologie LMV-OPGC, UMR 6524, Clermont-Ferrand

1. Processus éruptifs et écoulements volcaniques

Participants LMV permanents : T. Druitt, K. Kelfoun, J.-L. LePennec, C. Robin, O. Roche, P. Samaniego, J.-C. Thouret, B. van Wyk de Vries.

Objectifs. Cet axe concerne la dynamique des éruptions (processus de conduit) et les mécanismes de mise en place des écoulements pyroclastiques, des lahars, et des avalanches de débris en combinant des travaux de terrain, expérimentaux et théoriques. Ce résumé se focalise uniquement sur nos travaux concernant les écoulements.

Dynamique des écoulements pyroclastiques. Nous avons effectué un programme d'expériences pour mieux comprendre le comportement physique de propagation et de sédimentation des mélanges denses air-particules (Figure 1). Nous avons montré que de tels écoulements se propagent comme des fluides inertiels, à la faveur d'une forte pression de fluide interstitiel, avant d'être en régime granulaire-frictionnel lors d'une courte phase d'arrêt [183, 334]. Dans le cas de mélanges obtenus avec des cendres volcaniques, nous avons déterminé : les lois d'échelle pour la distance parcourue par les écoulements en fonction de leur expansion initiale, le champ de vitesse interne des écoulements et le mode de formation des dépôts [75, 149]. Les travaux de modélisation numérique ont suivi deux approches. La première a consisté à déterminer des lois de comportement au premier ordre pour les écoulements pyroclastiques, en comparant des données de terrain avec des résultats théoriques pour des rhéologies données [234]. Il s'est avéré qu'un comportement plastique (friction constante) était le mieux adapté pour simuler des écoulements naturels. La seconde approche a consisté à développer un modèle numérique 2D, testé à l'aide d'expériences de laboratoire, pour des écoulements denses en tenant compte des interactions entre les particules solides et le fluide interstitiel [326]. L'ensemble des résultats de ces travaux expérimentaux et théoriques apporte des contraintes pour l'interprétation des mécanismes des écoulements pyroclastiques à partir des observations des dépôts [342].

Mesure des propriétés des lahars. Des données obtenues sur le terrain ont permis de mieux comprendre les régimes d'écoulement des lahars et constituent une base de données utile pour de futures simulations de ces phénomènes naturels [297, 116, 117]. Des mesures faites à l'aide de capteurs géophysiques ont permis de déterminer la profondeur, le débit, et la concentration en particules des lahars du Volcan Semeru (Java). Elles ont montré que ces lahars sont caractérisés par une initiation rapide puis par des bouffées instables, et que les particules sont le plus souvent concentrées vers le cœur de l'écoulement. De plus, les lahars incorporent du substrat ou bien sédimentent lorsque leur débit est respectivement élevé ou faible, pouvant ainsi causer d'importantes variations de leur volume.

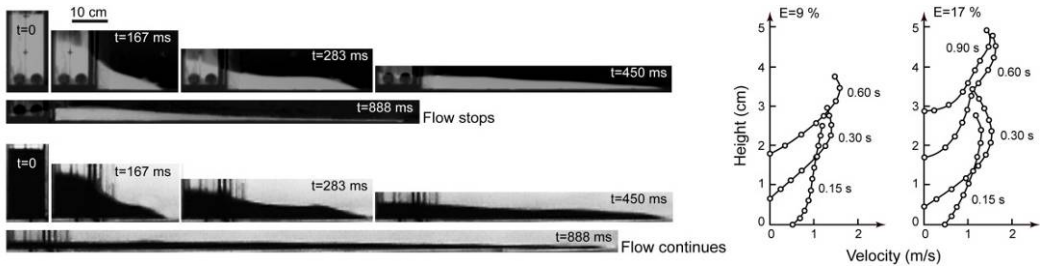

Figure 1. Gauche : transition entre régime inertiel (t<450 ms) et frictionnel pour un écoulement air-particules (haut), déduite par comparaison avec un écoulement d'eau (bas). Droite : champs de vitesse dans des écoulements de cendres (E : expansion initiale), avec formation d'un dépôt basal (vitesse nulle).

Mécanismes des avalanches de débris. Une première étude a porté sur une comparaison entre des résultats de simulations numériques et d'analyses structurales de dépôts naturels à partir d'images satellites haute résolution [158]. Il a pu être démontré que l'avalanche de Socompa (Chili) était constituée d'une partie interne au comportement fluide, expliquant ainsi sa forte mobilité, surmontée d'une croûte rigide cassante. Une seconde étude a été réalisée en couplant des expériences analogiques et des travaux sur le terrain (Mombacho, Chimborazo). Les expériences et les études de terrain ont mis en évidence les mécanismes par lesquels des structures préexistantes dans les édifices volcaniques peuvent contrôler le déclenchement des avalanches [284, 134, 190].

2. Processus volcano-tectoniques

Participants LMV permanents : P. Labazuy, J.-F. Lénat, O. Merle, JC Thouret, B. van Wyk de Vries.

Objectifs. Une thématique importante de l'équipe de volcanologie est la compréhension des dynamiques structurales de l'édifice liées à la gravité, la tectonique régionale, l'activité du magma (vidange et remplissage d'un réservoir, injections de magma dans les filons), le développement du système hydrothermal (altération des produits volcaniques par circulation de fluides chauds), les déstabilisations de flanc et l'action de l'érosion.

Construction et destruction d'un volcan bouclier. Le volcan bouclier de l'Ile de La Réunion sert de laboratoire naturel à notre groupe depuis plusieurs décennies. Pendant ce quadriennal, les résultats spectaculaires obtenus sur la formation et l'histoire de cette ile océanique proviennent de la mise en œuvre et de la confrontation de multiples méthodes, principalement la tomographie sismique [261], l'analyse des anomalies magnétiques, gravimétriques et géo-électriques [223], la bathymétrie [171, 242], la géologie structurale [142, 325], la stratigraphie et la géochronologie des laves [241]. Ces méthodes ont permis (1) de montrer que l'étalement du panache mantellique de La Réunion a été canalisé entre deux failles transformantes parallèles, provoquant la formation d'un haut topographique prononcé, strictement limité au compartiment lithosphérique situé entre ces deux failles transformantes et se mettaient en place sous forme d'intrusion vis, (2) de mettre en évidence que ce volcan bouclier a été régulièrement affecté par de spectaculaires effondrements de flancs, dans toutes les directions, effondrements qui entourent les deux édifices volcaniques du Piton des Neiges et du piton de la Fournaise sur une superficie supérieure à l'Ile elle-même, (3) de tracer la limite interne entre le volcan des Alizés sous-jacent et sa superstructure constituée par

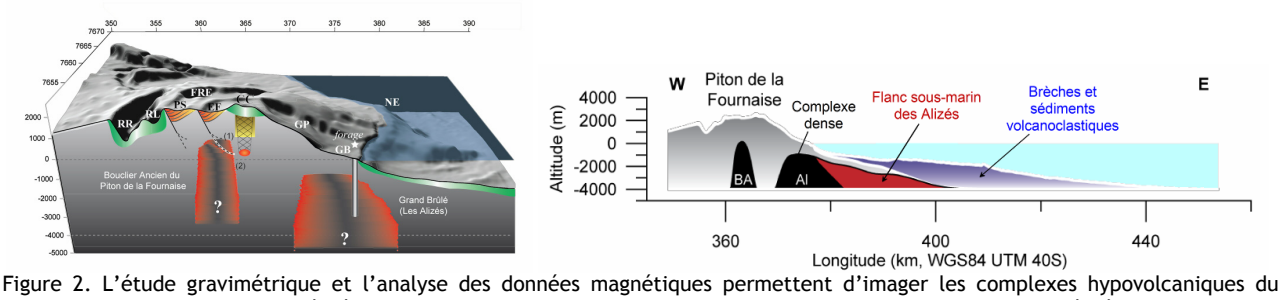

Figure 2. L'étude gravimétrique et l'analyse des données magnétiques permettent d'imager les complexes hypovolcaniques du Piton de la fournaise et des Alizés (à gauche) et de visualiser l'extension en mer du flanc Est du volcan des Alizés (à droite).

le Piton de la Fournaise, (4) d'imager en carte et en coupe les complexes hypovolcaniques denses du volcan des Alizés et du Piton de la Fournaise, (5) de préciser l'extension du système hydrothermal à l'échelle de la caldera de l'Enclos et de visualiser l'épaisseur des terrains résistants correspondants au remplissage de la caldera, enfin (6) de montrer que la morphologie actuelle de ce volcan dépend étroitement de l'interaction entre l'érosion et les épisodes volcano-tectoniques (calderas, paléo-canyons et remplissages par les coulées, glissements), la permanence et la constance de cette interaction au cours du temps étant une des caractéristiques essentielles de ce type de volcan bouclier.

Formation des calderas. Le modèle standard de formation des calderas implique la vidange du réservoir magmatique sous-jacent et l'effondrement du toit rigide dans l'espace ainsi libérée. Dans de nombreux cas, les volcans ne possèdent pas un réservoir de taille suffisante pour expliquer la formation des grandes calderas pluri-kilométriques, en particulier pour les volcans basaltiques. Un nouveau modèle structural, alternatif au modèle standard, a été proposé. Les études de polarisation spontanée révèlent que les calderas sont le siège d'une intense circulation de fluides hydrothermaux contrôlée par les discontinuités structurales [197]. Des modélisations analogiques ont montré que le cœur altéré d'un édifice volcanique pouvait fluer provoquant l'effondrement vertical du couvercle résistant et former des structures caldériques de grande taille [64, 324]. Ce nouveau modèle de formation des calderas a été appliqué à la caldera de l'Enclos au Piton de la Fournaise, ainsi qu'à d'autres volcans.

3. Dynamique et suivi des panaches de cendres volcaniques

Participants LMV permanents : F. Donnadieu, P. Labazuy, S. Moune, A. Harris, J.-L. LePennec, L. Gurioli.

Objectifs : Le Laboratoire possède une combinaison unique de techniques de télédétection sol et satellite très favorable à l'étude de la dynamique, de la charge et de la dispersion des panaches de cendres. Quelques résultats tirés des radars Doppler sol et de l'imagerie satellitaire MSG sont présentés.

Quantifier la dynamique des panaches de cendres par radar Doppler sol. La modélisation des signaux radar d'éruptions de l'Etna en 2001 a permis d'améliorer l'interprétation des signaux temporels et spectraux en termes de paramètres éruptifs. L'analyse statistique possible grâce à la continuité des enregistrements et la haute résolution temporelle, permet de caractériser les vitesses initiales et leur évolution, voire des flux de gaz minimums, la distribution spatiale des éjectas (uniforme vs. Gaussienne, [305]). L'inversion de la puissance

radar pour quantifier les masses de pyroclastes, les flux massiques, les concentrations particulaires, les énergies cinétique et thermique des explosions est un résultat majeur [150]. Il ouvre la voie à une quantification de la dynamique et de la charge des panaches de cendres, en particulier à l'Etna où un radar Doppler de l'OPGC effectue la surveillance continue des cratères sommitaux depuis 2009. Le couplage des méthodes géophysiques [232], géochimiques [327] et texturales [308] est un autre outil puissant pour donner une image plus complète de la dynamique éruptive, depuis les processus de dégazage en profondeur jusqu'à l'activité en surface. A l'Arenal les caractéristiques des signaux radars sont en accord avec le modèle de clarinette magmatique suggéré pour la genèse du tremor, mais l'association du radar avec des sismomètres LB et des capteurs acoustiques montre une grande variabilité des signaux [1025] et un caractère non systématique des corrélations et des répartitions d'énergie, qui conduisent à envisager des processus de dégazage plus complexes que ceux des modèles de conduit actuels (S. Valade, thèse en cours).

Etude et surveillance de l'activité volcanique par télédétection spatiale et sol infrarouge. Ce projet d'étude a été initié depuis 2006, en synergie avec les autres thématiques de télédétection spatiale et in-situ, développées au LMV. L'étude de l'éruption de l'Eyjafjöll (Islande) en avril-mai 2010 (Figure 3) est une démonstration claire de l'expertise de notre groupe en télédétection spatiale basée sur l'imagerie satellitale, dans l'infrarouge et l'ultraviolet, pour la caractérisation et la quantification des émissions volcaniques (cendres, aérosols, …) liées à une activité éruptive.

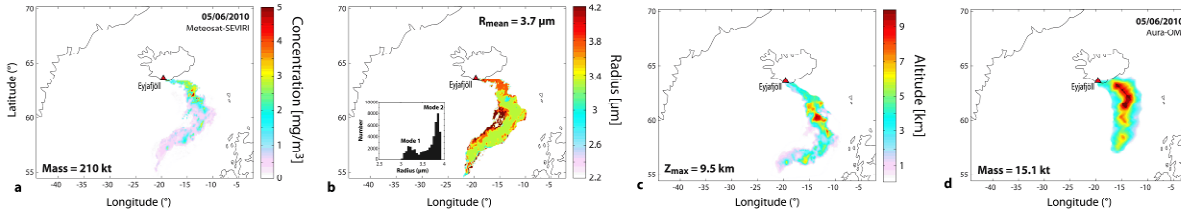

Figure 3. Distribution quantitative des produits volcaniques. L'inversion des données Météosat-SEVIRI IR permet l'estimation de divers produits volcaniques, comme (a) la concentration en cendres, (b) le rayon des cendres, (c) l'altitude du panache de cendres et (4) and (d) la teneur en SO_2.

Les travaux engagés récemment (Y. Guéhenneux, thèse en cours) s'appuient sur les données à basse résolution spatiale et haute résolution temporelle des satellites géostationnaires, qui sont d'un intérêt majeur pour la surveillance quasi temps réel de l'activité volcanique. Les satellites météorologiques Météosat Seconde Génération (MSG), à très haute répétitivité temporelle (une image toutes les 15 minutes) et grande couverture spectrale, représentent de formidables outils pour la détection, la surveillance et l'analyse des anomalies thermiques volcaniques et des panaches de cendres volcaniques (Gouhier et al., soumis). Ce volet est renforcé par la formidable opportunité de disposer d'une série de données de référence unique, grâce à la base de données en cours de constitution au sein du Service d'Observation HotVolc à l'OPGC.

Un autre axe de recherche (Postdoc M. Gouhier) concerne la détection et l'estimation quantitative des produits de panaches volcaniques (cendres, eau/glace, SO_2, …), par les méthodes d'analyse spectrale, dans les domaines de l'infrarouge et de l'ultraviolet. Les modèles d'inversion des données satellites, développés au LMV permettent l'estimation quantitative au premier ordre de la teneur des différents produits de l'éruption (Figure 3 ; Gouhier et al., soumis).

4. Géophysique volcanique : Transferts de magma

Participants LMV permanents. J. Battaglia, V. Cayol, J.-L. Froger, T. Souriot.

Objectifs. Cette thématique concerne la détection des transferts de magma et la compréhension des mécanismes qui gouvernent ces transferts. Pour cela, nous mesurons les déplacements et les accélérations du sol et les variations de gravité. Nous analysons également des données de géologie structurale. Afin d'interpréter ces différentes données, nous utilisons des méthodes combinant modélisations 3D et inversions ou des modélisations analogiques.

Détection de transferts de magma. La méthode principale utilisée au LMV pour la détermination des transferts de magma est la mesure des déplacements de surface par interférométrie radar (InSAR). Cette méthode permet de déterminer les déplacements sur de grandes surfaces avec une précision centimétrique. Les sites que nous avons étudiés avec cette méthode sont les suivants :

- Le Piton de la Fournaise (île de la Réunion). Ce volcan est l'objet d'une surveillance particulière puisque, depuis 2003, des images satellitales radar sont systématiquement acquises sur le volcan. Elles ont permis de caractériser les déplacements du sol associés à une vingtaine d'éruptions. Ces données, traitées dans le cadre du Service d'Observation OPGC VOLInSAR, sont mises à disposition de la communauté via l'interface web CASOAR (https://wwwobs.univ-bpclermont.fr/lmv/RV/casoar/), conçue pour la gestion

et la consultation de grandes bases de données.

- Sur le complexe volcanique Cordon del Azufre – Lastaria (Chili-Argentine), des données d'interférométrie radar ont permis de détecter une inflation de grande étendue dont la modélisation a montré qu'elle était due à la mise en pression d'une source magmatique profonde [82].

En parallèle, des données de sismicité très large bande sont utilisées pour déterminer les mouvements de magma. Toutefois, ces données sont surtout sensibles aux variations d'inclinaisons et il faut les utiliser en les combinant à d'autres données pour obtenir des interprétations fiables [205].

Interprétations des données. Afin d'analyser les mesures de déplacements, nous combinons des modélisations numériques 3D à des inversions par méthodes d'optimisation locales (algorithme de Levenberg-Marquardt) ou globales (proches voisins). Ces analyses ont été utilisées pour diverses études.

- Au Piton de la Fournaise, ces inversions ont été utilisées pour les éruptions qui se sont produites entre mars 1998 et juin 2000. Nous avons montré [301] qu'après une phase de propagation verticale, les dikes se propageaient latéralement à environ 1000 m sous la topographie (Figure 4). Il est probable que ces changements dans la direction de propagation du magma soient guidés par la présence d'un niveau de flottabilité neutre.

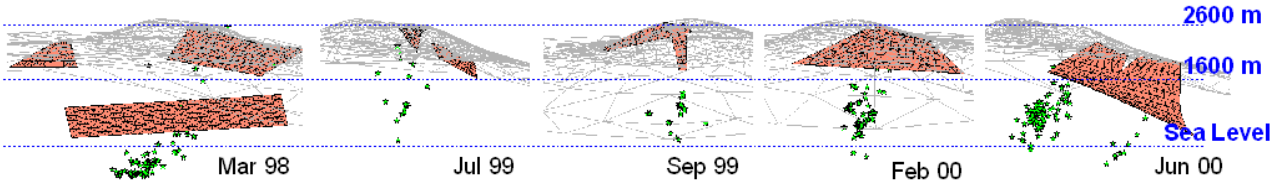

Figure 4. L'analyse de données d'interférométrie radar par une méthode combinant modélisations 3D et inversions a permis de modéliser les dikes mis en place entre 1998 et 2000

- Au Nyiragongo (Thèse C. Wauthier) pour l'éruption de février 2002, nous avons montré que les déplacements enregistrés par InSAR dans la région de Goma, étaient dus à l'action combinée du dike associé à la fissure éruptive, et d'un autre dike plus profond situé sous le lac Kivu.

Ces méthodes 3D sont précises mais lentes numériquement. Aussi, une autre méthode d'analyse des déplacements basée sur la superposition de sources ponctuelles, et faisant une hypothèse de faible topographie et de continuité des sources a été développée et testée pour l'étude des déplacements post-effondrement de 2007 de la zone sommitale du Piton de la Fournaise (Thèse A. Augier).

List of publications

2010

1. Andrade SD, van Wyk de Vries B (2010) Structural analysis of the early stages of catastrophic stratovolcano flank-collapse using analogue models. *Bulletin of Volcanology* **72**, 771-789, doi 10.1007/s00445-010-0363-x.
2. Applegarth LJ, James MR, van Wyk de Vries B, Pinkerton H (2010) The influence of surface clinker on the crustal structures and dynamics of `a`a- lava flows. *Journal of geophysical Research* **115**, B07210, doi:10.1029/2009JB006965.
3. Borgia A, Aubert M, Merle O, van Wyk de Vries B (2010) What is a volcano? *Geological Society of America, special publications* **479**, 1-9, doi: 10.1130/2010.2470(01).
4. Burgisser A, Poussineau S, Arbaret L, Druitt TH, Giachetti T, Bourdier JL (2010) Pre-explosive conduit conditions of the 1997 Vulcanian explosions at Soufrière Hills Volcano (Montserrat): I. Pressure and vesicularity distributions. *Journal of Volcanology and Geothermal Research* **194**, 27-41, doi:10.1016/j.jvolgeores.2010.04.008.
5. Calvari S, Lodato L, Steffke A, Cristaldi A, Harris AJL, Spampinato L, Boschi E (2010) The 2007 Stromboli eruption: event chronology and effusion rates using thermal infrared data. *Journal of Geophysical Research* **115**, B04201, doi:10.1029/2009JB006478.
6. Davies A, Keszthelyi L, Harris AJL (2010) The Thermal Signature of Volcanic Eruptions on Io and Earth. *Journal of Volcanology and Geothermal Research* **194**, 75-99, doi:10.1016/j.jvolgeores.2010.04.009.
7. Davies T, McSaveney M, Kelfoun K (2010) Runout of the Soccompa volcanic debris avalanche, Chile: a mechanical explanation for low basal shear resistance. *Bulletin of Volcanology* **72**, 933-944, doi 10.1007/s00445-010-0372-9.
8. Delle Donne D, Harris AJL, Ripepe M, Wright R (2010) Earthquake-induced thermal anomalies at active volcanoes. *Geology* **38**, 771-774, doi: 10.1130/G30984.1.
9. Doyle EE, Cronin SJ, Cole SE, Thouret JC (2010) The coalescence and organization of lahars at Semeru volcano, Indonasia. *Bulletin of Volcanology* **72**, 961-970, doi 10.1007/s00445-010-0381-8.
10. Dumaisnil C, Thouret JC, Chambon G, Doyle EE, Cronin SJ (2010) Hydraulic, physical and rheological characteristics of rain-triggered lahars at Semeru volcano, Indonesia. *Earth Surface Processes and Landforms* **35**, 1573-1590, doi: 10.1002/esp.2003.

11. Elitok, O., Ozgür, N., Drüppel, K., Dilek, Y., Platevoet, B., Guillou, H., Poisson, A., Scaillet, S., Satir, M., Siebel, W., Bardintzeff, J.M., Deniel**, C.** & Yilmaz, K. (2010). Origin and geodynamic evolution of Late Cenozoic potassium-rich volcanism in the Isparta area, southwestern Turkey. International Geology Review, 52, 4-6, 454-504. DOI: 10.1080/00206810902951411.
12. Favalli M, Fornaciai A, Mazzarini F, Harris A, Neri M, Behncke B, Pareschi MT, Tarquini S, Boschi E (2010) Evolution of an active lava flow field using a multitemporal LIDAR acquisition. *Journal of geophysical Research* **115**, B11203, doi:10.1029/2010JB007463.
13. Favalli M, Harris AJL, Fornaciai A, Pareschi MT, Mazzarini F (2010) The distal segment of Etna's 2001 basaltic lava flow. *Bulletin of Volcanology* **72**, 119-127, doi:10.1007/s00445-009-0300-z.
14. Fukushima Y, Cayol V, Durand P, Massonnet D (2010) Evolution of magma conduits during the 1998–2000 eruptions of Piton de la Fournaise volcano, Réunion Island. *Journal of Geophysical Research* **115**, B10204, doi:10.1029/2009JB007023.
15. *Giachetti T*, Druitt TH, Burgisser A, Arbaret L, Galven C (2010) Bubble nucleation and growth during the 1997 Vulcanian explosions of Soufrière Hills Volcano, Montserrat. *Journal of Volcanology and Geothermal Research* **193**, 215-231, doi:10.1016/j.jvolgeores.2010.04.001.
16. Girolami L, Roche O, Druitt TH, Corpetti T (2010) Particle velocity fields and depositional processes in laboratory ash flows, with implications for the sedimentation of dense pyroclastic flows. *Bulletin of Volcanology* **72**, 747-759, doi:10.1007/s00445-010-0356-9.
17. Gouhier M, Donnadieu F (2010) The geometry of Strombolian explosions: insights from Doppler radar measurements. *Geophysical Journal International* **183**, 1376–1391 doi: 10.1111/j.1365-246X.2010.04829.x.
18. Gunnell Y, Thouret JC, Brichau S, Carter A, Gallagher K (2010) Low-temperature thermochronology in the Peruvian Central Andes: implications for long-term continental denudation, timing of plateau uplift, canyon incision, and lithosphere dynamics. *Journal of the Geological Society, London* **167**, 803-815 Doi:10.1144/0016-76492009-166.
19. Gurioli L, Sulpizio R, Cioni R, Sbrana A, Luperini W, Santacroce R, Andronico D (2010) Pyroclastic flow hazard assessment at Somma-Vesuvius based on the geological record. *Bulletin of Volcanology* **72**, 1021-1038, doi 10.1007/s00445-010-0379-2.
20. Harris AJL, Favalli M, Steffke A, Fornaciai A, Boschi E (2010) A relation between lava discharge rate, thermal insulation, and flow area set using lidar data. Geophysical Research *Letters,* **37**, L20308, doi:10.1029/2010GL044683.
21. Kelfoun K, Giachetti T, Labazuy P (2010) Landslide–generated tsunamis at Réunion Island. *Journal of Geophysical Research, Earth Surface* **115**, F04012, doi:10.1029/2009JF001381.
22. Kervyn M, Boone MN, van Wyk de Vries B, Lebas E, Cnudde V, Fontijn K, Jacobs P (2010) 3D imaging of volcano gravitational deformation 3 by computerized X-ray micro-tomography. *Geosphere* **6**, 482-498; doi: 10.1130/GES00564.1.
23. Mangeney A, Roche O, Hungr O, Mangold N, Faccanoni G, Lucas A (2010) Erosion and mobility in granular collapse over sloping beds. *Journal of Geophysical Research – Earth Surface* **115**, F03040, doi:10.1029/2009JF001462.
24. Merle O, Barde-Cabusson S, van Wyk de Vries B (2010) Hydrothermal calderas. *Bulletin of Volcanology* **72**, 131-147, doi: 10.1007/s00445-009-0314-6.
25. Merle O, Mairine P, Michon L, Bachèlery P, Smietana M (2010) Calderas, Landslides and Paleo-canyons on Piton de la Fournaise Volcano (La Réunion Island, Indian Ocean). *Journal of Volcanology and Geothermal Research* **189**, 131-142.
26. Meruane C, Tamburrino A, Roche O (2010) On the role of the ambient fluid on gravitational granular flow dynamics. *Journal of Fluid Mechanics* **648**, 381-404, doi: 10.1017/S0022112009993181.
27. Miallier D., Boivin P., Deniel C., Gourgaud A., Lanos P., Sforna M., Pilleyre, T. (2010) : The ultimate summit eruption of Puy de Dôme volcano (Chaîne des Puys, French Massif Central) about 10,700 years ago. C R Geoscience 342, 847-854, doi:10.1016/j.crte.2010.09.004.
28. Moune S, Gauthier P-J, Delmelle P (2010) Trace elements in the particulate phase of the plume of Masaya volcano, Nicaragua. *Journal of Volcanology and Geothermal Research* **193**, 232-244, doi:10.1016/j.jvolgeores.2010.04.004.
29. Ripepe M, Marchetti E, Bonadonna C, Harris AJL, Pioli L, Ulivieri G (2010) Monochromatic Infrasonic Tremor Driven by Lava Lake Degassing and Convection at Villarrica Volcano, Chile. *Geophysical Research Letters* **37**, L15303, doi:10.1029/2010GL043516.
30. Rivera M, Thouret J-C, Marino J, Berolatti R, Fuentes J (2010) Characteristics and management of the 2006-2008 volcanic crisis at the Ubinas volcano (Peru). *Journal of Volcanology and Geothermal Research* **198**, 19-34, doi:10.1016/j.jvolgeores.2010.07.020.
31. Robin C, Samaniego P, Le Pennec JL, Fornari M, Mothes P, van der Plicht J (2010) New radiometric and petrological constraints on the evolution of the Pichincha volcanic complex (Ecuador). *Bulletin of Volcanology* **72**, 1109-1129, doi: 10.1007/s00445-010-0389-0.
32. Roche O, Montserrat S, Niño Y, Tamburrino A (2010) Pore fluid pressure and internal kinematics of gravitational laboratory air-particle flows : insights into the emplacement dynamics of pyroclastic flows. *Journal of Geophysical Research – Solid Earth* **115**, B09206, doi:10.1029/2009JB007133.
33. Samaniego P, Robin C, Chazot G, Bourdon E, Cotten J (2010) Evolving metasomatic agent in the Northern Andean subduction zone, deduced from magma composition of the long-lived Pichincha volcanic complex (Ecuador). *Contribution to Mineralogy and Petrology*, doi 10.1007/s00410-009-0475-5

34. Schiano P, Monzier M, Eissen J-P, Martin H, Koga KT (2010) Simple mixing as the major control of the evolution of volcanic suites in the Ecuadorian Andes. *Contribution to Mineralogy and Petrology* **160**, 297-312, doi: 10.1007/s00410-009-0478-2.
35. Shea T, Gurioli L, Larsen J, Houghton BF, Hammer JE, Cashman KV (2010) Linking experimental and natural textures in Vesuvius 79AD white pumice. *Journal Volcanology and Geothermal Research* **192**, 69-84, doi: 10.1016/j.jvolgeores.2010.02.013.
36. Shea T, Houghton BF, Gurioli L, Cashman KV, Hammer JE, Hobden BJ (2010) Textural studies of vesicles in volcanic rocks: an integrated methodology. *Journal Volcanology and Geothermal Research*, doi:10.1016/j.jvolgeores.2009.12.
37. Shea T, van Wyk de Vries B (2010) Collapsing volcanoes: the sleeping giants' threat: Geohazards Explained. *Geology Today* **26**, 72-77.
38. Silva Parejas C, Druitt TH, Robin C, Moreno H, Naranjo JA (2010) The holocene Pucon eruption of volcan Villarrica, Chile: deposit architecture and eruption chronology. *Bulletin of Volcanology* **72**, 677-692.
39. Singh RP, Medhi W, Gauta R, Senthil Kumar J, Zlotnicki J, Kafatos M (2010) Precursory Signals Using Satellite and Ground data Associated with the Wenchuan Earthquake of 12 May, 2008. *International Journal of Remote Sensing* **31**, 3341-3354.
40. Steffke AM, Fee D, Garces M, Harris A (2010) Eruption chronologies, plume heights and eruption styles at Tungurahua Volcano: Integrating remote sensing techniques and infrasound. *Journal of Volcanology and Geothermal Research* **193**, 143-160, doi:10.1016/j.jvolgeores.2010.03.004.
41. Temel A, Yürür T, Alici P, Varol E, Gourgaud A, Bellon H, Demirbag H (2010) Alkaline series related to early-Middle Miocene intra-continental rifting in a collision zone: an example from Polatli, Central Anatolia, Turkey. *Journal of Asian Earth Sciences* **38**, 289-306.
42. Thouret JC (2010) Volcanic hazards and ricks: a geomorphological perspective. In: eIA-AaAS Goudie (ed.)*Geomorphological Hazards and Disaster Prevention*. pp. 13-32. Cambridge University Press.
43. Thouret JC, Gupta A, Lube G, Cronin SJ, Surono (2010) Analysis of the 2006 eruption deposits of Merapi Volcano, Java, Indonesia, using high-resolution IKONOS images and complementary ground based observations. *Remote Sensing of Environment* **114**, 1949-1967, doi: 10.106/j.rse.2010.03.016.
44. Vargas Franco R, Thouret JC, Delaite G, van Westen C, Sheridan MF, Siebe C, Mariño J, Souriot T, Stinton A (2010) *Mapping and assessing volcanic hazards and risks in the city of Arequipa, Peru, based on GIS techniques*. In G Groppelli & L. Viereck-Goette, eds.,'Stratigraphy and Geology of volcanic areas', Geological Society of America Special Publication SPE464.
45. Zlotnicki J, Li F, Parrot M (2010) Signals recorded by DEMETER satellite over active volcanoes during the period September 2004 – December 2007. *Geophysical Journal International* **183**, 1332-1347, doi: 10.1111/j.1365-246X.2010.04785.x.

2009

1. Aldanmaz E, Schmidt MW, Gourgaud A, Meisel T (2009) Mid-ocean ridge and supra-subduction geochemical signatures in spinel–peridotites from the Neotethyan ophiolites in SW Turkey: Implications for upper mantle melting processes. *Lithos* **113**, 691-708, doi:10.1016/j.lithos.2009.03.010.
2. Barde-Cabusson S, Levieux G, Lénat, J.F., Finizola, A., Revil, A., Chaput, M., Dumont, S., Duputel, Z., Guy , A., Mathieu, L., Saumet, S., Sorbadère, F., Vieille, M. (2009) Transient self-potential anomalies associated with recent lava flows at Piton de la Fournaise volcano (Réunion Island, Indian Ocean). *Journal of Volcanology and Geothermal Research* **187**, 158-166, doi:10.1016/j.jvolgeores.2009.09.003.
3. Battaglia J, Cayol V (2009) A comment on "Hidden dykes detected on ultra long period seismic signals at Piton de la Fournaise volcano?" by N. Houlié and J.-P. Montagner, EPSL 261, (2007). *Earth and Planetary Science Letters* **287**, 284-287, doi:10.1016/j.epsl.2009.06.023.
4. Bernard B, van Wyk de Vries B, Leyrit H (2009) Distinguishing volcanic debris avalanche deposits from their reworked products: the Perrier sequence (Franch Massif Central). *Bulletin of Volcanology* **71**, 1041-1056, doi: 10.1007/s00445-009-0285-7.
5. Byrne PK, van Wyk de Vries B, Murray JB, Troll VR (2009) The geometry of volcano flank terraces on Mars. *Earth and Planetary Science Letters* **281**, 1-13, doi:10.1016/j.epsl.2009.01.043.
6. Deniel C. (2009): Heterogeneous initial Sr isotope compositions of highly evolved volcanic rocks from the Main Ethiopian Rift, Ethiopia. Bull Volc, 71, 5, 495-508, doi:10.1007/s00445-008-0228-8.
7. Finizola A, Aubert M, Revil A, Schütze C, Sortino F (2009) Importance of structural history in the summit area of Stromboli during the 2002–2003 eruptive crisis inferred from temperature, soil CO2, self-potential, and electrical resistivity tomography. *Journal of Volcanology and Geothermal Research* **183**, 213-227, doi:10.1016/j.jvolgeores.2009.04.002.
8. Gailler LS, Lénat JF, Lambert M, Levieux G, Villeneuve N, Froger JL (2009) Gravity structure of Piton de la Fournaise volcano and inferred mass transfer during the 2007 crisis. *Journal of Volcanology and Geothermal Research* **184**, 31-48, doi:10.1016/j.jvolgeores.2009.01.024.
9. Gonzales K, Froger JL, Audin L, Orlando M (2009) Ejemplos de deformación producto de la tectonica extensiva de los Andes Centrales, zonas de Huambo-Cabanaconde (Arequipa) y Calacoa-Huaytire (Moquegua), Vistos Por Interferometria Radar – InSAR. *Earth and Planetary Science Letters* **255**.
10. Grosse P, van Wyk de Vries B, Petrinovic IA, Euillades PA, Alvarado GE (2009) Morphometry and evolution of arc volcanoes. *Geology* **37**, 651-654, doi: 10.1130/G25734A.1.
11. Harris AJL, Baloga SM (2009) Lava discharge rates from satellite-measured heat flux. *Geophysical Research Letters* **36**, L19302, doi:10.1029/2009GL039717.

12. Kelfoun K, Samaniego P, Palacios P, Barba D (2009) Testing the suitability of frictional behaviour for pyroclastic flow simulation by comparison with a well-constrained eruption at Tungurahua volcano (Ecuador). *Bulletin of Volcanology* **71**, 1057-1075, doi: 10.1007/s00445-009-0286-6.
13. Kervyn M, Ernst GGJ, van Wyk de Vries B, Mathieu L, Jacobs P (2009) Volcano load control on dyke propagation and vent distribution: Insights from analogue modeling. *Journal of Geophysical Research* **114**, B03401, doi:10.1029/2008JB005653.
14. Lénat JF, Boivin P, Deniel C, Gillot P-Y, Bachèlery P, 1 FT (2009) Age and nature of deposits on the submarine flanks of Piton de la Fournaise (Reunion Island). *Journal of Volcanology and Geothermal Research* **184**, 199-207, doi:10.1016/j.jvolgeores.2009.01.013.
15. Lénat JF, Merle O, Lespagnol L (2009) La réunion: An example of channeled hot spot plume. *Journal of Volcanology and Geothermal Research* **184**, 1-13, doi:10.1016/j.jvolgeores.2008.12.001.
16. Mathieu L, Van Wyk de Vries B (2009) Edifice and substrata deformation induced by intrusive complexes and gravitational loading in the Mull volcano (Scotland). *Bulletin of Volcanology* **71**, 1133-1148, doi: 10.1007/s00445-009-0295-5.
17. Michon L, Cayol V, Letourneur L, Peltier A, Villeneuve N, Staudacher T (2009) Edifice growth, deformation and rift zone development in basaltic setting: Insights from Piton de la Fournaise shield volcano (Réunion Island). *Journal of Volcanology and Geothermal Research* **184**, 14-30, doi:10.1016/j.jvolgeores.2008.11.002.
18. Michon L, Villeneuve N, Catry T, Merle O (2009) How summit calderas collapse on basaltic volcanoes: New insights from the April 2007 caldera collapse of Piton de la Fournaise volcano. *Journal of Volcanology and Geothermal Research* **184**, 138-151, doi:10.1016/j.jvolgeores.2008.11.003.
19. Mora M, Lesage P, Donnadieu F, Valade S, Schmidt A, Soto G, Taylor W, Alvarado G (2009) Joint Seismic, Acoustic and Doppler Radar observations at Arenal Volcano, Costa Rica: preliminary results. In: CJ Bean, Braiden, A. K., Lokmer, I., Martini, F., O'Brien, G. S. (ed.)*Volume project / Volcanoes: Understanding subsurface mass movement*. pp. 330-340.
20. Moune S, Holtz F, Botcharnikov RE (2009) Sulphur solubility in andesitic to basaltic melts: implications for Hekla volcano. *Contributions to Mineralogy and Petrology* **157**, 691-707, doi: 10.1007/s00410-008-0359-0.
21. Murray JB, van Wyk de Vries B, al. e (2009) Late-stage water eruptions from Ascraeus Mons volcano, Mars: Implications for its structure and history. *Earth and Planetary Science Letters*, doi:10.1016/j.epsl.2009.06.020.
22. Peltier A, Hurst T, Scott B, Cayol V (2009) Structures involved in the vertical deformation at Lake Taupo (New Zealand) between 1979 and 2007: New insights from numerical modelling. *Journal of Geophysical Research* **181**, 173–184, doi:10.1016/j.jvolgeores.2009.01.017.
23. Peltier A, Staudacher T, Bachèlery B, Cayol V (2009) Formation of the April 2007 caldera collapse at Piton de La Fournaise volcano: Insights from GPS data. *Journal of Volcanology and Geothermal Research* **184**, 152-163, doi:10.1016/j.jvolgeores.2008.09.009.
24. Prôno E, Battaglia J, Monteiller V, Got JL, Ferrazzini V (2009) P-wave velocity structure of Piton de la Fournaise volcano deduced from seismic data recorded between 1996 and 1999. *Journal of Volcanology and Geothermal Research* **184**, 49-62, doi:10.1016/j.jvolgeores.2008.12.009.
25. Robin C, Eissen J, Samaniego P, Martin H, Hall M, Cotten J (2009) Evolution of the late Pleistocene Mojanda–Fuya Fuya volcanic complex (Ecuador), by progressive adakitic involvement in mantle magma sources. *Bulletin of Volcanology* **71**, 233-258, doi: 10.1007/s00445-008-0219-9.
26. Sahetapy-Engel ST, Harris AJL (2009) Thermal structure and heat loss at the summit crater of an active lava dome. *Bulletin of Volcanology* **71**, 15-28, doi: 10.1007/s00445-008-0204-3.
27. Sahetapy-Engel ST, Harris AJL (2009) Thermal-image-derived dynamics of vertical ash plumes at Santiaguito volcano, Guatemala. *Bulletin of Volcanology* **71**, 827-830, doi: 10.1007/s00445-009-0284-8.
28. Shea T, Larsen J, Gurioli L, Houghton B, Hammer J, Cioni R (2009) Leucite crystals: surviving witnesses of the pre-eruptive magma chamber of the 79AD eruption at Vesuvius, Italy. *Earth Planetary Science Letters*, doi:10.1016/j.epsl.2009.02.014.
29. Thouret JC (2009) Volcanic Hazards and Risks: a Review with a geomorphological Perspective. In: IGA Alcantayala (ed.)*Geomorphological Hazards, chap 3*. pp. 13-32. Cambridge University Press.
30. Thouret JC, Gupta A, Lube G, Cronin SJ, Surono (2009) Analysis of the 2006 eruption deposits of Merapi Volcano, Java, Indonesia, using high-resolution IKONOS images and complementary ground based observations. *Remote Sensing of Environment*, doi:10.1016/j.rse.2010.03.016.
31. Vargas Franco R, Thouret JC, Delaite G, van Westen C, Sheridan MF, Siebe C, Marino J, Souriot T, Stinton A (2009) Mapping and Assessing Volcanic Hazards and Risks in the city of Arequipa, Peru, based on GIS techniques. In: GG Viereck-Goette (ed.)*Stratigraphy and Geology of volcanic areas*. Geological Society of America Special Publication SPE464, Chap 13.
32. Vlastelic I., Deniel C., Bosq C., Telouk P., Boivin P., Bachelery P., Famin V., Staudacher T. (2009): Pb isotope geochemistry of Piton de la Fournaise historical lavas. J Volcanol Geotherm Res, 184, 1-2, 63-78, doi:10.1016/j.jvolgeores.2008.08.008.
33. Wooler L, van Wyk de Vries B, Cecchi E, Rymer H (2009) Analogue models of the effect on long-term basement fault movement on volcanic edifices. *Bulletin of Volcanology* **71**, 1111-1131, doi 10.1007/s00445-009-0289-3.
34. Zlotnicki J, Sasai Y*, et al.* (2009) Combined electromagnetic, geochemical and thermal surveys of Taal volcano (Philippines) during the period 2005–2006. *Bulletin of Volcanology* **71**, 29-47, doi: 10.1007/s00445-008-0205-2.
35. Zlotnicki J, Sasai Y*, et al.* (2009) Electromagnetic and geochemical methods applied to investigations of hydrothermal/volcanic unrests: Examples of Taal (Philippines) and Miyake-jima (Japan) volcanoes. *Physics and Chemistry of the Earth* **34**, 394-408, doi:10.1016/j.pce.2008.09.012.

2008

1. Arellano SR, Hall M, Samaniego P, Le Pennec JL, Ruiz A, Molina I, Yepes H (2008) Degassing patterns of Tungurahua volcano (Ecuador) during the 1999–2006 eruptive period, inferred from remote spectroscopic measurements of SO2 emissions. *Journal of Volcanology and Geothermal Research* **176**, 151-162, doi:10.1016/j.jvolgeores.2008.07.007.
2. Aubert M, Diliberto S, Finizola A, Chébli Y (2008) Double origin of hydrothermal convective flux variations in the Fossa of Vulcano (Italy). *Bulletin of Volcanology* **70**, 743-751, Doi:10.1007/s00445-007-0165-y.
3. Barba D, Robin C, Samaniego P, Eissen JP (2008) Recurrent Pyroclastic flows at Chimborazo Volcano, between ~8000 and ~1000 yr BP. *Journal of Volcanology and Geothermal Research* **176**, 27-35.
4. Battaglia J, Zollo A, Virieux J, Iacono D (2008) Merging active and passive data sets in traveltime tomography: the case study of Campi Flegrei caldera (Southern Italy). *Geophysical Prospecting* **56**, 555-573.
5. Bernard B, Wyk de Vries van B, Barba D, Leyrit H, Robin C, Alcaraz S, Samaniego P (2008) The Chimborazo sector collapse and debris avalanche: Deposit characteristics as evidence of emplacement mechanisms. *Journal of Volcanology and Geothermal Research* **176**, 36-73, doi:10.1016/j.jvolgeores.2008.03.012.
6. Buisson C, Merle O (2008) A universal method to compute the finite strain ellipsoid for any strain combination. In: SJLaGM Hammler (ed.)*Structural Geology : New Research*. Nova Sciences publisher Inc., chapter 7.
7. Cesca S, Battaglia J, Dahm T, Tessmer E, Heimann S, Okubo P (2008) Effects of topography and crustal heterogeneities on the source estimation of LP event at Kilauea volcano. *Geophysical Journal International* **172**, 1219-1236, doi:10.1111/j.1365-246X.2007.03695.x.
8. Delcamp A, Van Wyk de Vries B, James MR (2008) The influence of edifice slope and substrata on volcano spreading. *Journal of Volcanology and Geothermal Research* **177**, 925-943, doi:10.1016/j.jvolgeores.2008.07.014.
9. Ersoy O, Aydar E, Gourgaud A, Bayhan H (2008) Quantitative analysis on volcanic ash surfaces : application of extended depth-of-field (focus) algorithm for light and scanning electron microscopy and 3D reconstruction. *Micron* **39**.
10. Girolami L, Druitt TH, Roche O, Khrabrykh Z (2008) Propagation and hindered settling of laboratory ash flows. *Journal of Geophysical Research* **113**, B02202, doi/10.1029/2007JB005074.
11. Gouhier M, Donnadieu F (2008) Mass estimations of ejecta from Strombolian explosions by inversion of Doppler radar measurements. *Journal of Geophysical Research* **113**, B10202, doi:10.1029/2007JB005383.
12. Hall M, Samaniego P, Le Pennec JL, Johnson JS (2008) Ecuadorian Andes volcanism: A review of Late Pliocene to present activity. *Journal of Volcanology and Geothermal Research* **176**, 1-6, doi:10.1016/j.jvolgeores.2008.06.012.
13. Hoffer G, Eissen JP, Beate B, Bourdon E, Fornari M, Cotten J (2008) Geochemical and petrological constraints on rear-arc magma genesis processes in Ecuador: The Puyo cones and Mera lavas volcanic formations. *Journal of Volcanology and Geothermal Research* **176**, 107-118.
14. Holohan EP, Troll VR, van Wyk de Vries B, Walsh JJ, Walter TR (2008) Unzipping Long Valley: an explanation for vent migration patterns during an elliptical ring fracture eruption. *Geology* **36**, 323-326.
15. Holohan EP, Wyk de Vries van B, Troll VR (2008) Analogue models of caldera collapse in strike-slip tectonic regimes. *Bulletin of Volcanology* **70**, 773-796, DOI 10.1007/s00445-007-0166-x.
16. Kelfoun K, Druitt TH, Wyk de Vries van B, Guilbaud MN (2008) Topographic reflection of Socompa debris avalanche, Chile. *Bulletin of Volcanology* **70**, 1169-1187, doi:10.1007/s00445-008-0201-6.
17. Le Pennec JL, Java D, Samaniego P, Ramón P, Moreno Yánez S, Egred J, van der Plicht J (2008) The AD 1300–1700 eruptive periods at Tungurahua volcano, Ecuador, revealed by historical narratives, stratigraphy and radiocarbon dating. *Journal of Volcanology and Geothermal Research* **176**, 70-81, doi:10.1016/j.jvolgeores.2008.05.019.
18. Liew SC, Thouret JC, Gupta A, Kwoh LK (2008) First Satellite Image of a Moving Pyroclastic Flow. *EOS, Transactions American Geophysical Union* **89**, doi:10.1029/2008EO220002.
19. Loock S, Diot H, Van Wyk de Vries B, Launeau P, Merle O, Vadeboin F, Petronis MS (2008) Lava flow internal structure found from AMS and textural data: An example in methodology from the Chaîne des Puys, France. *Journal of Volcanology and Geothermal Research* **177**, 1092-1104, doi:10.1016/j.jvolgeores.2008.08.017.
20. Mathieu L, van Wyk de Vries B, Holohan EP, Troll VR (2008) Dykes, cups, saucers and sills: analogue experiments on magma intrusion into brittle rocks. *Earth and Planetary Science Letters* **271**, 1-13, doi:10.1016/j.epsl.2008.02.020.
21. Merle O, Michon L, Bachèlery P (2008) Caldera rim collapse: A hidden volcanic hazard. *Journal of Volcanology and Geothermal Research* **177**, 525-530, doi:10.1016/j.jvolgeores.2008.06.011.
22. Paquereau-Lebti P, Fornari M, Roperch P, Thouret JC, Macedo O (2008) Paleomagnetism, magnetic fabric, and 40Ar/39Ar dating of Pliocene and Quaternary ignimbrites in the Arequipa area, southern Peru. *Bulletin of Volcanology* **70**, 977-997, DOI 10.1007/s00445-007-0181-y.
23. Peltier A, Famin V, Bachèlery P, Cayol V, Fukushima Y, Staudacher T (2008) Cyclic magma storages and transfers at Piton de La Fournaise volcano (La Réunion hotspot) inferred from deformation and geochemical data. *Earth and Planetary Science Letters* **270**, 180-188, doi:10.1016/j.epsl.2008.02.042.
24. Robin C, Samaniego P, Le Pennec JL, Mothes P, Van der Plicht J (2008) Late Holocene phases of dome growth and Plinian activity at Guagua Pichincha volcano (Ecuador). *Journal of Volcanology and Geothermal Research* **176**, 7-15, doi:10.1016/j.jvolgeores.2007.10.008.
25. Roche O, Montserrat S, Nino Y, Tamburrino A (2008) Experimental observations of water-like behavior of initially fluidized, dam break granular flows and their relevance for the propagation of ash-rich pyroclastic flows. *Journal of Geophysical Research* **B113**, B12203, doi:10.1029/2008JB005664.

26. Samaniego P, Eissen JP, Le Pennec JL, Robin C, Hall M, Mothes P, Chavrit D, Cotten J (2008) Pre-eruptive physical conditions of El Reventador volcano (Ecuador) inferred from the petrology of the 2002 and 2004–05 eruptions. *Journal of Volcanology and Geothermal Research* **176**, 82-93, doi:10.1016/j.jvolgeores.2008.03.004.
27. Shea T, Van Wyk de Vries B (2008) Structural analysis and analogue modeling of the kinematics and dynamics of rockslide avalanches. *Geosphere* **4**, 657-686, doi: 10.1130/GES00131.1.
28. Shea T, Wyk de Vries van B, Pilato M (2008) Emplacement mechanisms of contrasting debris avalanches at Volcan Mombacho (Nicaragua), provided by structural and facies analysis. *Bulletin of Volcanology* **70**, 899-921, doi 10.1007/s00445-007-0177-7.
29. Smellie JL, Johnson JS, McIntosh WC, Esser R, Gudmundsson MT, Hambrey MJ, Van Wyk de Vries B (2008) Six million years of glacial history recorded in volcanic lithofacies of the James Ross Island Volcanic Group, Antarctic Peninsula. *Palaeogeography, Palaeoclimatology, Palaeoecology* **260**, 122-148, doi:10.1016/j.palaeo.2007.08.011.
30. Ulusoy I, Labazuy P, Aydar E, Ersoy O, Cubukçu E (2008) Structure of the Nemrut caldera (Eastern Anatolia, Turkey) and associated hydrothermal fluid circulation. *Journal of Volcanology and Geothermal Research* **174**, 269-283, doi:10.1016/j.jvolgeores.2008.02.012.
31. Varol E, Temel A, Gourgaud A (2008) Textural and compositional evidence for magma mixing in the evolution of th Camhdere volcanic rocks (Galatean volcanic province), Central Anatolia, Turkey. *Turkish Journal of Earth Sciences* **17**, 709-727.

2007

1. 1 Barde-Cabusson S, Merle O (2007) From steep-slope volcano to flat caldera floor. *Geophysical Research Letter* **34**, L10305, doi: 10.1029/2007GL029784.
2. Bogoutdinov SR, Agayan SM, Gvishiani AD, Graeva EM, Rodkin MV, Zlotnicki J, Le Mouël JL (2007) Fuzzy Logic Algorithms in the Analysis of Electrotelluric Data with Reference to Monitoring of Volcanic Activity. Izvestiya. *Physics of the Solid Earth* **43**, 597-609.
3. Borgia A, Grieco G, Brondi F, Badali M, Merle O, Pasquarè G, Martielli L, di Nardo T (2007) Reply to comment by V. Picotti and F.J Pazzaglia on Shale diapirism in the Quaternary tectonic evolution of the Northern Apenine, Bologna, Italy. *Journal of geophysical Research* **112**, doi: 10.1029/20034JB003375.
4. Carter A, Van Wyk de Vires B, Kelfoun K, Bachèlery P, Briole P (2007) Pits, rifts and slumps: the summit structure of Piton de la Fournaise. *Bulletin of Volcanology* **69**, 741-756, doi:10.1007/s00445-006-0103-4.
5. Cubuckçu E, Aydar E, Gourgaud A (2007) Comments on « Volcanostratigraphy and petrogenesis of the Nemrut stratovolcano (East Anatolian High plateau) : the most recent post-collisional volcanism in Turkey » by Ozdemir et al. (Chemical Geology 226 (2006) 189-211. *Chemical Geology* **245**, 120-129.
6. Delacour A, Gerbe MC, Thouret JC, Wörner G, Paquereau-Lebti P (2007) Magma evolution of Quaternary minor volcanic centres in southern Peru, Central Andes. *Bulletin of Volcanology* **69**, 581-608. doi10.1007/s00445-006-0096-z.
7. Druitt TH, Avard G, Bruni G, Lettieri P, Maez F (2007) Gas retention in fine-grained pyroclastic flow materials at high temperatures *Bulletin of Volcanology* **69**, 881-901, doi 10.1007/s00445-007-0116-7.
8. Ersoy O, Aydar E, Gourgaud A, Artuner H, Bayhan H (2007) Clustering of volcanic ashes arising from different fragmentation mechanisms using Kohonen self-organizing maps. *Computer and Geosciences* **33**, 821-828.
9. Ersoy O, Gourgaud A, Aydar E, Chinga G, Thouret JC (2007) Quantitative scanning-electron microscope analysis of volcanic ash surfaces : application to the 1982-83 Galunggung eruption (Indonesia). *Geological Society of America Bulletin* **119**, 743-752.
10. Froger JL, Remy D, Bonvalot S, Legrand D (2007) Two scales of inflation at Lastarria-Cordon del Azufre volcanic complex, central Andes, revealed from ASAR-ENVISAT interferometric data. *Earth and Planetary Science Letters* **255**, 148-163.
11. Garcia-Aristizabal A, Kumagai H, Samaniego P, Mothes P, Yepes H, Monzier M (2007) Seismic, petrologic, and geodetic analyses of the 1999 dome-forming eruption of Guagua Pichincha volcano, Ecuador. *Journal of Volcanoloy and Geothermal Research* **161**, 333-351.
12. Holohan E, Van Wyk de Vries B, Troll TR (2007) Caldera collapse in strike-slip environments. *Bulletin of Volcanology* **7**, 773-776.
13. Hradecky P, Sébasta J, Havelick, P., Hrubes, M., Kyck, P., Mloch, B., Mrazova, S., Novack, Z., Opletal, M., Prichystal, A., Rapprich, V., Stanick, E., van wyk de Vries, B. *et al.* (2007) Map of the Nicarguan volcanic chain 1:200 000 eds. Hradecky P, Sebasta J. Czech Geological Survey ISBN 978-80-7075-671-3.
14. Huggel C, Ceballos JL, Pulgarin B, Ramirez J, Thouret JC (2007) Review and reassessment of hazards owing to volcano glacier interactions in Colombia. *Annals of Glaciology/ (The International Symposium on Earth and Mars Ice-Volcano Interactions, Reykjavik, Iceland, June 2006)* **45**, 115-127.
15. Kuentz A, Galán de Mera A, Ledru MP, Thouret JC (2007) Phytogeographical data and modern pollen rain of the puna belt in southern Peru (Nevado Coropuna, Western Cordillera). *Journal of Biogeography* **34**, 1762-1776.
16. Lénat JF (2007) Retrieving Self Potential anomalies in a complex volcanic environment : a SP/elevation gradient approach. *Near Surface Geophysics*, 161-170.
17. Meloni A, Zlotnicki J (2007) Electromagnetic Studies of Earthquakes and Volcanoes,. *Annals of Geophysics* **50**.
18. Moune S, Faure F, Gauthier PJ, Sims K (2007) Pele's hairs and tears: natural probe of volcanic plume. *Journal of Volcanology and Geothermal Research* **164**, 244-253.
19. Moune S, Sigmarsson O, Thordarson T, P.J. G (2007) Recent volatile evolution in the magmatic system of Hekla volcano, Iceland. *Earth and Planetary Science Letters* **255**, 373-389.
20. Oehler JF, Lénat JF, Labazuy P (2007) Growth and collapse of the Reunion Island volcanoes. *Bulletin of Volcanology*, 717-742, doi 10.1007/s00445-007-0163-0.

21. Sasai Y, Johnston MJS, Tanaka, Y., Mueller, R., Hashimoto, T., Utsugi, M., Sakanaka, M., Uyeshima, M., Zlotnicki, J., Yvetot, P. (2007) Drag-out effect of piezomagnetic signals due to a borehole: The Mogi source as an example. *Annals of Geophysics* **1**, 93-104.
22. Shea T, Wyk de Vries van B, Pilato M (2007) Emplacement mechanisms of contrasting debris avalanches at Volcan Mombacho (Nicaragua), provided by structural and facies analysis. *Bulletin of Volcanology* **70**, 899-921, doi: 10.1007/s00445-007-0177-7.
23. Thouret JC, Lavigne F, Suwa H, Sukatja B, Surono (2007) Volcanic hazards at Mount Semeru, East Java (Indonesia), with emphasis on lahars. *Bulletin of Volcanology* **70**, 221-244.
24. Thouret JC, Ramirez C, Gibert-Malengreau B, Vargas CA, Naranjo JL, Vandemeulebrouck J, Valla F, Funk M (2007) Volcano-glacier interactions on composite cones and lahar generation: Nevado del Ruiz, Colombia, case study. *Annals of Glaciology* **45**, 115-127.
25. Thouret JC, Ramirez J, Naranjo JL, Gibert-Malengreau B, Vandemeulebrouck J, Funk M, Valla F (2007) The Nevado del Ruiz ice cap, Colombia, 21 years after: volcano-glacier interactions, meltwater generation, and lahar hazards. *Annals of Glaciology* **45**, 115-127.
26. Thouret JC, Wörner G, Gunnell Y, Singer B, Zhang X, Souriot T (2007) Geochronologic and stratigraphic constraints on canyon incision and Miocene uplift of the Central Andes in Peru. *Earth and Planetary Science Letters* **263**, 151-166.
27. Varol E, Temel A, Gourgaud A, Bellon H (2007) Early Miocene adakite-like volcanism in the Balkuyumcu region, central Anatolia, Turkey : petrology and geochemistry. *Journal Asian Earth Sciences* **30**, 613-628.

Groupe des Sciences de la Terre, LPS, CNRS-CEA, Saclay

(rattaché à l'IPGP en en 2010)

Mécanismes et bilans de transferts des fluides magmatiques

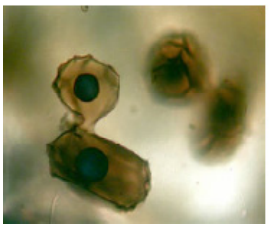
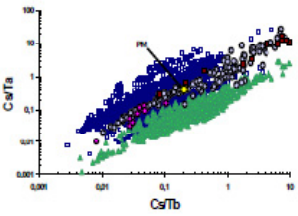


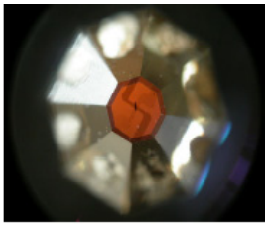

Les constituants volatils majeurs - H_2O, CO_2, S (SO_2, H_2S), et halogènes (Cl, F) – exercent une influence majeure sur les propriétés rhéologiques des magmas (viscosité, densité, température de liquidus) et, par leur exsolution sous forme des bulles de gaz lors de la remontée des magmas, constituent la force motrice des éruptions volcaniques. Les recherches ont été développées sur différents aspects : comportement des volatils dissous et des processus de dégazage magmatique, composition chimique et des flux émissions gazeuses volcaniques, géochimie des magmas à la frontière des plaques Africaine et Européenne, développement ou/et acquisition de nouveaux outils analytiques. Différents volcans actifs ont été étudiés, notamment l'Etna et le Stromboli, mais aussi des volcans de l'arc du Vanuatu (Yasur, Ambrym, Ambae), de l'arc des Antilles (St. Vincent, Grenade), le Piton de la Fournaise, et l'éruption 2010 de l'Eyjafjallajökull en Islande. Parmi les avancées majeures, on peut citer :

- La modélisation du comportement des volatils dissous et exsolvés dans les magmas en fonction de la pression, grâce à leur étude dans les inclusions vitreuses des cristaux d'olivine par microfaisceaux (microsondes électronique, ionique et nucléaire).
- La quantification des dégazages magmatiques par analyses couplées des volatils dans les magmas et des émissions gazeuses magmatiques en surface (outils spectroscopiques).
- Les développements analytiques : dosage quantitatif et rapide de l'eau dissoute dans les verres et inclusions vitreuses par micro-spectroscopie Raman, et dans les verres volcaniques et minéraux mantéliques par ERDA ; le dosage des éléments en trace des laves par ICP-MS sur des microquantités d'échantillon; et l'acquisition/utilisation d'un spectromètre infrarouge à transformée de Fourier en parcours ouvert (OP-FTIR) pour la mesure à distance et en temps réel de la composition chimique des gaz magmatiques pendant les éruptions.

Ces recherches ont été développées en collaborations avec différents partenaires français (CRPG, LMV, IPGP, LMPP, LSCE, IRD) et étrangers (notamment l'INGV et les Universités de Palerme et Pise, en Italie, DGMWR au Vanuatu, VSI en Islande), dans le cadre de projets ANR (EXPLANT, VOLGASPEC, Arc Vanuatu, MIME), de projets INSU, et de collaborations bilatérales. On en donne ci-dessous quelques illustrations.

1. Caractérisation des volatils dans les magmas

1.1 Spéciation du soufre en fonction de la composition et de l'état redox des magmas

Participants : Métrich N., Berry A.(Imperial College of London), O'Neill H.(ANU, Australie), Susini J.(ESRF)

La solubilité du soufre dans les magmas est liée directement à son état redox et représente un paramètre important à déterminer pour comprendre les processus géologiques (dégazage magmatique, formation des gîtes métallifères, géochimie des éléments chalcophiles..).
Les séries de mesures réalisées par micro-spectrométrie d'absorption X ([μXANES*) au seuil K du soufre, sur la ligne ID21 de l'ESRF, ont permis d'identifier sans ambiguïté les espèces soufrées présentes dans les verres et les inclusions vitreuses silicatées. On a ainsi pu démontrer que la proportion de soufre dissous sous forme sulfate prédomine dans les magmas basaltiques d'arc, oxydés et riches en eau (*Bonnin-Mosbah et al., 2002, Métrich et al., 2002*). La spéciation du soufre semble plus complexe dans des inclusions basaltiques représentatives de magmas moins oxydés et saturés vis à vis du globule de sulfure. L'ensemble des spectres acquis sur ces inclusions vitreuses montre la coexistence systématique de sulfate (S^{VI}) et sulfure ($S^{I}I$), la présence possible d'autres espèces soufrées, ainsi qu'un pic à 2469.4 eV, non identifié (Figure ci-contre).

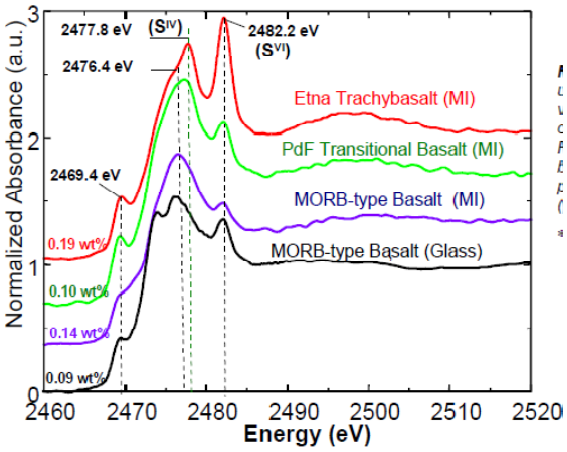

Pour comprendre cette variabilité nous avons mené une étude systématique de la spéciation du soufre dans des verres de compositions variables (basaltiques à liquides riches en Ca-Na-Mg), synthétisés sous différentes conditions d'oxydation. Les verres synthétisés en conditions réductrices (log fO_2 -8.8 à -10.9; log fS_2 -1.9) à 1200-1400°C et 1 bar, sont caractérisés par un pic à 2476.3 eV, identifiant l'espèce sulfure. Dans les verres oxydés (log fO_2 -0.49 à - 0.30; log fS_2 -0.18 à -0.31; log fSO_2 -1.5 à -2.1), le soufre est dissous sous forme sulfate (pic à 2482 eV). Nous montrons aussi que l'espèce sulfite (S^{IV}) est présente dans les verres très oxydés, mais peut aussi résulter de la réduction des sulfates par photo-réduction en cours d'analyse (*Métrich et al., 2009)*.

1.2. Dosage quantitatif de l'eau dissoute par spectroscopie micro-Raman

Participants : Di Muro A, M. Mercier, Métrich N., O. Belhadj, D. Massare

H_2O jouant un rôle majeur dans les processus magmatiques, il est essentiel de disposer d'un outil analytique permettant son dosage rapide et précis. Dans le cadre du projet et d'un doctorat (*M. Mercier*, 2009), l'analyse quantitative de l'eau dans les verres volcaniques par spectroscopie micro-Raman a été développée en trois étapes: a) quantification et calibration de l'influence des effets de matrice, dus à la composition complexe des verres volcaniques, sur les spectres Raman de l'hydrogène (H_2O_{tot}) mais aussi du carbone (CO_2) dissous; b) inter-comparaison des résultats aux données jusque-là obtenues par spectroscopie FTIR; et c) application des nouveaux protocoles à l'analyse des produits vitreux de différents volcans. Les résultats ont donné lieu à 6 publications de rang A et à 5 communications à congrès internationaux.
Les effets de matrice ont été étudiés et calibrés sur une large série de verres de synthèse (>60 compositions différentes), produits pour la plupart à partir des matériaux naturels (*Mercier et al.*, 2008, 2009, 2010; *Di Muro et al.*, 2009, 2010). Ont été étudiés: des verres anhydres avec un degré de dépolymérisation croissant, couvrant la presque totalité du spectre de composition des magmas (à l'exception des magmas exotiques ultra-alcalins ou carbonatitiques); des verres anhydres mafiques avec un degré d'oxydation croissant; et des verres hydratés à moyenne-basse pression (<2 kb) et haute pression (jusqu'à 20 kbar), ayant des teneurs en eau (0.1-7 % poids) caractéristiques de la diversité des magmas naturels. Des verres siliceux (haplogranite) synthétisés à haute pression nous ont permis d'étudier la dissolution de H et C en fonction de la pression à composition constante (*Ardia et al.*, 2011). Les résultats ont permis de quantifier, pour des verres naturels et synthétiques, l'effet sur la topologie des spectres Raman et infrarouges de plusieurs paramètres tels que : a) le degré de polymérisation, b) l'état redox du fer, c) la teneur en eau dissoute et d) la pression. Une équation générale a été formulée qui permet prédire avec précision la teneur en eau dissoute des verres naturels d'après les spectres micro-Raman (*Mercier et al.*, 2009), en bon accord avec les mesures par spectroscopie FTIR (Figure ci-dessous). La méthode a été appliquée avec succès à différents magmas et produits (basaltes riches en fer; inclusions vitreuses vésiculées de l'andésite de Montserrat (*Williamson et al.*, 2010); micro-cheveux de Pelé du Piton de la Fournaise; inclusions vitreuses du Yasur).

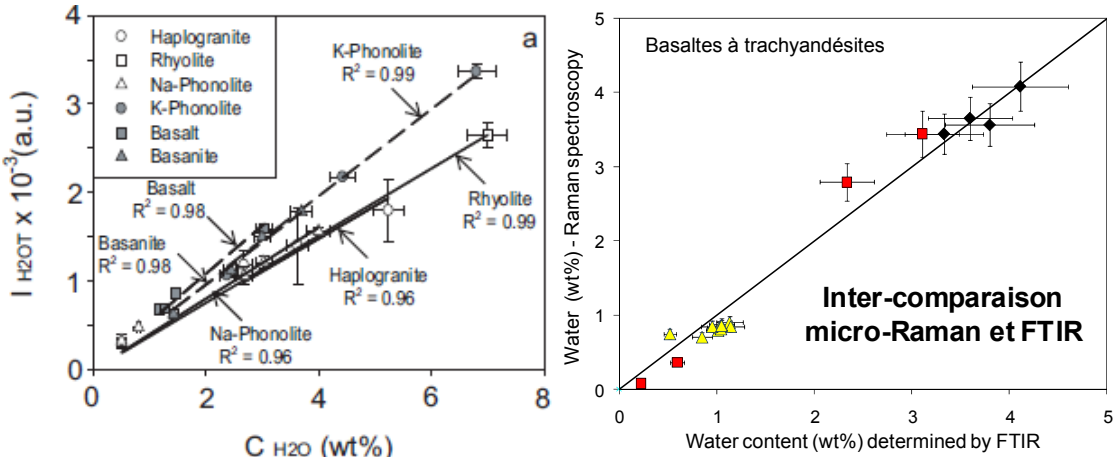

Figure – Analyse de l'eau dissoute dans les verres volcaniques par spectroscopie micro-Raman : a) Calibration externe de l'intensité du pic H_2O_T (3550 cm^{-1}) dans les spectres Raman en fonction de la concentration en eau pour 6 verres synthétiques de composition différente (basanite à rhyolite); b) Inter-comparaison entre contenus en eau dans des verres naturels mesurés par spectroscopies micro-Raman et FTIR (*Mercier et al.*, 2010).

2. Signature géochimique de la source des magmas

2.1 Etna (éléments traces, teneur en eau et rapport isotopique D/H)

Participants : Métrich N., Allard P.; Collaborations: E. Deloule (CRPG-Nancy), Kamenetsky V. (Univ. Tasmanie), Pompilio M. (INGV-Pise, Italie), Sobolev A. et Kuzmin D.W. (Max Planck Institute, Germany).
L'Etna est situé dans un contexte géodynamique complexe, à la frontière des plaques Africaine et Européenne et à l'arrière de la subduction ionienne. La source des magmas etnéens a fait l'objet de nombreux débats et publications. Pour approfondir cette question nous avons premièrement étudié le magma picritique riche en olivine (Fo90) de l'éruption explosive sub-plinienne datée à 3900 ans BP, l'un des magmas plus primaires de l'histoire récente du volcan. On montre que les roches totales et les inclusions vitreuses des olivines ont des teneurs en éléments en traces et des rapports entre ces éléments parfaitement comparables (*Kamenetsky et al., 2007; Métrich et al., 2007*). Ces picrites et les basaltes actuels ou historiques de l'Etna ont des rapports Th/U et Ce/Th compatibles avec leur dérivation d'une source de mantélique de type OIB à affinité HIMU. Leurs rapports U/Nb, Sr/Nd et H2O/Ce indiquent cependant une contamination de cette source par un fluide métasomatique (lié ou non à la subduction de la lithosphère ionienne), avec un enrichissement marqué du magma picritique en eau et CO_2 (Figure ci-contre). Les pressions de piégeage du liquide magmatique, comprises entre 400 et 500 MPa, correspondent à des profondeurs comprises entre le manteau et la croûte inférieure sous l'Etna.

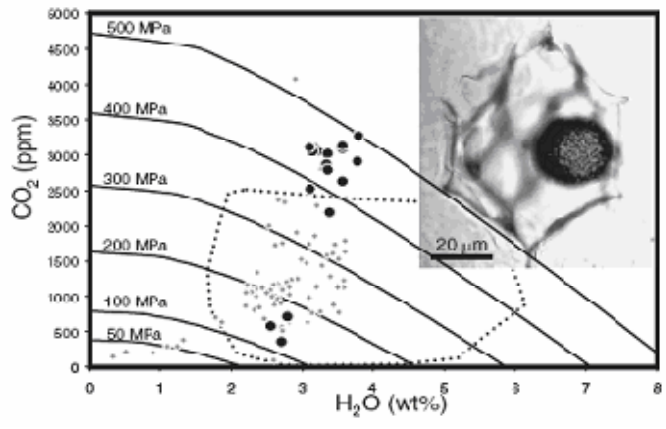

Le rapport isotopique de l'eau dissoute dans les magmas étnéens a ensuite été mesuré par SIMS dans les inclusions vitreuses des olivines des du magma picritique de 3900 BP et dans les basaltes primitifs produits par les deux puissantes éruptions de 2001 et 2002. Les résultats révèlent une eau magmatique enrichie en deutérium (δD ~ -30‰) comparée aux valeurs caractéristiques du manteau supérieur (δD ~ -60‰), indiquant une source enrichie en eau recyclée par subduction. De plus, l'évolution des δD en fonction de la pression permet de tracer les fractionnements isotopiques associés au dégazage en système fermé ou ouvert des magmas lors de leur remontée vers la surface (*Allard et al.*, 2009 and in prep.).

2.2. Géochimie isotopique des magmas primaires de l'arc des Antilles (St Vincent, Grenade)

Participants : Bouvier A.S., Métrich N. Collaborations : E. Deloule (CRPG-Nancy), ANR-UD Antilles.
Ce travail est entrepris dans le cadre de l'ANR-UD-Antilles (2006-2008) a fait l'objet de la thèse d'Anne Sophie Bouvier co-dirigée avec E. Deloule. L'arc volcanique des Petites Antilles résulte de la subduction de la plaque Atlantique sous la plaque Caraïbes, à une vitesse relativement lente de 2 à 4 cm par an. Les laves sont à dominante andésitiques, les basaltes primaires riches en MgO (HMB) n'étant présents qu'au sud de l'arc. Les

magmas aux Antilles sont engendrés par la fusion d'un manteau type MORB modifié par des fluides provenant de la croûte océanique altérée et des sédiments subductés. Cependant, la nature des fluides contaminants issus de la plaque en subduction varie du nord au sud de l'arc et fait l'objet de débats. Nous avons donc étudié les magmas primaires de l'arc pour clarifier cette question. Les scories basaltiques magnésiennes (MgO ~ 12 à 15%) de Grenade et St Vincent (sud de l'arc) ont été échantillonnées puis, après sélection, ont été analysées pour leurs inclusions vitreuses les plus représentatives des magmas primaires (Figure 23). Les concentrations en H2O, Li, B, Cl, F et S des inclusions, ainsi que les compositions isotopiques de Li, B, O et S, ont été systématiquement déterminées par microsonde ionique (IMS 1270) au CRPG.

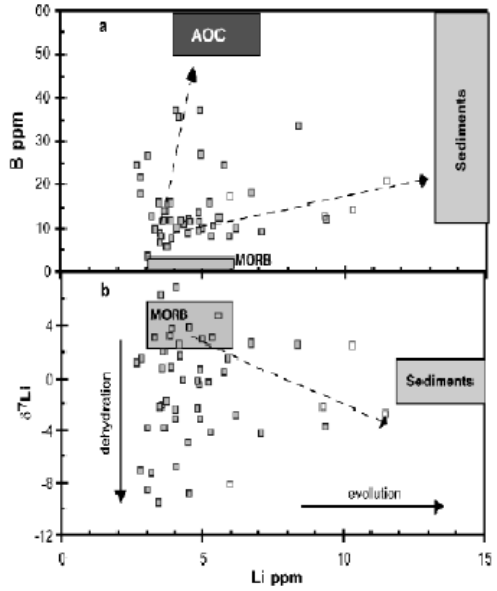

Figure 22 *: Inclusions vitreuses et spinelles piégés par une olivine riche en MgO (Mg# 0.90) provenant de lapilli basaltiques (dépôts pré-Somma) de l'île de St Vincent*

Figure 23 *: Variations des teneurs en B et Li (**a**) et de δLi (**b**) dans les inclusions vitreuses piégées par les olivines Fo_{90} des basaltes de St Vincent Les pôles représentés sont ceux des MORB, de la croûte océanique altérée (AOC) et des sédiments subductés.*
Sont reportées les inclusions représentatives des magmas primaires (symboles pleins) et évolués par cristallisation (symboles) évidés

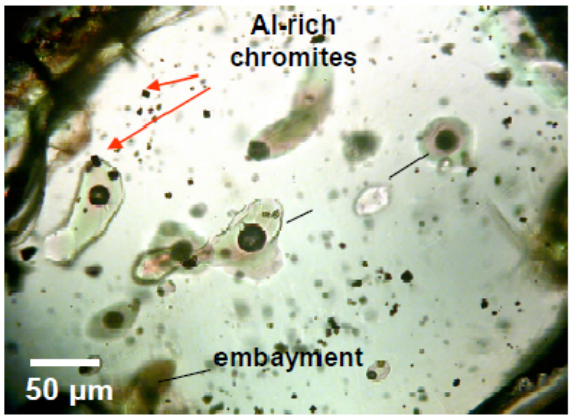

Les résultats acquis sur les basaltes magnésiens de St Vincent sont extrêmement intéressants. Les inclusions ont des compositions très variables, compatibles avec la contamination d'une source type MORB par deux fluides : l'un issu de la déshydratation de la croûte océanique, et l'autre des sédiments subductés sous le sud de l'arc (Figure 22). Les teneurs en eau des inclusions, rapportés aux travaux expérimentaux (Pichavant & McDonald, 2007), permettent de contraindre les conditions de pression et température de genèse des magmas (*Bouvier et al., 2008*). Un travail identique mené sur les liquides primaires de l'île de Grenade, piégés en inclusions vitreuses, conforte ces observations nouvelles (*Bouvier et al., 2010*).

3. Comportement de la phase gazeuse et dynamismes éruptifs

Ce paragraphe regroupe et résume différents travaux effectués sur les dégazages magmatiques et les dynamismes éruptifs, étudiés tant à partir des abondances et du comportement des éléments volatils dissous dans les magmas, qu'à partir des mesures de composition chimique et de flux massique des émissions gazeuses volcaniques en surface.

3.1 Mécanismes à l'origine de l'activité explosive et des paroxysmes du Stromboli. Dualité magma/gaz.

Participants : P. Allard, N. Métrich, A. Di Muro, O. Belhadj, D. Massare. Collaborations : A. Bertagnini, P. Landi, M. Burton (INGV-Pise, Italie), M. Rosi (Univ. Pise, Italie), A. La Spina, F. Murè (INGV-Catane, Italie), A. Aiuppa (CFTA, Univ. Palerme, Italie)

Stromboli est fameux pour son activité explosive récurrente (activité strombolienne) qui, chaque 10 à 20 minutes, donne lieu à des jets de gaz et de scories denses (riches en cristaux : 50% de plagioclase, pyroxène, olivine) aux cratères sommitaux, et ceci depuis environ 1500 ans. Cependant, Stromboli produit aussi des paroxysmes explosifs isolés, particulièrement dangereux, dont la fréquence moyenne varie de 1 à 3 par an pour les explosions 'majeures', et de 1-2 par décennie pour les plus violents paroxysmes de type vulcaniens. Une caractéristique unique et commune à ces paroxysmes est l'éruption, sous forme de ponce aphyrique et vésiculée, du basalte shoshinitique riche en gaz qui alimente le volcan (Bertagnini et al., 2003; Métrich et al., 2005).

Nos travaux ont permis de caractériser la source (profondeur) des différents évènements explosifs du Stromboli et de proposer des modèles quantitatifs pour leur genèse.

L'activité explosive strombolienne est engendrée par l'ascension puis la rupture de poches de gaz (slugs) formées en profondeur par coalescence de bulles plus petites. La profondeur d'origine de ces poches de gaz était estimée à environ 250-400 m sous les cratères d'après les signaux sismiques et acoustiques associés aux explosions. Or, nos mesures des gaz par spectroscopie infrarouge à transformée de Fourier en parcours ouvert (OP-FTIR) ont permis de montrer (i) que les slugs gazeux responsables des explosions étaient notablement enrichis en CO_2 par rapport au dégazage calme persistant (Figure ci-dessous) et (ii) se forment à des profondeurs allant de 1 à 3 km sous les cratères, soit entre la base du volcan et le niveau de la mer, bien supérieures aux estimations admises jusque là. Ces résultats ont été publiés dans Science (*Burton et al., 2007)*.

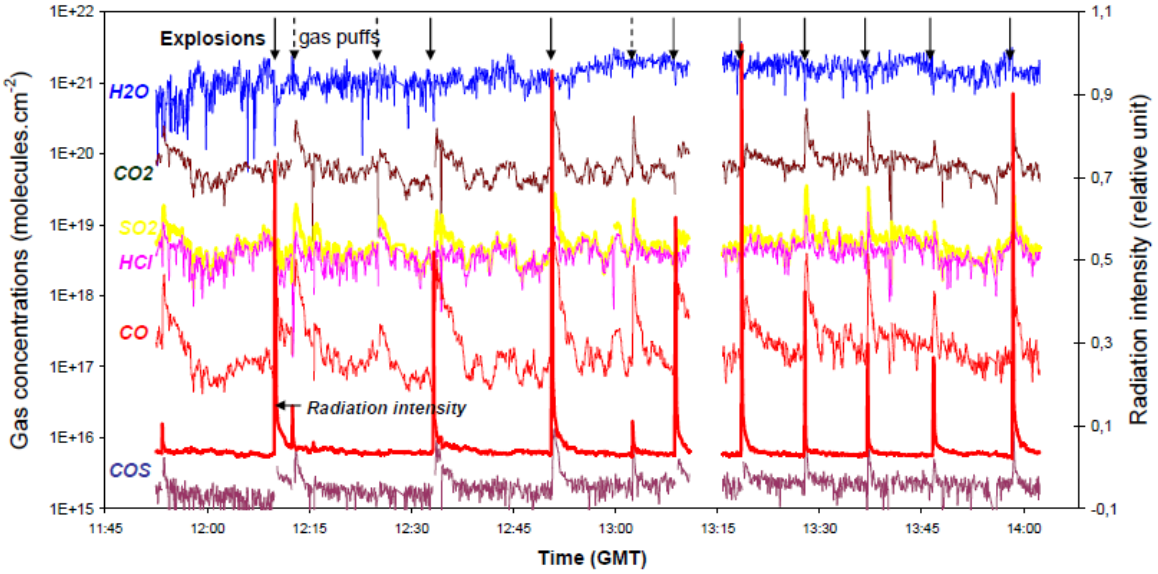

Figure 10 *: Analyse OP-FTIR à distance (240 m) de la composition chimique des gaz émis pendant et entre les explosions récurrentes du Stromboli (1 spectre chaque 4 sec). Variations de concentrations (et rapports) des espèces gazeuses lors des explosions (pics d'intensité radiative) et des bouffées de gaz ('puffs'). (Burton et al., 2003, 2007)*

La genèse des paroxysmes explosifs a fait l'objet d'études minutieuses de leurs produits solides et des volatils piégés dans les inclusions vitreuses de leurs cristaux d'olivine (*Bertagnini et al., 2008 ; Francalanci et al., 2008 ; Landi et al., 2008 ; Métrich et al., 2010 ; Aiuppa et al., 2010*). Il en ressort un modèle de remontée rapide de 'blobs' de magma primitif, riche en gaz (≥3% poids de H_2O+CO_2+S+Cl), depuis des pressions de 240-250 MPa (environ 7-8 km de profondeur sous le sommet du volcan). Ce modèle rend bien compte des explosions paroxysmales historiques mais aussi de l'explosion paroxysmale du 5 Avril 2003.
Toutefois, sur la base de différentes observations et d'un modèle de dégazage du magma basaltique basé sur le comportement des volatils en fonction de la pression, un modèle alternatif a été proposé (*Allard, 2010*) qui fait jouer un rôle moteur au dioxyde de carbone exsolvé et accumulé en profondeur. Les explosions majeures, mais aussi certaines explosions paroxysmales au moins, seraient principalement déclenchées par de larges poches de gaz riches en CO_2 accumulées aux discontinuités du système d'alimentation. Ce modèle est compatible avec les anomalies de tremor sismique décelées une quinzaine d'heures avant le paroxysme du 5 Avril 2003 (*Pino et al., in press*), ainsi qu'avec des variations de flux de CO_2 enregistrées depuis quatre ans avant chaque explosion 'majeure' (*Aiuppa et al., soumis*). Il est possible, cependant, que les deux mécanismes proposés opèrent

séparément ou simultanément selon les circonstances et la profondeur de genèse des paroxysmes, les différences portant sur les rôles respectifs de la phase gazeuse et du liquide magmatique.

3.2 Processus et bilans de dégazage magmatique dans l'arc du Vanuatu (Yasur et Ambrym)

Participants : P. Allard, N. Métrich, A. Di Muro, O. Belhadj, D. Massare, G. Sawyer. Collaborations: P. Bani, B. Pelletier (IRD, Noumea), Bertagnini, M. Burton (INGV-Pise, Italie), A. Aiuppa, F. Parello (CFTA, Univ. Palerme, Italie), E. Garaebiti (DGMWR, Vanuatu)

Les dégazages magmatiques aux deux volcans Yasur (trachyandésite) et Ambrym (basalte) ont été étudiés en détail dans le cadre des contrats ANR 'Arc Vanuatu' et 'Volgaspec' (2007-2010).

- Yasur :

L'analyse des produits solides anciens et actuels du complexe volcanique à caldera Siwi-Yasur (ignimbrite de Siwi, produits explosifs du Yasur depuis 1400 ans) et de ses émissions gazeuses nous a permis de démontrer (Métrich et al., 2008, 2009, 2011; Allard et al., 2008, 2011 et en prép.): (i) son alimentation, depuis au moins 2 millions d'années, par un même basalte parent, relativement anhydre, qui se différencie en magma trachyandésitique par 50% de cristallisation fractionnée; (ii) un dégazage continu, partiellement ouvert du magma trachyandésitique (1107±15°C) entre 5-4 km de profondeur et la surface, associé à un flux de chaleur intense; (iii) un flux total de $15x10^3$ tonnes/jour de gaz magmatique (97 mol% d'H_2O), dont ~700 tonnes/jour de SO_2 et 165 tonnes/jour de HCl, qui, normé aux teneurs pré-éruptives en soufre et chlore dissous, implique un taux moyen d'alimentation en basalte de 0.05 km^3/an; enfin, (iv) l'accumulation de 26 km^3 de magma trachyandésitique dégazé en 1000 ans sous la caldera de Siwi, qui suffirait amplement à expliquer la résurgence cumulée (2.8 km^3) du horst du Yenkahe dans le même temps (Figure 1, ci-dessus).

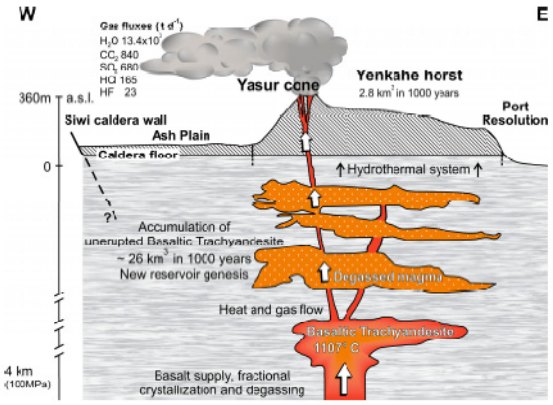

- Ambrym :

Des investigations fines ont été menées (i) sur le contenu en volatils des basaltes du volcan Ambrym (H_2O-CO_2-S-Cl-F dissous en inclusion vitreuses des olivines) et (ii) sur les gaz émis par ce volcan à lac de lave (Post-doc ANR Volgaspec de G. Sawyer). Les inclusions ont été analysées par spectroscopie micro-Raman (H_2O), microsonde nucléaire (CO_2) et microsonde électronique (éléments majeurs, S, Cl et F). Les résultats obtenus, les tout premiers sur ce volcan, révèlent: (i) une grande homogénéité chimique des liquides basaltiques d'Ambrym, vérifiée par l'analyse des roches totales; (ii) l'existence, cependant, de liquides calciques riches en volatils (olivine Fo88), communs à d'autres volcans d'arc mais dont l'origine reste mal comprise; (iii) des concentrations massiques relativement modestes en CO_2 (0.1%), H_2O (1.2%), S (0.15-0.17%) et Cl (~0.1%) des liquides basaltiques les moins évolués (olivine Fo83); et (iv) une exsolution rapide, lors de la décompression, du CO_2 par rapport à l'eau et du soufre par rapport au chlore (Figure ci-contre qui va faire varier les rapports entre ces espèces dans la phase gazeuse en fonction de la pression.

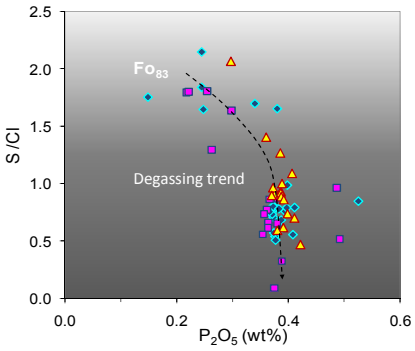

Figure – Inclusions vitreuse dans les olivines des basaltes d'Ambrym: évolution du rapport soufre sur chlore lors de la décompression et différenciation (P_2O_5) du liquide basaltique

Les pressions totales de fluides calculées à partir des teneurs en CO_2 et H_2O dissous indiquent une alimentation à plus de 6 km de profondeur (olivine Fo83) et un réservoir magmatique superficiel situé à ~4 km sous le volcan, en bon accord avec les premières données sismiques existantes (Legrand et al., 2005). C'est ce réservoir qui alimente le dégazage continu et l'activité à lacs de lave d'Ambrym (*Allard et al.*, 2009, et en soumission), dont la composition a pu être mesurée pour la première fois par spectroscopie OP-FTIR (Figure page suivante).

Les flux de gaz, normés au flux de SO_2 mesuré par spectroscopie DOAS aéroportée, montrent qu' Ambrym est l'un des plus forts émetteurs volcaniques de matière volatile dans l'atmosphère, produisant environ 10% des flux volcaniques globaux de SO_2, HF, Cu, As, Se, ^{210}Po et ^{210}Pb (*Allard et al.*, 2008,2009, et en soumission) et une fraction importante du budget total en SO_2 de l'arc du Vanuatu (*Bani et al., en révision*). Combinés aux analyses du soufre dissous en inclusions vitreuses, les flux de SO_2 permettent de calculer un taux d'alimentation magmatique moyen de 10 m^3/s (*Allard et al., 2009*).

.

Figure – Composition chimique des gaz magmatiques émis par le lac de lave basaltique du volcan Ambrym, Vanuatu, enregistrée chaque 4 secondes par spectroscopie OP-FTIR (*Allard et al.*, en soumission).

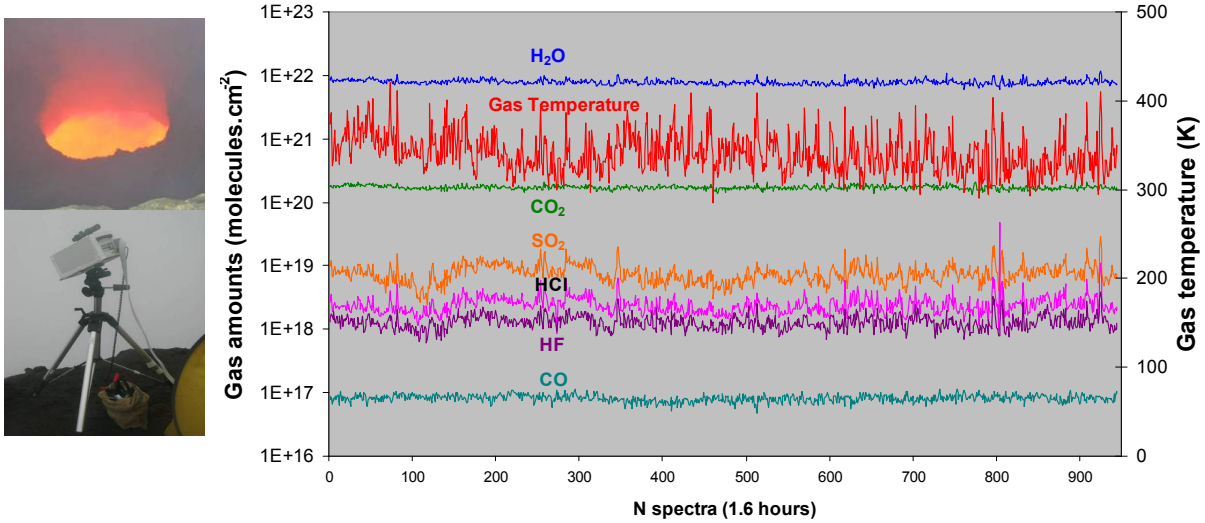

3.3 Un archétype des éruptions basaltiques dues à la propagation latérale de dykes d'origine profonde: l'éruption de l'Etna en février-avril 1974

Participants: N. Métrich, P. Allard, Fourmentraux C. ; collaborations: R. Corsaro, D. Andronico, L. Miraglia (INGV, Catania, Italy)

L'Etna, comme les autres stratovolcans basaltiques, produit des éruptions latérales, dont les coulées de lave constituent un risque majeur pour les populations avoisinantes. Ces éruptions résultent de la propagation du magma dans des fractures (dykes) qui, soit drainent les conduits centraux, soit se propagent depuis un réservoir sous le volcan indépendamment des conduits centraux. Quelques rares éruptions appartenant à cette seconde catégorie ont eu lieu en 1763, 1974, 2001 et 2002. Elles ont eu en commun une très forte explosivité et la particularité d'avoir produit des magmas riches en gaz et très peu cristallisés. Appelées 'excentriques', ces éruptions peuvent cependant se produire en différents points du volcan, selon le lieu et l'altitude d'émergence des dykes. L'origine et les conditions de remontée de leurs magmas restent de plus mal connues.

Ceci nous a conduit à étudier en détail les produits de l'éruption latérale de 1974 (1650 m, sur le flanc ouest), évènement 'clef' dans l'histoire de l'Etna en raison de son explosivité, de son déroulement en deux phases séparées, et surtout de la composition anormale de son magma basaltique, enrichi en alcalins (K, Rb), en ^{226}Ra et strontium radiogénique. L'éruption fut précédée et accompagnée par deux fortes crises sismiques. Elle a produit 4.5x10^{6} m^{3} de lave et formé deux nouveaux cônes de scories (Mt. De Fiore I et II, Figures 6-7).

Figure 6 : *Vue du Nord Est du cône de scories (Mt. De Fiore II) construit en ~3 jours Projection de lambeaux de lave incandescente et de cendres (Photo: B. Puglisi)*

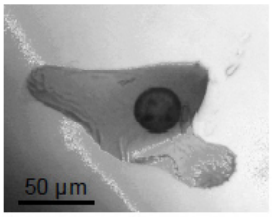

Figure 7 : *Inclusions vitreuses piégées par une olivine des scories de Mt Fiori*

Nous avons repris et développée l'étude minéralogique et géochimique des laves et scories de l'éruption, ainsi que celle des inclusions vitreuses de leurs cristaux d'olivine (Figure :7). Combinés aux données sismiques, les résultats obtenus nous permettent de démontrer que l'éruption de 1974 a résulté successivement de : (i) la fracturation tectonique du flanc ouest du volcan puis de la croûte profonde, (ii) la décompression du système d'alimentation intermédiaire et la nucléation, à environ 15 km de profondeur, d'un dyke qui s'est propagé vers la surface à une vitesse moyenne de l'ordre du centimètre par seconde, et enfin (iii) la remontée rapide, en système fermé du magma et des gaz jusqu'à faible profondeur (1 km) sous le site de l'éruption. La richesse initiale en eau (3% poids) du basalte et son ascension rapide ont empêché la cristallisation du plagioclase. La composition du basalte démontre l'injection d'un nouveau magma enrichi en alcalin dans le système d'alimentation de l'Etna, mélangé à 75%/25% au magma préexistant, qui fut émis pour la première fois en 1974. Pour cette éruption, archétype des éruptions 'excentriques' de l'Etna, nous proposons une nouvelle nomenclature qui peut être généralisée à d'autres volcans basaltiques (*Corsaro et al., 2009*).

.

4. Autres activités

- Traçage isotopique de la source des magmas ou/et des interactions fluides magmatiques/aquifères par les isotopes de l'hélium

- Premières analyses isotopiques de l'hélium dans les fluides volcaniques hydrothermaux de l'archipel des Açores (*Jean-Baptiste et al., EPSL 2009* ; collab. avec l'Univ. des Açores et programme CNRS-JNICT).
- Premières analyses isotopiques de l'hélium dans les fluides et les olivines de l'arc volcanique du Vanuatu (*Jean-Baptiste et al., 2009,* et en cours).
- Etude des eaux thermales de Tunisie et premières analyses isotopiques de l'hélium dissous (*Fourré et al., en révision;* collaboration avec l'Univ. Al Manar de Tunis*).*

- Spéciations et flux volcaniques de mercure

- Soufrière de Guadeloupe et Italie (*Bagnato et al., 2008, 2009*)
- Flux volcaniques globaux (*Bagnato et al., 2010*)

List of publications

2010

Aiuppa, A., Bertagnini A., Métrich N., Moretti R., Liuzzo M., &. Tamburello G. (2010) A model of degassing for Stromboli volcano. *Earth Planet. Sci. Let.* 295, 195-204, doi: 1.1016/j.epsl2010.03.040

Allard P. (2010) A CO_2-rich gas trigger of explosive paroxysms at Stromboli basaltic volcano. *J. Volcan. Geotherm. Res.*, 189, 363–374.

Bagnato E., Aiuppa A., Parello F., Allard P., Shinohara H., Liuzzo M., Giudice G. (2010) New clues on the contribution of Earth's volcanism to the global mercury cycle. *Bull. of Volcanology*, DOI 10.1007/s00445-010-0419.

Bouvier A.-S., Deloule E. & Métrich N. (2010) Fluid inputs to magma sources of St. Vincent and Grenada (Lesser Antilles): new insights from trace elements in olivine-hosted melt inclusions. *J. Petrol.* 51/8, 1597-1615, doi:10.1093/petrology/egq031.

Bouvier A.-S., Métrich N, & Deloule E (2010). Light elements, volatiles, and stable isotopes in basaltic melt inclusions from Grenada, Lesser Antilles. Inferences for magma genesis. *Geochim. Geophys. Geosyst*, 11, Q09004, doi: 10.1029/2010GC003051.

Mercier M., Di Muro A., Métrich N., Giordano, D., Belhadj O., Mandeville C. W. (2010). Spectroscopic analysis (FTIR, RAMAN) of water in mafic and intermediate glasses and glass inclusions. *Geochim. Cosmochim. Acta* 74, 5641-5656, doi: 10.1016/j.gca.2010.06.020.

Métrich N., Bertagnini A., Di Muro A. (2010) Conditions of Magma Storage, Degassing and Ascent at Stromboli: New Insights into the Volcano Plumbing System with Inference on the Eruptive Dynamics. *J. Petrol.* 51/3, 603-626.

Métrich N. and Mandeville C.W. (2010) Sulfur in magmas. *Elements* 6, 81-86.

Métrich N., Allard P., Aiuppa A., Bani P., Bertagnini A., Belhadj O., Di Muro A., Garaebiti E., Massare D., Parello F., and Shinohara H. (2010) Magma and volatile supply to post-collapse renewed volcanism and block resurgence in Siwi caldera (Tanna island, Vanuatu arc). *Journal of Petrology*, in press.

Pino A., Moretti R., Allard P., Boschi E., Seismic precursors of a basaltic paroxysmal explosion track deep gas accumulation and slug upraise. *J. Geophys. Research – Solid Earth*, 2009JB000826R, in press.

Williamson B.J., Di Muro A., Horwell C.J., Spieler O., and Llewellin (2010) Injection of vesicular magma into an andesitic dome at the effusive-explosive transition. *Earth and Planetary Science Letters*, 295, 83-90.

2009

Bagnato M., Allard P., Parello F., Aiuppa A., Calabrese S., Hammouya G. (2009) Mercury gas emissions from La Soufrière volcano, Guadeloupe (lesser Antilles). *Chemical Geology*, 226, 276-282.

Catinon M., Ayrault S., Clocchiatti R., Boudouma O., Asta J. Tissut M., Ravanel P. (2009) The anthropogenic atmospheric elements fraction: A new interpretation of elemental deposits on tree barks. *Atmos. Env.* 43, 1124-1130.

Corsaro R.A., N. Métrich , P. Allard, D. Andronico, L. Miraglia, C. Fourmentraux (2009) The 1974 eruption of Mount Etna: a milestone in the recent volcano evolution and an archetype for sub-volcano dyke (SVD) eruptions on basaltic strato-volcanoes. *J. Geophys. Res. Solid Earth,* 114, B07204, doi:10.1029/2008JB006013.

Di Muro A., Métrich N., Mercier M., Giordano G., Massare D. & Montagnac G. (2009) Micro-Raman Determination of Iron Redox State in Dry Natural Glasses: Application to Peralkaline Rhyolites and Basalts. *Chem. Geol.* 259, 78-88

Jean-Baptiste P., Allard P., Fourré E., Ferreira T., Coutinho R., Queiroz G., Gaspar J. (2009) Helium isotopes in hydrothermal volcanic fluids of the Azores Archipelago. *Earth Plan. Sci. Letters*, 281, 70-80.

Mercier M., Di Muro A., Giordano D., Métrich N., Lesne P., Pichavant M., Scaillet B., Clocchiatti R., & Montagnac G. (2009) Influence of glass polymerisation and oxidation on microRaman water analysis in alumino-silicate glasses. *Geochim. Cosmochim. Acta* 73, 197-217. doi:10.1016/j.gca.2008.09.030.

Métrich N., A. J. Berry, H. St. C O'Neill & J. Susini (2009) Oxidation state of sulphur in synthetic and natural glasses determined by X-ray absorption spectroscopy. *Geochim. Cosmochim. Acta.* 73, 2382-2399. doi:10.1016/j.gca.2009.01.025.

2008

Allard P., Aiuppa A., Burton M., Caltabiano T., Federico C., Salerno G., La Spina A. (2008) Crater Gas Emissions and the Magma Feeding System of Stromboli Volcano. In: Learning from Stromboli Volcano: insights from the 2002-2003 eruption (eds. S. Calvari, S. Inguaggiato, G. Puglisi, M. Ripepe, M. Rosi), *AGU Geophys. Monograph. Series*, vol. 182, Washington DC, Chap. 1.5, 65-80.

Allard P., Aiuppa A., Bani P., Parello P., Shinohara H., Gauthier P-J., Bagnato M., Bertagnini A., Métrich N. (2008) Magma-derived Volatile Emissions from Ambrym and Yasur Volcanoes (Vanuatu Arc). IAVCEI Gen. Assembly, Reykjavik, Iceland, 17-23 August 2008, 513 (invited talk).

Allard P., Métrich N., Deloule E., Spilliaert N., Mandeville C. (2008) Water and Sulfur Isotopic Ratios of Olivine-hosted Melt Inclusions in Primitive Etna Basalts: Magma Degassing Processes and Volatile Source(s). RST-2008, Nancy, 8-e.

Bagnato E., Aiuppa A., Parello F., D'Alessandro W., Allard P., Calabrese S. (2008) Mercury concentration and speciation in volcanic aquifers: measurements in Italy and Guadeloupe (West Indies). *J. Volcanol. Geotherm. Res.*, 179, 96-106.

Bertagnini A., Métrich N., Francalanci L., Landi P., Tommasini S., & Conticelli S. (2008) Volcanology and magma geochemistry of the present-day activity: constraints on the feeding system. *In:* Learning from Stromboli, (eds. S. Calvari, S. Inguaggiato, G. Puglisi, M. Ripepe, M. Rosi), *AGU Geophys Monograph*, vol. 182, Washington DC, pp. 399.

Bouvier AS, Métrich N, & Deloule E (2008) Slab-derived fluids in magma sources of St Vincent (Lesser Antilles Arc): volatiles and light element imprints. *J. Petrology* 49, 1427-1448, doi:10.1093/petrology/egn031.

Burton M., Allard P., Murè F., La Spina A. (2008) Lessons learnt from 8 years of FTIR measurements on Mt. Etna. Europ. Geophys. Union Assembly, Vienna, Austria, April 2008.

Burton M., Allard P., Puglisi G. (2008) Ground deformations and magma degassing at Mt. Etna. IAVCEI Gen. Assembly, Reykjavik, Iceland, 17-23 August 2008, 765.

Francalanci L., Bertagnini A., Métrich N., Renzulli A., Vannucci R., Landi P., Del Moro S., Menna M., Petrone C.M., & Nardini I. (2008) Mineralogical, Geochemical and Isotopic characteristics of the ejecta from the 5 April 2003 paroxysm at Stromboli, Italy: Inferences on the understanding of the eruptive dynamism. *In:* Learning from Stromboli, (eds. S. Calvari, S. Inguaggiato, G. Puglisi, M. Ripepe, M. Rosi), *AGU Geophys Monograph*, vol. 182, Washington DC, pp. 399.

Landi P., Métrich N., Bertagnini A., & Rosi M. (2008) Recycling and "re-hydration" of degassed magma inducing transient dissolution/crystallization events at Stromboli (Italy). *J. Volcanol. Geotherm. Res.* 174, 325-336.

Mariet C., Belhadj O., Leroy S., Carrot F., & Métrich N. (2008) Relevance of NH_4F in acid digestion before ICPMS analysis. *Talanta,* doi:10.1016/j.talanta.2008.07.007

Métrich N. & Wallace P. (2008) Volatile abundances in basaltic magmas and their degassing paths tracked by melt inclusions. *In:* Minerals, Inclusions & Volcanic Processes, (eds K. Putirka & F. Tepley), *Rev. Mineral. Geochem.* 69, Chapter 10, pp. 363-402.

2007

Allard P., Volcanic fluxes of water from Mount Etna and Stromboli (Italy): measurements and implications. Union Gen. Assemb., April 2007, Vienna, Austria, GMPV8-09799, Abstract (2007).

Allard P., Burton M., Puglisi G. (2007) Reconciling ground deformation and degassing at Mount Etna. IUGG Gen. Assembly, Perugia, Italy, 2-13 July 2007, VS005-10.

Allard P., Métrich N., Deloule E., Belhadj O., Spilliaert N., Mandeville C. (2007) D/H isotope Ratios of Olivine-hosted Melt Inclusions in Mount Etna Primitive Basalt. IUGG Gen. Assembly, Perugia, Italy, 2-13 July 2007, VW003-13, 2007.

Bureau H., B. Ménez, V. Malavergne, A. Somogyi, A. Simionovici, D. Massare, H. Khodja, L. Daudin, J.-P. Gallien, C. Shaw, M. Bonnin-Mosbah (2007) In situ mapping of high-pressure fluids using hydrothermal diamond anvil cells. *High Pressure Research* 27, N°2, 1-13.

Burton M., Allard P., Muré F., La Spina A. (2007) Magmatic gas composition reveals the source depth of slug-driven Strombolian explosive activity*, Science*, 317, 227, DOI: 10.1126/science.114190.

Halama R., Joron J.L., Villemant B., Markl G. and Treuil M. (2007) Trace element constraints on mantle sources during mid-Proterozoic magmatism: Evidence for a link between the Gardar (South Greenland) and Abitibi (Canadian Shield) mafic rocks. *Can. J. Earth Sci.* 44, 459-478.

Kamenetsky V, M. Pompilio, N. Métrich, A.V. Sobolev, D.V. Kuzmin and R. Thomas (2007) Arrival of extremely volatile-rich high-Mg magmas changes explosivity of Mount Etna. *Geology*, 35, 255-258; doi: 10.1130/G23163A.1.

Malavergne V., M. Tarrida, R. Combes, H. Bureau, J. Jones, C. Schwandt (2007) New High-Pressure and High-Temperature Metal/Silicate partitioning of U and Pb : Implication for the Cores of the Earth and Mars. *Geochimica et Cosmochimica Acta* 71, 2637-2655.

Ménez B., H. Bureau, J. Cauzid, V. Malavergne, A. Somogyi, A. Simionovici, M. Munoz, L. Avoscan, C. Rommevaux-Jestin and B. Gouget (2007) In Situ X-Ray Microscopy at High Temperature and Pressure, *in Modern Research and Educational Topics in Microscopy,* sous presse.

Mercier N., Valladas H., Froget L., Joron J.L., Reyss J.L., Weiner S., Golberg P., Meignen L., bar-Yosef O., KuhnS.L., STiner M.C., Tillier A.M., Arensburg B., Vandermeersch B. (2007) Hayonim Cave: a TL-based chronology for this Levantine Mousterain sequence. *Journal of Archaeological Science*.

Métrich N., V. Kamenetsky, P. Allard, M. Pompilio (2007) Trace element and volatile signature of Etna magma source(s): a melt inclusion approach. (*Invited*) Goldschmidt conference. Cologne 19-24 August 2007, Germany.

Richter D., Mercier N., Valladas H., Jaubert J., Texier P.J., Brugal J.P., Kervazo B., Reyss J.L., Joron J.L. and Wagner G.A. Thermoluminescence dating of heated flint from the Mousterian site of Bérigoule, Murs, Vaucluse, France. *Journal of Archaeological Science*, vol. 34, issue 4, pp 532-539.

Géophysique des volcans, ISTerre, LGIT, Chambéry

Composition de l'équipe

Nom	Statut	Thématique principale
Byrdina Svetlana	CR	Systèmes hydrothermaux
Collombet Marielle	MCF	Modélisation des écoulements
Got Jean-Luc	PR	Sismologie et mécanique
Lesage Philippe	MCF	Sismologie volcanique
Métaxian Jean-Philippe	CR	Sismologie volcanique
Pinel Virginie	CR	Modélisation mécanique et déformation
Revil André	DR	Méthodes électriques
Vandemeulebrouck Jean	MCF	Systèmes hydrothermaux

1. Introduction

Dans les dernières années, la volcanologie a connu de rapides progrès dans plusieurs domaines. Les systèmes d'observation, qu'ils soient permanents ou temporaires, se sont grandement améliorés, entraînant une augmentation de la qualité, de la quantité et de la variété des données disponibles. Pour exploiter la masse d'information obtenue, des méthodes d'analyse détaillée et de traitement systématique des signaux ont été développées. Des observations multi-méthodes se multiplient et l'interprétation conjointe des différents types de données permet de mieux comprendre les phénomènes dans les systèmes magmatiques et hydrothermaux. Ces résultats apportent des contraintes à des modèles physiques de ces systèmes. Par exemple, des modèles de dynamique des écoulements de magma dans des conduits et de l'évolution des dômes de lave rendent compte de nombreux aspects du comportement complexe des éruptions de volcans andésitiques. D'autres études montrent que les effets du dégazage des colonnes magmatiques jouent un rôle fondamental dans l'évolution des systèmes et dans leur réponse sismique (Collombet, 2009). Une meilleure compréhension des processus physique dans les volcans repose donc sur le développement de modèles conceptuels et numériques ainsi que sur des expériences analogiques. En parallèle, les études de structure ont été l'objet de développements remarquables. La résolution des méthodes d'imagerie a été améliorée grâce à la densification des réseaux de capteurs et à l'amélioration des méthodes. Sur des volcans très actifs et particulièrement bien instrumentés comme l'Etna, des tomographies à 4D ont mis en évidence des évolutions temporelles de la structure en relation avec des intrusions magmatiques. Toutefois, malgré les progrès mentionnés ci-dessus, la connaissance partielle que l'on a des structures génère de fortes incertitudes sur la localisation et le mécanisme des sources sismiques.

2. Sismo-mécanique et structure des volcans

Notre effort a porté sur la mise au point d'une méthode de tomographie en doubles-différences (Monteiller, 2005). Cette méthode permet l'utilisation de décalages temporels d'ondes P premières arrivées, mesurés très précisément par méthode interspectrale dans le cas de séismes semblables, pour une tomographie en vitesse sismique du milieu de propagation. Cette méthode nécessite un calcul direct très précis (effectué par retracé des rais dans le champ des temps de parcours calculé par un algorithme Podvin-Lecomte) et une inversion robuste, une attention particulière étant portée aux problèmes de conditionnement du système d'équations à inverser. Elle a nécessité la mise en œuvre d'un algorithme d'inversion Tarantola-Valette dans l'espace des paramètres, et donc une approximation correcte de l'inverse de la matrice de covariance des paramètres (vitesses), réalisée grâce à une relation de récurrence originale. L'application réalisée sur le volcan Kilauea a permis de mettre en évidence, à petite échelle, le système d'approvisionnement magmatique du volcan avec une résolution et une stabilité jamais atteintes jusqu'ici (Monteiller et al., 2005).
Deux autres résultats notables de cette étude ont été la mise en évidence dans le volcan et ses rifts d'un noyau rapide (donc dense, mis en place par intrusion) entouré de matériau lent (léger, mis en place par extrusion), et d'un système plan de décollement (au toit de la croûte océanique) – faille inverse (dans la croûte océanique) à la limite du noyau rapide. Une modélisation mécanique des déformations du volcan a été effectuée en différenciant le noyau dense et élastique de la couverture périphérique, légère et élasto-plastique. Elle permet de retrouver une faille inverse dans la croûte, créée sous l'action du poids du noyau et des contrastes de propriétés mécaniques noyau/remplissage. Un édifice de la taille du Mauna Loa peut atteindre la masse critique permettant de poinçonner profondément la croûte océanique, en engendrant un système de faille qui

traverse la croûte, créant les conditions pour l'ascension du magma et la naissance d'un nouvel édifice volcanique (le Kilauea et ses rifts).

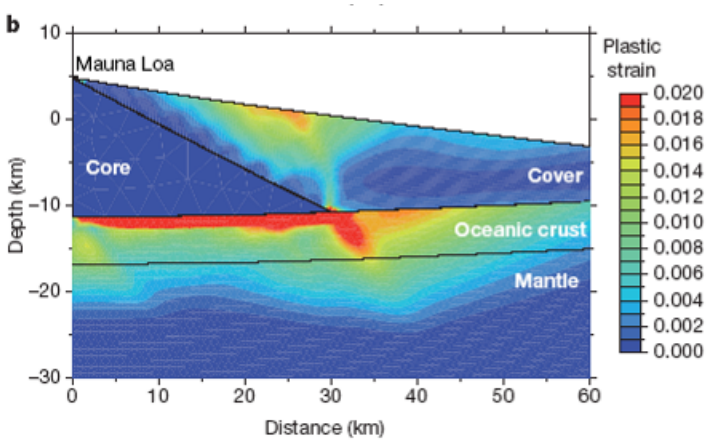

Modélisation mécanique du volcan Mauna Loa, Hawaii, et de la lithosphère sous-jacente (Got et al., 2008)

L'introduction d'une poussée horizontale du magma provoque un poinçonnement de la couverture d'origine effusive, légère et élasto-plastique par le noyau dense et plus rigide, engendrant une zone de déformation intense exactement à l'endroit où l'on observe les gigantesques escarpements de failles d'Hilina Pali, dont les mouvements sont à l'origine de tsunamis (Got et al., 2008).
La même méthode, comportant une nouvelle paramétrisation en Vp, Vp/Vs et un nouveau test de validation de la position des séismes localisés, a été utilisée pour étudier la structure des volcans Cotopaxi (Equateur) et Etna (Italie). Pour le Cotopaxi, l'étude a nécessité la mise au point d'un modèle de vitesse régional à l'échelle de l'Equateur, puis à celle du volcan Cotopaxi. Le résultat montre une zone de vitesse plus élevée au Sud-Est du Cotopaxi, dans la région où Molina et al. (2009) ont localisé un essaim de séismes très longue période accompagnant une intrusion. Cette zone rapide délimite probablement le système d'alimentation du volcan.

3. Etude et modélisation des sources sismo-volcaniques

Nous avons étudié les sources sismo-volcaniques et la sismicité des volcans en combinant plusieurs méthodes.
En collaboration avec l'OPGC, Nous avons développé une approche multi-méthode pour observer en détail des explosions volcaniques. Elle consiste à déployer simultanément un réseau de sismomètres large-bande, des antennes sismiques, des capteurs acoustiques, un radar Doppler, complétés si possible par des mesures de flux de gaz par spectromètres UV (DOAS) et des enregistrements vidéo. Cette approche permet de mieux mettre en évidence la complexité et la variabilité des phénomènes et aussi de mieux contraindre les modèles interprétatifs. Des expériences de ce type ont été menées sur les volcans Arenal (Costa rica), Popocatépetl (Mexique) et Yasur (Vanuatu). Les données obtenues sont en cours d'analyse (Mora et al., 2009) et montrent une grande complexité des phénomènes. Nous avons proposé un modèle conceptuel de la source des trémors volcaniques de l'Arenal (Lesage et al., 2006). Ce modèle fait intervenir un couplage entre un flux intermittent de gaz à travers des fractures du bouchon de lave et la résonance du conduit magmatique. Les observations multi-méthodes effectuées récemment sur ce volcan sont en accord avec ce modèle.
Les localisations de sources d'événements émergents, tels que les séismes LP et les trémors, que l'ont peut effectuer à l'aide d'antennes sismiques, sont fortement perturbées par les hétérogénéités de la structure. Nous avons étudié et pris en compte les effets de topographie et des couches superficielles à faibles vitesses en calculant les sismogrammes synthétiques complets par la méthode Lattice-Boltzman de O'Brien et Bean (2004). Nous avons montré ainsi que l'on peut améliorer les localisations et mieux choisir les sites d'installation des antennes (Métaxian et al., 2009).

La localisation, le mécanisme et la fonction temporelle des sources sont des informations essentielles pour mieux comprendre la dynamique des systèmes éruptifs. Nous avons abordé le problème de la détermination du tenseur des moments sismiques des sources associées aux explosions par l'inversion des formes d'onde. Ce travail est mené en collaboration avec l'University College of Dublin et l'INGV de Pise. Nous avons appliqué cette méthodologie aux explosions de l'Ubinas (Pérou) qui présentent des formes d'onde très similaires suggérant une source non destructive. Dans ce cas, le modèle de source le plus probable correspond à une fracture de 40° de pendage (Monteiller et al., 2008). D'autres applications sur les volcans Arenal (Davi et al., 2008, 2010) et Yasur (thèse de Laurence Perrier) sont en cours.

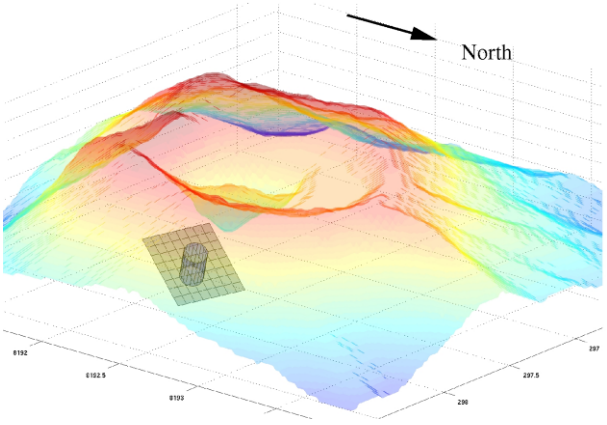

Modèle de source sismique dans le volcan Ubinas

Par ailleurs, nous avons développé divers outils d'analyse. Un logiciel dédié au traitement des signaux sismo-volcaniques avec interfaces graphiques a été réalisé et distribué dans des observatoires et des groupes de recherche (Lesage, 2008 ; 2009). Un système de classification automatique de signaux basé sur les Chaînes de Markov Cachées (Benitez et al., 2009) a été mis au point en collaboration avec l'Universidad de Granada (Espagne) et l'Universidad de Colima (Mexique). Celui-ci sera intégré dans des systèmes de surveillance pour améliorer les diagnostiques en temps réel. De plus, ce système sera utilisé pour classer l'ensemble des événements enregistrés sur plusieurs volcans et obtenir des catalogues complets et cohérents de sismicité par classe d'événement.

4. Evolution temporelle des signaux géophysiques (sismicité, déformation) associée au stockage et au transport du magma.

Des modèles mécaniques prenant en compte le couplage entre la roche encaissante et le magma fluide ont été développés afin d'expliquer l'évolution temporelle de la sismicité et de la déformation induite par le stockage et le transport du magma. Ces modèles ont été appliqués avec succès à plusieurs volcans basaltiques. Lengliné et al. (2009) montrent une évolution exponentielle de la sismicité et de la déformation au Kilauea (Hawaii) et au Piton de la Fournaise (La Réunion) compatible avec un stockage de magma dans un réservoir superficiel alimenté par une source profonde ayant une pression constante. La constante de temps déterminée apporte une information sur les dimensions du système d'alimentation profond. Traversa & Grasso (2009) et Traversa et al. (2010) montrent une stationnarité de la sismicité lors de l'épisode de propagation de dyke sur plusieurs volcans basaltiques (par ex. Etna, Piton de la Fournaise) compatible avec un flux d'injection de magma constant dans le temps. Ce modèle apporte des contraintes sur la taille et la surpression du réservoir superficiel nourrissant l'intrusion magmatique. Par ailleurs, Albino et al. (2010) ont montré que l'étude des déformations enregistrées sur un cycle éruptif et des volumes de magma émis permettait d'obtenir une estimation de la résistance à la fracturation en tension des roches et de la compressibilité du magma. Enfin, Pinel et al. (2010) montrent que ces modèles peuvent également servir à interpréter des données pétrologiques obtenues à des échelles de temps beaucoup plus grandes : ils permettent d'expliquer des variations temporelle de flux magma émis en surface.

Un travail important a été effectué sur les effets des perturbations externes au système volcanique. Nous avons caractérisé la déformation induite par une variation superficielle de charge. Ceci a apporté une estimation du module de Young caractérisant la croûte superficielle en Islande (Pinel et al., 2007; Grapenthin et al., 2006) et de séparer la déformation induite par un apport de magma de celle due à des phénomènes externes (Sturkell et al., 2008 ; Pinel et al., 2009). Nous avons estimé les perturbations de pression induite dans une zone de stockage superficielle et les conséquences pour la sismicité enregistrée et le déclenchement des éruptions (Pinel et al., 2009 ; Albino et al., 2010). Les modèles développés apportent une information sur la forme du réservoir magmatique, sa taille et sa profondeur.

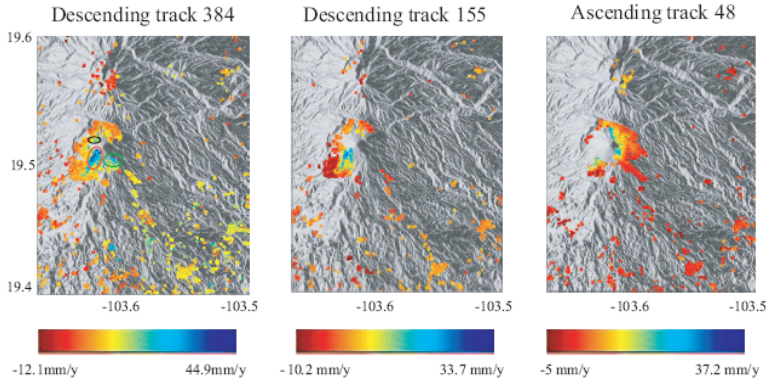

Vitesse moyenne dans la ligne de visée du satellite pour le volcan de Colima (les valeurs positives correspondent à un éloignement du satellite). Les résultats sont présentés sur le Modèle Numérique de Terrain SRTM. (d'après Pinel et. al, 2008).

Les modèles développés ayant montré l'intérêt d'avoir une bonne information sur l'évolution temporelle de la déformation, nos efforts ont également porté sur l'acquisition de données de déformation par InSAR dans le cas des strato-volcans andésitiques. Ces volcans présentent des changements rapides et mal compris de leur dynamisme éruptif et leur étude par interférométrie présente des difficultés certaines principalement due à la topographie importante des édifices. Nous avons travaillé sur des séries temporelles de données SAR en incorporant des corrections des artéfacts atmosphériques par apport d'informations météorologiques. Cette étude a été appliquée à deux volcans Mexicains : le Popocatepetl et le Colima (Pinel et al., 2008).

5. Dynamique des fluides hydrothermaux

Cet axe de recherche vise à reconnaître et comprendre les processus physiques qui régissent le fonctionnement des systèmes hydrothermaux. Il s'appuie d'une part sur l'observation et l'imagerie géophysique de ces systèmes, et d'autre part sur la modélisation analogique et numérique.
L'observation des processus naturels a été réalisée par des suivis temporels et des **campagnes d'imagerie géophysique multi-méthodes** (a) à grande échelle sur des volcans actifs, (b) à petite échelle, sur des zones laboratoires choisies pour leur activité cyclique comme la zone hydrothermale de Waimangu (thèse A. Legaz, 2008) ou les geysers de Yellowstone (thèse en cours d'E. Cros). Les techniques d'imagerie utilisées, acoustique, thermique et électrique, se sont révélés très complémentaires et bien applicables aux champs hydrothermaux (Revil et al., 2008). L'application des méthodes géophysiques est allé de pair avec des **développements méthodologiques** en acoustique et électrique, comme par exemple l'application de techniques acoustiques sous-marines, comme le Matched Field Processing (Legaz et al, 2008) en liaison avec l'équipe acoustique du LGIT, le développement de méthodes inverses en polarisation spontanée (Jardani et al., 2008) et en méthode sismo-électrique, et le développement d'un modèle mécanistique en polarisation provoquée.
La **modélisation analogique** des systèmes hydrothermaux a tout d'abord permis de caractériser leurs instabilités intrinsèques, ces systèmes étant gravitationnellement instables à cause de leur structuration thermique (liquide au dessus de vapeur). En utilisant des milieux poreux saturés soumis à des conditions thermiques similaires aux systèmes naturels, on a d'abord pu montrer qu'ils pouvaient présenter une activité cyclique naturelle (Vandemeulebrouck et al., 2005), similaire à celle observée sur plusieurs sites volcaniques dont Waimangu (Vandemeulebrouck et al., 2008). Dans un deuxième temps, nous avons étudié la réponse mécanique et thermique d'un système hydrothermal à un forçage externe, comme un dégazage d'origine magmatique. L'injection instantanée de vapeur à la base du milieu poreux étudié précédemment provoque une rapide surrection du milieu, suivie d'une lente subsidence sur laquelle viennent se superposer des oscillations amorties. Une telle évolution est tout à fait semblable aux variations du mouvement du sol observées depuis 1980 aux Champs Phlégréens (Italie), comme le montre la figure ci-dessous, et prouve que la réponse hydrothermale est complexe et contient des composantes non magmatiques. Une coopération en cours avec M. Todesco de l'INGV Bologne sur l'application du **code numérique** TOUGH2 va permettre d'étudier le passage à grande échelle des processus observés analogiquement à petite échelle.

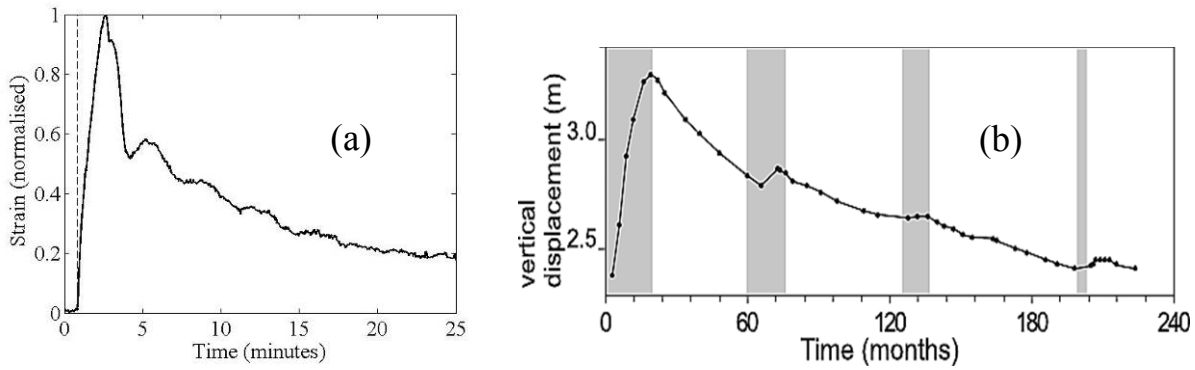

Comparaison (a) de la déformation verticale obtenue suite à d'un injection de vapeur (trait pointillé) sur un modèle poreux analogique avec (b) le déplacement vertical du sol mesuré aux Champs Phlégréens, d'après Chiodini et al., 2003 . Le modèle analogique montre qu'une seule injection suffit pour générer la totalité de l'évolution observée, y compris les épisodes de mini-uplifts.

List of publications

Albino F, Pinel V, Sigmundsson F (2010) Influence of surface load variations on eruption likelihood: application to two Icelandic subglacial volcanoes, Grimsvotn and Katla. Geophysical Journal International 181(3):1510-1524

Ball LB, Ge SM, Caine JS, Revil A, Jardani A (2010) Constraining fault-zone hydrogeology through integrated hydrological and geoelectrical analysis. Hydrogeology Journal 18(5):1057-1067.

Barde-Cabusson S, Finizola A, Revil A, Ricci T, Piscitelli S, Rizzo E, Angeletti B, Balasco M, Bennati L, Byrdina S, Carzaniga N, Crespy A, Di Gangi F, Morin J, Perrone A, Rossi M, Roulleau E, Suski B, Villeneuve N (2009) New geological insights and structural control on fluid circulation in La Fossa cone (Vulcano, Aeolian Islands, Italy). Journal of Volcanology and Geothermal Research 185(3), 231-245.

Barde-Cabusson, S., G. Levieux, J-F. Lénat, A. Finizola, A. Revil, M. Chaput, S. Dumont, Z. Duputel, B. Fragnol, A. Guy, F. Lorion, L. Mathieu, S. Saumet, F. Sorbadère, and M. Vieille (2009) Transient self-potential anomalies associated with recent lava flows at Piton de la Fournaise volcano (Réunion Island, Indian Ocean), Journal of Volcanology and Geothermal Research, 187, 158–166.

Benítez, M.C., Lesage, P., Cortés, G., Segura, J.C., Ibáñez, J.M., de la Torre, A. (2009) Automatic recognition of volcanic-seismic events base on Continuous Hidden Markov Models. *In*: Bean, C. J., Braiden, A. K., Lokmer, I., Martini, F., O'Brien, G. S. The VOLUME project, EU PF6 (No. 018471). ISBN 978-1-905254-39-2, VOLUME Project Consortium, Dublin.

Boleve A., Revil A., Janod F., Mattiuzzo J. L., and Jardani A. (2007) Forward modeling and validation of a new formulation to compute self-potential signals associated with ground water flow. Hydrology and Earth System Sciences 11 (5), 1661-1671.

Bolève A., A. Revil, F. Janod, J. L. Mattiuzzo, and J.-J. Fry (2009) Preferential fluid flow pathways in embankment dams imaged by self-potential tomography, Near Surface Geophysics, 7(5), 447-462, doi: 10.3997/1873-0604.2009012.

Bonnardot MA, Hassani R, Tric E (2008) Numerical modelling of lithosphere-asthenosphere interaction in a subduction zone. Earth and Planetary Science Letters 272(3-4), 698-708.

Bonnardot MA, Hassani R, Tric E, Ruellan E, Regnier M (2008) Effect of margin curvature on plate deformation in a 3-D numerical model of subduction zones. Geophysical Journal International 173(3), 1084-1094.

Byrdina S., Revil A., Contraires S., Perrier F., Pant S., Gautam U., Koirala B., Shrestha P., Tiwari D.R. and Sapkota S.N., Dipolar Self-Potential anomaly associated with carbon dioxide and radon exhalation at Syabru-Bensi hot springs in Central Nepal, *J. Geophys. Res.,* in press.

Byrdina, S., A. Revil, S. R. Pant, B. P. Koirala, P. L. Shrestha, D. R. Tiwari, U. P. Gautam, K. Shrestha, S. N. Sapkota, S. Contraires, and F. Perrier, Dipolar self-potential anomaly associated with carbon dioxide and radon flux at Syabru-Bensi hot springs in central Nepal, J. Geophys. Res., 114, B10101, doi:10.1029/2008JB006154, 2009.

Cardiff M., W. Barrash, P. Kitanidis, B. Malama, A. Revil, S. Straface, E. Rizzo, and T. Johnson (2009) Inverse modeling of dipole hydrologic testing for an unconfined aquifer, Ground Water, 47(2), 259-270.

Castermant J, Mendonca CA, Revil A, Trolard F, Bourrie G, Linde N (2008) Redox potential distribution inferred from self-potential measurements associated with the corrosion of a burden metallic body. Geophysical Prospecting 56(2), 269-282.

Collombet, M. (2009) Two dimensional gas loss for silicic magma flows: toward more realistic numerical models. Geophys. J. Int., 177: 309-318, doi: 10.1111/j.1365-246X.2008.04086.x.

Cortés, G., Arámbula, R., Álvarez, I., Benítez, C. M., Ibáñez, J. M., Lesage, P., González Amezcua, M., and Reyes Davila, G. (2009) Analysis of Colima, Popocatépetl and Arenal volcanic seismicity using an automatic CHMM-based recognition. *In*: Bean, C. J., Braiden, A. K., Lokmer, I., Martini, F., O'Brien, G. S. The VOLUME project, EU PF6 (No. 018471). ISBN 978-1-905254-39-2, VOLUME Project Consortium, Dublin.

Cosenza P, Ghorbani A, Revil A, Zamora M, Schmutz M, Jougnot D, Florsch N (2008) A physical model of the low-frequency electrical polarization of clay rocks. Journal of Geophysical Research-Solid Earth 113(B8).

Courboulex F., Larroque C., Deschamps A., Kohrs Sansorny C., Gelis C., Got J. L., Charreau J., Stephan J. F., Bethoux N., Virieux J., Brunel D., Maron C., Duval A. M., Perez L., and Mondielli P. (2007) Seismic hazard on the French Riviera: observations, interpretations and simulations. Geophysical Journal International 170(1), 387-400.

Crespy A, Revil A, Linde N, Byrdina S, Jardani A, Boleve A, Henry P (2008) Detection and localization of hydromechanical disturbances in a sandbox using the self-potential method. Journal of Geophysical Research-Solid Earth 113(B1).

Davi R, O'Brien GS, Lokmer I, Bean CJ, Lesage P, Mora MM (2010) Moment tensor inversion of explosive long period events recorded on Arenal volcano, Costa Rica, constrained by synthetic tests. Journal of Volcanology and Geothermal Research 194(4):189-200.

De Barros L, Pedersen HA, Metaxian JP, Valdes-Gonzalez C, Lesage P (2008) Crustal structuree below Popocatepetl Volcano (Mexico) from analysis of Rayleigh waves. Journal of Volcanology and Geothermal Research 170(1-2), 5-11.

De Barros L, Bean CJ, Lokmer I, Saccorotti G, Zuccarello L, O'Brien GS, Metaxian JP, Patane D (2009) Source geometry from exceptionally high resolution long period event observations at Mt Etna during the 2008 eruption. Geophysical Research Letters 36.

Finizola A, Aubert M, Revil A, Schutze C, Sortino F (2009) Importance of structural history in the summit area of Stromboli during the 2002-2003 eruptive crisis inferred from temperature, soil CO_2, self-potential, and electrical resistivity tomography. Journal of Volcanology and Geothermal Research 183(3-4), 213-227.

Finizola A, Ricci T, Deiana R, Cabusson SB, Rossi M, Praticelli N, Giocoli A, Romano G, Delcher E, Suski B, Revil A, Menny P, Di Gangi F, Letort J, Peltier A, Villasante-Marcos V, Douillet G, Avard G, Lelli M (2010) Adventive hydrothermal circulation on Stromboli volcano (Aeolian Islands, Italy) revealed by geophysical and geochemical approaches: Implications for general fluid flow models on volcanoes. Journal of Volcanology and Geothermal Research 196(1-2):111-119.

Gelis C, Revil A, Cushing ME, Jougnot D, Lemeille F, Cabrera J, De Hoyos A, Rocher M (2010) Potential of Electrical Resistivity Tomography to Detect Fault Zones in Limestone and Argillaceous Formations in the Experimental Platform of Tournemire, France. Pure and Applied Geophysics 167(11):1405-1418.

Ghorbani A, Cosenza P, Revil A, Zamora M, Schmutz M, Florsch N, Jougnot D (2009) Non-invasive monitoring of water content and textural changes in clay-rocks using spectral induced polarization: A laboratory investigation. Applied Clay Science 43(3-4), 493-502.

Goncalves J., Rousseau Gueutin P., and Revil A. (2007) Introducing interacting diffuse layers in TLM calculations: A reappraisal of the influence of the pore size on the swelling pressure and the osmotic efficiency of compacted bentonites. Journal of Colloid and Interface Science 316(1), 92-99.

Got J. L., Monteiller V., Virieux J., and Okubo P. (2006) Estimating crustal heterogeneity from double-difference tomography. Pure and Applied Geophysics 163(2-3), 405-430.

Got JL, Monteiller V, Monteux J, Hassani R, Okubo P (2008) Deformation and rupture of the oceanic crust may control growth of Hawaiian volcanoes. Nature 451(7177), 453-456.

Got JL, Monteiller V, Virieux J, Operto S (2008) Potential and limits of double-difference tomographic methods. Geophysical Prospecting 56(4), 477-491.

Got JL, Mourot P, Grangeon J (2010) Pre-failure behaviour of an unstable limestone cliff from displacement and seismic data. Natural Hazards and Earth System Sciences 10(4):819-829.
Haas, A., and A. Revil (2009) Electrical signature of pore scale displacements, Water Resources Research, 45, W10202, doi:10.1029/2009WR008160.
Jardani A, Revil A, Boleve A, Dupont JP (2008) Three-dimensional inversion of self-potential data used to constrain the pattern of groundwater flow in geothermal fields. Journal of Geophysical Research-Solid Earth 113(B9).
Jardani A., Revil A., Boleve A., Dupont J. P., Barrash W., and Malama B. (2007) Tomography of groundwater flow from self-potential (SP) data. Geophysical Research Letters 34, L24403, doi:10.1029/2007GL031907.
Jardani A, Revil A (2009) Stochastic joint inversion of temperature and self-potential data. Geophysical Journal International 179(1), 640-654.
Jardani A, Revil A, Barrash W, Crespy A, Rizzo E, Straface S, Cardiff M, Malama B, Miller C, Johnson T (2009) Reconstruction of the Water Table from Self-Potential Data: A Bayesian Approach. Ground Water 47(2), 213-227.
Jardani A, Revil A, Slob E, Solllner W (2010) Stochastic joint inversion of 2D seismic and seismoelectric signals in linear poroelastic materials: A numerical investigation. Geophysics 75(1):N19-N31.
Johnson TC, Versteeg RJ, Ward A, Day-Lewis FD, Revil A (2010) Improved hydrogeophysical characterization and monitoring through parallel modeling and inversion of time-domain resistivity and induced-polarization data. Geophysics 75(4):WA27-WA41.
Jougnot D, Revil A, Leroy P (2009) Diffusion of ionic tracers in the Callovo-Oxfordian clay-rock using the Donnan equilibrium model and the formation factor. Geochimica Et Cosmochimica Acta 73(10), 2712-2726.
Jougnot D, Ghorbani A, Revil A, Leroy P, Cosenza P (2010) Spectral induced polarization of partially saturated clay-rocks: a mechanistic approach. Geophysical Journal International 180(1):210-224.
Jougnot D, Revil A (2010) Thermal conductivity of unsaturated clay-rocks. Hydrology and Earth System Sciences 14(1):91-98.
Jougnot D, Revil A, Lu N, Wayllace A (2010) Transport properties of the Callovo-Oxfordian clay rock under partially saturated conditions. Water Resources Research 46
Knight R, Pyrak-Nolte LJ, Slater L, Atekwana E, Endres A, Geller J, Lesmes D, Nakagawa S, Revil A, Sharma MM, Straley C (2010) Geophysics at the interface: response of geophysical properties to solid-fluid, fluid-fluid, and solid-solid interfaces. Reviews of Geophysics 48.
Legaz A., Revil A., Roux P., Vandemeulebrouck J., Gouedard P., Hurst T., and Bolève A. (2008) Self potential and passive monitoring of hydrothermal activity: A case study at Iodone Pool, Waimangu geothermal Valley, New-Zealand, Journal of Volcanology and Geothermal Research 179(1-2), 11-18.
Legaz A, Revil A, Roux P, Vandemeulebrouck J, Gouedard P, Hurst T, Boleve A (2009) Self-potential and passive seismic monitoring of hydrothermal activity: A case study at Iodine Pool, Waimangu geothermal valley, New Zealand. Journal of Volcanology and Geothermal Research 179(1-2), 11-18
Legaz A, Vandemeulebrouck J, Revil A, Kemna A, Hurst AW, Reeves R, Papasin R (2009) A case study of resistivity and self-potential signatures of hydrothermal instabilities, Inferno Crater Lake, Waimangu, New Zealand. Geophysical Research Letters 36, L12306, doi:10.1029/2009GL037573.
Lengline O, Marsan D, Got JL, Pinel V, Ferrazzini V, Okubo PG (2008) Seismicity and deformation induced by magma accumulation at three basaltic volcanoes. Journal of Geophysical Research-Solid Earth, 113(B12).
Lengline O, Marsan D (2009) Inferring the coseismic and postseismic stress changes caused by the 2004 M-w=6 Parkfield earthquake from variations of recurrence times of microearthquakes. Journal of Geophysical Research-Solid Earth, 114.
Leroy P, Revil A, Kemna A, Cosenza P, Ghorbani A (2008) Complex conductivity of water-saturated packs of glass beads. Journal of Colloid and Interface Science 321(1), 103-117.
Leroy P, Revil A (2009) A mechanistic model for the spectral induced polarization of clay materials. Journal of Geophysical Research-Solid Earth 114.
Lesage P., Mora M. M., Alvarado G. E., Pacheco J., and Metaxian J. P. (2006) Complex behavior and source model of the tremor at Arenal volcano, Costa Rica. Journal of Volcanology and Geothermal Research 157 (1-3) Special Iss. SI, 49-59.
Lesage P (2008) Automatic estimation of optimal autoregressive filters for the analysis of volcanic seismic activity. Natural Hazards and Earth System Sciences 8(2), 369-376.
Lesage P. (2009) An interactive Matlab software for the analysis of seismic volcanic signals, Computer and Geosciences 35, 2137-2144, DOI: 10.1016/j.cageo.2009.01.010.
Macedo, O., J.-P. Métaxian, E. Taipe, D. Ramos, and A. Inza (2009) Seismicity associated with the 2006-2008 eruption, Ubinas volcano. VOLUME project, EU PF6 (No. 018471). ISBN 978-1-905254-39-2, VOLUME Project Consortium, Dublin.
Malama, B., A. Revil, and K.L. Kulhman (2009) A semi-analytical solution for trensient streaming potentials associated with confined aquifer pumping tests, Geophysical Journal International, 176, 1007-1016, doi: 10.1111/j.1365-246X.2008.04014.x.
Malama, B., K.L. Kuhlman, and A. Revil (2009) Theory of transient streaming potentials associated with axial-symmetric flow in unconfined aquifers, Geophysical Journal International, 179, 990–1003, doi: 10.1111/j.1365-246X.2009.04336.x.
Marsan D, Lengline O (2008) Extending earthquakes' reach through cascading. Science 319(5866), 1076-1079.
Martinez-Pagan P, Jardani A, Revil A, Haas A (2010) Self-potential monitoring of a salt plume. Geophysics 75(4):WA17-WA25

Metaxian JP, O'Brien GS, Bean CJ, Valette B, Mora M (2009) Locating volcano-seismic signals in the presence of rough topography: wave simulations on Arenal volcano, Costa Rica. Geophysical Journal International 179(3):1547-1557 .

Monteiller V., Got J.-L., J. Virieux and P. Okubo (2005) An efficient algorithm for double-difference tomography and location in heterogeneous media, with an application to Kilauea volcano, J. Geophys. Res., 110, B12306, doi:10.1029/2004JB003466.

Monteiller V., J.-L. Got, D. Patané, G. Barberi, and O. Cocina (2009) Double-difference tomography at Mt Etna volcano: Preliminary results. VOLUME project, EU PF6 (No. 018471). ISBN 978-1-905254-39-2, VOLUME Project Consortium, Dublin.

Monteiller V., J.-P. Métaxian, O. Macedo, G.S. O'Brien, I. Lokmer, and E. Taipe (2009) Moment-tensor inversion of very long period explosion events recorded at the Ubinas volcano, Peru. VOLUME project, EU PF6 (No. 018471). ISBN 978-1-905254-39-2, VOLUME Project Consortium, Dublin.

Mora M. M., Lesage P., Valette B., Alvarado G. E., Leandro C., Metaxian J. P., and Dorel J. (2006) Shallow velocity structure and seismic site effects at Arenal volcano, Costa Rica. Journal of Volcanology and Geothermal Research 152(1-2), 121-139.

Mora, M., Lesage, P., Donnadieu, F., Valade, S., Schmidt, A., Soto, G., Taylor, W., Alvarado, G. (2009) Joint Seismic, Acoustic and Doppler Radar observations at Arenal Volcano, Costa Rica: preliminary results. *In*: Bean, C. J., Braiden, A. K., Lokmer, I., Martini, F., O'Brien, G. S. VOLUME project, EU PF6 (No. 018471). ISBN 978-1-905254-39-2, VOLUME Project Consortium, Dublin.

Narteau C.**,** Byrdina S., Shebalin P. and Schorlemmer D., Common dependency on stress for the two fundamental laws of statistical seismology, *accepted to Nature.*

Narteau, C., S. Byrdina, P. Shebalin and D. Schorlemmer, 2009. Common dependency on stress for the two fundamental laws of statistical seismology, Nature (in press)

Nowack, R. L., T. Parsons, and A. Revil (2009) Editorial: Exploring New Frontiers with JGR-Solid Earth, J. Geophys. Res., 114, B10001, doi:10.1029/2009JB006977.

Perrier F., Richon P., Byrdina S., Rajaure S., France-Lanorde C., Revil A., Contraires S.**,** Bureau S., Gautam U., Koirala B., Shrestha P., Tiwari D.R., Bollinger L., Sapkota S. N., A direct evidence for high carbon dioxide and radon-222 gas exhalation at the Syabru-Bensi hot springs in Central Nepal, *EPSL, 278,198-207, doi:10.1016/j.epsl.2008.12.008,* 2009.

Perrier F, Richon P, Byrdina S, France-Lanord C, Rajaure S, Koirala BP, Shrestha PL, Gautam UP, Tiwari DR, Revil A, Bollinger L, Contraires S, Bureau S, Sapkota SN (2009) A direct evidence for high carbon dioxide and radon-222 discharge in Central Nepal. Earth and Planetary Science Letters 278(3-4), 198-207

Pinel V., Sigmundsson F., Sturkell E., Geirsson H., Einarsson P., Gudmundsson M. T., and Hognadottir T. (2007) Discriminating volcano deformation due to magma movements and variable surface loads: application to Katla subglacial volcano, Iceland. Geophysical Journal International 169(1), 325-338.

Pinel, V., Albino F., Sigmundsson F., Sturkell E. , Geirsson H., Einarsson P., Gudmundsson M. T. , Consequences of local surface load variations for volcanoes monitoring: Application to Katla subglacial volcano, Iceland, in VOLUME project, EU PF6 (No. 018471), edited by : C. J. Bean, A. K. Braiden, I. Lokmer, F. Martini, G. S. O'Brien, ISBN 978-1-905254-39-2, Publisher: VOLUME Project Consortium, Dublin, March 2009.

Pinel V, Jaupart C, Albino F (2010) On the relationship between cycles of eruptive activity and growth of a volcanic edifice. Journal of Volcanology and Geothermal Research 194(4):150-164.

Prono E, Battaglia J, Monteiller V, Got JL, Ferrazzini V (2009) P-wave velocity structure of Piton de la Fournaise volcano deduced from seismic data recorded between 1996 and 1999. Journal of Volcanology and Geothermal Research 184(1-2), 49-62.

Revil A, Finizola A, Piscitelli S, Rizzo E, Ricci T, Crespy A, Angeletti B, Balasco M, Cabusson SB, Bennati L, Boleve A, Byrdina S, Carzaniga N, Di Gangi F, Morin J, Perrone A, Rossi M, Roulleau E, Suski B (2008) Inner structure of La Fossa di Vulcano (Vulcano Island, southern Tyrrhenian Sea, Italy) revealed by high-resolution electric resistivity tomography coupled with self-potential, temperature, and CO2 diffuse degassing measurements. Journal of Geophysical Research-Solid Earth 113(B7) .

Revil A., C. Gevaudan, N. Lu, and A. Maineult (2008) Hysteresis of the self-potential response associated with harmonic pumping tests. Geophysical Research Letters, 35(16) L16402

Revil A, Jougnot D (2008) Diffusion of ions in unsaturated porous materials. Journal of Colloid and Interface Science 319(1), 226-235.

Revil A., F., Trolard, G. Bourrié, J. Castermant, A. Jardani, and C.A. Mendonça (2009) Ionic contribution to the self-potential signals associated with a redox front, Journal of Contaminant Hydrology, 109, 27-39.

Revil A (2010) Comment on "Review of self-potential methods in hydrogeophysics" by L. Jouniaux et al. C. R. Geoscience 341 (2009) 928-936. Comptes Rendus Geoscience 342(10):807-809.

Revil A, Cosenza P (2010) Comment on "Generalized effective-medium theory of induced polarization" (Michael Zhdanov, 2008, GEOPHYSICS, 73, F197-F211). Geophysics 75(2):X7-X9.

Revil A, Florsch N (2010) Determination of permeability from spectral induced polarization in granular media. Geophysical Journal International 181(3):1480-1498.

Revil A, Jardani A (2010) Seismoelectric response of heavy oil reservoirs: theory and numerical modelling. Geophysical Journal International 180(2):781-797.

Revil A, Jardani A (2010) Stochastic inversion of permeability and dispersivities from time lapse self-potential measurements: A controlled sandbox study. Geophysical Research Letters 37.

Revil A, Johnson TC, Finizola A (2010) Three-dimensional resistivity tomography of Vulcan's forge, Vulcano Island, southern Italy. Geophysical Research Letters 37.

Revil A, Mendonca CA, Atekwana EA, Kulessa B, Hubbard SS, Bohlen KJ (2010) Understanding biogeobatteries: Where geophysics meets microbiology. Journal of Geophysical Research-Biogeosciences 115.
Roux PF, Marsan D, Metaxian JP, O'Brien G, Moreau L (2008) Microseismic activity within a serac zone in an alpine glacier (Glacier d'Argentieire, Mont Blanc, France). Journal of Glaciology 54(184), 157-168.
Schmutz M, Revil A, Vaudelet P, Batzle M, Vinao PF, Werkema DD. (2010) Influence of oil saturation upon spectral induced polarization of oil-bearing sands. Geophysical Journal International 183(1):211-224.
Sigmundsson F, Pinel V, Lund B, Albino F, Pagli C, Geirsson H, Sturkell E (2010) Climate effects on volcanism: influence on magmatic systems of loading and unloading from ice mass variations, with examples from Iceland. Philosophical Transactions of the Royal Society a-Mathematical Physical and Engineering Sciences 368(1919):2519-2534.
Slob E, Snieder R, Revil A (2010) Retrieving electric resistivity data from self-potential measurements by cross-correlation. Geophysical Research Letters 37.
Sturkell E, Einarsson P, Roberts MJ, Geirsson H, Gudmundsson MT, Sigmundsson F, Pinel V, Guomundsson GB, Olafsson H, Stefansson R (2008) Seismic and geodetic insights into magma accumulation at Katla subglacial volcano, Iceland: 1999 to 2005. Journal of Geophysical Research-Solid Earth 113(B3).
Thouret J. C., Ramírez J. C., Gibert-Malengreau B., Vargas C. A., Naranjo J. L., Vandemeulebrouck J., Valla F., and Funk M. (2007) Volcano-glacier interactions on composite cones and lahar generation: Nevado del Ruiz, Colombia, case study. Annals of Glaciology 45(1), 115-127.
Traversa P, Grasso JR (2009) Brittle Creep Damage as the Seismic Signature of Dyke Propagations within Basaltic Volcanoes. Bulletin of the Seismological Society of America 99(3), 2035-2043.
Traversa, P., J.-R. Grasso, O. Lengliné, and V. Ferrazzini, 2009. Seismic signature of magma reservoir dynamics at basaltic volcanoes, lessons from the Piton de la Fournaise volcano. VOLUME project, EU PF6 (No. 018471). ISBN 978-1-905254-39-2, VOLUME Project Consortium, Dublin.
Traversa P, Pinel V, Grasso JR (2010) A constant influx model for dike propagation: Implications for magma reservoir dynamics. Journal of Geophysical Research-Solid Earth 115.
Vandemeulebrouck J, Hurst AW, Scott BJ (2008) The effects of hydrothermal eruptions and a tectonic earthquake on a cycling crater lake (Inferno Crater Lake, Waimangu, New Zealand). Journal of Volcanology and Geothermal Research 178(2), 271-275.
Vandemeulebrouck J, Roux P, Gouedard P, Legaz A, Revil A, Hurst AW, Boleve A, Jardani A (2010) Application of acoustic noise and self-potential localization techniques to a buried hydrothermal vent (Waimangu Old Geyser site, New Zealand). Geophysical Journal International 180(2):883-890.
Wang M, Revil A (2010) Electrochemical charge of silica surfaces at high ionic strength in narrow channels. Journal of Colloid and Interface Science 343(1):381-386.
Woodruff WF, Revil A, Jardani A, Nummedal D, Cumella S (2010) Stochastic Bayesian inversion of borehole self-potential measurements. Geophysical Journal International 183(2):748-764.

Institut de Physique du Globe, UMR7154 (CNRS-Univ. Paris Diderot) et LGSR (Université de la Réunion, St. Denis)

L'Institut de Physique du Globe de Paris exerce la responsabilité de la surveillance des volcans français d'Outre-mer (Antilles et Réunion) et est actuellement co-tutelle de l'Observatoire volcanologique de Montserrat. Il développe en même temps des recherches dans différentes disciplines de la volcanologie. Les travaux mentionnés ci-dessous ne font état que des rapports reçus.

1. Modélisation des transferts et stockages magmatique au Piton de La Fournaise à partir de leur signature géophysique de surface

A. Peltier et collaborateurs (IPG, UMR 7154 CNRS-Univ. Paris Diderot, Paris)

La thématique abordée aux travers de ces études est de mieux contraindre et comprendre le fonctionnement du système d'alimentation du Piton de La Fournaise, allant de son système de stockage superficiel à la propagation des dykes vers la surface.
Au Piton de La Fournaise, cette étude jouit d'une activité volcanique soutenue (1 à 2 éruptions par an depuis 20 ans) ainsi que d'un large nombre de données géophysiques de surface collectées par l'observatoire volcanologique. L'analyse croisée des données de déformation et de leur modélisation numérique, des données sismologiques ainsi que des données géochimiques de la période 1998-actuel a permit d'imager un réservoir superficiel localisé aux alentours de 2000-2500m de profondeur et contraindre les différents chemins préférentiels empruntés par les dykes se situant aux limites structurales est et ouest du cratère Dolomieu.
Les études les plus récentes (post 2007) des déformations de surface ont permis également de caractériser l'influence de l'effondrement du cratère Dolomieu d'Avril 2007 sur l'activité actuelle du volcan. Les résultats préliminaires suggèrent que l'augmentation de la fréquence des intrusions avortées en 2008 et 2009, serait influencée par les conséquences de l'effondrement du cratère Dolomieu (Peltier et al., 2010). Les changements

de distribution de contrainte dans l'édifice suite à l'effondrement, ont temporairement au moins, favorisés l'arrêt des dykes en profondeur.

Publications

Peltier, A., P. Bachèlery, T. Staudacher (2011), Early detection of large eruptions at Piton de La Fournaise volcano (La Réunion Island): contribution of a distant tiltmeter station, J. Volcano. Geotherm. Res, 199, Issues 1-2, 96-104.

Peltier, A., M. Bianchi, E. Kaminski, J-C Komorowski, A. Rucci, T. Staudacher (2010), PSInSAR as a new tool to monitor pre-eruptive volcano ground deformation: validation using GPS measurements on Piton de la Fournaise, Geophys. Res. Lett., 37, L12301, doi:10.1029/2010GL043846.

Peltier, A., T. Staudacher, P. Bachèlery (2010), New behaviour of the Piton de La Fournaise volcano feeding system (La Réunion Island deduced from GPS data: influence of the 2007 Dolomieu crater collapse, J. Volcano. Geotherm. Res, 192, 48-56.

Peltier, A., P. Bachèlery, T. Staudacher (2009), Magma transfer and storage at Piton de La Fournaise (La Réunion Island) between 1972 and 2007: a review of geophysical and geochemical data, J. Volcano. Geotherm. Res., 184(1-2), 93-108.

Staudacher, T., V. Ferrazzini, A. Peltier, P. Kowalski, P. Boissier, P. Catherine, F. Lauret, F. Massin (2009), The April 2007 eruption and the Dolomieu crater collapse, two major events at Piton de la Fournaise, J. Volcano. Geotherm. Res.,184(1-2), 126-137.

Michon L., V. Cayol, L. Letourneur, A. Peltier, N. Villeneuve, T. Staudacher (2009), Edifice growth, deformation and rift-zone development in basaltic setting: insights from Piton de La Fournaise basaltic shield volcano (La Réunion Island, Indian Ocean), J. Volcano. Geotherm. Res., 184(1-2), 14-30.

Peltier, A., T. Staudacher, P. Bachèlery, V. Cayol (2009), Formation of the April 2007 caldera collapse at Piton de La Fournaise volcano: insights from GPS data, J. Volcano. Geotherm. Res., 184 (1-2), 152-163.

Peltier, A., V. Famin, P. Bachèlery, V. Cayol, Y. Fukushima. T. Staudacher (2008), Cyclic magma storages and transfers at Piton de La Fournaise volcano (La Réunion hotspot) inferred from deformation and geochemical data, Earth and Planetary Science Letters, 270 (3-4), 180-188.

Letourneur, L., A. Peltier, T. Staudacher, A. Gudmundsson (2008), The effects of rock heterogeneities on dyke paths and asymmetric ground deformation: The example of Piton de la Fournaise (Réunion Island), J. Volcano. Geotherm.Res.,173 (3-4), 289-302.

Vlastélic, I., A. Peltier, T. Staudacher (2007), Short-term (1998-2006) fluctuations of Pb isotopes at Piton de la Fournaise volcano (Reunion Island): Origins and constrains on the size and shape of the magma reservoir, Chemical Geology, 244, 202-220.

Peltier A., T. Staudacher, P. Bachèlery (2007), Constraints on magma transfers and structures involved in the 2003 activity at Piton de La Fournaise from displacement data, J. Geophys. Res., 112, B03207, doi:10.1029/2006JB004379.

2. Modélisation

a. Développement d'un modèle de turbulence mieux adapté à la dynamique des panaches volcaniques, prenant en compte notamment l'impact de l'échelle de ces écoulements et l'effet de la flottabilitédans les jets volcaniques. Nous avons mis en oeuvre des expériences analogiques pour valider ces modèles avant de les appliquer aux cas géologiques.
b. Développement d'un modèle théorique pour l'extraction des liquides magmatiques dans les milieux visco-élastiques.
c. Modèle de détection des liquides magmatiques dans le manteau par l'anisotropie sismique.

Publications

E. Kaminski, A.-L. Chenet, C. Jaupart and V. Courtillot, Rise of volcanic plumes to the stratosphere aided by penetrative convection above large lava flows, Earth Planet. Sci. Lett., 10.1016/j.epsl.2010.10.037, 2011.

A. Peltier, M. Bianchi, E. Kaminski, J.-C. Komorowski, A. Rucci and T. Staudacher, PSInSAR as a new tool to monitor pre-eruptive volcano ground deformation: Validation using GPS measurements on Piton de la Fournaise, Geophys. Res. Lett., 37, L12301, doi:10.1029/2010GL043846, 2010.

G. Carazzo, E. Kaminski and S. Tait, The rise and fall of turbulent fountains: a new model for improved quantitative predictions, J. Fluid Mech., 2010.

G. Carazzo, E. Kaminski and S. Tait, On the dynamics of volcanic columns: a comparison of field data with a new model of negatively buoyant jets, J. Volcanol. Geotherm. Res., in press, doi:10.1016/j.jvolgeores.2008.01.002, 2008.

B. Chauveau and E. Kaminski, Porous compaction in transient creep regime and implications for melt, petroleum, and CO2 circulation, J. Geophys. Res., 113, B09406, doi:10.1029/2007JB005088. 2008.

G. Carazzo, E. Kaminski and S. Tait, On the Rise of Turbulent Plumes: Quantitative Effects of Variable Entrainment for Submarine Hydrothermal Vents, Terrestrial and Extra Terrestrial Explosive Volcanism, J. Geophys. Res., 113, B09201, doi:10.1029/2007JB005458, 2008.

E. Kaminski, The interpretation of seismic anisotropy in terms of mantle flow when melt is present, Geophys. Res. Lett., 33, L02304, doi:10.1029/2005GL024454, 2006.

G. Carazzo, E. Kaminski and S. Tait, The route to self-similarity in turbulent jets and plumes, J. Fluid Mech., 547 - pp. 137-148, 2006.

3. Synthèse de la recherche en volcanologie menée entre 2007 et 2010 par le Laboratoire Géosciences Réunion de l'Université de la Réunion.

Préambule:
Le laboratoire GéoSciences Réunion comprend 6 enseignants-chercheurs, 1 chercheur CNRS depuis juillet 2010, et entre 6-8 doctorants. Depuis 2005, les membres du laboratoire ont intégré l'équipe Géologie des Systèmes Volcaniques de l'UMR 7154 de l'IPGP. Notre recherche s'articule autour de plusieurs thématiques qui ont pour finalité de renforcer notre compréhension globale des systèmes volcaniques.

1- Structure Mantellique des points chauds

La mise en commun des données PLUME (2001-2005) et BBOBS a permis d'obtenir une couverture suffisante pour effectuer une tomographie du Pacifique sud par les ondes de volume. 1500 temps d'arrivées (P et PP) ont été utilisés (Tanaka et al., 2008) dans une tomographie régionale et dans un modèle de tomographie globale du manteau. La tomographie régionale met en évidence une anomalie lente à 400 km sous le point chaud de la Société et s'enracinant dans le manteau inférieur (Figure 1). Une large anomalie lente est visible sous le centre du superswell jusqu'à 1600 Km de profondeur. La prise en compte de données sismologiques temporaires (Suetsugu *et al.*, 2009) enregistrées dans le Pacifique Sud dans un modèle de tomographie globale (Fukao et al., 2003) a mis en évidence une anomalie lente de vitesse sismique culminant à 1000 Km de profondeur (Tanaka et al., 2009a; Tanaka et al., 2009b), c'est à dire bien en dessous de l'interface à 660 Km qui avait été proposée comme limite supérieure d'un "superplume" dans le manteau inférieur. La modélisation du superswell à partir de ces données tomographiques (Adam et al., 2010) montre que l'anomalie bathymétrique est très bien expliquée par les anomalies de densité dans le manteau supérieur.

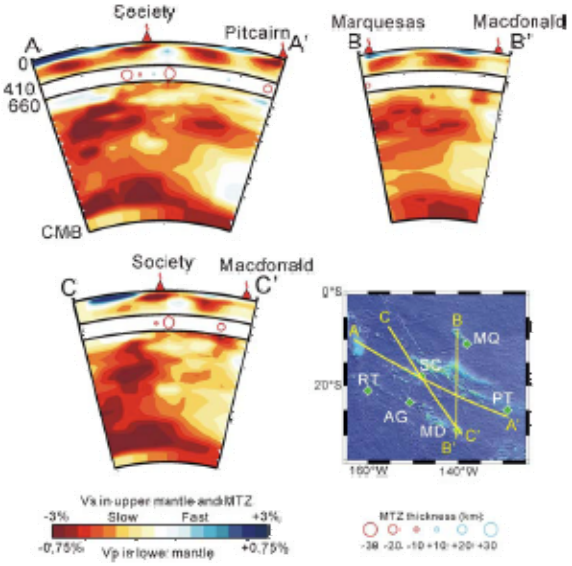

Figure 1: Coupes de l'ensemble du manteau sous le pacifique Sud à travers le modèle tomographique global en prenant en compte les données PLUME (2001-2005) et BBOBS (Suetsugu et al., 2009; Tanaka et al., 2008). La tomographie régionale met en évidence une anomalie lente à 400 km sous le point chaud de la Société et s'enracinant dans le manteau inférieur. Le modèle de tomographie globale (Fukao et al., 2003) a mis en évidence une anomalie lente de vitesse sismique culminant à 1000 Km de profondeur (Tanaka et al., 2009a; Tanaka et al., 2009b), c'est à dire bien en dessous de l'interface à 660 Km qui avait été proposée comme limite supérieure d'un "superplume" dans le manteau inférieur.

L'utilisation des ondes SKS dans le Pacifique sud est rendue complexe par le faible nombre de données utilisables. En effet, il faut être situé à des distances épicentrales supérieures à 85° pour pouvoir utiliser les phases SKS et caractériser l'anisotropie du manteau. Le Pacifique ouest et sud ne sont pas des endroits les plus propices à ces mesures (couleurs bleues sur la carte) (Barruol et al., 2002).

Malgré un nombre assez réduit de données aux stations temporaires, nous avons pu caractériser l'anisotropie sous la plupart des stations du Pacifique sud. L'anisotropie a été détectée sous toutes les stations temporaires excepté sous Tahiti, malgré un grand nombre de données analysées.

Les mesures effectuées montrent des directions rapides proches de celle du déplacement de la plaque Pacifique (N120°) qui peuvent être expliquée par un **cisaillement asthénosphérique** induit par le déplacement de la plaque, et des directions parallèles aux failles transformantes (N70°), parallèles aux anciennes directions d'expansion (Figure 2). Des variations azimutales des paramètres anisotropes observées en certaines stations sont compatibles avec la présence de **deux couches d'anisotropie** (Fontaine et al., 2007) actuelle (dans l'asthénosphère) et ancienne (dans la lithosphère).

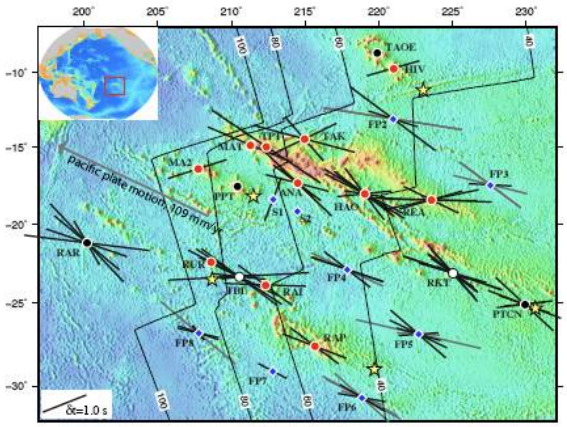

Figure 2: Carte d'anisotropie sous le Pacifique sud (déphasage d'ondes SKS) aux stations permanentes et temporaires PLUME (Fontaine et al., 2007) ainsi qu'aux OBS (Barruol et al., 2009; Suetsugu et al., 2009). Les points chauds sont indiqués par les étoiles jaunes. Les mesures effectuées montrent des directions rapides proches de celle du déplacement de la plaque Pacifique (N120°) qui peuvent être expliquée par un **cisaillement asthénosphérique** induit par le déplacement de la plaque, et des directions parallèles aux failles transformantes (N70°), parallèles aux anciennes directions d'expansion. Des variations azimutales des paramètres anisotropes observées en certaines stations sont compatibles avec la présence de **deux couches d'anisotropie** (Fontaine et al., 2007) actuelle (dans l'asthénosphère) et ancienne (dans la lithosphère).

Les mesures des déphasage des ondes SKS incluant les données des OBS ont montré que l'anisotropie observée sur les fonds océaniques non affectés par les points chauds est très semblable à celle observée sur les îles. Les stations localisées au dessus du point chaud de la Société semblent dépourvues d'anisotropie, ce qui peut être expliqué par un flux mantellique vertical, ou bien par la présence d'un flux asthénosphérique parabolique lié à l'étalement du panache sous la lithosphère en mouvement (Barruol *et al.*, 2009).

2- Interaction points chauds édifices

L'influence du point chaud sur le développement des édifices volcaniques a été évaluée par l'étude multi-échelle des structures volcano-tectoniques des volcans réunionnais (Michon et al., 2007). Ce travail a révélé un fort parallélisme entre les structures lithosphériques héritées de l'accrétion océanique, des failles majeures recoupant le Piton des Neiges et la majorité des rifts zones des Piton de Neiges et Piton de la Fournaise. Une telle superposition des orientations a été interprétée comme le résultat d'un contrôle structural de la lithosphère sur le développement et l'évolution du Piton des Neiges et du Piton de la Fournaise.

Par ailleurs, les données sismiques acquises pendant la campagne REUSIS suggéraient une absence de flexure lithosphérique au droit de la Réunion (de Voogd et al., 1999). Cette caractéristique, bien différente des points chauds du Pacifique (Hawaii et Marquises) où la lithosphère s'infléchit sous la charge des édifices (Figure 3a), serait liée à l'érosion thermique de la base de la lithosphère réunionnaise (Figure 3b). La capacité d'un point chaud à éroder la lithosphère dépendrait à la fois de l'ampleur de l'anomalie de température et de la vitesse de déplacement de la plaque (Michon et al., 2007).

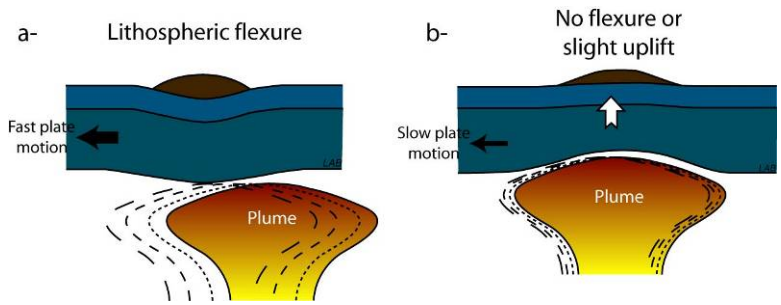

Figure 3: a) Impact de l'emplacement d'un plume mantellique sous une plaque se déplaçant rapidement. Le déplacement rapide empêche une érosion thermique efficace de la base de la lithosphère. La charge liée à l'édifice provoque donc une flexure lithosphérique comme à Hawaii ou aux Marquises. Les formes en pointillés représentent l'anomalie à différentes périodes. b) Erosion thermique efficace d'une lithosphère se déplaçant lentement. L'érosion thermique induit un déséquilibre isostatique et un bombement qui contre-balance la charge de l'édifice comme à la Réunion.

3- Dynamique de chambre, intrusions et déformation

En grande majorité, les compositions de laves du Piton de la Fournaise ont pu être expliquées par trois mécanismes de différenciation magmatique distincts, à partir d'un seul et unique magma source (Famin et al., 2009; Figure 4). La première différentiation privilégie la cristallisation de clinopyroxène et de plagioclase, dans le réservoir le plus profond (> 7,5 km). La deuxième différentiation favorise la cristallisation d'olivine à 0,5 – 2,6 km, ce qui explique son abondance dans les éruptions d'océanites comme la coulée de février 2005. La troisième différentiation se produit lors de la remontée des magmas en surface ou dans des poches à très faible profondeur (0,5 km), et se traduit à nouveau par la cristallisation d'un assemblage clinopyroxène + plagioclase. Le passage d'un mode de différentiation au suivant dépend principalement de la pression.

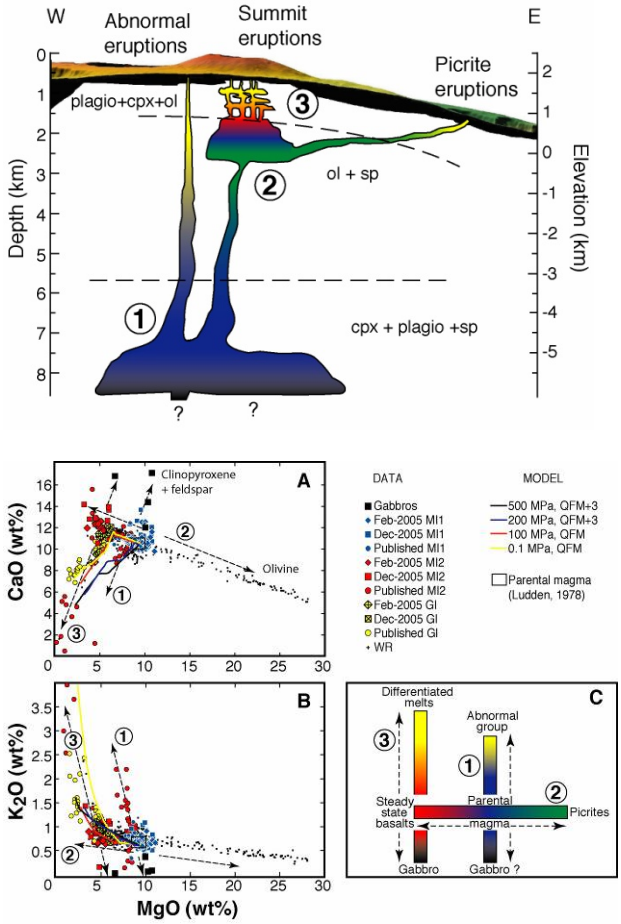

Figure 4 : Profondeur des réservoirs de magma sous le piton de la Fournaise et style de différentiations chimiques. Les couleurs correspondent aux compositions des laves, qui indiquent trois styles de différentiation magmatique en fonction de la profondeur des réservoirs (Famin et al. 2009).

Les cristaux d'olivine des éruptions récentes montrent des textures associées à des cycles rapides de refroidissement et de réchauffement (Figure 5). Ceci suggère que le réservoir situé entre 0,5 et 2,6 km de la surface entre en convection thermique juste avant les éruptions. Il est donc possible d'imaginer que ce sont les instabilités thermiques qui engendrent les éruptions (Welsch et al., 2009).

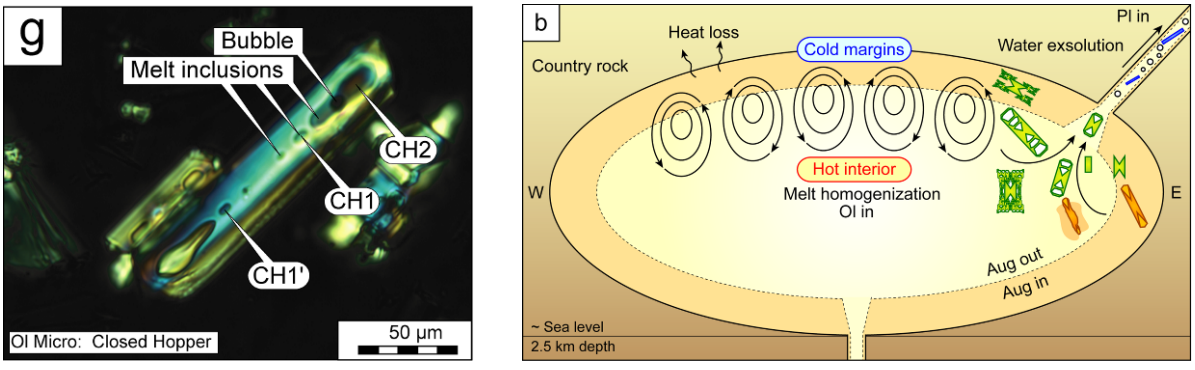

Figure 5 : a) Microcristal d'olivine à croissance symétrique ayant piégé une paire d'inclusions vitreuses à chaque cycle de refroidissement-réchauffement. Ce cristal a subi trois cycles. b) Modèle de convection dans le réservoir magmatique à olivine, d'après la texture des microcristaux. La convection se produit au toit de la chambre car c'est la zone où l'instabilité thermique se développe (Welsch et al., 2009).

L'étude des éruptions depuis 1981 nous a permis de montrer qu'au Piton de la Fournaise le magma s'injectait le long de deux rift zones perpendiculaires orientées N25-30 et N120 (Michon et al., 2007a). La majorité des intrusions entraine le développement de fissures éruptives qui s'organisent selon une géométrie en échelon sur le cône actif. Nous avons montré que cette distribution ne traduisait pas un cisaillement latéral associé au déplacement co-éruptif du flanc est du volcan mais résultait du champ de contraintes prévalant en sub-surface (Michon et al. 2009a).

La modélisation numérique d'intrusions récurrentes le long des rift zones N25-30 et N120 a montré que cette activité intrusive produisait une déformation asymétrique du cône actif du Piton de la Fournaise, identique à celle observée par GPS et au niveau de la topographie (Michon et al., 2009a; Figure 6).

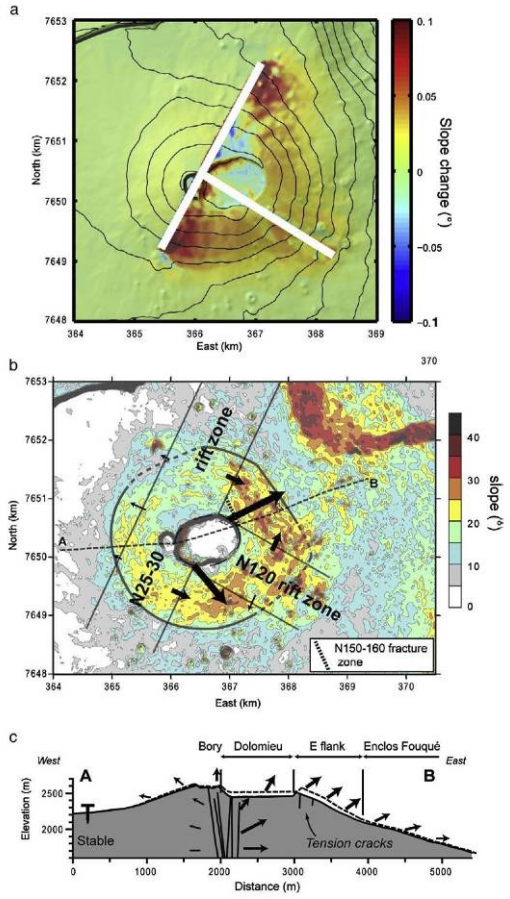

Figure 6: a) Modélisation des changements de pente dus à l'intrusion répétée de dykes dans les rift zones N25-30 et N120. La trace des dykes en surface est représentée par une ligne blanche. b) Carte de pente suggérant l'effet des dykes dans le développement des flancs est et sud-est du cône actif. c) Coupe E–W présentant l'inflation de la moitié est du cône.

Parallèlement, nos travaux menés dans le cœur du Piton des Neiges ont révélé qu'en profondeur, les intrusions magmatiques se développaient essentiellement sous forme de sills faiblement inclinés vers l'extérieur. Un niveau de forte concentration en sills, mis en place dans la partie nord, entre un massif gabbroïque et des dépôts d'avalanche de débris, a été reconnu comme un détachement ayant contrôlé la déstabilisation latérale du volcan (Famin et Michon, 2010; Figure 7). Ce type de structure et de processus, jamais observé sur les autres volcans boucliers car localisé en profondeur, constitue une alternative mécanique au modèle d'injections de dykes le long des rift zones.

Figure 7: Coupe géologique au niveau du gabbro de l'îlet à Vidot montrant la zone de déformation (vert) sur laquelle le flanc nord du Piton des Neiges a continuellement glissé (Famin et Michon, 2010).

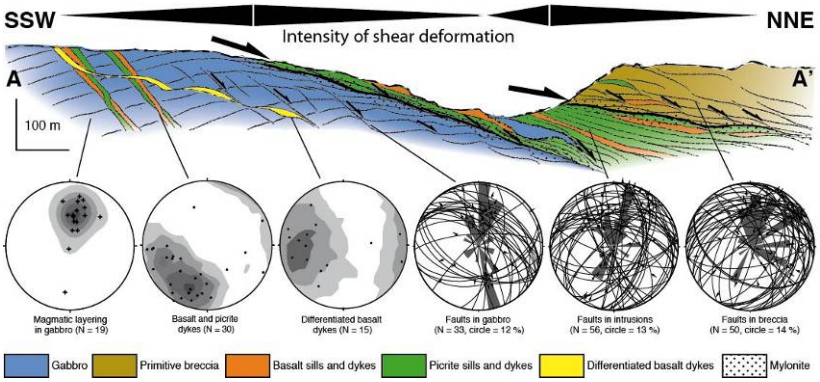

4- Structuration et dynamique des systèmes hydrothermaux

Les systèmes hydrothermaux correspondent à la zone d'interaction entre le système purement magmatique et les fluides météoriques descendants. Les nombreuses campagnes géophysiques (tomographie de résistivité électrique, polarisation spontanée et température du sol) et d'analyse de gaz (CO_2 dans le sol) ont permis d'imager les systèmes hydrothermaux du Stromboli, de Vuclano, du Piton de la Fournaise et des volcans Santa Maria, Cerro Quemado et Zunil au Guatemala (Finizola et al., 2008, 2009, 2010; Revil et al. 2008, 2010). Sur ces différents systèmes, nous avons pu mettre en évidence le contrôle étroit des limites structurales sur la remontée de fluides et dans le confinement latéral du système hydrothermal (Figure 8). A Stromboli, la récurrence des campagnes de mesure a permis de suivre les variations du système hydrothermal lors des phases d'activité "normales" ou exceptionnelles, comme lors de la crise éruptive de 2002-2003.

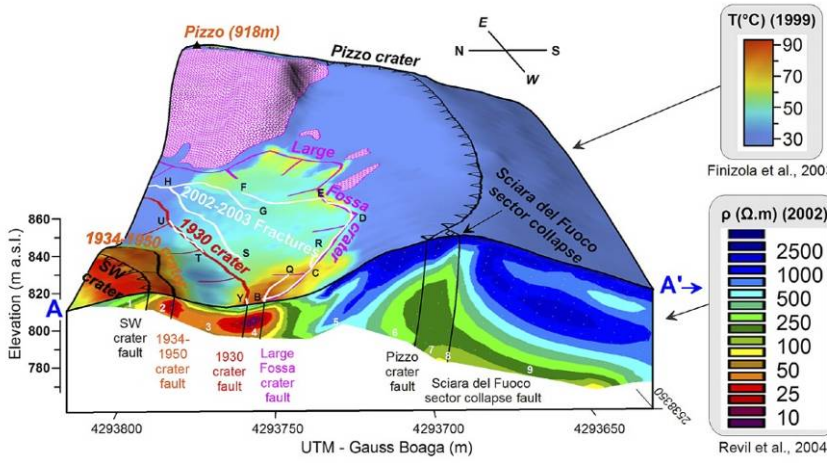

Figure 9: Représentation 3D de la Fossa, à Stromboli, avec en coupe un profil de tomographie de résisitivité électrique et en surface une carte de température du sol. Cf Finizola et al., (2009) pour une description détaillée.

5- Dynamique des calderas magmatiques

L'effondrement du cratère Dolomieu d'avril 2007 au Piton de la Fournaise constitue l'exemple le plus récent d'effondrement caldérique. La déformation péri-caldérique a été enregistrée par un dense réseau GPS. Les déplacements associés à cet événement, pluri-métriques pour certains, ont été maximum le long de la bordure sud du Dolomieu (Michon et al., 2009b; Figure 8). La décroissance rapide des déplacements depuis la bordure vers l'extérieur a entrainé la formation d'un dense réseau de fractures concentriques, fragilisant cette partie du sommet.

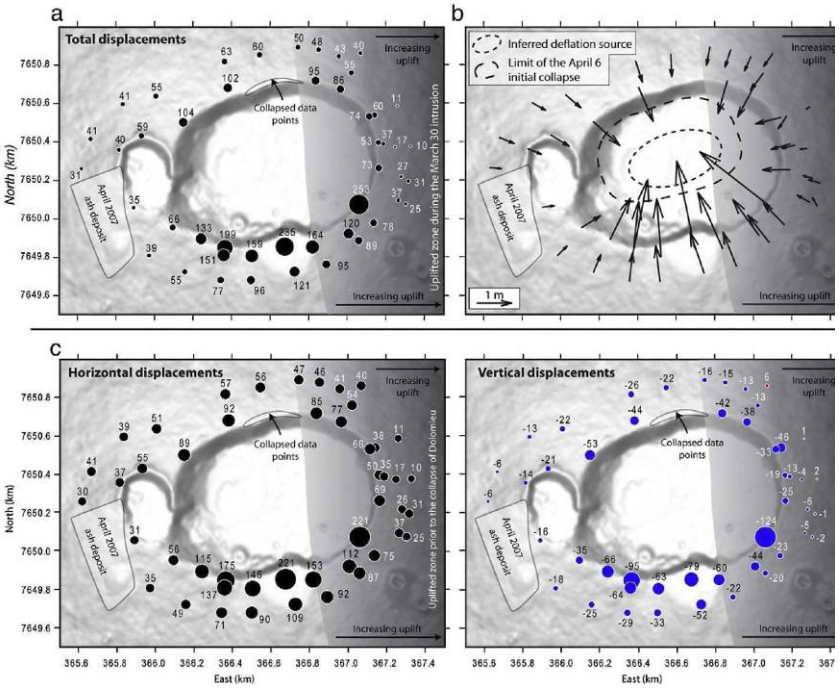

Figure 8: Déplacements enregistrés sur la bordure du Dolomieu entre mars et mai 2007. a) Déplacements totaux (en cm). b) Vecteurs déplacement pour la composante horizontale. c) Composantes horizontale et verticale du déplacement (en cm).

La dynamique d'effondrement du Dolomieu a été comparée à celle enregistrée lors des effondrements caldériques du Fernandina en 1968 et du Miyakejima en 2000. Nous avons pu montrer que ces trois événements s'étaient produits de manière similaire, i.e. en un effondrement incrémental d'un piston dans la chambre magmatique (Michon et al., 2009b). L'intégration des données sismiques et de déformation a permis de déterminer le déplacement vertical du piston lors de chaque incrément d'effondrement, et incidemment les taux de vidange magmatique pour ces trois volcans (Michon et al., 2011). La dynamique d'effondrement observée dans le cas des calderas basaltiques est identique à celle, supposée, des calderas siliceuses.

6- Erosion des volcans insulaires et transfert sédimentaire

L'exploitation des données acquises lors des campagnes à la mer, FOREVER (2006) et ERODER (2006, 2008, 2010), a permis une caractérisation précise des processus mis en jeu dans la construction des pentes sous-marines de La Réunion. En particulier, la découverte de plusieurs systèmes turbiditiques en connexion avec les grandes rivières de l'île de La Réunion démontre l'efficacité du transfert sédimentaire depuis la zone émergée vers le domaine marin. Le système de Cilaos a été bien étudié (thèses de Saint-Ange – 2009 et Sisavath – en cours, Saint-Ange et al. 2011; Figure 9). Il constitue le plus bel exemple de système volcanoclastique sous-marin décrit autour d'une île. Loin de toute source continentale, il fournit des informations uniques sur l'architecture et les processus associés à la mise en place de ce type de formation, dont l'importance était jusqu'alors largement minimisée dans le volcanisme insulaire intraplaque.

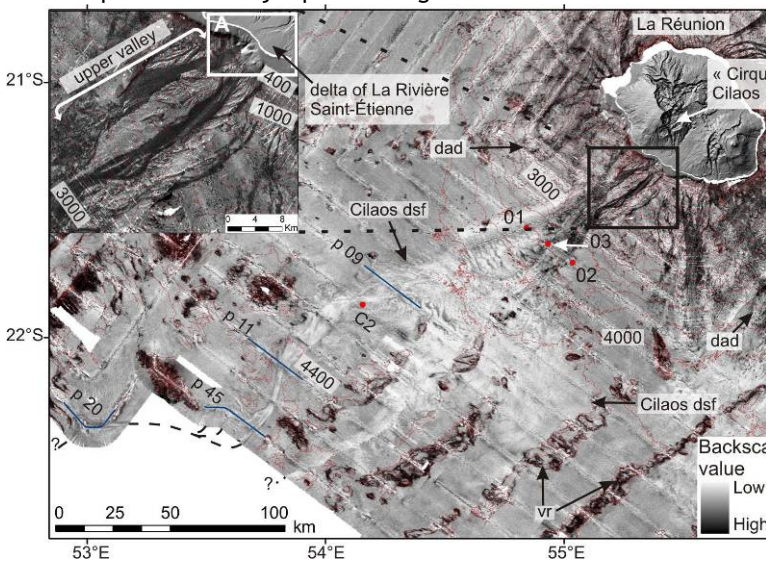

Figure 9: Le système turbiditique de Cilaos : Imagerie acoustique au sud-ouest de l'île de La Réunion acquise durant les campagnes FOREVER ET ERODER (in Saint-Ange et al., Geology, 2011). Abbreviations: dad—Dépôts d'avalanche de débris; dsf—deep-sea fan; vr—rides volcaniques.

Publications

- **Finizola A.**, Ricci T., Deiana R., Barde-Cabusson S., Rossi M., Praticelli N., Giocoli A., Romano G., Delcher E., Suski B., Revil A., Menny P., Di Gangi F., Letort J., Peltier A., Villasante-Marcos V., Douillet G., Avard G., Lelli M. (2010). Adventive hydrothermal circulation on Stromboli volcano (Aeolian Islands, Italy) revealed by geophysical and geochemical approaches: Implications for general fluid flow models on volcanoes. *J. Volcanol. Geotherm. Res.*, 196, 111-119. doi: 10.1016/j.jvolgeores.2010.07.022.
- Komorowski, J.-C., Y. Legendre, T. Christopher, M. Bernstein, R. Stewart, E. Joseph, N. Fournier, L. Chardot, **A. Finizola,** G. Wadge, R. Syers, C. Williams, V. Bass (2010), Insights into processes and deposits of hazardous vulcanian explosions at Soufrière Hills Volcano during 2008 and 2009 (Montserrat, West Indies), *Geophys. Res. Lett.*, 37, L00E19, doi:10.1029/2010GL042558.
- **Drouin, M.**, Ildefonse, B., Godard, M. (2010), A microstructural imprint of melt impregnation in slow-spread lithosphere: the olivine-rich troctolites from the Atlantis Massif (Mid-Atlantic Ridge 30°N, IODP Hole U1309D). *Geochem. Geophys. Geosyst.*, 11, Q06003, doi:10.1029/2009GC002995.
- Revil, A., T.C. Johnson, **A. Finizola** (2010), Three-dimensional resistivity tomography of Vulcan's forge, Vulcano Island, southern Italy, Geophys. Res. Lett., 37, L15308, doi:10.1029/2010GL043983.
- Merle, O., Ph. Mairine, **L. Michon, P. Bachèlery, M. Smietana** (2010), Calderas, Landslides and Paleo-canyons at Piton de la Fournaise Volcano (La Réunion Island, Indian Ocean), *J. Volcanol. Geotherm. Res.*, 189, 131-142, doi:10.1016/j.jvolgeores.2009.11.001
- **Famin V., Michon L.** (2010), Volcano desabilization by magma injection in a detachment, *Geology*, 38, 219-222.
- Peltier A., Staudacher T., **Bachèlery P.** (2010), New behaviour of the Piton de La Fournaise volcano feeding system (La Réunion Island) deduced from GPS data: Influence of the 2007 Dolomieu caldera collapse, *J. Volcanol. Geotherm. Res.*, 192 (1-2), 48-56.

2009

- **Welsch B.,** Faure F., **Bachèlery P., Famin V.** (2009), Microcrysts record transient convection at Piton de la Fournaise volcano (La Réunion hotspot). *Journal of Petrology*, 50, 2287-2305.
- Barruol, G., D. Suetsugu, H. Shiobara, H. Sugioka, S. Tanaka, G. H. R. Bokelmann, **F. R.Fontaine**, and D. Reymond (2009), Mapping upper mantle flow beneath French Polynesia from broadband ocean bottom seismic observations, *Geophys. Res. Lett.*, 36, L14301, doi:10.1029/2009GL038139.
- Barde-Cabusson, S., Levieux, G., Lénat, J.-F., **Finizola A**., Revil, A., **Chaput, M**., Dumont, S., Duputel, Z., Guy, A., Mathieu, L., Saumet, S., Sorbadère, F. and Vieille, M., (2009). Transient self-potential anomalies associated with recent lava flows at Piton de la Fournaise volcano (Réunion Island, Indian Ocean). *J. Volcanol. Geotherm. Res.*, vol. 187, 3-4, 158-166.
- Bani P., **Join J.-L.,** Cronin S. J., Lardy M., Rouet I. Garaebiti E. (2009). Characteristics of the summit lakes of Ambae volcano and their potential for generating lahars. *Nat. Hazards Earth Syst. Sci.*, 9, p 1471-1478.
- **Morin J.**, Lavigne F., **Bachèlery P., Finizola A., Villeneuve N.** Institutional and social responses to hazards related to Karthala volcano, Comoros. Part I - Analysis of the May 2006 eruptive crisis. *SHIMA The International Journal of Research into Island Cultures*, vol 3, n° 1, 33 – 53.
- **Morin J.**, Lavigne F. Institutional and people's response in the face of volcanic hazards in island environment: Case of Karthala volcano, Comoros Archipelago. Part II - Deep-seated root causes of Comorian vulnerabilities. *SHIMA The International Journal of Research into Island Cultures*, vol 3, n°1, 54-71.
- Antoine R., Baratoux D., Rabinowicz M., Fontaine F., **Bachèlery P.**, Staudacher T., Saracco G., **Finizola A.**, (2009). Thermal infrared image analysis of a quiescent cone on Piton de la Fournaise volcano: Evidence of convective air flow within an unconsolidated soil. *J. Volcanol. Geortherm. Res.*, 183, 228-244, doi: 10.1016/j.jvolgeores.2008.12.003
- Boivin P. and **P. Bachèlery** (2009). Petrology of 1977 to 1998 eruptions at Piton de la Fournaise, la Réunion Island. *J. Volcanol. Geortherm. Res.*, 184, p 109-125, doi: 10.1016/j.jvolgeores.2009.01.012
- **Drouin, M.**, Godard, M., Ildefonse, B., Bruguier, O., Garrido, C. J. (2009). Geochemical and petrographic evidence for magmatic impregnation in the oceanic lithosphere at Atlantis Massif, Mid-Atlantic Ridge (IODP Hole U1309D, 300N), *Chem. Geol.*, doi: 10.1016/j.chemgeo.2009.02.013
- **Famin V.**, **B. Welsch**, S. Okumura, **P. Bachèlery** and S. Nakashima (2009). Three differentiation stages of a single magma at Piton de la Fournaise (Reunion hotspot). *G-Cubed.* 10(1) Q01007, doi: 10.1029/2008GC002015
- **Fontaine, F. R.**, G. Barruol, B. L. N. Kennett, G. H. R. Bokelmann, and D. Reymond (2009). Upper mantle anisotropy beneath Australia and Tahiti from P wave polarization: Implications for real-time earthquake location, *J. Geophys. Res.*, 114, B03306, doi:10.1029/2008JB005709
- Gailler L.-S., J.-F. Lénat, M. Lambert, G. Levieux, **N. Villeneuve**, J.-L. Froger (2009). Gravity structure of Piton de la Fournaise volcano and inferred mass transfer during the 2007 crisis. *J. Volcanol. Geortherm.*

Res., 184, 199-207, doi:10.1016/j.jvolgeores.2009.01.024
- Lénat J.-F., P. Boivin, C. Deniel, P.-Y. Gillot, **P. Bachèlery** and Fournaise 2 Team (2009). Age and nature of deposits on the submarine flanks of Piton de la Fournaise (Reunion Island). *J. Volcanol. Geortherm. Res.*, 184, 199-207, doi:10.1016/j.jvolgeores.2009.01.013
- **Michon L.**, V. Cayol, L. Letourneur, A. Peltier, **N. Villeneuve**, T. Staudacher (2009). Edifice growth, deformation and rift zone development in basaltic setting: insigths from Piton de la Fournaise shield volcano (La Réunion Island, Indian Ocean). *J. Volcanol. Geortherm. Res.*, 184, 14-30, doi: 10.1016/j.jvolgeores.2008.11.002.
- **Michon L.**, **N. Villeneuve**, **Th. Catry**, O.Merle (2009). How summit calderas collapse on basaltic volcanoes: new insights from the April 2007 caldera collapse of Piton de la Fournaise volcano. *J. Volcanol. Geortherm. Res.*, 184, 138-151, doi: 10.1016/j.jvolgeores.2008.11.003
- Peltier, A., T. Staudacher, **P. Bachèlery**, V. Cayol (2009). Formation of the April 2007 caldera collapse at Piton de La Fournaise volcano: insights from GPS data. *J. Volcanol. Geortherm. Res.*, 184, 152-163, doi:10.1016/j.jvolgeores.2008.09.009
- Peltier, A., **P. Bachèlery**, T. Staudacher (2009). Magma transport and storage at Piton de La Fournaise (La Réunion) between 1972 and 2007: A review of geophysical and geochemical data. *J. Volcanol. Geortherm. Res.*, 184, 93-108, doi:10.1016/j.jvolgeores.2008.12.008
- Staudacher T., V. Ferrazzini, A. Peltier, P. Kowalski, P. Boissier, P. Catherine, F. Lauret, **F. Massin** (2009). The April 2007 eruption and the Dolomieu crater collapse, two major events at Piton de la Fournaise. *J. Volcanol. Geortherm. Res.*, 184, 126-137, doi:10.1016/j.jvolgeores.2008.11.005
- Vlastélic, I., C. Deniel, C. Bosq, P. Télouk, P. Boivin, **P. Bachèlery**, **V. Famin**, T. Staudacher (2009). Pb isotope geochemistry of Piton de la Fournaise historical volcanism. *J. Volcanol. Geortherm. Res.,* 184, 63-78, doi:10.1016/j.jvolgeores.2008.08.008
- Barde-Cabusson S., **Finizola A.**, Revil A., Ricci T., Piscitelli S., Rizzo E., Engeletti B., Balasco M., Bennati L., Byrdina S., Carzaniga N., Crespy A., Di Gangi F., **Morin J.**, Perrone A., Rossi, M., Roulleau E., Suski B., **Villeneuve N.** (2009). New geological insights and structural control on fluid circulation in La Fossa cone (Vulcano, Aeolian Islands, Italy). *J. Volcanol. Geortherm. Res.*, 185, 3, 231-245.
- **Finizola A.**, Aubert M., Revil A., Schütze C., Sortino F. (2009). Importance of structural history in the summit area of Stromboli during the 2002–2003 eruptive crisis inferred from temperature, soil CO2, self-potential, and electrical resistivity tomography. *J. Volcanol. Geortherm. Res.*, 183, 3-4, p. 213-227.

2008
- **Michon, L.**, and F. Saint-Ange (2008), Morphology of Piton de la Fournaise basaltic shield volcano (La Réunion island): Characterization and implication in the volcano evolution. *J. Geophys. Res.*, 113, B03203, doi:101029/2005JB0044118.
- Merle, O., **L. Michon, P. Bachèlery** (2008). Caldera rim collapse : a hidden volcanic hazard, *J. Volcanol. Geotherm. Res.*, 177, 525-530. doi:10.1016/j.jvolgeores.2008.06.011
- **Peltier, A., V. Famin, P. Bachèlery**, V. Cayol, Y. Fukushima, and Th., Staudacher (2008), Cyclic magma storages and transfers at Piton de La Fournaise volcano (La Réunion Island) inferred from deformation and geochemical data. *Earth. Planet. Sci. Lett.* doi:10.1016/j.epsl.2008.02.042, 270,180-188.
- Revil, A., **A. Finizola**, S. Piscitelli, E. Rizzo, T. Ricci, A. Crespy, B. Angeletti, M. Balasco, S. B. Cabusson, L. Bennati, A. Boleve, S. Byrdina, N. Carzaniga, F. Di Gangi, **J. Morin**, A. Perrone, M. Rossi, E. Roulleau, and B. Suski (2008). The inner structure of La Fossa di Vulcano (Vulcano Island, southern Tyrrhenian Sea, Italy) revealed by high resolution electric resistivity tomography coupled with self-potential, temperature, and CO2 diffuse degassing measurements, *J. Geophys. Res.*, doi:10.1029/2007JB005394.
- Lavigne F., B. De Coster, N. Juvin, F. Flohic, JC. Gaillard, P. Texier, **J. Morin**, J. Sartohadi (2008). People's behaviour in the face of volcanic hazards: Perspectives from Javanese communities, Indonesia, *J. Volcanol. Geortherm. Res.*, 172, 273-287, doi : 10.1016/j.jvolgeores.2007.12013.
- **Morin J**., De Coster B., Flohic F., Lavigne F., Le Floch D., Paris R., 2008. Assessment and prevention of tsunami risk in Indonesia. *Disaster Prevention and Management*, vol.17:3, pp. 430-446.
- **Villeneuve N.**, Neuville D., Boivin P., **Bachèlery P.**, Richet P., Magma crystallization and viscosity: A study of molten basalts from the Piton de la Fournaise volcano (La Réunion island), *Chemical Geology*, 256, 242-251.

2007
- Aubert, M., S. Diliberto, **A. Finizola**, and Y. Chébli (2007), Double origin of hydrothermal convective flux variations in the Fossa of Vulcano (Italy), *Bull. Volcanol.*, doi: 10.10007/s00445-007-0165-y.
- Carter, A., B. van Wyk de Vries, K. Kelfoun, **P. Bachèlery**, P. Briole (2007), Pits, rifts and slumps: the summit structure of Piton de la Fournaise, *Bull. Volcanol.*, 69, 741-756, 10.1007/s00445-006-0103-4.
- **Michon, L., F. Saint-Ange, P. Bachèlery, N. Villeneuve**, and Th. Staudacher (2007), Role of the structural inheritance of the oceanic lithosphere in the magmato-tectonic evolution of Piton de la Fournaise volcano (La Réunion Island). *J. Geophys. Res.* 112, B4, B04205, 10.1029/2006JB004598.

- **Michon, L.**, Th. Staudacher, V. Ferrazzini, **P. Bachèlery**, J Marti, (2007), April 2007 collapse of Piton de la Fournaise: a new example of caldera formation, *Geophys. Res. Lett.*, 34, L21301, doi:10.1029/2007GL031248.
- **Peltier, A.**, T. Staudacher, **P. Bachèlery** (2007), Constraints on magma transfers and structures involved in the 2003 activity at Piton de La Fournaise from displacement data. *J. Geophys. Res.*, 112, B3, B03207, 10.1029/2006JB004379.
- Vlastelic, I., **A. Peltier**, and T. Staudacher, Short-term (1998-2006) fluctuations of Pb isotopes at Piton de la Fournaise volcano (Reunion Island): origins and constrains on the size and shape of the magma reservoir. *Chemical Geology*, 244, 202-220.
- **Fontaine F. R.**, **Barruol G.,** Tommasi A., and Bokelmann G. H. R. (2007), Upper mantle flow beneath French Polynesia from shear-wave splitting, vol 170, 1262-1288, *Geophys. J. Int*, doi:10.1111/j.1365-246X.2007.03475.x.

Autres publications IPG

Cortés, A., Garduño, V.H., Navarro-Ochoa, C., **Komorowski, J-C**., Saucedo R., Macias J. L., and Gavilanes J. C. (2009) Geologic mapping of the Colima Volcanic Complex (Mexico), and implications for hazard assessment. Geological Society of America Book Series, "Stratigraphy and geology in volcanic areas", Edited by G. Groppelli, L. Viereck-Goette and A. Basu, in press.

Drouin, M., Godard, M., Ildefonse, B., Bruguier, O., Garrido, C. J. (2009). Geochemical and petrographic evidence for magmatic impregnation in the oceanic lithosphere at Atlantis Massif, Mid-Atlantic Ridge (IODP Hole U1309D, 300N), *Chem. Geol.*, doi: 10.1016/j.chemgeo.2009.02.013.

Mehl, C., F. Gueydan, **V Famin.**, L. Jolivet, Fluid-rock interaction and strain localization in the middle crust, *Earth. Planet. Sci. Lett.* (accepté

Massin F., **Ferrazzini V.,**Bachelery P., Nercessian A., Duputel Z., **Staudacher T**., Seismological study of the structure and the evolution of le Piton de la Fournaise plumbing system from the April 2007 major eruption, 2009 submitted to J.G.R.

Morin J., Lavigne F. Institutional and people's response in the face of volcanic hazards in island environment: Case of Karthala volcano, Comoros Archipelago. Part II - Deep-seated root causes of Comorian vulnerabilities. *SHIMA The International Journal of Research into Island Cultures*, in press.

Pascal, M.L., **A. Di Muro,** M. Fonteilles, C. Principe, (2008) Zirconolite and calzirtite in skarn ejecta from Vesuvius 1631 eruption - inferences for the magma - wallrock zoneography. *The Mineralogical Magazine,* in press.

Vigouroux N., Williams-Jones A.E., Wallace P., **Staudacher Th.,** The November 2002 eruption of Piton de la Fournaise, Reunion : Tracking the pre-eruptive thermal evolution of magma using melt inclusions., Bull. Volc., 2009.

Coppola D., James M.R., **Staudacher T.** and Cigolini C., A comparison of field- and satellite-derived thermal flux at Piton de la Fournaise: implications for the calculation of lava discharge rate, Bulletin of Volcanology, 2009

Wada K., Heggy E., **Staudacher T.,** Yarai H., L-band interferometric observations of the Fournaise Volcano: Monitoring and modeling the displacements of the 2007 major eruption, GRL 2009.

Bhugwant C., Siéja B., Bessafi M., **Staudacher T.,** Ecormier J. (2009). Atmospheric sulfur dioxide measurements during the 2005 and 2007 eruptions of the Piton de La Fournaise volcano: Implications for human health and environmental changes *J. Volcanol. Geotherm. Res.*, special issue: Piton de La Fournaise, doi: 10.1016/j.jvolgeores.2008.04.012, 184, 208–224.

Balcone-Boissard H., A. Michel, B. Villemant, **(2009). Simultaneaous determination of Fluorine, Chlorine, Bromine and Iodine in six Geochemical Reference Materials Using Pyrohydrolysis, Ion Chromatography and Inductively Coupled Plasma Mass Spectrometry.** ***Geostandards and Geoanalytical Research***

Barde-Cabusson, S., **Finizola, A.,** Revil, A., Ricci, T., Piscitelli, S., Rizzo, E., Angeletti, B., Balasco,M., Bennati, L., Byrdina, S., Carzaniga, N., Crespy, A., Di Gangi, F., Morin, J., Perrone, A., Rossi, M., Roulleau, E., Suski, B., Villeneuve, N., (2009). New geological insights and structural control on fluid circulation in La Fossa cone (Vulcano, Aeolian Islands, Italy). *J. Volcanol. Geotherm. Res.*, doi: 10.1016/j.jvolgeores.2009.06.002, 185, 231–245.

Barde-Cabusson S., Levieux G., Lénat J.-F., **Finizola, A.**, Revil A., Chaput M., Dumont S., Duputel Z., Guy A., Mathieu L., Saumet S., Sorbadère F., Vieille M. (2009). Transient self-potential anomalies associated with recent lava flows at Piton de la Fournaise volcano (Réunion Island, Indian Ocean). *Journal of Volcanology and Geothermal Research*,

Boivin P., **Bachèlery P.**, Petrology of 1977-1998 Eruptions of Piton de la Fournaise, La Reunion Island. *J. Volcanol. Geotherm. Res.* , special issue: Piton de La Fournaise, doi: 10.1016/j.jvolgeores.2009.01.012, 184, 109-125.

Bhugwant, C., B. Siéja, L. Perron, E. Rivière, and **Th. Staudacher,** Regional transport of polluants emitted from the June-July 2001 eruption of Piton de la Fournaise volcano (Reunion Island), *Atmospheric research*, in press.

Coppola D., Piscopo D., **Staudacher T.,** Cigolini C., (2009). Lava discharge rate and effusive pattern at Piton de la Fournaise from MODIS data, *J. Volcanol. Geotherm. Res.* , special issue: Piton de La Fournaise, doi: 10.1016/j.jvolgeores.2008.11.031, 184 174–192.

Deroussi S., Diament M., Feret J.B., Nebut T., **Staudacher T.**, (2009). Localization of cavities in a thick lava flow by microgravimetry, *J. Volcanol. Geotherm. Res.*, special issue: Piton de La Fournaise, doi: 10.1016/j.jvolgeores.2008.10.002, 184, 193–198.

Duputel Z., **Ferrazzini V.,** Brenguier F., Shapiro N., Campillo M., Nercessian A. (2009). Real time monitoring of relative velocity changes using ambient seismic noise at the Piton de la Fournaise volcano (La Réunion) from January 2006 to June 2007 *J. Volcanol. Geotherm. Res.*, special issue: Piton de La Fournaise, doi: 10.1016/j.jvolgeores.2008.11.02', 184, 164–173.

Famin V., B. Welsh, S. Okumura, **P. Bachèlery,** S. Nakashima (2009), Three differentiation stages of a single magma at Piton de la fournaise volcano (Reunion hotspot). G-Cubed, 10(1) Q01007, doi: 10.1029/2008GC002015.

Finizola A., Aubert M., Revil A., Schütze C., Sortino F. (2009). Importance of structural history in the summit area of Stromboli during the 2002–2003 eruptive crisis inferred from temperature, soil CO_2, self-potential, and electrical resistivity tomography. *J. Volcanol. Geotherm. Res.*, doi:10.1016/j.jvolgeores.2009.04.002, 183, 213–227

Hill, B., Connor, C., Aspinall, W.P., Komorowski, J-C., Nakada, S. (2009) Chapter 25: Recommendations for Assessing Volcanic Hazards of Nuclear Installations. In : C. Connor, N. Chapman, L. Connor (Eds), Volcanism and Tectonism in siting of Nuclear Power Plants, Cambridge University Press, Cambridge, United Kingdom, pp. 566-592.

Le Friant, A., G. Boudon, A. Arnulf, R. Robertson (2009). Debris Avalanche Deposits Offshore St Vincent (West Indies): Impact Of Flank-Collapse Events On The Morphological Evolution Of The Island. J. Volcanol. Geotherm. Res., DOI: 10.1016/J.VOLGEORES.2008.09.022, 179, 1-10.

Le Friant A., C. Deplus, **G. Boudon,** R.S.J. Sparks, J. Trofimovs, P. Talling (2009). Submarine deposition of volcaniclastic material from the 1995-2005 eruptions of Soufrière Hill Volcano, Montserrat, *Geol. Soc. London* 166, doi: 10.1144/0016-76492008-047

Lénat J.-F., Boivin P., Deniel C., Gillot P.-Y., **Bachèlery P.** and Fournaise 2 Team (2009). Age and nature of deposits on the submarine flanks of Piton de la Fournaise (Reunion Island) *J. Volcanol. Geotherm. Res.* , special issue: Piton de La Fournaise, doi: 10.1016/j.jvolgeores.2009.01.013, 184, 199–207.

Michon L., V. Cayol, L. Letourneur, **A. Peltier, N. Villeneuve**, T. Staudacher (2009). Edifice growth, deformation and rift zone development in basaltic setting: insigths from Piton de la Fournaise shield volcano (Réunion Island). *J. Volcanol. Geortherm. Res.*, special issue: Piton de La Fournaise, doi: 10.1016/j.jvolgeores.2008.11.002, 184, 14-30.

Michon L., Villeneuve N., Catry Th, Merle O. (2009). How summit calderas collapse on basaltic volcanoes: New insights from the April 2007 caldera collapse of Piton de la Fournaise volcano, *J. Volcanol. Geortherm. Res.*, special issue: Piton de La Fournaise special issue: Piton de La Fournaise, doi: 10.1016/j.jvolgeores.2008.11.003, 184, 138-151.

Morin J., Lavigne F., **Bachèlery P., Finizola A.,** Villeneuve N., 2009. Institutional and social responses to hazards related to Karthala volcano, Comoros. Part I: Analysis of the May 2006 eruptive crisis. *Shima: The International Journal of Research into Island Cultures,* 3-1, 33-53.

Peltier A., Bachèlery P., Staudacher T., Magma transport and storage at Piton de La Fournaise (La Réunion) between 1972 and 2007: A review of geophysical and geochemical data, *J. Volcanol. Geotherm. Res.* , special issue: Piton de La Fournaise, doi: 10.1016/j.jvolgeores.2008.12.008, 184 (2009) 93–108.

Peltier, A., T. Staudacher, P. Bachèlery, V. Cayol, (2009). Formation of the April 2007 caldera collapse at Piton de La Fournaise volcano: insights from GPS data. *J. Volcanol. Geortherm. Res.*, special issue: Piton de La Fournaise, doi: 10.1016/j.jvolgeores.2008.09.009, 184, 152-163.

Peltier, A, T. Hurst, B. Scott, V. Cayol (2009), Structures involved in the vertical deformation at LakeTaup (New Zealand) between 1979 and 2007: New insights from numerical modelling *J. Volcanol. Geotherm. Res.* 181, 207-219.

Peltier, A., B. Scott, T. Hurst (2009), Ground deformation patterns at White Island volcano (New Zealand) between 1967 and 2008 deduced from levelling data, *J. Volcanol. Geotherm. 181, 207-219.*

Staudacher T., V. Ferrazzini, A. Peltier, P. Kowalski, P. Boissier, P. Catherine, F. Lauret, **F. Massin** (2009). The April 2007 eruption and the Dolomieu crater collapse, two major events at Piton de la Fournaise (La Réunion Island, Indian Ocean). *J. Volcanol. Geortherm. Res.*, special issue: Piton de La Fournaise, doi: 10.1016/j.jvolgeores.2008.11.005, 184, 126-137.

Perrier F., **Richon P.,** Sabroux J.C. (2009), Temporal variations of radon concentration in the saturated soil of Alpine grassland: The role of groundwater flow. Science of the Total Environment, 407: 2361-1371.

Perrier F., **Richon P.,** Byrdina S., France-Lanord C., Rajaure S., Koirala B., Shrestha P., Gautam U., Tiwari D. R., Revil A., Bollinger L., Contraires S., Bureau S., Sapkota S. N. (2009). A direct evidence for high carbon dioxide and radon-222 discharge in Central Nepal. *Earth and Planetary Science Letters*, doi:10.1016/j.epsl.2008.12.008, 278: 198-207.

Prôno E., Battaglia J., Monteiller V., Got J.-L., **Ferrazzini V.** (2009). P-wave velocity structure of Piton de la Fournaise volcano deduced from seismic data recorded between 1996 and 1999. *J. Volcanol. Geortherm. Res.*, special issue: Piton de La Fournaise, doi: 10.1016/j.jvolgeores.2008.12.009, 184, 49-62.

Richon P., Perrier F., Pili E. and Sabroux J.C., (2009), Detectability and significance of 12h barometric tide in radon-222 signal, dripwater flow rate, air temperature and carbon dioxide concentration in an underground tunnel. Geophysical J. Int., doi: 10.111/j.13654-246X.2008.04000.x, 176: 683-694.

Toutain J.-P, Sortino F., Baubron J.-C, **Richon P**., Surono, Sumarti S., Nonell A. (2009). Structure and CO2 budget of Merapi volcano during inter-eruptive periods. Bull. Volcanol., doi: 10.1007/s00445-009-0266-x.

Samper A., X. Quidelleur, **J.-C. Komorowski,** P. Lahitte, G**. Boudon,** Effusive History Of The Grande Découverte Volcanic Complex, Southern Basse-Terre (Guadeloupe, French West Indies) From New K-Ar Cassignol-Gillot AGES *J. VOLCANOL. GEOTHERM. RES.*, DOI: 10.1016/J.VOLGEORES.2009.08.016.

Sulem, J., **V. Famin**, Thermal decomposition of carbonates in fault zones: slip-weakening and temperature limiting effects, J. Geoph. Res. 114, B03309, doi:10.1029/2008JB006004.

Viane C., Bhugwant C., Sieja B., **Staudacher T.,** Demoly P., Étude comparative des émissions de gaz volcanique du Piton de la Fournaise et des hospitalisations pour asthme de la population réunionnaise de 2005 à 2007, Revue française d'allergologie (2009), doi:10.1016/j.reval.2009.02.010.

Villemant B., Salaün A., Staudacher T., Evidence for a homogeneous primary magma at Piton de la Fournaise (La Réunion): A geochemical study of matrix glass, melt inclusions and Pélé's hairs of the 1998–2008 eruptive activity, *J. Volcanol. Geotherm. Res.*, special issue: Piton de La Fournaise, doi: 10.1016/j.jvolgeores.2009.03.015, 184 (2009) 79–92.

Vlastélic I., Deniel C., Bosq C., Télouk P., Boivin P., **Bachèlery P., Famin V., Staudacher T.,** Pb isotope geochemistry of Piton de la Fournaise historical lavas, *J. Volcanol. Geotherm. Res.* , special issue: Piton de La Fournaise, doi: 10.1016/j.jvolgeores.2008.08.008, 184 (2009) 63–78.

• **2008**

Antoine R., Baratoux D., Rabinowicz M., Fontaine F., **Bachèlery P., Staudacher Th**., Saracco G., **Finizola A**., Thermal infrared analysis of a quiescent cone on Piton de la Fournaise volcano : evidence of convective air flow within an unconsolidated soil, doi:10.1016/j.chemgeo.2008.08.018

Baker D.R., **H. Balcone-Boissard**, (2008), Halogen diffusion in magmatic systems. Special Issue, "Halogens in Volcanic Systems and Their Environmental Impacts" *Chemical Geology, doi:*10.1016/j.chemgeo.2008.10.010.

Balcone-Boissard, H., D.R. Baker, **B. Villemant, G. Boudon,** (2008), F and Cl diffusion inphonolitic melts : Influence of the Na/K ratio. Special Issue, "Halogens in Volcanic Systems and Their Environmental Impacts" *Chemical Geology,* doi:10.1016/j.chemgeo.2008.08.018

Balcone-Boissard, H., B. Villemant, G. Boudon, and A. Michel, (2008), Non-volatile vs volatile behaviours of halogens during the 79 AD plinian eruption of Vesuvius, Italy. *Earth. Planet. Sci. Lett.*, doi:10.1016/j.epsl.2008.02.003, 269 (1-2), 66-79

Boichu, M., B. Villemant, G. Boudon, (2008). A Model For Episodic Degassing Of An Andesitic Magma Intrusion. *J. Geophys. RES.* DOI:10.1029/2007JB005130.

Boudon, G., J.-C. Komorowski, B. Villemant, M.P. Semet, (2008). A new scenario for the last magmatic eruption of La Soufrière de Guadeloupe (Lesser Antilles) in 1530 A.D.: evidence from stratigraphy, radiocarbon dating and magmatic evolution of erupted products. *J. Volcanol. Geortherm. Res.*, doi: 10.1016/j.jvolgeores.2008.03.006, 178:474-490.

Brenguier F., Shapiro N.M., Campillo M., **Ferrazzini V.**, Duputel Z., Coutant O., Nercessian A. (2008), Toward forecasting volcanic eruptions using seismic noise, *Nature,* doi:1001038/ngeo104

Coppola D., Piscopo D., **Staudacher Th..,** Cigolini, C., Lava discharge rate and effusive pattern at Piton de la Fournaise from MODIS data, *J. Volcanol. Geortherm. Res.*, special issue: Piton de La Fournaise doi : 10.1016/j.jvolgeores.2008.11.031

Davies, A.G., Castaño, R., Chien, S., Tran, D.Q., Mandrake, L., Wright, R., Kyle, P., **Komorowski, J-C**., Mandl, D., Frye, S. Rapid Response to Volcanic Eruptions with an Autonomous Volcano Sensor Web: the Nyamulagira Eruption of 2006, *Aerospace Conference, 2008, IEEE,* 1-8 March 2008, paper 1180, pp 1-11, DOI : 10.1109/AERO.2008.4526456

Deroussi S., Diament M, Ferret M., Nebut J.B. **Staudacher Th**., Localisation of cavities in a thick lava flow by microgravity, *J. Volcanol. Geortherm. Res.*, special issue: Piton de La Fournaise. doi : 10.1016/j.jvolgeores.2008.10.002

Di Muro, A., J. Palister, **B. Villemant,** C. Newhall**, M. Semet,** M., Martinez, C. Mariet , (2008), Pre-1991 sulfur transfer between mafic injections and dacite magma in the Mt. Pinatubo reservoir. *J. Volcanol. Geortherm. Res.*, doi: 10.1016/j.jvolgeores.2008.02.025.

Di Muro, A., M. Rosi, E. Aguilera, R. Barbieri, G. Massa, F. Mundula, F. Pieri, (2008) Transport and sedimentation dynamics of transitional explosive eruption columns: the exemple of the 800 BP Quilotoa plinian eruption (Ecuador). *J. Volcanol. Geotherm. Res.*, 174, 307-324.

Duputel Z., **V Ferrazzini**, F. Brenguier, N. Shapiro, M. Campillo, A. Nercessian, Real Time Monitoring of Relative Velocity Changes Using Ambient Seismic Noise on the Piton de la Fournaise Volcano (La Réunion) from January 2006 to June 2007. *J. Volcanol. Geortherm. Res.*, special volume, doi : 10.1016/j.jvolgeores.2008.11.024

Famin, V., S. Nakashima, A. M. Boullier, K. Fujimoto and T. Hirono (2008). Earthquakes produce carbon dioxide in crustal faults *Earth. Planet. Sci. Lett.* doi:10.1016/j.epsl.2007.10.041, 270 (1-2), 487-497.

Hirono, T., T. Yokoyama, Y. Hamada, W. Tanikawa, T. Mishima, M. Ikehara, **V. Famin,** M. Tanimizu, W. Lin, W. Soh, and S. Song (2008). Correction to "A chemical kinetic approach to estimate dynamic shear stress during the 1999 Taiwan Chi-Chi earthquake" *Geophys. Res. Lett.*, 35, L02301, doi:10.1029/2007GL032512.

Komorowski, J.-C., Y. Legendre, B. Caron, And **G. Boudon** (2008), Reconstruction And Analysis Of Sub-Plinian Tephra Dispersal During The 1530 A.D. Soufrière (Guadeloupe) Eruption: Implications For Scenario

Definition And Hazards Assessment *J. VOLCANOL. GEORTHERM. RES*. DOI: 10.1016/J.JVOLGEORES.2007.11.022, 178: 491-515.

Lavigne F., B. De Coster, N. Juvin, F. Flohic, JC. Gaillard, P. Texier, **J. Morin**, J. Sartohadi, People's behaviour in the face of volcanic hazards: Perspectives from Javanese communities, Indonesia, *J. Volcanol. Geortherm. Res.*, 172, 273-287, doi : 10.1016/j.jvolgeores.2007.12013.

Le Friant, A., E.J. Lock, M.B. Hart, **G. Boudon,** R.S.J. Sparks, M.J. Leng, C.W. Smart, **J.C. Komorowski,** C. Deplus, and J.K. Fisher (2008), Late Pleistoicene tephrochronology of marine sediments adjacent to Montserrat, Lesser Antilles volcanic arc. *J. Geol. Soc. London*, 165, 279-289.

Le Friant, A., P. Heinrich, **G. Boudon** (2008). Field survey and numerical simulation of the 21 November 2004 tsunami at Les Saintes (Lesser Antilles), *Geophys. Res. Lett*. doi:10.1029/2008GL034051

Letourneur, L., **A. Peltier, Th. Staudacher,** and A. Gudmundsson (2008). The effects of rock heterogeneities on dyke paths and asymmetric ground deformation; the example of Piton de la Fournaise (Réunion Island), *J. Volcanol. Geotherm. Res., doi*10.1016/j.jvolgeores.2008.01.018, 173, 289-302

Merle, O., **L. Michon**, **P. Bachèlery** (2008). Caldera rim collapse : a hidden volcanic hazard, J. Volcanol. Geotherm. Res., doi: 10.1016/j.jvolgeores.2008.06.011, 177, 525-530.

Michon L., L. V. Cayol, Letourneur, **A. Peltier**, N. Villeneuve, **T. Staudacher** (2008), Edifice growth, deformation and rift zone development in basaltic setting: insights from Piton de la Fournaise shield volcano (La Réunion Island). *J. Volcanol. Geortherm. Res.*, special issue: Piton de La Fournaise doi: 10.1016/j.jvolgeores.2008.11.02

Michon, L., And F. Saint-Ange (2008), Morphology Of Piton De La Fournaise Basaltic Shield Volcano (La Réunion Island): Characterization And Implication In The Volcano Evolution. *J. Geophys. Res.*, 113, B03203, DOI:101029/2005JB0044118.

Michon L., Villeneuve N., Catry Th, Merle O. (2008), How summit calderas collapse on basaltic volcanoes: new insights from the April 2007 caldera collapse of Piton de la Fournaise volcano, *J. Volcanol. Geortherm. Res.*, special issue: Piton de La Fournaise doi: 10.1016/j.jvolgeores.2008.11.003.

Morin J., De Coster B., Flohic F., Lavigne F., Le Floch D., Paris R., (2008), Assessment and prevention of tsunami risk in Indonesia. Disaster Prevention and Management, vol.17:3, pp. 430-446.

Peltier, A., V. Famin, P. Bachèlery, V. Cayol, Y. Fukushima, and **Th.**, **Staudacher** (2008), Cyclic magma storages and transfers at Piton de La Fournaise volcano (La Réunion Island) inferred from deformation and geochemical data. *Earth. Planet. Sci. Lett*. doi:10.1016/j.epsl.2008.02.042, 270,180-188.

Pili E., S. Bureau, F. Perrier, D. Patriarche, L. Charlet, P. M. Adler, **P. Richon** (2008). Reactive transport and residence times in unsaturated fractured rocks from field-scale experiments, American Chemical Society Developments in Earth & Environmental Sciences, M. Barnett and D. Kent (Editors), 7, 445-473, 2008. DOI 10.1016/S1571-9197(07)07016-4.

Prono E., J. Batttaglia, V. Monteiller, J.L. Got**, V. Ferrazzini** (2008). P-wawe veolocity structure of piton de la Fournaise volcano deduced from seismic data recorded between 1996 and 1999. *J. Volcanol. Geotherm. Res.* special issue: Piton de la Fournaise, doi: 10.1016/j.jvolgeores.2008.12.009.

Revil A., **Finizola A.**, Piscitelli S., Rizzo E., Ricci T., Crespy A., Angeletti B., Balasco M., Barde Cabusson S., Bennati L., A. Bolève., Byrdina S., Carzaniga N., Di Gangi F., Morin J., Perrone A., Rossi M., Roulleau E., Suski B. Inner structure of La Fossa di Vulcano (Vulcano Island, southern Tyrrhenian Sea, Italy) revealed by high resolution electric resistivity tomography coupled with self-potential, temperature, and CO2 diffuse degassing measurements. Journal of Geophysical Research, Vol. 113, B07207, doi:10.1029/2007JB005394.

Samper, A., X. Quidelleur, **G. Boudon, A. Le Friant,** and **J.C. Komorowski** (2008). Radiometric dating of three large volume flank-collapses in the Lesser Antilles Arc, *J. Volcanol. Geortherm. Res.* doi: 10.1016/j.jvolgeores.2008.02.028.

Spence, R., **J-C. Komorowski,** K. Saito, A. Brown, A. Pomonis, G. Toyos, and P. Baxter (2008), Modelling the impact of a hypothetical sub-Plinian eruption at la Soufrière of Guadeloupe (West Indies). *J. Volcanol. Geotherm. Res.,* doi: 10.1016/j.jvolgeores.2008.03.016, 178:516-528

Staudacher T., V. Ferrazzini, A. Peltier, P. Kowalski, P. Boissier, P. Catherine, F. Lauret, **F. Massin** , The April 2007 eruption and the Dolomieu crater collapse, two major events at Piton de la Fournaise. *J. Volcanol. Geortherm. Res.*, special issue: Piton de La Fournaise doi: 10.1016/j.jvolgeores.2008.11.005

Villemant, B., J. Mouatt, and **A. Michel** (2008), Andesitic Magma Degassing Investigated Through H2O Vapour-Melt Partitioning of Halogens at Soufrière Hills Volcano, Montserrat (Lesser Antilles) *Earth. Planet. Sci. Lett.*, doi:10.1016/j.epsl.2008.02.014, 269 (1-2), 212-229.

Vlastelic I., Deniel C. Bosq C., Télouk P., Boivin P., **Bachèlery P., Famin V., Staudacher Th**. (2008), Pb isotopic geochemistry of Piton de la Fournaise historical lavas, change *J. Volcanol. Geortherm. Res.*, special issue: Piton de La Fournaise, doi: 10.1016/j.jvolgeores.2008.08.008.

Villeneuve N., Neuville D., Boivin P., **Bachèlery P.,** Richet P., Magma crystallization and viscosity: A study of molten basalts from the Piton de la Fournaise volcano (La Réunion island), *Chemical Geology*, 256, 242-251.

• **2007**

Aubert, M., S. Diliberto, A. **Finizola,** and Y. Chébli (2007), Double origin of hydrothermal convective flux variations in the Fossa of Vulcano (Italy), *Bull. Volcanol.*, doi: 10.10007/s00445-007-0165-y.

Bernard, M.L., M. Zamora, Y. Géraud, and **G. Boudon** (2007), Transport properties of pyroclastic rocks from Montagne Pelée volcano (Martinique, Lesser Antilles). *J. Geophys. Res., 112(* B5), B05205, 10.1029/2006JB004385.

Boudon, G., A. Le Friant, J.-C. Komorowski, C. Deplus, and **M.P. Semet** (2007), Volcano flank instability in the Lesser Antilles Arc: diversity of scale, processes, and temporal recurrence. *J. Geophys. Res. 112,* B08205, doi:10.1029/2006JB004674

Bouhifd, M.A., **P. Besson,** P. Courtial, C. Gérardin, A. Navrotsky and P. Richet (2007), Thermochemistry and melting properties of basalt. *Contrib. Mineral. Petrol. 153,* 689-698.

Brenguier, F., N.M. Shapiro, M. Campillo, A. Nercessian, and **V. Ferrazzini** (2007), 3-D surface wave tomography of the Piton de la Fournaise volcano using seismic noise correlations. *Geophys. Res. Lett., 34,* L02305, doi:10.1029/2006GL028586.

Carter, A., B. van Wyk de Vries, K. Kelfoun, **P. Bachèlery,** and P. Briole (2007). Pits, rifts and slumps: the summit structure of Piton de la Fournaise. *Bull. Volcanol.* doi 10.007/s00445-006-0103-4

Chopart JL., **N. Payet**, H. Saint Maccary, M. Vauclin, Is maize root growth affected by pig slurry application on a tropical acid soil?, *Plant Root*, 1: 75-84,doi: 10.3117/plantroot.1.75

Coppola D, **Th. Staudacher,** and C. Cigolini (2007), Field thermal monitoring during the August 2003 eruption at Piton de la Fournaise (La Réunion). *J. Geophys. Res., 112,* B5, B05215, 10.1029/2006JB004659.

Halama, R., J.L. Joron, **B. Villemant,** G. Markl, and M.Treuil (2007), Trace element constraints on mantle sources during mid-Proterozoic magmatism: Evidence for a link between the Gardar (South Greenland) and Abitibi (Canadian Shield) mafic rocks. *Can. Jour. Sci., 44,* 459-478.

Hirono, T., T. Yokoyama, Y. Hamada, W. Tanikawa, T. Mishima, M. Ikehara, **V. Famin,** M. Tanimizu, W. Lin, W. Soh, and S. Song (2007). A chemical kinetic approach to estimate dynamic shear stress during the 1999 Taiwan Chi-Chi earthquake, *Geophys. Res. Lett.,* 34, L19308, doi:10.1029/2007GL030743.

Longpré, M.-A., **Th. Staudacher** and J. Stix (2007), The November 2002 eruption at Piton de la Fournaise volcano, La Réunion Island: ground deformation, seismicity, and pit crater collapse, *Bull. Volcanol.* doi: 10.1007/s00445-006-0087-0.

Michon, L., F. Saint-Ange, P. Bachèlery, N. Villeneuve, and **Th. Staudacher** (2007), Role of the structural inheritance of the oceanic lithosphere in the magmato-tectonic evolution of Piton de la Fournaise volcano (La Réunion Island). *J. Geophys. Res. 112,* B4, B04205, 10.1029/2006JB004598.

Michon, L., Th. Staudacher, V. Ferrazzini, P. Bachèlery, J Marti, (2007), April 2007 collapse of Piton de la Fournaise: a new example of caldera formation, *Geophys. Res. Lett.,* 34, L21301, doi:10.1029/2007GL031248.

Nicollin, F., D.Gibert, **F. Beauducel, G. Boudon,** and **J.-C. Komorowski** (2007), Reply to comment on " Electrical Tomography of La Soufrière of Guadeloupe Volcano: Field Experiments, 1D Inversion and Qualitative Interpretation by N. Linde and A. Revil. *Earth Planet. Sci. Lett. 258,* 623-626.

Peltier, A., T. Staudacher, P. Bachèlery (2007), Constraints on magma transfers and structures involved in the 2003 activity at Piton de La Fournaise from displacement data. *J. Geophys. Res., 112,* B3, B03207, 10.1029/2006JB004379.

Perrier F., **P. Richon**, U. Gautam, D.R. Tiwari, P. Shrestha, and S.N. Sapkota (2007), Seasonal variations of natural ventilation and radon-222 exhalation in a slightly rising dead-end tunnel. *J. Environmental Radioactivity, 97,* 220-235.

Remusat, L., F. Robert, and S. Derenne (2007), The Insoluble Organic Matter in carbonaceous chondrites: chemical structure, isotopic composition and origin. *C.R. Geosciences,* doi:10.1016/j.crte.2007.10.001, 339, 895-906.

Richon P., P. Bernard, V. Labed, J.-C. Sabroux, A. Beneïto, D. Lucius, S. Abbad, and M.C. Robe (2007), Results of monitoring 222Rn in soil gas of the Gulf of Corinth region, Greece. *Radiation Measurements 42,* 87 – 93.

Touboul, M., B. Bourdon, **B. Villemant, G. Boudon,** J.L. Joron (2007) ^{238}U-^{230}Th-^{226}Ra disequilibria in andesitic to dacitic lavas of the 1440 Soufrière eruption (Guadeloupe): processes and timescales of magma differentiation. *Chemical Geology, 246,*181-206.

Urai, M., N. Geshi, and **T. Staudacher** (2007), Size and volume evaluation of the caldera collapse on Piton de la Fournaise volcano during the April 2007 eruption using ASTER stereo imagery, *Geophys. Res. Lett.,* 34, L22318, doi: 10.1029/2007GL031551

Vlastelic, I., **A. Peltier, and T. Staudacher,** Short-term (1998-2006) fluctuations of Pb isotopes at Piton de la Fournaise volcano (Reunion Island): origins and constrains on the size and shape of the magma reservoir. *Chemical Geology,* 244, 202-220.

Equipe Géochronologie - Dynamique des Systèmes Volcaniques
UMR IDES 8148, Université Paris-Sud 11, Orsay.

Les recherches de l'équipe géochronologie-dynamique des systèmes volcaniques (GDSV) portent principalement sur la reconstruction de l'histoire des systèmes éruptifs en tous types de contextes géodynamiques et l'analyse des différents facteurs de risque liés à leur évolution (aléas éruptifs et gravitaires). Ces recherches mettent en œuvre des compétences et des approches variées, à l'interface entre les différentes disciplines des Sciences de la Terre et des Planètes (cartographie des systèmes volcaniques,

géochronologie, géomorphologie quantitative, géochimie des magmas et des fluides crustaux, modélisations numériques). Une part importante des travaux est également consacrée à la calibration des échelles des temps géologiques et des inversions magnétiques et à la datation des grandes crises de l'histoire de la Terre. L'originalité du groupe GDSV est en effet fondée sur des techniques de mesure d'âge exploitant le K-Ar et le $^{40}Ar/^{39}Ar$. Les techniques de datation sont mises au point et les appareils conçus et réalisés par les chercheurs afin d'atteindre la meilleure performance analytique adaptée aux besoins des études. Les recherches du groupe sont réalisées en partenariat avec des collègues français et étrangers dans le cadre de programmes nationaux (ANR, DYETI, INSU-relief, CNES) et internationaux (UFI, TEAMINT, GTS-Next, MEGA-HAZARDS). Ces financements servent actuellement de support à la réalisation de cinq thèses en cours, dont 1 en cotutelle, et quatre thèses soutenues ces quatre dernières années. Les travaux de l'équipe ont donné lieu à la publication de plus de 30 articles de rang A dans des revues internationales entre 2007 et 2010.

English summary

Research topics of the team geochronology-dynamics of volcanic systems in Orsay are mostly focussed on the reconstruction of the history of volcanic systems in all types of geodynamic settings and on the analysis of natural hazards linked to their evolution (eruptive and mass-wasting processes). This research involves Earth scientists with complementary skills and expertise (geological mapping of volcanic systems, geochronology, quantitative geomorphology, geochemistry of magma and crustal fluids, numeric modelling). An important part of our work is also devoted to the calibration of the geological and paleomagnetic timescales, and to dating of the major crises in the history of the Earth. The originality of our group relies on the development of high-precision accurate geochronology including conventional unspiked K/Ar and $^{40}Ar/^{39}Ar$. The techniques and instruments are designed and developed in-house to reach the best performance adapted to the requirements of our different studies. Our research is conducted in collaboration with partners from France and abroad in the framework of national and international programs (e.g., UFI, TEAMINT, GTS-Next, MEGA-HAZARDS). Such funding is presently supporting 5 ongoing PhDs, including one in co-supervision with academics from foreign universities, and 4 thesis defended during the last four years. The research from our team for the 2007-2010 period has been published as more than 30 articles in peer-reviewed international journals.

List of IDES publications

Germa A., Quidelleur X., Lahitte P., Labanieh S, and Chauvel C, 2011. The K-Ar Cassignol-Gillot technique applied to western Martinique lavas: A record of the evolution of the recent Lesser Antilles island arc activity from 2 Ma to Mount Pelée volcanism, Quaternary Geochronology, accepté.

Lahitte, P., Samper, A. and **Quidelleur X**, 2011. DEM-based reconstruction of Southern Basse Terre volcanoes (Guadeloupe archipelago, FWI): a contribution to the Lesser Antilles Arc volumetric extrusion and erosion rates. Geomorphology, accepté.

Germa A., Quidelleur X , Labanieh S, **Lahitte P**. and Chauvel C, 2010. The eruptive history of Morne Jacob volcano (Martinique Island, French West Indies): geochronology, geomorphology and geochemistry of the earliest volcanism in the recent Lesser Antilles arc. J. Volcanol. Geotherm. Res., 198, 297-310.

Quidelleur, X., Holt, J.W., **Salvany, T**. and Bouquerel H., 2010. New K-Ar ages from La Montagne massif, Réunion Island (Indian Ocean) supporting two geomagnetic events in the time period 2.2 – 2.0 Ma. Geophys. J. Int., 182 : 699-710.

Germa, A., Quidelleur, X., Gillot, P.Y., Tchilingurian, P., 2010. Volcanic evolution of the back-arc Pleistocene Payun Matru volcanic field (Argentina). J. South Am. Earth Sci., 29 : 717-730.

Samper, A., Quidelleur X, Komorowski, J.C., **Lahitte, P.**, Boudon, G, 2009. Effusive history of the Grande Découverte Volcanic Complex, southern Basse-Terre (Guadeloupe, French West Indies) from new K-Ar Cassignol-Gillot ages. J. Volcanol. Geotherm. Res., 187: 117-130.

Hildenbrand, A., Madureira, P., Ornelas Marques, F., Cruz, I., Henry, B., and P. Silva, 2008. Multi-stage evolution of a sub-aerial volcanic ridge over the last 1.3 Myr: S. Jorge Island, Azores Triple Junction. Earth Planet. Sci. Lett., 273: 289-298.

Samper, A., Quidelleur X, Boudon, G., Le Friant, A., Komorowski, J.C., 2008. Radiometric dating of three large volume flank collapses in the Lesser Antilles arc. J. Volcanol. Geotherm. Res., 176: 485-492.

Rouchon, V., Gillot, P.Y., Quidelleur, X., Chiesa, S., Floris, B., 2008. Temporal Evolution of the Roccamonfina volcanic complex (Plesitocene), Central Italy. J. Volcanol. Geotherm. Res., 177 : 500-514.

Quidelleur, X., Hildenbrand, A., Samper, A., 2008 ; Link between paleoclimatic changes and oceanic islands evolution. Geophys. Res. Lett., 35: L02303.

Hildenbrand, A., Gillot, P.Y. and Marlin, C., 2008. Geomorphological study of long-term erosion on a tropical volcanic ocean island: Tahiti-Nui (French Polynesia), Geomorphology, 93 (3-4) : 460-481.

Samper, A., Quidelleur X, Lahitte, P., Mollex, D., 2007. Timing of effusive volcanism whithin the whole Basse Terre Island (Guadeloupe, F.W.I.) from new K-Ar Cassignol-Gillot Ages. Earth Planet. Sci. Lett., 258: 175-191.

Guérin, G and **Gillot, P-Y**, 2007. Nouveaux éléments de chronologie du volcanisme Pléistocène du Bas-Vivarais (Ardèche, France) par thermoluminescence. C.R. Geosciences, 339, 40-49.

DATATIONS DES ACTIVITES VOLCANIQUES HISTORIQUES

M. Condomines (Montpellier), J-C. Tanguy (St Maur)

L'essentiel de nos résultats concerne la succession des éruptions des derniers millénaires pour les volcans italiens par la méthode archéomagnétique de haute précision particulière au laboratoire de St Maur (Tanguy *et al.*, 2007, 2009, Figure 1). Dans de nombreux cas cependant il a été nécessaire de recourir à la méthode ^{226}Ra-^{230}Th (Condomines et al., 2005, Fig. 2) pour discriminer entre des directions géomagnétiques semblables à des époques différentes.

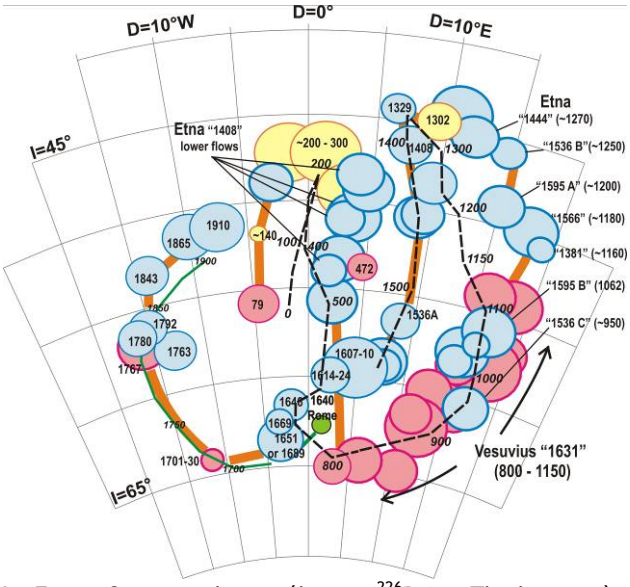

Figure 1

La Figure 1 montre la variation de la direction du champ géomagnétique en Sicile (ligne orange) au cours des derniers 2000 ans, en bon accord avec la courbe archéomagnétique en France (tireté noir). Les cercles de confiance à 95% de probabilité des directions magnétiques figées dans les laves (Etna en bleu, Vésuve en rouge, Ischia en jaune), permettent des datations très précises (±40 ans en moyenne). On voit cependant qu'il est impossible de discriminer les périodes 600-800 et 1600-1650 où le champ montrait des orientations très voisines.

La Figure 2 montre la corrélation $(^{226}Ra)_0$ - Th obtenue à partir de coulées historiques d'âges connus, et qui sert de référence pour la datation des coulées d'âge indéterminé. $(^{226}Ra)_0$ est l'activité du ^{226}Ra en désintégrations par minute et par gramme, recalculée au moment de l'éruption.

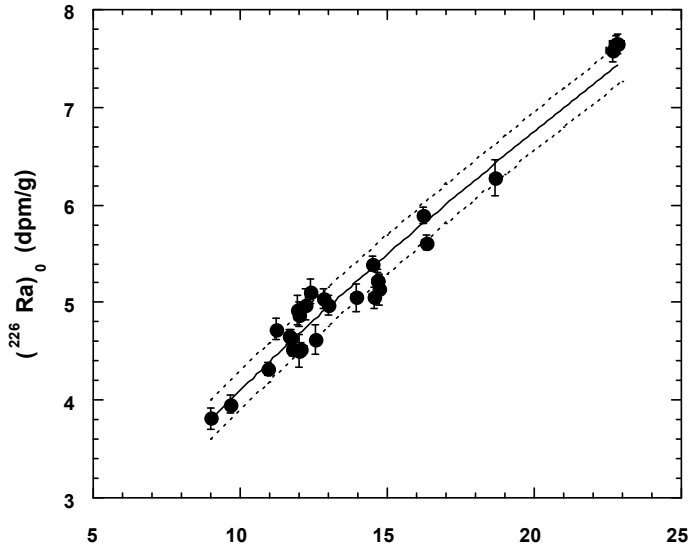

L'identification des produits volcaniques par ces méthodes montre que beaucoup de laves « historiquement datées » (80% de celles antérieures à 1700, dates entre guillemets sur la fig. 1) sont dues en réalité à d'autres éruptions (dates entre parenthèses), souvent non enregistrées par les documents écrits, les écarts atteignant plusieurs siècles et parfois plus d'un millénaire. Cette révision de l'histoire des volcans italiens a des implications importantes sur la cartographie, les statistiques, les mécanismes éruptifs, la protection civile.

Un autre aspect des travaux basés sur les déséquilibres ^{226}Ra-^{230}Th récents concerne un modèle d'accumulation du ^{222}Rn (Radon) dans les magmas, qui peut expliquer les excès de ^{210}Pb observés dans beaucoup de roches volcaniques actuelles (Condomines et al., 2010). Ce modèle vient compléter celui établi par Gauthier et Condomines (1999) pour le dégazage du ^{222}Rn. Il a été appliqué au cas de Santorin et de Surtsey, et les

résultats suggèrent que l'accumulation de Rn peut en effet expliquer les forts excès de ^{210}Pb, aussi bien dans une chambre zonée (Santorin) que dans les vésicules de ségrégation d'une coulée de lave (Surtsey).

Publications

CONDOMINES M., GAUTHIER P. J., TANGUY J. C., GERTISSER R., THOURET J.C., BERTHOMMIER P., CAMUS G. (2005) ^{226}Ra or ^{226}Ra/Ba dating of Holocene volcanic rocks: Application to Mt Etna and Merapi volcanoes. Earth and Planet. Sci. Lett. 230, 289-300.

CONDOMINES M., SIGMARSSON O., GAUTHIER P. J. (2010). A simple model of ^{222}Rn accumulation leading to ^{210}Pb excesses in volcanic rocks. Earth and Planet. Sci. Lett. 293, 331-338.

LIOTARD J. M., DAUTRIA J. M., BOSCH D., CONDOMINES M., MEHDIZADEH H., RITZ J. F. (2008). Origin of the absarokite-banakite association of the Damavand volcano (Iran). Trace element and Sr, Nd, Pb isotope constraints. Int. J. of Earth Sciences, 97/1, 89-102.

TANGUY J.C., CONDOMINES M., LE GOFF M., CHILLEMI V., LA DELFA S., PATANÈ G. (2007) - *Mount Etna eruptions of the last 2750 years: revised chronology and location through archeomagnetic and ^{226}Ra-^{230}Th dating*. Bull. of Volcanology 70: 55-83.

TANGUY J.C., LE GOFF M., ARRIGHI S., PRINCIPE C., LA DELFA S., PATANÈ G. (2009) – *The History of Italian Volcanoes revised by Archeomagnetism*. EOS, vol. 90, n. 40, 349-350.

VEZZOLI L., PRINCIPE C., MALFATTI J., ARRIGHI S., TANGUY J.C., LE GOFF M. (2009) – *Modes and times of caldera resurgence : The <10 ka evolution of Ischia Caldera, Italy, from high-precision archeomagnetic dating*. J. Volcanol. Geotherm. Res. 186, 305-319.

TANGUY J.C., BACHÈLERY P., LE GOFF M. (in press). *Archeomagnetism of Piton de la Fournaise: bearing on volcanic activity at La Réunion Island and geomagnetic secular variation in Southern Indian Ocean*. Earth Planet. Sci. Letters, accepted for publication.

COOPERATION FRANCO-INDONESIENNE EN VOLCANOLOGIE

Avec le partenaire
DVGHM Center of Volcanology and Geologic Hazards Mitigation
Bandung, Java, Indonesia
---

1 RAPPORT D'ACTIVITE 2010

Coordonnateur : Jean-Claude THOURET
PRES Clermont, Université Blaise Pascal, Laboratoire Magmas et Volcans UMR 6524
CNRS et IRD, OPGC
5 rue Kessler, 63038 Clermont-Ferrand cedex
(J.C.Thouret@opgc.univ-bpclermont.fr)

INTRODUCTION

Avec plus de 120 volcans actifs répartis sur les 4000 km de l'archipel et une densité de population de l'ordre de 120 habitants/km^2 (830 à Java), l'Indonésie est le pays au monde où le risque volcanique est le plus élevé. L'Indonésie est par ailleurs un terrain d'activité exceptionnel pour la communauté volcanologique française. La coopération franco-indonésienne en volcanologie, initiée en 1986 sous l'égide de Haroun Tazieff, alors secrétaire d'Etat à la Prévention des Risques Majeurs, s'est développée sous

l'impulsion du MAEE (Ministère des Affaires Etrangères et Européennes). Outre les activités de formation et de transfert de technologies vers le partenaire indonésien, les équipes françaises ont obtenu des résultats scientifiques remarquables qui se traduisent par une bibliographie fournie et une reconnaissance internationale incontestable. Le partenaire privilégié en Indonésie est le Center of Volcanology and Geological Hazards Mitigation (CVGHM, ex-VSI : Volcanological Survey of Indonesia). Il est chargé de la gestion des risques naturels et est l'autorité de tutelle des observatoires répartis dans l'archipel. Il contribue à la mise en place et soutient les missions et la maintenance des équipements.

L'Ambassade de France, dans le cadre de son programme de coopération culturelle et scientifique, co-finance pour partie les activités de recherche appliquée et d'échanges (équipements et fonctionnement, missions). Elle finance également des bourses d'étude pour les étudiants indonésiens pour la réalisation de mémoires de M2 et de thèses dans les laboratoires français.

Cette coopération poursuit trois objectifs :

1) la formation à la recherche à l'intention des Indonésiens (thèses, stages, collaborations sur site), l'aide à la surveillance opérationnelle (mise en place de réseaux de surveillance) et le transfert de technologie ;
2) Une contribution essentielle à l'évaluation de l'aléa et du risque volcanique grâce à la surveillance des volcans dangereux, la prévision de certains phénomènes précurseurs et l'aide à la prévention, qui incombe à notre partenaire DVGHM en Indonésie ;
3) un retour d'expérience fondamental pour la France : compréhension des processus, mise au point d'instrumentation et de protocoles expérimentaux, formation de scientifiques français (chercheurs, doctorants), apprentissage de la confrontation aux situations de crise sur les volcans explosifs.
4)

ACTEURS DE LA COOPERATION

Responsables de thématiques intervenus en 2010 :

Franck LAVIGNE (LGP, aspect sociétal du risque) : francklavigne@yahoo.fr
Philippe LESAGE (OSUG-LGIT, sismologie) : lesage@univ-savoie.fr
Jean-Philippe METAXIAN (OSUG-LGIT, sismologie) : Jean-Philippe.Metaxian@univ-savoie.fr
Patrick RICHON (CEA-DASE, géochimie gaz) : patrick.richon@cea.fr
Coordonnateur : Jean-Claude THOURET (LMV-OPGC, dynamique coulées pyroclastiques et lahars) : J.C.Thouret@opgc.univ-bpclermont.fr
Jean-Paul TOUTAIN (OMP-LMTG et IRD, géochimie) : toutain@lmtg.obs-mip.fr

Impliqués également dans la coopération, n'étant pas intervenus en 2010, mais susceptibles d'intervenir dans les années prochaines :

François BEAUDUCEL (IPGP, déformations, GPS) : beauducel@ipgp.jussieu.fr
Anastasia BORISSOVA (LMTG, pétrologie) : borisova@lmtg.obs-mip.fr
Hélène Celle-JEANTON (LMV-OPGC, hydrogéologie) : h.celle-jeanton@opgc.univ-bpclermont.fr
Catherine DENIEL (LMV-OPGC, géochimie) : deniel@opgc.univ-bpclermont.fr
Alain GOURGAUD (LMV-OPGC, dynamique des dômes) : A.Gourgaud@opgc.univ-bpclermont.fr
Philippe JOUSSET (BRGM), p.jousset@brgm.fr

Karim KELFOUN (LMV-OPGC, dynamique des dômes) : K.Kelfoun@opgc.univ-bpclermont.fr
Jean-Luc LE PENNEC (LMV-IRD, volcanologie physique) : J.L.Lepennec@opgc.univ-bpclermont.fr
Séverine MOUNE (LMV-OPGC, géochimie gaz, flux de SO_2) : S.Moune@opgc.univ-bpclermont.fr
Dominique REMY (LMTG-OMP, télédétection, INSAR) : remy@lmtg.obs-mip.fr
Jacques ZLOTNICKI (LMV-OPGC, électromagnétisme) : jacques.zlotnicki@wanadoo.fr

Affiliations :

LMV-OPGC : Observatoire de Physique du Globe de Clermont-Ferrand, Laboratoire Magmas et Volcans CNRS et IRD, Université Blaise Pascal (Clermont-Ferrand)
LMTG-OMP : Observatoire Midi-Pyrénées, Laboratoire d'Etude des Mécanismes de Transfert en Géologie (Toulouse)
OSUG-LGIT : Observatoire des Sciences de l'Univers de Grenoble, Laboratoire de Géophysique Interne et de Tectonophysique (Grenoble) et Université de Savoie à Chambéry
IPGP : Institut de Physique du Globe de Paris (Paris)
CEA-DASE : Département Analyse Surveillance Environnement, Commissariat à l'Energie Atomique
LGP : Laboratoire de Géographie Physique, CNRS UMR 8591, Meudon et Université Panthéon-Sorbonne.

ACTIVITES EN 2010 : OBJECTIFS

Nos activités en 2010 se sont plus particulièrement concentrées sur les volcans Merapi et Semeru. Elles ont inclus trois thèmes de recherche appliquée et une action de valorisation et de diffusion du savoir.

1. **Surveillance des appareils actifs**
   - Etude des gaz des sols au volcan Merapi, actuellement en état d'alerte (éruption le 26 octobre 2010),
   - Sismologie et exploration pour un projet ANR
2. **Mesures des lahars au Semeru et télédétection haute résolution** :
   - suivi de l'évolution de l'appareil sommital par télédétection,
   - étude des écoulements pyroclastiques de l'éruption du Merapi en 2006 par télédétection.
3. **Evaluation des aléas et des risques, utilisation des matériaux volcaniques**
4. **Valorisation et diffusion du savoir et des savoir faires**.

MISSIONS effectuées en 2010

P. Richon et J.-P. Toutain (septembre 2010), F. Lavigne (septembre 2010), J.-Ph. Metaxian (octobre 2010) ; J.-C. Thouret et A. Solikhin (février 2010).

ACTIVITE 1 : SURVEILLANCE DES APPAREILS ACTIFS

1.1. MESURE DES GAZ DES SOLS SUR LE MERAPI, ^{222}RN, TEMPERATURE ET CO_2, DEVELOPPEMENT D'UN NOUVEL OUTIL DE SURVEILLANCE.

P. Richon (CEA), J.P. Toutain (IRD) - CEA-DASE & BPPTK, VSI, BMKG

Le Mérapi est l'un des volcans les plus actifs et plus explosifs (VEI = 2-4) d'Indonésie. Il menace directement l'une des zones les plus densément peuplées de Java (Yogyakarta et sa région). Ses éruptions paroxysmales dans le passé, associées à des écroulements de flancs, ont recouvert toute la région d'épais dépôts pyroclastiques (ensevelissement du temple de Borobudur). En dépit d'une longue surveillance, ses éruptions font toujours des victimes, un millier en 1930 et une vingtaine en 1994. Depuis 1872, l'activité continue du volcan consiste en des phases de croissance puis démantèlement (effondrement ou/et explosion) de dômes andésitiques, avec émission de coulées pyroclastiques et de lahars. Le Merapi est considéré comme le volcan de référence pour l'émission de coulées pyroclastiques engendrées par écroulement gravitaire de dôme. Il présente également un intense dégazage magmatique, matérialisé par un panache permanent issu du dôme de lave (>900 °C) et d'évents fumerolliens latéraux (> 600 °C). C'est un des volcans de référence pour la géochimie des gaz volcaniques et l'étude des processus de dégazage. Son éruption très spectaculaire en 2006, qui a fortement affecté le tissu socio-économique javanais, fut atypique, avec un dôme de volume inhabituel, d'étroites interactions avec la sismicité régionale et une phénoménologie inhabituelle des coulées pyroclastiques. Il est surveillé par l'Observatoire du Merapi (BPPTK) qui relève de l'autorité du DVGHM.
L'intérêt pour le Mérapi est dicté d'abord par la nécessité d'apporter un soutien aux autorités scientifiques indonésiennes, et ensuite par la forte ressemblance de cet appareil avec les volcans français antillais à dômes explosifs (Soufrière, Montagne Pelée). L'objectif est donc d'obtenir également un retour d'expérience directement utilisable en cas de crise volcanique en Guadeloupe ou Martinique.

Dans le cadre de la collaboration Franco-Indonésienne, le CEA-DASE participe depuis 2002 à des campagnes de mesure des gaz des sols sur le Merapi. Notre collaboration sur place s'effectue essentiellement avec les scientifiques de l'Observatoire Volcanologique du Merapi (BPPTK) et son directeur, mais aussi, historiquement, avec le BMKG, Badan Meteorologi Klimatologi dan Geofisika, Institut national de Météorologie et de Géophysique où un VIE du CEA-DASE y est en poste permanant.

Notre domaine d'intervention réside essentiellement dans la prospection et le suivi des émanations gaz des sols (T°, ^{222}Rn, CO_2), cf. Fig. 1, ainsi que dans l'étude de leurs relations avec les structures volcano-tectoniques et les fluctuations d'activité volcanique.

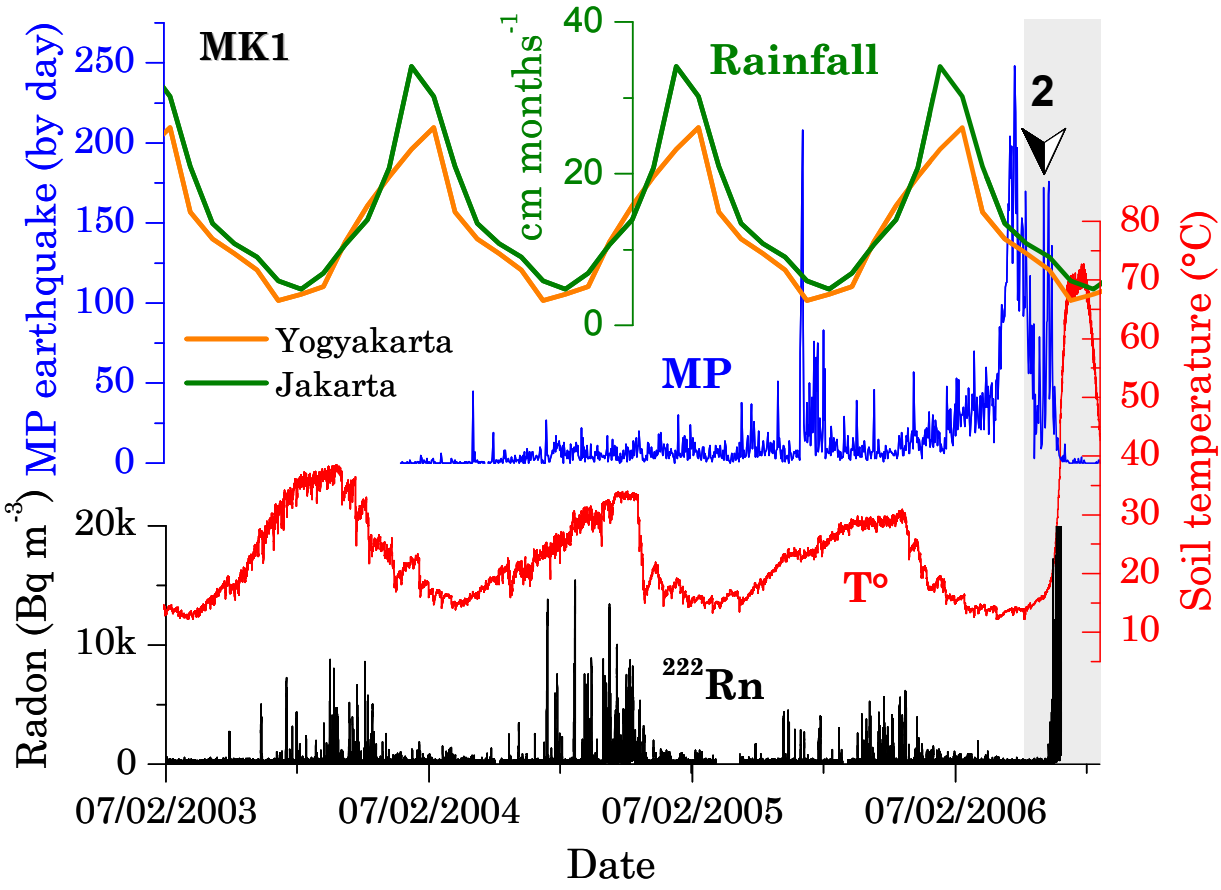

Figure 1. Totalité des données enregistrées à la station MK1 (Kawha Mati crater) de 2002 à 2006, juste avant l'éruption de Juin 2006 et le séisme de Yogyakarta (Mw 6.4).

L'objectif, à terme, est d'obtenir un outil de surveillance des phases de pressurisation du dôme de lave qui nous permettrait d'anticiper les épisodes d'écroulements catastrophiques qui se produisent de façon récurrente et qui menacent la sécurité des populations environnantes. Les objectifs principaux de cette collaboration sont :

1) La mise en place de réseaux de surveillance novateurs (mesures T°, ^{222}Rn et météorologie).
2) L'expérimentation et la validation de nouvelles stratégies de prospection des zones de gaz summitales (mesure de flux par chambre d'accumulation et par imagerie thermique basse température, Testo^{TM}).
3) La surveillance par la mesure ponctuelle du radon-222 et du thoron (radon-220) dans les gaz fumerolliens de Woro et Gendol.
4) La formation des chercheurs du MVO, sur la thématique du radon-222 des gaz des sols, formation devant déboucher à terme à la maitrise de la métrologie par les chercheurs de l'observatoire.
5) Une cartographie thermique des zone de dégazage, et choisir ainsi plus judicieusement les point intéressants pour le déploiement des 4 sondes radon et des dix capteurs de températures.
6) Les données météorologiques sont nécessaires pour interpréter les signaux des réseaux électromagnétiques et géochimie. La station actuelle hors service depuis

l'éruption de 2006 sera redéfinie, se limitant à un pluviomètre équipé d'un capteur de température de l'air + pression atmosphérique (T°air, Patm, pluviométrie).
Un des objectifs à terme, une fois que la dynamique de chaque station sera bien comprise, est de transmettre en temps réel, les données collectées directement à l'observatoire, afin que les chercheurs du MVO prennent possession du réseau.
Le planning prévisionnel débutera en Septembre 2011 pour les opérations de prospection et de remise en place du réseau et ce jusqu'à la prochaine éruption.

Intervenants :

Patrick Richon, Ingénieur-Chercheur au CEA-DASE ; Jean-Paul Toutain (IRD, Jakarta) ; VIE DASE (BMKG Jakarta).

References

Richon P., J.-C. Sabroux, M. Halbwachs, J. Vandemeulebrouck, N. Poussielgue, J. Tabbagh, R. Punongbayan, Radon anomaly in the soil of Taal volcano, the Philippines: A likely precursor of the M 7.1 Mindoro earthquake (1994), Geophys. Res. Lett., 30 (9), 1481, doi:10.1029/2003GL016902, 2003.

Toutain J. P., Sortino F., Baubron J. C., Richon P., Surono, Sumarti S., Nonell A., 2009. Structure and CO_2 budget of Merapi volcano during inter-eruptive periods. B. Volcanol. 71(7), 815-826.

Richon P., Toutain J.-P., Baubron J.-C., Labat D., Radtmatopurbo A., 2010. Radon-222 and thermal transient related to the 2006 seismo-volcanic event at Merapi volcano, Indonesia. Geophys. Res. Lett., Submitted.

1.2. Mission en sismologie et exploration pour un projet ANR en Indonésie

(Octobre 2010) **-Jean-Philippe Métaxian,** IRD et LGIT

Objectifs

Cette mission avait pour objectifs 1) l'évaluation des besoins en sismologie volcanique ; 2) la préparation d'un projet ANR sur le thème de la modélisation de la dynamique des dômes volcaniques appliquée au Merapi. Ce projet se place dans le cadre du développement des activités scientifiques de VELI. 3) l'analyse de données en collaboration avec des collègues du CVGHM.

Calendrier

4 octobre 2010 : arrivée à Bandung.
5-8 Octobre : Séjour à Bandung, discussions avec le Dr Surono et le Dr Hendra Gunawan, travaux sur un logiciel de transformation de format de données sismiques.
8-14 Octobre : Séjour à l'Observatoire de Yogyakarta, discussion avec le directeur et les responsables de la surveillance. Analyse de données sismiques du volcan Merapi.
15 octobre : Visite au Service de Coopération et d'Action Culturelle à Jakarta.

Préparation d'un projet ANR Modélisation de la croissance de dômes : Application au Merapi

Le Merapi est un volcan emblématique et un laboratoire international. Les conséquences de l'éruption actuelle montre, s'il était nécessaire, que cet appareil est le plus dangereux de l'Indonésie. Il s'agit aussi d'un volcan dont le dôme est actif, c'est-à-dire que l'extrusion de lave, lente, y est permanente. L'édification et la destruction de ce dôme, dont les pentes sont très raides au-dessus des flancs densément peuplés,

entraîne des écoulements pyroclastiques qui sont les processus volcaniques les plus meurtriers, avec les lahars.
Ce projet consiste à contraindre les modèles de dégazage, d'évolution rhéologique et de comportement mécanique d'extrusion et d'évolution de dômes magmatiques par des observations géochimiques, qui apportent par ailleurs des informations sur les processus magmatiques, des mesures géophysiques (déformations, activité sismique) et topographiques ainsi que par des données pétrologiques. Ce projet est en cours d'élaboration. Le produit devrait être un ou des modèles numériques d'écoulement du magma dans le conduit et de formation des dômes magmatiques. Le projet comporte également un volet surveillance. Il regroupe plusieurs laboratoires, le Laboratoire Magmas et Volcans ; (LMV), le laboratoire des mécanismes et transferts en Géologie (LMTG), L'institut de Sciences de la Terre d'Orléans (ISTO), l'Institut de Physique du Globe de Paris (IPGP) et le Laboratoire de Géophysique Interne et Tectonophysique (LGIT). Le partenaire indonésien est le CVGHM.
Les grandes lignes du projet ont été présentées au Dr Surono, directeur du CVGHM, et au directeur de l'Observatoire du Merapi à Yogyakarta. Ils ont donnés leur accord de principe pour l'accès à des données anciennes, l'installation de nouveaux équipements, une participation du personnel du CVGHM à la maintenance des équipements sur le terrain pendant la durée du projet. J'ai recueilli des informations concernant les données géophysiques et géochimiques existantes : type d'instrument, mode d'enregistrement des données, périodes de fonctionnement. La plupart de ces données sont inexploitées. C'est le cas notamment des données sismologiques. Le catalogue de données débute en 1990, ce qui englobe 6 éruptions du Merapi. L'analyse de ces données pour une meilleure définition des précurseurs éruptifs, la recherche de corrélations entre les différents cycles pré-éruptifs et éruptifs constituera une partie du projet. Les diverses informations recueillies nous permettent d'alimenter la réflexion concernant la structuration du projet et seront exploitées pour sa rédaction.

Analyse de données sismiques du Merapi, propositions d'amélioration du système de surveillance

Mon séjour à l'observatoire de Yogya a coïncidé avec le début d'une crise du Merapi. Le niveau 2 a été déclaré fin septembre 2010. Cela a été l'occasion d'observer le fonctionnement du service de surveillance et noter des améliorations qui pourraient être apportées.
Le système de surveillance se compose d'un réseau sismique dont les données sont transmises par radio en temps réel. Il existe un réseau de mesures de déformations (EDM). Plusieurs réflecteurs sont installés autour du cône. Les mesures sont faites depuis les observatoires lorsque la visibilité le permet. Il y a aussi des capteurs de température proches du sommet au nord (coulée 1956) et au sud (WORO). Ces données sont aussi transmises par radio. Les autres mesures (GPS, gaz) sont faîtes ponctuellement sur le terrain. Le réseau sismique se compose de 4 stations équipées de capteurs courte période et d'une transmission analogique (réseau le plus ancien), de 3 stations large bande Guralp CMG-3ESP (60 sec) du projet MIA VITA équipés d'une transmission numérique (4 ou 5 stations sont prévues) et d'une station équipée d'un capteur large bande STS2 (120 sec) et d'une télémétrie numérique. Or ces 3 systèmes ont des temps différents. C'est un problème technique majeur qui doit être résolu dès que possible car les séismes ne peuvent être localisés à l'heure actuelle qu'avec les 4 stations du réseau analogique.

Par ailleurs, le personnel de l'Observatoire n'est pas formé à la localisation des séismes. J'ai travaillé avec Agus Budi Santoso sur ce thème en installant un programme de pointé des phases sismiques (pickev) et un programme de localisation (Hypoellipse). Les figures 1 et 2 représentent les résultats des localisations effectuées pendant mon séjour avec 4 stations.

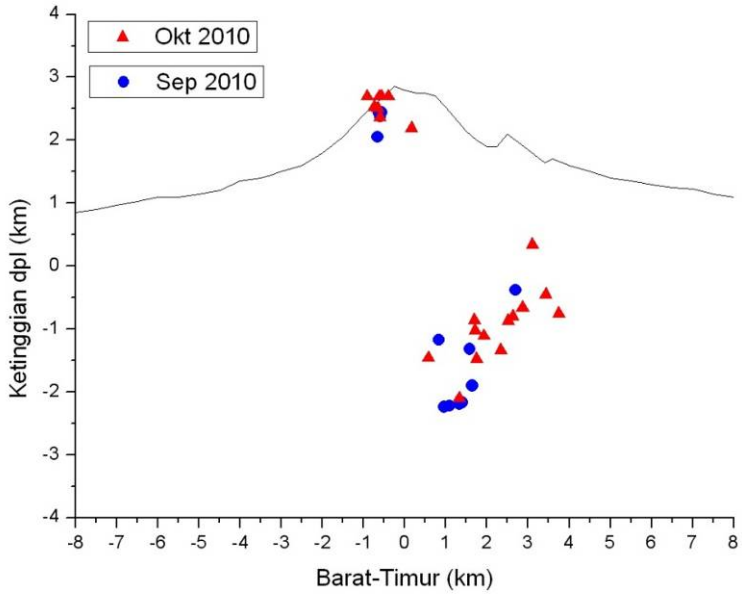

Figure 1 : Localisation de séismes volcano-tectoniques pendant la période fin Septembre-début Octobre. Coupe Ouest-Est

Figure 2 : Localisation de séismes volcano-tectoniques pendant la période fin Septembre-début Octobre. Coupe horizontale.

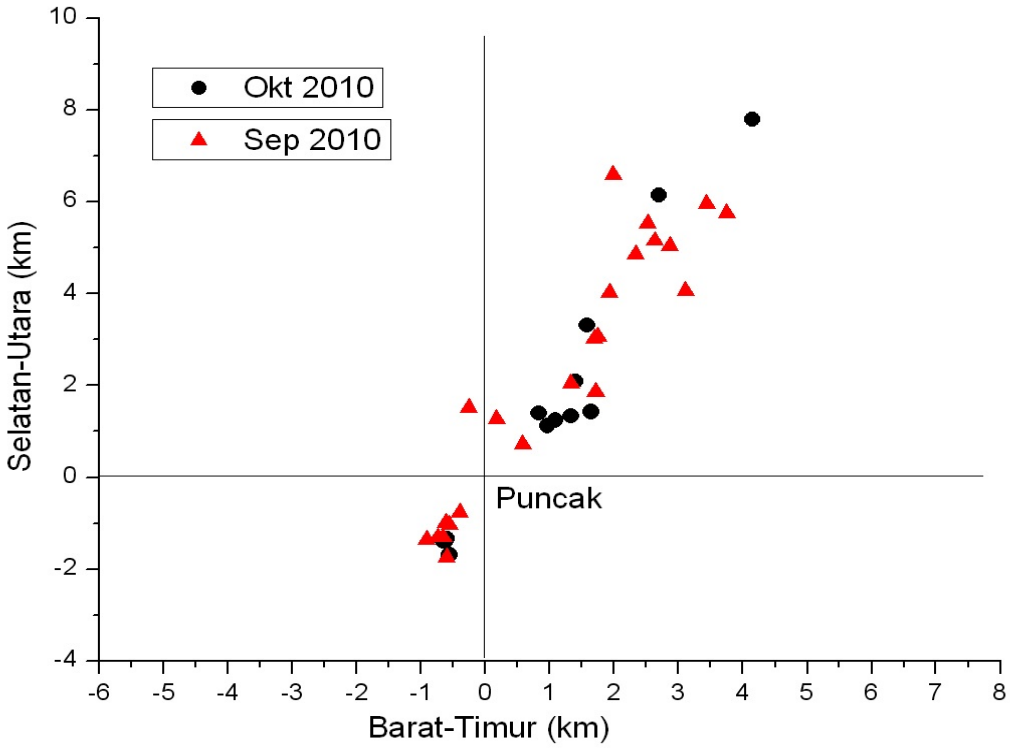

Les résultats mettent en évidence 2 zones distinctes, une au sommet correspondant à la zone du dôme et l'autre plus profonde. On observe un manque de sources sismiques entre le niveau de la mer et 2 km d'altitude. La distribution horizontale de la sismicité correspond aux résultats obtenus lors de l'éruption de 2006. Ce résultat est très préliminaire, il reste à confirmer ou à infirmer en utilisant plus de stations.

Le comptage des séismes par type est effectué manuellement sur les enregistrements papier. Les signaux précurseurs caractéristiques d'une intrusion sont principalement des signaux de fracturation type VA (profonds) et type VB (superficiels), et des signaux associés au mouvements du magma de type MP (Multi-phase). Ce travail effectué manuellement est long et fastidieux. Il peut y avoir plusieurs centaines à plusieurs milliers de signaux en une journée pendant une éruption. La figure 3 représente la sismicité depuis début 2009. Ce système de comptage pourrait être amélioré en utilisant un programme qui intègre la visualisation de signaux numériques, le pointé de phases pour identifier l'heure de début, la durée, de l'analyse spectrale permettant de différencier les différents types de sources et enfin des calculs d'énergie. La demande d'un outil de ce type a été formulée par Agu Budi Santoso. Des programmes existant au LGIT seront adaptés au cas du Merapi pour améliorer le processus de comptage et la classification des séismes. Cet outil permettra de créer un catalogue de données qui pourra être utilisé ultérieurement comme entrée d'un système de classification automatique.

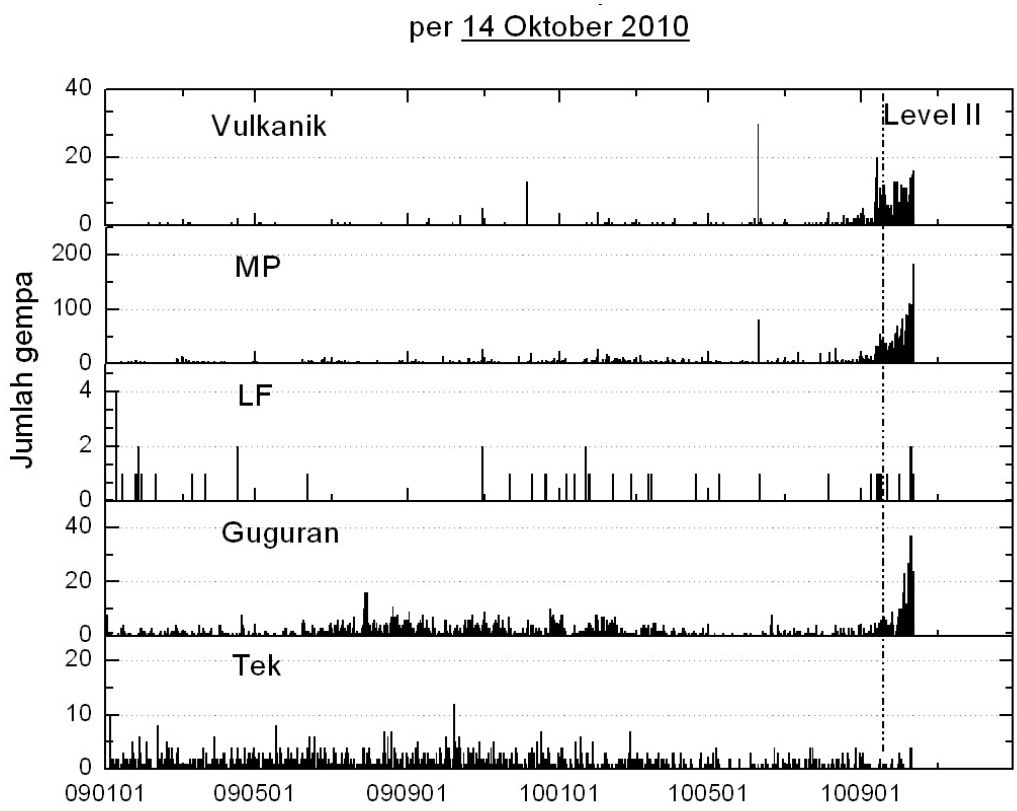

Figure 3 : Nombre de séismes par jour entre le 1er janvier 2009 et le 14 octobre 2010. Vulkanik : séismes volcano-tectoniques types A (profonds) et B (superficiels) ; MP : séismes Multi-Phase ; LF : séismes basse fréquence ; Guguran : éboulements ; Tek : séismes tectoniques.

Conclusions
Cette mission a permis de préparer le projet ANR modélisation de la dynamique de dômes volcaniques appliqué au Merapi en collaboration avec le CVGHM. Elle a aussi permis de mettre en évidence des améliorations à apporter au système de surveillance du Merapi.

ACTIVITE 2
LAHARS ET TELEDETECTION, VOLCANS SEMERU ET MERAPI

2.1. Mesures et surveillance des lahars au Semeru

J.-C. Thouret et A. Solikhin (CVGHM, futur doctorant au LMV en 2011)

Les lahars ou coulées de débris et de boue sont les phénomènes volcaniques les plus dangereux, avec les écoulements pyroclastiques qui les engendrent souvent durant la saison des pluies. Les lahars sont d'autant plus dangereux qu'ils se déclenchent en dehors des éruptions (fortes pluies) ou par la rupture d'un lac, etc. En outre, ils se propagent dans les vallées à plus grande distance que les écoulements pyroclastiques ; leur volume et parfois leur vitesse augmentent lors de leur propagation par entraînement des matériaux issus du lit et des berges de la vallée qu'ils empruntent. Comprendre les modalités de leur initiation, de leur propagation est fondamental dans le but d'alerter les populations très nombreuses sur les flancs et le long des vallées qui drainent les volcans indonésiens. Cartographier et mesurer la part des matériaux qui sont remobilisés par ces lahars dans les vallées lors des saisons des pluies après chaque éruption permettront d'évaluer plus précisément les zones affectées par les prochains lahars sur les volcans actifs (Semeru et Merapi).

Depuis quelques années, nous avons installé temporairement **un équipement de mesures et surveillance des lahars dans la vallée de Lengkong sur le volcan actif Semeru à Java**. L'un des posters joints (PDF) montre le thème de l'étude des lahars en Indonésie, le site choisi sur le Semeru, les outils et méthodes utilisés et enfin les résultats des mesures effectuées.

Nous installons une batterie de capteurs afin de mesurer les caractéristiques des écoulements et leur propagation entre deux stations distantes de 500 m : les capteurs de pression interstitielle (espace entre grains solides occupés par l'eau) et les géophones permettent d'estimer le débit, les capteurs de charge mesurent la force aplliquée sur le lit du chenal, un sismomètre à large bande permet d'analyser les fréquences induites par les vibrations dans le sol dues aux lahars, les cameras aident à mesurer la vitesse de l'écoulement et à enregistrer les phénomènes d'instabilité à la surface des écoulements, l'échantillonnage dans l'écoulement à intervalles réguliers fournit des valeurs de la concentration en solides, etc. (Doyle *et al.,* 2010a,b ; Dumainsil *et al.,* 2010)

Notre étude expérimentale "grandeur nature" poursuit quatre objectifs : 1. Acquérir des mesures in situ pendant ces écoulements particuliers ; 2. Comprendre les caractéristiques hydrauliques des flux, physiques des dépôts et matériaux, et leur comportement comparable à celui des "laves torrentielles" des Alpes ; 3. Suivre l'évolution d'une vallée qui convoie des lahars fréquents et estimer le bilan de l'érosion ; 4. Prévoir l'extension et l'impact des lahars sur les piémonts du Semeru où vit un million d'habitants.

Les données analysées sont le débit, la concentration en solides, la vitesse d'arrivée du front du lahar, la propagation et la vitesse des pulsations ou "bouffées" qui se succèdent pendant 1 à 2 heures. Ces données permettront de comprendre les processus d'entraînement ou de charge des matériaux dans le lahar, de sédimentation et d'érosion le long du chenal pendant l'écoulement. Les processus d'érosion et d'accumulation sont suivis annuellement depuis 2006 grâce aux levés topographiques effectués avec des GPS et au moyen de MNT (voir la dernière carte à droite). Toutes ces données serviront à calibrer des modèles d'écoulement de lahar. Les résultats sont rassemblés dans 3 publications en 2010.

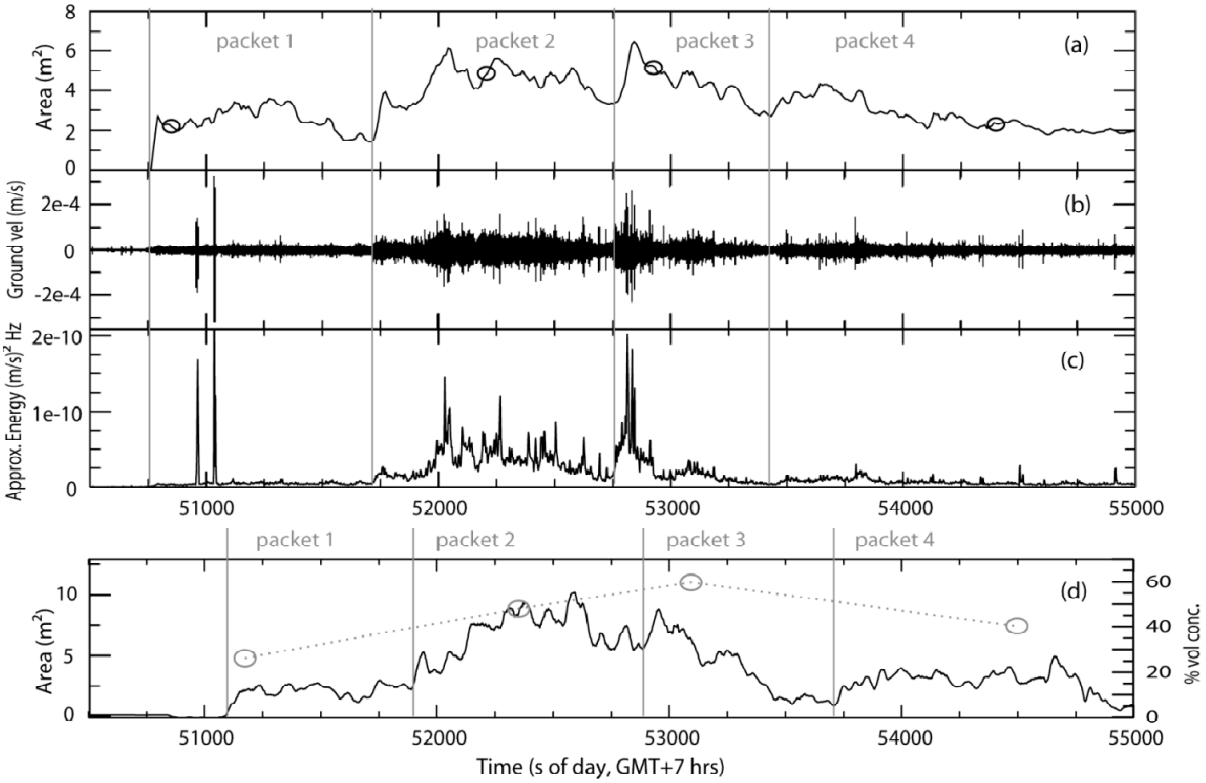

Fig ; 1. Quatre enregistrements acquis durant le lahar du 5 mars 2008 : la première et la dernière courbes représentent quatre parties de l'écoulement lors de leur passage aux stations amont et aval et les variations de leur concentration en sédiments (ellipses et trait fin interrompu). Le spectre noir indique la vitesse du mouvement du sol et la troisième ligne est l'énergie induite par les vibrations des écoulements dans le lit, deux données mesurées par un sismomètre situé à la station amont.

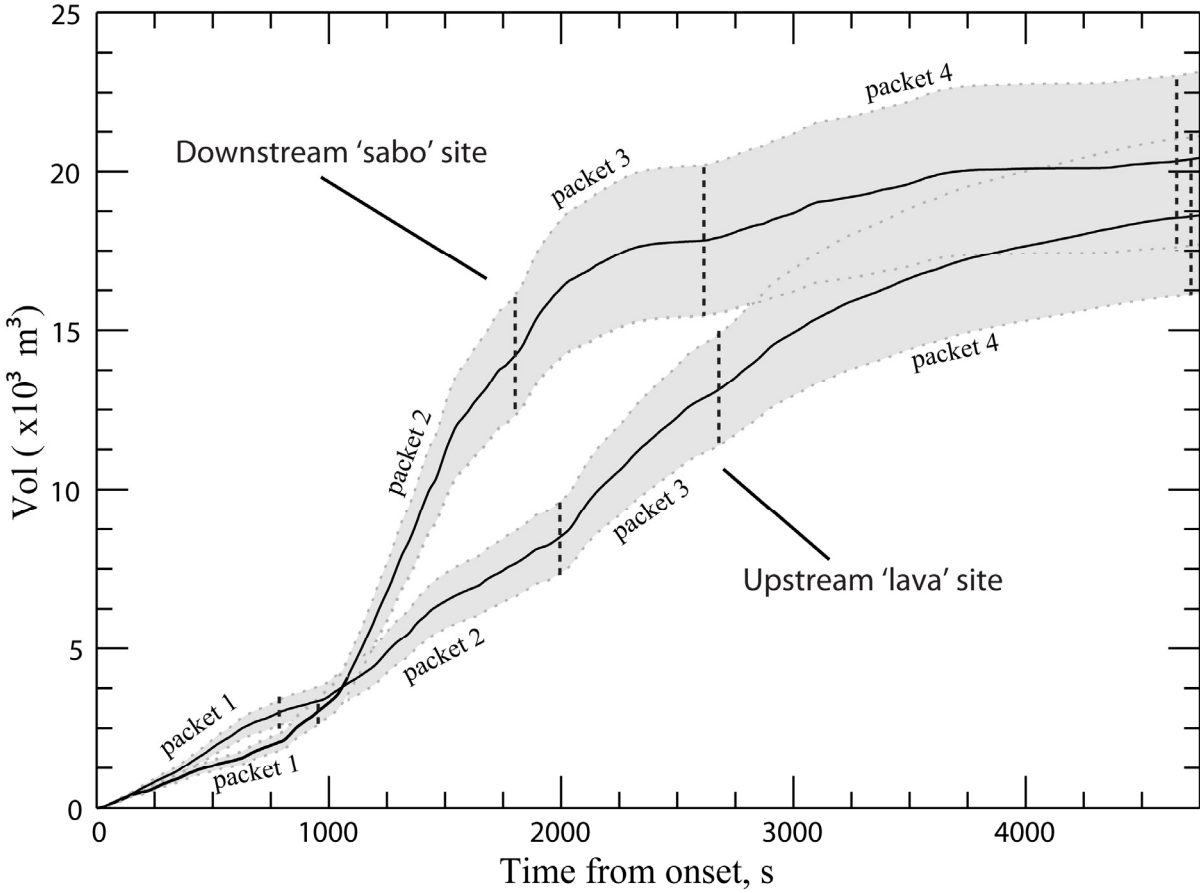

Fig. 2. L'évolution du volume du lahar du 5 mars 2008 entre les 2 stations amont « lava » et aval « sabo » . « Packet » = segment ou pulsation. Les variations de volume et de concentration en sédiments (en %) sont liées. Ces variations sont dues aux processus d'entraînement (incorporation de matériaux) et de sédimentation (dilution). La courbe et la zone grise du bas montre qu' au passage du lahar à la station amont le volume croît peu entre les paquets (= bouffées ou pulsations du lahar). Au contraire, la courbe et la zone grise du haut montre qu'au passage du lahar à la station aval, le volume des paquets 3 et 4 a cru 4 fois. Ceci reflète l'entraînement de matériaux des berges et peut-être du lit.

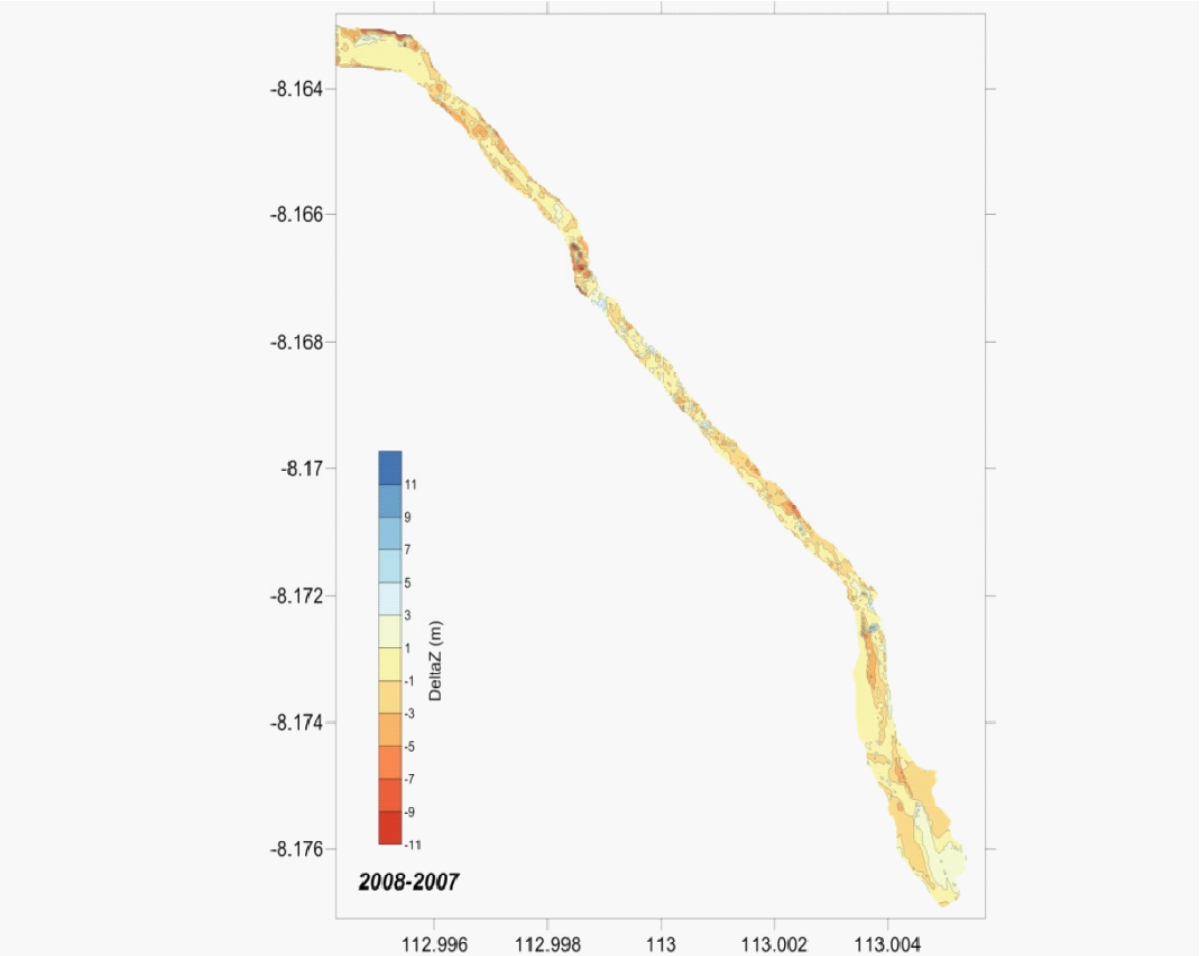

Fig ; 3. Acquisition de données topographiques avec GPS différentiel, comparaison inter-annuelle de Modèles Numériques de Terrain de 2006 à 2008 : les zones d'érosion (en rouge) et d'accumulation (en bleu) de matériaux sont montrées dans le chenal de la vallée de Lengkong sur 2 km de distance.

En 2011, nous voudrions effectuer trois tâches sur ce site expérimental grandeur nature :

1. **Mesurer les lahars** en février-mars pendant la saison des pluies avec l'équipement décrit plus haut durant au mois 3 semaines. Le but est d'acquérir des caractéristiques hydrauliques des écoulements et des matériaux afin de les utiliser dans les modèles d'écoulement à tester (à Grenoble, au Cemagref)
2. Acquérir une nouvelle **topographie du chenal de la rivière Lengkong** (avec GPS différentiel et avec des photos prises à basse altitude avec un ULM). Le but est de suivre l'évolution du chenal et surtout de mesurer les processus d'érosion et de dépôt en détail. Ce paramètre (érosion ou incorporation de matériau et dépôt ou dilution de l'écoulement) est fondamental pour comprendr e le phénomène et pour prévoir la propagation vers les zones peuplées à l'aval et autour du site expérimental.
3. Collaborer avec des économistes de Montpellier qui étudient **les attitudes et les réponses** (assurance, etc.) **face aux risques d'inondation et de coulées de boue**, et qui analysent le **type de gestion de ces risques par les autorités**

locales. Ceci se fera par l'intermédiaire d'enquêtes sur place avec l'aide d'un doctorant ou post-doctorant Indonésien.

2.2. TELEDETECTION HAUTE RESOLUTION AU MERAPI ET AU SEMERU

L'imagerie satellitaire est largement utilisée pour surveiller les volcans actifs et analyser l'évolution des édifices. Les progrès des techniques instrumentales et la résolution des images actuellement disponibles (1 m pour Ikonos, 50 cm pour GeoEye) nous permettent, selon les conditions météorologiques, d'appliquer cet outil aux deux volcans dangereux choisis pour cible. Sur le Merapi, volcan laboratoire, l'interprétation des images de haute résolution nous aide à suivre l'évolution du dôme et les effets des écoulements pyroclastiques induits par les effondrements (par ex. juin 2006, octobre 2010) en direction des flancs S et SW densément peuplés. Sur le Semeru, l'activité permanente, quotidienne et les conditions d'accès difficiles nous interdisent une approche répétée de la zone sommitale et du cratère. Nous exploitons donc les images des satellites Ikonos et SPOT5 afin de détecter des modifications au sommet et afin de délimiter sur des cartes détaillées les effets actuels et futurs des écoulements pyroclastiques et des lahars sur les piémonts densément peuplés.

En 2009 et 2010, nous avons utilisé l'imagerie satellitaire de haute résolution Ikonos (1m) et Spot (5 2,5 m) disponible à CRISP (National University of Singapore) avec trois objectifs :

- Détecter les différents types d'écoulements pyroclastiques issus de l'éruption de 2006 au Merapi (effondrement de dôme, coulées de blocs et cendres, déferlantes). Nous avons détecté leurs effets sur les versants et la forêt de la vallée de Gendol et déduit les causes de débordement des écoulements hors de la vallée principale en direction du village de Kaliadem (Thouret *et al.,* 2010). Ces débordements sont dus aux facteurs morphologiques de la vallée (sinuosité, obstacles), au changement de la capacité du chenal vis-à-vis des écoulements répétés, et aux obstacles d'origine anthropique (*Sabo dam* récemment construit à l'amont du village), à l'origine de débordements meurtriers vers Kaliadem en 2006 et 2010°. Ce constat remet en cause l'utilité des ouvrages de défense de type *Sabo dam* (Lube *et al*., 2010). Ceci débouche sur une évaluation des effets et des dommages lors des éruptions, qui surviennent tous les 4 ans en moyenne depuis 1904 au Merapi.
- Suivre l'évolution du sommet du Semeru et des bassins versants fréquemment empruntés par les écoulements pyroclastiques et surtout les lahars. Ceci se fera avec A. Solikhin (CVGHM, procahin doctorant au LMV).
- Reconnaître les formations géologiques du volcan, surtout les plus récentes, inventorier les produits principaux et le contexte structural de l'édifice, notamment les flancs instables comme celui exposé à l'est (A. Solikhin, Master2, 2009 à Clermont).

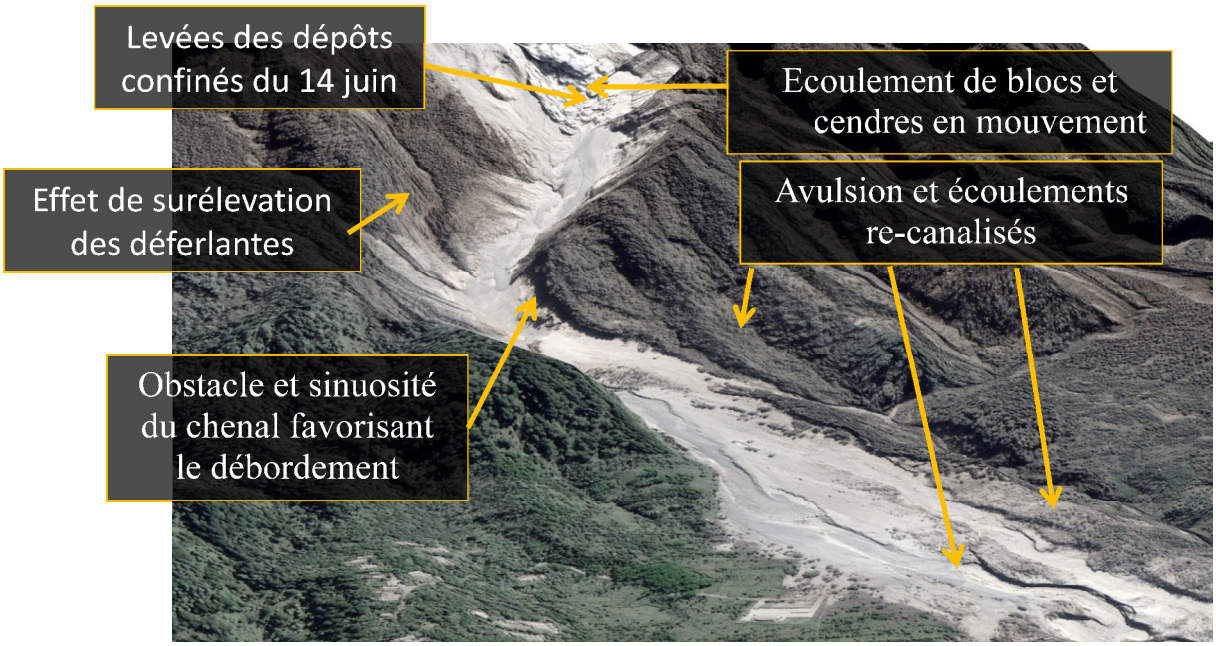

Fig. 4. Image Ikonos drapée sur un MNT du flanc sud du Merapi (vallée de Gendol). Les types, les effets et les processus liés aux écoulements pyroclastiques mis en place lors de l'éruption de 2006 sont indiqués. NB. Un écoulement de blocs et cendres se propage à l'amont de la vallée de Gendol au moment même où le satellite IKONOS acquérait cette image le 16 juin 2006.

Références

Thouret J.-C., Gupta A., Lube G., Cronin S.J., Surono, 2010. Analysis of the 2006 eruption deposits of Merapi Volcano, Java, Indonesia, using high-resolution IKONOS images and complementary ground based observations. *Remote Sensing of Environment, 114, 1949-1967* DOI:10.1016/j.rse.2010.03.016.

Dumaisnil C., Thouret J.-C., Chambon G., Doyle E.E., Cronin S.J., 2010. Hydraulic, physical and rheological characteristics of rain-triggered lahars at Semeru volcano, Indonesia. *Earth Surface Processes and Landforms, online2 June,* DOI: 10.1002/esp.2003.

Doyle E.E., Cronin S.J., Cole S.E., Thouret J.-C., 2010a. The coalescence and organization of lahars at Semeru, Indonesia. *Bulletin of Volcanology, 72, 8, 961-970.* DOI: 10.1007/s00445-010-0381-8.

Doyle E., Cronin S.J., Thouret J.-C., 2010b. Cycles of bulking and debulking in lahars at Semeru, Indonesia. *Geol Soc Amer Bull, Accepted August 2010, in the press.*

Lube G., Cronin J.S., Thouret J.-C., Surono, 2010. Kinematic characteristics of pyroclastic density currents at Merapi and controls on their avulsion from natural and engineered channels. *Geological Society America Bulletin, accepted September 2010.*

ACTIVITE 3 :
MISSION D'EVALUATION DES RISQUES, UITILSATION DES MATERIAUX VOLCANIQUES ET VALORISATION DE LA RECHERCHE

Franck Lavigne, LGP et Université Paris 1

Activités de coordination de la recherche

1. Rencontres avec Dr Surono, directeur DVGHM, Bandung

- Mercredi 7 et jeudi 8 juillet 2010, Jeudi 26 août 2010, Bandung, Lundi 20 septembre 2010, Paris, Mercredi 29 septembre 2010, Bandung.

2. Rencontres avec Dr Subandryio, directeur BPPTK, Yogyakarta en juillet - août 2010

Activité de valorisation de la recherche

1. Conférence « Le risque volcanique en Indonésie »
   - Lundi 27 septembre 2010, Lycée International Français (LIF) de Jakarta
     Classes de 4e (Ecole Internationale Française de Bali) et de 1ère (LIF)
   - Jeudi 30 septembre2010, Résidence de l'ambassadeur de France à Jakarta
     Une soixantaine de personnes de la communauté française et francophone de Jakarta. Conférence avec J.P. Toutain et Dr Surono.
   - Vendredi 12 novembre 2010, Section française de l'Indonesian Heritage Society (IHS). Communauté française et francophone de Jakarta.
2. Visite du Musée de la Géologie et projection de film à Bandung
   - Mardi 28 septembre 2010 : accompagnement de la classe de 4e de l'Ecole Internationale Française de Bali.

   Projection du film de F. Lecuyer « Volcans d'Indonésie, Java sur l'échine du dragon ».

Activités de recherche

1. Photographie haute résolution par ULM (*Ultra-Light Motorized*)

Une série de 116 photographies à haute résolution a été acquise par ULM fin août 2010 (Fig. 5).

Objectifs :

- Disposer de vues 2D et 3D des vallées Gendol et Woro en anticipant les prochains écoulements pyroclastiques du Merapi. Un second survol est prévu au lendemain de la prochaine éruption (2011 ?).
- Cartographier les impacts géomorphologiques liés aux extractions au fond des vallées.
- Compter les camions au moment du survol afin d'estimer les volumes de matériaux extraits en un temps donné.

Méthodes

- Photointerprétation et cartographie 2D des vallées.
- Construction d'un Modèle Numérique de Terrain (MNT) à partir de couples d'images par stéréophotogrammétrie (réalisée à l'Ecole Nationale des Sciences Géographiques – ENSG).

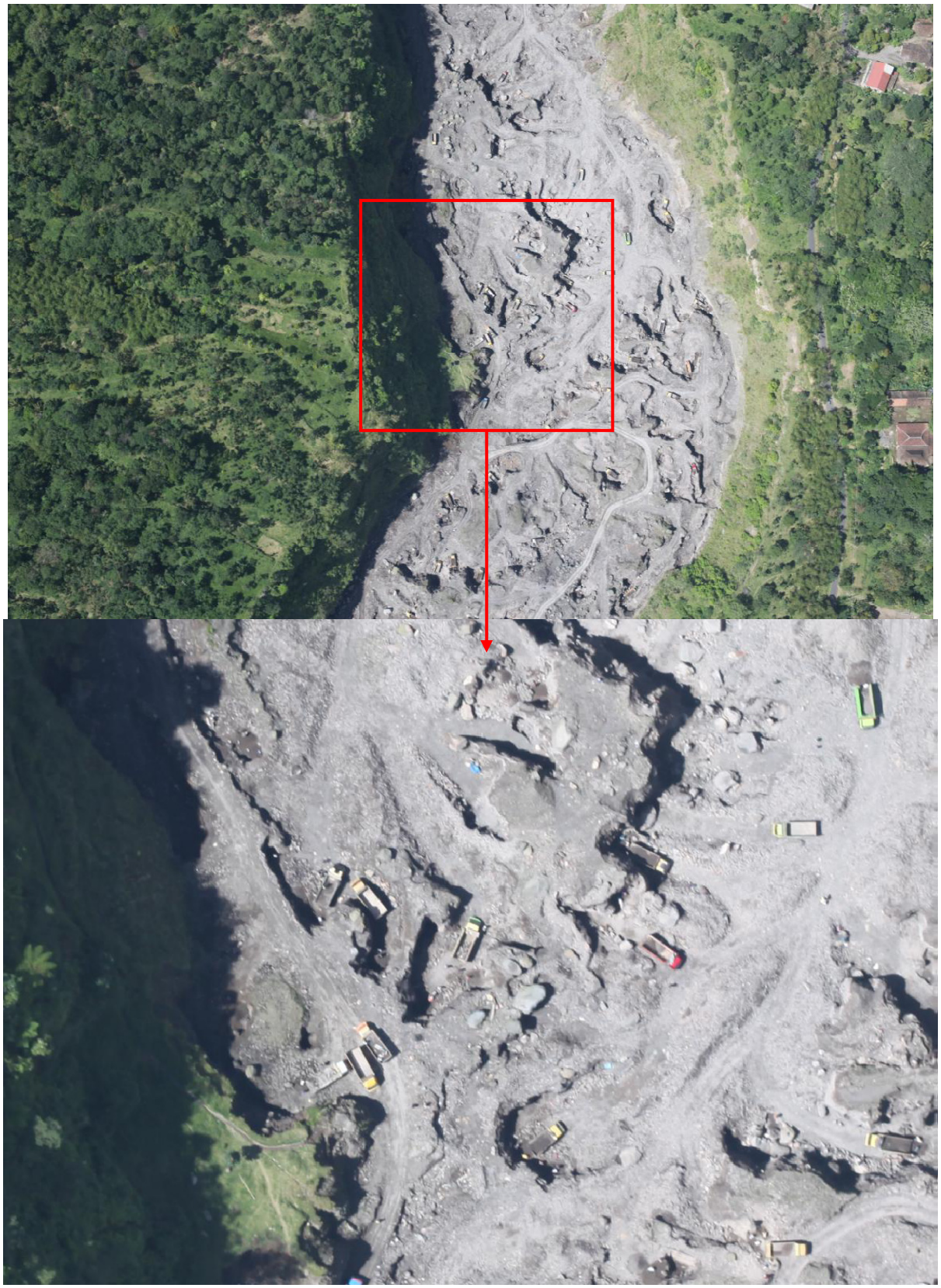

Fig. 5. Photographie haute résolution par ULM dans la vallée Gendol.

2. Relevés topographiques d'un tronçon de la vallée Gendol (Fig. 6)
Des relevés topographiques par station totale TRIMBLE ont été effectués en août 2010 (Fig. 6) afin de construire un Modèle Numérique de Terrain (Fig. 7) dans deux tronçons de la vallée : Kaliadem dam et un second site à 2 km plus en aval. Les objectifs étaient identiques que ceux présentés stéréophotogrammétrie ne s'étant concrétisés que récemment.

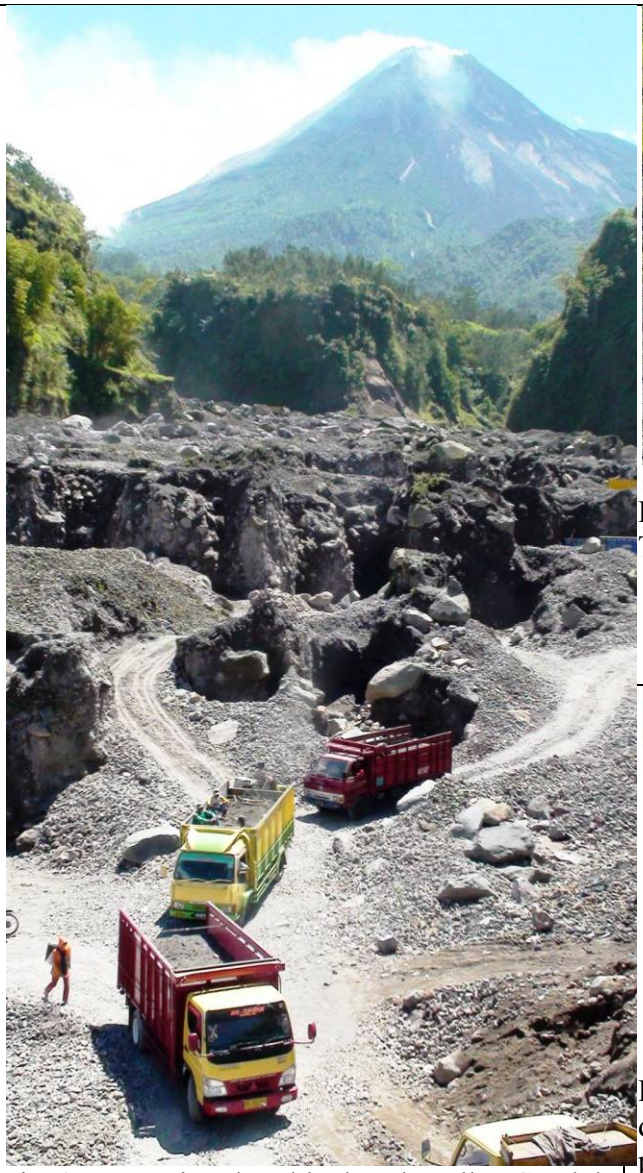

Fig. 2. Extraction de sable dans la vallée Gendol, août 2010

Fig. 6. Relevés topographiques par Station Totale. Dans la vallée Gendol, août 2010.

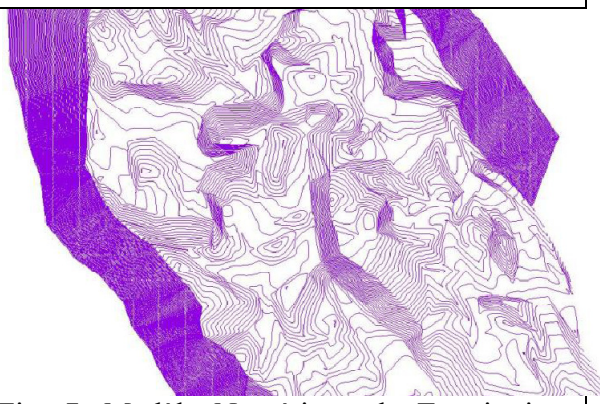

Fig. 7. Modèle Numérique de Terrain issu d'une campagne de relevés topographiques par Station Totale.

3. Cartographie des facteurs de vulnérabilité sur les flancs du Merapi
Travaux entrepris dans le cadre du programme européen MIA VITA.

ACTIVITE 4
VALORISATION ET DIFFUSION DU SAVOIR ET DES SAVOIR FAIRE

Plusieurs posters destinés à la diffusion des savoir faires et des résultats acquis en Indonésie depuis quelques années ont été remis à l'Ambassade de France en juillet 2010. Les titres de ces 8 posters sont les suivants :

1) Coopération franco-indonésienne : historique, objectifs et moyens (J.-P. Toutain)
2) Emanations gazeuses à hautes et basses températures sur un volcan actif, moyen de surveillance (J.-C. Baubron, J.-P. Toutain, P. Richon, F. Sortino)
3) Mesure du radon et de la température du gaz des sols ; au sommet du Merapi (P. Richon)
4) Coopération franco-indonésienne en sismologie volcanique (Ph. Lesage et J.-Ph. Metaxian)
5) Utiliser l'imagerie satellitaire de haute résolution afin de suivre l'activité et l'évolution des deux appareils les plus actifs et dangereux en Indonésie (J.-C. Thouret et A. Solikhin)
6) Coopération franco-indonésienne en volcanologie : les lahars (J.-C. Thouret, A. Solikhin et collaborateurs)
7) Dômes du Merapi et écoulements pyroclastiques associés (K. Kelfoun)
8) Volcans et sociétés en Indonésie : vivre avec les risques (F. Lavigne, D. Grancher, E. De Bélizal, E. Mei et A. Picquout)

D'autres activités de valorisation des acquis de la recherche ont été mentionnées dans le rapport de F. Lavigne ci-dessus.

Jean-Claude Thouret, Clermont le 28 octobre 2010.

UNION GEODESIQUE ET GEOPHYSIQUE INTERNATIONALE
INTERNATIONAL UNION OF GEODESY AND GEOPHYSICS

2009-2010 GRANT PROGRAMME

Project title:

Monitoring Taal volcano unrest in Philippines with joint Electromagnetic and multi-disciplinary educational EMSEV-PHIVOLCS program

FINAL REPORT
December 2010

EMSEV Inter- Association (ElectroMagnetic Studies of Earthquakes and Volcanoes)
http://www.emsev-iugg.org/emsev/

Jacques Zlotnicki, Chairperson
CNRS-France
(UMR6524-Clermont-Ferrand Observatory, France)
Email: Jacques.zlotnicki@wanadoo.fr

Yoichi Sasai, IAVCEI Liaison member
Tokyo Metropolitan Government
The Disaster Prevention Division
Email: yosasai@zag.att.ne.jp

Toshiyasu Nagao, EMSEV Secretary
Tokai University, Shimizu
Earthquake Prediction Research Center
Email: nagao@scc.u-tokai.ac.jp

Renato Solidium, PHIVOLCS Director
Philippines Institute of Volcanology and Seismology
PHIVOLCS
Email: renato_solidum@yahoo.com

Malcolm Johnston, EMSEV vice-Chair, IASPEI Liaison
U.S. Geological Survey, Menlo Park, USA
Earthquake and Volcano Hazards
Email: mal@usgs.gov

Introduction

Following an international workshop held in Manila in January 2003 for 'Initiating seismic and volcanic electromagnetic monitoring in Asian countries' the Inter-Association Working Group EMSEV has developed a scientific cooperation in the electromagnetic field and other geophysical methods with the Philippines Institute of Volcanology and Seismology (http://www.phivolcs.dost.gov.ph/). Priority was given to Taal volcano which may involve large eruptions with pyroclastic flows, base surges and violent phreatic explosions. The volcano has always shown signs of sporadic activity since the last period of activity (1965-1977) during which about 200 people were killed. In 1991, 1992, 2000-2004, 2006, and 2010 major seismic crises were recorded inducing occasionally felt earthquakes, opening of fissures, cyclic ground surface uplifts, increase in ground and water temperatures, bubbling in the acidic inner crater lake, and surface activity. Based on local authorities and PHIVOLCS researches, about 10,000 inhabitants should be concerned by a mild activity within a radius of only 7 km while more than 650,000 people should be affected in case of a violent eruption as that in 1749.

To respond and mitigate to this high level volcanic risk, EMSEV and PHIVOLCS have joined their best efforts for (1) understanding the interactions between the magma feeding system and the hydrothermal system buffered by both the hot acidic inner Crater Lake (MCL) and the cold outer Taal Lake(TL), the geological discontinuities along which heat and soil degassing prevail, (2) evaluating scenarios of activities, (3) monitoring the volcanic activity, and (4) constituting an electromagnetic scientific community at PHIVOLCS.

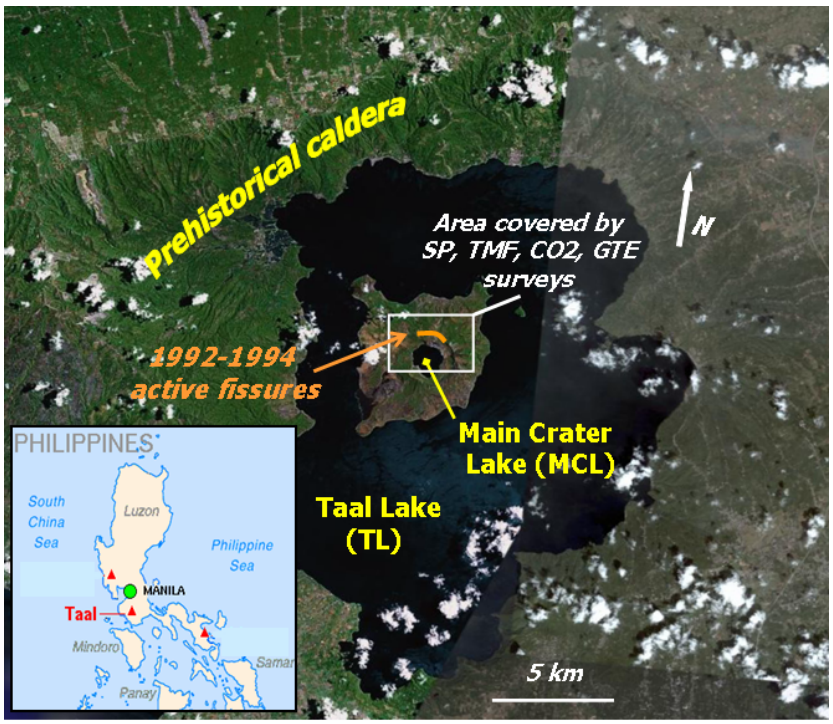

Figure 1: Topographic map of Taal volcano. White rectangle is the main area where EM and other geophysical field studies have been performed.

Time line of the cooperation

- **2003**

International EMSEV-PHIVOLCS workshop in Manila held in January 2003 on 'Initiating seismic and volcanic electromagnetic monitoring in Asian countries'
Formation an international electromagnetic (EM) EMSEV team based on Japanese and French counterparts.

- **2004**

Memorandum of agreement signed by PHIVOLCS and EMSEV on 'The understanding of the geotectonics, seismicity and volcanism of the southern Luzon region'

- **2005**

PHIVOLCS designs an initial EM team. First joint field campaign on Taal.
Magnetic (TMF), self-potential (SP), ground temperature (GT) and soil degassing surveys (CO_2) are performed.
A first continuous multi-parametric station located across the active fissures opened during the 1991-92 seismic activities is set. Data are recorded locally.

- **2006**

Two joint field campaigns are led. During the first January campaign, felt earthquakes incite people living on the volcanic Island to spontaneously evacuate for a few days.
A network of magnetic benchmarks is achieved on which the total magnetic field is regularly measured.

- **2007**

Two tasks were simultaneously performed during the two multiparty field works. One is to extend the electromagnetic, soil degassing and temperature surveys on the ground through the two identified geothermal fields. The second task is to build a new continuous multi-parametric station located inside the crater above the second geothermal field.
A real telemetry system was implemented between the two multi-parametric stations and the local Taal observatory. Data can be visualized and analyzed by PHIVOLCS.

Two continuous stations recording the total magnetic field were installed in the immediate vicinity of the two multi-parametric stations. Data which are recorded locally are collected every month by PHIVOLCS members.
One cross section of 13 audio-magnetotelluric soundings along a North-South direction highlights the rooting and the interconnection of the two geothermal fields.
During field work, particular attention is made to educate EM-PHIVOLCS team to the methods which are applied. EM-PHIVOLCS team is advised on best techniques to make measurements .
Reports were written, and meetings were held at PHIVOLCS headquarter.

- **2008**

Two years IUGG grant is obtained. It greatly allows the cooperation to speed up research.
A memorandum of agreement was made on the use of geomagnetic data from Muntinlupa magnetic observatory in the Philippines. It was signed by the National Mapping and Resources Information Authority (Philippines), the Ocean Hemisphere Research Center, the Earthquake Research Institute (University of Tokyo) the Japan Agency for Marine-Earth Science and Technology, PHIVOLCS, and EMSEV. This memorandum allows EMSEV and PHIVOLCS to use Muntinlupa magnetic data as remote reference.
Magnetic and bathymetry surveys of the inner Crater Lake were performed during the two joint 2008 campaigns.
Water level and temperature of the Crater Lake are now recorded thanks to a combined sensor located in the middle of the Crater Lake.
Reports were, and meetings at PHIVOLCS were held.

- **2009**

Meetings at PHIVOLCS, and two common field work efforts were organized.
Detail and large scale magnetic, self-potential, soil degassing and ground temperature surveys are done.
Because of the relative quietness of the surface activity of the Crater Lake, water temperatures (WTE) at the bottom of the Lake were measured. Detail bathymetry was updated.
An outstanding effort was made by both parties to install a more reliable internet connection between the computer recording multi-parametric data at the local observatory and PHIVOLCS headquarter, and the French server. Automatic transfers were set, and data can now be visualized and processed routinely on the Virtual ElectroMagnetic Laboratory (VEML; http://virtual-electromagnetic-laboratory.com/).

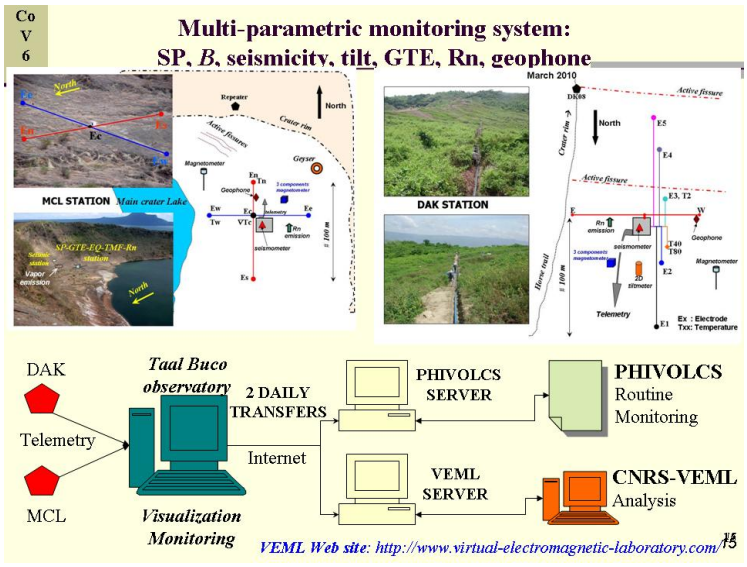

Figure 2: At MCL station, self-potential, ground temperature and gradient, seismic noise, components of the magnetic field, seismicity, , and Rn emission are recorded. At DAK station, in addition to the same parameters, two components of the tilt are also recorded (2010). 2 seconds

sampled data are radio-transmitted in real time.

♦ **2010**

Thanks to IUGG grant, PHIVOLCS and French Embassy supports, a second international workshop was held at PHIVOLCS. Title is 'Monitoring active volcanoes by electromagnetic and other geophysical methods; Application to Asian volcanoes'. About 60 participants attended the meeting (http://www.emsev-iugg.org/emsev/).

A new memorandum of agreement was signed between PHIVOLCS and EMSEV for the period 2010-2014.

Following the meeting, a large field campaign was organized:

- Resistivity, Very Low Frequency soundings are performed along the tracks followed by SP, ground temperature and soil degassing surveys (Greek participation).
- A borehole tiltmeter is installed at the northern multi-parametric station (DAK, USGS participation).
- Magnetic surveys were measured along the magnetic network of benchmarks, and new SP profiles allow building a complete map describing the extent of the hydrothermal field including the two geothermal fields.

In October and November 2010, a new step in the cooperation was achieved:

- Three magnetotelluric stations are installed under the framework of a JICA support (Japan).
- A new EMSEV multi-parametric station was build on the northwestern edge of the crater rim, at the limit of the northern geothermal field. Data recorded on site will be telemetered in real time in 2011.

From mid-April to the end of July, Taal volcano exhibited an abrupt and strong seismic crisis. PHIVOLCS raised the alert level from 1 to 2 temporarily and included a possible plan to partially evacuate the volcanic Island. Thanks to the real-time multi-parametric network, EMSEV was able to regularly process data and to inform PHIVOLCS about the observed signals and the interpretation. Two reports were sent to PHIVOLCS during this period. This several months of activity were useful for all the participants who rapidly communicate data, evaluation of the activity and so forth.

♦ **2011 prospective**

Two main field campaigns should be done during the year.

- Magnetotelluric soundings should be performed on the volcanic Island in order to study the deep structure,
- A fourth EMSEV multi-parametric station should be installed on the volcano. The objectives of this new station are multiple. First, parameters similar to those at the other stations (SP, temperature, gradient of temperature, seismic noise …) will be recorded, and, second, a current system which will allow dipole-dipole resistivity soundings on the basis of the multi-parametric network will be implemented.
- Depending on the budgets that each foreign EM team will get, theoretical and applied studies and stages will be proposed to PHIVOLCS EM team members.

Main results and achievements

Combined SP, GT, WTE, soil degassing and TMF surveys indicate that the northern part of the volcano is undergoing strong thermal transfers and degassing. The activity takes place along E-W fissures that could be linked to the root of the northern border of the Crater (MC) at a depth of some hundreds of metres, and also connected to a thermal source near the MCL shore line. This thermal source location could be the initial spot of the next eruptive activity. In such a case, strong activity could induce a collapse of a part of the northern MC rim into the MCL, due to mechanical weakening by the active 1992-1994 fissures. To the south, this system appears to be bounded by a NW-SE fault suspected from the NW-SE alignment of negative SP and WT anomalies in the MC. Seismic activity and dike injection may be taking place along this alignment. Changes in SP, TMF

and GT are measured by means of repeat profiles, suggesting that potentially hazardous phreatic/and gas eruptions may be associated with future seismic unrest in these geothermal areas.
The two geothermal fields are linked at several hundreds meters depth and the hydrothermal/volcanic fluids are prevailing in the northern part of the crater. Bathymetry and bottom water temperature of MCL clearly show that a bulge of 5 to 10 m high is present and is cut by active hot springs located along a N.NW-S.SE direction.
Resistivity soundings outline that hydrothermal fluids have mineralized and altered the northern rim of the crater which make it unconsolidated.
When one considers the background seismicity on the volcano, it is clear that seismic crises appear abruptly and are accompanied by rapid ground deformation as observed on many similar volcanoes. High levels of activity can be quickly reached. Therefore, real time monitoring and data analysis systems are a necessity for anticipating the level of hazard expected.
Earthquakes during the April-July 2010 crisis have again re-activated the 1991-94 fissures, which might unconsolidate the northern outer rim of the crater. Many data indicate that the region beneath the northern Crater Lake is still active. During this crisis, the near-surface activity in MCL is apparent, and one may consider that the general hydrothermal activity will again be similar to that observed in 2007 or before. Taking into consideration all the available data, it seems that is new crisis is serious although the details of the deep activity and its potential are not clear. Magmatic intrusion, together with hydrostatic overpressure, could be reactivating the region below the northern part of the volcano. Under this hypothesis, any depressurization, resulting from faulting triggered by teleseismic or local earthquakes, landsliding, etc, could destabilize the system and lead to a phreatic explosion on the volcano.
Four real time multi-parametric EMSEV stations will be operating in 2011. They allow continuous monitoring of the volcanic activity and greatly contribute to improved understanding of the on-going activity. The program adds further value to the seismic networks, geophysical and geochemical surveys operated by PHIVOLCS. PHIVOLCS already integrate some of our results in the information planning to Local authorities and inhabitants.
Several PHIVOLCS members are now aware of EM methods and they would go further in the next years in the study of the EM field. Some of the methodologies developed during the cooperation may already be integrated in the monitoring of other volcanoes in the Philippines.

PHIVOLCS and International EMSEV consortium and evolution

♦ PHIVOLCS team

From the beginning of the cooperation PHIVOLCS (Director R. Solidum) made a huge effort to mobilize active researchers, engineers and technicians in the EMSEV-PHIVOLCS cooperation. The Institute has always largely contributed to providing adequate numbers of personnal in the field in order to complete joint field campaigns. PHIVOLCS has also financially supported the contribution of PHIVOLCS members on the field.

About 8 to 10 PHIVOLCS members may be regularly involved in the cooperation. Most of them are coming from the Volcanological section (directed by J. Sincioco). Two groups were constituted and each of them has focused his interest in the 'Magnetic field monitoring' (J.M. Gordon, Jr, P. Alanis, Freddy)or in the 'Electric field monitoring' (E. Villarcorte, L. Bong, P. Reniva). During each field visit, a representative (J.P. Sabit) of the volcanological section accompanies PHIVOLCS members on the field. The local support is given by Taal observatory (A. Loza Loic, L.A. C. Banes).

♦ EMSEV team and other contributions

EMSEV team has largely increased during the past years.

- Initially the cooperation was supported by two teams mainly belonging to the Earthquake Prediction Research Centre (T. Nagao, M. Harada located at Tokai University, Shimizu) and Tokyo Metropolitan City (Y. Sasai) in Japan, and to the French National Research Centre in France (J. Zlotnicki, F. Fauquet, and P. Yvetot positioned at the Observatory of Physics of

Globe, Clermont-Fd). About 6 researchers and engineers, experts in the EM field, were involved.

From these countries other research teams joint the cooperation, bringing their own expertise: For instance the Aso observatory for total field magnetometers, and J.P. Toutain from the Laboratoire de Mécanismes de Transfert en Géologie for geochemical studies and soil degassing.

- Later on, F. Sortino from the Istituto Nazionale per la Vulcanologia of Palermo (INGV, Italy) contributed to heat fluxes and CO_2 degassing measurements, while A. Bernard from the Laboratoire de Géochimie et Minéralogie (Université Libre de Bruxelles, Belgium) focuses on Thermal Aster imagery of Taal Crater Lake.

- In 2010, G. Vargemezis from the Aristotle University of Thessaloniki entered the scientific consortium and manages the resistivity soundings on the volcano with J.R. Puertollano, R.C. Pigtain from PHIVOLCS. US Geological Survey greatly enlarges the monitoring of the volcano by setting a borehole tiltmeter at a first multi-parametric station (DAK). Now, M.J.S. Johnston is deeply involved in the monitoring of the volcano as the French and Japanese teams.

- Satellite observations progressively enlarge the multi-disciplinarity of the EMSEV consortium. EM observations by DEMETER are active til the end of the experiment. MOPITT observations are done by R.P. Singh working at Chapman University (USA). V. Tramutoli and N. Pergola from Department of Engineering and Physics of The Environment (DIFA, University of Basilicata) are presently setting a time domain analysis of robust satellite techniques (RST) for near real-time monitoring of active volcanoes and thermal precursor identification.

Dissemination of results

♦ Articles

M. Harada, Julio P. Sabit, Y. Sasai, Paul K. B. Alanis, Jr. Juan M. Cordon, Ernesto G. Corpuz, J. Zlotnicki, T. Nagao and Jane T. Punongbayan, 2005. Magnetic and Electric Field Monitoring of Taal Volcano, Philippines. Part I: Magnetic Measurements, Japan Acad. Sci., 81, B, 261-266.

J. Zlotnicki, Y. Sasai, J.P. Toutain, E.U. Villacorte, A. Bernard, Julio P. Sabit, Juan M. Gordon Jr, Ernesto G. Corpuz, M. Harada, J.T. Punongbayan, H. Hase and T. Nagao, 2008. Combined Electromagnetic, geochemical and thermal surveys of Taal volcano (Philippines) during the period 2005-2006. Bull Volcanol., doi: 10.1007/s00445-008-0205-2.

Y. Sasai, M. Harada, J.P. Sabit, J. Zlotnicki, Y. Tanaka, J.M. Cordon Jr., S. Uyeda, T. Nagao, J.S. Sincioco, 2008, Geomagnetic and topographic survey of the Main Crater Lake in Taal Volcano (Philippines): preliminary report, J. Geography, 117, 894-900 (in Japanese with English abstract).

M. Harada, Y. Sasai, J. Zlotnicki, Y. Tanaka, H. Hase, J.P. Sabit, J.T. Punongbayan, J.M. Cordon Jr, E.U. Villacorte, E.G. Corpuz, and T. Nagao, 2008. Monitoring of volcanic activity of Taal volcano (Philippines) by electromagnetic methods, Bull. Inst. of Oceanic Res. and Dev., Tokai University, 29, 9-28, 2008 (in Japanese with English abstract).

J. Zlotnicki, Y. Sasai, J.P. Toutain, E. Villacorte, PHIVOLCS team, P. Yvetot, F. Fauquet, A. Bernard, 2009. Electromagnetic and Geochemical methods applied to investigations of Hydrothermal/magmatic unrests: Examples of Taal (Philippines) and Miyake-jima (Japan) volcanoes, Physics and Chesmistry of the Earth, 34, 394-408. doi:10.1016/j.pce.2008.09.012.

I. Fikos, G. Vargemezis, J. Zlotnicki, J.R. Puertollano, R.C. Pigtain, P.B. Alanis and Y. Sasai, 2011. Shallow structure of the hydrothermal system at Taal volcano (Philippines) inferred by detailed electrical resistivity tomography, in preparation to Bull. Volcanol.

M. Harada, J. Zlotnicki, Y. Sasai, 2011. Magnetic maaping and bathymetry of Taal Crater Lake (the Philippines). In preparation.

♦ Conferences

J. Zlotnicki, 2003. Invited conference. Electromagnetic investigations on Volcanoes : What to observe ? Workshop for initiating seismic and volcanic electromagnetic monitoring in Asian countries, organisé par IUGG et EMSEV, Manille (Philippines), 14-16 jan., 2003.

M. Harada, Y. Sasai, J. Zlotnicki, J.P. Sabit, J.T. Punongbayan, J.M. Cordon, E.U. Villacorte, P.K.B. Alanis, Ishmael C. Narag[4]; Raymond Patrick R. Maximo[4]; Teodorico, A. Sandoval, E.G. Corpuz, B.C. Bautista, R.U. Solidum, T. Nagao, S. Uyeda, 2005.

Magnetic and SP measurements in Taal Volcano, Philippines. Joint meeting for Earth and Planetary Science, May 22-26, 2005, Tokyo, Japan.
E.U. Villacorte, J. Zlotnicki, Y. Sasai, J.P. Toutain, A. Bernard, M. Harada, B.J.T. Punongbayan, I.C. Narag, R.P.R. Maximo, E.G. Corpuz and EM PHILVOLCS team, 2005. Taal volcano (Philippines): Gearing toward a new eruption? Combined land based self-potential, ground temperature and CO2 soil degassing surveys with the crater lake temperature monitored by satellite imagery. IAGA meeting, Toulouse July 18-29, France.
J. Zlotnicki, Y. Sasai, J.P. Toutain, E.U. Villacorte, A. Bernard, J.T. Punongbayan, H. Hase, M. Harada, Ernesto G. Corpuz, Julio P. Sabit, T. Nagao, 2006. Taal volcano (Philippines): Gearing toward a new eruption? Combined land based self-potential, magnetic, ground temperature and CO2 soil degassing surveys with the Crater Lake temperature monitored by satellite imagery. International Workshop on Demeter. Toulouse, June 14-16.
J. Zlotnicki, Y. Sasai, J.P. Toutain, E.U. Villacorte, A. Bernard, J.T. Punongbayan, H. Hase, M. Harada, Ernesto G. Corpuz, Julio P. Sabit, T. Nagao, 2006. Taal volcano (Philippines): Gearing toward a new eruption? Combined land based self-potential, magnetic, ground temperature and CO2 soil degassing surveys with the Crater Lake temperature monitored by satellite imagery, 2006. IWMEEMSV Workshop, India, Nov. 20-22.
J. Zlotnicki, Y. Sasai, J.P. Toutain, E.U. Villacorte, J.M Cordon Jr., A. Bernard, J. P. Sabit, M. Harada, H. Hase, J. Sincioco, J.T. Punongbayan, and T. Nagao, 2007. Electromagnetic and Geochemical monitoring of the slow unrest of Taal volcano (Philippines). IUGG, Perugia, Italy, July 2-13.
SenthilKumar, R.P. Singh J. Zlotnicki, Y. Sasai, and J. Sincioco, 2007. Monitoring slow unrest of Taal volcano (Philippines) Using Carbon Monoxide from MOPITT satellite. IUGG, Perugia, Italy, July 2-13.
J. Zlotnicki, J.P. Toutain, Y. Sasai, E.U. Villacorte, A. Bernard, J. Sincioco, J.M Cordon Jr., Senthilkumar, J. P. Sabit, M. Harada, H. Hase, J.T. Punongbayan, and T. Nagao. Electromagnetic and Geochemical monitoring of the slow unrest of Taal volcano (Philippines). IGOS, GeoHazards 2007. Frascati, Italy Nov. 6-9
Sasai, Y., J. P. Sabit, J. M. Cordon Jr., E. U. Villacorte, J. Zlotnicki, J-P. Toutain, M. Harada, H. Hase, J. Sincioco, T. Nagao: Electromagnetic and geochemical monitoring of Taal volcano, the Philippines: 2005-2007. The 5th International Congress of Cities on Volcanoes; COV-07), Shimabara, Nov. 2007.
J. Zlotnicki, J.P. Toutain, Y. Sasai, E.U. Villacorte, A. Bernard, J.M Cordon Jr., F. Sortino, J. P. Sabit, M. Harada, PHIVOLCS EM team, J. Sincioco, H. Hase, T. Nagao, 2008. Invited conference "Volcanic lakes". Integrated Electromagnetic and Geochemical methods applied to volcanic hydrothermal systems: Application to Taal volcano (Philippines). IAVCEI GA Assembly, Reykjavik, Iceland, Aug. 18-25, 2008.
J. Zlotnicki, Y. Sasai, J.P. Toutain, E. Villacorte, PHIVOLCS team, P. Yvetot, F. Fauquet, A. Bernard. Electromagnetic and Geochemical methods applied to investigations of Hydrothermal/magmatic unrests: Example of Miyake-jima (Japan) volcano, 2008. IAVCEI meeting, Reykjavik, Iceland, Aug. 18-25, 2008.
M. Harada, J.P. Sabit, Y. Sasai, J.M. Cordon Jr., J. Zlotnicki, Y. Tanaka, E.U. Villacorte, H. Hase, J.S. Sincioco and T. Nagao, 2008. Monitoring of volcanic activity in Taal volcano (Philippines) by electromagnetic methods: geomagnetic observations. EMSEV-DEMETER joint workshop, Sinaia, Romania, Sept. 7-12, 2008.
J. Zlotnicki, J.P. Toutain, Y. Sasai, E.U. Villacorte, M. Harada, A. Bernard, Paul Yvetot, F. Fauquet, J.M. Cordon Jr., F. Sortino, J. P. Sabit, J. Sincioco, PHIVOLCS EM team, H. Hase, T. Nagao, 2008. Integrated Electromagnetic and Geochemical methods applied to the volcanic hydrothermal system of Taal volcano (Philippines). EMSEV-DEMETER joint workshop, Sinaia, Romania, Sept. 7-12, 2008.
P.K.B. Alanis, J. Zlotnicki, J.P. Sabit, Y. Sasai, J.M. cordon Jr., M. Harada, J.P. Toutain, E.U. Villacorte, A. Bernard, H. Hase, J.T. Punongbayan, T. Nagao, R.U. Solidum Jr., 2009, Electromagnetic, geochemical and thermal studies on Taal Volcano (Philippines) from 2005 to present, AOGS conference, Singapore, August 11-15, 2009.
J. Zlotnicki, J.P. Toutain, Y. Sasai, E.U. Villacorte, M. Harada, A. Bernard, P. Yvetot, F. Fauquet, 4, F. Sortino, PHIVOLCS EM team, T. Nagao, and R. Solidium, 2009. Electromagnetic, Geochemical and thermal anomalies related to the hydrothermal activity of Taal volcano (Philippines). IAGA meeting, Sopron (Hungary), August 22-29, 2009.
M. Harada, Y. Sasai, J.P. Sabit, J.M. Cordon Jr., J. Zlotnicki, J.Sincioco, Y. Tanaka, T. Nagao, 2009. Magnetic and topographic studies on the main crater lake of Taal volcano (Philippines). IAGA meeting, Sopron (Hungary), August 22-29, 2009.
J. Zlotnicki, **Organisation du workshop EMSEV-PHIVOLCS International Meeting** on Monitoring active volcanoes by Electromagnetic and other geophysical methods, Mainla (Philippines), Feb. 25-27, 2010.
J. Zlotnicki, Y. Sasai, J.P. Toutain, E. Villacorte, M. Harada, PHIVOLCS team, P. Yvetot, F. Fauquet, A. Bernard, T Nagao, 2010. Electromagnetic, geochemical and thermal investigations of Taal volcano, 2010. EMSEV-PHIVOLCS Intern. Meeting on Monitoring active volcanoes by Electromagnetic and other geophysical methods, Mainla (Philippines), Feb. 25-27, 2010.
J. Zlotnicki, and EMSEV bureau, 2010. EMSEV project and its activities. EMSEV-PHIVOLCS Intern. Meeting on Monitoring active volcanoes by Electromagnetic and other geophysical methods, Mainla (Philippines), Feb. 25-27, 2010
P.K.B. Alanis, J.P. Sabit, Y. Sasai, J.M. Cordon, Jr., **J. Zlotnicki**, M. Harada, E.U. Villacorte, H. Hase, J.T. Punongbayan, T. Nagao, J.S. Sincioco and R.U. Solidum Jr, 2010. Magnetic observations on Taal Volcano (Philippines) in combination with other geophysical and geochemical methods from 2005 to present. Meeting on Monitoring active volcanoes by Electromagnetic and other geophysical methods, Mainla (Philippines), Feb. 25-27, 2010.
J.P. Toutain, F. Sortino, **J. Zlotnicki**, Phivolcs team, 2010. soil gas and heat flow assessment at Taal hydrothermal system. Meeting on Monitoring active volcanoes by Electromagnetic and other geophysical methods, Mainla (Philippines), Feb. 25-27, 2010.
J. Zlotnicki, 2010. Electromagnetic and Geochemical methods applied to the investigation of Taal hydrothermal system (Philippines). 6th International meeting Cities on Volcanoes, Tenerife, May 31- June 4, 2010.
J. Zlotnicki, 2010. Taal volcano (Philippines): gearing towards a new eruption? European Open Forum, EOSF-2010, Turino, July 3-7, 2010.
J. Zlotnicki, Y. Sasai, EM PHIVOLCS team, M.J.S. Johnston, J.P. Toutain, and G. Vargemezis, 2010. Five years of cooperation between EMSEV and PHIVOLCS for understanding and monitoring Taal volcano. EMSEV International 2010 workshop, Santa Ana, USA, 3-6 October, 2010.

Comité National Français de Géodésie et Géophysique

French National Committee of Geodesy and Geophysics

RAPPORT QUADRIENNAL DU CNFGG A l'UGGI

QUADRENNIAL REPORT OF CNFGG TO IUGG

SECTION 4 – GÉOMAGNÉTISME ET AÉRONOMIE

SECTION 4 - GEOMAGNETISM AND AERONOMY

Comité National Français de Géodésie et Géophysique

Section IV - Aéronomie et Géomagnétisme

Rapport Quadriennal 2007-2011

The following pages aim describing some of the recent scientific progresses in the area of aeronomy and geomagnetism that were authored or co-authored by the French community. Rather than putting the emphasis on a very limited number of results, we chose to gather in this report very synthetic and brief notes on different topics, in the area of geomagnetic field measurements, data processing, modeling, intepretation, paleo- and archeomagnetism, bio- and rock magnetism, experimental and numerical dynamo, interactions with climate, solar wind, high atmosphere studies, troposhere, ionosphere, and planetary magnetic fields.

We are very thankful to thoses who unselfishly accepted to spend some time to this report. These are Hagay Amit, Pierre-Louis Blelly, Annick Chauvin, Arnaud Chulliat, Jean Pascal Cogné, Jérôme Dyment, Alexandre Fournier, Yves Gallet, Agnès Genevey, Gauthier Hulot, Aude Isambert, France Lagroix, Philippe Lanos, Guillaume Le Hir, Aurélie Marchaudon, Jean-François Pinton and Yoann Quesnel.

Erwan Thébault (Secretary)
Jean-Baptiste Renard (Vice-President)
Benoit Langlais (President)

Earth's magnetic field measurements

Arnaud Chulliat, Jérôme Dyment, and Gauthier Hulot

Institut de Physique du Globe de Paris, INSU/CNRS, F-75005 Paris

Abstract The French community contributes to the international effort of monitoring the Earth's magnetic field. The "Bureau Central de Magnétisme Terrestre" (BCMT) gathers French institutions contributing to ground observations. As of Feb. 2011, 18 INTERMAGNET observatories are affiliated to BCMT, among which 8 are in collaboration with foreign institutions. During 2007-2011, BCMT developed its instrument technical abilities, installed two new observatories (Easter Island and Antarctica), and upgrade the data processing procedures to provide quasi-definitive data within one month. Regarding marine measurements, new techniques were developed and marine campaigns were conducted. The French community has also an important role in the soon-to-be-launched SWARM ESA mission, with an instrument-PIship.

Magnetic observatories

The BCMT, founded in 1921 and attached to the Institut de Physique du Globe de Paris (IPGP), is in charge of coordinating ground observations of the Earth's magnetic field by French institutions. Three French institutions are currently operating magnetic observatories: the IPGP, the École et Observatoire des Sciences de la Terre (EOST) and the Institut de Recherche pour le Développement (IRD). A fourth institution, the Observatoire Versailles Saint Quentin (OVSQ), attached to Institut Pierre Simon Laplace (IPSL) and Université Versailles Saint Quentin (UVSQ), hosts the International Service of Geomagnetic Indices (ISGI), which provides data products derived from magnetic observatory data. The BCMT currently operates a network of 18 observatories throughout the world (including 8 observatories in cooperation with foreign institutions) and a network of 30 repeat stations in metropolitan France. All BCMT observatories belong to INTERMAGNET (www.intermagnet.org), the global network of magnetic observatories transmitting their data in near real time and fulfilling high quality standards. In addition, the BCMT develops, builds and calibrates its own lines of vector and scalar magnetometers (Figure 1), providing significant flexibility to its variations of the Earth's magnetic field having time scales from a few seconds to several decades [Matzka et al., 2010]

Over the time interval 2007-2011, the BCMT has made the following strides: New magnetometers and data acquisition systems were developed in order to acquire data every second [Chulliat et al., 2009], as opposed to every minute which was the previous international standard. New 1 Hz systems were installed in 13 observatories (as of February 2011), thus providing new data for investigations of rapid geomagnetic variations (such as geomagnetic pulsations, tsunami generated magnetic fields, etc.) Two new INTERMAGNET-type observatories were installed in challenging locations, one in Easter Island (Chile) [Chulliat et al., 2009, Manoj et al., 2011] and the other one in Dome C (Antarctica) [Schott and Rasson, 2007, Chambodut et al., 2009, Chambodut and Schott, 2010]. Forty years of data from the Parc St Maur and Val Joyeux observatories, covering the period 1883-1922, were digitized from yearbooks, quality-controlled and distributed on the internet [Fouassier and Chulliat, 2007, 2009]. The World Monthly Means Database maintained by IPGP was upgraded [Chulliat and Telali, 2007]. Data processing procedures were upgraded [Schott and Linthe, 2007, Truong et al., 2009] and so-called quasi-definitive data are now available in one month time delay (Figure 2) [Peltier and Chulliat, 2010]. This new data product, recently endorsed by INTERMAGNET and IAGA, has been used to validate IGRF-11 candidate models [Chulliat and Thebault, 2010] and will be used during the upcoming ESA Swarm mission.

Marine measurements

Instrumental developments have been carried out in deep-sea magnetometry, with the design and operations of a deep-tow scalar magnetometer and a vector magnetometer attached to deep-sea vehicles such as manned sub-

Figure 1: The IPGP VM391 tri-axis fluxgate magnetometer.

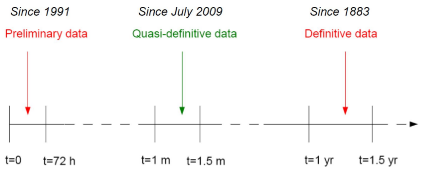

Figure 2: Latencies of the BCMT data products.

mersible, remotely operated vehicles (ROV), or autonomous underwater vehicles (AUV). A long, high-resolution magnetic profile across the whole Cretaceous Quiet Zone in the Central Atlantic Ocean off Africa has been collected by the deep-tow magnetometer and reveals variations in the geomagnetic regime during this 35 My period of constant polarity [Dyment et al., 2009]. Magnetic profiles acquired on the seafloor by deep-sea submersible Nautile have provided important constraints on the structure of slow-spreading ridge segment [Honsho et al., 2009] and on the detailed age of the seafloor, allowing a fine description of magmatic processes [Cordier et al., 2010]. Detailed magnetic and topographic surveys have been achieved by ROV Victor on several hydrothermal sites with ultramafic basement. Unlike the sites lying on basalt, associated to magnetic lows due to the alteration of basalt titanomagnetite to titanomaghemite and non-magnetic minerals, the sites lying on serpentinite exhibit a magnetic high due to the formation of magnetite as part of the serpentinisation process and its conservation in a reducing environment [Tivey and Dyment, 2010]. This result will help to detect and characterized potential mineral resources associated to inactive hydrothermal sites on the seafloor.

Satellite measurements

France has also taken a very active role in the development of Low Earth Orbit (LEO) space magnetometry over the past decade, even more so over the past four years. It contributed to the two very successful Danish Oersted and German Champ missions, both of which carried OVH absolute scalar magnetometers built by CEA/LETI (and provided by CNES, in the case of Oersted). These missions provided a wealth of high quality data until very recently, well beyond the nominal lifetime of both these missions (Champ re-entered the atmosphere on September 19, 2011, after more than ten years of good and faithful service, Oersted is still in orbit). These remarkable data have allowed much progress in our ability to identify and recover the various types of magnetic signals [Hulot et al., 2007], particularly those of internal origin: the main field and its secular variation [Gillet et al., 2010], and the field of lithospheric origin [Thébault et al., 2010]. But these missions also revealed the limits of single satellite magnetometry missions and the need for more advanced concepts [Olsen et al., 2010]. Such an advanced concept, SWARM, was selected by ESA as the fifth Earth Explorer Mission in 2004, following a joint proposal by DNSC (now DTU) in Denmark, GFZ in Germany and IPGP in France [Friis-Christensen et al., 2006, 2009].

The SWARM mission is to involve two satellites orbiting side by side (Fig. 3) on a low polar orbit to measure the East-West gradient of the magnetic field, and a third satellite to be launched (with the same launcher) at a slightly higher altitude. The orbital plane of this third spacecraft will progressively shift with respect to the orbital plane of the lower spacecraft pair, to provide data at different local times [see e.g. Olsen et al., 2010, for a full justification of this constellation configuration]. It will carry similar but more advanced instruments as the Champ mission. In particular, the absolute scalar magnetometers, again built by CEA/LETI, provided by CNES as a Customer Furnished Instrument under the scientific responsibility of IPGP, is now a latest generation Helium 4 optical pumping absolute magnetometer. It will make it possible to reach an accuracy of 0.3 nT. The French scientific community has been very active in both the technical and scientific preparation of this mission, which is now due to be launched in the summer of 2012 for a nominal lifetime of five years.

SWARM will provide both so-called level 1b data

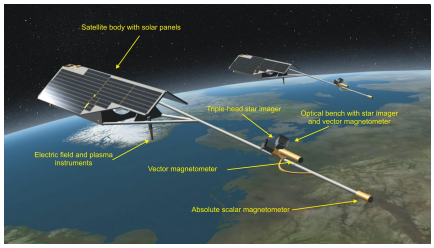

Figure 3: Two (out of three) Swarm satellites.

(calibrated 1Hz and 50 Hz vector and scalar field values from each satellite) and level 2 products, such as core field, lithospheric field and ionospheric field models, but also local estimates of ionospheric parameters such as the Eastward Electrical Field that drives much of the ionosphere's equatorial dynamics. These level 2 products will be prepared by IPGP and several other institutions within an international consortium led by DTU in Denmark. Both level 1b data and level 2 products will be made freely available by ESA to the scientific community and are expected to considerably enhance our knowledge of the various sources of the Earth's magnetic field.

The perspective of the SWARM mission has also prompted much related scientific development in geomagnetism (for a recent review see e.g. [Hulot et al., 2010, 2011, and references therein], in particular investigations of short timescale dynamics [Finlay et al., 2010], initiation of data assimilation techniques in geomagnetism [Fournier et al., 2010], and the construction of maps of the lithospheric field by merging satellite, airborne, marine and ground-based magnetic data [Hemant et al., 2007]. All these areas of research are expected to considerably benefit from the future SWARM data.

References

A. Chambodut and J.-J. Schott. Current status of permanent magnetic observatories in French Austral and Antarctic Territories. volume Proceedings of i-DUST (Inter-Disciplinary Underground Science and Technology Conference, pages 15–26, 2010.

A. Chambodut, D. Di Mauro, J.-J. Schott, P. Bordais, L. Agnoletto, and P. di Felice. Three years of continuous record of the Earth s magnetic field at Concordia station (Dome C, Antarctica). *Ann. Geophys.*, 52:15–26, 2009.

A. Chulliat and K. Telali. World monthly means database project. In J. Reda, editor, *Proc. of the XIIth IAGA Workshop on Geomagnetic Observatory Instruments, Data Acquisition and Processing*, volume C-99 of *Publs. Inst. Geophys. Pol. Acad. Sc.*, pages 268–274, 2007. 19-24 June 2006, Belsk, Poland.

A. Chulliat and E. Thebault. Testing IGRF-11 candidate models against CHAMP data and quasi-definitive observatory data. *Earth Planets Space*, 62:805–814, 2010. doi: 10.5047/eps.2010.06.004.

A. Chulliat, J. Savary, K. Telela, and X. Lalanne. Acquisition of 1-second data in ipgp magnetic observatories. volume Proceedings of the XIIth IAGA Workshop on geomagnetic observatory instruments, data acquisition and processing. U.S. Geological Survey, 2009. Open-File Report 2009-1226.

C. Cordier, M. Benoit, C. Hemond, J. Dyment, B. Le Gall, A. Briais, and M. Kitazawa. Distribution of lava compositions across a ridge axis reveals timescales of melt extraction. *Geochem., Geophys., Geosyst.*, 11, 2010. doi: 10.1029/2010GC003074.

J. Dyment, Y. Gallet, E. Hoise, and The Magofond 08 scientific party. First complete high-resolution record of the Cretaceous Normal Superchron. *AGU Fall Meeting Abstracts*, 2009.

C. C. Finlay, M. Dumberry, A. Chulliat, and M. Pais. Short timescale core dynamics: theory and observations. *Space Sci. Rev.*, 155, 2010. doi: 10.1007/s11214-010-9691-6.

D. Fouassier and A. Chulliat. The new BCMT magnetic database. In J. Reda, editor, *Proc. of the XIIth IAGA Workshop on Geomagnetic Observatory Instruments, Data Acquisition and Processing*, volume C-99, pages 128–134, 2007.

D. Fouassier and A. Chulliat. Extending backwards to 1883 the french magnetic hourly data series. volume Proceedings of the XIIIth IAGA Workshop on geomagnetic observatory instruments, data acquisition and processing. U.S. Geological Survey, 2009. Open-File Report 2009-1226.

A. Fournier, G. Hulot, D. Jault, W. Kuang, A. Tangborn, N. Gillet, E. Canet, J. Aubert, and F. Lhuillier. An Introduction to Data Assimilation and Predictability in Geomagnetism.

Space Sci. Rev., 155(1-4):247–291, 2010. doi: 10.1007/s11214-010-9669-4.

E. Friis-Christensen, H. Lühr, and G. Hulot. A constellation to study the Earth's magnetic field. *Earth Planets Space*, 58:351–358, 2006.

E. Friis-Christensen, H. Lühr, G. Hulot, R. Haagmans, and M. E. Purucker. Past as Prologue: SWARM and the Decade of Geopotential Research. *EOS, Trans. Amer. Geophys. Union*, 90, 2009. doi: 10.1029/2009EO250002.

N. Gillet, V. Lesur, and N. Olsen. Geomagnetic Core Field Secular Variation Models. *Space Sci. Rev.*, 155:129–145, 2010. doi: 10.1007/s11214-009-9586-6.

K. Hemant, E. Thébault, M. Mandea, D. Ravat, and S. Maus. Magnetic anomaly map of the world: merging satellite, airborne, marine and ground-based magnetic data sets. *Earth Planet. Sci. Lett.*, 260, 2007. doi: 10.1016/j.epsl.2007.05.040.

C. Honsho, J. Dyment, K. Tamaki, M. Ravilly, H. Horen, and P. Gente. Magnetic structure of a slow-spreading ridge segment: insights from near-bottom magnetic measurements onboard a submersible. *J. Geophys. Res.*, 114, 2009. doi: 10.1029/2008JB0059151.

G. Hulot, N. Olsen, and T. J. Sabaka. The present field. In M. Kono, editor, *Treatise on Geophysics*, volume 5, Geomagnetism, pages 33–75. Elsevier, Amsterdam, The Netherlands, 2007.

G. Hulot, A. Balogh, U. R. Christensen, C. G. Constable, M. Mandea, and N. Olsen. The Earth's Magnetic Field in the Space Age: An Introduction to Terrestrial Magnetism. *Space Sci. Rev.*, 155:1–7, 2010. doi: 10.1007/s11214-010-9703-6.

G. Hulot, A. Balogh, U. R. Christensen, C. G. Constable, M. Mandea, and N. Olsen. *Terrestrial Magnetism*, volume 36. Space Science Series of ISSI, 2011.

C. Manoj, S. Maus, and A. Chulliat. Observation of magnetic fields generated by tsunamis. *EOS, Trans. Amer. Geophys. Union*, 92:13–14, 2011.

J. Matzka, A. Chulliat, M. Mandea, C. Finlay, and E. Qamili. Geomagnetic observations for main field studies: from ground to space. *Space Sci. Rev.*, 155, 2010. doi: 10.1007/s11214-010-9693-4.

N. Olsen, G. Hulot, and T. J. Sabaka. Measuring the Earth's Magnetic Field from Space: Concepts of Past, Present and Future Missions. *Space Sci. Rev.*, 155:65–93, 2010. doi: 10.1007/s11214-010-9676-5.

A. Peltier and A. Chulliat. On the feasibility of promptly producing quasi-definitive magnetic observatory data. *Earth Planets Space*, 62, 2010. doi: 10.5047/eps.2010.02.002.

J. J. Schott and J. Linthe. The hourly mean computation problem revisited. In J. Reda, editor, *Proc. of the XIIth IAGA Workshop on Geomagnetic Observatory Instruments, Data Acquisition and Processing*, volume C-99, pages 135–143, 2007.

J. J. Schott and J. Rasson. Magnetic observatories in antarctica. In D. Gubbins and E. Herrero-Bervera, editors, *Enc. Geomag. Paleomag.*. Springer, Netherlands, 2007.

E. Thébault, M. Purucker, K. A. Whaler, B. Langlais, and T. J. Sabaka. The Magnetic Field of the Earthś Lithosphere. *Space Sci. Rev.*, 155, 2010. doi: 10.1007/s11214-010-9667-6.

M. Tivey and J. Dyment. *The magnetic signature of hydrothermal systems in slow spreading environments*, pages 43–66. Diversity of hydrothermal systems on slow spreading ocean ridges, P. Rona, C. Devey, J. Dyment and B. Murton (Eds.), AGU Monograph, 2010.

F. Truong, X. Lalanne, and A. Chulliat. Magis: The information system of ipgp magnetic observatories. volume Proceedings of the XIIIth IAGA Workshop on geomagnetic observatory instruments, data acquisition and processing. U.S. Geological Survey, 2009. Open-File Report 2009-1226.

Processing of Magnetic Field Measurements from Ground to Space

Erwan Thébault (1) and Yoann Quesnel (2)

(1) Institut de Physique du Globe de Paris, Université Paris-Cité, INSU/CNRS, F-75005 Paris
(2) Université Aix Marseille, CEREGE, CNRS, F-13545 Aix En Provence

Abstract Satellite and near-surface measurements are by nature different. Satellites travel at hundreds kilometers altitude and do not detect all details pertaining to the magnetic signal of the crust. However, they allow a global view, provide homogeneous vector and scalar measurements and survey almost the entire Earth, including remote and inhospitable regions. To the contrary, near-surface aeromagnetic and marine data are restricted to regions, are scalar only, but offer views at meters to kilometer resolutions. Reconciling both source of information is essential to study the Earth's magnetic crust but this requires developing very different tools.

One important resolution of the Working Group V-MOD of the International Association of Geomagnetism and Aeronomy is to encourage the production of a World Digital Magnetic Anomaly Map (WDMAP). In this framework, the French community collaborated closely with other international groups. On Earth, magnetic anomalies are defined as the vector, or scalar, differences between the measured magnetic field and an estimate of the main field originating from the core that dominates up to SH degree 13 (Figure 1). Magnetic anomalies, also known as the lithospheric field, are commonly assumed to reflect the magnetic properties of rocks lying in the Earth's crust. Therefore, a product like WDMAM should help to better identify and connect widely separated geological units. The first WDMAM was released during the IUGG meeting in Peruggia in 2007 [Thebault, 2011]. This composite map was built upon measurements from space, airplanes and ships collected during more than 60 years by researchers of all nationalities worldwide.

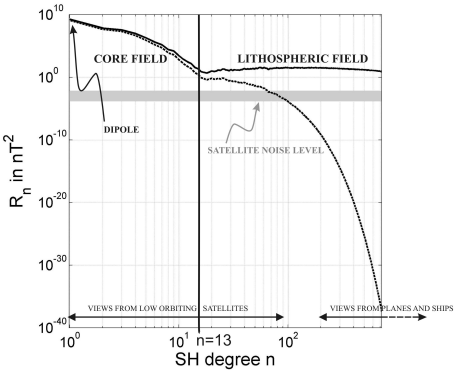

Figure 1: Synthetic view of the crustal field power spectrum at satellite altitude (400-km; dashed line) and aeromagnetic altitude (5-km; solid line). The noise at satellite altitudes does not allow seeing scales smaller than SH degree 100, or so (400-km), while airplanes poorly detect features larger than about 200 -km (SH degree 200, or so). After [Thebault, 2011]

During the last four years, significant efforts were made to improve the first version of the WDMAM at both ends of the magnetic field spectrum and to try filling the spectral gap between large and small scales (SH degree 100 to about 200; Figure 1). The French community was involved in collecting new data. In the oceanic regions, for instance, high resolution magnetic field profiles were recorded over the whole Cretaceous Quiet Zone offshore Africa [Dyment et al., 2009]. In addition, an effort was made to retrieve old aeromagnetic maps over the French territory that are now ready to be digitized. These new data will be included in future versions of the WDMAM map.

Many technical difficulties were faced in the first WDMAM version because of the nature of the considered data. This was further investigated. First, the available raw scalar marine measurements acquired at very different epochs are noisy. A first step consisted in screening 20 millions of GEODAS data and in removing the unrealistic spikes. Then, improved corrections for the diurnal external and the main fields were performed (see Geomagnetic Field Models) to bet-

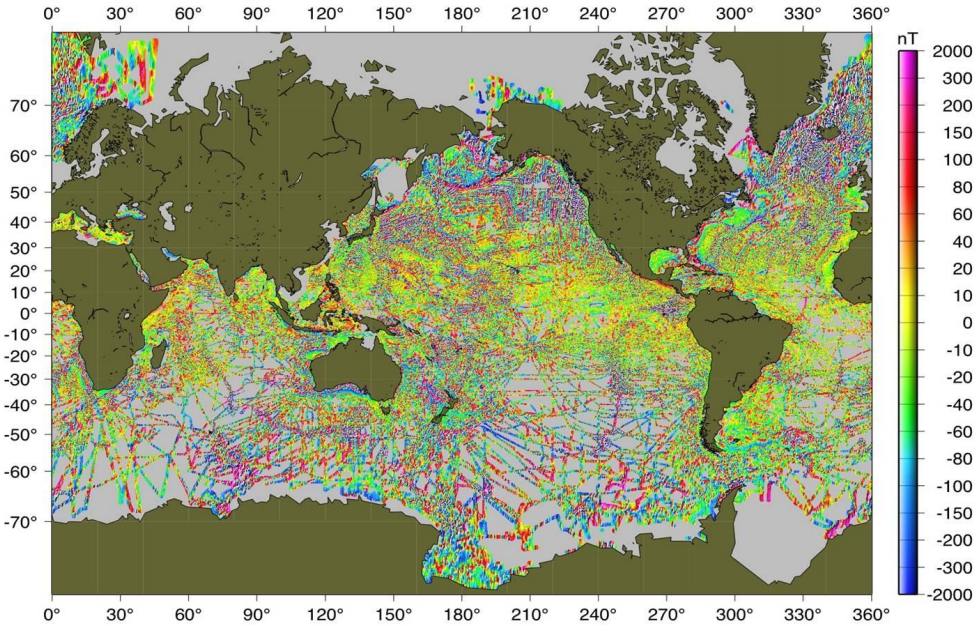

Figure 2: Reprocessed oceanic compilation. After [Quesnel et al., 2009]

ter delineate the structures of the lithospheric field. This work was compiled in a new oceanic world compilation [Quesnel et al., 2009] (Figure 2). Secondly, the CHAMP satellite data were also better processed. It appeared, thanks to the development of high-resolution modelling techniques (see Geomagnetic Field Models) that corrections for the magnetospheric field could introduce artifacts in the satellite based final anomaly maps. These artifacts may be visually distracting when they coincidentally align along oceanic ridges and could lead to wrong geophysical interpretations [Thébault et al., 2011]. It is therefore important to correct for these errors when satellite and near-surface data are merged together in a by-product such as WDMAM. Recognizing the importance of these works, a new tentative map was produced. This was performed outside the official WDMAM project because the new map intends to test prototype techniques of data analysis, such as line levelling, gridding by colocation, and an anisotropic interpolation between sparse marine track lines using a strong prior information concerning the direction of the oceanic chrons based on a model of the age of the oceanic crust [Maus et al., 2009].

References

J. Dyment, Y. Gallet, E. Hoise, and The Magofond 08 scientific party. First complete high-resolution record of the Cretaceous Normal Superchron. *AGU Fall Meeting Abstracts*, 2009.

S. Maus, U. Barckhausen, H. Berkenbosch, N. Bournas, J. Brozena, V. Childers, F. Dostaler, J. D. Fairhead, C. Finn, R. R. B. von Frese, C. Gaina, S. Golynsky, R. Kucks, H. Lühr, P. Milligan, S. Mogren, R. D. Müller, O. Olesen, M. Pilkington, R. Saltus, B. Schreckenberger, E. Thébault, and F. Caratori Tontini. EMAG2: A 2 arc min resolution Earth Magnetic Anomaly Grid compiled from satellite, airborne, and marine magnetic measurements. *Geochem., Geophys., Geosyst.*, 10, 2009. doi: 10.1029/2009GC002471.

Y. Quesnel, M. Catalán, and T. Ishihara. A new global marine magnetic anomaly data set. *J. Geophys. Res.*, 114, 2009. doi: 10.1029/2008JB006144.

E. Thebault. Magnetic anomalies, interpretation. In H. Gupta, editor, *Encyclopedia of Solid Earth Geophysics*. Springer, Netherlands, 2011.

E. Thébault, F. Vervelidou, V. Lesur, and M. Hamoudi. The shortcomings of the along-track satellite filtering in planetary magnetism. *Submitted*, 2011.

Geomagnetic Field Models

Erwan Thébault

Institut de Physique du Globe de Paris, Université Paris-Cité, INSU/CNRS, F-75005 Paris

Abstract Magnetic field measurements are not available everywhere on Earth. Therefore, mathematical tools must be applied and developed to estimate the field outside the dominion of data. Measurements are traditionally carried out on the Earth's surface but the availability of satellite data during the last decade allowed stupendous progresses in predicting the geomagnetic field anywhere between ground and space altitudes. Modeling the geomagnetic field is important for practical and scientific applications. It is an essential tool for aeronautic navigation, resource exploration, and fundamental research related to the dynamics of the Earth's core.

The Earth's magnetic field is traditionally represented in Spherical Harmonics when data are available worldwide. Every five years, an international team of scientists produces and releases an International Geomagnetic Reference Field model (IGRF). This activity is supervised by the working group V-MOD of the International Association of Geomagnetism and Aeronomy (IAGA). The aim of this working group is to promote and coordinate international efforts to model the main geomagnetic field and its secular variation. The French community has been significantly involved in deriving the 11 th generation of IGRF models [Finlay et al., 2010]. The complete process took about a year. After submission of two French candidate models [Chambodut et al., 2010, Thebault et al., 2010] (Figure 1), and models in collaborations with other teams [Olsen et al., 2010], a phase of evaluation and validation was completed [Finlay et al., 2010]. The IGRF model was released in January 2010 in a special issue published in the journal Earth Planets and Space.

During the construction of the IGRF candidate models interesting methodological and geophysical researches were conducted. For instance, comparisons between main geomagnetic field models developed during the previous decade [Gillet et al., 2010] showed how both the information contained in the data, particularly the satellite ones, and the a priori constraints introduced by their modeling could result in artificial geomagnetic spatial and time variations. Keeping in mind these limitations, independent observatory data were used to assess the occurrence of a pulse of geomagnetic field acceleration around 2006 that could be responsible of two geomagnetic jerks observed around 2003 and 2007 [Chulliat et al., 2010]. This core field acceleration pulse might be the relevant phenomenon to be investigated from the point of view of rapid core dynamics rather than the jerks (see Numerical Dynamo Modelling). Theoretical studies were also carried out in order to estimate the extent to which the secular variation could be predicted in space and forward in time. It was concluded that the minimum spatial resolution achievable for the secular variation is estimated to be about 1800 -km at the Earth's surface [Hulot et al., 2009], which confirms the need in the near future to develop alternative strategies to infer the physical properties of the Earth's core at higher resolutions using, in particular, the framework of data assimilation (see Geomagnetic Data Assimilation).

The derivation of main field models like IGRF is also of utmost importance for correcting the data for a main field in order to highlight the permanent structures of the Earth's lithospheric field that are poorly detected from space [Thébault et al., 2010] but almost invisible in near-surface data because of their poor lateral extent. After dedicated processing and the merging satellite and ground based data, it was possible to produce an integrated picture of the magnetic field contribution of the Earth's crust at 5-km altitude (see Processing the satellite and near-surface data for geomagnetic field models). The problem of reconciling surface, near-surface, and satellite measurements at high spatial resolution in Spherical Harmonics is a long standing problem because of computational burden and uneven data distribution. The French community has contributed to develop very specific tools to address these problems using local functions like wavelets, spherical caps, etc. (see Schott

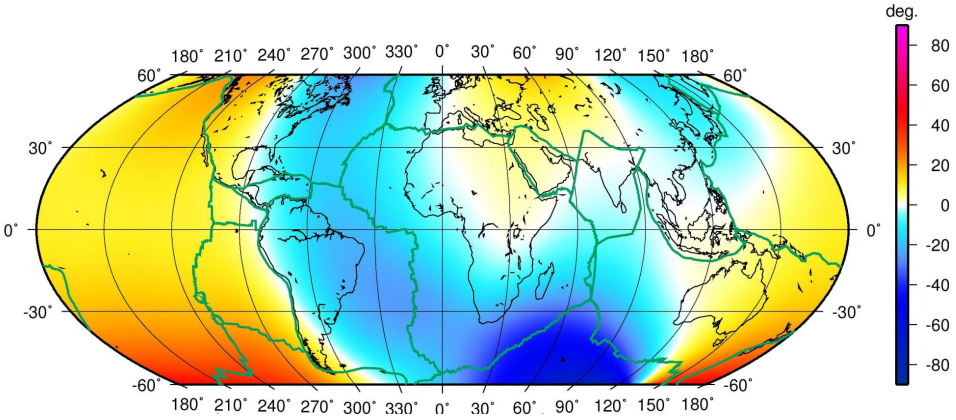

Figure 1: Declination map in 2010.0 at the Earth's mean radius and mid-latitudes derived from a french candidate model to the 11th generation of IGRF Thebault et al. [2010]

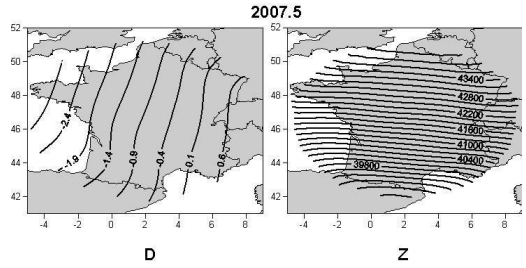

Figure 2: The declination (D in degrees) and vertical (Z in nT) components of the magnetic field in France in 2007.5 [Thébault, 2008]

and Thebault [2011] for a review). For instance, a technique based on Spherical Cap Harmonic Analysis was specifically developed to model the Earth's magnetic field variations in France over 40 years [Thébault, 2008] (Figure 2). When the problem arises from the amount of available data, but at global scales, local expansion may be derived to speed up the computational process and to perform data compression [Minchev et al., 2009].

References

A. Chambodut, B. Langlais, M. Menvielle, E. Thebault, A. Chulliat, and G. Hulot. Candidate models for the IGRF-11th generation making use of extrapolated observatory data. *Earth Planets Space*, 62:745–751, 2010. doi: 10.5047/eps.2010.06.006.

A. Chulliat, E. Thebault, and G. Hulot. Core field acceleration pulse as a common cause of the 2003 and 2007 geomagnetic jerks. *Geophys. Res. Lett.*, 37, 2010. doi: 10.1029/2009GL042019.

C. C. Finlay, S. Maus, C. D. Beggan, M. Hamoudi, F. J. Lowes, N. Olsen, and E. Thebault. Evaluation of candidate geomagnetic field models for IGRF-11. *Earth Planets Space*, 62:787–804, 2010. doi: 10.5047/eps.2010.11.005.

C. C. Finlay, S. Maus, C. D. Beggan, T. N. Bondar, A. Chambodut, T. A. Chernova, A. Chulliat, V. P. Golovkov, B. Hamilton, M. Hamoudi, R. Holme, G. Hulot, W. Kuang, B. Langlais, V. Lesur, F. J. Lowes, H. Luehr, S. Macmillan, M. Mandea, S. McLean, C. Manoj, M. Menvielle, I. Michaelis, N. Olsen, J. Rauberg, M. Rother, T. J. Sabaka, A. Tangborn, L. Toffner-Clausen, E. Thebault, A. W. P. Thomson, I. Wardinski, Z. Wei, and T. I. Zvereva. International Geomagnetic Reference Field: the eleventh generation. *Geophys. J. Int.*, 183(3):1216–1230, 2010. doi: 10.1111/j.1365-246X.2010.04804.x.

N. Gillet, V. Lesur, and N. Olsen. Geomagnetic Core Field Secular Variation Models. *Space Sci. Rev.*, 155:129–145, 2010. doi: 10.1007/s11214-009-9586-6.

G. Hulot, N. Olsen, E. Thébault, and K. Hemant. Crustal concealing of small scale core field secular variation. *Geophys. J. Int.*, 177, 2009. doi: 10.1111/j.1365-246X.2009.04119.x.

B. Minchev, A. Chambodut, M. Holschneider, I. Panet, E. Schoell, M. Mandea, and G. Ramillien. Local multi-polar expansions in potential field modeling. *Earth Planets Space*, 61:1127–1141, 2009.

N. Olsen, M. Mandea, T. Sabaka., and L. Tøffner-Clausen. The CHAOS-3 geomagnetic field model and candidates for the 11th generation IGRF. *Earth Planets Space*, 62:719–727, 2010. doi: 10.5047/eps.2010.07.003.

J. J. Schott and E. Thebault. *Geomagnetic Observations and Models*, volume 5, chapter Modelling the earth's magnetic field from global to regional scales, pages 229–264. IAGA Book Series, 2011.

E. Thébault. A proposal for regional modelling at the Earth's surface, R-SCHA2D. *Geophys. J. Int.*, 174, 2008. doi: 10.1111/j.1365-246X.2008.03823.x.

E. Thebault, S. Maus, A. Chulliat, G. Hulot, B. Langlais, A. Chambodut, and M. Menvielle. IGRF candidate models at times of rapid changes in core field acceleration. *Earth Planets Space*, 62:753–763, 2010. doi: 10.5047/eps.2010.05.004.

E. Thébault, M. Purucker, K. A. Whaler, B. Langlais, and T. J. Sabaka. The Magnetic Field of the Earthś Lithosphere. *Space Sci. Rev.*, 155, 2010. doi: 10.1007/s11214-010-9667-6.

Geomagnetic Data Assimilation

Alexandre Fournier

Institut de Physique du Globe de Paris, Sorbonne Paris Cité, Univ. Paris Diderot, INSU/CNRS, F-75005 Paris

Abstract Geomagnetic data assimilation aims at combining the information contained in present and past measurements of the Earth's magnetic field with the information contained in numerical models describing the dynamics of the Earth's core, where the main geomagnetic field is generated and sustained by means of a dynamo process. It aims at bringing new constraints on the physical processes occurring in the core responsible for the geomagnetic secular variation, in light of the available data. (Note that we are only interested in this short review with the secular variation whose origin is rooted in the core, and which occurs on interannual to millenial time scales.) In addition to the fundamental issues that such an approach could help address, it could have more practical applications, regarding for instance the design of geomagnetic field models in which the time-dependency would need not be parameterized or approximated as currently done, since it would be controlled by the numerical model. This field has recently come to the fore in geomagnetism for two main reasons: 1) the continuous increase in quality and size of the databases of geomagnetic measurements on the recent, historical, and archeomagnetic time scales and 2) our increased ability to model numerically Earth's core dynamics. It is a young field, and most studies published during the past few years are concerned with the feasibility of applying techniques routinely used in the fields of meteorology, climate dynamics or physical oceanography to the field of terrestrial magnetism. During the past year the first geophysical applications of geomagnetic data assimilation appeared. They are very encouraging and indicate that the field will continue to develop in the years to come. This development will hopefully trigger fruitful collaborations between observers and theoreticians of the geomagnetic field.

The principle of data assimilation is illustrated in Fig. 1. Starting from an unconstrained model trajectory, data assimilation aims at correcting the trajectory in order to provide an optimal fit to the available observations (the stars), given their error bars. This is an inverse problem set in a dynamical context, for which time t is a variable.

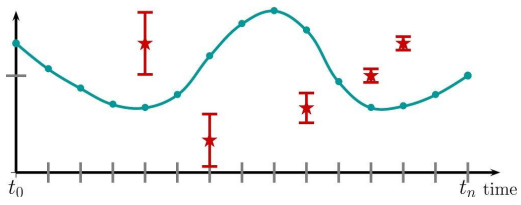

Figure 1: Assimilation starts with an unconstrained model trajectory over the time window of interest. It aims at correcting this initial model trajectory in order to provide an optimal fit to the available observations (the stars), given their error bars. Adapted from Fournier et al. [2010].

In geomagnetism, early studies have focused on the feasibility of implementing data assimilation algorithms to the problem of the geomagnetic secular variation, by analyzing the response and behavior of the assimilating system in a well-controlled environment, using databases of synthetic observations, starting from one-dimensional toy models [Fournier et al., 2007, Sun et al., 2007], and moving on to systems of higher complexity [Liu et al., 2007, Kuang et al., 2008, Canet et al., 2009]. Those studies are generically referred to in the literature as "observing system simulations experiments" (OSSEs), or, equivalently, "twin experiments". More recent applications have considered "level-2" observations (geomagnetic field models coefficients, also known as Gauss coefficients), thereby permitting to make some inference on the state of the core [Kuang et al., 2009]. The approaches followed nowadays, reviewed in Fournier et al. [2010], differ by the choice of the physical and numerical model employed to describe core dynamics, and the form of assimilation they resort to (sequential or variational, see Fig. 2 for an illustration). Let us stress that specific to the core problem is the remote, blurred and incomplete observation of its state. Accordingly, we lack a well-defined background state (the equivalent of a "climatological" mean), about which the dynamics of the secular variation is

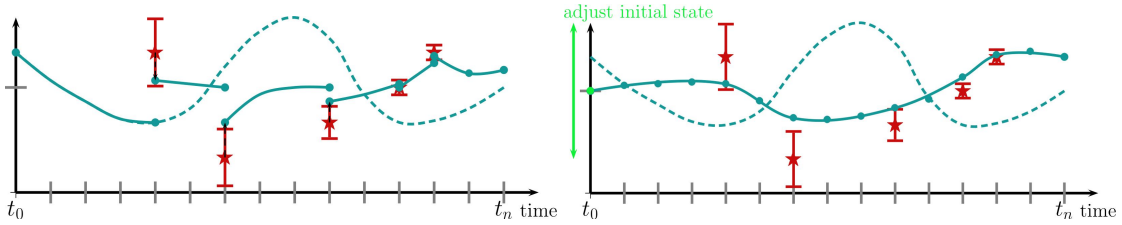

Figure 2: Left: The sequential approach to data assimilation. Starting from the initial time, the model trajectory follows the initial forecast. As soon as the first observation is available, the analysis is performed. The same cycle is repeated anytime an observation is available, with the assimilated trajectory deviating from the initial guess (the dashed line). Right: the variational approach to data assimilation. After adjustment of the initial condition (the green bullet on the t=t0 axis) by means of an iterative minimization algorithm, the model trajectory is corrected over the entire time window, in order to provide an optimal fit to the data (in a generalized least squares sense). The dashed line corresponds to the initial (unconstrained) guess of the model trajectory introduced in Fig. 1.

likely to take place, even though we have a fairly good idea of the large to medium length scales of the poloidal field at the top of the core over a 400 year period, and for the largest scales much longer back in time (e.g. Hulot et al. [2010]).

All the preliminary results obtained so far show that, in the assimilation framework, surface measurements of the radial component of the field at the core surface can provide some information and constraints about the structure of the field and the flow within the core. The propagation of the information (the innovation) from the core-mantle boundary to the bulk of the core is achieved either through the non-linear interactions between the dynamical actors (the various components of the state vector, which include the poloidal field), when operating with a three-dimensional (3D) model of the geodynamo, or by some a priori constraint imposed on the nature of the dynamics (under the quasi-geostrophic assumption, the invariance of the flow in the direction of rotation). This propagation can also be made more effective through the use of a background error covariance matrix coupling effectively the surface of the core with its interior.

The last year has witnessed the first geophysical applications of geomagnetic data assimilation techniques. Using geomagnetic field models spanning the past 7,000 years as observations and an iterative predictor-corrector time scheme to reduce model errors, Kuang et al. [2010] contributed to the 2010 release of the IGRF (for the secular variation); Beggan and Whaler [2010] also contributed to the same IGRF. They predict the evolution of the geomagnetic field over the next 5 years, their secular variation being based on an ensemble of steady core flows.

On a more fundamental level, Gillet et al. [2010]

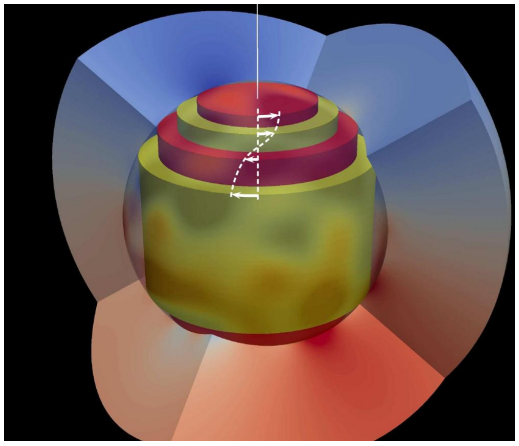

Figure 3: Sketch illustrating the propagation of torsional Alfvén waves in the Earth's core interior.

were able to estimate the strength of the magnetic field in the core interior (on the order of 4 mT). This represents the first application of variational data assimilation to geomagnetism. That study uses time series of core flow streamfunctions calculated with the quasi-geostrophic assumption. A recurring signal of period about 6 years was detected in the time series for the zonal flow. It can be interpreted as the result of Alfvén waves propagating in the fluid outer core. These special AlfvÃľn waves consist in the motion of nested cylinders aligned with the rotation axis and linked by the magnetic field that threads them (see Figure 3); the stronger the field, the faster the wave. This promising study reconciles observations and theoretical estimates of the strength of the field based on scaling laws [Christensen and Aubert, 2006]. It also leaves many questions unanswered. These will likely be addressed in the years to come within the frame-

work of data assimilation.

References

C. Beggan and K. Whaler. Forecasting secular variation using core flows. *Earth Planets Space*, 62, 2010. doi: 10.5047/eps.2010.07.004.

E. Canet, A. Fournier, and D. Jault. Forward and adjoint quasi-geostrophic models of the geomagnetic secular variation. *J. Geophys. Res.*, 114, 2009. doi: 10.1029/2008JB006189.

U. R. Christensen and J. Aubert. Scaling properties of convection-driven dynamos in rotating spherical shells and application to planetary magnetic fields. *Geophys. J. Int.*, 166:97–114, 2006.

A. Fournier, C. Eymin, and T. Alboussière. A case for variational geomagnetic data assimilation: Insights from a one-dimensional, nonlinear, and sparsely observed mhd system. *Nonlin. Proc. Geophy*, 14, 2007. doi: 10.5194/npg-14-163-2007.

A. Fournier, G. Hulot, D. Jault, W. Kuang, A. Tangborn, N. Gillet, E. Canet, J. Aubert, and F. Lhuillier. An Introduction to Data Assimilation and Predictability in Geomagnetism. *Space Sci. Rev.*, 155(1-4):247–291, 2010. doi: 10.1007/s11214-010-9669-4.

N. Gillet, D. Jault, E. Canet, and A. Fournier. Fast torsional waves and strong magnetic field within the Earth's core. *Nature*, 465:74–77, 2010. doi: 10.1038/nature09010.

G. Hulot, C. C. Finlay, C. G. Constable, N. Olsen, and M. Mandea. The Magnetic Field of Planet Earth. *Space Sci. Rev.*, 152:159–222, 2010. doi: 10.1007/s11214-010-9644-0.

W. Kuang, A. Tangborn, W. Jiang, D. Liu, Z. Sun, J. Bloxham, Z. Wei, Z. , R. Holme, and A. Tangborn. Mosst_das: the first generation geomagnetic data assimilation framework. *Commu. Comp. Phys.*, 3, 2008.

W. Kuang, A. Tangborn, Z. Wei, and T. Sabaka. Constraining a numerical geodynamo model with 100 years of surface observations. *Geophys. J. Int.*, 179, 2009. doi: 10.1111/j.1365-246X.2009.04376.x.

W. Kuang, Z. Wei, R. Holme, and A. Tangborn. Prediction of geomagnetic field with data assimilation: a candidate secular variation model for igrf-11. *Earth Planets Space*, 62, 2010. doi: 10.5047/eps.2010.07.008.

D. Liu, A. Tangborn, and W. Kuang. Observing system simulation experiments in geomagnetic data assimilation. *J. Geophys. Res.*, 112, 2007. doi: 10.1029/2006JB004691.

Z. Sun, A. Tangborn, and W. Kuang. Data assimilation in a sparsely observed one-dimensional modeled mhd system. *Nonlin. Proc. Geophy*, 14, 2007.

Numerical Dynamo Models

Hagay Amit

Univrsité de Nantes and CNRS, Laboratoire de Planétologie et Géodynamique de Nantes, 44322 Nantes cedex 3

Abstract Studies of numerical dynamo models by researchers in France in the period 2006-2010 focused on (a) scaling laws and extrapolations of model results to the planets, (b) core-mantle thermal interactions and their impact on the dynamo, (c) dipole polarity reversals, and (d) short-term secular variation (SV) with implications to core flow inversions. Other studies include Earth-like field morphology, inner core super-rotation, dynamo predictability time, dynamos generated by shear flows and inner core size affecting stellar or planetary dynamo behavior. Here we briefly note these studies.

Numerical dynamos operate in a parameter regime very far from Earth's core (due to computational limitations), so any inference to the geodynamo is questionable. Extrapolations of scaling laws may bridge the models and the Earth. Christensen and Aubert [2006] used a large data base of dynamo models to derive scaling laws based on a buoyancy-flux Rayleigh number independent of any diffusivities. They found that inertial effects define the transition between dipole-dominated non-reversing to multipolar reversing dynamos. The magnetic field strength is controlled by the buoyancy flux. They also predicted a slow inner core growth rate and a relatively old inner core. Aubert et al. [2009] combined numerical dynamos with varying inner core sizes and different convective styles with thermal history models to expand the scaling laws to early Earth conditions. They argued that a thermally-driven dynamo acting prior to the inner core could produce a dipole moment comparable to today's field. They predicted that the early Earth field reversed less frequently due to lower convective power.

Non-axisymmetric geodynamo observations suggest that the heterogeneous mantle affects the dynamics in Earth's core. Aubert et al. [2007] used numerical dynamos with heterogeneous core-mantle boundary (CMB) heat flux to study mantle control on the dynamo. They compared long-term time-average flow below the CMB with intermediate averages corresponding to the length of available geomagnetic data. The statistically significant correlation between the intermediate and long-term flows suggests that a signature of the mantle heterogeneity on time-average core flows inverted from the historical geomagnetic SV is expected. Aubert et al. [2008a] demonstrated that the steady part of a numerical dynamo model with tomographic CMB heat flux pattern inferred from a lower mantle seismic tomography recovers important features of geophysical observations, including the locations of high-latitude paleomagnetic flux patches, large cyclones in the time-average core flow from geomagnetic SV, and hemispheric seismic anomalies in the upper inner core. The mantle heterogeneity is coupled to the inner core via columnar convection that concentrates magnetic flux at high-latitudes of the CMB and extracts anomalous buoyancy flux from the inner-core boundary (ICB) at the same longitude on the equatorial plane. Amit and Choblet [2009] examined different interpretations of lower mantle seismic shear velocities in terms of thermal and post-Perovskite origins. Comparing their numerical dynamo time-average properties to geophysical observations, they found that accounting for post-Perovskite in the lower mantle tomography may generally improve the agreement. They also proposed that quasi-axial convective rolls may reconcile dominant rotational effects and deviations from equatorial symmetry in the CMB heat flux prescribed by the lower mantle. Amit et al. [2010] used tomographic numerical dynamos and a tracking algorithm to study the time-dependence of the robust high-latitude intense magnetic flux patches. They found that the patches oscillate about preferred locations prescribed by the mantle, with episodic drifts from one location to another. The drift events correspond to azimuthal motions of fluid downwelling structures that concentrate magnetic flux. Their models reconcile the correlation of the patches location in historical and paleomagnetic field

models together with their weaker signature in the paleomagnetic field and their mobility in archeomagnetic field models.

The mechanisms controlling geomagnetic polarity reversals are not fully understood. Aubert et al. [2008b] designed a Dynamical Magnetic Fieldlines Imaging (DMFI) algorithm to study reversals in numerical dynamos. They showed that magnetic upwellings originating in the ICB produce reversed flux patches on the CMB that subsequently trigger reversals. Olson et al. [2009] compared two dipole collapse events in a numerical dynamo model, one that reversed and one that did not reverse. They found that prior to the dipole collapse, the ratio of reversed/normal flux contributions to the axial dipole is much larger in the reversing case and may therefore serve as a possible reversal precursor. Application of their criterion to the current geomagnetic dipole decrease suggests that the present field will not reverse. Gissinger et al. [2010] found in numerical dynamos where the viscosity is smaller than the magnetic diffusivity that the reversal can be simplified to the interaction among the axial dipole, the axial quadrupole and a symmetry breaking zonal flow. In their low order system, reversals are triggered by deterministic chaos.

Numerical dynamos may assess the reliability of core flow inversions and improve their quality. Amit et al. [2007] tested their helical-geostrophic core flow inversion method against synthetic SV data generated by numerical dynamos. They found decent agreement between the true dynamo flow and their inverted flow for large-scale dynamos, but deteriorating correlations for smaller scale dynamos. They attributed the discrepancies to magnetic diffusion and data truncation effects. Amit and Christensen [2008] showed in dynamo models a correlation between radial and tangential diffusion contributions to magnetic SV. They extrapolated the ratio of the two diffusive terms to Earth-like conditions and incorporated magnetic diffusion in core flow inversions. They concluded that a thin magnetic boundary layer at the top of the core might cause strong radial diffusion and significant non frozen-flux SV.

The plethora of numerical dynamo models provide different field morphologies which one is most Earth-like? Christensen et al. [2010] defined quantitative criteria for field morphology characterization and ranked the semblance of their large data base of dynamo models to the observed geomagnetic field. They found that Earth-like dynamo models exist all the way from accessible simulations to the geodynamo.

Some seismic observations suggest inner core super-rotation. Aubert and Dumberry [2010]used high-resolution low-viscosity numerical dynamos where the inner core is allowed to differentially rotate with respect to the mantle by viscous and magnetic torques applied by the liquid outer core and gravitational restoring torque exerted by the mantle. They found that time-dependent fluctuations dominate steady drift, and that the observed seismic signal is likely part of a fluctuation.

Assuming complete knowledge of all dynamo variables, how far in time can the field be predicted? Hulot et al. [2010] introduced small perturbations to numerical dynamo models and measured the time until the system deviates from the unperturbed models. They found that this time, i.e. the predictability time of the dynamo, depends on the magnetic Reynolds number. Applying their results to Earth's core, they found one century as the maximum predictability time, precluding the possibility to discover whether the current dipole decrease is a beginning of a reversal or not.

Spherical Couette flows may generate dynamos. Guervilly and Cardin [2010] imposed such mechanical boundary condition on a numerical dynamo. They found that non-axisymmetric flow is required to excite a dynamo. Without global rotation, the critical magnetic Reynolds number is very high. Their study has important implications for MHD laboratory experiments.

The size of the inner core may dramatically alter dynamo action. Goudard and Dormy [2008] compared numerical dynamos with different inner to outer core aspect ratios. They showed that varying the aspect ratio may cause a sharp transition from Earth-like steady dynamos to Sun-like dynamo waves.

References

H. Amit and G. Choblet. Mantle-driven geodynamo features-effects of post-Perovskite phase transition. *Earth Planets Space*, 61(11): 1255–1268, 2009.

H. Amit and U. R. Christensen. Accounting for magnetic diffusion in core flow inversions from geomagnetic secular variation. *Geophys. J. Int.*, 175(3):913–924, 2008. doi: 10.1111/j.1365-246X.2008.03948.x.

H. Amit, J. Aubert, and G. Hulot. Stationary, oscillating or drifting mantle-driven geomagnetic flux patches? *J. Geophys. Res.*, 115, JUL 27 2010. doi: 10.1029/2009JB006542.

H. Amit, P. Olson, and U. Christensen. Tests of core flow imaging methods with numerical dynamos. *Geophys. J. Int.*, 168(1):27–39, 2007. doi: 10.1111/j.1365-246X.2006.03175.x.

J. Aubert and M. Dumberry. Steady and fluctuating inner core rotation in numerical geodynamo models. *Geophys. J. Int.*, 184:162–170, 2010.

J. Aubert, H. Amit, and G. Hulot. Detecting thermal boundary control in surface flows from numerical dynamos. *Phys. Earth Planet. Int.*, 160(2):143–156, 2007. doi: 10.1016/j.pepi.2006.11.003.

J. Aubert, H. Amit, G. Hulot, and P. Olson. Thermochemical flows couple the Earth's inner core growth to mantle heterogeneity. *Nature*, 454(7205):758–U80, 2008a. doi: 10.1038/nature07109.

J. Aubert, J. Aurnou, and J. Wicht. The magnetic structure of convection-driven numerical dynamos. *Geophys. J. Int.*, 172:945–956, 2008b.

J. Aubert, S. Labrosse, and C. Poitou. Modelling the paleo-evolution of the geodynamo. *Geophys. J. Int.*, 179:1414–1428, 2009.

U. R. Christensen and J. Aubert. Scaling properties of convection-driven dynamos in rotating spherical shells and application to planetary magnetic fields. *Geophys. J. Int.*, 166:97–114, 2006.

U. R. Christensen, J. Aubert, and G. Hulot. Conditions for Earth-like geodynamo models. *Earth Planet. Sci. Lett.*, 296(3-4):487–496, 2010. doi: 10.1016/j.epsl.2010.06.009.

C. Gissinger, E. Dormy, and S. Fauve. Morphology of field reversals in turbulent dynamos. *Euro. Phys. Lett.*, 90(4), 2010. doi: 10.1209/0295-5075/90/49001.

L. Goudard and E. Dormy. Relations between the dynamo region geometry and the magnetic behavior of stars and planets. *Euro. Phys. Lett.*, 83(4), 2008. doi: 10.1029/0295-5075/83/59001.

C. Guervilly and P. Cardin. Numerical simulations of dynamos generated in spherical Couette flows. *Geophys. Astrophys. Fluid Dyn.*, 104(2-3):221–248, 2010. doi: 10.1080/03091920903550955.

G. Hulot, F. Lhuillier, and J. Aubert. Earth's dynamo limit of predictability. *Geophys. Res. Lett.*, 37, 2010. doi: 10.1029/2009GL041869.

P. Olson, P. Driscoll, and H. Amit. Dipole collapse and reversal precursors in a numerical dynamo. *Phys. Earth Planet. Int.*, 173(1-2):121–140, 2009. doi: 10.1016/j.pepi.2008.11.010.

Laboratory dynamo experiments

Jean-François Pinton

Laboratoire de Physique de l'École Normale Supérieure de Lyon, CNRS & Université de Lyon, F-69364 Lyon, France

Abstract Since the turn of the century, experiments have produced laboratory fluid dynamos which enable a study of the effect in controlled conditions. The most recent one, the VKS experiment, demonstrate the possibility of dynamo generation from turbulent motions and exhibits a rich variety of time dynamics.

Although dynamo research is essentially motivated by observations from planetary and stellar dynamos, the conditions that prevail in such natural objects cannot be reproduced in the laboratory. Experiments and numerics can only be run in quite different parameter regimes, but they both provide useful insights into the features of natural dynamos. Experiments cannot be rotated as fast as real systems do, convective motion cannot be as strong, etc, but they run with real fluids and probe quantities that cannot be accessed from remote observations of natural dynamos.

In order for a dynamo to be self-sustained, the production of induced currents by fluid motions must overcome the resistive Joule dissipation. This condition sets an instability threshold, requiring that the magnetic Reynolds number of the flow ($R_M = UL/\lambda$) exceeds a critical value R_M^c – U and L are characteristic velocity and length and λ is the magnetic diffusivity. Assuming R_M^c values of the order of 10 to 100 (a value often quoted for the Earth), and given the fact that all liquid metals have magnetic Prandtl numbers (ratio of kinetic to magnetic diffusivities) of the order of $P_M \sim 10^{-5}$, one realizes that dynamo flows are associated with huge kinetic Reynolds number values $R_V = R_M/P_M$, typically exceeding 10^6. Such high R_V values are associated with fully developed turbulence, an observation that raises several central issues for dynamo experiments. Turbulence is often synonymous of (a) disordered motions, and (b) strongly diffusive features. In this context, (a) means that the specific motions that favor dynamo action maybe disrupted by the randomness of the flow. In addition, the small magnetic Prandtl number values impose that the Joule resistive scale is very much larger than the hydrodynamic viscous length. It is therefore tempting to perform some kind of sub-scale average

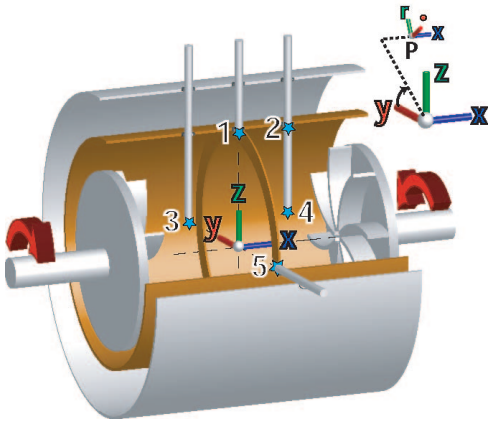

Figure 1: Sketch of the VKS flow configuration. The flow is generated by rotating two impellers 371 mm apart in a thin cylindrical copper vessel, $2R = 412$ mm in inner diameter and 524 mm in length. The impellers are fitted with 8 curved blades of height $h = 41.2$ mm; in most experimental runs, the impellers are rotated so that the blades move in a *non-scooping* direction, defined as the positive direction by arrows. Positions 1 to 5 correspond to points where magnetic measurements have been made, using 3D Hall probes.

of the action of the turbulent velocity field. Then (b) leads to an effective magnetic diffusivity that could be much larger than the molecular value. These considerations have raised doubts on the very existence of fully turbulent dynamos.

One alternative is to engineer flow configurations that will preserve flow patterns which are essential for the dynamo generation. The design of the Riga and Karlsruhe experiments have been made to ensure that the time-averaged flow field resembles laminar flows which are kinematic dynamo solutions [Moreau and Pinton, 2008]. These pioneering studies have validated the principle of a *fluid* dynamo, and have

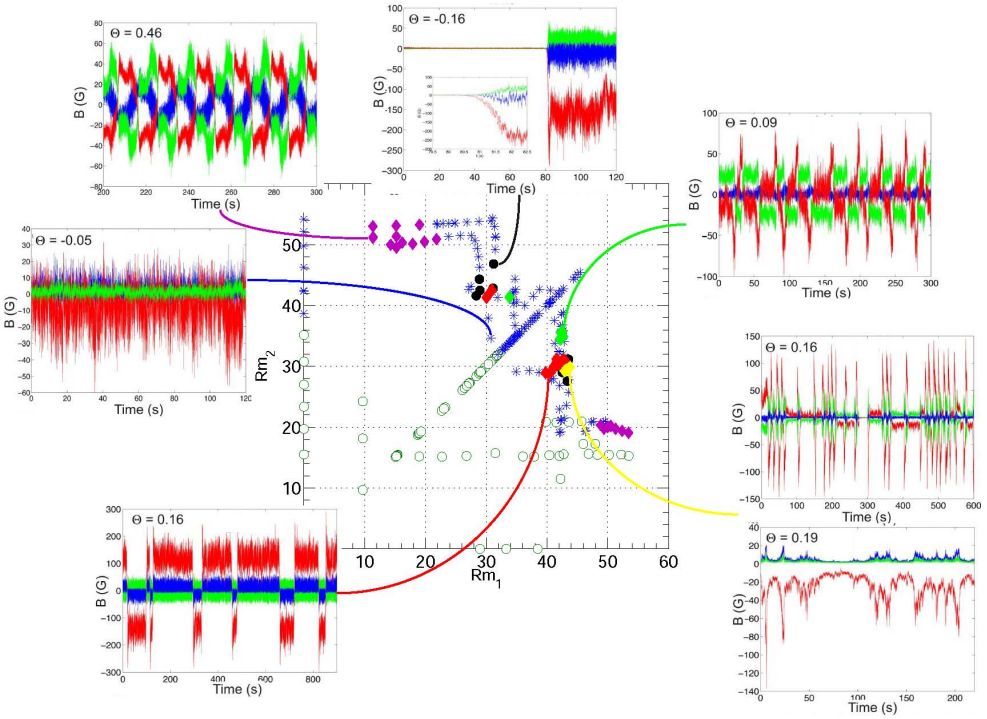

Figure 2: Dynamical regimes observed in the von Kármán sodium experiment when the impellers driving the flow rotate at varying rates: the coordinates in the main plot are the magnetic Reynolds numbers built from the velocity of each impeller. The insets give examples of time signals of the 3 components of the magnetic field recorded in the mid-plane of the cylinder.

shown many fundamental dynamo properties. The threshold for dynamo action has been found to be in good agreement with predictions, showing the predominance of the large scales in their dynamo processes.

Another possibility, often explored in the geophysics community, is provided by strongly rotating flows. In this case, the Proudman-Taylor constrain may be able to prevent the development of strong three-dimensional turbulent fluctuations. This effect may even be strengthened by the generation of a dynamo dipole with its axis parallel to the rotation vector. Experiments in rotating Couette flows are studied in Grenoble and Maryland [Schmitt et al., 2008, Kelley et al., 2007]. Preliminary studies have not shown self-generation, but have pointed to the existence of *waves* in these strong rotating and magnetized flows: inertial, magneto-rotational, Alfvèn, etc. Their role regarding dynamo self-generation has yet to be elucidated.

The VKS experiments have shown that it is possible to generate a dynamo from fully turbulent motions, with non-trivial dynamics [Monchaux et al., 2009]. The existence of fully turbulent motions has a major impact on the power requirements of the experiment. In the limit of very high R_V values, the hydrodynamic power consumption (below dynamo threshold) scales as $P = \rho L^2 U^3$ (ρ is the fluid's density), leading to magnetic Reynolds number $R_M = \mu\sigma(PL/\rho)^{1/3}$ (μ and σ are the magnetic permeability and electrical conductivity of the fluid, so that $\lambda = 1/\mu\sigma$ is its magnetic diffusivity). Engineering difficulties typically scale with the size L of the experiment, while operational costs are best associated with the power input P. Then, the above scaling shows that in order to reach high R_M values, one should use a fluid with the best electrical conductivity and lowest density (hence the use of liquid sodium), with size and power consumption only contributing to the one-third power. This is a noteworthy peculiarity of the study of this hydromagnetic instability: energy and engineering constrains are such that one is not able to increase at will the control parameter of the instability; one must also choose conditions such that the thresholds is within the capacity of the selected setup. In the case of the VKS experiment this is ensured when ferromagnetic impellers are used to drive the flow. When rotating, they promote a strong omega effect in their vicinity. Cou-

pled with local sources of alpha processes (helical flow structures, turbulence gradients), this arrangement generates a dynamo at $R_M^c \sim 30$. A stationary dynamo is produced when one impeller rotates while the other is kept at rest. The main magnetic mode has the shape of an axial dipole. When both are set into (counter) rotation, a rich variety of regimes are observed from the interactions of the dynamos generated from the rotation of each impeller. As shown in [Monchaux et al., 2008] they share many properties with the dynamics of low dimensional systems.

Liquid metal flows reach magnetic Reynolds numbers of the order of 100, at most. Using a plasma as the working fluid is a possibility currently explored to generate laboratory dynamos at significantly higher R_M values [Spence et al., 2009]. This may enable the observation in the lab of small scale fluctuating dynamos which prevail in many astrophysical situations.

References

D. H. Kelley, S. A. Z. Triana, D. S., A. Tilgner, and D. P. Lathrop. Inertial waves driven by differential rotation in a planetary geometry. *Geophys. Astrophys. Fluid Dyn.*, 101, 2007.

R. Monchaux, M. Berhanu, S. Aumaître, A. Chiffaudel, F. Daviaud, B. Dubrulle, F. Ravelet, M. Bourgoin, P. Odier, J.-F. Pinton, N. Plihon, R. Volk, S. Fauve, N. Mordant, and F. Pétrélis. Chaotic dynamos generated by a turbulent flow of liquid sodium. *Phys. Rev. Lett.*, 101, 2008.

R. Monchaux, M. Berhanu, S. Aumaître, A. Chiffaudel, F. Daviaud, B. Dubrulle, L. Marié, F. Ravelet, S. Fauve, N. Mordant, F. Pétrélis, M. Bourgoin, P. Odier, J.-F. Pinton, N. Plihon, and R. Volk. The vks experiment: turbulent dynamical dynamos. *Phys. Fluids*, 21, 2009.

R. Moreau and J. Pinton. (eds), dynamo effect: experimental progress and geo- and astro-physical challenges, special issue. *C. R. Phys.*, 9, 2008.

D. Schmitt, T. Alboussiere, D. Brito, P. Cardin, N. Gagniere, D. Jault, and H.-C. Nataf. Rotating spherical couette flow in a dipolar magnetic field: experimental study of magneto-inertial waves. *J. Fluid Mech.*, 604:175–197, 2008.

E. Spence, K. Reuter, and C. Forest. A spherical plasma dynamo experiment. *Astrophys. J.*, 700, 2009.

Paleomagnetism and Rock Magnetism

Jean Pascal Cogné and France Lagroix

Université Paris Diderot, Institut de Physique du Globe de Paris
PRES Sorbonne Paris-Cité, INSU/CNRS, F-75005 Paris

Abstract Paleomagnetism has proven a powerful tool providing valuable constraints on Plate Tectonics, depicting history and helping theory of continental drift. In France, Paleomagnetism and rock magnetism have grown following pioneering works of Profs. Emile Thellier and Louis NÃl'el in the middle of the XXth century, giving rise to the establishment of several paleomagnetic labs in the country at present. Since the time of Plate Tectonics theory and establishment of magnetic field reversal evidences, french labs have largely contributed and developped use of magnetic memory of rocks, synthetic materials and other human ancient artifacts. Here we cite some significant french contributions.

Archeomagnetism pioneered by St Maur lab, later joined by IPGP, is currently being developped by most paleomag labs in France. Archeomagnetism allows recovery of magnetic field direction and intensity as recorded by baked archeological artifacts (e.g. potteries, ovens...) at a given location. As a result, high resolution directional and intensity variation curves for a given region, Gallet et al. [2009] (Fig. 1) provide constraints for geomagnetic studies, and, for archeologist, a dating tool [eg Kovacheva et al., 2009, Schnepp et al., 2009].

Magnetostratigraphy, paleointensity and geomagnetic field behaviour polarity timescales are progressively obtained from more and more ancient eras, as far back as the Paleozoic and Proterozoic. They have noticeably revealed a long normal superchron in the Ordovician [Pavlov and Gallet, 2010], or periods of high reversal frequencies in the Proterozoic, possibly larger than 5-10 reversals per Myr [Pavlov and Gallet, 2009]. The last element defining the geomagnetic field vector, its intensity, is uneasy to evaluate. In marine sediments, relative paleointensity methods provide important contribution to the study of the geomagnetic field, particularly in its reversals and excursions history [eg Valet et al., 2008, Laj et al., 2006]. Absolute paleointensity is the last parameter which allows full definition of magnetic field vector and its changes through geological times. This parameter can be defined in effusive formations only, mainly basalts. Experimental determination of this parameter is still uneasy. Therefore, methodological developments are still being held, together with data acquisition [Biggin and Perrin, 2007, Valet et al., 2010, Thouveny et al., 2008].

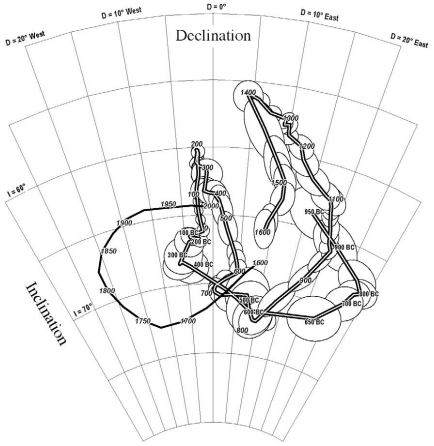

Figure 1: Directional evolution of the Earth's magnetic field in France (Paris) during the past three millennia, from [Gallet et al., 2009].

Plate tectonics and continental deformation Paleomagnetism remains a powerful tool in deciphering deformation of continents and their movements at the Earth' surface. Beyond continuing establishement of reference Apparent Polar Wandering Paths (APWP) [Moreau et al., 2007], some significant efforts, which deserve attention, have focused on tectonics of recent mountain chains such as the Andes [Arriagada et al., 2008, Fig 2.](Fig. 2) or the Asian system (Tibet, China, Mongolia... [Hankard et al., 2007, Cogne et al., 2011, Fig. 3.].

Fig. 2 and 3 illustrate tectonic analyses which

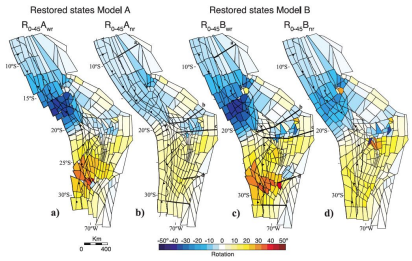

Figure 2: Two-dimensional map-view restorations of the central Andes using paleomagnetically derived shortening and block rotation models [Moreau et al., 2007].

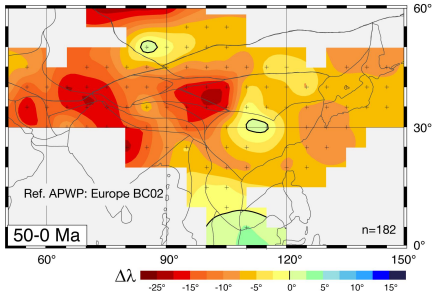

Figure 3: Cenozoic paleolatitude anomaly over Asia, resulting from anomalously shallow paleomagnetic inclinations. The origin, geomagnetic and/or tectonic [Hankard et al., 2007] of this anomaly is still hotly debated [Cogne et al., 2011]

are now possible, due to increasing density and coverage (but far from being sufficient and of homogeneous coverage and quality) of paleomagnetic database, to which french labs have significantly contributed.

True Polar Wander (TPW) and global dynamics Using a geodynamic model based on plate reconstructions that estimates the location and rate of subducted slabs, and taking into account the effect of large-scale upwellings as evidenced by tomography, it is shown that temporal variation of the mantle density heterogeneities is essentially due to changes in the subduction history of plates. Since 120 Myr, both the maximum and intermediate Principal Inertia Axes have moved in a plane perpendicular to Africa, along a circle corresponding to the low of geoid induced by subduction around the Pacific. The minimum PIA seems to be relatively stable since 120 Myr, and close to the maximum degree 2 geoid high under Africa. This can account for observed TPW or African APW in the last 200 Myr [Rouby et al., 2010, Fig. 4].

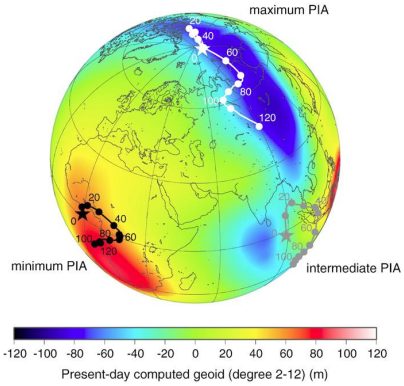

Figure 4: Principal Inertia Axes since 120 Myr [Rouby et al., 2010] (dots every 10 Myr, stars denote present day values) for a mantle density heterogeneities model arising from circum-Pacific subductions. The corresponding present-day geoid (degrees 2-12) is also shown.

Rock magnetism To end this brief overview, we finally underline that a significant part of scientific activity in paleomagnetism deals with magnetic properties of natural, synthetic and/or anthropogenic materials. The aim is to further understand the remanence acquisition processes, its alteration through time and in different geological settings together with applying mineral magnetic properties to investigate a variety of questions, such as rock formation processes (weathering, deposition etc... [e.g. Lagroix and Banerjee, 2004a, Ricordel-Prognon et al., 2010], characterization of extra-terrestrial materials [Rochette et al., 2009], or environmental studies such as heavy metal pollution evaluations [Franke et al., 2009], and paleoclimate [e.g. Lagroix and Banerjee, 2004b, Blanchet et al., 2009].

References

C. Arriagada, P. Roperch, C. Mpodozis, and P. R. Cobbold. Paleogene building of the Bolivian Orocline: Tectonic restoration of the central Andes in 2-D map view. *Tectonics*, 27, 2008. doi: 10.1029/2008TC002269.

A. J. Biggin and M. Perrin. The behaviour and detection of partial thermoremanent magnetisation (PTRM) tails in Thellier palaeointensity experiments. *Earth Planets Space*, 59:717–725, 2007.

C. L. Blanchet, N. Thouveny, and L. Vidal. Formation and preservation of greigite (Fe3S4)

in sediments from the Santa Barbara Basin: Implications for paleoenvironmental changes during the past 35 ka. *Paleooceano.*, 24, 2009. doi: 10.1029/2008PA001719.

J.-P. Cogne et al. A new Meso-Cenozoic East Asia APWP: an alternative solution to decipher the tertiary inclination anomaly issue - Implications on plate tectonics and continental deformation of Central and SE Asia, East Europe and Arctic regions of Eurasia. *Geophys. J. Int.*, Submitted:–, 2011.

C. Franke, C. Kissel, E. Robin, P. Bonte, and F. Lagroix. Magnetic particle characterization in the seine river system: Implications for the determination of natural versus anthropogenic input. *Geochem., Geophys., Geosyst.*, 10, 2009. doi: 10.1029/2009GC002544.

Y. Gallet, A. Genevey, M. Le Goff, N. Warme, J. Gran-Aymerich, and A. Lefevre. On the use of archeology in geomagnetism, and vice-versa: Recent developments in archeomagnetism. *C. R. Phys.*, 10, 2009. doi: 10.1016/j.crhy.2009.08.005.

F. Hankard, J.-P. Cogne, V. A. Kravchinsky, L. Carporzen, A. Bayasgalan, and P. Lkhagvadorj. New Tertiary paleomagnetic poles from Mongolia and Siberia at 40, 30, 20, and 13 Ma: Clues on the inclination shallowing problem in central Asia. *J. Geophys. Res.*, 112, 2007. doi: 10.1029/2006JB004488.

M. Kovacheva, A. Chauvin, N. Jordanova, P. Lanos, and V. Karloukovski. Remanence anisotropy effect on the palaeointensity results obtained from various archaeological materials, excluding pottery. *Earth Planets Space*, 61, 2009.

F. Lagroix and S. K. Banerjee. Cryptic post-depositional reworking in aeolian sediments revealed by the anisotropy of magnetic susceptibility. *Earth Planet. Sci. Lett.*, 224, 2004a. doi: 10.1016/j.espl.2004.05.029.

F. Lagroix and S. K. Banerjee. The regional and temporal significance of primary aeolian magnetic fabrics preserved in Alaskan loess. *Earth Planet. Sci. Lett.*, 225, 2004b. doi: 10.1016/j.epsl.2004.07.003.

C. Laj, C. Kissel, and A. P. Roberts. Geomagnetic field behavior during the Iceland Basin and Laschamp geomagnetic excursions: A simple transitional field geometry? *Geochem., Geophys., Geosyst.*, 7, 2006. doi: 10.1029/2005GC001122.

M.-G. Moreau, J. Besse, F. Fluteau, and M. Greff-Lefftz. A new global Paleocene-Eocene apparent polar wandering path loop by "stacking" magneto stratigraphies: Correlations with high latitude climatic data. *Earth Planet. Sci. Lett.*, 260, 2007. doi: 10.1016/j.epsl.2007.05.025.

V. Pavlov and Y. Gallet. Variations in geomagnetic reversal frequency during the Earth's middle age. *Geochem., Geophys., Geosyst.*, 11, 2010. doi: 10.1029/2009GC002583.

V. E. Pavlov and Y. Gallet. Superchron at the Mesoproterozoic-Neoproterozoic transition. *Dokl. Earth Sci.*, 426, 2009. doi: 10.1134/S1028334X09040278.

C. Ricordel-Prognon, F. Lagroix, M.-G. Moreau, and M. Thiry. Lateritic paleoweathering profiles in French Massif Central: Paleomagnetic datings. *J. Geophys. Res.*, 115, 2010. doi: 10.1029/2010JB007419.

P. Rochette, B. P. Weiss, and J. Gattacceca. Magnetism of Extraterrestrial Materials. *Elements*, 5, 2009. doi: 10.2113/gselements.5.4.223.

H. Rouby, M. Greff-Lefftz, and J. Besse. Mantle dynamics, geoid, inertia and TPW since 120 Myr. *Earth Planet. Sci. Lett.*, 292, 2010. doi: 10.1016/j.epsl.2010.01.033.

E. Schnepp, P. Lanos, and A. Chauvin. Geomagnetic paleointensity between 1300 and 1750 AD derived from a bread oven floor sequence in Lubeck, Germany. *ggg*, 10, 2009. doi: 10.1029/2009GC002470.

N. Thouveny, D. L. Bourles, G. Saracco, J. T. Carcaillet, and F. Bassinot. Paleoclimatic context of geomagnetic dipole lows and excursions in the Brunhes, clue for an orbital influence on the geodynamo? *Earth Planet. Sci. Lett.*, 275, 2008. doi: 10.1016/j.epsl.2008.08.020.

J.-P. Valet, G. Plenier, and E. Herrero-Bervera. Geomagnetic excursions reflect an aborted polarity state. *Earth Planet. Sci. Lett.*, 274, 2008. doi: 10.1016/j.epsl.2008.07.056.

J.-P. Valet, E. Herrero-Bervera, J. Carlut, and D. Kondopoulou. A selective procedure for absolute paleointensity in lava flows. *Geophys. Res. Lett.*, 37, 2010. doi: 10.1029/2010GL044100.

Recent French activity in archeomagnetism

Annick Chauvin (1), Yves Gallet (2) Agnès Genevey (3), and Philippe Lanos (4)

(1) Géoscience Rennes, Université de Rennes 1, F-35000 Rennes
(2) Institut de Physique du Globe de Paris, INSU/CNRS, F-75005 Paris
(3) Centre de Recherche et de Restauration des Musées de France, F-75001 Paris
(1) Centre de Recherches en Physique Appliquée à l'Archéologie, Université Bordeaux 3 et Université Rennes 1

Abstract Archeomagnetism is a very active domain of research in France thanks to several French laboratories involved in magnetic property analyses of baked clay archeological artifacts. Here we list some recent results.

Recent archeomagnetic studies have been focused on the evolution, both in direction and in intensity, of the geomagnetic field over the past few centuries and/or millennia in several regions, in Western Europe [Gomez-Paccard et al., 2008, Genevey et al., 2009, Schnepp et al., 2009, Gallet et al., 2009a, Hervé et al., 2011], in the Middle East [Gallet et al., 2008] or in Central and Southern America [Hartmann et al., 2010]. In particular, these studies led to the acquisition of numerous high-quality archeointensity data, allowing one to gradually compensate for the lack of data of this nature, which existed until now. Hence, a 3000 year-long full (direction and intensity) geomagnetic field record is progressively emerging for Western Europe. Studies performed in Brazil further brought important new information on the geomagnetic field behavior in southern hemisphere where archeointensity results are still rare, representing as a whole less than 5% of all available intensity data [Genevey et al., 2008]. Other investigation is being conducted in Syria in order to pursue the construction of a detailed regional archeointensity variation curve encompassing a large part of the Holocene.

The main objectives of these studies are threefold. The first target concerns geomagnetism. The new data greatly contribute to the development of more reliable and accurate regional or global archeomagnetic field models [Valet et al., 2008]. Our interest is to recover the millennial-scale evolution of the geomagnetic field with a sub-centennial temporal resolution. This ambitious objective makes necessary the acquisition of numerous archeomagnetic data from carefully selected well-dated archeological artifacts. Whatever the periods, our data sets show the important regional geomagnetic field variability. Regarding intensities, the occurrence of several peaks in intensity was detected from Western European data, with a prominent maximum during the High Middle Age ($\sim$800 AD) and two other peaks during the second half of the XIVth century and around 1600 AD (Figure 1 and Gomez-Paccard et al. [2008], Genevey et al. [2009], Schnepp et al. [2009]).

The second target of the French archeomagnetic studies is to strengthen the possibility of using the geomagnetic field secular variation as a dating tool for archeological purposes. Archeomagnetic dating relying on geomagnetic directional variations are being currently made in close collaboration with archeologists from firing *in situ* structures, such as pottery and domestic kilns. The analyses are particularly frequent for domestic kilns dated to the High Middle Age found in abundance in the Ile-de-France region and for which the archeological dating constraints are generally scarce [Warmé, 2009]. On another hand, the large number of archeointensity data recently obtained from French and Syrian objects gives rise to the possibility of further using the geomagnetic field intensity fluctuations for deriving dating constraints. The interest would be to be able to use the archeomagnetic dating technique on virtually all archeological artifacts, either found in situ or in displaced context from their original firing position (potsherds, bricks and tiles).

Our archeomagnetic studies also penetrated the domains of environmental and climatic sciences. Trends in secular variation recognized in carbonate concretions sampled in Roman water conducts were for instance used to put temporal constraints on climatic indicators obtained from the same concretions [Carlut et al., 2009]. Other studies were focused on the possible causal

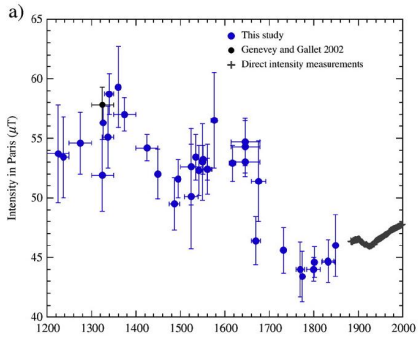

Figure 1: French archeointensity data over the past eight centuries after Genevey et al. [2009].

link existing between geomagnetic secular variation and regional and/or global climatic fluctuations during the Holocene [Gallet et al., 2009a, Hartmann et al., 2010]. This challenging topic is closely connected to the necessity of better knowing the geomagnetic field behavior over centennial time scales, including new constraints on the origin of the so-called archeomagnetic jerks [Gallet et al., 2009b], and, from this point of view, joins the first theme discussed above.

The interest for the different applications of archeomagnetism in geomagnetism, archeology and climatology rapidly and significantly grew over the past few years within the French and international communities of Paleomagnetism and Geomagnetism; there is no doubt that this interest will be even more important in the near future.

References

J. Carlut, G. Chazot, H. Dessales, and E. Letellier. Trace element variations in an archeological carbonate deposit from the antique city of ostiaă: Environmental and archeological implications. *C. R. Geosciences*, 341:10–20, 2009.

Y. Gallet, M. Le Goff, A. Genevey, J. Margueron, and P. Matthiae. Geomagnetic field intensity behavior in the middle east between 3000 bc and 1500 bc. *Geophys. Res. Lett.*, 2008.

Y. Gallet, A. Genevey, M. Le Goff, N. Warme, J. Gran-Aymerich, and A. Lefevre. On the use of archeology in geomagnetism, and viceversa: Recent developments in archeomagnetism. *C. R. Phys.*, 10, 2009a. doi: 10.1016/j.crhy.2009.08.005.

Y. Gallet, G. Hulot, A. Chulliat, and A. Genevey. Geomagnetic field hemispheric asymmetry and archeomagnetic jerks. *Earth Planet. Sci. Lett.*, 284:179–186, 2009b. doi: 10.1016/j.epsl.2009.04.028.

A. Genevey, Y. Gallet, C. Constable, M. Korte, and G. Hulot. Archeointă: An upgraded compilation of geomagnetic field intensity data for the past ten millennia and its application to the recovery of the past dipole moment. *Geochem., Geophys., Geosyst.*, 2008.

A. Genevey, Y. Gallet, R. J., and M. Le Goff. Evidence for rapid geomagnetic field intensity variations in western europe over the past 800 years from new archeointensity french data. *Earth Planet. Sci. Lett.*, 2009.

M. Gomez-Paccard, A. Chauvin, P. Lanos, and J. Thiriot. New archeointensity data from spain and the geomagnetic dipole moment in western europe over the past 2000 years. *J. Geophys. Res.*, 2008.

G. Hartmann, A. Genevey, Y. Gallet, R. Trindade, C. Etchevarne, M. Le Goff, and M. Afonso. Archeointensity in northeast brazil over the past five centuries. *Earth Planet. Sci. Lett.*, 296:340–352, 2010.

G. Hervé, E. Schnepp, A. Chauvin, P. Lanos, and N. Nowaczik. Archaeomagnetic results on three early iron age salt-kilns from moyenvic (france). *Geophys. J. Int.*, 2011.

E. Schnepp, P. Lanos, and A. Chauvin. Geomagnetic paleointensity between 1300 and 1750 AD derived from a bread oven floor sequence in Lubeck, Germany. *ggg*, 10, 2009. doi: 10.1029/2009GC002470.

J.-P. Valet, E. Herrero-Bervera, J.-L. Le Mouël, and G. Plénier. Secular variation of the geomagnetic dipole during the past 2000 years. *Geochem., Geophys., Geosyst.*, 9, 2008.

N. Warmé. L'archéomagnétisme appliqué aux fours culinaires du haut moyen âge: dix ans d'activité. L'habitat rural du haut Moyen Âge en Île de France, 2ème supplément au Bulletin archéologique du Vexin Français et du Val d'Oise, Guiry-en -Vexin„ 2009.

Paleomagnetism and Climate

Guillaume Le Hir

Université Paris D. Diderot, Institut de Physique du Globe de Paris, Université Paris-Cité, INSU/CNRS, F-75005 Paris

Abstract The Earth's surface has undergone successive episodes of formation of continental landmasses through Wilson cycles, which formed supercontinents, such as Pangea, followed by their dispersal. As a consequence, the land-sea distribution, as well as its distribution with respect to latitude has evolved. Using oceanic magnetic anomalies and palaeomagnetic data, we are able to reconstruct the locations of continents in the past until the Late Jurassic. If paleomagnetic methods are used by many researchers, very few work on the potential influence of the continental drift on the climate change. A French team of scientists has intensively investigated this interplay, and has shown that the paleogeography is among the first mechanisms proposed to explain the climate change at the long term scale.

Indeed it has long been recognized that paleogeography may potentially influence the climate via the continental silicate weathering which is the main carbon sink at the long term scale [Francois and Walker, 1992]. The two climatic factors affecting the rate of continental silicate weathering are the air temperature and the continental runoff, both of these factors being strongly linked to atmospheric pCO_2 via the greenhouse effect. The essence of the mechanism is that accumulation of CO2 in the atmosphere would be compensated by an increase in its removal through silicate weathering under enhanced greenhouse conditions, the pCO_2 increase would halt at the point where the silicate weathering rate balances the rate of input by volcanic outgassing. On the basis of the existence of this relationship, the continental silicate weathering feedback governs the pCO_2 and therefore the Earth's climate at the geological timescale [Walker et al., 1981].

Five years ago, a French team has developed a new tool to investigate the interplays between tectonic and climate [Donnadieu et al., 2006]. This model, named GEOCLIM, includes a General Circulation Model (GCM) [Jacob, 1997] coupled to a box model of the geological carbon-alkalinity cycles (COMBINE) [Godderis et al., 2005]. The spatial resolution of GEOCLIM allows to capture the evolution of the main features of geographies and their impacts on the carbon cycle. To illustrate the potential magnitude of continental drift control on the long term atmospheric CO_2 and climate, an international team, mainly composed by French researchers [Donnadieu et al., 2006] has quantified the pCO_2 evolution in response of the waltz of continents over the course of the Mesozoic. It should be noted that, regarding the abundance of the oceanic crust, paleogeographies prior the Jurassic are less well constrained.

Looking for the Fig. 1, we see that the general pattern of the simulated CO_2 curve illustrates the fundamental importance of the paleogeography in controlling atmospheric CO_2 and then the Earth climate. From a global point of view, the breakup of Pangea causes a transition from a generally dry climatic regime during the Triassic to a wetter one during the Cretaceous. In the same time, global and continental air temperature largely decreases in response of the pCO_2 reduction. Hence the paleogeography, by influencing the continental weathering pattern, governs the global climate and could explain the Earth cooling or warming at the long-term scale.

As shown with this brief example, the paleomagnetism is an essential tool to reconstruct the past land-sea distributions and therefore the Earth climate. However, three years ago, a second paleomagnetism application has emerged, allowing us to capture the Deccan trap impact on the global climate. Indeed, by a flow-by-flow analysis of paleomagnetic directions, Chenet et al. [2009] have reconstructed the eruptive history of the Deccan trap. They have discovered that the volcanism duration was shorter than previously expected and constituted by volcanic pulses. Using this fact, climate modelers are now able to reconstruct the climatic consequences of the Deccan eruption, and determinate its potential impact on the Life. In conclusion, the paleomagnetism and its recent developments contribute to

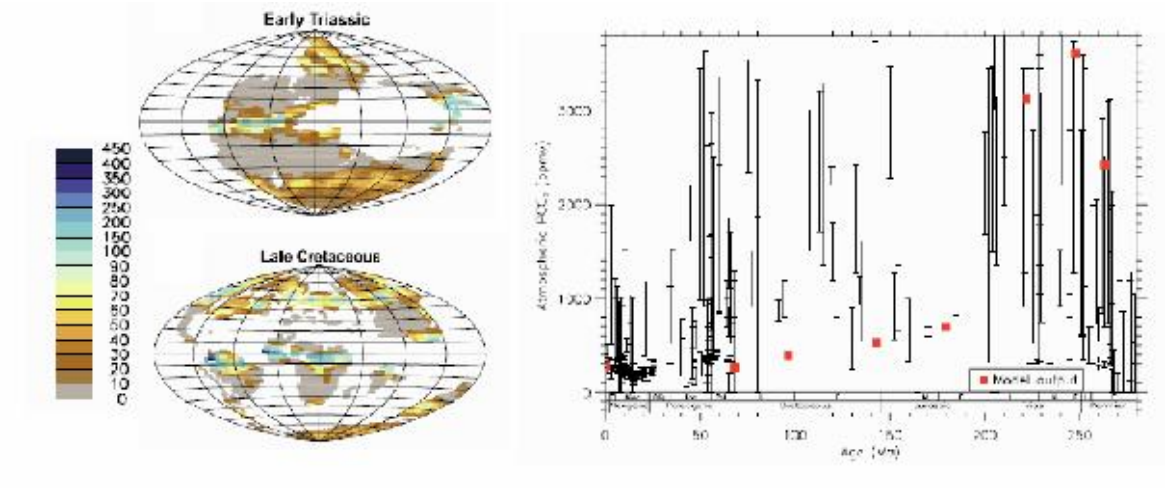

Figure 1: (left) Links between paleogeography and runoff using a climate model. Mean annual runoff (cm/yr) for two paleogeographies spanning the Mesozoic obtained in fixing the pCO_2 at the same level (here 1680ppmv). (right) Evolution of atmospheric CO2 through the Mesozoic. Bars represent atmospheric CO_2 estimates (min/max values) coming from the data sets built by [Royer et al., 2004] and available online at http://www.geosociety.org/pubs/ft2004.htm. The squares represent the modeled atmospheric CO_2 in the reference run under boundary conditions (full description available in [Donnadieu et al., 2006]).

increase our understanding of the past climate changes and the Earth evolution.

References

A.-L. Chenet, V. Courtillot, F. Fluteau, M. Gerard, X. Quidelleur, S. F. R. Khadri, K. V. Subbarao, and T. Thordarson. Determination of rapid deccan eruptions across the cretaceous-tertiary boundary using paleomagnetic secular variation: 2. constraints from analysis of eight new sections and synthesis for a 3500-m-thick composite section. *J. Geophys. Res.*, 114, 2009. doi: 10.1029/2008JB005644.

Y. Donnadieu, Y. Godderis, R. Pierrehumbert, G. Dromart, F. Fluteau, and R. Jacob. A GEOCLIM simulation of climatic and biogeochemical consequences of Pangea breakup. *Geochem., Geophys., Geosyst.*, 7, 2006. doi: 10.1029/2006GC001278.

L. Francois and J. Walker. Modeling the phanerozoic carbon-cycle and climate constraints from the sr-87-sr-86 isotopic ratio of seawater. *Am. J. Sci.*, 292:81–135, 1992.

Y. Godderis, Y. Donnadieu, M. Tombozafi, R. Pierrehumbert, J. Gaillardet, L. R. Kump, and B. Dupre. Links between climate, paleogeography and silicate rock weathering: A cretaceous vs present day comparative study with the geoclim model. *gca*, 69:688–688, 2005.

R. L. Jacob. *Low frequency variability in a simulated atmosphere ocean system*. PhD thesis, The University of Wisconsin - Madison, 1997.

D. L. Royer, R. A. Berner, I. P. Montanez, N. J. Tabor, and D. J. Beerling. Co2 as a primary driver of phanerozoic climate. *GSA Today*, 14 (3):4–10, 2004.

J. C. G. Walker, P. B. Hays, and J. F. Kasting. A negative feedback mechanism for the long-term stabilization of earths surface- temperature. *J. Geophys. Res.*, 86:9776– 9782, 1981.

Environmental Magnetism and Magnetotactic Bacteria

Aude Isambert

Institut de Physique du Globe de Paris, Sorbonne Paris Cité, UniversitÃľ Paris Diderot, INSU/CNRS, F-75005 Paris

Abstract Studying the crystallographic and magnetic properties of magnetite crystals produced by magnetotactic bacteria present a great interest in many fields such as physics of fine particles, biomineralization, medicine and environmental and planetary sciences. Indeed, (1) biomagnetites represent an interesting object of study in the field of fine particles magnetism and a source of potential medical application, (2) studying the biological mechanisms implied in the formation of magnetite crystals is a means to better understand the different processes of biomineralization in living organisms, (3) and last, fossil magnetosomes could significantly contribute to magnetic properties of sediments and soils, their spatial organisation in chains being considered as a potential biomarker in terrestrial or extraterrestrial environments.

Magnetotactic bacteria mineralize nanometer-sized magnetite (Fe_3O_4) or greigite (Fe_3S_4) crystals in intracellular vesicles, also called magnetosomes. The sizes, morphologies, crystallographic characteristics, and chemical compositions of the biogenic crystals of magnetite are controlled by the bacteria and can thus be used as potential biosignatures (Fig. 1). Magnetosomes are generally arranged in chains that act as compass needles so that the bacteria tend to align passively along the Earth's magnetic field lines. This phenomenon called magnetotaxis, coupled with flagellar motility and aerotaxis, allows the cells to locate and maintain an optimal position for their growth in vertical chemical gradients within aquatic environments.

The French community studying magnetotactic bacteria, due to the transversal aspect of this subject of research, is composed of specialists of different domains including biophysicists, biochemists, microbiologists and geophysicists. One first aim of the working group is to better understand the contribution of fossil magnetosomes to magnetic properties of sediments. Various morphotypes of magnetotactic bacteria have been observed in aqueous environments. The freshwater magnetotactic population found in the Seine River [Isambert et al., 2007] is an example of the variety of both magnetic cells and crystals shapes. Different morphotypes were recognized using morphological criteria, which rely on the number of magnetite crystals and their organization within cells, the size and shape of the cells and their statistical distribution. Among the collected rod-shaped bacteria, a type similar to Magnetobacterium bavaricum has been found (Fig. 2). This species is indeed easily recognizable by the fact that these large rod-shaped magnetic cells, up to 12 μm in length, may contain more than 600 highly anisotropic bullet-shaped magnetosomes in a unique cell, arranged in 3 up to 5 bundles of magnetosomes chains. Those bullet-shaped magnetites may contribute significantly to sedimentary magnetism. To begin to answer, magnetic measurements on enrichments of freshly collected natural living cells and on magnetic extracts of river sediments are in progress.

In parallel, to improve the knowledge of MTB distribution and ecology, we have just started to investigate the temporal variation of MTB communities in the Seine River by combining the study of phenotypic criteria with phylogenetic analysis and cultivation-independent molecular techniques [Gerard et al., 2005]. This technology, applied for the first time to natural samples could give us specific information on MTB species. Indeed, the biomineralization process of bullet shaped magnetites is still poorly understood and culturing these bacteria has been unsuccessful until now.

A second aim is to better understand the anthropogenic effect on the development of magnetotactic populations and to precise the natural (biomagnetite, sedimentary magnetite) versus anthropogenic input in magnetic particles in the Seine River system. A challenge is to trace both geological, biological and human induced processes and particularly to identify the potential effect of pollution on fine magnetic particles present in these fluvial sediments. A first analysis of the regional distribution of suspended mag-

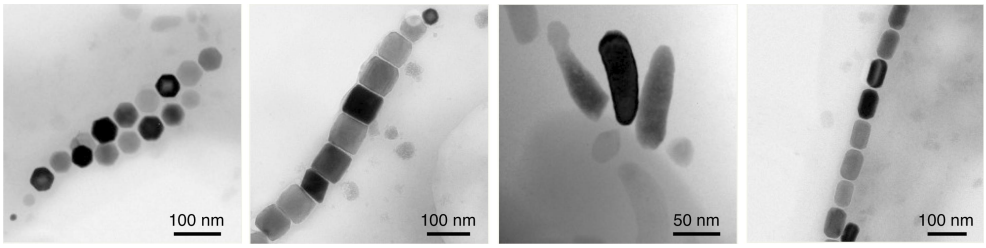

Figure 1: TEM images showing the diversity of magnetosomes morphologies observed in the Seine River (from left to right : cuboctahedral, truncated prismatic, tooth-shaped and elongated prismatic magnetite).

netic material has been conducted on sediment trap samples [Franke et al., 2009]. A combination of rock magnetic and advanced scanning electron microscopic techniques has shown an increase in magnetic concentration coupled with a coarsening in magnetic grain size downstream of the Seine river system. A significant correlation between anthropogenic antimony-rich iron oxide particles and the magnetic concentration has been observed. In the continuity of this study, it seems important to determine the contribution of magnetic fine grains of biological origin at nanometre scale, which are the principal carriers of remanence in sediment, and to observe the potential adsorption of pollutant on those magnetic nanograins.

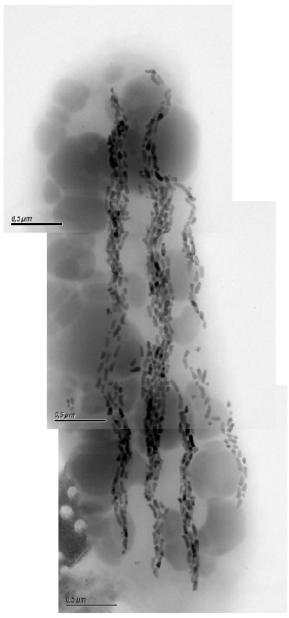

Figure 2: Rod-shaped bacteria extracted from the Seine River, similar to Magnetobacterium bavaricum, containing more than 600 highly anisotropic bullet-shaped magnetites.

In addition to microscopic approach [Isambert et al., 2007], magnetic measurements, because of the nature of the studied object, represent a useful analysis tool able to serve to identify the contributions of individual tributaries in the Seine river system [Alphandery et al., 2010, Vasiliev et al., 2008].

References

E. Alphandery, L. Liejour, Y. Lalatonne, and L. Motte. Different signatures between chemically and biologically synthesized nanoparticles in a magnetic sensor: a new technology for multiparametric detection. *Sensors & Actuators B*, 147:786–790, 2010.

C. Franke, C. Kissel, E. Robin, P. Bonte, and F. Lagroix. Magnetic particle characterization in the seine river system: Implications for the determination of natural versus anthropogenic input. *Geochem., Geophys., Geosyst.*, 10, 2009. doi: 10.1029/2009GC002544.

E. Gerard, F. Guyot, P. Philippot, and P. Lopez-Gardia. Fluorescence in situ hybridisation coupled to ultra-small immunogold detection to identify prokaryotic cells using transmission and scanning electron microscopy. *J. Microbiol. Methods*, 63:20–28, 2005.

A. Isambert, N. Menguy, E. Larquet, F. Guyot, and J. P. Valet. Transmission electron microscopy study of magnetites in a freshwater population of magnetotactic bacteria. *Amer. Min.*, 92:621 630, 2007.

I. Vasiliev, C. Franke, J. D. Meeldijk, M. J. Dekkers, C. G. Langereis, and W. Krijgsma. Putative greigite magnetofossils from the pliocene epoch. *Nature Geoscience*, 1: 782–786, 2008.

Planetary Magnetic Fields and Magnetized Environments

Benoit Langlais

Univrsité de Nantes and CNRS, Laboratoire de Planétologie et Géodynamique de Nantes, 44322 Nantes cedex 3

Abstract There exists magnetic fields around other planets than the Earth. The closest body, the Moon, possesses a weak remanent magnetic field, of the order of a few nT at 10 km altitude or so. Mars has a similars magnetic field in origin, but its anmplitude reaches up to 1500 nT at 90 km, as it was measured by Mars Global Surveyor. These intense crustal fields strongly interact with the light Martian atmosphere and the solar wind, creating minimagnetospheres. Mercury has the most 'earth-like' magnetic signature, with a magnetic field of core origin. Observations and models of these planetary magnetic fields, as well as measurements on extraterrestrial samples, help to better understand the geodynamo processes.

The existence of a global magnetic field around a planet is important, as it may help to protect and shield the atmosphere against the solar wind [Dehant et al., 2007]. Thus, the magnetic exploration of our solar system is important, as it brings constraints on the conditions under which dynamo action is possible [Breuer et al., 2010]. Here we briefly review some recent results dealing both with planetary magnetic fields and their effects on their environment.

Mars

The Martian magnetic field was measured by the Mars Global Surveyor (MGS, 1996-2006) probe, with a very good accuracy and a very good and complete coverage. Soon after the first measurements, the nature of the martian field revealed its complexity: intense and large magnetic anomalies are heterogeneously located, mainly above the southern and highly cratered highlands. The northern hemisphere, as well as the largest volcanic provinces and the largest impact craters, seems to be devoid of significant anomalies, meaning that the dynamo which was active when units acquired a remanent magnetization shut down early in Mars' history [Langlais and Quesnel, 2008], although this was recently challenged [Michel and Forni, 2011].

Recently, the absence of magnetization above the northern lowlands were tentatively reinterpreted. Rather than invoking a giant impact, possibly affecting a whole hemisphere, Quesnel et al. [2009] suggested large scale serpentinization processes, affecting the southern hemisphere only. This metamorphic process produces magnetite, and also decrease the density,

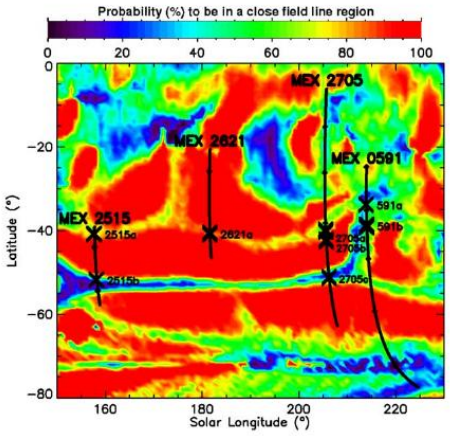

Figure 1: Map of the probability to be in a closed field line region at 400 km in altitude on the Martian nightside as calculated from MGS-ER. Also plotted are the trajectories of Mars Express (black line) below 1000 km altitude for four orbits with aurora events (crosses). After Leblanc et al. [2008].

which may explain the topographic dichotomy. Another explanation may be the existing oxydation conditions that existed at Mars' surface while the dynamo was active [Hood et al., 2010]. This would explain why some volcanic units, postdating the large demagnetized impacts, are still magnetized. An alternate is a different dynamo regime: recently, computations proved that a heat flux dichotomy at the CMB creates a hemispherical dynanmo [Amit et al., 2011].

The existence of these strong localized magnetic field modify the way the planet and its environment interacts with the solar wind. For instance,

aurorae were recorded by SPICAM on board Mars Express above areas where crustal magnetic field lines are not closed, i.e. organized into cusp-like structures [Leblanc et al., 2008]. 3-D hybrid simulations of the solar wind/Mars interaction were also performed, to quantify the importance of the solar wind source to the helium balance of the Martian atmosphere [Chanteur et al., 2009]. The importance of the dayside induced magnetic field in the ionosphere were also studied [Akalin et al., 2010].

Mercury

Mercury's magnetic field will be partially monitored by the US probe MESSENGER very soon, giving the first hemispheric (but not global) view of the Hermean magnetic field. While it is of core origin [Wicht et al., 2007], the exact conditions under which a dynamo action is possible in such a small planet remain unknown. Recently, Malavergne et al. [2010] suggested a layered core, due to the presence of sulfur and silicon. Such a structure would indeed limit the area in which the dynamo action is possible, explaining the weak observed magnetic field.

Lunar and other rocks

Measurements and experiments on extraterrestrial rocks may constrain the nature and the extent of the lunar magnetic fields. The origin of the weak lunar magnetic field is still unknown [Langlais et al., 2010]. Has it a core, external or in-situ origin? [Gattacceca et al., 2010] performed experimental acquisition of shock remanence by lunar rocks in the 0.1-2 GPa range, and showed that shock explanation is plausible as the origin of lunar magnetization. This is confirmed by analyses of lunar Apollo and Luna returned samples [Rochette et al., 2010].

Paleomagnetic studies of chondritic and small-body achondritic meteorites have revealed a diversity of magnetic field records [Weiss et al., 2010]. When coupled with new theoretical insights into the possibility of dynamo generation on small bodies, these records indicate that some planetesimals formed metallic cores and early dynamos within just a few million years of solar system formation.

Titan

The Cassini mission has provided much information about the Titan environment, with numerous low altitude encounters with the moon. The structure of its ionosphere was studied by Ågren et al. [2009], who highlighted the dependence of electron number density and electron temperature w.r.t. the Solar Zenith Angle. The atmospheric escape is strongly related to these quantities too [Edberg et al., 2010], as it was predicted by a hybrid model [Modolo and Chanteur, 2008].

References

K. Ågren, J. Wahlund, P. Garnier, R. Modolo, J. Cui, M. Galand, and I. Müller-Wodarg. On the ionospheric structure of Titan. *Planet. Space Sci.*, 57, 2009. doi: 10.1016/j.pss.2009.04.012.

F. Akalin, D. D. Morgan, D. A. Gurnett, D. L. Kirchner, D. A. Brain, R. Modolo, M. H. Acuna, and J. R. Espley. Dayside induced magnetic field in the ionosphere of Mars. *Icarus*, 206, 2010. doi: 10.1016/j.icarus.2009.03.021.

H. Amit, U. R. Christensen, and B. Langlais. The influence of degree-1 mantle heterogeneity on the past dynamo of Mars. *Phys. Earth Planet. Int.*, Submitted, 2011.

D. Breuer, S. Labrosse, and T. Spohn. Thermal Evolution and Magnetic Field Generation in Terrestrial Planets and Satellites. *Space Sci. Rev.*, 152(1-4):449–500, 2010. doi: 10.1007/s11214-009-9587-5.

G. M. Chanteur, E. Dubinin, R. Modolo, and M. Fraenz. Capture of solar wind alpha-particles by the Martian atmosphere. *Geophys. Res. Lett.*, 36, 2009. doi: 10.1029/2009GL040235.

V. Dehant, H. Lammer, Y. N. Kulikov, J.-M. Grießmeier, D. Breuer, O. Verhoeven, Ö. Karatekin, T. van Hoolst, O. Korablev, and P. Lognonné. Planetary magnetic dynamo effect on atmospheric protection of early Earth and Mars. *Space Sci. Rev.*, 129, 2007. doi: 10.1007/s11214-007-9163-9.

N. J. T. Edberg, J. Wahlund, K. Ågren, M. W. Morooka, R. Modolo, C. Bertucci, and M. K. Dougherty. Electron density and temperature measurements in the cold plasma environment of Titan: Implications for atmospheric

escape. *Geophys. Res. Lett.*, 37, 2010. doi: 10.1029/2010GL044544.

J. Gattacceca, M. Boustie, L. Hood, J.-P. Cuq-Lelandais, M. Fuller, N. S. Bezaeva, T. de Resseguier, and L. Berthe. Can the lunar crust be magnetized by shock: Experimental groundtruth. *Earth Planet. Sci. Lett.*, 299, 2010. doi: 10.1016/j.epsl.2010.08.011.

L. L. Hood, K. P. Harrison, B. Langlais, R. J. Lillis, F. Poulet, and D. A. Williams. Magnetic anomalies near Apollinaris Patera and the Medusae Fossae formation in Lucus Planum, Mars. *Icarus*, 208, 2010. doi: 10.1016/j.icarus.2010.01.009.

B. Langlais and Y. Quesnel. New Pespectives on Mars' Crustal Magnetic Field. *C. R. Geosciences*, 340, 2008. doi: 10.1016/j.crte.2008.08.006e.

B. Langlais, V. Lesur, M. E. Purucker, J. E. P. Connerney, and M. Mandea. Crustal Magnetic Fields of Terrestrial Planets. *Space Sci. Rev.*, 152, 2010. doi: 10.1007/s11214-009-9557-y.

F. Leblanc, O. Witasse, J. Lilensten, R. A. Frahm, A. Safaenili, D. A. Brain, J. Mouginot, H. Nilsson, Y. Futaana, J. Halekas, M. Holmström, J. L. Bertaux, J. D. Winningham, W. Kofman, and R. Lundin. Observations of aurorae by SPICAM ultraviolet spectrograph on board Mars Express: Simultaneous ASPERA-3 and MARSIS measurements. *J. Geophys. Res.*, 113, 2008. doi: 10.1029/2008JA013033.

V. Malavergne, M. J. Toplis, S. Berthet, and J. Jones. Highly reducing conditions during core formation on Mercury: Implications for internal structure and the origin of a magnetic field. *Icarus*, 206, 2010. doi: 10.1016/j.icarus.2009.09.001.

N. Michel and O. Forni. Mars mantle convection: Influence of phase transitions with core cooling. *Planet. Space Sci.*, In Press, 2011. doi: 10.1016/j.pss.2011.02.013.

R. Modolo and G. M. Chanteur. A global hybrid model for Titan's interaction with the Kronian plasma: Application to the Cassini Ta flyby. *J. Geophys. Res.*, 113, 2008. doi: 10.1029/2007JA012453.

Y. Quesnel, C. Sotin, B. Langlais, S. Costin, M. Mandea, M. Gottschalk, and J. Dyment. Serpentinization of the martian crust during Noachian. *Earth Planet. Sci. Lett.*, 277, 2009. doi: 10.1016/j.epsl.2008.10.012.

P. Rochette, J. Gattacceca, A. V. Ivanov, M. A. Nazarov, and N. S. Bezaeva. Magnetic properties of lunar materials: Meteorites, Luna and Apollo returned samples. *Earth Planet. Sci. Lett.*, 292, 2010. doi: 10.1016/j.epsl.2010.02.007.

B. P. Weiss, J. Gattacceca, S. Stanley, P. Rochette, and U. R. Christensen. Paleomagnetic Records of Meteorites and Early Planetesimal Differentiation. *Space Sci. Rev.*, 152, 2010. doi: 10.1007/s11214-009-9580-z.

J. Wicht, M. Mandea, F. Takahashi, U. R. Christensen, M. Matsushima, and B. Langlais. The Origin of Mercury's Internal Magnetic Field. *Space Sci. Rev.*, 132, 2007. doi: 10.1007/s11214-007-9280-5.

Balloon Campaigns Dedicated to the Study of the Dynamics and the Chemistry of the Atmosphere

Jean-Baptiste Renard

Université Orléans and CNRS, LPC2E, F-45071 Orléans 2, France

Abstract Several campaigns involving different kinds of balloons were dedicated to the study of the atmosphere between 2006 and 2010. These campaigns were conducted by CNES. The main campaigns were the ENVISAT validation missions between 2006 and 2008, VASCO (climate variability above the Indian Ocean) in 2007, SCOUT (troposhere - stratosphere interactions in tropical areas) in 2008, StrapolEté (summertime polar stratosphere), Kiruna 2010 (water vapour, ozone, nitrogen dioxide and carbon dioxide in the stratosphere), and Concordiasi (validation campaign of the IASI instrument).

Envisat validation (2006)

Since its launch in 2002, several validation campaigns of the European satellite Envisat have been conducted at various latitudes using stratospheric balloons [Renard et al., 2008]. The 2006 campaign, conducted from Kiruna, Sweden, was mainly dedicated to the validation of NOx measurements, in particular in the lower stratosphere by combining in situ and remote sensing measurements.

It has been show that remote-sensing measurements can be biased in the lower stratosphere when the stratosphere is dynamically perturbed, as in the outer part of the winter polar vortex [Berthet et al., 2007].

VASCO (2007)

This camapgin was dedicated to better undestand the climate variability in the Indian Ocean [Vialard et al., 2009]. In tropical regions, the atmosphere undergoes marked fluctuations of temperature, pressure and humidity. These fluctuations, which are particularly intense in the Indian Ocean, cause disturbances over differing time-scales.

The method involves using low-flying aeroclippers and stratospheric balloons that drift with disturbances over the oceans and in the atmosphere's boundary layer, where the circulation of airstreams is influenced by surface relief and by thermal exchanges with the surface, both land and sea. The programme will run for several years in the form of annual campaigns during which balloons will be launched from January until mid-February.

SCOUT / Envisat validation (2008)

7 flights were performed. The campaign was in the (sub)tropical regions with the following objectives [Cairo et al., 2010]:

- to investigate transport from the tropical tropopause layer into the stratosphere;
- to study the role of deep convection on the transport of species into the stratosphere;
- to investigate the microphysics of aerosols and clouds and their impact on the composition of this atmospheric region.

As Teresina (Brasil) is truly tropical (lat 5S), the campaign adds value and gives more insight into the tropical trace gas distribution in the upper troposphere, lower and middle stratosphere. The Quasi-Biennal Oscillation (QBO) is an important modulator for the transport insight the tropical pipe. Because of the QBO modulation of the wind direction and speed in the equatorial stratosphere, it is often possible to manage rather long balloon flights by taking advantage of different wind directions at different layers and using the valve and ballast to stabilize the balloon at the preferred altitude levels.

Flight were also dedicated to the validation of the MIPAS instrument onboard the Envisat satellite. The SCOUT project is funded by the European commission, and the Envisat valuation is funded by the European Space Agency.

Figure 1: Launch of a stratospheric balloon from Kiruna (Sweden).

Strapolet é (2009)

The summer polar stratosphere was poorly documented in the past, since most of the previous polar campaigns were dedicated to the ozone-hole studies [Huret, 2010].

The core of the project is based on measurements obtained during an Arctic campaign involving seven flights of balloon-borne instruments in August-September 2009 from Kiruna, Sweden (Fig. 1). The data set obtained from balloon-borne instruments and satellites will allow us to provide a detailed picture of the polar stratosphere in August for the content in NOx and halogenes species, and in aerosols

Concerning the modelling approach the goal is twofold with firstly an assessment of their operational results from comparisons with measurements, and secondly detailed investigations to highlight key processes controlling the stratosphere composition and to improve the model calculations. The project is funded by ANR (French National Research Agency) and IPEV (Institut polaire français Paul Emile Victor).

Kiruna (2010)

This small campaign was mainly dedicated to the study of the water vapour and aerosol content trend in the stratosphere.

In particular, a flight was performed up to an altitude of 42 km, has unambiguously confirmed the presence of (solid) aerosols in significant amount at such altitude [Renard et al., 2010].

Concordiasi (2010)

Concordiasi [Rabier et al., 2010] is an international project, currently supported by the following agencies: MÃľtÃľo-France, CNES, CNRS/INSU, NSF, NCAR, University of Wyoming, Purdue University, University of Colorado, the Alfred Wegener Institute, the Met Office and ECMWF. Three field experiments are part of Concordiasi, two which have occurred during the autumn 2008 and 2009 (Austral spring) in Antarctica and a third one planned in Austral spring 2010.

Additional in-situ measurements include radiosoundings at the Concordia station at Dome C and at Dumont d'Urville in 2008, at Concordia in 2009 and high altitude balloons able to drop dropsondes, launched on demand under a parachute and measuring atmospheric parameters on their way down over Antarctica in 2010. Some of the balloons will carry experimental instruments measuring ozone and particles at flight level. Some will also be enhanced to carry GPS receivers in order to perform radio-occultation measurements.

Numerical simulations will be use to complete the experiment data. The main goal is to provide validation data to improve the usage of polar-orbiting satellite data over Antarctica, in particular IASI radiances (IASI is a sounder instrument onboard the Metop sateliite measuring the infrared spectrum with an improved accuracy for temperature and humidity sounding in the troposphere and stratosphere).

References

G. Berthet, J.-B. Renard, V. Catoire, M. Chartier, C. Robert, N. Huret, F. Coquelet, Q. Bourgeois, E. D. Riviere, B. Barret, F. Lefevre, and A. Hauchecorne. Remote-sensing measurements in the polar vortex: Comparison to in situ observations and implications for the simultaneous retrievals and analysis of the NO2 and OCIO species. *J. Geophys. Res.*, 112, 2007. doi: 10.1029/2007JD008699.

F. Cairo, J. P. Pommereau, K. S. Law, H. Schlager, A. Garnier, F. Fierli, M. Ern, M. Streibel, S. Arabas, S. Borrmann, J. J. Berthelier, C. Blom, T. Christensen, F. D'Amato, G. Di Donfrancesco, T. Deshler, A. Diedhiou, G. Durry, O. Engelsen, F. Goutail, N. R. P. Harris, E. R. T. Kerstel, S. Khaykin, P. Konopka, A. Kylling,

N. Larsen, T. Lebel, X. Liu, A. R. MacKenzie, J. Nielsen, A. Oulanowski, D. J. Parker, J. Pelon, J. Polcher, J. A. Pyle, F. Ravegnani, E. D. Riviere, A. D. Robinson, T. Rockmann, C. Schiller, F. Simoes, L. Stefanutti, F. Stroh, L. Some, P. Siegmund, N. Sitnikov, J. P. Vernier, C. M. Volk, C. Voigt, M. von Hobe, S. Viciani, and V. Yushkov. An introduction to the SCOUT-AMMA stratospheric aircraft, balloons and sondes campaign in West Africa, August 2006: rationale and roadmap. *Atm. Chem. Phys.*, pages 2237–2256, 2010.

N. Huret. Le projet strapolété pour l'étude de la stratosphère polaire en été. *Météorologie*, 68, 2010.

F. Rabier, A. Bouchard, E. Brun, A. Doerenbecher, S. Guedj, V. Guidard, F. Karbou, V. H. Peuch, L. El Amraoui, D. Puech, C. Genthon, G. Picard, M. Town, A. Hertzog, F. Vial, P. Cocquerez, S. A. Cohn, T. Hock, J. Fox, H. Cole, D. Parsons, J. Powers, K. Romberg, J. VanAndel, T. Deshler, J. Mercer, J. S. Haase, L. Avallone, L. Kalnajs, C. R. Mechoso, A. Tangborn, A. Pellegrini, Y. Frenot, J. N. Thepaut, A. McNally, G. Balsamo, and P. Steinle. The Concordia project in Antarctica. *Bull. Am. Met. Soc.*, 91, 2010. doi: 10.1175/2009BAMS2764.1.

J.-B. Renard, G. Berthet, C. Brogniez, V. Catoire, D. Fussen, F. Goutail, H. Oelhaf, J.-P. Pommereau, H. K. Roscoe, G. Wetzel, M. Chartier, C. Robert, J.-Y. Balois, C. Verwaerde, F. Auriol, P. Francois, B. Gaubicher, and P. Wursteisen. Validation of GOMOS-Envisat vertical profiles of O-3, NO2, NO3, and aerosol extinction using balloon-borne instruments and analysis of the retrievals. *J. Geophys. Res.*, 113, 2008. doi: 10.1029/2007JA012345.

J.-B. Renard, G. Berthet, V. Salazar, V. Catoire, M. Tagger, B. Gaubicher, and C. Robert. In situ detection of aerosol layers in the middle stratosphere. *Geophys. Res. Lett.*, 37, 2010. doi: 10.1029/2010GL044307.

J. Vialard, J. P. Duvel, M. J. McPhaden, P. Bouruet-Aubertot, B. Ward, E. Key, D. Bourras, R. Weller, P. Minnett, A. Weill, C. Cassou, L. Eymard, T. Fristedt, C. Basdevant, Y. Dandonneau, O. Duteil, T. Izumo, C. Montegut, S. Masson, F. Marsac, C. Menkes, and S. Kennan. CIRENE Air-Sea Interactions in the Seychelles-Chagos Thermocline Ridge Region. *Bull. Am. Met. Soc.*, 90, 2009. doi: 10.1175/2008BAMS2499.1.

French Satellite Programme for the Study of the Troposphere and Climate

Jean-Baptiste Renard

Université Orléans and CNRS, LPC2E, F-45071 Orléans 2

Abstract Four main programmes have been conducted during the last years by the French Space Agency for the study of the troposphere and climate from space. The objectives is a better understanding of the water vapour cycle, the better detection of the aerosols, pollutions studies, meteorological previsions, and role of solar irradiance on climate. These programmes are CALLISPSO (tropospheric aerosols), PARASOL (clouds and aerosols properties), IASI (study weather forecast and atmospheric chemistry), and PICARD (effects of sun irradiance on climate).

CALIPSO

The Franco-American CALIPSO mission (Cloud Aerosol Lidar and Infrared Pathfinder Satellite Observations) was selected by the NASA for the Earth System Science Pathfinder (ESSP) program to supply a unique data set of atmosphere vertical profiles measured by a Lidar on-board a satellite [Vernier et al., 2009, Winker et al., 2010]. The CALIPSO satellite has a payload composed of one backscattering Lidar at 532 and 1,060 nm, with polarization measurements, a 1 meter telescope, a visible camera, and an infrared imager provided by CNES. This minisatellite provides vertical distribution of the properties of aerosols and thin clouds to better understand the aerosol-cloud-radiation interactions. In particular, CALIPSO has detected the ashes of the Eyjafjöll volcano above Paris (Figure 1). CALIPSO has been launched on 28 April 2006.

CALIPSO flies in tandem with CLOUDSAT radar satellite, and both integrated the A-TRAIN, constellation of satellites dedicated to the observation of clouds, aerosols and the water cycle (Fig. 2).

PARASOL

PARASOL, for *Polarization and Anisotropy of Reflectances for Atmospheric Science coupled with Observations from a Lidar* is the second microsatellite in the Myriade series, developed by CNES. It carries the POLDER widefield radiometer (Polarization and Directionality of the Earth's Reflectances), designed with the support of the LOA atmospheric optics laboratory (CNRS-USTL). POLDER measures the directional characteristics and polarization of light reflected by the Earth and atmosphere to further our understanding of the radiative and microphysical properties of clouds and aerosols. For example, this innovative observing technique will allow scientists to distinguish natural and manmade aerosols more accurately [Fan et al., 2008]. PARASOL is also in the A-Train. PARASOL was launched on 18 December 2004.

IASI

IASI, Infrared Atmospheric Sounding Interferometer, is a key payload element of the METOP series of European meteorological polar-orbit satellites. It is developed by CNES in the framework of a co-operation agreement with EUMETSAT. The first flight model was launched in 2006 onboard the first European meteorological polar-orbiting satellites, METOP-A. The second and third instruments will be mounted on the METOP-B and C satellites with launches scheduled in April 2012 and October-November 2016.

IASI has been designed for operational meteorological soundings with a very high level of accuracy (specifications on Temperature accuracy of 1K for 1 km and 10% for humidity) being devoted to improved medium range weather forecast. It is also designed for atmospheric chemistry aiming at estimating and monitoring trace gases like ozone, methane or carbon monoxide on a global scale [Clerbaux et al., 2009]. The IASI system includes the 3 instruments. The measurement technique is based on passive IR remote sensing using an accurately calibrated

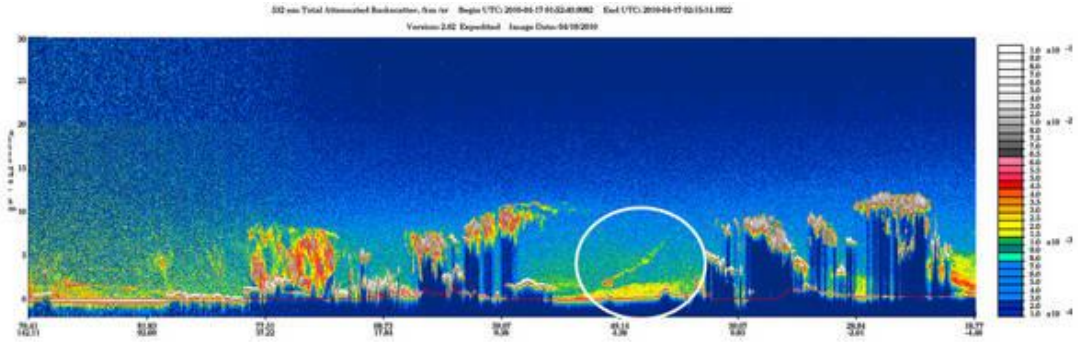

Figure 1: Ashes of the Eyjafjöll volcano above Paris (from IPSL, NASA and CNES).

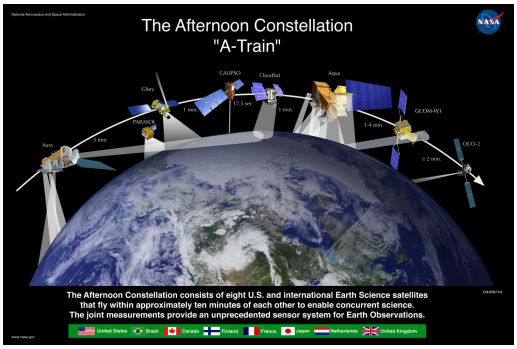

Figure 2: The "A-Train".

Fourier Transform Spectrometer operating in the 3.7 - 15.5 μm spectral range and an associated infrared imager operating in the 10.3 - 12.5 μm spectral range. The optical configuration of the sounder is based on a Michelson interferometer. The integrated infrared imager allows the co registration of the IASI sounder with AVHRR imager on-board METOP.

METOP (Fig. 3) was launched on 19 October 2006.

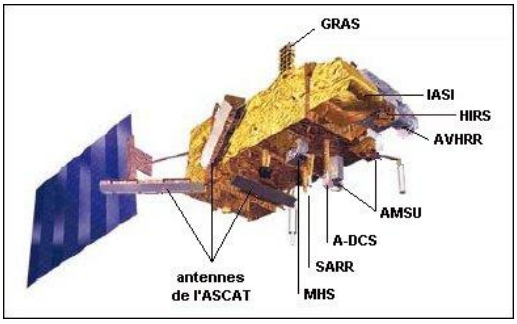

Figure 3: The METOP satellite.

PICARD

PICARD is a micro-satellite dedicated to the simultaneous measurement of the absolute total and spectral solar irradiance, the diameter and solar shape, and to the Sun's interior probing by the helioseismology method [Thuillier et al., 2009, Schmutz et al., 2009]. These measurements obtained all along the mission will allow to study their variations as a function of the solar activity. The PICARD payload is composed of the following instruments: SOVAP SOlar VAriability PICARD: composed of a differential absolute radiometer and a bolometric sensor to measure the total solar irradiance (previously called solar constant) ; PREMOS PREcision MOnitor Sensor: a set of 3 photometers to study the ozone formation and destruction, and to perform helioseismologic observations, and an absolute differential radiometer to measure the total solar irradiance; SODISM SOlar Diameter Imager and Surface Mapper: an imaging telescope accurately pointed and a CCD which allows to measure the solar diameter and shape with an accuracy of a few milliarc second, and to perform helioseismologic observations to probe the solar interior.

The PICARD measurements will help to better understand the effect of the Sun irradiance on Earth climate. PICARD was launched on 15 June 2010.

References

C. Clerbaux, A. Boynard, L. Clarisse, M. George, J. Hadji-Lazaro, H. Herbin, D. Hurtmans, M. Pommier, A. Razavi, S. Turquety, C. Wespes, and P. F. Coheur. Monitoring of atmospheric composition using the thermal infrared

IASI/MetOp sounder. *Atm. Chem. Phys.*, 9: 6041–6054, 2009.

X. Fan, P. Goloub, J. L. Deuze, H. Chen, W. Zhang, D. Tanre, and Z. Li. Evaluation of PARASOL aerosol retrieval over North East Asia. *Rem. Sens. Env.*, 112, 2008. doi: 10.1016/j.rse.2007.06.010.

W. Schmutz, A. Fehlmann, G. Huelsen, P. Meindl, R. Winkler, G. Thuillier, P. Blattner, F. Buisson, T. Egorova, W. Finsterle, N. Fox, J. Groebner, J. F. Hochedez, S. Koller, M. Meftah, M. Meisonnier, S. Nyeki, D. Pfiffner, H. Roth, E. Rozanov, M. Spescha, C. Wehrli, L. Werner, and J. U. Wyss. The PREMOS/PICARD instrument calibration. *Metrologia*, 46, 2009. doi: 10.1088/0026-1394/46/4/S13.

G. Thuillier, T. Foujols, D. Bolsee, D. Gillotay, M. Herse, W. Peetermans, W. Decuyper, H. Mandel, P. Sperfeld, S. Pape, D. R. Taubert, and J. Hartmann. SOLAR/SOLSPEC: scientific objectives, instrument performance and its absolute calibration using a blackbody as primary standard source. *Sol. Phys.*, 257, 2009. doi: 10.1007/s11207-009-9361-6.

J. P. Vernier, J. P. Pommereau, A. Garnier, J. Pelon, N. Larsen, J. Nielsen, T. Christensen, F. Cairo, L. W. Thomason, T. Leblanc, and I. S. McDermid. Tropical stratospheric aerosol layer from CALIPSO lidar observations. *J. Geophys. Res.*, 114, 2009. doi: 10.1029/2009JD011946.

D. M. Winker, J. Pelon, J. A. Coakley Jr., S. A. Ackerman, R. J. Charlson, P. R. Colarco, P. Flamant, Q. Fu, R. M. Hoff, C. Kittaka, T. L. Kubar, H. Le Treut, M. P. McCormick, G. Megie, L. Poole, K. Powell, C. Trepte, M. A. Vaughan, and B. A. Wielicki. The CALIPSO mission, a global 3D view of aerosols and clouds. *Bull. Am. Meteo. Soc.*, 91, 2010. doi: 10.1175/2010BAMS3009.1.

The terrestrial ionosphere and its connections

Pierre-Louis Blelly (1) and the French community in ionospheric physics

(1) Institut de Recherche en Astrophysique et Planétologie, Toulouse, France

Abstract The ionosphere is a good tracer of the interactions between the Sun and the terrestrial environment, as it is connected to the different regions of the magnetospheric system and it is in strong interaction with the thermosphere. Our studies aim at taking advantage of this specificity to access the different levels of couplings within the Earth system in the frame of the scientific part of an international Space Weather program. For doing that we jointly use experimental facilities and complex numerical models of the ionospheric subsystem.

The community is strongly involved in studies aiming at understanding the key role of the thermosphere-ionosphere subsystem within the magnetospheric system, in the frame of Solar-Terrestrial connection programs. The activity of the community is based on a combined use of experiment facilities and numerical models, with clear scientific objectives related to the couplings at high latitudes and applications to the Space Weather. Moreover, our scientific interests evolve towards the couplings at low latitude (interhemispheric dynamics) and couplings with low and mid-altitude regions which may be significant contributors to the overall dynamics.

Experimentation

The instruments we base our studies on are basically EISCAT incoherent scatter radars, SuperDARN coherent scatter radars, satellites (DEMETER, Cluster) and optical instruments. However, the four-year period has been marked by the death of Jean-Paul Villain, the Principal Investigator of the French contribution to SuperDARN chain. This imposed us to reconsider our involvement in SuperDARN community and we decided to refocus our activity around Kerguelen radar. Moreover, France decided to withdraw from EISCAT association and our involvement is now restricted to the purchase of radar hours around dedicated campaigns. Beside this, a new optical instrument devoted to the measurement the polarity of the oxygen red line emission has been developed and deployed in the polar region (Svalbard) for joint campaigns with EISCAT-ESR radar.

These facilities are located at high latitudes, and our studies mainly deal with solar-wind / magnetosphere couplings. In particular, the penetration within the magnetosphere of particles and energy coming from the solar wind, observed at high altitude with Cluster, has been studied in term of ionospheric signatures in radar measurement, either on EISCAT or SuperDARN. Following this, a mapping at ionospheric level of the different regions of the magnetosphere has been handled. In connections with these couplings, we have made several studies on the dynamics of the ionospheric plasma:

- ULF waves, which are observed on ionospheric profiles and magnetometer radars at either local scales or global scales;
- relationships between convection and plasma field aligned transport in the vicinity of auroral arcs.

The red line emission is polarized because of the existence of a static magnetic field, and we were able to detect, for the first time this polarity, with the new optical instrument.

More recently, the eclipse au August 1st 2008 was a good opportunity to study the couplings of the ionospheric plasma with the atmosphere in the auroral and polar regions by using our numerical tools (Fig. 1).

Numerical models

Numerical models are important part of our contribution, as they help us in analyzing and interpreting the experimental data (see figure 1). We have developed a series of ionospheric model, the TRANSCAR family, which are intended to provide a very good insight of the ionospheric plasma dynamics, controlled by the couplings with the atmosphere and the magnetosphere.

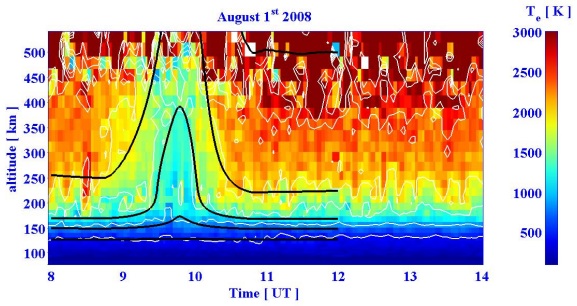

Figure 1: temporal profiles of the electron temperature at ESR during the eclipse period. The black lines are the contours between 500 and 3000 K (by step of 550 K) of our simulation-with TRANSCAR and should be compared to the same contours for the experiment (in white).

Two new models were built, one dedicated to the inclusion of the impact of energetic protons on the atmosphere and one dedicated the inter-hemispheric transport of plasma within the plasmasphere. Beside this, we also built a new model for the runaway electrons which are one of the energetic contributions of the ionosphere to the global system.

Space Weather activity

Space weather is the physical and phenomenological state of natural space environments which focus on the possible impacts on biological and technological systems. Our contribution to the Solar-Terrestrial physics is completely embedded in the scientific aspects of this large program. We made some efforts to provide some parameters, like proxies, characteristics of the magnetospheric system activity which may help to forecast the solar and non-solar driven perturbations that affect Sun-Earth system.

Low and mid-atmosphere couplings

There are more and more evidences that the couplings between the ionosphere and the middle and low atmosphere play a significant role in the dynamics of the Earth system. Thus, we decided to extend our studies to the low ionosphere (D region) where chemical processes can produce molecules (e.g. NOx) that can be transported to lower regions (in the stratosphere). In this perspective we are involved in TARANIS project which will study the couplings between thunderstorms and the magnetosphere.

References

P.-L. Blelly, D. Alcayde, and A. P. van Eyken. A new analysis method for determining polar ionosphere and upper atmosphere characteristics from ESR data: Illustration with IPY period. *J. Geophys. Res.*, 115, 2010. doi: 10.1029/2009JA014876.

G. Garcia and F. Forme. A kinetic model of the ionospheric return currents. *Geophys. Res. Lett.*, 36, 2009. doi: 10.1029/2009GL039972.

C. Hanuise, J. C. Cerisier, F. Auchere, K. Bocchialini, S. Bruinsma, N. Cornilleau-Wehrlin, N. Jakowski, C. Lathuillere, M. Menvielle, J.-J. Valette, N. Vilmer, J. Watermann, and P. Yaya. From the Sun to the Earth: impact of the 27-28 May 2003 solar events on the magnetosphere, ionosphere and thermosphere. *Ann. Geophys.*, 24:129–151, 2006.

T. Johansson, G. Marklund, T. Karlsson, S. Lileo, P.-A. Lindqvist, A. Marchaudon, H. Nilsson, and A. Fazakerley. On the profile of intense high-altitude auroral electric fields at magnetospheric boundaries. *Ann. Geophys.*, 24:1713–1723, 2006.

A. Kullen, S. Buchert, T. Karlsson, T. Johansson, S. Lileo, A. Eriksson, H. Nilsson, A. Marchaudon, and A. N. Fazakerley. Plasma transport along discrete auroral arcs and its contribution to the ionospheric plasma convection. *Ann. Geophys.*, 26:3279–3293, 2008.

C. Lathuillere and W. Kofman. A short review on the F1-region ion composition in the auroral and polar ionosphere. 37, 2006. doi: 10.1016/j.asr.2005.12.014.

C. Lathuillere and M. Menvielle. Comparison of the observed and modeled low- to mid-latitude thermosphere response to magnetic activity: Effects of solar cycle and disturbance time delay. *Adv. Spa. Res.*, 45, 2010. doi: 10.1016/j.asr.2009.08.016.

C. Lathuillere, M. Menvielle, A. Marchaudon, and S. Bruinsma. A statistical study of the observed and modeled global thermosphere response to magnetic activity at middle and low latitudes. *J. Geophys. Res.*, 113, 2008. doi: 10.1029/2007JA012991.

J. Lilensten, C. Simon, M. Barthelemy, J. Moen, R. Thissen, and D. A. Lorentzen. Considering the polarization of the oxygen ther-

mospheric red line for space weather studies. *Space Weather*, 4, 2006. doi: 10.1029/2006SW000228.

J. Lilensten, J. Moen, M. Barthelemy, R. Thissen, C. Simon, D. A. Lorentzen, O. Dutuit, P. O. Amblard, and F. Sigernes. Polarization in aurorae: A new dimension for space environments studies. *Geophys. Res. Lett.*, 35, 2008. doi: 10.1029/2007GL033006.

S. Lileo, G. T. Marklund, T. Karlsson, T. Johansson, P.-A. Lindqvist, A. Marchaudon, A. Fazakerley, C. Mouikis, and L. M. Kistler. Magnetosphere-ionosphere coupling during periods of extended high auroral activity: a case study. *Ann. Geophys.*, 26:583–591, 2008.

G. Lointier, T. D. de Wit, C. Hanuise, X. Vallieres, and J.-P. Villain. A statistical approach for identifying the ionospheric footprint of magnetospheric boundaries from SuperDARN observations. *Ann. Geophys.*, 26:305–314, 2008.

R. Lukianova, C. Hanuise, and F. Christiansen. Asymmetric distribution of the ionospheric electric potential in the opposite hemispheres as inferred from the SuperDARN observations and FAC-based convection model. *J. Atmo. Terr. Phys.*, 70, 2008. doi: 10.1016/j.jastp.2008.05.015.

A. Marchaudon, J.-C. Cerisier, J.-M. Bosqued, C. J. Owen, A. N. Fazakerley, and A. D. Lahiff. On the structure of field-aligned currents in the mid-altitude cusp. *Ann. Geophys.*, 24:3391–3401, 2006.

M. Menvielle, C. Lathuillere, S. Bruinsma, and R. Viereck. A new method for studying the thermospheric density variability derived from CHAMP/STAR accelerometer data for magnetically active conditions. *Ann. Geophys.*, 25: 1949–1958, 2007.

M. Messerotti, F. Zuccarello, S. L. Guglielmino, V. Bothmer, J. Lilensten, G. Noci, M. Storini, and H. Lundstedt. Solar Weather Event Modelling and Prediction. *Space Sci. Rev.*, 147, 2009. doi: 10.1007/s11214-009-9574-x.

Cluster's insights in solar wind-magnetosphere coupling

Aurélie Marchaudon

Laboratoire de Physique et Chimie de l'Environnement et de l'Espace, CNRS, Orléans

Abstract Despite more than 10 years spent in space, the four spacecraft Cluster mission is still making important progress on the understanding of the Earth's solar-wind magnetosphere coupling. The multi-point nature of this mission allows discriminating between temporal and spatial structures. Recent results include new insights on large-scale and small-scale properties of magnetopause reconnection, dynamics of polar cusp, polar cap and of its boundaries.

Reconnection process at the magnetopause

Magnetopause reconnection has long been recognized as the main process by which energy momentum and plasma can be transferred from the solar wind to the magnetosphere. The Cluster mission flying in tetrahedron configuration through the high-latitude magnetopause has improved our understanding of this region and of the reconnection process, especially when used in conjunction with other missions, such as the Chinese Double Star mission.

Berchem et al. [2008] have compared Cluster and Double Star magnetopause data to results of MHD model. They have been able to discriminate between anti-parallel and 'component' reconnection models; in the latter magnetic fields do not need to be strictly anti-parallel for reconnection to occur. Pitout et al. [2008] investigated properties of the magnetosheath at different altitudes with Cluster and Double Star showing that unlike predictions from gasdynamic modeling, the density is found lower near the nose of the magnetopause than further downstream.

Pitout et al. [2008] and Owen et al. [2008] also used the four-point measurement capability of Cluster to discriminate between sporadic reconnection signatures known as Flux Transfer Events (FTE) and magnetopause pressure pulses caused by solar wind/magnetosheath compressions. Owen et al. [2008] confirmed for the first time without ambiguity that specific magnetopause signatures, known as 'Crater' FTE, are caused by reconnection.

Magnetopause studies for very quiet and very disturbed solar wind conditions have also been possible with Cluster. Maggiolo et al. [2008] showed that very efficient magnetopause reconnection process can occur even during extremely low solar wind density conditions, explaining why the plasmasheet and magnetotail regions are maintained during such conditions. Dandouras et al. [2009] studied unusual dayside magnetosphere compression, penetration of high-energy particles in the magnetotail, and ring current development following Interplanetary Coronal Mass Ejections (ICME) shock arrival on the magnetopause.

Dynamics of the polar cusp

Cluster is also a powerful tool for studying polar cusp dynamics, region providing direct access to solar wind plasma into the magnetosphere via magnetopause reconnection process. When crossing the cusp at mid-altitude, the Cluster spacecraft adopt a string-of-pearl configuration following each other on the same orbit with a certain time delay (usually several minutes). With this configuration, temporal variations of the cusp precipitation can be studied and location of the magnetopause reconnection site with respect to Interplanetary Magnetic Field (IMF) variations can be inferred.

By means of statistical analysis, Pitout et al. [2006] studied the size and location of the polar cusp. Pitout et al. [2009] recently completed this study by investigating large-scale cusp morphology. They showed that the occurrence of clearly dispersed ion structures in the cusp, caused by magnetopause reconnection, is 48% and corresponds generally to stable IMF conditions. In all other cases, the cusp exhibits a more disturbed behaviour in terms of ion structures and generally correlates with variable or rotating IMF.

By studying evolution of cusp precipitation with the four Cluster spacecraft, Escoubet et al. [2008a,b] showed that the cusp responds quickly to IMF rotation causing generally a relocation

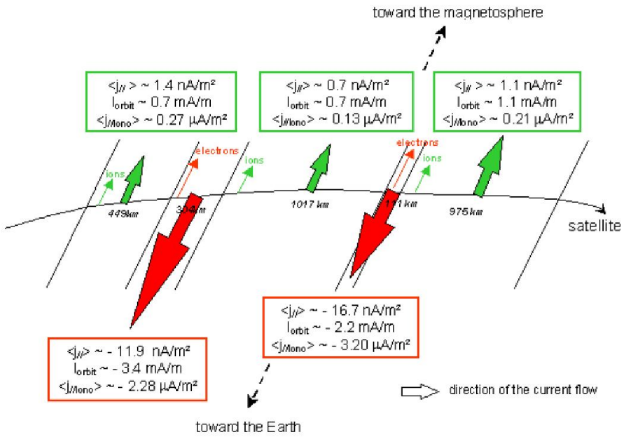

Figure 1: Summary sketch of the suggested current geometry for a polar cap crossing by northward IMF. The red (green) arrows point toward the Earth (magnetosphere) and represent the downgoing (upgoing) currents mostly carried by the electron beams (ion structures) [Teste et al., 2007].

of the magnetopause reconnection site. During the transition period between two different stable IMF orientations, particles coming from two distinct magnetopause reconnection sites are simultaneously observed.

Marchaudon et al. [2009] used a conjunction between Cluster, Double Star and ionospheric SuperDARN radars, to study properties of cusp reconnected flux tubes issued from magnetopause reconnection. Using a method develop in a previous paper [Marchaudon et al., 2006], they determined the transverse sizes (0.5-2 RE), the bean-shape like, the velocity (20-40 km.s-1) and the field-aligned current distribution (upward/downward current pair) of these flux tubes. They thus gained a complete picture of the flux tubes electrodynamics.

Electrodynamics of the polar cap and of its boundaries

Field-aligned electron and ion beams have long been observed in the auroral zones. On the other hand, polar cap mainly connected to the magnetospheric lobe region, has long been regarded as an almost void region, apart from weak ion outflows originating from the dayside region and transported anti-sunward with the solar wind flow.

Cluster, crossing the polar cap between 5 and 9 RE altitude, discovered complex particles signatures associated with broadband electrostatic emissions during northward IMF periods. The polar ionosphere suddenly appeared as a wide region of successive extended particle populations forming a complex electrodynamical circuit in the polar cap. Maggiolo et al. [2006] first identified ion outflows originating from the ionosphere and accelerated locally by potential drop as confirmed by their inverted-V shaped energy-time signatures. Teste et al. [2007] identified exactly between these ion outflow structures, narrow upward electrons beams with large fluxes, also escaping the ionosphere and responsible for broadband electrostatic emissions (Fig. 1). Teste et al. [2010] showed recently that these beams are likely to destabilize Langmuir waves and could be responsible for the appearance of electrostatic solitary waves above the polar cap.

A large set of phenomena occur at polar cap boundaries and can be observed by Cluster combined with ionosphere measurements (EISCAT radars, ground-based magnetometers, low-latitude spacecraft...). Aikio et al. [2008] observed zig-zag motion of the polar cap boundary (PCB) with a 30 minutes period during substorm late expansion phase. They proposed that the poleward motions of the PCB are produced by bursts of enhanced reconnection at the near-Earth neutral line (NENL) in the magnetotail. The subsequent equatorward motions of the PCB represent the recovery of the merging line towards the equilibrium state. Echim et al. [2009] studied a stable discrete auroral arc associated with fluxes of field-aligned accelerated electrons and ions at the interface of the polar cap. They compared Cluster and DMSP observations with a quasi-stationary magnetosphere-ionosphere coupling model. The matching data

and model results suggest a quasi-stationary field-aligned acceleration of auroral electrons and ions, probably associated with a convergent perpendicular electric field at the polar cap boundary.

References

A. T. Aikio, T. Pitkanen, D. Fontaine, I. Dandouras, O. Amm, A. Kozlovsky, A. Vaivdas, and A. Fazakerley. EISCAT and Cluster observations in the vicinity of the dynamical polar cap boundary. *Ann. Geophys.*, 26, 2008.

J. Berchem, A. Marchaudon, M. Dunlop, C. P. Escoubet, J. M. Bosqued, H. Reme, I. Dandouras, A. Balogh, E. Lucek, C. Carr, and Z. Pu. Reconnection at the dayside magnetopause: Comparisons of global MHD simulation results with Cluster and Double Star observations. *J. Geophys. Res.*, 113, 2008. doi: 10.1029/2007JA012743.

I. S. Dandouras, H. Reme, J. Cao, and C. P. Escoubet. Magnetosphere response to the 2005 and 2006 extreme solar events as observed by the Cluster and Double Star spacecraft. *Adv. Spa. Res.*, 43, 2009. doi: 10.1016/j.asr.2008.10.015.

M. M. Echim, R. Maggiolo, M. Roth, and J. De Keyser. A magnetospheric generator driving ion and electron acceleration and electric currents in a discrete auroral arc observed by Cluster and DMSP. *Geophys. Res. Lett.*, 36, 2009. doi: 10.1029/2009GL038343.

C. P. Escoubet, J. Berchem, J.-M. Bosqued, K. J. Trattner, M. G. G. T. Taylor, F. Pitout, H. Laakso, A. Masson, M. Dunlop, I. Dandouras, H. Reme, A. N. Fazakerley, and P. Daly. Effect of a northward turning of the interplanetary magnetic field on cusp precipitation as observed by Cluster. *J. Geophys. Res.*, 113, 2008a. doi: 10.1029/2007JA012771.

C. P. Escoubet, J. Berchem, J.-M. Bosqued, K. J. Trattner, M. G. G. T. Taylor, F. Pitout, C. Vallat, H. Laakso, A. Masson, M. Dunlop, H. Reme, I. Dandouras, and A. Fazakerley. Two sources of magnetosheath ions observed by Cluster in the mid-altitude polar cusp. *Adv. Spa. Res.*, 41, 2008b. doi: 10.1016/j.asr.2007.04.031.

R. Maggiolo, J.-A. Sauvaud, D. Fontaine, A. Teste, E. Grigorenko, A. Balogh, A. Fazakerley, G. Paschmann, D. Delcourt, and H. Reme. A multi-satellite study of accelerated ionospheric ion beams above the polar cap. *Ann. Geophys.*, 24, 2006.

R. Maggiolo, J. A. Sauvaud, I. Dandouras, E. Luceck, and H. Reme. A case study of dayside reconnection under extremely low solar wind density conditions. *Ann. Geophys.*, 26, 2008.

A. Marchaudon, J.-C. Cerisier, J.-M. Bosqued, C. J. Owen, A. N. Fazakerley, and A. D. Lahiff. On the structure of field-aligned currents in the mid-altitude cusp. *Ann. Geophys.*, 24, 2006.

A. Marchaudon, J.-C. Cerisier, M. W. Dunlop, F. Pitout, J.-M. Bosqued, and A. N. Fazakerley. Shape, size, velocity and field-aligned currents of dayside plasma injections: a multi-altitude study. *Ann. Geophys.*, 27, 2009.

C. J. Owen, A. Marchaudon, M. W. Dunlop, A. N. Fazakerley, J.-M. Bosqued, J. P. Dewhurst, R. C. Fear, S. A. Fuselier, A. Balogh, and H. Reme. Cluster observations of "crater" flux transfer events at the dayside high-latitude magnetopause. *J. Geophys. Res.*, 113, 2008. doi: 10.1029/2007JA012701.

F. Pitout, C. P. Escoubet, B. Klecker, and H. Reme. Cluster survey of the mid-altitude cusp: 1. size, location, and dynamics. *Ann. Geophys.*, 24, 2006.

F. Pitout, M. W. Dunlop, A. Blagau, Y. Bogdanova, C. P. Escoubet, C. Carr, I. Dandouras, and A. Fazakerley. Coordinated Cluster and Double Star observations of the dayside magnetosheath and magnetopause at different latitudes near noon. *J. Geophys. Res.*, 113, 2008. doi: 10.1029/2007JA012767.

F. Pitout, C. P. Escoubet, B. Klecker, and I. Dandouras. Cluster survey of the mid-altitude cusp - Part 2: Large-scale morphology. *Ann. Geophys.*, 27, 2009.

A. Teste, D. Fontaine, J.-A. Sauvaud, R. Maggiolo, P. Canu, and A. Fazakerley. CLUSTER observations of electron outflowing beams carrying downward currents above the polar cap by northward IMF. *Ann. Geophys.*, 25, 2007.

A. Teste, D. Fontaine, P. Canu, and G. Belmont. Cluster observations of outflowing electron distributions and broadband electrostatic emissions above the polar cap. *Geophys. Res. Lett.*, 37, 2010. doi: 10.1029/2009GL041593.

Comité National Français de Géodésie et Géophysique

French National Committee of Geodesy and Geophysics

RAPPORT QUADRIENNAL DU CNFGG A l'UGGI

QUADRENNIAL REPORT OF CNFGG TO IUGG

SECTION 5 – METÉOROLOGIE ET SCIENCES DE L'ATMOSPHÈRE

SECTION 5 – METEOROLOGY AND ATMOSPHERIC SCIENCES

Cette section n’a pas fourni de rapport au 01/07/2011

This section has not provided report on 01/07/2011

Comité National Français de Géodésie et Géophysique

French National Committee of Geodesy and Geophysics

RAPPORT QUADRIENNAL DU CNFGG A l'UGGI

QUADRENNIAL REPORT OF CNFGG TO IUGG

SECTION 6 – SCIENCES HYDROLOGIQUES

SECTION 6 – HYDROLOGICAL SCIENCES

Cette section n’a pas fourni de rapport au 01/07/2011

This section has not provided report on 01/07/2011

Comité National Français de Géodésie et Géophysique

French National Committee of Geodesy and Geophysics

RAPPORT QUADRIENNAL DU CNFGG A l'UGGI

QUADRENNIAL REPORT OF CNFGG TO IUGG

SECTION 7 – SCIENCES PHYSIQUES DE L'OCÉAN

SECTION 7 – PHYSICAL SCIENCES OF THE OCEAN

Rapport quadriennal de la Section VII Sciences physiques des Océans

pour le congrès IUGG 2011

Contenu

Rapport quadriennal IUGG de la Section 7 "Sciences Physiques de l'Ocean"

Observations of the ACC across the Kerguelen Plateau: TRACK project

PI: Young-Hyang Park (yhpark@mnhn.fr)
LOCEAN/DMPA, Muséum National d'Histoire Naturelle, Paris, France

Rational and objectives

The Kerguelen Plateau is the largest near-meridional submarine topographic obstacle, diverting the Antarctic Circumpolar Current (ACC) over a great distance between the subtropical and subpolar regions. It acts as a natural barrier for closing the eastern boundary of the Weddell Gyre to the west and developing the western boundary of the Australian-Antarctic Gyre to the east of the plateau, thus providing an important meridional pathway for the equatorward evacuation of transformed subpolar water masses. Despite its indisputable role in the ACC dynamics and the Southern Ocean meridional circulation, our knowledge on the physics and dynamics of the ACC across the Kerguelen Plateau has been seriously hampered until recently due to lacking of high-quality oceanographic observations. The TRACK (Transport across the Kerguelen Plateau) cruises carried out as part of a French contribution to the International Polar Year activities, were designed to measure directly the top-to-bottom physical properties, currents and transport over the Kerguelen Plateau, especially across the Fawn Trough and the Deep Western Boundary Current (DWBC) on the eastern flank of the southern plateau.

TRACK cruises and preliminary results

In February-March 2009 closely-spaced, full-depth hydrographic and direct current measurements in the Fawn Trough area were made during the TRACK cruise (Chief Scientist: Y.-H. Park) on R/V Marion Dufresne II. This cruise occupied in particular a near-meridional section across the Fawn Trough and repeated the western boundary segment of the WOCE I8S section at 58°S (Fig. 1). Three lines of current meter mooring with a total of 12 current meters were maintained for about 1 year across the Southern ACC Front (SACCF), which were recovered in January 2010 during the TRACK recovery cruise (Chief Scientist: F. Vivier). The preliminary results from the 2009 TRACK cruise (Park et al., 2009) are summarised below, while the velocity time series data from recovered current meters are under analysis as part of a thesis work.

Vertical profiles of cross-track lowered acoustic Doppler current profiler (LADCP) velocities and corresponding transport across the western (SACCF) and southern (DWBC) sections are shown in Figure 2. In the western section most of the eastward flow is tightly concentrated in the Fawn Trough, with the strongest flow of 0.6 m s-1 at the surface decreasing to 0.3 m s-1 at 1000 m, below which the velocity is nearly constant reaching >0.2 m s-1 at 2000 m, indicating that both the baroclinic and barotropic components of current are equally important. A secondary eastward flow branch with a depth-averaged velocity on the order of 0.2 m s-1 is observed on the near-shore slope just south of the Heard/McDonald Islands. The net transport across this 750 km-long western section amounts to 50 Sv (1 Sv = 106 m3 s-1) northeastward, 43 Sv of which are concentrated at the SACCF and 6 Sv immediately south of the Heard/McDonald Islands. In the southern section the northwestward flowing DWBC is highly barotropic and mostly confined within a narrow (~75 km) continental slope. It is also characterized by a bottom-intensified flow, with the highest velocity >0.3 m s-1 being found at the bottom at station 48. The total transport of the DWBC amounts to 43 Sv, which is largely compensated by a poleward recirculation transport of 34 Sv in the offshore area.

The TRACK cruise has permitted us to evaluate for the first time reliable transport values of different ACC branches crossing the Kerguelen Plateau (Fig. 3). Including ~2 Sv inferred at the Polar Front (PF) branch south of the Kerguelen Islands, the net ACC transport to the south of the islands amounts to 58 Sv: 43 Sv at the SACCF passing through the Fawn Trough; 6 Sv south of the Heard/McDonald Islands; 7 Sv at the Southern Boundary (SB) of ACC through the northern Princess Elizabeth Trough. The latter 7 Sv was obtained by considering only those stations in the southern section where the bottom water has a temperature >0.1°C, while the major component (36 Sv) of the DWBC with a bottom temperature <0.1°C should be fed by the northward turning of the Antarctic Slope Current along the western limb of the cyclonic subpolar gyre. According to previous work, the ACC main branch associated with the Subantarctic Front (SAF) should carry 89-94 Sv north of the Kerguelen Islands and ~6 Sv at the PF just east of the islands. Combining these with the TRACK transports sums up to 147-152 Sv as the total ACC transport in the Kerguelen area, which are not significantly different from the 147±10 Sv at 140°E south of Australia and the Drake Passage transport of 137±8 Sv augmented by 10-15 Sv of the Indonesian Throughflow.

Reference

PARK Y.-H., VIVIER F., ROQUET F. & KESTENARE E., 2009. - Direct observations of the ACC transport across the Kerguelen Plateau, Geophys. Res. Lett., 36: L18603, doi:10.1029/2009GL039617.

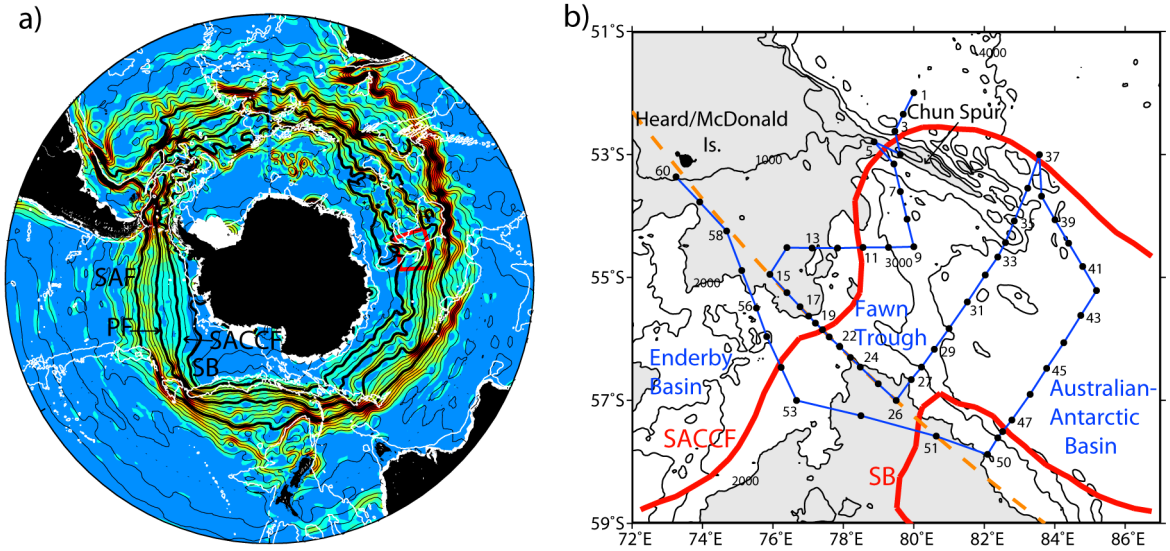

Fig.1_Park. (a) Surface streamlines from the altimetry-derived mean dynamic height, with bold streamlines standing for four circumpolar fronts and a red box for the TRACK cruise area. (b) the 2009 TACK cruise map showing the grid of 60 CTD stations, with two southernmost circumpolar fronts being superimposed. A dotted line is the Jason altimeter ground track #94. Adapted from Park et al. (2009).

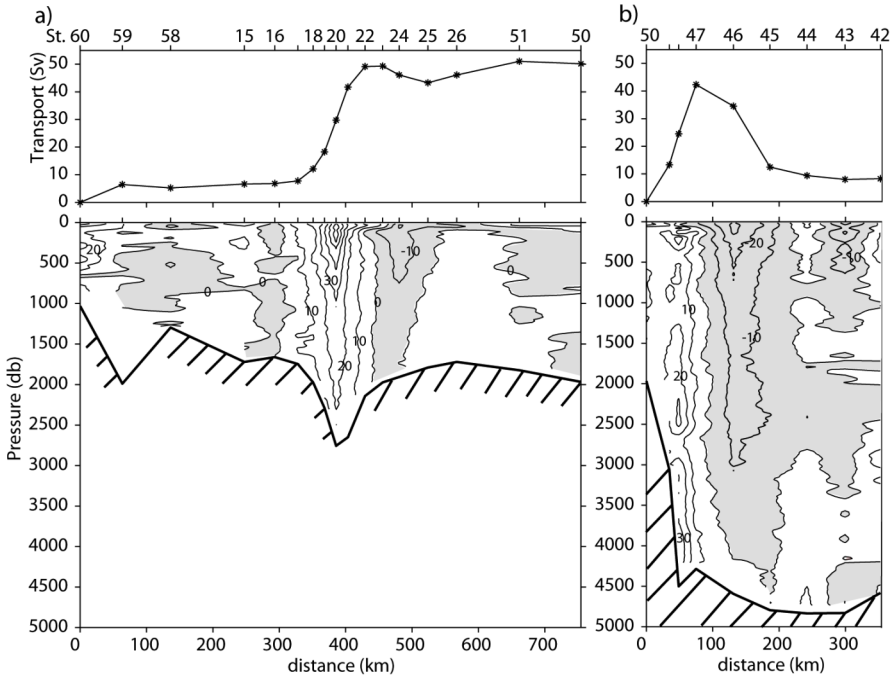

Fig. 2_Park. Vertical profiles of cross-track LADCP velocities and cumulative top-to-bottom transport in the (a) western (Fawn Trough) and (b) southern (DWBC) sections. Adapted from Park et al. (2009).

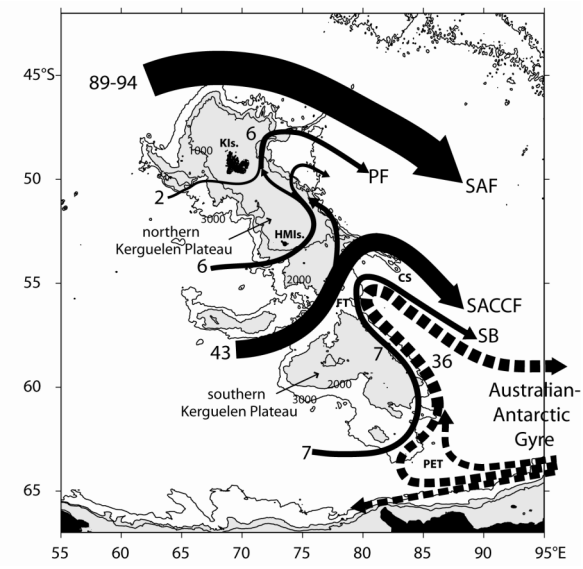

Fig. 3_Park. Schematic of major pathways and transports (in Sv) of the ACC system (bold continuous lines) and DWBC of the Australian-Antarctic Gyre (bold discontinuous lines). Adapted from Park et al. (2009).

Figure captions

Fig.1_Park. (a) Surface streamlines from the altimetry-derived mean dynamic height, with bold streamlines standing for four circumpolar fronts and a red box for the TRACK cruise area. (b) the 2009 TACK cruise map showing the grid of 60 CTD stations, with two southernmost circumpolar fronts being superimposed. A dotted line is the Jason altimeter ground track #94. Adapted from Park et al. (2009).

Fig. 2_Park. Vertical profiles of cross-track LADCP velocities and cumulative top-to-bottom transport in the (a) western (Fawn Trough) and (b) southern (DWBC) sections. Adapted from Park et al. (2009).

Fig. 3_Park. Schematic of major pathways and transports (in Sv) of the ACC system (bold continuous lines) and DWBC of the Australian-Antarctic Gyre (bold discontinuous lines). Adapted from Park et al. (2009).

The DRAKE project - Experimental aims and design

Christine Provost

The DRAKE project is a recently concluded experiment consisting of in situ measurements made over a period of about 3 years (February 2006 to April 2009), which are tightly coupled to satellite altimetry (TOPEX/POSEIDON and Jason). A major goal of DRAKE is to attempt to combine in situ current meter observations with simultaneous satellite data from Jason to gain a better understanding of the relationship between sea surface height (SSH) and volume transport. The measurement array consisted of 10 subsurface current meter moorings deployed below Jason track 104, with individual moorings located at altimeter crossover points (Fig. 1). High resolution hydrography and LADCP measurements were made on the cruises that serviced the moorings [Provost et al., 2011]. All cruises were performed from R.V. Polarstern. A total of 5 full-depth hydrographic sections were performed.

DRAKE early results

Early results from analyses of satellite data and the Drake hydrographic data are summarized below, while the time series from the moorings are under analysis as parts of two Ph.D. thesis.

The altimetric time-series documented the long-term trends in sea surface height, the recurrence of major frontal meanders and statistical links between them (Barré et al., 2011). Trends are not homogeneous in Drake Passage, rather they change sign, suggesting a regional effect caused by the complicated bathymetry and geometry (Fig. 2). Topography favors the recurrence of some meanders and eddies in specific spots in Drake Passage. For example a dipole occurring with a close to annual periodicity is observed at the entrance to DP over the Phoenix Antarctic Ridge (PAR) and corresponds to adjacent meanders of the SAF and PF (Barré et al., 2011) (Fig. 3). An anticyclonic meander of the PF was found to be recurrent over the Ona sea floor depression (OSD) to the northwest of the Ona Basin (54°W, 58°S) and constitutes an important element of the cyclonic recirculation in the Ona Basin (Barré et al., 2008).

Barre et al. [2011] used isolines of absolute dynamic topography from satellite altimetry data to map out locations of fronts and eddies, providing a temporal and spatial context for the 2006 DRAKE mooring deployment cruise. Multiple branches of ACC fronts were observed to merge into single jets in the narrowest part of the passage, with two branches of the SAF merging at about 61°W and three branches of the PF merging over the Shackleton Fracture Zone (SFZ) (Fig. 4 a and b). The SACCF branches could also be traced using altimetry. The agreement between the location of the frontal branches and eddies detected by altimetry and the patterns observed in sea surface temperature and ocean color is remarkable in spite of the differences in spatial and temporal resolution (Fig. 4 c, d, e). The crest of the SFZ constitutes a barrier in the south of DP, causing the two SACCF branches to separate by about 400 km, creating sheltered conditions in partial isolation from the ACC, while promoting an active recirculation region in the Ona Basin (Fig. 4 c, d, e). This recirculation, marked by cyclonic eddies carrying cold fresh and oxygenated water from south of the Southern Boundary of the ACC (Fig. 4 c, d, e), causes effective ventilation of the whole Circumpolar Deep Water (CDW) density range (Provost et al., 2011).

The 2006 cruise comprised a hydrographic section under Jason-1 track 104 repeated within 3 weeks, providing a unique opportunity to document full depth in situ variability at about a 10-day interval. Between the two occupations, the contributions of frontal meanders and eddies to the total volume transport changed notably, although the net transport changed by only 10% and agreed within confidence limits with prior WOCE and ISOS estimates [Renault et al., 2011]. Due to high quality of the data and a fine horizontal resolution, transport was estimated (143 Sv) with the best accuracy ever achieved of 7-10 Sv.

Considerable differences in properties between the 10-day-apart sections are observed throughout the whole water column with values as high as 0.2°C in temperature, 0.01 in salinity, 0.03 kg.m-3 in neutral density and 10 μmol.kg-1 in dissolved-oxygen concentration found below a depth of 3000 m [Provost et al., 2011; Sudre et al., 2011]. Only part of the differences is attributable to frontal or eddy displacements along the section. The other part results from the spatial heterogeneity of water properties upstream the section and the funnelling of the flow due to the topographic constraints of the Shackleton Fracture Zone (SFZ). The considerable short-term differences in water properties in rather large-scale structures that cannot be accounted for by frontal motions along the section, call for caution when interpreting differences in hydrographical properties obtained by oceanographic cruises that are years apart in terms of climatic signals.

References:

Barré N., C. Provost, N. Sennéchael, J. Hak Lee, 2008: Circulation in the Ona Basin, southern Drake Passage. J. Geophys. Res., 113, doi:10.1029/2007JC004549

Barré N., C. Provost, A. Renault, N. Sennéchael, 2011: Mesoscale activity in Drake Passage during the January-February 2006 cruise: a satellite perspective. Deep Sea Res., Part II, Topical Studies in Oceanography (in press)

Provost C., A. Renault, N. Barré, N. Sennéchael, V. Garçon, J. Sudre and O. Huhn, 2011: Two repeat crossings of Drake Passage in austral summer 2006: short term vatiations and evidence for considerable ventilation of intermediate and deep waters. Deep Sea Res., Part II, Topical Studies in Oceanography.

Renault A., C. Provost, N. Sennéchael, N. Barré and A. Kartavtseff, 2011: Two LADCP surveys in the Drake Passage in 2006: transport estimates. Deep Sea Res., Part II, Topical Studies in Oceanography, (in press).

Sudre J., V. Garçon, C. Provost, N. Sennéchael, O. Huhn, and M. Lacombe, 2011: Short-term variations of deep water masses in Drake Passage revealed by a multiparametric analysis of the ANT-XXIII/3 bottle data Deep Sea Res., Part II, Topical Studies in Oceanography, (in press).

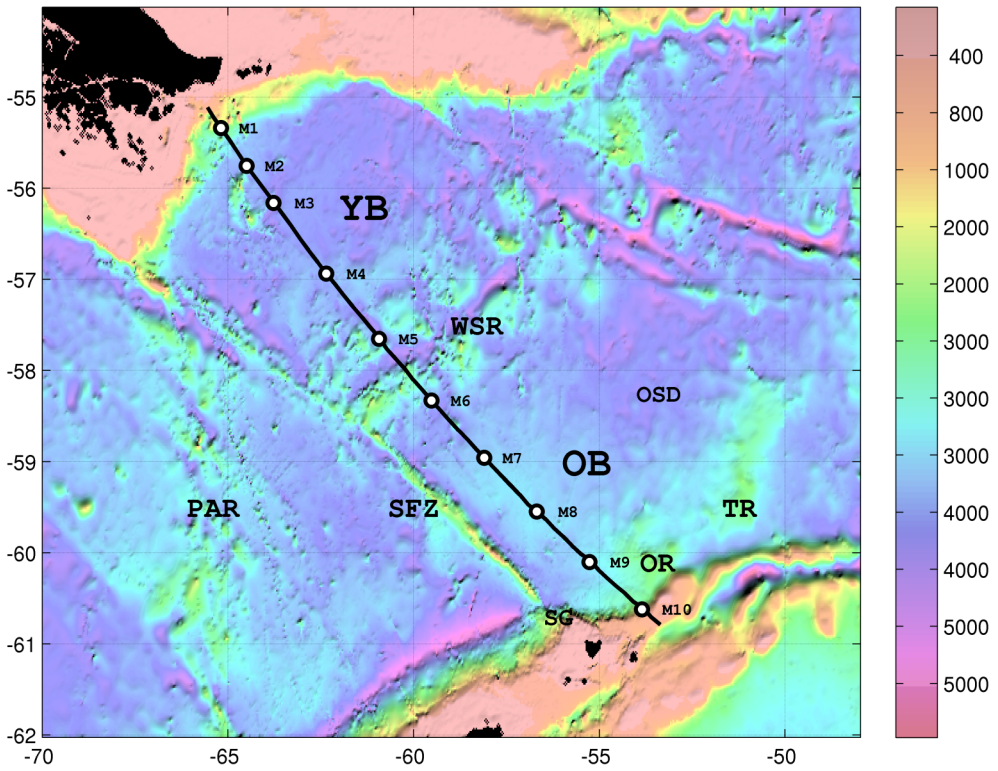

Figure 1: Location of the 10 Drake current meter moorings M1 through M10)along Jason ground track #104. Background is bathymetry in meters. Major bathymetric features are labeled: YB Yaghan Basin, OB Ona Basin, PAR: Phoenix Antarctic Ridge, SFZ: Shackleton Fracture Zone, WSR: West Scotia Ridge, OSD: Ona Sea floor Depression,.

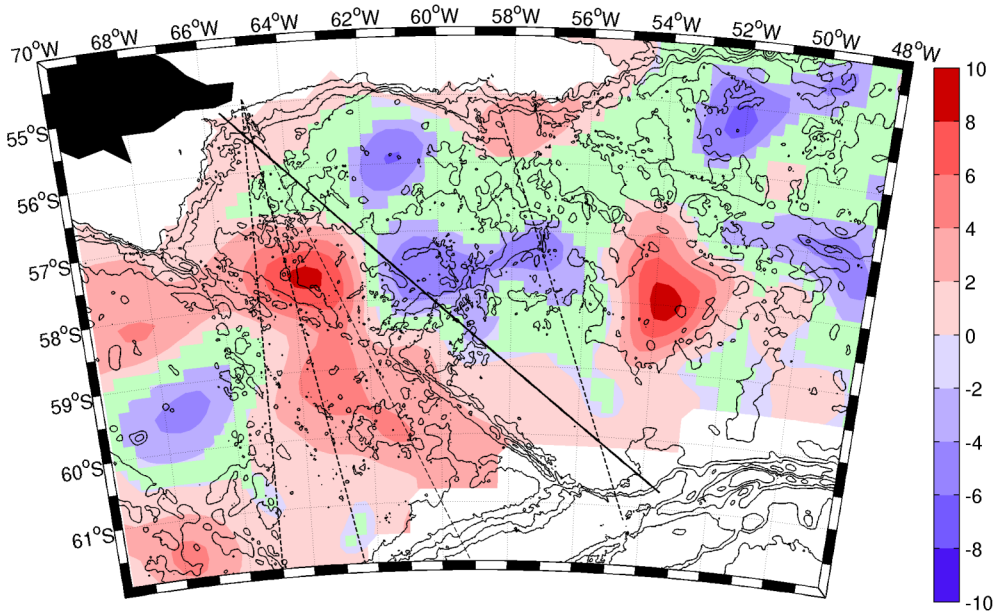

Figure 2: Linear trends in dynamic topography (mm per year) from January 1993 to December 2009. The significance of the trend was computed using a two-sided Student t-test with a confidence limit of 99%. Areas where the trend is not significant are colored in green. White areas correspond to the regions where the time series are incomplete and the data from over the continental slope (depth less than 500 m) are disregarded. Black contours represent the bathymetry between 4000 m and 1000m with contour intervals of 500 m. The black diagonal line indicates the Jason track 104. Black dashed lines represent XBT surveys from the US Antarctic supply vessel (west of track 104) and the repeat hydrographic section SR1b (east of track 104). (updated from Barré et al, 2011).

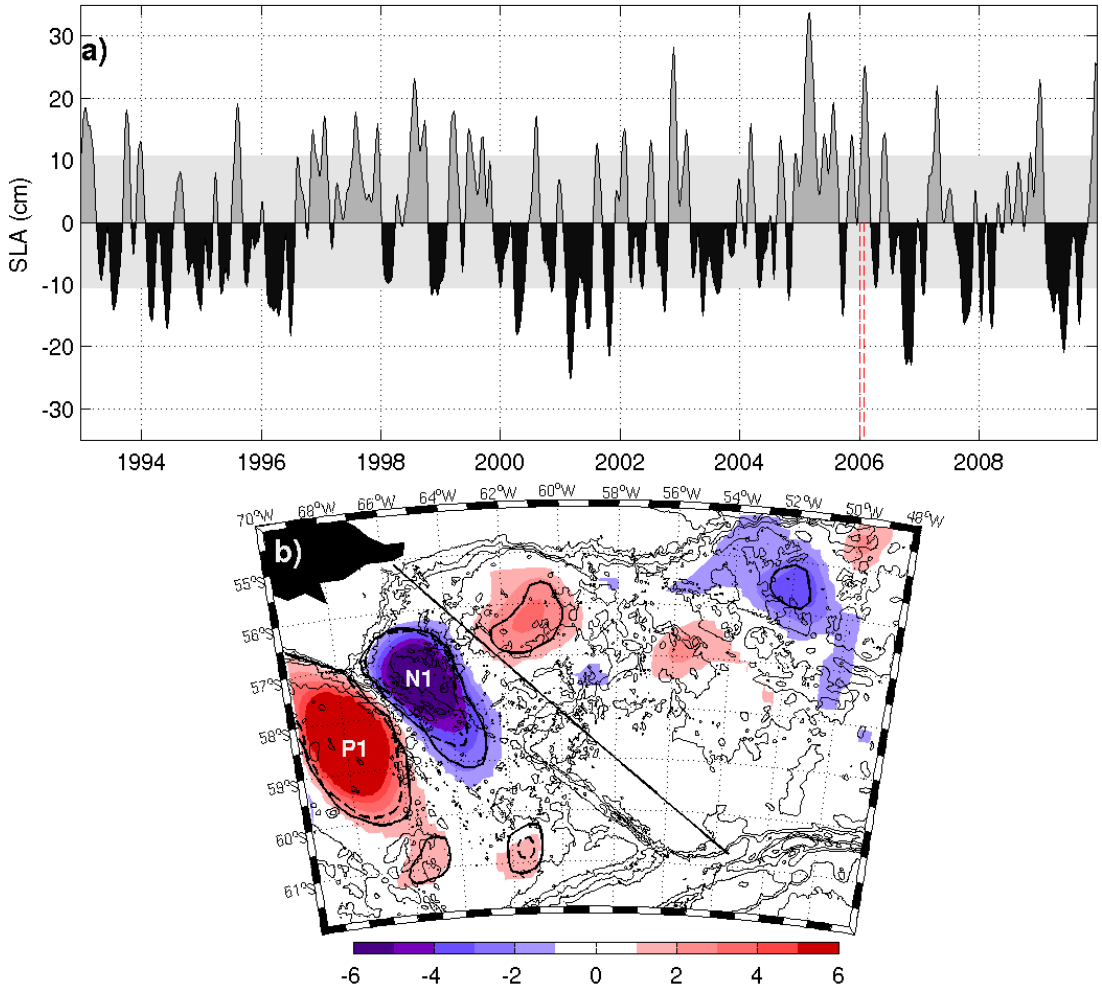

Figure 3:

a Time series of sea level anomaly (SLA) over a 1°x1° box centered at 68°W and 58.5°S (location P1). The linear trend has been removed.

b Regression of SLA, in Drake Passage, on the normalized time-series in Fig.3a. Solid black contours represent the correlation at the 90% confidence level; dashed black contours represent the 95% confidence level. The regression map suggests that the strong anomaly (P1) on the western side of the PAR can be associated with an anomaly of the opposite sign (N1) on the eastern side of the PAR. Thin black lines are bathymetry isobaths (2000, 3000 and 4000m). (updated from Barré et al., 2011)

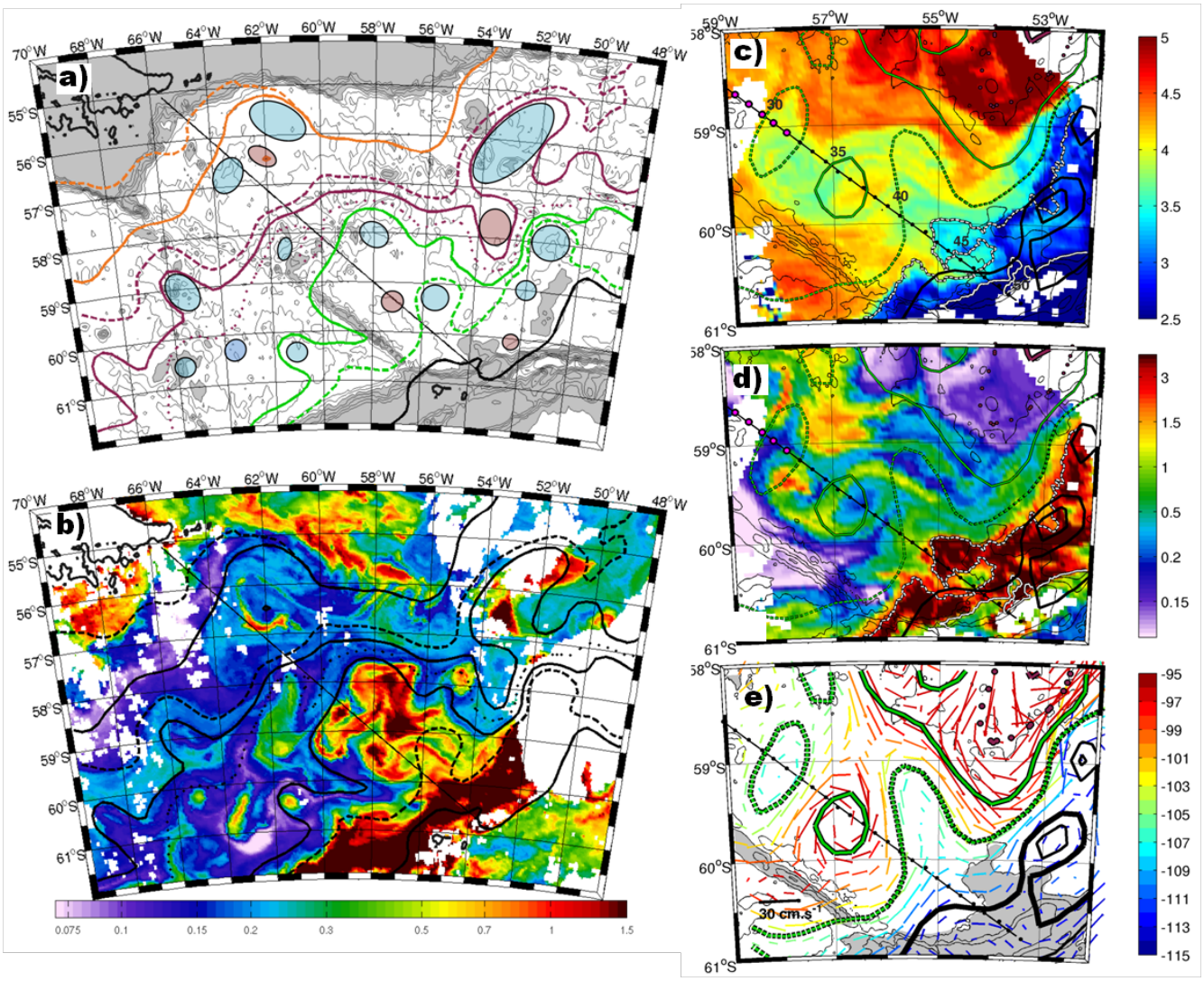

Figure 4:

a Schematic of the frontal branch and eddy location during the ANT-XXIII/3 cruise period derived from altimetry (composite map from 15 to 21 January 2006). SAF branches in orange; PF branches in purple; SACCF branches in green; and SB, in black. Blue patches are the major cyclonic eddies and red patches are the major anticyclonic eddies.

b One-week (17-24 January 2006) composite image of chlorophyll-a concentration (mg.m-3) from MODIS. Black contours are the branches of the ACC fronts and eddies like in a.

c, d, e :Satellite views of the Ona Basin late January 2006:

c: Sea surface temperature (°C) from 22 January 2006 (MODIS). Superimposed are the front and eddy locations derived from the 7-day composite altimetry map centered on January 25: PF-S (purple dotted line); SACCF-N (green solid line), SACCF-S (green dashed line); and SB (black line). The white dotted line is the 2.36 mg.m-3 isoline in Chlorophyll-a concentration and the continuous white line the northern limit to surface waters colder than 2.3°C.

d: Chlorophyll-a concentration (mg.m-3) from 22 January 2006 (MODIS). Contours like in c.

e: Surface geostrophic velocity field derived from the 7-day composite map of altimetric absolute dynamic topography centered on January 25. The color code indicates absolute dynamic topography values (in centimeters). Schematics of the front and eddy locations correspond to the date of the map (same color code as in c and d).

On all maps, thin black contours represent the bathymetry between 4000m and 1000m with contour intervals of 500m. Bottom depths shallower than 3000 m are shaded in grey. The black diagonal line indicates the Jason track 104. (adapted from Provost et al., 2011)

The OVIDE Project
Documenting and understanding the inter annual to decadal variability of the North Atlantic Subpolar gyre

Herlé Mercier, Pascale Lherminier, Nathalie Daniault, Virginie Thierry, Bruno Ferron, Thierry Huck
Laboratoire de Physique des Océans, CNRS, Ifremer, IRD, UBO, Plouzané, France

Since 2002, the Ovide project occupies every other year, in June-July, the A25 hydrographic section between the southern tip of Greenland at 60°N and Portugal at 40°N (Figure 1). This is a repeat of a line that was previously occupied during the International Geophysical year and, in the framework of the Fourex project, in September 1997. The Ovide project is a contribution to CLIVAR. During each cruise, CTDO2 and L-ADCP measurements are conducted from the surface down to the sea-floor at about 95 hydrographic stations and VM-ADCP is running during all cruises. Nutrients, CFCs, pH and alkalinity are measured from water samples obtained from the 28 bottle rosette. The Ovide cruises also contributes to maintaining the Argo array by deploying ~15 floats during each cruise. The cruises are a collaborative work with P. Morin (station biologique de Roscoff, France) and A. Rios and F. Perez (IIM Vigo, Spain). We summarize below one of the results obtained from the analysis of the Ovide data set that was complemented by a reanalysis of Fourex.

For the first time in the subpolar North Atlantic, a large variability in the amplitude of the meridional overturning circulation (MOC) and the associated heat flux (HF) has been documented. Estimates are based on an inverse model analysis of the Ovide and Fourex hydrographic sections (Lherminier et al., 2007, Lherminier et al. 2010, Gourcuff et al. 2011). Figure 2 shows that across the Fourex/Ovide hydrographic section the main balance in terms of transport is between the North Atlantic Current (NAC, $\sigma 1 < 32.1$), east of the subarctic front (SAF) and the net transport of dense water ($\sigma 1 > 32.1$) west of the SAF. This balance defines the MOC and shows that the NAC transport variability is a good proxy of the MOC variability. Focussing now on the MOC, the maximum amplitudes were observed in September 1997 (19 Sv and 0.69 PW for the MOC and the HF, respectively) and the minimum amplitudes were observed in June 2006 (11 Sv and 0.29 PW for the MOC and the HF). Values for 2002, 2004 and 2008 are in between. Although it is tempting to relate the decrease in the MOC amplitude between Fourex and Ovide 2006 to the spin-down of the subpolar gyre that has been reported by Hakkinen and Rhines (2009), it should be stressed here that those measurements quantify the variability of the MOC and associated heat flux but the associated time scales have still to be determined. For instance, Daniault et al. (2011) showed from an analysis of a current meter array in the East Greenland Irminger Current that at the time of the Ovide 2006 the transport of this current, which is an essential component of the MOC, reached a minimum that lasted for a few weeks, associated with a relatively weak wind stress curl in the Irminger Gyre (as compared to the 20-year average).

Références

Daniault, N., P. Lherminier, H. Mercier, 2011: Circulation and transport at the south east tip of Greenland. J. Phys. Oceanogr., in press.

Gourcuff, C., P. Lherminier, H. Mercier, P. Y. LeTraon, 2011: Altimetry combined with hydrography for ocean transport estimation. J. Atmosph. Ocean. Tech., submitted.

Hakkinen, S., P. Rhines, 2004: Decline of the subpolar North Atlantic Circulation during the 1990's. Science, 304, 555-559.

Lherminier, P., H. Mercier, C. Gourcuff, M. Alvarez, S. Bacon, C. Kermabon, 2007: Transports across the 2002 Greenland-Portugal Ovide section and comparison with 1997. J. Geophys. Res. Oceans., 112, C07003, doi:10.1029/2006JC003716.

Lherminier, P. H. Mercier, T. Huck, C. Gourcuff, F. F. Perez, P. Morin, A. Sarafanov, 2010: The Atlantic Meridional Overturning Circulation and the subpolar gyre observed at the A25-OVIDE section in June 2002 and 2004. Deep Sea Res. I, doi:10.1016/j.dsr.2010.07.009.

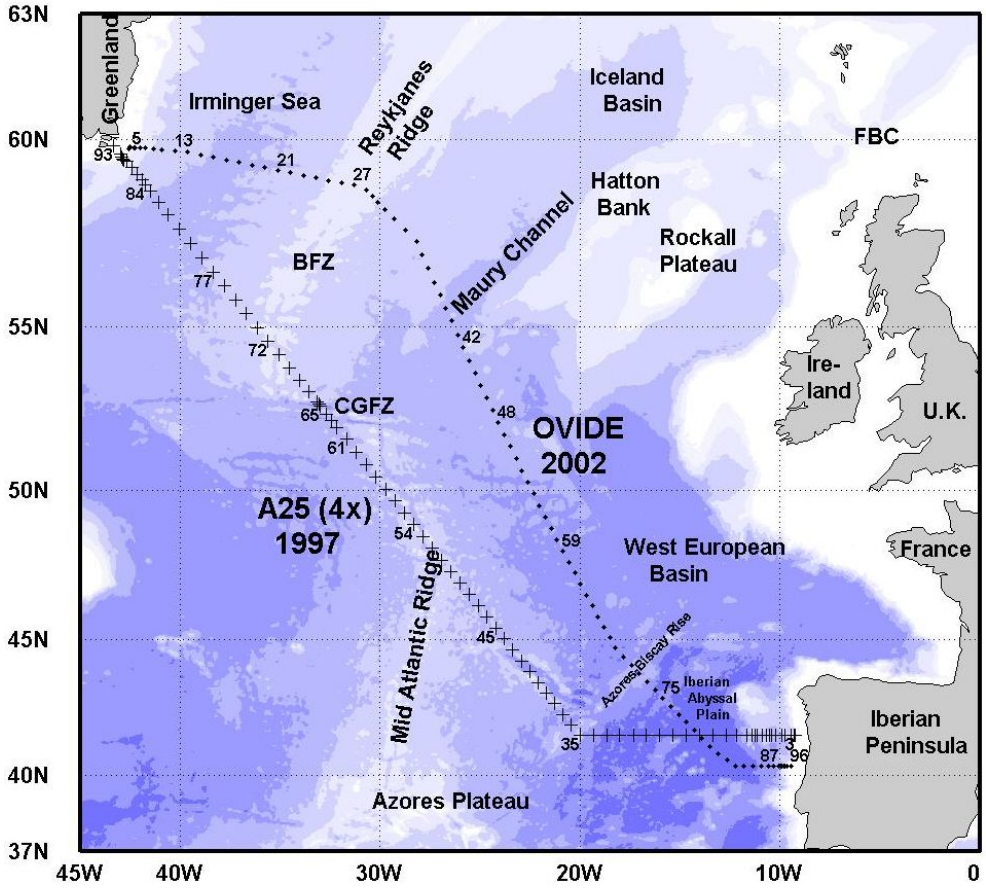

Figure 1: The Fourex (1997) and the Ovide (2002, 2004, 2006, 2008, 2010) hydrographic lines

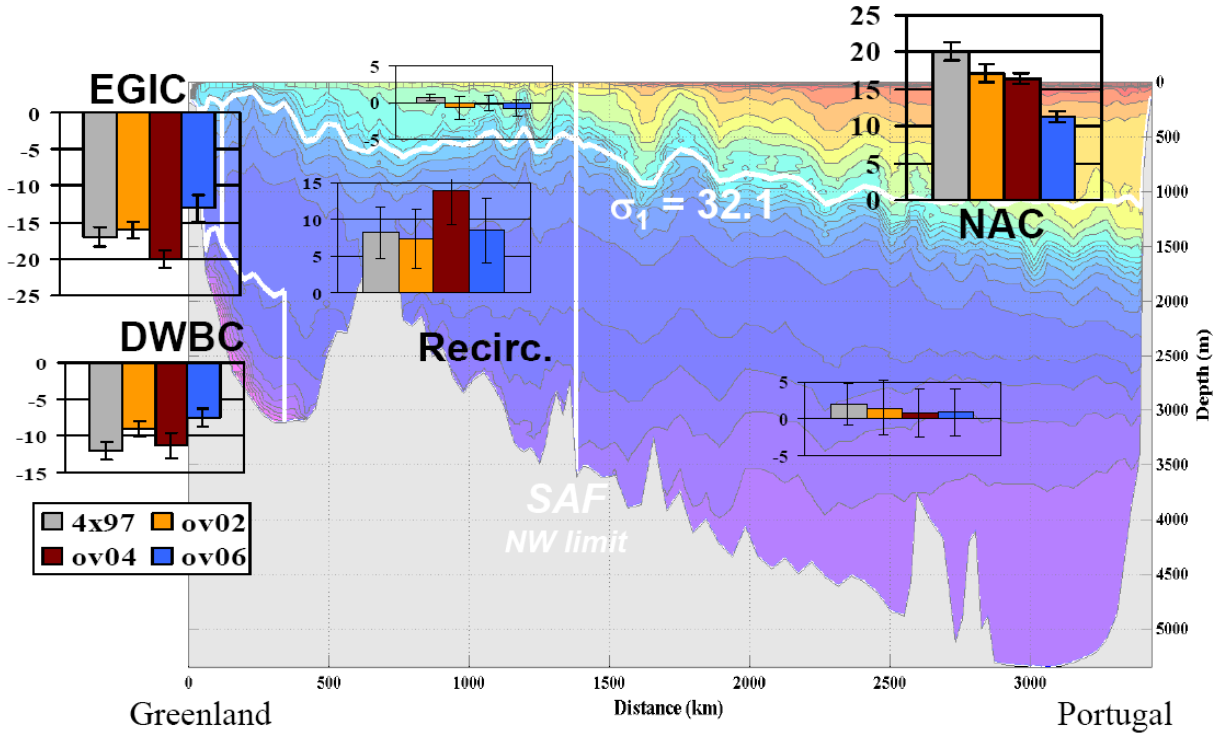

Figure 2 : Transport variability in Sv (1 Sv = 106 m3 s-1) contributing to the MOC obtained from an inverse model analysis of Fourex (1997) and OVIDE (2002, 2004, 2006) hydrographic sections. Northward transports are positive. EGIC : East-Greenland Irminger Current ; DWBC : Deep Western Bourndary Current ; Recirc. : Deep recirculation in the Island basin and the eastern Irminger Sea; NAC: North Atlantic Current. SAF: Sub-arctic front. The σ1 = 32.1 isopycnal is the limit between the upper and lower limbs of the MOC.

Ocean fine scales – micro-scales horizontal and vertical mixing

Gilles Reverdin (LOCEAN, Paris), Pascale Bouruet-Aubertot (LOCEAN, Paris), Bruno Ferron (LPO, Brest), Louis Marié (LPO, Brest), Ariane Koch-Larrouy (LEGOS, Toulouse)

During the last 4 years, the French contribution in this field of research has been more extensive on the vertical dimension with studies of fine and micro-scales in different environments.

This includes investigations during cruises aimed at better understanding large scale or meso-scale circulation and their role on climate or biogeochemical cycles. We can refer to the Ovide cruises in the North Atlantic subpolar gyre (in particular in 2008), with emphasis on finding a structuration of vertical mixing related to bathymetry and understanding how it influences large scale ocean circulation, the Indomix cruise in the Indonesian seas (2010) with emphasis on vertical mixing related to the internal wave field, in particular in the Banda Sea, and its relation to the large internal tides found in these seas. During cruise Boum (summer 2007 in the Mediterranean Sea), the emphasis was on vertical transport of nutrients in the thermocline and the mixed layer during summer in the oligotrophic environment of anti-cyclonic surface eddies of the eastern Mediterranean Sea. During cruise Keops (early 2007, Kerguelen plateau in the Austral Ocean), the emphasis was on understanding the contribution of vertical mixing associated to the internal waves to vertical transport of micro-nutrient over the Kerguelen plateau in the south Indian Ocean. Mixing related to the generation of internal tidal waves near the shelf Break has been investigated during the Mouton summer 2008 cruise in the Bay of Biscay. Some of these data contribute to the parameterization of mixing in numerical models of the regional to large scale ocean circulation.

Other investigations focused on mixing in deep sill environments, in particular near the Lucky Strike segment of the Mid-Atlantic Ridge where deep flows strongly constrained by topography are associated with large vertical mixing, and a very active internal wave field, with a strong contribution of internal tides and background vertical shear to mixing.

A new field of investigation appeared during this period: vertical mixing on the deep shelves surrounding France. This was in particular structured over the Bay of Biscay shelves with the EPIGRAM project, within which the generation of internal waves was investigated in 2010, the dilution by mixing of the freshwater spring plume of the Gironde in 2009-2010, and in 2010, the structuration of mixing near a front (Ushant Front west of Brittany) and how tidal mixing interfers with the structure of this front. This is a fairly new field of research in France, strongly based on the collection of new observations.

Investigation of small horizontal scales and the associated mixing, on the other hand, has been mostly driven by ocean modeling, and surface satellite observations. These satellite observations and model simulations strongly suggest a continuity of scales that structure the ocean dynamics, but also ecosystems and biogeochemical processes. On which scales these structures mix, and the role of small scale vertical processes on this mixing has only been barely touched by the French community on an in situ basis (for example: Gogasmos Bay of Biscay cruises in 2009 and Latex cruise in the Gulf of Lion in 2010).

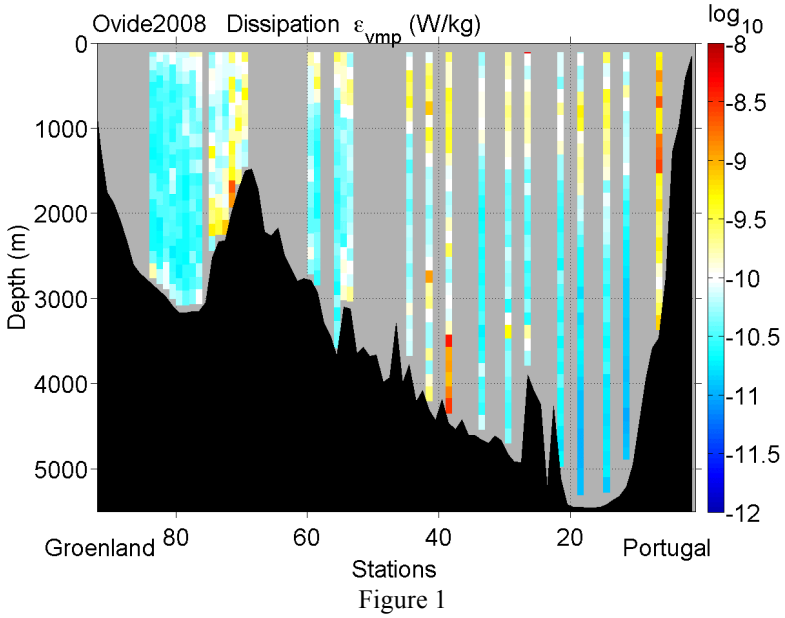

Figure 1

Turbulent kinetic energy Dissipation (log-scale W/kg) measured by VMP micro-structure profiled along Ovide summer 2008 section between Portugal and Greenland Notice the large values near 4000m (station 40), as well along the Portugal continental slope, and the slightly larger values within the thermocline (east of station 60).

MESOSCALE AND SUBMESOSCALE TURBULENCE

Patrice Klein (LPO, Plouzané, France) and Guillaume Lapeyre (LMD, Paris, France)

The first 500-1000m of the upper ocean have been known for many years to be crucial for the biogeochemical and the atmosphere-ocean coupling systems. At the end of the 20th century, data from conventional satellite altimeters (that capture O(100km) structures) and global-scale oceanic simulations with a 10km resolution have unveiled the strong turbulent character of the mesoscale eddy field in many oceanic regions. These oceanic mesoscale eddies (the ocean weather system), characterized by horizontal scales of O(100km) and depths between 500m and 1000m constitute the dominant part of the total kinetic energy and are known to significantly contribute to the lateral transport of heat, momentum and tracers (Ferrari and Wunsch, ARFM, 2009) and to the biogeochemical system (McGillicuddy, GGC, 2003).

Since 2005 a bunch of studies, both numerical and experimental, have profoundly changed our « turbulent » vision of the upper oceanic layers. They reveal the importance of submesoscales (such as filaments with a 10km width and small-scale vortices with a 5-40km diameter) that are ubiquitous on the Sea Surface Temperature (SST) and Ocean Color images but whose dynamical impacts were totally ignored before. Dynamics of the first 500m of the ocean can now be viewed as captured by a sea of interacting mesoscale eddies and submesoscale structures (Klein et al., JPO, 2008, Capet et al., JPO, 2008, Klein and Lapeyre, ARMS, 2009). These new studies have offered an unprecedented insight on the dramatic impact of these submesoscales. These submesoscales are associated with vertical velocities that can reach 100m/day (typically one order of magnitude larger than those associated with mesoscale eddies) down to 200-500m below the surface (Legal et al., JPO, 2007; Nagai et al., JGR 2006; Klein et al., JPO, 2008; Capet et al., JPO, 2008). As a consequence they impact much more significantly, than previously thought, the global ocean circulation and the biogeochemical system. Such new insight has been made possible because of the development of instruments mounted on towed vehicles, new float devices in the upper layer but, principally, because of the fast development of supercomputers.

Quantification on a global scale indicates that, in oceanic regions overcrowded with mesoscale eddies such as in the Gulf Stream, the Kuroshio and the Antartic Circumpolar Current, the vertical velocity field associated with submesoscales represent almost 70% of the total vertical velocity field (Lapeyre and Klein, JMR, 2006; Klein et al., JPO, 2008). The remaining 30% being located inside mesoscale eddies. As a result submesoscales explain more than 60% of the total nutrient vertical fluxes. This may provide an answer to the ongoing debate about which physical processes can close the nutrient balance in the ocean (McGillicuddy, GGC, 2003). Furthermore the presence of submesoscales make the primary production in the ocean to be multiplied by a factor 2 (Levy, 2005; Martin et al., GGC, 2006; Klein and Lapeyre, ARMS, 2009). High resolution primitive equation simulations (1km) in large domain performed on the Earth simulator have unveiled the impact of submesoscales on the ocean dynamics at larger scales. Kinetic energy associated with these submesoscales is globally smaller than that associated with mesoscale eddies but their presence explains that the mesoscale kinetic energy is multiplied by a factor 2 (Klein et al., JPO, 2008; and Capet et al., JPO, 2008) and that the sea surface temperature increase by almost 1o K (due to ageostrophic motions) (Klein et al., JPO, 2008)! Roullet and Klein (PRL, 2010) further point out that the submesoscales accelerates the ocean energy circuit – between potential and kinetic energy among the different (large and small) scales - through the vertical velocity field.

The physics that explains the importance of submesoscales in the upper ocean is frontogenesis (the same mechanism that drives atmospheric fronts): density anomalies are stretched by mesoscale eddies into small-scale elongated patterns which increases the density gradient they are associated with and triggers frontogenesis. The resulting vertical velocity field affects the first 500m and provides a pathway between the surface boundary layer (or the surface mixed-layer) and the ocean interior. These submesoscales are part of a surface dynamical mode, first introduced by Blumen (JAS, 1978), extended to the ocean by Held et al. (JFM,1995) and Lapeyre and Klein (JPO, 2006) and to the atmosphere by Hakim et al. (JAS, 2002) and Tulloch and Smith (JAS, 2009). This mesoscale/submesoscale turbulence in the upper ocean is driven by the surface potential vorticity (that can be estimated from the Sea Surface Height) and by the interior potential vorticity (Lapeyre and Klein, JPO, 2006). The high resolution simulations performed by the French scientists on the Earth Simulator and by the UCLA scientists have provided unvaluable insights on the importance of this mesoscale/submesoscale turbulence. Global observations of the dynamics this mesoscale/submesoscale turbulence are presently lacking but are highly needed to constrain future realistic numerical simulations at these resolutions. Sea Surface Temperature and Ocean Color satellites images have such a high resolution but they are much affected by the clouds and, when available, do not provide any dynamical information. Future satellite altimeter missions (such as the Surface Water and Ocean Topography (SWOT) mission, see Fu and Ferrari, EOS, 2009) should allow to get dynamical information at the ocean surface at a resolution ten times higher than the conventional altimeters and, therefore, reduce the gap between numerical and data resolutions. But one major challenge is how to exploit the full potential information

provided by these new high resolution satellite data - when combined with existing data (such as the Global Argo float database- to retrieve and diagnose these new dynamical impacts related to the submesoscales in particular those related to the vertical velocity field in the first 500m and to the air-sea fluxes. This is one of the major challenge of the present decade.

A global numerical model to study the interannual variability of the ocean

Anne Marie Treguier, CNRS
Laboratoire de Physique des Oceans, UMR 6523 CNRS-IFREMER-IRD-UBO, IUEM

The DRAKKAR project is a collaboration between French research laboratories (LEGI, Grenoble; LPO, Brest; LOCEAN, Paris), Mercator-Ocean, and other teams in Europe (Southampton, U.K; Kiel, Germany) and Canada. In 2006-2010 a global ocean and sea ice model has been developed, based on the NEMO platform (www.nemo-ocean.eu), with a ¼° resolution: a grid scale ranging from 27 km at the equator to an average of 12 km in the Arctic ocean. A new representation of bottom topography and numerical schemes have brought improvements in the representation of the main current systems and the associated eddies (Barnier et al, 2006; figure 1). Simulations of the ocean variability over the past decades (1958-2007) have been performed, forced by atmospheric data based on ECMWF reanalysis and analyses (Brodeau et al, 2010). The results of these simulations have been distributed to a wide international community. Variability mechanisms have been analyzed globally or regionally (in the Arctic, the Mediterranean sea, the Southern Ocean, the North Atlantic…). Only two examples are given here.

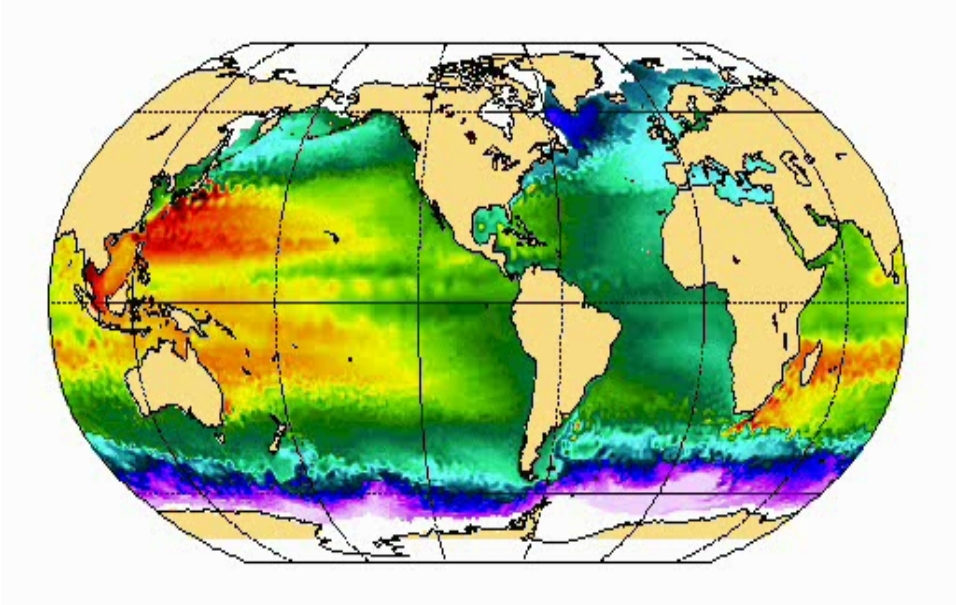

Figure 1: Map of a 5-day average of sea level in the DRAKKAR ¼° model (the ice cover is indicated in white). The model reproduces well some eddying regions like the Agulhas retroflection or the Zapiola Anticyclone south of the Brazil-Malvinas confluence zone. The ¼° resolution is still too coarse in other areas, for example in the Gulf stream, the Kuroshio, or west of Australia in the Indian Ocean

Mechanisms of regional sea level trends (1993-2001).

Lombard et al (2008) have compared the trend in sea level in DRAKKAR simulations and observations. The good agreement (figure 2) allows to use the model to analyse the possible causes of the observed trends. The model (which has no assimilation of satellite nor in situ data) demonstrates that regional changes in sea level over that period are largely forced by the atmosphere. They are mainly due to thermosteric changes in the upper 750m. Wind stress trends over that period explain some of the sea level trends, especially in the tropical Pacific and Indian Ocean.

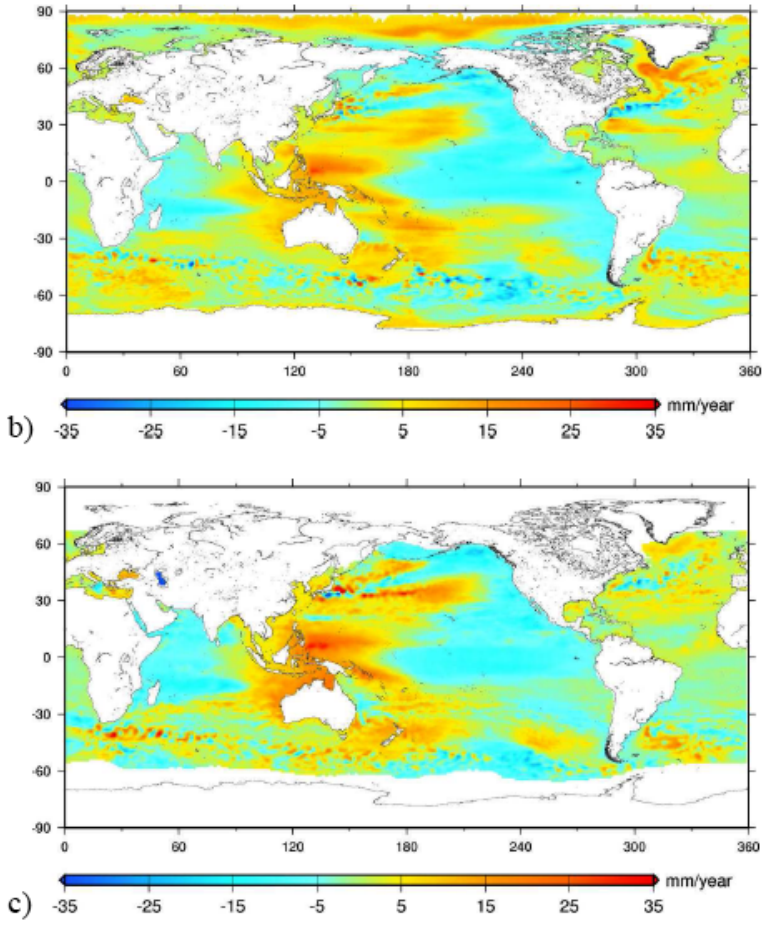

Figure 2: Regional trends of sea level between 1993 and 2001 (mm/year). Top: ORCA025; bottom: observation by satellite altimetry. From Lombard et al, 2008.

Ice and freshwater transport variability along both sides of Greenland

The ¼° global DRAKKAR model simulates the variability of the Arctic Ocean and its interaction with the Pacific and Atlantic Oceans, with a mesh fine enough to resolve Bering Strait and the main pathways through the Canadian Archipelago. The model allows to propose a quantitative estimate of the liquid freshwater and ice fluxes from the Arctic to the Atlantic (Lique et al, 2009; figure 3). Regarding the mechanisms of interannual variability, the model suggests a striking difference between both sides of Greenland. At Davis Strait to the west, the variability is due to the volume transport, while on the east side at Fram Strait, the variability is due in equal parts to the variations of the volume transport and to variations of the salinity, linked with interannual variability of the ice-ocean exchanges north of Fram Strait.

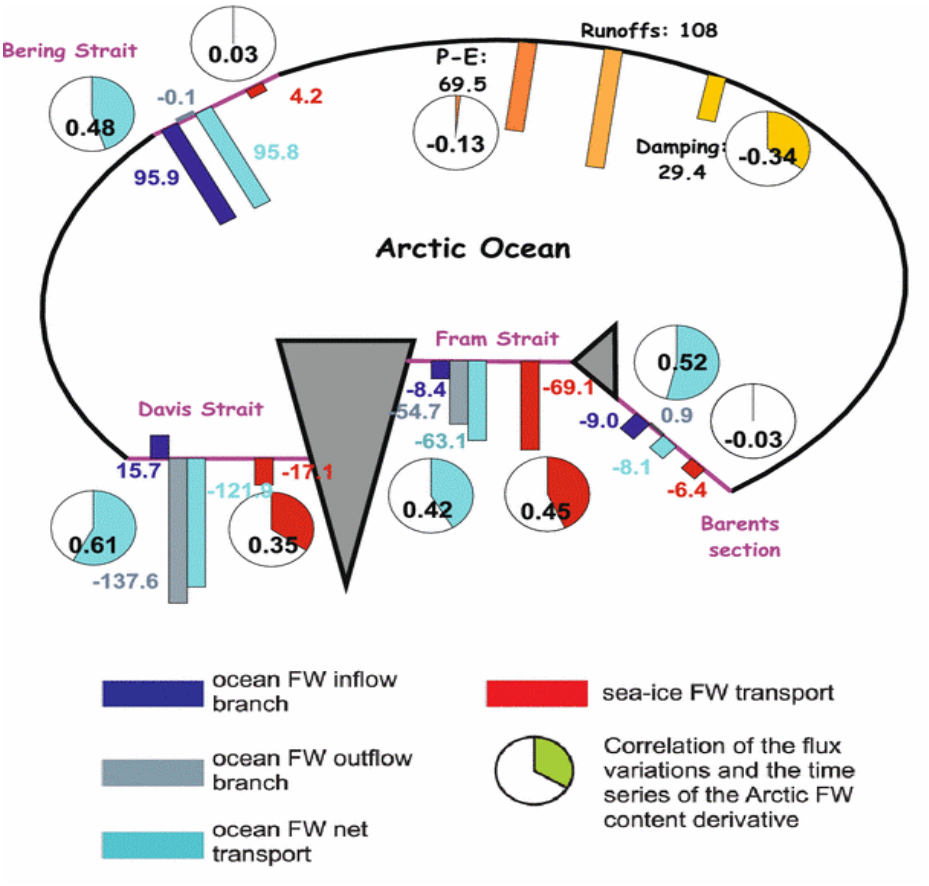

Figure 3 (Lique et al, 2009). Schematic view of the Arctic freshwater balance. Mean value of each source and sink is represented (bar, in mSv), as well as the correlation of its variations with the times series of the Arctic freshwater content derivative (circular diagrams). The sign of the freshwater

fluxes indicates if the flux represents a sink or a source of freshwater for the Arctic Ocean, regardless the direction of the volume fluxes (For instance, the inflow branch through Fram Strait brings waters with salinity higher than 34.8, and thus has a negative sign)

Barnier B., G. Madec, T. Penduff, J.-M. Molines, A.-M. Treguier, J. Le Sommer, A. Beckmann, A. Biastoch, C. Böning, J. Dengg, C. Derval, E. Durand, S. Gulev, E. Remy, C. Talandier, S. Theetten, M. Maltrud, J. McClean, and B. De Cuevas, 2006: Impact of partial steps and momentum advection schemes in a global ocean circulation model at eddy permitting resolution. Ocean Dynamics, Vol 4, DOI 10.1007/s10236-006-0082-1.

Brodeau, L., B. Barnier, A.M. Treguier, T. Penduff, S. Gulev, 2009: An ERA40-based atmospheric forcing for global ocean circulation models. Ocean Modelling, 31, 88-104, doi: 10.1016/j.ocemod.2009.10.005

Lombard, A., G. Garric, and T. Penduff, 2009 : «Regional patterns of observed sea level change: Insights from a 1/4° global ocean/sea-ice hindcast ». Ocean Dynamics, 59, 3, 433-449.

Lique, C., Treguier, A.M., Scheinert, M., Penduff, T., 2009: A model-based study of ice and freshwater transport variabilities along both sides of Greenland. Climate Dynamics, 33 (5), 685-705, DOI: 10.1007/s00382-008-0510-7.

Inter-decadal modulation of ENSO nonlinearity and its evolution in a warming climate

Boucharel J. (1), Dewitte B. (1) (2), du Penhoat Y. (1) (2), Garel B. (3), Yeh, S.-W. (4), Kug J.-S. (5)
(1) Université de Toulouse; UPS (OMP-PCA); LEGOS, 14 Av. Edouard Belin, F-31400 Toulouse, France.
(2) IRD; LEGOS, F-31400 Toulouse, France.
(3) Université de Toulouse; INP-ENSEEIHT, Institut de Mathématiques de Toulouse (UPS) France.
(4) Department of Environmental Marine Science, Hanyang University, Ansan, South Korea
(5) Korea Ocean Research and Development Institute, Ansan, South Korea.

1. Introduction

El Niño Southern Oscillation (ENSO) is the dominant mode of tropical climate variability, whose variations influence climate and ecosystems as well as many societies around the globe. It is therefore of great interest to understand its past, present and future variations. Over the last century, ENSO properties including amplitude, frequency and propagating features underwent significant changes at decadal to interdecadal timescales (An, 2004), which are partly revealed by the presence of climate shifts (Guilderson and Schrag, 1998) within ENSO typical timeseries. For instance, the two decades after the 1976/77 climate shift were characterised by more frequent and stronger El Niño events compared to previous decades (An and Wang, 2000; An, 2004; Moon et al., 2004). These changes in ENSO characteristics are intimately linked to changes in the mean state of the tropical Pacific because the dominant feedback processes associated with ENSO, namely the zonal advective and thermocline feedbacks, depend explicitly on the zonal mean Sea Surface Temperature (SST) and thermocline gradients, respectively (Zebiak and Cane, 1987; An and Jin, 2001).

Another recently documented characteristic of ENSO is its asymmetry, which reflects the nonlinearity of the tropical Pacific system (An and Jin, 2004). ENSO asymmetry also fluctuates over decadal to interdecadal timescales that are related to changes in mean state (Rodgers et al, 2004; Dewitte et al., 2007). In particular, the latter can result from the residual effect of the ENSO asymmetry variability (Schopf and Burgman, 2006; Dewitte et al., 2007), potentially leading to a tropical Pacific natural coupled mode over decadal timescales (Choi et al., 2009).

Because of this complex interaction between mean state and ENSO at a wide range of frequencies, it is difficult to provide an unambiguous explanation for the impact of global warming on ENSO. As a matter of fact, the current generation of models exhibits a wide range of behaviours with regards to their sensitivity to global warming (Guilyardi et al., 2009). In particular, the evolution of tropical Pacific SST, especially the mean zonal equatorial gradient remains a noteworthy source of uncertainty (DiNezio et al., 2009).

Recently, Yeh et al. (2009) showed, with a group of IPCC models, that most consistent changes in ENSO characteristics due to global warming take place in the central equatorial Pacific (i.e. the Niño4 region (150°E-150°W; 5°S-5°N)). They showed that global warming leads to increased SST variability over the central tropical Pacific in the form of an increased occurrence of the so-called Modoki or Central Pacific (CP) El Niño (Ashok et al., 2007) relatively to the traditional so-called Eastern Pacific (EP) El Niño characterized by positive SST departure from normal in the Niño3 region (150°W-90°W; 5°S-5°N).

In this study, we further examine the relationships between changes in mean state and changes in ENSO properties, especially El Niño flavours and the importance of associated nonlinear mechanisms through an alternative statistical measure. These analyses are carried out on both reconstructed historical datasets and CGCMs outputs.

2. Statistical diagnosis of ENSO nonlinearity

Whereas ENSO nonlinearity has usually been considered through its asymmetric character (in particular as El Niño events are stronger and more numerous than La Niña's), recent studies indicate that ENSO also has a signature on higher-order statistical moments (Timmermann, 1999). This tends to emphasize the highly nonlinear nature of the tropical Pacific system and calls for the use of statistical tools that can effectively measure ENSO nonlinearity.

We propose here an alternative to classic Gaussian statistics, namely the □-stable laws, to explicitly consider 2 main features of the ENSO Probability Density Function (PDF) (Figure 1): the asymmetry and the weight of the distribution tail associated with warm strong El Niño episodes.

In brief, non-Gaussian α-stable laws, (heavy tailed laws) are characterized by four main parameters. The main ones, $0 < \alpha \leq 2$ and $-1 \leq \beta \leq 1$, respectively allow to diagnose the "non-Gaussian degree" (the PDF tails weight) and the asymmetry (~ skewness) of the set to be measured. Simply put, the analyses of these two parameters allow measuring the deviation of a distribution from a Normal law; this deviation being representative of the underlying nonlinear processes. When $\alpha = 2$ and $\beta = 0$, the result is a Gaussian law. The lower α, the more α-stable the distribution and the more nonlinear the associated mechanisms. See Mandelbrot (1963) and Boucharel et al. (2009) for a more complete

description. It is noteworthy that the measurement of nonlinearity through the α parameter does not discriminate between nonlinear processes. Actually, the sources of nonlinearities of the tropical Pacific system remain numerous ranging from turbulent and ocean-mixing processes in the form of tropical instability waves for instance, to high frequency atmospheric forcing (An, 2009).

Koutrouvelis (1980) proposed a trustful regression method to estimate α-stable laws parameters.

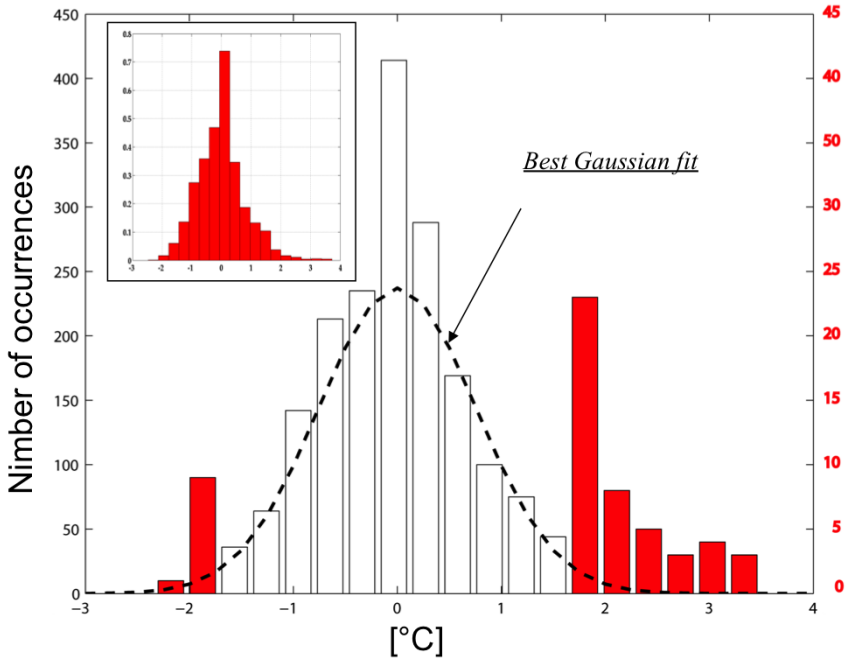

Figure 1. Histogram of Niño3 SST anomalies from Kaplan et al. (1998) reconstructed dataset. The y-axis of red bars (events greater than standard deviation) has ten times increased scale. Normalized histogram I the upper left quadrant.

3. Inter-decadal modulation of ENSO nonlinearity (statistics).

Over the inter-shift periods detected in Boucharel et al. (2009) (statistically confident ruptures detected in 1903, 1976 and 1998 through a bivariate test elaborated by Maronna and Yohai, 1978), the results of the estimation of □ and □ on distinct warm/cool periods (Figure 2) indicate that the ENSO statistics experienced significant changes. In particular, warm periods were characterised by stronger asymmetry and a greater deviation from Gaussianity (smaller α and □ ~ 1) whereas the cool period exhibited a Gaussian symmetrical pattern on average over the tropical Pacific (α ≈ 2 and □ ~ 0). A comparable tendency was found in the intermediate complexity Zebiak and Cane (ZC) model. In particular the ZC model had increased (reduced) nonlinearity quantified through nonlinear advection within the mixed layer (Nonlinear Dynamical Heating (NDH)) during warm (cool) periods (An and Jin, 2004; Boucharel et al., 2009). Consistently with recent studies, nonlinear dynamics is found to be responsible for rectification of ENSO variability through changes in ocean background. Although current measures of ENSO nonlinearities (through NDH) have provided meaningful information on the rectification of ENSO variability by changes in mean state, they may not fully account for the complexity of the rectified effect.

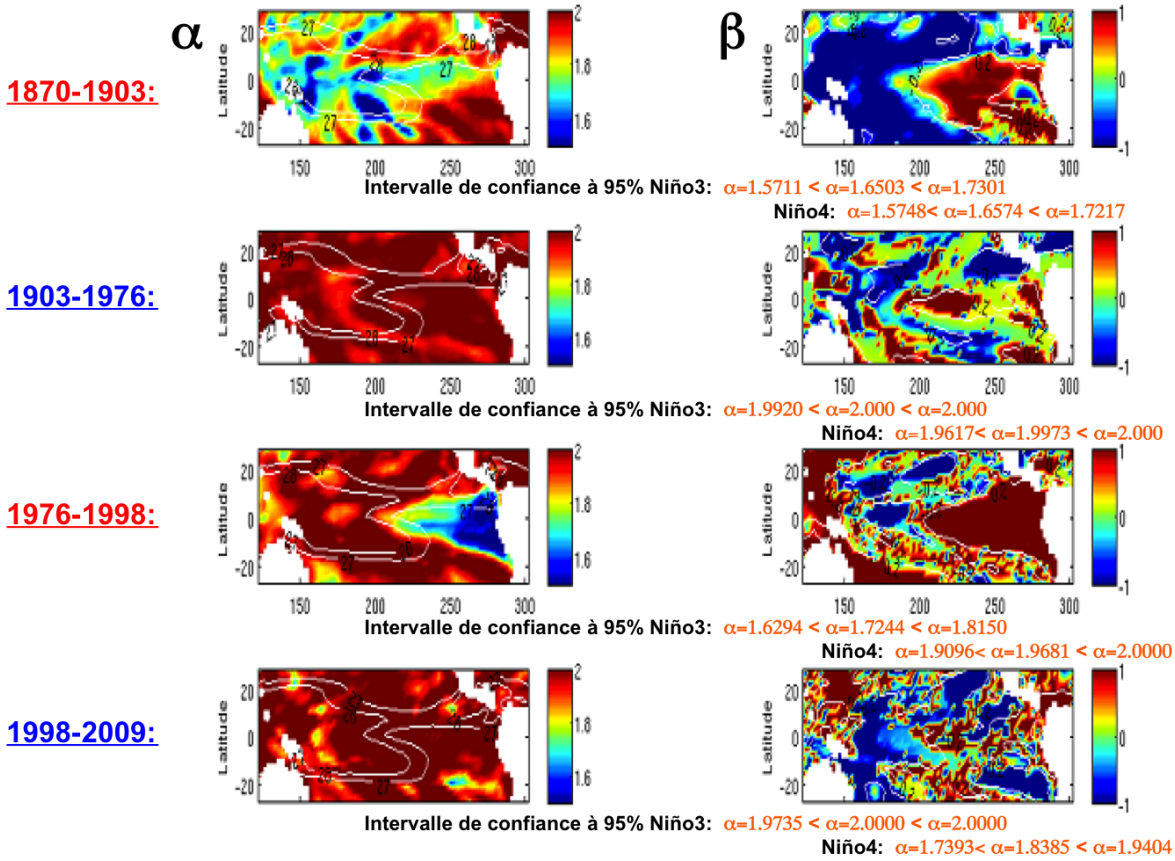

Figure 2. □ and □ parameters on distinct warm (1870-1903 and 1976-1998) and cool (1903-1976 and 1998-2009) inter-shifts periods estimated from Kaplan et al. (1998) reconstructed dataset. Confidence intervals for parameters estimation on Niño3 and Niño4 indices are provided below each plot.

In order to test further the relationships between ENSO nonlinearity and the tropical Pacific mean state, we took advantage of the CMIP3 Coupled General Circulation Models (CGCMs) database and the different scenario experiments provided by the fourth version of the assessment report of the IPCC. We selected a set of models available through the CMIP3-IPCC-AR4 data centre at the Program for Climate Model Diagnosis and Intercomparison (PCMDI) and tested them in different configurations in terms of greenhouse gases concentration (respectively the Pre-Industrial reference -PICTRL-, the doubling -2xCO2- and quadrupling -4xCO2- greenhouse gases concentration). In particular, since the focus of the study deals with the diagnostic of high-order statistics and their response to changes in mean state, we followed the classification established in Table 5 in Boucharel et al. (2009). The latter evaluates the performances of the whole CMIP3 database in simulating irregular (nonlinear, □-stable) ENSO timeseries along with a noteworthy low frequency modulation of the tropical Pacific mean state (revealed by the presence of climate shifts). Interestingly, models able to represent a significant decadal to inter-decadal variability are also strongly nonlinear (with regards to the α parameter analysis). These models (in bold in Table 5 in Boucharel et al. (2009)) will be the models of interest in the present study. Interestingly, this "nonlinear" classification is consistent with other recent studies dedicated to intercomparison (Belmadani et al., 2010 among others).

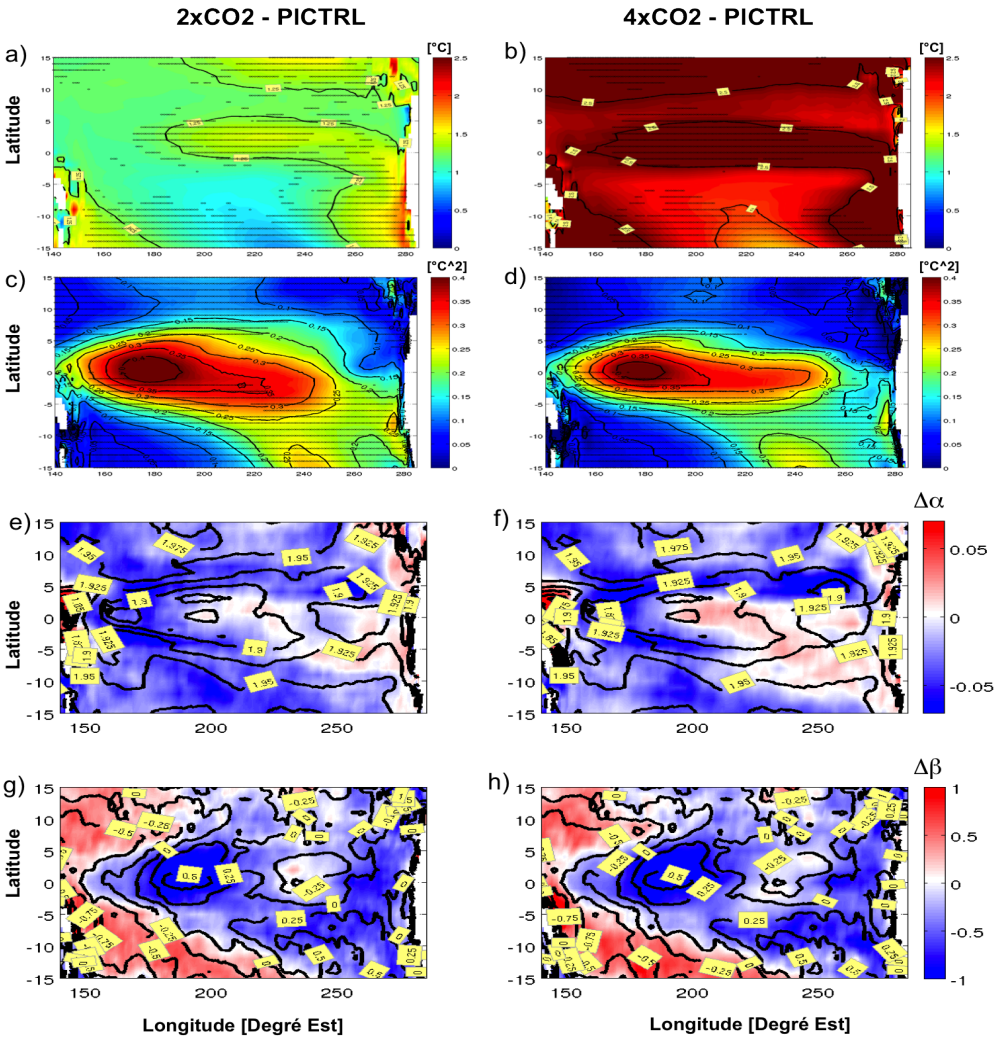

Figure 3. Changes in tropical Pacific statistics between different IPCC scenarios for the multi model ensemble mean (2xCO2 – PICTRL on left panels and 4xCO2 – PICTRL on right panels). Changes in: mean SST a) and b), RMS SST c) and d). Dots denote 95% statistical confidence level based on a Student's t-test. Changes in: □parameter e) and f), □ parameter g) and h). Contours in e), f), g) and h) panels denote □ and □ parameters values for the multi models mean for the PICTRL experiment.

Figure 3 displays the change in mean state for the model ensemble mean considered in this study for the $2xCO_2$ and $4xCO_2$ scenario. It consists of an El Niño-like pattern (i.e. maximum mean SST changes over the Cold Tongue region, Figure 3a). Interestingly, for the $4xCO_2$ scenario, models simulate an enhanced equatorial warming (Figure 3b), rather than an El Niño-like warming. These changes in mean SST are associated with changes in ENSO variability as evidenced by Figures 3cd. Interestingly, the largest changes for these quantities are observed over the Warm Pool region similarly to the study by Yeh et al. (2009) and are less sensitive to the concentration of greenhouse gases, suggesting a nonlinear response of the tropical Pacific.

Figure 3 also displays changes in α and β parameters induced by global climate change under different projection scenarios for the multi-model ensemble mean. The pattern of maps for the β parameter (Figures 3fh) denotes increase (decrease) in negative (positive) asymmetry associated with global warming in the Warm Pool (Cold Tongue) region. Interestingly, for the α parameter, a peculiar pattern of changes associated with increased GHG concentrations emerges (Figure 3eg): it consists of a region of decreased α-stability (decrease in deviation from Gaussianity i.e. $\Delta\alpha>0$) in the Cold Tongue region and a region of increased α-stability ($\Delta\alpha<0$) in the Warm Pool. In the far western equatorial Pacific the rising concentration of GHG tends to favour a more Gaussian-type behaviour ($\Delta\alpha>0$). The decrease in □over the Warm Pool region indicates a tendency towards more EEs in a warmer climate over this region. See Boucharel et al. (2011) for more explanations and details about the statistical confidence (and consistency among models) of Figure 3efgh.

This is consistent with the recent results by Yeh et al. (2009) who diagnosed an increase of the CP to EP El Niño ratio in a warmer climate. The increase in negative asymmetry over the Warm Pool region also suggests a tendency towards more and/or "stronger" cold events (relative to a warmer climate mean state) consistently with Timmermann (1999).

This raises the question of whether the tendency towards more El Niño events over the Warm Pool region (new "Modoki flavour" of El Niño) is directly related to the tropical Pacific mean state change associated with global warming (seen as an external forcing) or whether it is associated with changes in nonlinearity as an intermediate step in the process. In the next section, we will explore the relationships between the different types of El Niño and tropical Pacific nonlinearity, as measured by the parameter.

4. El Niño flavours and tropical Pacific nonlinearity.

In this section, we investigate the extent to which the change in El Niño type under global warming can be related to the change in nonlinearity. Whereas Yeh et al. (2009) suggest that the increase of CP El Niño frequency in a warmer climate may be associated with changes in mean state (mean thermocline depth and slope), we hypothesize here that it is also related to changes in nonlinearity of the tropical Pacific system. It is noteworthy that timescale interactions (low frequency mean state changes versus ENSO variability) through nonlinear processes are subject to decadal or inter-decadal modulation (see the review by An (2009)) so that diagnostics of global warming on such processes are not straightforward.

In particular, although observational records suggest a tendency towards more frequent CP El Niño in recent years, this may hide fluctuations in statistics on decadal to inter-decadal timescales. For instance, Kug et al. (2010) found a clear phase relationship between the frequency of occurrence of CP El Niño and low frequency changes in mean state in the Warm Pool region in the GFDL-CM2.1 model (see their Figure 13). It is therefore important to verify whether such low frequency variability can also be found in ENSO nonlinearity and the extent to which it can be influenced by global greenhouse warming.

The simple detection test proposed by Yeh at al. (2009) for distinguishing a CP El Niño from an EP El Niño is applied to data and model outputs. However, instead of using a fixed threshold of +0.5°C for the ENSO indices (Niño3 and Niño4 averaged over the boreal winter months of December-January-February) to account for El Niño, we used a threshold that depends on model variability (see Boucharel et al., 2011)

For sake of clarity, we chose to present results for one model among the most sensitive to global warming (seen as a change in tropical SST mean state), i.e. the MRI-CGCM2.3.2.A.

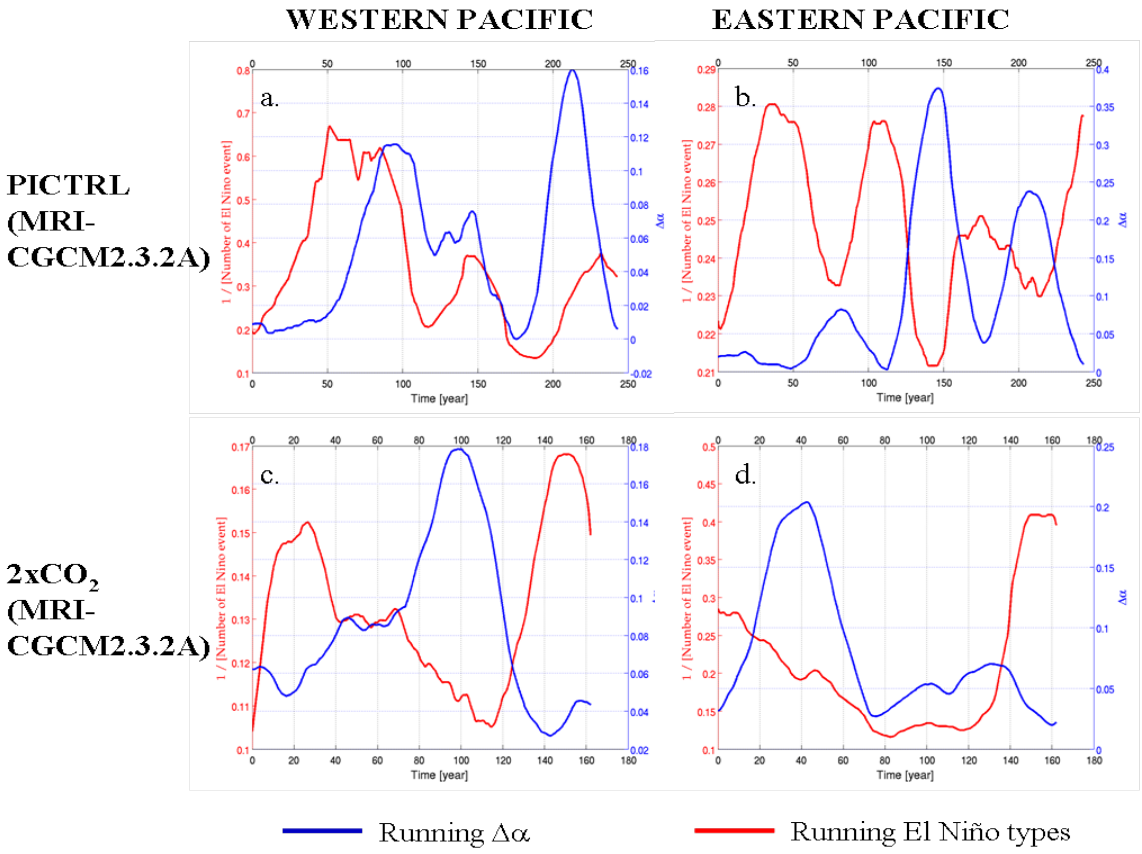

Figure 4. Running α parameter (27-year running windows) in blue lines (right panels for Niño3 and left panels for Niño4W) and running El Niño types frequency in red lines (left panels for Central Pacific and right panels for Eastern Pacific)

MRI-CGCM2.3.2.A PICTRL run (a. and b.)

MRI-CGCM2.3.2.A 2xCO2 run (c. and d.)

Figure 4 presents results for this model for the PICTRL and $2xCO_2$ scenarios. While the occurrence of so-called Modoki events does not seem to be related to nonlinear processes in a Pre-Industrial climate (correlation of -0.10, Figure 4a.), EP El Niño and over the Niño3 region exhibits a clear out of phase relationship (-0.66, Figure 4b.). Interestingly, the picture is reversed for this particular model under anthropogenic warming hypothesis. The correlation between El Niño Modoki and Niño4 index nonlinearity increases up to -0.80 (Figure 4c.), while the relationship between EP El Niño and $\Delta\alpha$ over the Niño3 region falls to 0.16 (Figure 4d.). This relationship between $\Delta\alpha$ and El Niño "flavours" appears to be a robust feature of the Tropical Pacific coupled system as it is clearly simulated by the majority of the selected models (Table 3 of Boucharel et al., 2011).

This raises the question of the evolution of low frequency tropical Pacific coupled modes under global warming hypothesis. Actually, beyond the inter-decadal alternation of favourable EP and CP El Niño periods (e.g. see the out of phase relationships between the red curves in the upper panels of Figure 4), Yeh et al. (2009) and Boucharel et al. (2011) diagnosed a dominance of the "Modoki/CP" mode in a warmer climate. The present study highlights the possible significant role of nonlinear mechanisms in driving this low frequency modulation of El Niño flavours.

5. Summary and Discussion

In the present study, we examined the response of ENSO statistics, particularly the high-order statistical moments through an alternative statistical framework, to abrupt changes in the mean climate background. Reconstructed data for the 20th century exhibited a clear modulation of ENSO nonlinearity (deviation of its statistics from a Gaussian distribution) according to the mean state. In particular, warm (cool) periods tend to favour more (less) nonlinear processes. This sensitivity to changes in mean state was further investigated in the CMIP3 database, using different scenario experiments provided by IPCC-AR4 to characterize different mean state. We found drastic changes in ENSO nonlinearity patterns in a warmer climate. The activity of nonlinear mechanisms tends to be translated from the Cold Tongue region to the central equatorial Pacific under greenhouse climate hypothesis.

This is consistent with recent studies which indicate that global warming may have a significant impact on El Niño characteristics, leading in particular to an increased occurrence of the so-called Modoki El Niño located in the central Pacific (Yeh et al., 2009). There are many processes that may be responsible for such changes. They involve complex interactions between mean state, ENSO variability and nonlinearity.

We evidenced here a low frequency modulation of the different El Niño flavours, namely the EP and CP El Niño, both in a Pre-Industrial and in a warmer climate. We found that the EP flavour was directly related to the Eastern Pacific nonlinearity in the PICTRL experiments, whereas the CP flavour does not seem to be driven by the central/western pacific nonlinear mechanisms. Interestingly, the picture is reversed in a warmer climate. These findings provide further arguments to the existence of a tropical Pacific natural coupled mode oscillating on decadal to inter-decadal timescales.

Further study is required to diagnose which of the numerous nonlinear processes is more influential in this low frequency modulation.

5. Bibliography

An, S.-I., and B. Wang, 2000: Interdecadal change of the structure of the ENSO mode and its impact on the ENSO frequency. J. Climate, 13, 2044-2055.

An, S.-I., and F.-F. Jin, 2001: Collective role of thermocline and zonal advective feedbacks in the ENSO mode. J. Climate, 14, 3421-3432.

An, S.-I., 2004: Interdecadal changes in the El Niño-La Niña asymmetry. Geophys. Res. Lett., 31:L23210, doi:101029/2004GL021299.

An, S.-I., and F.-F. Jin, 2004: Nonlinearity and asymmetry of ENSO. J. Climate, 17, 2399-2412.

An, S.-I., 2009: A review of interdecadal changes in the nonlinearity of the El Nino-Southern Oscillation. Theor. Appl. Climatol., 97, 29-40.

Ashok, K., S.K. Behera, S.A. Rao, H. Weng, and T. Yamagata, 2007: El Niño Modoki and its possible teleconnection. J. Geophys. Res., 112, C11007.

Belmadani, A., B. Dewitte, and S.-I. An, 2010: ENSO feedbacks and associated time scales of variability in a multi-model ensemble. J. Climate, accepted.

Boucharel, J., B. Dewitte, B. Garel, and Y. du Penhoat, 2009: ENSO's non-stationary and non-Gaussian character: The role of climate shifts. Nonlin. Proc. Geophys., 16, 453-473.

Boucharel, J., B. Dewitte, Y. du Penhoat, B. Garel, S.-W. Yeh, an J.-S Kug 2009: ENSO nonlinearity in a warming climate. In revision in Clim. Dynam.

Choi J., S.-I. An, B. Dewitte, and W.W. Hsieh, 2009: Interactive feedback between the tropical Pacific decadal oscillation and ENSO in a coupled general circulation model. J. Climate, 22, 6597-6611.

Dewitte, B., C. Cibot, C. Périgaud, S.-I. An, and L. Terray, 2007: Interaction between near-annual and ENSO modes in a CGCM simulation: Role of the equatorial background mean state. J. Climate, 20, 1035-1052.

DiNezio, P.N., A.C. Clement, G.A. Vecchi, B.J. Soden, B.P. Kirtman, and S-K. Lee, 2009: Climate response of the equatorial Pacific to global warming. J. Climate, 22, 4873-4892.

Guilderson, T.P., and Schrag D.P., 1998: Abrupt shift in subsurface temperatures in the tropical pacific associated with changes in El Niño. Science, 281, 5374, 240-243.

Guilyardi, E., A. Wittenberg, A. Fedorov, M. Collins, C. Wang, A. Capotondi, G.J. van Oldenborgh, and T. Stockdale, 2009: Understanding El Niño in Ocean–Atmosphere General Circulation Models: Progress and Challenges. Bull. Amer. Meteor. Soc., 90, 325-340.

Kaplan, A., M. Cane, Y. Kushnir, A. Clement, M. Blumenthal, and B. Rajagopalan, 1998: Analyses of global sea surface temperature 1856-1991. J. Geophys. Res., 103, 18,567-18,589.

Koutrouvelis, I.A., 1980: Regression-Type Estimation of the parameters of stable laws. J. Amer. Statist. Assoc., 75, N 372.

Kug, J.-S., J. Choi, S.-I. An, F.-F. Jin, and A.T. Wittenberg, 2010: Warm Pool and Cold Tongue El Nino events as simulated by the GFDL 2.1 coupled GCM. J. Climate 23, 1226-1239

Moon, B.-K., S.-W. Yeh, B. Dewitte, J.-G. Jhun, I.-S. Kang and B.P. Kirtman, 2004: Vertical structure variability in the equatorial Pacific before and after the Pacific climate shift of the 1970s. Geophys. Res. Lett. 31:L03203, doi: 10.1029/2003GL018829.

Rodgers, K.B., P. Friederichs, and M. Latif, 2004: Tropical Pacific Decadal Variability and Its Relation to Decadal Modulations of ENSO. J. Climate., 17, 3761-3774.

Schopf, P.S., and R.J. Burgman, 2006: A Simple Mechanism for ENSO Residuals and Asymmetry. J. Climate, 19, 3167–3179.

Timmermann, A., 1999: Detecting the nonstationary response of ENSO to greenhouse Warming. J. Atmos. Sci., 56, 2313-2325.

Timmermann, A., F.-F. Jin, and J. Abshagen, 2003: A nonlinear theory of El Niño bursting. J. Atmos. Sci., 60, 152-165.

Yeh, S.-W., J.-S. Kug, B. Dewitte, M.-H. Kwon, B.P. Kirtman, and F.-F. Jin, 2009: El Niño in a changing climate. Nature, 461, 511-514.

Zebiak, S.E., and M.A. Cane, 1987: A model of El Niño Southern Oscillation. Mon. Wea. Rev., 115, 2262,-2278

Observed freshening and warming of the western Pacific Warm Pool

Sophie Cravatte, Thierry Delcroix, Dongxiao Zhang, Michael McPhaden and Julie Leloup

Published in Climate Dynamics, 2009

Cravatte,S., T. Delcroix, D. Zhang, M. McPhaden and J. Leloup (2009), Observed Freshening of the warming Western Tropical Pacific and extension of the Warm/Fresh Pool in recent decades, Clim Dyn, doi 10.1007/s00382-009-0526-7.

The Warm Pool (WP) of the western tropical Pacific Ocean is characterized by some of the warmest seawaters of the global ocean, with Sea Surface Temperatures (SST) warmer than 28–29°C. Reaching depths of 100 m, the WP covers a large surface area of about 159106 km2 and contains an important warm water volume. Its warm waters supply the atmosphere with water vapor and heat, releasing latent heat and leading to convection and heavy rainfall in excess of 2–3 m per year. This high precipitation rate, associated with light winds in the region, induces Sea Surface Salinity (SSS) lower than 35 pss, and results in the formation of a relatively low density and stable oceanic mixed layer.

At the equator, the Warm and low-salinity waters of the WP are separated from the cold and saltier waters of the central Pacific by a sharp salinity front. The position of the eastern edge of the Warm Pool in the equatorial band, associated with an oceanic convergence zone and a salinity front, is a key parameter for ENSO dynamics and ocean–atmosphere interactions.

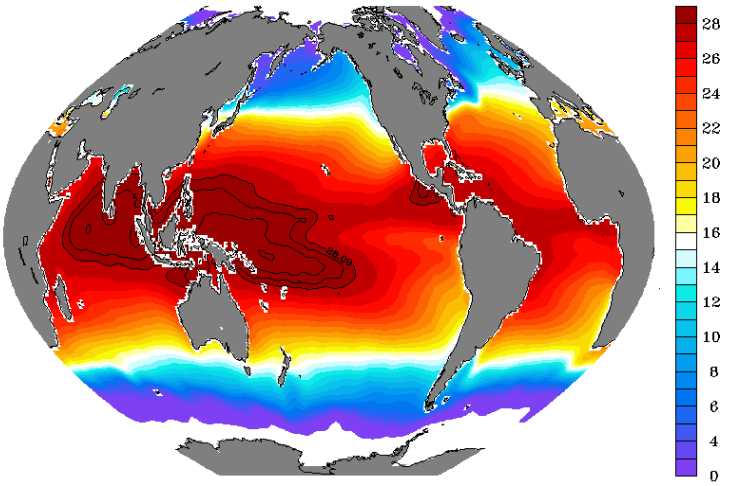

Figure 1: Mean SST from WOA2000

In a paper published in Climate Dynamics in 2009, S. Cravatte, T. Delcroix from IRD-LEGOS and coauthors from NOAA/PMEL and RSMAS used sea surface temperature and in situ sea surface salinity (SSS) data to address the central questions of whether Warm/Fresh Pool size, eastern extent and properties have changed in recent decades. Their results are striking: a significant surface freshening (up to 0.75 pss per 50 years) concurrent with an important surface warming (up to 1.2°C per 50 years, but typically from 0.2°C to 1°C per 50 years) was detected in the western tropical Pacific since 1955. Both warming and freshening are highly significant, since they reach at some locations five interannual standard deviations of the signal per 50 years. An increase in SSS is, in contrast, observed in regions of high evaporation, in the western Coral Sea and in the subtropical regions. Both geographical and seasonal SSS patterns are enhanced.

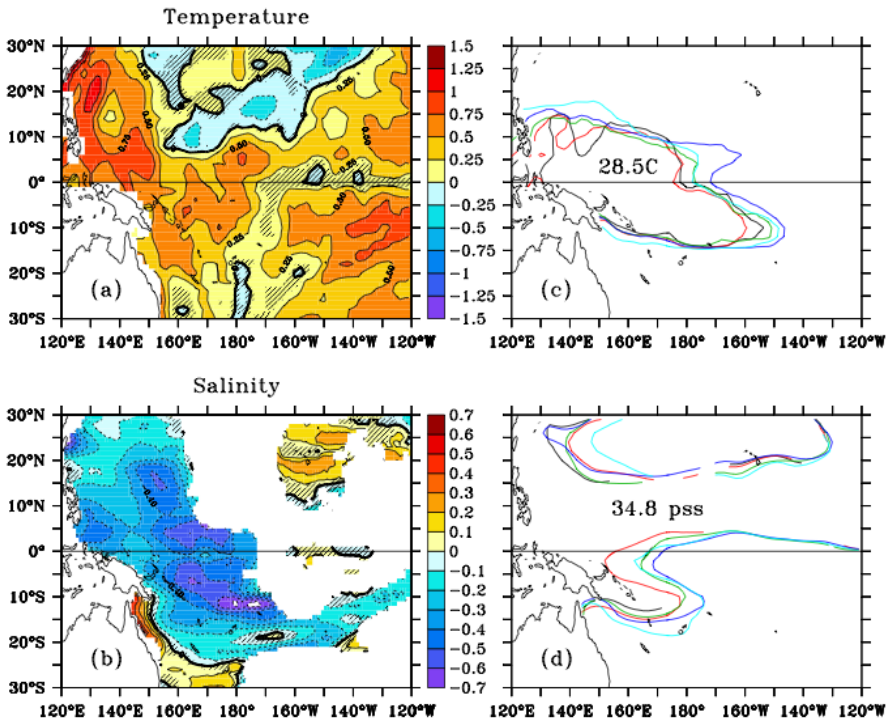

Figure 2 (@Climate Dynamics): Linear trends in SST (a) and SSS (b). Units are °C/50 years and pss/50 years. Positions of the 28.5°C isotherms (c) and of the 34.8 isohalines (d), averaged during 1956–1965 (black), 1966–1975 (red), 1976–1985 (green), 1986–1995 (blue) and 1996–2003 (light blue). The regions where the linear trends are not significant at the 90% confidence level are hatched in black

In response to these warming and freshening trends, the Warm/Fresh Pool extended both latitudinally and longitudinally at the surface during the past few decades. Interestingly, the warmest and freshest waters expanded the most in relative terms. The eastern edge of the Warm/Fresh Pool migrated eastward along the equator, as indicated by displacements of isohalines and isotherms. Strong decadal variability of the same magnitude as the long-term trend leads to a stronger eastward displacement from 1955 to the mid-1990s, and to a rather negligible displacement from 1978 to 2003. In the Southwestern tropical Pacific, the salinity front located under the South Pacific Convergence Zone also migrated southward and eastward. At decadal timescales, its longitudinal movements are opposite to those of the equatorial front, as they are at interannual timescales. Long-term trends are in the same direction though, which emphasizes that they are not simply the result of decadal variability or increased interannual variability.

Forcing fields that could be used to tentatively explain the observed freshening are not reliable. Alternatively, the " wet get wetter and dry get drier" paradigm associated with quasi-uniform tropical SST warming can provide useful guidance for the interpretation of the long-term SSS trends. Increased heating will enhance evaporation, while increased air moisture due to increase in saturation vapour pressure with temperature will produce more intense precipitation. They use a very simple model to predict the SSS changes using Clausius–Clapeyron scaling. Their results suggest that the increase of the mean hydrological cycle predicted by a simple Clausius–Clapeyron scaling is already happening, consistent with other recent works.

Following many previous studies, the paper suggests that salinity is an important indicator of climate change in the tropics. However, in some regions, decadal variability appears greater or on the same order of magnitude than longer term trends.

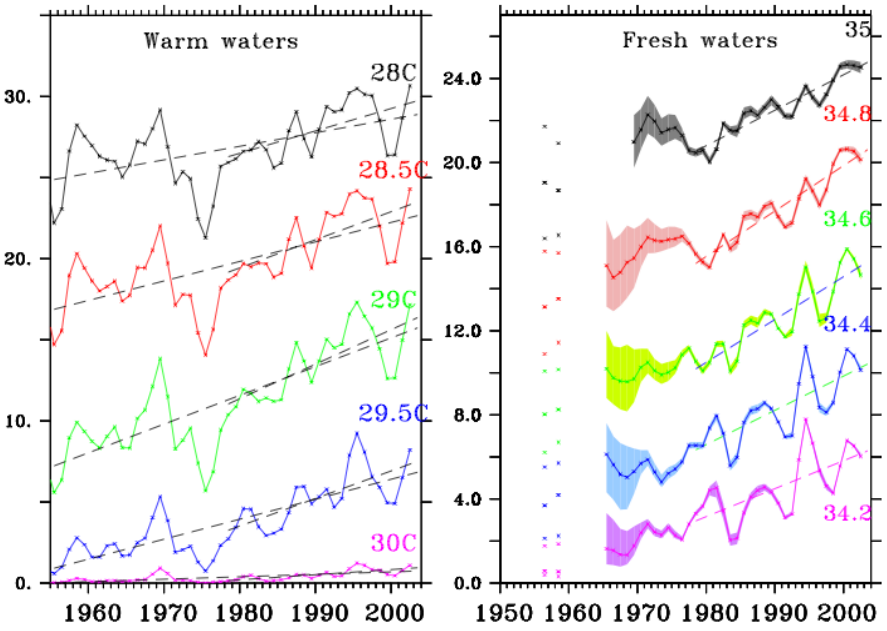

Figure 3 (@Climate Dynamics): Left: Time series of the surface area covered by waters warmer than SST thresholds. Right: Time series of surface area covered by waters fresher than SSS thresholds.

Low-frequency variations of the large-scale ocean circulation and heat transport in the North Atlantic from 1955–2008 in situ temperature and salinity data

T. Huck, A. Colin de Verdière, P. Estrade, F. Gaillard, R. Schopp, P. Bellec, R. Dussin

Laboratoire de Physique des Océans (UMR 6523 CNRS IFREMER IRD UBO), Brest, France

Abstract

On interdecadal timescales, the Atlantic meridional overturning circulation (AMOC) is thought to be in phase with the North Atlantic Sea Surface Temperatures (as measured by the Atlantic Multidecadal Oscillation – AMO – index). However, it appears that we have entered a positive phase of the AMO since 1995-2000 although we fear the Atlantic meridional overturning may be on a declining trend, as suggested by several observational and modelling studies. Here we constrain ocean models with temperature and salinity fields built on observations, and compare the results with various simple methods (namely diagnostic, robust diagnostic and prognostic), models (North Atlantic and global configurations at various resolutions), and forcings. Mean transports of heat and mass are sensitive to the method and model configuration, but their decadal variability is much more coherent and does not depend explicitly on the variations of the surface forcing, its influence being imprinted in the thermohaline structure. Multidecadal variations are of the order of 20% (0.15 PW in heat transport and 4 Sv in overturning), with large transports in the subpolar gyre in the early 1960's and mid 1990's, and low values in the mid 1970's. Declining transports of heat and mass are coherent in several models and methods since 1995, especially in the subpolar gyre, and opposite to the long term tendency from 1958 to 2008.

1. Introduction

Variations in the oceanic thermohaline structure have been documented over the last decades: surface intensified warming and changes in salinity, as well as deep water properties and formation rates [Dickson et al. 1996, 2002]. However the associated changes in the large-scale ocean circulation are poorly known, and deserve much interest in the context of the ongoing global warming and possible decay of the thermohaline circulation [Bryden et al. 2005; Gregory et al. 2005], or recent decline observed in the North Atlantic subpolar gyre [Häkkinen and Rhines 2004]. Several ocean models have been forced by atmospheric reanalysis forcings, but these forcings have significant uncertainties and well-known heterogeneities over the last 50 years. The main model deficiencies lie in formulation of subgrid-scale mixing with consequences on deep-water formation, usually impacting the overturning circulation on the long term. In situ data assimilation in such models on long time scales requires complex tools and delicate choices on the method, that largely influence the results. On the other hand, to avoid the need for accurate surface fluxes of heat and freshwater, one can use the observed temperature and salinity (TS) fields. Density providing the baroclinic velocities through the thermal wind relation, the barotropic part is obtained from the vorticity equation forced by the wind and a bottom pressure torque [Sarkisyan and Keonjiyan 1975]. Mellor et al. [1982] integrated this equation along f /H contours, whereas Holland and Hirschman [1972] used the dynamical part of numerical ocean models, although some adjustment of the bottom density field may be necessary [Ezer and Mellor 1994]. These methods have been applied to compare the pentads 1955–59 and 1970–74 [Greatbatch et al. 1991; Ezer et al. 1995], and more recently for 7 pentads from 1950 to 1994 using a finite element formulation [Myers et al. 2005]. NODC has made available global fields of TS pentadal anomalies from 1955–59 to 1994–98 based on hydrographic data. We will diagnose mean ocean currents from these fields to investigate the low-frequency variations of mass and heat transports in the North Atlantic. We first use three simple, well-documented methods: constant tracers, robust diagnostic, and short prognostic. Although the methods provide different results on the mean state, the low-frequency variations are rather coherent. Then, we implement only the robust diagnostic method in a global model continuous simulation with the seasonal cycle and TS anomaly fields updated to 2008.

2. First methodological step in a North Atlantic configuration with ROMS

The Regional Ocean Modeling System ROMS [Shchepetkin and McWilliams 2005] is used here, based on topography-following sigma coordinates. A smoothed bottom topography is required for accurate calculations of pressure gradients [Barnier et al. 1998 DSR]. We used a 1/2° resolution and 50 sigma levels to reproduce correctly the ocean bottom topography and capture the signature of the boundary currents in the TS climatologies. The model configuration spans from 10°N to 66°N in the Atlantic. The model is used to produce mean fields of T, S and velocities for each 5-yr period from 1955–59 to 1994–98. The initial TS fields were optimally interpolated on the model grid from the pentadal fields available on a 1°x1° grid and 33 z-levels. These pentadal fields were constructed from objectively analyzed anomalies of T and S down to 3000 m [Levitus et al. 2005; Boyer et al. 2005] and from the associated mean climatology (down to the bottom). Wind stress and surface fluxes are provided by the atmospheric reanalyses from NCEP [Kalnay et al. 1996

BAMS] and ECMWF ERA-40 [Uppala et al. 2005 QJRMS], averaged over the corresponding 5-yr periods. Three semi-diagnostic methods are implemented. Constant Tracers (hereafter CT): T and S are kept constant during the model integration, only the momentum equations are integrated in time and reach a steady state within months [Holland and Hirschman 1972]; the final velocity fields are averaged over months 6 to 12. Robust Diagnostic (RD): the tracer equations are now integrated in time with an additional relaxation to initial values with a timescale of 30 days [Sarmiento and Bryan 1982]; kinetic and potential energy adjusts within 6 months, and the final fields are averaged over the second year of integration. Short Prognostic (PR): the full dynamics and tracer equations are integrated for 45 days such that the barotropic velocities adjusts but the tracers do not drift away from the initial state [Ezer and Mellor 1994]; the final fields are averaged over the days 31 to 45. Rms differences between the initial and final TS fields are similar for both RD and PR methods (around 0.3 K at 100 m, 0.05 K at 1000 m and less than 0.01 K below 2000 m), although the former is in steady-state while the latter drifts rapidly from the initial state and longer prognostic integration would lead to much larger differences. Because the use of annual mean fields instead of seasonal cycle may be arguable, we have tested that the diagnostic transports of mass and heat on the annual mean climatology very closely resemble the mean of these diagnostics for the seasonal climatologies. Results are shown in Fig.1 for 1957-1996.

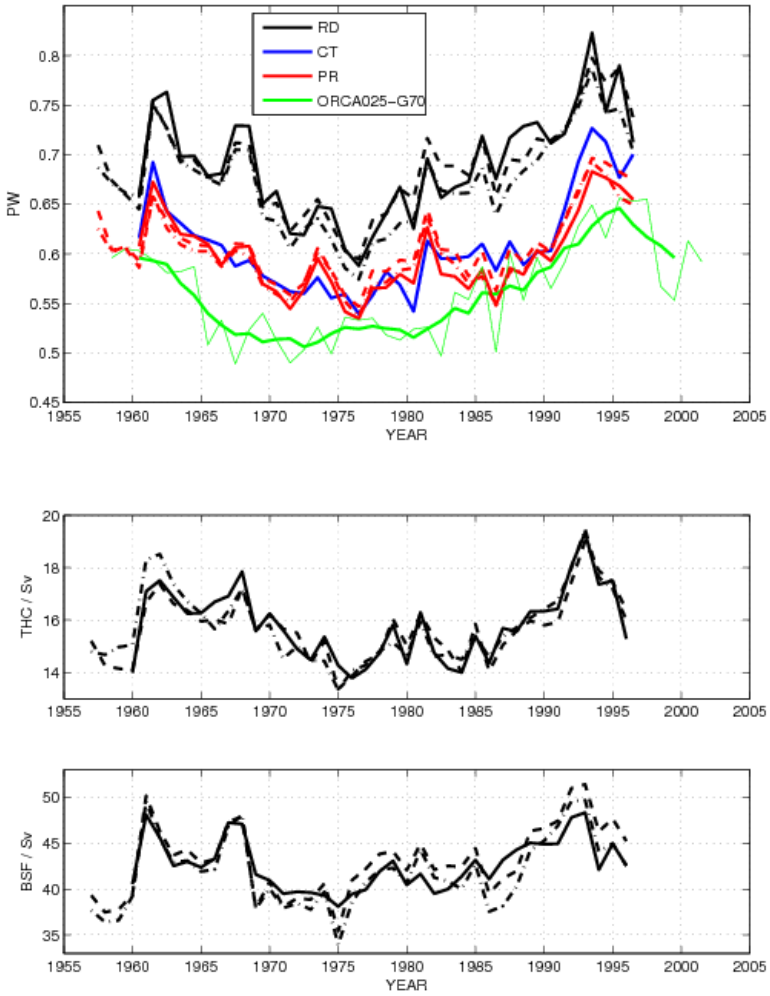

Figure 1: (top) Poleward heat transport maximum in the subpolar gyre (45-60°N) for the 3 diagnostic methods (RD robust diagnostic, CT constant tracers, SP short prognostic) implemented in a North Atlantic ROMS configuration using NODC pentadal TS anomalies and various forcings: ERA-40 (solid) or NCEP (dashed) 5-yr averaged surface fluxes, ERA-40 40-yr-averaged fields (dash-dotted); global prognostic reference simulation of the Drakkar project, ORCA025-G70, annual and pentadal means (green). (middle) Thermohaline circulation and (bottom) barotropic subpolar gyre intensity at 48°N, here for the RD method, show coherent variations with the poleward heat transport. Source: Huck et al. (2008).

3. Implementation of the robust diagnostic method in a global model configuration

Several limitations of the previous methods are addressed in this next step. First, to avoid open boundaries, a global model configuration is used with a ½° resolution, refined towards the equator: OPA ORCA05 [Molines et al. 2006]. The model integration is now continuous in time from 1958 to 2008. The surface forcing set is DFS4 [Brodeau et al. 2010] based on ERA-40 atmospheric reanalysis. The robust diagnostic method is implemented with relaxation time scale of 50 days in the upper 800m and 1 year in the deep ocean [Madec and Imbard 1996], although comparison with a uniform restoring field of 120 day shows no major change. The restoring TS fields, now varying in time and according to the seasonal cycle, are reconstructed from the annual or pentadal anomaly added to the monthly mean climatology. NODC pentadal fields are used for the period 1958 to 1996 as in the previous section. From 1997 to 2008, annual anomaly fields are used down to 2000m [von Schuckmann et al. 2009, Gaillard et al. 2009]. A twin prognostic experiment (ie. with no restoring in the ocean interior) is run for the same period. The restoring term efficiently removes incorrect trends in heat and salt content (not shown), and the evolutions of MOC and MHT diverge within 15 yr but show similar decadal variability (Fig. 2). Comparison is also performed with the Drakkar project reference experiment at ¼° resolution, ORCA025-G70 [Barnier et al. 2006]. In general, although the mean values of heat and mass transport

significantly vary from one model to the other, especially at 24°N, the decadal and longer variations show more coherence.

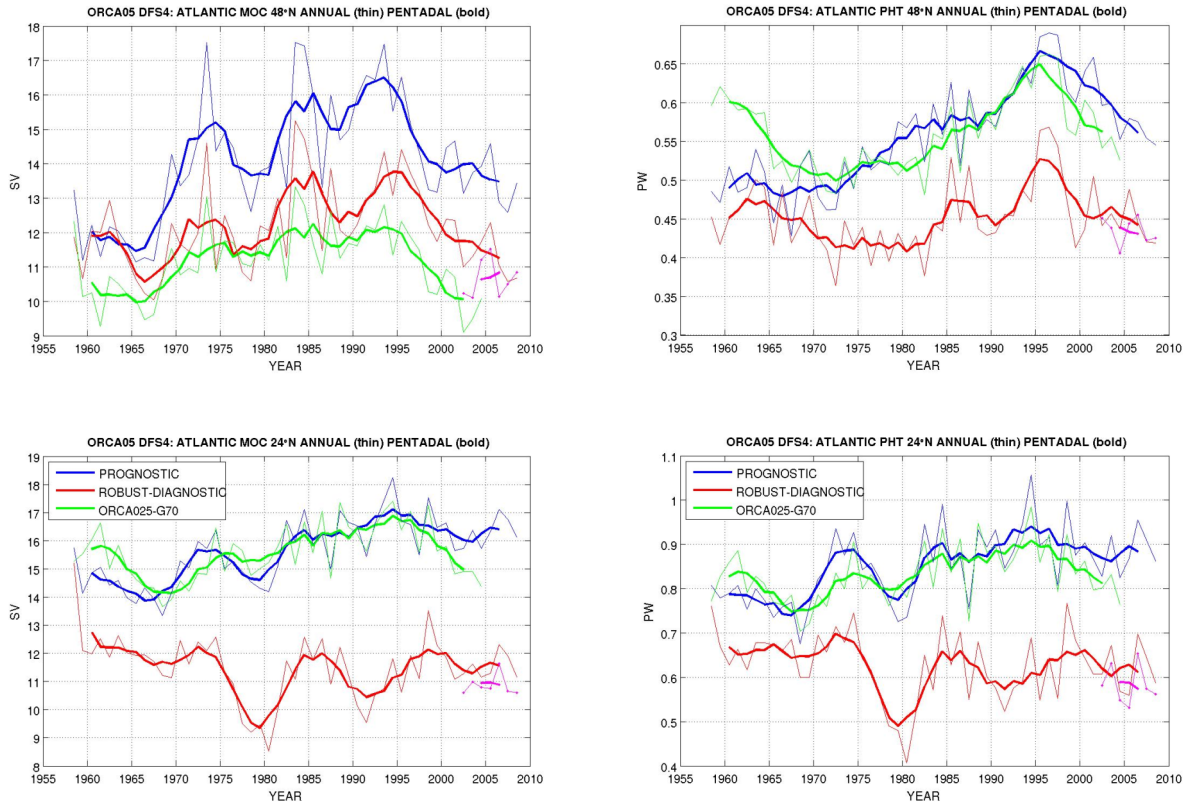

Figure 2: Synthesis of global ORCA05 simulations, prognostic (blue) and robust diagnostic (red), and comparison with Drakkar reference simulation (ORCA025-G70, green) for the evolution of the maximum meridional overturning circulation (MOC) and meridional heat transport (PHT) at 24°N (bottom) and 48°N (top) in the Atlantic. Thin (bold) lines are annual (pentadal) means. Dots correspond to average over the last 2 years for "equilibrium" 12-yr long simulations with restoring and DFS4 forcing of the year repeated (magenta). The decline of mass and heat transport at 48°N since 1995, opposite to the long term 1958-2008 tendency, appears as the most robust signal.

4. Discussion and conclusion

This work provides an estimate of the low-frequency variability in the North Atlantic circulation based on in situ TS data using simple methods: diagnostic, robust-diagnostic and short prognostic. Without finely tuning the model configuration or parameterizations, the variability in mass and heat transports associated with the thermohaline changes has been successfully captured in the subpolar gyre, as compared to state-of-the-art prognostic models: energetic barotropic and overturning circulations drive high heat transport in the early 60's and mid 90's, whereas both circulations and heat transport are at the lowest in the mid 70's, and declining since 1995, in agreement with observational estimates attributed to NAO forcing [Curry and McCartney, 2001]. Our methods also point out an apparent phase opposition in heat transport between the subtropical and subpolar gyres, that could result from the delayed adjustment of the meridional overturning at lower latitude to the low-frequency NAO forcing [Eden and Jung 2001]. The original idea of relying on in situ observations rather than changes in the surface forcing to investigate the variations of the ocean circulation provides an alternative to prognostic hindcast models, with or without assimilation, that avoids potential model drift associated with uncertainties in both subgrid-scale processes parameterizations and surface fluxes. Yet let us recall that these are dynamical and not thermodynamical methods: they allow only limited insight in heat or salt budgets for instance. The pentadal/annual TS fields are certainly not perfectly constrained over the last decades, especially at depth, and due to the scarcity of salinity data: the robustness of our results should be investigated with the use of alternative products, analyzed on isopycnal surfaces for instance. The large smoothing in the NODC data set, as discussed by Myers et al. [2005], may also have some influence on our results, as well as the transition from NODC to LPO fields. A radical change occurred in the observing system since 2003 with Argo, that allows to build reliable annual fields of TS for the upper 2000m, and we have shown this is sufficient to reconstruct most of the large-scale circulation changes. See Huck et al. [2008] for a detailed analysis of the results.

References

Barnier, B., et al., 2006: Impact of partial steps and momentum advection schemes in a global ocean circulation model at eddy permitting resolution. Ocean Dyn., 56, 1616-7341.

Boyer, T. P., et al., 2005: Linear trends in salinity for the world ocean, 1955–1998, Geophys. Res. Lett., 32, L01604.

Brodeau, L., et al., 2010: An ERA40-based atmospheric forcing for global ocean circulation model. Ocean Model., 31, 3-4, 88-104.

Bryden, H. L., H. R. Longworth, S. A. Cunningham, 2005: Has the Atlantic overturning circulation slowed?, Nature, 438, 655 – 657.
Curry, R. G., M. S. McCartney, 2001: Ocean gyre circulation changes associated with the NAO, J. Phys. Oceanogr., 31, 3374– 3400.

Dickson, B., et al., 2002: Rapid freshening of the deep North Atlantic Ocean over the past four decades, Nature, 416, 832– 837.

Dickson, R., et al., 1996: Long-term coordinated changes in convective activity of the North Atlantic, Prog. Oceanogr., 38, 241– 295.

Eden, C., T. Jung, 2001: North Atlantic interdecadal variability: Oceanic response to the NAO (1865-1997). J. Clim., 14, 676– 691.

Ezer, T., G. L. Mellor, 1994: Diagnostic and prognostic calculations of the North Atlantic circulation and sea level using a sigma coordinate ocean model, J. Geophys. Res., 99, 14,159–14,172.

Ezer, T., et al., 1995: On the interpentadal variability of the North Atlantic Ocean. J. Geophys. Res., 100, 10,559 – 10,566.

Gaillard, F., et al., 2009: Quality control of large Argo datasets. J. Atmos. Ocean. Technol., 26 (2),. 337-351.

Greatbatch, R. J., J. Xu, 1993: On the transport of volume and heat through sections across the North Atlantic: Climatology and the pentads 1955 – 1959, 1970 – 1974, J. Geophys. Res., 98, 10,125 – 10,142.

Gregory, J. M., et al., 2005: A model intercomparison of changes in the Atlantic thermohaline circulation in response to increasing atmospheric CO2 concentration, Geophys. Res. Lett., 32, L12703, doi:10.1029/2005GL023209.

Häkkinen, S., P. B. Rhines, 2004: Decline of subpolar North Atlantic circulation during the 1990s, Science, 304, 555 – 559.

Holland, W. R., A. D. Hirschman, 1972: A numerical calculation of the circulation in the North Atlantic Ocean, J. Phys. Oceanogr., 2, 336 – 354.

Huck, T., et al., 2008: Low-frequency variations of the large-scale ocean circulation and heat transport in the North Atlantic from 1955-1998 in-situ temperature and salinity data. Geophys. Res. Let., 35, L23613.

Levitus, S., J. Antonov, T. Boyer, 2005: Warming of the world ocean, 1955 – 2003, Geophys. Res. Lett., 32, L02604.

Madec, G., M. Imbard, 1996: A global ocean mesh to overcome the North Pole singularity. Clim. Dyn., 12, 381-388.

Mellor, G. L., et al., 1982: A diagnostic calculation of the general circulation of the Atlantic Ocean, Deep Sea Res. A, 29, 1171-1192.

Molines, B. et al., 2006: Definition of the global 1/2° experiment with CORE forcing, ORCA05-G50. LEGI report DRA-1-11-2006.

Myers, P. G., S. Grey, K. Haines, 2005: A diagnostic study of interpentadal variability in the North Atlantic Ocean using a finite element model, Ocean Modell., 10, 69–81.

Sarkisyan, A. S., V. P. Keonjiyan, 1975: Review of numerical ocean circulation models using the observed density field, Numerical Models of Ocean Circulation, pp. 76– 93, Natl. Acad. of Sci., Washington, D. C.

Sarmiento, J. L., K. Bryan, 1982: An ocean transport model for the North Atlantic, J. Geophys. Res., 106, 16,711 – 16,728.

Shchepetkin, A., J. C. McWilliams, 2005: The Regional Oceanic Modeling System: A split-explicit, free-surface, topography-following coordinate ocean model, Ocean Modell., 9, 347– 404.

von Schuckmann, K., F. Gaillard, P.-Y. Le Traon, 2009: Global hydrographic variability patterns during 2003-2008. J. Geophys. Res., 114, C9, C09007, doi:10.1029/2008JC005237.

Ocean wave research in France, 2007-2010

Fabrice Ardhuin, Ifremer, Brest, France

Recent developments in the investigations of ocean waves are marked by their connections with other geophysical disciplines, from air-sea interactions and remote sensing to seismology, through coastal oceanography. Indeed the current wave of progress toward ever more realistic numerical models of sea states (e.g. WISE group 2007) has been based on the analysis of a wider range of observations from various types of instruments. Among these, the space-borne synthetic aperture radar data acquired in "wave mode" by the Advanced SAR on board ESA's Envisat mission, a legacy of the ERS 1 and 2 missions thanks to Klaus Hasselmann, has been used to measure the dissipation rates of trans-oceanic swells, with unprecedented accuracy (Ardhuin et al. 2009). The e-folding scales of swells was found to vary systematically with wave steepness and period, from 2000 to over 20000 km for wave periods in the range 13 to 18s. This measurement gave us the biggest missing piece in the energy balance of wave fields at global scale. A tentative theory has been proposed for the observed nonlinear dissipation rate, with stronger dissipation for steeper swells, which may reconcile observations of wave-driven winds and the persistence of swells at global scales. Yet a full understanding of the air-sea boundary layer is still missing.

Based on this observation, the parameterizations of wave dissipation processes have been re-established, with more accurate numerical wave models (Ardhuin et al. 2010). This accuracy was verified against measurements of wave heights, directional wave parameters spectral distributions which include some parameters relevant for many geophysical applications. In particular the mean square slopes of the sea surface can now be estimated with a relative accuracy of about 15% r.m.s., which thus includes the long wave contribution to the slopes. This opens new perspectives for the processing of remote sensing data, in particular for the sea surface salinity retrievals from the SMOS and Aquarius missions, for which the slopes induced by the long waves can produce deviations in the measured quantities (brightness temperatures) equivalent to a salinity change by up to 3 P.S.U. Likewise, these effort make it now possible to improve the sea state bias estimates for more accurate estimates of sea level using altimetry (Tran et al. 2010).

A more challenging area of application, because of the poor knowledge of the directional wave properties, is the estimation of seismic noise sources from ocean wave spectra. Ardhuin et al. (manuscript submitted to J. Geophys. Res.) have demonstrated the capability to reproduce observed seismic spectra with unprecedented accuracy, for most of the global seismic network stations (e.g. figure 1). Using the theory by Hasselmann (1963), this numerical model has revealed that seismic noise sources are strongest in the middle of ocean basins, although many land-based seismometers are mostly sensitive to coastal sources only. This determination of seismic source locations is an important step for better interpretations of seismic noise correlations (Shapiro and Campillo 2004). This seismic noise model was also used to refine estimates of sea states from seismic noise which should provide more accurate analyses of past wave climates, as already proposed by Bernard (1990) or Grevemeyer et al. (2000).

There has also been strong developments in the theoretical formulation of the interaction of waves, currents and turbulence (e.g. Ardhuin et al. 2008), which are now being implemented in three-dimensional primitive equation models for the investigation of nearshore flows with a wide variety of applications: from sediment dynamics to water quality or storm surges. In this area the parameterization of bottom friction and mixing will still require more work, while observations are still scarce and limited. The general improvement in our understanding of wave dynamics should not conceal the formidable questions that are still unaswered. These include the effect of breaking waves on fluxes across the ocean surface. This is probably the most important problem at hand, either for upper ocean mixing (e.g. Rascle and Ardhuin 2009) or for the production of marine aerosols which have a key role in the climate regulation by clouds. On this front we can mention the remarkable measurements by Reul et al. (2008) of modifications of the wind stress by breakers. These observations and others made internationally are feeding the development of the next generation of wave model parameterization, which should aim at predicting wave breaking statistics for many geophysical and other applications.

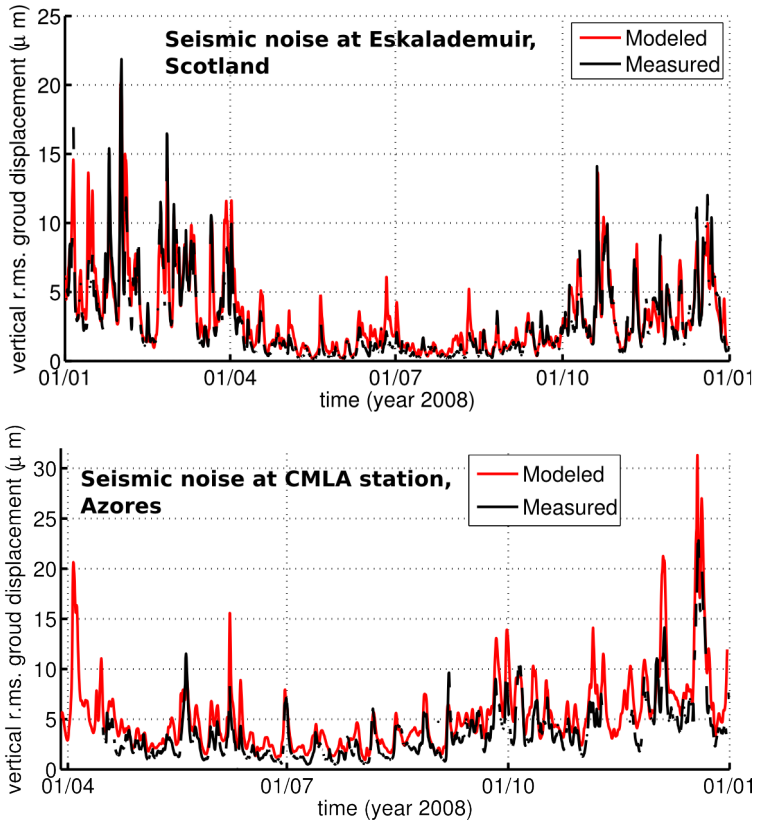

Figure 1: Observed and modelled ground motion caused by secondary microseisms in the North Atlantic, as recorded by two seismic stations. The model is described in Ardhuin et al. (submitted) using the latest improvements in numerical wave modelling. Earthquakes have been filtered out from the measured time series.

References

Ardhuin F., B. Chapron, and F. Collard, "Observation of swell dissipation across oceans," Geophys. Res. Lett., vol. 36, p. L06607, 2009a.

Ardhuin F., E. Rogers, A. Babanin, J.-F. Filipot, R. Magne, A. Roland, A. van der Westhuysen, P. Que□eulou, J.-M. Lefevre, L. Aouf, and F. Collard, "Semi-empirical dissipation source functions for wind-wave models: part I, definition, calibration and validation," J. Phys. Oceanogr., vol. 40, p. in press, 2010.

F. Ardhuin, E. Stutzmann, M. Schimmel, and A. Mangeney, "Revealing ocean wave sources of seismic noise," J. Geophys. Res., 2010. submitted.

F. Ardhuin, N. Rascle, and K. A. Belibassakis, "Explicit waveaveraged primitive equations using a generalized Lagrangian mean," Ocean Modelling, vol. 20, pp. 35–60, 2008.

P. Bernard, "Historical sketch of microseisms from past to future," Phys. Earth Planetary Interiors, vol. 63, pp. 145–150, 1990.

I. Grevemeyer, R. Herber, and H.-H. Essen, "Microseismological evidence for a changing wave climate in the northeast Atlantic Ocean," Nature, vol. 408, pp. 349–1129, 2000.

K. Hasselmann, "A statistical analysis of the generation of microseisms," Rev. of Geophys., vol. 1, no. 2, pp. 177–210, 1963.

Rascle N. and F. Ardhuin, "Drift and mixing under the ocean surface revisited. stratified conditions and model-data comparisons," J. Geophys. Res., vol. 114, p. C02016, 2009. doi:10.1029/2007JC004466.

N. Reul, H. Branger, and J.-P. Giovanangeli, "Air flow structure over short-gravity breaking water waves," Boundary-Layer Meteorol., vol. 126, pp. 477–705, 2008.

Shapiro, N. M. & Campillo, M. 2004 Emergence of broadband Rayleigh waves from correlations of the ambient seismic noise. Geophys. Res. Lett. 31, L07614. doi:10.1029/2004GL019491

Tran N., D. Vandemark, S. Labroue, H. Feng, B. Chapron, H. L. Tolman, J. Lambin, and N. Picot, “The sea state bias in altimeter sea level estimates determined by combining wave model and satellite data,” J. Geophys. Res., vol. 115, p. C03020, 2010.

WISE Group: «Wave modelling - the state of the art». Progress in Oceanography Vol. 75, pp. 603-674, 2007.

Coastal patterns tracking: a lagrangian approach

Philippe FRAUNIE

Several investigations have been recently conducted in coastal areas in the framework of collaborative field campaigns granted and organized by research agencies and national oceanography administrations (INSU, SHOM, IFREMER) together with university laboratories.

Process oriented measurements and modeling have been performed concerning wind induced and baroclinic small scale features including vortices, filaments, fronts, alongshore current stability, internal tides and waves for better prediction of retention structures and confinement barriers.

In addition to high resolution RV cruises, satellite and HF radar synoptic mapping of the sea surface and vertical profilers and moorings, lagrangian measurements from drifting buoys and gliders have been extensively analysed. Especially, complementary deployment strategy allowed to validate each other measurements and models for high frequency patterns and sudden events both in tidal (bay of Biscay) and microtidal (Gulf of Lions, Adriatic sea) coastal environments. Figures 1 to 3 give examples of investigations in different coastal areas.

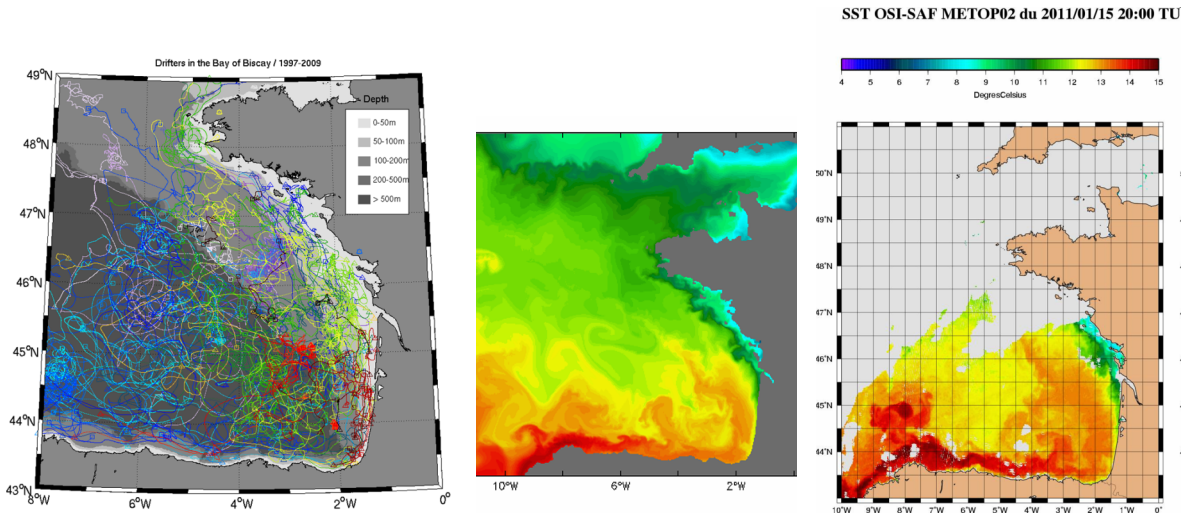

Fig 1. Drifted buoys trajectories in the bay of Biscay (EPIGRAM project, 2009-2012) (Charria et al) and Navidad event (southern warm waters inflow on the shelf) (Le Cann, Serpette et al)

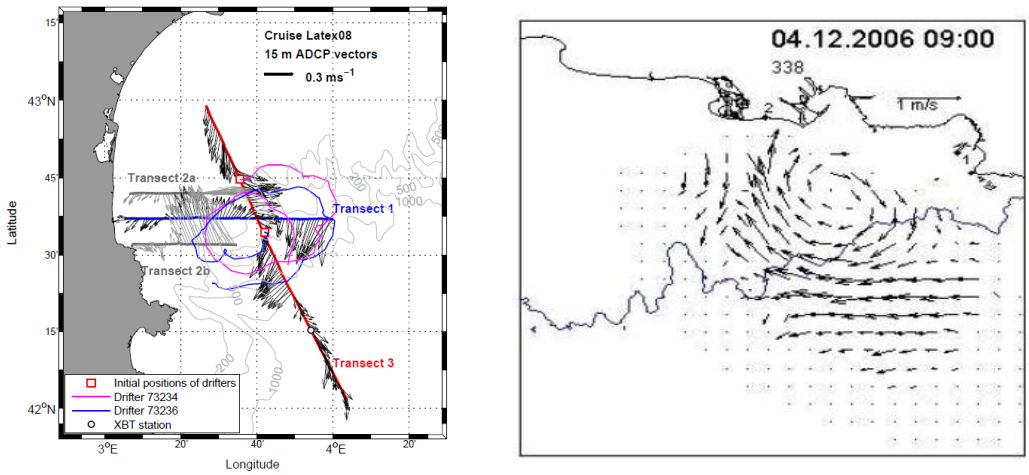

Fig 2. Anticyclonic vortices in the Gulf of Lions (LATEX and ECOLO experiments) ADCP, drifters and HF radar measurements) (Hu et al., 2010, Allou et al 2009)

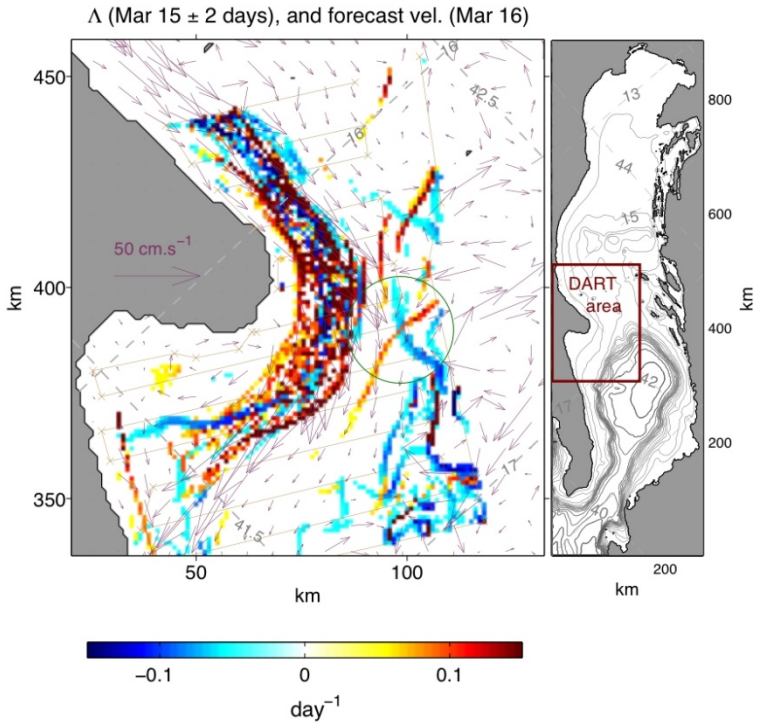

Fig. 3 Model-based directed drifter launches in the Adriatic Sea:
Results from the DART experiment, Haza et al., 2007.

New projects are concerning better understanding of coastal and internal waves from theoretical and high resolution long series measurements (Bouruet Aubertot et al, Zeitline et al).

Selected references :

Bay of Bisacy project :

Marsaleix P., Ulses C., Pairaud I., Herrmann M.J., Floor J.W., Estournel C., Auclair F., 2009. Open boundary conditions for internal gravity wave modelling using polarization relations. Ocean Modelling, 29, 27-42.

Le Hénaff M., De Mey P., Marsaleix P., 2009. Assessment of observational networks with the Representer Matrix Spectra method-application to a 3D coastal model of the Bay of Biscay. Ocean Dynamics, 59, 3-20

Philippe Grosso, Marc Le Menn, Jean-Louis De Bougrenet De La Tocnaye, Zong Van Wu, Damien Malarde, 2009. Deep-Sea Research 1 57 (2010) 151- 156. Practical versus absolute salinity measurements: New advances in high performance seawater salinity sensors.

G. Reverdin, J. Boutin, N. Martin, A. Lourenco, P. Bouruet-Aubertot, A. Lavin, J. Mader, P. Blouch, J. Rolland, F. Gaillard, P. Lazure, 2010. accepted JAOT-O. Temperature measurements from surface drifters.

Michel S., Vandermeirsch F. and Lorance, P., 2009. Aquat. Living Resour., volume 22, 447-461. DOI: 10.1051/alr/2009054. Evolution of upper layer temperature in the Bay of Biscay during the last 40 years.

Bonneton, P., Bruneau, N., Marche, F. and Castelle, B. 2010. DCDS-S, in press. Large-scale vorticity generation due to dissipating waves in the surf zone.

Cienfuegos, R., Barthelemy, E. and Bonneton, P. 2010. J. Waterway, Port Coastal and Ocean Engrg, 136, 10-26. A wave-breaking model for Boussinesq-type equations including mass-induced effects.

Bruneau, N., Castelle, B., Bonneton, P., Pedreros, R., Almar, R., Bonneton, N., Bretel, P., Parisot, J-P. and Sénéchal, N. 2009. Continental Shelf Res, 29,1650–1662, doi:10.1016/j.csr.2009.05.005. Field observations of an evolving rip current on a meso-macrotidal well-developed inner bar and rip morphology.

Lannes D., Bonneton P. 2009. Physics of Fluids 21 (1), 016601 (9 pages), DOI: 10.1063/1.3053183. Derivation of asymptotic two-dimensional time-dependent equations for surface water wave propagation.

Ardhuin, F., B. Chapron, and F. Collard, 2009. Geophysical Research Letters, vol. 36, p. L06607. Strong decay of steep swells observed across oceans.

Ardhuin, F., L. Marié, N. Rascle, P. Forget, and A. Roland, 2009. Journal of Physical Oceanography, 39, 2820—2838. Observation and estimation of Lagrangian, Stokes and Eulerian currents induced by wind and waves at the sea surface.

Collard, F., Ardhuin, F., B. Chapron, 2009. Journal of Geophysical Research, 114, C07023. Routine monitoring and analysis of ocean swell fields using a spaceborne SAR.

V. Rossi, C. Lopez, E. Hernandez-Garcia, J. Sudre, V. Garcon, and Y. Morel, 2009. Nonlin. Processes Geophys., 16, 557–568. Surface mixing and biological activity in the four Eastern Boundary Upwelling.

Cécile Renaudie, Rémy Baraille, Yves Morel, Gwenaëlle Hello, Hervé Giordani, 2009. Ocean Modelling, 30, 178-189. Adaptation of the vertical resolution in the mixed layer for HYCOM.

V. Rossi, Y. Morel and V. Garçon, 2009. Ocean Modelling, doi : 0.1016/j.ocemod.2009.10.002. Effect of the wind on the dynamics of the shelf : formation of a secondary upwelling along the continental margin.

B. Le Cann and A. Serpette, 2009. Continental Shelf Research, doi:10.1016/j.csr.2008.11.015. Intense warm and saline upper ocean inflow in the southern Bay of Biscay in autumn-winter 2006-2007.

Le Boyer A., Cambon G., Daniault N., Herbette S., Le Cann B., Marié L., Morin P, 2009. Cont. Shelf. Res. (29) 1026-1037. Observations of the Ushant tidal front in september 2007

L. Marié, 2009. Nonlin. Processes Geophys. (17), 49-63, 2010. A study of the phase instability of quasi-geostrophic Rossby waves on the infinite beta-plane to zonal flow perturbations.

Rascle, N., F. Ardhuin, 2009. Journal of Geophysical Research, 114, C02016, doi:10.1029/2007JC00446. Drift and mixing under the ocean surface. Part 2: Stratified conditions and model-data comparisons.

Y. Morel and L. Thomas, 2009. Ocean Modelling, doi:10.1016/j.ocemod.2009.01.002. Ekman drift and vortical structures.

Mediterranean sea projects :

Hu, Z.H., Petrenko, A.A., Doglioli, A.M., Dekeyser, I. (2011), Numerical Study of eddy generation in the western part of the Gulf of Lion, JGR, submitted

Hu, Z.H., Petrenko, A.A., Doglioli, A.M., Dekeyser, I. (2010), Study of coastal eddies : application in the Gulf of Lion. J. Marine Syst., accepted.

Hu, Z.H., Doglioli, A.M., Petrenko, A.A., Marsaleix, P., Dekeyser, I. (2009), Numerical simulations of eddies in the Gulf of Lion. Ocean Model., Vol. 28/4, pp. 203-208, doi : 10.1016/j.ocemod.2009.02.004

Allou A., Forget P. and J.L. Devenon (2009) Submesoscale vortex structures at the entrance of the Gulf of Lions in the Northwestern Mediterranean Sea. Cont. Shelf Res., 30: 724-732

André G., Garreau P., Fraunié P. (2009) Mesoscale slope current variability in the Gulf of lions. Interpretation of in-situ measurements using a 3D model, Cont. Shelf Res. 29: 407-423

Casella E., Molcard A., Provenzale A. , Simulations of sub-mesoscale eddies in the Ligurian Sea. J. Mar. Syst., to appear.

Dufois F., Garreau P., Le Hir P., Forget P. (2008), Wave and current-induced bottom shear stress distribution in the Gulf of Lions. Continental Shelf Res., 28(15), pp.1920-1934.

Forget P. and G. André (2007), Can satellite-derived chlorophyll imagery be used to trace surface dynamics in coastal zone ? A case study in the Northwestern Mediterranean Sea. Sensors 7 884-904.

Forget, P., M. Saillard, and P. Broche, (2006) Observations of the sea surface by coherent L band radar at low grazing angles in a nearshore environment, J. Geophys. Res., 111 C09015, doi:10.1029/2005JC002900.

Haza A., Ozgokmen T.M., Griffa A., Molcard A., Poulain P.-M., Peggion G. (2010), Transport properties in small scale coastal flows : relative dispersion from VHF radar measurements in the Gulf of La Spezia, Ocean Dynam.,sous presse.

Haza, A. C.,A. Griffa, P. Martin, A. Molcard, T. M. Ozgokmen, A. C. Poje, R. Barbanti, J. Book, P. M. Poulain, M. Rixen, P. Zanasca (2007), Model-based directed drifter launches in the Adriatic Sea: Results from the DART Experiment, Geophys. Res. Letters 34 L10605 , doi:10.1029/2007GL029634

Jouon A., Douillet P., Ouillon S., Fraunié P. (2006), Calculations of hydrodynamic time parameters in a semi-opened coastal zone using a 3D hydrodynamical model, Cont. Shelf Res., 26, 1395-1415.

Langlais C., Barnier B., Molines J.M., Fraunié P., Jacob D., Kotlarski S. (2009) Evaluation of dynamically downscalled atmospheric reanalysis in the prospect of forcing long term simulations of the ocean circulation in the Gulf of Lions.,Ocean Modelling 30: 270-286

Maps F, Plourde S, Zakardjian B (2010) Control of dormancy by lipid metabolism in Calanus finmarchicus: a population model test , Mar. Ecol. Progr. Ser. 403 165-180), doi:10.3354/meps08525

Molcard A., Poulain P.M., Forget P., Griffa A., Barbin Y., Gaggelli J., De Maistre J.C., Rixen M. (2009), Comparison between VHF radar observations and data from drifter clusters in the Gulf of La Spezia (Mediterranean Sea), J. Mar. Sys., 78:79-89./

Taillandier, V., A. Griffa, A. Molcard (2006) A variational approach for the reconstruction of regional scale Eulerian velocity fields from Lagrangian data, Ocean Modelling 13(1): 1-24

F. Bouchut and V. Zeitlin, A robust well-balanced scheme for multi-layer shallow water equations, 2010, Discr. and Cont. Dyn. Systems, 13, 739 – 758 .

F. Bouchut, E. Scherer, and V. Zeitlin, Nonlinear adjustment of a front over escarpment, 2008, Phys. Fluids, 20, 016602-1 – 016602-12.

Bouruet-Aubertot, P., van Haren, H., Lelong, M.P. 2010 "Stratified inertial subrange in the boundary layer of Rockall channel", J. Phys. Oceanogr., 40, 2401- 2417..

Bouruet-Aubertot, P., Mercier, H., Gaillard, F., Lherminier, P. 2005. Evidence of strong inertio-gravity waves during POMME experiment, J. Geophys. Res., 110, doi 10-1029/2004JC002747

Ferrarri, R., Wunsch, C. 2010. The distribution of eddy kinetic and potential energies in the global ocean. Tellus, 62A, 92-108.

J. Gula, R. Plougonven, and V. Zeitlin, Ageostrophic instabilities of fronts in a channel in a stratified rotating fluid, 2009, J. Fluid. Mech., 627, 485 - 507 .

J. Gula and V. Zeitlin, Instabilities of buoyancy-driven coastal currents and their nonlinear evolution in the two-layer rotating shallow water model. I. Passive lower layer, 2010, J. Fluid Mech. 659, 69 - 93.

J. Gula , V. Zeitlin and F. Bouchut, Instabilities of buoyancy-driven coastal currents and their nonlinear evolution in the two-layer rotating shallow water model. II. Active lower layer, 2010, J. Fluid Mech. – in press.

Komori, N., Ohfuchi, W., Taguchi, B., Sasaki H., Klein, P. 2008 « Deep ocean inertia-gravity waves simulated in a high-resolution global coupled atmosphere-ocean gcm » Geophys. Res. Lett., 35, 1897-1915.

Le Vaillant, X., Cuypers, Y., Bouruet-Aubertot, P., Vialard, J., McPhaden, M. 2010. «Generation and propagation of near-inertial baroclinic waves during Cirene experiment : energy fluxes and impact on vertical mixing", submitted to J. Geophys. Res.

Medvedev, S.B., Zeitlin, V. "Turbulence of near-inertial waves in the continuously stratified fluid" Phys. Letters A, v. 371, p.221-227

G. Reznik and V. Zeitlin, Resonant excitation of trapped waves by free inertia-gravity waves in coastal waveguide, and their nonlinear evolution, 2010 J. Fluid Mech. – accepted.

Scherer E. and V. Zeitlin, Stability and nonlinear evolution of coupled geostrophic density fronts, 2008, J. Fluid. Mech., 613, 309 - 327.

Winters, K., Bouruet-Aubertot, P., Gerkema, T. 2010. "Critical reflexion and abyssal trapping of near-inertial waves on a beta plane", submitted to J. Fluid Mech., in revision

Zervakis, V., Levine, M.D. 1995. Near-inertial energy propagation from the mixed layer: theoretical considerations. J. Phys. Oceanogr., 25, 2872-2889.

Comité National Français de Géodésie et Géophysique

French National Committee of Geodesy and Geophysics

RAPPORT QUADRIENNAL DU CNFGG A l'UGGI

QUADRENNIAL REPORT OF CNFGG TO IUGG

SECTION 8 – SCIENCES DE LA CRYOSPHERE

SECTION 8 – CRYOSPHERIC SCIENCES

IUGG 2011
Cryosphere report – France
March 2011

GPS measurements on Chhota Shigri, India (PhotoP. Wagnon)

In this report are found a selection of papers related to cryosphere with an important contribution of french scientists. The objective is to give a general view of the research conducted in France in this domain. The period of interest in 2007-2010.

The main contributors are from the following main laboratories:

- Laboratoire de Glaciologie et Géophysique de l'Environnement, Grenoble (**http://www-lgge.obs.ujf-grenoble.fr/**)
- Centre National de Recherche Météorologique, Météo-France, Toulouse et Grenoble (**http://www.cnrm-game.fr/**)
- Laboratoire des Sciences du Climat et de l'Environnement, Paris (**http://www.lsce.ipsl.fr/**)
- Laboratoire d'Etudes en Géophysique et Océanographie Spatiales, Toulouse (**http://www.legos.obs-mip.fr/**)
- Laboratoire des Transferts en Hydrologie et Environnement, Grenoble (**http://www.lthe.fr/LTHE/**)
- Laboratoire d'Océanographie et du Climat, Paris (**https://www.locean-ipsl.upmc.fr/**)
- Hydrosciences, Montpellier (**http://www.hydrosciences.org/**)
- GIPSA-LAB, Grenoble (**http://www.gipsa-lab.inpg.fr/**)

Papers were divided in a few main categories as follows.

1 – SNOW

1-1 Snow modelling (including snow-climate interactions)

1-1-1 Main references with abstracts

Lejeune, Y., P. Wagnon, L. Bouilloud, P. Chevallier, P. Etchevers, E. Martin, E. Sicart and F. Habets (2007) : **Melting of snow cover in a tropical mountain environment in Bolivia : Processes and modeling**. Journal of Hydrometeorology, 8(4), 922-937.

Abstract : To determine the physical processes involved in the melting and disappearance of transient snow cover in nonglacierized tropical areas, the CROCUS snow model, interactions between Soil–Biosphere–Atmosphere (ISBA) land surface model, and coupled ISBA/CROCUS model have been applied to a full set of meteorological data recorded at 4795 m MSL on a moraine area in Bolivia (16°17'S, 68°32'W) between 14 May 2002 and 15 July 2003. The models have been adapted to tropical conditions, in particular the high level of incident solar radiation throughout the year. As long as a suitable function is included to represent the mosaic partitioning of the surface between snow cover and bare ground and local fresh snow grain type (as graupel) is adapted, the ISBA and ISBA/CROCUS models can accurately simulate snow behavior over nonglacierized natural surfaces in the Tropics. Incident solar radiation is responsible for efficient melting of the snow surface (favored by fresh snow albedo values usually not exceeding 0.8) and also for the energy stored in snow-free areas (albedo = 0.18) and transferred horizontally to adjacent snow patches. These horizontal energy transfers (by conduction within the upper soil layers and by turbulent advection) explain most of the snowmelt and prevent the snow cover from lasting more than a few days during the wet season in this high-altitude tropical environment.

Brzoska, J.B., F. Flin and J. Barckicke (2008) : **Explicit iterative computation of diffusive vapour field in the 3-D snow matrix : some preliminary results for low flux metamorphism**. Annals of Glaciology, **48**, 13-18.

Abstract : The metamorphism of seasonal snow is classically considered as limited by vapour diffusion in the pore phase. To account for the lack of knowledge of the ice–vapour reaction coefficient near 0◦C, the assumption of a reaction-limited metamorphism was first tested in three-dimensional simulations at low and very low temperature gradients; however, the validity of such results is difficult to verify experimentally. By a reasoned use of traditional iterative schemes, vapour diffusion is now simulated in three dimensions on tomographic snow data, mapping the gradient of vapour pressure near the grains. Repeating this process may provide a way to simulate the isothermal metamorphism without grain packing at a reasonable expense of computation time. Preliminary results are compared with existing computations made within the reaction-limited hypothesis.

Flin, F. and J.B. Brzoska (2008) : **The temperature gradient metamorphism of snow: vapour diffusion model and application to tomographic images**. Annals of Glaciology, vol. **49**, pp 17-21.

Abstract : A simple physical model describing the temperature-gradient metamorphism of snow is presented. This model, based on Kelvin's equation and Fick's law, takes into account the local variation of the saturating vapour pressure

with temperature. It can determine locally whether the ice is condensing or subliming, depending on both the pressure and temperature fields in the snow structure. This model can also explain the formation of facets that occurs during the metamorphism. Using X-ray microtomographic images of snow samples obtained under low to moderate temperature-gradient conditions, this model has been tested and compared to the reaction-limited model proposed in a previous work.

Bouilloud, L.; Martin, E.; Habets, F.; Boone, A.; Moigne, P. L.; Livet, J.; Marchetti, M.; Foidart, A.; Franchistéguy, L.; Morel, S.; Noilhan, J. and Pettré, P. (2009), **Road Surface Condition Forecasting in France,** Journal of Applied Meteorology and Climatology, 48, 2513-2527.

Abstract : A numerical model designed to simulate the evolution of a snow layer on a road surface was forced by meteorological forecasts so as to assess its potential for use within an operational suite for road management in winter. The suite is intended for use throughout France, even in areas where no observations of surface conditions are available. It relies on short-term meteorological forecasts and long-term simulations of surface conditions using spatialized meteorological data to provide the initial conditions. The prediction of road surface conditions (road surface temperature and presence of snow on the road) was tested at an experimental site using data from a comprehensive experimental field campaign. The results were satisfactory, with detection of the majority of snow and negative road surface temperature events. The model was then extended to all of France with an 8-km grid resolution, using forcing data from a real-time meteorological analysis system. Many events with snow on the roads were simulated for the 2004/05 winter. Results for road surface temperature were checked against road station data from several highways, and results for the presence of snow on the road were checked against measurements from the Météo-France weather station network.

Durand, Y., G. Giraud, M. Laternser, P. Etchevers, L. Mérindol and B. Lesaffre (2009) : **Reanalysis of 47 years of climate in the French Alps (1958 – 2005): climatology and trends for snow cover.** Journal of Applied Meteorology and Climatology, 48(12), 2487-2512.

Abstract : Since the early 1990s, Météo-France has used an automatic system combining three numerical models to simulate meteorological parameters, snow cover stratification, and avalanche risk at various altitudes, aspects, and slopes for a number of mountainous regions in France. Given the lack of sufficient directly observed long-term snow data, this "SAFRAN"–Crocus–"MEPRA" (SCM) model chain, usually applied to operational avalanche forecasting, has been used to carry out and validate retrospective snow and weather climate analyses for the 1958–2002 period. The SAFRAN 2-m air temperature and precipitation climatology shows that the climate of the French Alps is temperate and is mainly determined by atmospheric westerly flow conditions. Vertical profiles of temperature and precipitation averaged over the whole period for altitudes up to 3000 m MSL show a relatively linear variation with altitude for different mountain areas with no constraint of that kind imposed by the analysis scheme itself. Over the observation period 1958–2002, the overall trend corresponds to an increase in the annual near-surface air temperature of about 1°C. However, variations are large at different altitudes and for different seasons and regions. This significantly positive trend is most obvious in the 1500–2000-m MSL altitude range, especially in the northwest regions, and exhibits a significant relationship with the North Atlantic Oscillation index over long periods.

Precipitation data are diverse, making it hard to identify clear trends within the high year-to-year variability.

Langlois, A., L. Brucker, J. Kohn, A. Royer, C. Derksen, P. Cliche, G. Picard, M. Fily and J.M. Willemet (2009) **: Simulation of Snow Water Equivalent (SWE) using Thermodynamic Snow Models in southern Québec between 2005 and 2006**. Journal of Hydrometeorology, 10(6), 1447-1462.

Abstract : Snow cover plays a key role in the climate system by influencing the transfer of energy and mass between the soil and the atmosphere. In particular, snow water equivalent (SWE) is of primary importance for climatological and hydrological processes and is a good indicator of climate variability and change. Efforts to quantify SWE over land from spaceborne passive microwave measurements have been conducted since the 1980s but a more suitable method has yet to be developped for hemispheric-scale studies, and tools such as snow thermodynamic models allow a better understanding of the snow cover and can potentially significantly improve existing snow products at the regional scale. In this study, the use of three snow models (SNOWPACK, CROCUS and SNTHERM) driven by local and reanalysis meteorological data for the simulation of SWE is investigated temporally through three winter seasons and spatially over intensively sampled sites across Northern Québec. Results show that the SWE simulations are in agreement with ground measurements through three complete winter seasons (2004–2005–2005–2006 and 2007–2008) in southern Québec, with higher error for 2007–2008. The correlation coefficients between measured and predicted SWE values ranged between 0.72 and 0.99 for the three models and three seasons evaluated in southern Québec. In subarctic regions, predicted SWE driven with the North American Regional Reanalysis (NARR) data fall within the range of measured regional variability. NARR data allow snow models to be used regionally, and this paper represents a first step for the regionalization of thermodynamic multi-layered snow models driven by reanalysis data for improved global SWE evolution retrievals.

Rutter N. et al. (2009), **Evaluation of forest snow processes models (SnowMIP2)**, J. Geophys. Res., 114, D06111, doi:10.1029/2008JD011063.

Abstract: Thirty-three snowpack models of varying complexity and purpose were evaluated across a wide range of hydrometeorological and forest canopy conditions at five Northern Hemisphere locations, for up to two winter snow seasons. Modeled estimates of snow water equivalent (SWE) or depth were compared to observations at forest and open sites at each location. Precipitation phase and duration of above-freezing air temperatures are shown to be major influences on divergence and convergence of modeled estimates of the subcanopy snowpack. When models are considered collectively at all locations, comparisons with observations show that it is harder to model SWE at forested sites than open sites. There is no universal ''best'' model for all sites or locations, but comparison of the consistency of individual model performances relative to one another at different sites shows that there is less consistency at forest sites than open sites, and even less consistency between forest and open sites in the same year. A good performance by a model at a forest site is therefore unlikely to mean a good model performance by the same model at an open site (and vice versa). Calibration of models at forest sites provides lower errors than uncalibrated models at three out of four locations. However, benefits of calibration do not translate to subsequent years, and benefits gained by models calibrated for forest snow processes are not translated to open conditions.

Wagnon, P., M. Lafaysse, Y. Lejeune, L. Maisincho, M. Rojas, and J. P. Chazarin (2009) : **Understanding and modeling the physical processes that govern the melting of snow cover in a tropical mountain environment in Ecuador**. Journal of Geophysical Research, 114, D19113.

Abstract : The ISBA/CROCUS coupled ground-snow model developed for the Alps and subsequently adapted to the outer tropical conditions of Bolivia has been applied to a full set of meteorological data recorded at 4860 m above sea level on a moraine area in Ecuador (Antizana 15 glacier, 0°28'S; 78°09'W) between 16 June 2005 and 30 June 2006 to determine the physical processes involved in the melting and disappearance of transient snow cover in nonglaciated areas of the inner tropics. Although less accurate than in Bolivia, the model is still able to simulate snow behavior over nonglaciated natural surfaces, as long as the modeled turbulent fluxes over bare ground are reduced and a suitable function is included to represent the partitioning of the surface between bare soil and snow cover. The main difference between the two tropical sites is the wind velocity, which is more than 3 times higher at the Antizana site than at the Bolivian site, leading to a nonuniform spatial distribution of snow over nonglaciated areas that is hard to describe with a simple snow partitioning function. Net solar radiation dominates the surface energy balance and is responsible for the energy stored in snow-free areas (albedo = 0.05) and transferred horizontally to adjacent snow patches by conduction within the upper soil layers and by turbulent advection. These processes can prevent the snow cover from lasting more than a few hours or a few days. Sporadically, and at any time of the year, this inner tropical site, much wetter than the outer tropics, experiences heavy snowfalls, covering all the moraine area, and thus limiting horizontal transfers and inducing a significant time lag between precipitation events and runoff.

Céron, J.-P. , Tanguy, G., Franchistéguy, L., Martin, E., Regimbeau, F. and Vidal, J.-P. (2010), **Hydrological seasonal forecast over France: feasibility and prospects**, Atmospheric Science Letters, 11, 78-82

Abstract: This article presents a first evaluation of a hydrological forecasting suite at seasonal time scales over France. The hydrometeorological model SAFRAN-ISBA-MODCOU is forced by seasonal forecasts from the DEMETER project for the March–April–May period. Despite a simple downscaling method, the atmospheric forcings are reasonably well represented at the finest scale. The computed soil moisture shows some predictability with large regions of correlation above 0.3. Probabilistic scores for soil moisture and river flows for four different catchments are higher than that for atmospheric variables. These results suggest to go further for building an operational hydrological seasonal forecast system.

Douville H. (2010) **Relative contributions of soil and snow hydrology to seasonal climate predictability: a pilot study.** Climate Dyn., 34, 797-818, doi: 10.1007/s00382-008-0508-1.

Abstract: Land surface hydrology (LSH) is a potential source of long-range atmospheric predictability that has received less attention than sea surface temperature (SST). In this study, we carry out ensemble atmospheric simulations driven by observed or climatological SST in which the LSH is either interactive or nudged towards a global monthly re-analysis. The main objective is to evaluate the impact of soil moisture or snow mass anomalies on seasonal climate variability and predictability over the 1986–1995 period. We first analyse the annual cycle of zonal mean potential (perfect model approach) and effective (simulated vs. observed

climate) predictability in order to identify the seasons and latitudes where land surface initialization is potentially relevant. Results highlight the influence of soil moisture boundary conditions in the summer mid-latitudes and the role of snow boundary conditions in the northern high latitudes. Then, we focus on the Eurasian continent and we contrast seasons with opposite land surface anomalies. In addition to the nudged experiments, we conduct ensembles of seasonal hindcasts in which the relaxation is switched off at the end of spring or winter in order to evaluate the impact of soil moisture or snow mass initialization. LSH appears as an effective source of surface air temperature and precipitation predictability over Eurasia (as well as North America), at least as important as SST in spring and summer. Cloud feedbacks and large-scale dynamics contribute to amplify the regional temperature response, which is however, mainly found at the lowest model levels and only represents a small fraction of the observed variability in the upper troposphere.

Eckert, N., C. Coleou, H. Castebrunet, M. Dechatres, G. Giraud and J. Gaume (2010), **Cross-comparison of meteorological and avalanche data for characterising avalanche cycles : The example of December 2008 in the eastern part of the French Alps**. Cold Regions Science and Technology, 64(2), 119-136.

Abstract : *In December 2008, an intense avalanche cycle occurred in the eastern part of the southern French Alps. Southerly atmospheric fluxes that progressively evolved into an easterly return caused important snowfalls with return periods up to 10 years. Cold temperatures and drifting snow had important aggravating effects. The return period for the number of avalanches was above 50 years in two massifs and some of the avalanche had very long runouts that exceeded historical limits recorded in the French avalanche atlas. Using this case study, this paper illustrates and discusses how avalanche reports, snow and weather data and results from numerical modelling of the snow cover can be combined to analyse abnormal temporal clusters of snow avalanches. For instance, it is shown how statistical techniques developed in other fields can be used to test the significance of different explanatory factors, extract spatio-temporal patterns, compare them with previous cycles and quantify the magnitude/frequency relationship at different scales.*

Peings Y., H. Douville (2010) **Influence of the Eurasian snow cover on the Indian summer monsoon variability in observations and CMIP3 simulations**. Climate Dyn., 34, 643-660, doi:10.1007/s00382-009-0565-0.

Abstract: The present study is aimed at revisiting the possible influence of the winter/spring Eurasian snow cover on the subsequent Indian summer precipitation using several statistical tools including a maximum covariance analysis. The snow–monsoon relationship is explored using both satellite observations of snow cover and in situ measurements of snow depth, but also a subset of global coupled ocean–atmosphere simulations from the phase 3 of the Coupled Model Intercomparison Project (CMIP3) database. In keeping with former studies, the observations suggest a link between an east–west snow dipole over Eurasia and the Indian summer monsoon precipitation. However, our results indicate that this relationship is neither statistically significant nor stationary over the last 40 years. Moreover, the strongest signal appears over eastern Eurasia and is not consistent with the Blanford hypothesis whereby more snow should lead to a weaker monsoon. The twentieth century CMIP3 simulations provide longer timeseries to look for robust snow–monsoon relationships. The maximum covariance analysis indicates that some models do show an apparent influence of the Eurasian snow cover on the Indian summer monsoon precipitation,

but the patterns are not the same as in the observations. Moreover, the apparent snow–monsoon relationship generally denotes a too strong El Niño- Southern Oscillation teleconnection with both winter snow cover and summer monsoon rainfall rather than a direct influence of the Eurasian snow cover on the Indian monsoon.

Peings Y., H. Douville, R. Alkama, B. Decharme (2010) **Snow contribution to springtime atmospheric predictability over the second half of the twentieth century.** Climate Dyn., in press, doi: 10.1007/s00382010-0884-1.

Abstract: A set of global atmospheric simulations has been performed with the ARPEGE-Climat model in order to quantify the contribution of realistic snow conditions to seasonal atmospheric predictability in addition to that of a perfect sea surface temperature (SST) forcing. The focus is on the springtime boreal hemisphere where the combination of a significant snow cover variability and an increasing solar radiation favour the potential snow influence on the surface energy budget. The study covers the whole 1950–2000 period through the use of an original snow mass reanalysis based on an off-line land surface model and possibly constrained by satellite snow cover observations. Two ensembles of 10-member AMIP-type experiments have been first performed with relaxed versus free snow boundary conditions. The nudging towards the monthly snow mass reanalysis significantly improves both potential and actual predictability of springtime surface air temperature over Central Europe and North America. Yet, the impact is confined to the lower troposphere and there is no clear improvement in the predictability of the large-scale atmospheric circulation. Further constraining the prescribed snow boundary conditions with satellite observations does not change much the results. Finally, using the snow reanalysis only for initializing the model on March 1st also leads to a positive impact on predicted low-level temperatures but with a weaker amplitude and persistence. A conditional skill approach as well as some selected case studies provide some guidelines for interpreting these results and suggest that an underestimated snow cover variability and a misrepresentation of ENSO teleconnections may hamper the benefit of an improved snow initialization in the ARPEGE-Climat model.

Rabier, F. et al. (2010), **The CONCORDIASI project in Antarctica**. Bull. Amer. Meteor. Soc.,91, 69-86.

Abstract: The Concordiasi project is making innovative observations of the atmosphere above Antarctica. The most important goals of the Concordiasi are as follows:

1. To enhance the accuracy of weather prediction and climate records in Antarctica through the assimilation of in situ and satellite data, with an emphasis on data provided by hyperspectral infrared sounders. The focus is on clouds, precipitation, and the mass budget of the ice sheets. The improvements in dynamical model analyses and forecasts are used in chemical-transport models that describe the links between the polar vortex dynamics and ozone depletion, and to advance the understanding of the Earth system by examining the interactions between Antarctica and lower latitudes.

2. To improve our understanding of microphysical and dynamical processes controlling the polar ozone, by providing the first quasi-Lagrangian observations of stratospheric ozone and particles, in addition to an improved characterization of the 3D polar vortex dynamics. Techniques for assimilating these Lagrangian observations are being developed.

A major Concordiasi component is a field experiment during the austral springs of 2008–10. The field activities in 2010 are based on a constellation of 19 long-duration stratospheric super-pressure balloons (SPBs) deployed from the McMurdo station. Six of these balloons carried GPS receivers and in situ instruments measuring temperature, pressure, ozone, and particles. Thirteen of the balloons released more than 600 drop-sondes on demand for measuring atmospheric parameters. Lastly, radiosounding measurements were collected at various sites, including the Concordia station. It is shown in the accompanying Figure that the appropriate use of IASI data in retrievals allowed the analysis to retrieve surface temperature at Concordia, in agreement with in situ measurements.

Rousselot, M., Y. Durand, G. Giraud, L. Mérindol, L. Daniel (2010) : ***Analysis and forecast of extreme new-snow avalanches : a numerical study of the avalanche cycle of February 1999 in France****. Journal of Glaciology, 56 (199), 758-770.*

Abstract : Snow and weather conditions typical of exceptional cycles of fresh-snow avalanches in the northern Alps are investigated using the numerical avalanche-hazard forecasting procedure of Météo-France. Sensitivity tests are performed on the events of February 1999 in the Chamonix France region, and resulting snowpack instability modeled at the massif scale is compared using adapted new indices and maps. Our results complete conclusions of earlier observation-based studies by providing new insights into the snow and weather conditions of February 1999. The large avalanches mainly resulted from large and very unstable fresh-snow accumulations. Moreover, the snowpack instability was increased locally by wind transport of light and fresh snow in February. The mechanical weaknesses resulting from the weather conditions prior to February were a key factor in explaining the unusual volumes of these avalanches. This study suggests that the operational numerical SAFRAN/Crocus/ME´PRA (SCM) chain provides reliable forecasts of extreme new-snow avalanche situations at the massif scale, but that local-scale simulations are still needed to improve the efficiency of risk mitigation and civil protection policies.

Jacobi, H.-W., F. Domine, W.R. Simpson, T.A. Douglas, and M. Sturm, **Simulation of the specific surface area of snow using a one-dimensional physical snowpack model: Implementation and evaluation for subarctic snow in Alaska,** *The Cryosphere* 4, 35-51, 2010.

Abstract : The specific surface area (SSA) of the snow constitutes a powerful parameter to quantify the exchange of matter and energy between the snow and the atmosphere. However, currently no snow physics model can simulate the SSA. Therefore, two different types of empirical parameterizations of the specific surface area (SSA) of snow are implemented into the existing one-dimensional snow physics model CROCUS. The parameterizations are either based on diagnostic equations relating the SSA to parameters like snow type and density or on prognostic equations that describe the change of SSA depending on snow age, snowpack temperature, and the temperature gradient within the snowpack. Simulations with the upgraded CROCUS model were performed for a subarctic snowpack, for which an extensive data set including SSA measurements is available at Fairbanks, Alaska for the winter season 2003/2004. While a reasonable agreement between simulated and observed SSA values is obtained using both parameterizations, the model tends to overestimate the SSA. This overestimation is more pronounced using the diagnostic equations compared to the results of the prognostic equations. Parts of the SSA deviations using both parameterizations can be attributed to

differences between simulated and observed snow heights, densities, and temperatures. Therefore, further sensitivity studies regarding the thermal budget of the snowpack were performed. They revealed that reducing the thermal conductivity of the snow or increasing the turbulent fluxes at the snow surfaces leads to a slight improvement of the simulated thermal budget of the snowpack compared to the observations. However, their impact on further simulated parameters like snow height and SSA remains small. Including additional physical processes in the snow model may have the potential to advance the simulations of the thermal budget of the snowpack and, thus, the SSA simulations.

Domine, F., A. S. Taillandier, and W. R. Simpson (2007) : **A parameterization of the specific surface area of seasonal snow for field use and for models of snowpack evolution**. Journal of Geophysical Research-Earth Surface, 112(F2), F02031.

Abstract : The specific surface area (SSA) of snow is needed to model air-snow exchange of chemical species. SSA is related to many snow physical properties, such as albedo and permeability. However, it is not described in models of snowpack evolution, in part because it is difficult to measure. Snowpack models often predict snow grain shape and snow density, and the goal of this paper is to propose parameterizations of snow SSA, based on snow density and grain shape. SSA values of 345 snow samples from snowpacks of the Alpine, maritime, tundra and taiga types are presented. Samples are regrouped into three main types: fresh (F), recent (R), and aged (A) snows, with several subtypes referring to grain shapes. Overall, there is a clear inverse correlation between SSA and density, d. Empirical equations of the form SSA = A ln(d) + B are proposed for the F and R types. For aged snows, separate correlations are proposed for subtypes A1 (rounded grains), A2 (faceted crystals), A3 (depth hoar), and A4 (lightly melted snow). Within subtypes A1, A2, and A3, more elaborate classifications are made by considering the snowpack type (Alpine, taiga, or tundra). For A1, A2, and A3 types, different trends are related to different intensities of wind action, which increases in the order taiga, Alpine, and tundra. We finally propose three parameterizations of snow SSA with increasing sophistication, by correlating SSA to snow type, then to snow type and density, and finally to snow type, density, and snowpack type.

Domine, F., A.-S. Taillandier, A. Cabanes, T. A. Douglas, and M. Sturm (2009) : **Three examples where the specific surface area of snow increased over time.** The Cryosphere, 3(1), 31-39.

Abstract : Snow on the ground impacts climate through its high albedo and affects atmospheric composition through its ability to adsorb chemical compounds. The quantification of these effects requires the knowledge of the specific surface area (SSA) of snow and its rate of change. All relevant studies indicate that snow SSA decreases over time. Here, we report for the first time three cases where the SSA of snow increased over time. These are (1) the transformation of a melt-freeze crust into depth hoar, producing an increase in SSA from 3.4 to 8.8 m2 kg−1. (2) The mobilization of surface snow by wind, which reduced the size of snow crystals by sublimation and fragmented them. This formed a surface snow layer with a SSA of 61 m2 kg−1 from layers whose SSAs were originally 42 and 50 m2 kg−1. (3) The sieving of blowing snow by a snow layer, which allowed the smallest crystals to penetrate into open spaces in the snow, leading to an SSA increase from 32 to 61 m2 kg−1. We discuss that other mechanisms for SSA increase are possible. Overall, SSA increases are probably not rare. They lead to enhanced uptake of chemical compounds and to

increases in snow albedo, and their inclusion in relevant chemical and climate models deserves consideration.

Taillandier, A. S., F. Domine, W. R. Simpson, M. Sturm, and T. A. Douglas (2007) : **Rate of decrease of the specific surface area of dry snow: Isothermal and temperature gradient conditions.** Journal of Geophysical Research-Earth Surface, 112(F3), F03003.

Abstract : The specific surface area (SSA) of snow is the surface area available to gases per unit mass. It is an important variable for quantifying air- snow exchange of chemical species, and it is closely related to other variables such as albedo. Snow SSA decreases during metamorphism, but few data are available to quantify its rate of decrease. We have performed laboratory experiments under isothermal and temperature gradient conditions during which the SSA of snow samples was monitored for several months. We have also monitored the SSA of snowfalls subjected to large temperature gradients at a field site in the central Alaskan taiga. The same snow layers were also monitored in a manipulated snowpack where the temperature gradient was greatly reduced. In all cases, the SSA decay follows a logarithmic equation with three adjustable variables that are parameterized using the initial snow SSA and the time- averaged temperature of the snow. Two parameterizations of the three adjustable variables are found: One applies to the isothermal experiments and to the quasi- isothermal cases studied in Alaska (equitemperature (ET) metamorphism), and the other is applicable to both the laboratory experiments performed under temperature gradients and to the natural snowpack in Alaska (temperature gradient (TG) metamorphism). Higher temperatures accelerate the decrease in SSA, and this decrease is faster under TG than ET conditions. We discuss the conditions of applicability of these parameterizations and use them to speculate on the effect of climate change on snow SSA. Depending on the climate regime, changes in the rate of decay of snow SSA and hence in snow albedo may produce either negative or positive feedbacks on climate change.

Morin**.,** S.**,** F. Domine, L. Arnaud and G. Picard (2010), **In-situ monitoring of the effective thermal conductivity of snow**, *Cold Reg. Sci. Technol.*, 64, 73–80.

Abstract : We report on a 3-month long time series of in-situ measurements of the effective thermal conductivity (k_{eff}) of snow at 6 heights in an Alpine snowpack in the Mont-Blanc mountain range, France, at an altitude of 2400 m. Measurements were carried out automatically every 2 days using heated-needle probes embedded in the snowpack. The experimental procedure used is presented in detail and demonstrates the applicability of single heated-needle probes for the evaluation of k_{eff} in snow, both for long-term measurements within the snowpack and occasional use in the field. Results based on 139 automatically collected data show k_{eff} values ranging between 0.04 and 0.35 $W\ m^{-1}\ K^{-1}$, and a consistent pattern of effective thermal conductivity increase throughout the measurements campaign. The temporal rate of change of k_{eff} varies up to 0.01 $W\ m^{-1}\ K^{-1} day^{-1}$, with maximum values just after snowfall.

1-1-2 – Other references without abstracts

King, C.and Pomeroy, J.; Gray, D. M.; Fierz, C.; Föhn, P.; Harding, R.; Jordan, R. & Martin, E.and Plüss, C. Armstrong, R. & Brun, E. (Eds.) (2008), **Snow-atmosphere energy and mass balance Snow and Climate: Physical Processes, Surface Energy Exchange and Modelling**, Cambrige University Press, 70-124.

1-2 Snow observation (including remote sensing).

1-2-1 Main references with abstracts

Brucker, L., Picard, G. and Fily, M. **Snow grain size profiles deduced from microwave snow emissivities in Antarctica**. *Journal of Glaciology*, 56(197), 514-526, 2010 TOC

ABSTRACT. Spaceborne microwave radiometers are an attractive tool for observing Antarctic climate because their measurements are related to the snow temperature. However, the conversion from microwave emission to snow temperature is not simple and strongly depends on the emissivity through snow properties. This difficulty in predicting the snow property profile for Antarctic conditions is the main bottleneck in the retrieval of accurate climate information from microwave radiometers. We attempt to explain the vertically polarized emissivity at 19.3 and 37GHz derived from brightness temperatures acquired by the Special Sensor Microwave/Imager (SSM/I) and physical temperature from the ERA-40 re-analysis. In Antarctica the snow emissivities at 19.3 and 37GHz are nearly equal, although a decrease with frequency is expected. To explain this, we consider various profiles of snow grain size and density and predict their emissivity using a dense-medium radiative transfer (DMRT) model. The results show that the emissivities cannot be explained by constant profiles of grain size and density. Heterogeneous snowpacks need to be considered. We first test random variations of snow density and grain radius with depth and then monotonic and continuous variations in the snow grain radius. In both cases, we show that an overall increase of the snow grain radius with depth is required to match the observed emissivity in Antarctica. In addition, two parameters characterizing the snow grain profiles are retrieved and compared with (1) in situ measurements of grain size at various locations in East Antarctica, (2) grain size estimated using visible spaceborne radiometers and (3) a semi-empirical relationship for grain growth.

J.-C. Gallet, F. Domine, C. Zender, and G. Picard **Measurement of the specific surface area of snow using infrared reflectance in an integrating sphere at 1310 and 1550 nm** *The Cryosphere* Vol.3, pp. 167-182, 2009

Abstract. *Even though the specific surface area (SSA) and the snow area index (SAI) of snow are crucial variables to determine the chemical and climatic impact of the snow cover, few data are available on the subject. We propose here a novel method to measure snow SSA and SAI. It is based on the measurement of the hemispherical infrared reflectance of snow samples using the DUFISSS instrument (DUal Frequency Integrating Sphere for Snow SSA measurement). DUFISSS uses the 1310 or 1550 nm radiation of laser diodes, an integrating sphere 15 cm in diameter, and InGaAs photodiodes. For SSA<60 m^2 kg^{-1}, we use the 1310 nm radiation, reflectance is between 15 and 50% and the accuracy of SSA determination is 10%. For SSA>60 m^2 kg^{-1}, snow is usually of low density (typically 30 to 100 kg m^{-3}), resulting in insufficient optical depth and 1310 nm radiation reaches the bottom of the sample, causing artifacts. The 1550 nm radiation is therefore used for SSA>60 m^2 kg^{-1}. Reflectance is then in the range 5 to 12% and the accuracy on SSA is 12%. We propose empirical equations to determine SSA from reflectance at both wavelengths, with that for 1310 nm taking into account the snow density. DUFISSS has been used to measure the SSA of snow and the SAI of snowpacks in polar and Alpine regions.*

G. Picard, L. Brucker, M. Fily, H. Gallée, G. Krinner, **Modeling timeseries of microwave brightness temperature in Antarctica.** *Journal of Glaciology*, 55 (191), pp 537-551, 2009.

ABSTRACT. This paper aims to interpret the temporal variations of microwave brightness temperature (at 19 and 37GHz and at vertical and horizontal polarizations) in Antarctica using a physically based snow dynamic and emission model (SDEM). SDEM predicts time series of top-of-atmosphere brightness temperature from widely available surface meteorological data (ERA-40 re-analysis). To do so, it successively computes the heat flux incoming the snowpack, the snow temperature profile, the microwaves emitted by the snow and, finally, the propagation of the microwaves through the atmosphere up to the satellite. Since the model contains several parameters whose value is variable and uncertain across the continent, the parameter values are optimized for every 50 km × 50 km pixel. Simulation results show that the model is inadequate in the melt zone (where surface melting occurs on at least a few days a year) because the snowpack structure and its temporal variations are too complex. In contrast, the accuracy is reasonably good in the dry zone and varies between 2 and 4 K depending on the frequency and polarization of observations and on the location. At the Antarctic scale, the error is larger where wind is usually stronger, suggesting either that meteorological data are less accurate in windy regions or that some neglected processes (e.g. windpumping, surface scouring) are important. At Dome C, in calm conditions, a detailed analysis shows that most of the error is due to inaccuracy of the ERA-40 air temperature (2 K). Finally, the paper discusses the values of the optimized parameters and their spatial variations across the Antarctic.

A. Mialon, Royer, A., Fily, M., Picard, G., 2007, **Daily Microwave-Derived Surface Temperature over Canada/Alaska** *Journal of Applied Meteorology and Climatology*, vol 46, issue 5 (May 2007), p 591-604.

The land surface temperature variation over northern high latitudes in response to the increase in greenhouse gases is challenging because of the lack of meteorological stations. A new method to derive the surface temperature from satellite microwave measurements that improves the frequency of measurements relative to that of infrared data is presented. The daily Special Sensor Microwave Imager 25 km × 25 km Equal-Area Scalable Earth Grid (EASE-Grid) dataset provided by the National Snow and Ice Data Center in Boulder, Colorado, is processed to derive the surface temperature using the method proposed by Fily et al. A normalization approach based on the 40-yr ECMWF reanalysis (ERA-40; 2.5°) temperature diurnal cycle fitted for each pixel is applied to overcome the time acquisition variation of measurements as well as to interpolate missing data. An adaptive mask for discriminating between ice-free pixels and snow-free pixels is also applied. The resulting database is thus a new consistent hourly series of near-surface air temperatures during the summer (without snow). The mean accuracy is on the order of 2.5–3 K when compared with the synchronous in situ air temperature and different gridded datasets over Canada and Alaska. The trend over the last 10 yr confirms observed climate evolution: an increase in summer surface temperature of +0.09° ± 0.04°C yr^{-1}, at the 90% confidence level, for Canada between 1992 and 2002, whereas a decrease of −0.15° ± 0.05°C yr^{-1}, at the 95% confidence level, is observed for Alaska. Spatial and temporal anomalies show regional impacts of meteorological phenomena such as the El Niño extreme warm summer episode of 1998, the decrease in temperatures in 1992 in Canada following the volcanic eruption of Mount Pinatubo in June 1991, and the strong drought in the

prairies in 2001. The annual sum of positive degree-days (thawing index) has been related to the permafrost distribution. The lower values of the derived thawing index (<1400 degree-days) are related well to the presence of continuous and dense discontinuous permafrost. The observed increase in the thawing index during the 1992–2002 period represents a decrease of classified permafrost area of 7%.

Bouchard, A., F. Rabier, V. Guidard, F. Karbou (2010), ***Enhancement of satellite data assimilation over Antarctica****, Monthly Weather Review, Vol. 138, No. 6., 2149–2173,doi : 10.1175/2009MWR3071.1.*

Abstract: The Concordiasi field experiment, which is took place in Antarctica, involved the launching of radiosoundings and stratospheric balloons. One of the main goals of this campaign is the validation of the Infrared Atmospheric Sounding Interferometer (IASI) radiance assimilation. Prior to the campaign, it was necessary to improve satellite data assimilation at high latitudes. Two types of sensors, microwave and infrared, have been considered to help with this issue. A major problem associated with microwave satellite data is the calculation of the surface emissivity. An innovative approach, based on satellite observations, improves the surface emissivity modeling over land and sea ice within the constraints of the four-dimensional variational data assimilation (4D-VAR) system. With this new calculation of emissivity, it has been possible to include many more microwave observations during the assimilation. In this study, this method has been applied to high latitudes, after some adjustments have been made to assimilate additional Advanced Microwave Sounding Unit-A/B (AMSU-A/B) data over sea ice and snow. The use of additional data from IASI and the Atmospheric Infrared Sounder (AIRS) sensors over land and sea ice has also been tested. The use of the microwave and infrared data over this polar area has modified the dynamical and thermodynamical model fields such as the snow precipitation quantity. Additional data have been found to have a positive impact on the skill of a model specially tuned for Antarctica (see the accompanying figure for some forecast scores).

Guedj, S., F. Karbou, F. Rabier, A. Bouchard (2010), **Microwave land emissivity over Antarctica : Impact of the surface approximation**, IEEE Trans. on Geoscience and Remote sensing, Vol. 48, Issue 4, 1976-1985, 10.1109/TGRS.2009.2036254

Abstract: This work is in direct line with the Concordiasi international project. It aims to better constrain atmospheric analyses by improving the assimilation of low-level Advanced Microwave Sounding Unit (AMSU)-A and AMSU-B microwave observations over Antarctica. So far, a very small amount of available AMSU observations is effectively assimilated over Antarctica. To assimilate more observations, different issues have to be dealt with. In this work, the surface emissivity issue over Antarctica is examined. In a first step, a thorough review of the use of a specular assumption to calculate emissivity from AMSU-A measurements has been undertaken. The effect of five different assumptions about the surface on retrieved AMSU emissivities has then been evaluated using a one-year database: specular, Lambertian, and three intermediate assumptions. Simulations of brightness temperatures at AMSU sounding frequencies have been produced using a radiative transfer model. The emissivities obtained using the five assumptions have been found very useful in improving these simulations (see the following figure). The most successful schemes are found to be the Lambertian scheme during the winter season and a specular or an intermediate scheme (50% specular, 50% Lambertian) during Antarctica's short summer.

Longepe, N., S. Allain, L. Ferro-Famil, E. Pottier and Y. Durand (2009) : **Snowpack Characterization in Mountainous Regions Using C-Band SAR Data and a Meteorological Model**. IEEE Transactions on Geoscience and Remote Sensing, 47(2), 406-418.

Abstract : This paper presents a method to characterize snow cover in mountainous regions using dual-polarization C-band synthetic aperture radar (SAR) data. It is demonstrated that an accurate modeling of the liquid water distribution inside the snowpack, using a multilayer meteorological snow model, is required to characterize snow with precision. A multilayer-snow electromagnetic (EM) backscattering model is developed based on the vector radiative transfer, the strong fluctuation theory, and physical parameters supplied by the meteorological model. However, the limited resolution of the meteorological snow model is insufficient for predicting a refined EM backscattering at a massif scale. An adequate spatial reorganization of these snow profiles, based on a comparison between simulated and measured dual-polarization SAR data, leads to a better estimation of some snowpack parameters. In particular, the monitoring of snow liquid water content is presented improving the capacity of wet snow mapping as compared to a classical SAR-based method. This methodology shows good capacities both for qualitative and quantitative snow assessments, opening the way for a new operational method.

1-2-2 – Other references without abstracts

Dumont, M., Brissaud, O., Picard, G., Schmitt, B., Gallet, J.-C., and Arnaud, Y. **High-accuracy measurements of snow Bidirectional Reflectance Distribution Function at visible and NIR wavelengths - comparison with modelling results,** *Atmos. Chem. Phys.*, 10, 2507-2520.

J.C. Gallet, F. Domine, L. Arnaud, G. Picard, and J. Savarino, **Vertical profiles of the specific surface area of the snow at Dome C, Antarctica,** *The Cryosphere Discussion*, 4, 1647-1708, 2010.

Langlois, A., Royer, A., Montpetit, B., Picard, G., Brucker, L., Arnaud, L., Goïta, K. and Fily, M. **On the relationship between snow grain morphology and in-situ near infrared calibrated reflectance photographs,** *Cold Regions Science and Technology*, 61, pp 34-42, 2010.

M. van den Broeke, G. König-Langlo, G. Picard, P. Kuipers Munneke and J. Lenaerts **Surface energy balance, melt and sublimation at Neumayer Station, East Antarctica**. *Antarctic Science*, 22 (01), pp 87-96, Feb 2010.

G. Picard, L. Arnaud, F. Domine, M. Fily, **Determining snow specific surface area from near-infrared reflectance measurements: numerical study of the influence of grain shape.** *Cold Region Science and Technology*, 56 (1), pp 10-17, 2009.

Lacroix, P., Legresy, B., Remy, F., Blarel, F., Picard, G. and Brucker, L. **Rapid change of the snow surface properties at Vostok, East Antarctica, revealed by altimetry and radiometry.** *Remote Sensing of Environment*, 113(12), pp 2633-2641, Dec 2009.

1-3 Snow chemistry (including water isotopes)

1-3-1 Main references with abstracts

Amoroso, A., et al. (2010): **Microorganisms in Dry Polar Snow Are Involved in the Exchanges of Reactive Nitrogen Species with the Atmosphere**, Environmental Science & Technology. 44(2), 714-719.

Abstract : The snowpack is a complex photochemical reactor that emits a wide variety of reactive molecules to the atmosphere. In particular, the photolysis of nitrate ions, NO3−, produces NO, NO2, and HONO, which affects the oxidative capacity of the atmosphere. We report measurements in the European High Arctic where we observed for the first time emissions of NO, NO2, and HONO by the seasonal snowpack in winter, in the complete or near-complete absence of sunlight and in the absence of melting. We also detected unusually high concentrations of nitrite ions, NO2−, in the snow. These results suggest that microbial activity in the snowpack is responsible for the observed emissions. Isotopic analysis of NO2− and NO3− in the snow confirm that these ions, at least in part, do not have an atmospheric origin and are most likely produced by the microbial oxidation of NH4+ coming from clay minerals into NO2− and NO3−. These metabolic pathways also produce NO. Subsequent dark abiotic reactions lead to NO2 and HONO production. The snow cover is therefore not only an active photochemical reactor but also a biogeochemical reactor active in the cycling of nitrogen and it can affect atmospheric composition all year round.

Domine, F., S. Houdier, A. S. Taillandier, and W. R. Simpson (2010) : **Acetaldehyde in the Alaskan subarctic snowpack**. Atmospheric Chemistry and Physics, 10(3), 919-929.

Abstract : Acetaldehyde is a reactive intermediate in hydrocarbon oxidation. It is both emitted and taken up by snowpacks and photochemical and physical processes are probably involved. Understanding the reactivity of acetaldehyde in snow and its processes of physical and chemical exchanges requires the knowledge of its incorporation mechanism in snow crystals. We have performed a season-long study of the evolution of acetaldehyde concentrations in the subarctic snowpack near Fairbanks (65 degrees N), central Alaska, which is subjected to a vigorous metamorphism due to persistent elevated temperature gradients in the snowpack, between 20 and 200 degrees C m(-1). The snowpack therefore almost entirely transforms into depth hoar. We have also analyzed acetaldehyde in a manipulated snowpack where temperature gradients were suppressed. Snow crystals there transformed much more slowly and their original shapes remained recognizable for months. The specific surface area of snow layers in both types of snowpacks was also measured. We deduce that acetaldehyde is not adsorbed onto the surface of snow crystals and that most of the acetaldehyde is probably not dissolved in the ice lattice of the snow crystals. We propose that most of the acetaldehyde measured is either trapped or dissolved within organic aerosol particles trapped in snow, or that acetaldehyde is formed by the hydrolysis of organic precursors contained in organic aerosols trapped in the snow, when the snow is melted for analysis. These precursors are probably aldehyde polymers formed within the aerosol particles by acid catalysis, but might also be biological molecules. In a laboratory experiment, acetaldehyde-di-n-hexyl acetal, representing a potential acetaldehyde precursor, was subjected to our analytical procedure and reacted to form acetaldehyde. This confirms our suggestion that acetaldehyde detected in snow could be produced during the melting of snow for analysis.

Domine, F., A. Cincinelli, E. Bonnaud, T. Martellini, and S. Picaud (2007) : **Adsorption of phenanthrene on natural snow**. Environmental Science & Technology, 41, 6033-6038.

Abstract : The snowpack is a reservoir for semivolatile organic compounds (SVOCs) and, in particular, for persistent organic pollutants (POPS), which are sequestered in winter and released to the atmosphere or hydrosphere in the spring. Modeling these processes usually assumes that SVOCs are incorporated into the snowpack by adsorption to snow surfaces, but this has never been proven because the specific surface area (SSA) of snow has never been measured together with snow composition. Here we expose natural snow to phenanthrene vapors (one of the more volatile POPs) and measure for the first time both the SSA and the chemical composition of the snow. The results are consistent with an adsorption equilibrium. The measured Henry's law constant is H-Phen(T) = 2.88 x 10(22) exp(-10660/T) Pa m(2) mol(-1), with Tin Kelvin. The adsorption enthalpy is Delta H-ads = -89 +/- 18 kJ mol(-1). We also perform molecular dynamics calculations of phenanthrene adsorption to ice and obtain Delta H-ads = -85 +/- 8 kJ mol(-1), close to the experimental value. Results are applied to the adsorption of phenanthrene to the Arctic and subarctic snowpacks. The subarctic snowpack, with a low snow area index (SAI = 1000), is a negligible reservoir of phenanthrene, but the colder Arctic snowpack, with SAI = 2500, sequesters most of the phenanthrene present in the (snow + boundary layer) system.

Savarino, J., J. Kaiser, S. Morin, D. M. Sigman, and M. H. Thiemens (2007), **Nitrogen and oxygen isotopic constraints on the origin of atmospheric nitrate in coastal Antarctica,** *Atmospheric Chemistry and Physics*, *7*, 1925-1945.

Throughout the year 2001, aerosol sam- ples were collected continuously for 10 to 15 days at the French Antarctic Station Dumont d'Urville (DDU) (66°40' S, l40°01' E, 40 m above mean sea level). The nitrogen and oxygen isotopic ratios of particulate nitrate at DDU exhibit seasonal variations that are among the most extreme observed for nitrate on Earth. In association with concentration measurements, the isotope ratios delineate four distinct periods, broadly consistent with previous studies on Antarctic coastal areas. Based on the measured isotopic composition, known atmospheric trans port patterns and the current understanding of kinetics and isotope effects of relevant atmospheric chemical processes, we suggest that elevated tropospheric nitrate levels during Period 3 are most likely the result of nitrate sedimentation from polar stratospheric clouds (PSCs), whereas elevated nitrate levels during Period 4 are likely to result from snow re-emission of nitrogen oxide species. We are unable to attribute the source of the nitrate during periods 1 and 2 to local production or long-range transport, but note that the oxygen isotopic composition is in agreement with day and night time nitrate chemistry driven by the diurnal solar cycle. A precise quantification is difficult, due to our insufficient knowledge of isotope fractionation during the reactions leading to nitrate formation, among other reasons.

Morin, S., J. Savarino, N. Yan, M. M. Frey, J. Bottenheim, S. Bekki, and J. Martins (2008), **Tracing the origin and fate of NOx in the Arctic atmosphere using stable isotopes**, *Science*, *322*, 730-732.

Atmospheric nitrogen oxides (NOx = NO + NO2) play a pivotal role in the cycling of reactive nitrogen (ultimately deposited as nitrate) and the oxidative capacity of the atmosphere. Combined measurements of nitrogen and oxygen stable isotope ratios of nitrate collected in the Arctic atmosphere were used to infer the origin and fate of NOx and nitrate on a seasonal basis. In spring, photochemically driven emissions of

reactive nitrogen from the snowpack into the atmosphere make local oxidation of NOx by bromine oxide the major contributor to the nitrate budget. The comprehensive isotopic composition of nitrate provides strong constraints on the relative importance of the key atmospheric oxidants in the present atmosphere, with the potential for extension into the past using ice cores.

Frey, M. M., J. Savarino, S. Morin, J. Erbland, and J. M. F. Martins (2009), **Photolysis imprint in the nitrate stable isotope signal in snow and atmosphere of East Antarctica and implications for reactive nitrogen cycling,** *Atmospheric Chemistry and Physics*, *9*, 8681–8696.

The nitrogen (δ15N) and triple oxygen (δ17O and δ18O) isotopic composition of nitrate (NO3-) was measured year-round in the atmosphere and snow pits at Dome C, Antarctica (DC, 75.1° S, 123.3° E), and in surface snow on a transect between DC and the coast. Comparison to the isotopic signal in atmospheric NO3- shows that snow NO3 is significantly enriched in δ15N by >200‰ and depleted in δ18O by <40‰. Post-depositional fractionation in δ17O(NO3-) is small, potentially allowing reconstruction of past shifts in tropospheric oxidation pathways from ice cores. Assuming a Rayleigh-type process we find fractionation constants of 60±15‰, 8±2 and 1±1‰, for δ15N, δ18O and δ17O, respectively. A photolysis model yields an upper limit for the photolytic fractionation constant 15 of δ15N, consistent with lab and field measurements, and demon- strates a high sensitivity of 15Îµ to the incident actinic flux spectrum. The photolytic 15 is process-specific and therefore applies to any snow covered location. Previously published 15 values are not representative for conditions at the Earth surface, but apply only to the UV lamp used in the reported experiment (Blunier et al., 2005; Jacobi et al., 2006). Depletion of oxygen stable isotopes is attributed to photolysis followed by isotopic exchange with water and hydroxyl radicals. Conversely, 15N enrichment of the NO3-fraction in the snow implies 15N depletion of emissions. Indeed, δ15N in atmospheric NO3- shows a strong decrease from background levels (4±7‰) to 35‰ in spring ng followed by recovery during summer, consistent with significant snowpack emissions of reactive nitrogen. Field and lab evidence therefore suggest that photolysis is an important process driving fractionation and associated NO3- loss from snow. The δ17O signature confirms previous coastal measurements that the peak of at- mospheric NOâ˙'3 in spring is of stratospheric origin. After sunrise photolysis drives then redistribution of NO3- from the snowpack photic zone to the atmosphere and a snow surface skin layer, thereby concentrating NO3 at the surface. Little NO3- appears to be exported off the EAIS plateau, still snow emissions from as far as 600 km inland can contribute to the coastal NO3- budget.

Legrand, M., S. Preunkert, B. Jourdain, H. Gallée, F. Goutail, R. Weller, and J. Savarino (2009), **Year-round record of surface ozone at coastal (Dumont d'Urville) and inland (Concordia) sites in East Antarctica**, *Journal of Geophysical Research*, *114*(D20), D20306,10.1029/2008jd011667.

Surface ozone is measured since 2004 at the coastal East Antarctic station of Dumont d'Urville (DDU) and since 2007 at the Concordia station located on the high East Antarctic plateau. Ozone levels at Concordia reach a maximum of 35 ppbv in July and a minimum of 21 ppbv in February. From November to January, sudden increases of the ozone level, up to 15–20 ppbbv above average, often take place. They are attributed to local photochemical ozone production as previously seen at the South Pole. The detailed examination of the diurnal ozone record in summer at Concordia

suggests a local photochemical ozone production of around 0.2 ppbv during the morning. The ozone record at DDU exhibits a maximum of 35 ppbv in July and a minimum of 18 ppbv in January. Mixing ratios at DDU are always higher than those at Neumayer (NM), another coastal Antarctic station. A noticeable difference in the ozone records at the two coastal sites lies in the larger ozone depletion events occurring from July to September at NM compared to DDU, likely due to stronger BrO episodes in relation with a larger sea ice coverage offshore that site. A second difference is the large day-to-day fluctuations which are observed from November to January at DDU but not at NM. That is attributed to a stronger impact at DDU than at NM of air masses coming from the Antarctic plateau. The consequences of such a high oxidizing property of the atmosphere over East Antarctica are discussed with regard to the dimethylsulfide (DMS) chemistry.

Larose, C., Dommergue, A., De Angelis, M., Cossa, D., Averty, B., Marusczak, N., Soumis, N., Schneider, D., Ferrari, C., 2010. **Springtime changes in snow chemistry lead to new insights into mercury methylation in the Arctic.** *Geochimica et Cosmochimica Acta* 74, 6263-6275.

Seasonal snow is an active media and an important climate factor that governs nutrient transfer in Arctic ecosystems. Since the snow stores and transforms nutrients and contaminants, it is of crucial importance to gain a better understanding of the dynamics of contaminant cycling within the snowpack and its subsequent release to catchments via meltwater. Over the course of a two-month field study in the spring of 2008, we collected snow and meltwater samples from a seasonal snowpack in Ny-Alesund, Norway (78_560N, 11_520E), which were analyzed for major inorganic ions and some organic acids, as well as total, dissolved, bioavailable mercury (THg, DHg, BioHg, respectively) and monomethylmercury (MMHg) species. We observe a seasonal gradient for ion concentrations, with surface samples becoming less concentrated as the season progressed. A significant negative correlation between BioHg and MMHg was observed in the snowpack. MMHg was positively and significantly correlated to methanesulfonate concentrations. Based on these results, we propose a new model for aerobic methylation of mercury involving species in the dimethylsulfoniopropionate cycle.

Dommergue, A., Larose, C., Faïn, X., Clarisse, O., Foucher, D., Hintelmann, H., Schneider, D., Ferrari, C.P., 2010. **Deposition of mercury species in the Ny-Ålesund area (79°N) and their transfer during snowmelt**. *Environmental Science and Technology* 44, 901-907.

Arctic snowpacks are often considered as temporary reservoirs for atmospheric mercury (Hg) deposited during springtime deposition events (AMDEs). The fate of deposited species is of utmost importance because melt leads to the transfer of contaminants to snowmelt-fed ecosystems. Here,we examined the deposition, fate, and transfer of mercury species (total Hg (THg) and methylmercury (MeHg)) in an arctic environment from the beginning of mass deposition of Hg during AMDEs to the full melt of the snow. Following these events, important amounts of THg were deposited onto the snow surface with concentrations reaching 373 ng · L-1 and estimated deposition fluxes of 200-2160 ng ·m-2. Most of the deposited Hg was reemitted to the atmosphere via photochemical reactions. However, a fraction remained stored in the snow and we estimated that the spring melt contributed to an input of 1.5-3.6 kg · year-1 of THg to the fjord (i.e., 8-21% of the fjord's THg content). A monitoring of MeHg in snow using a new technique (DGT sensors) is also presented.

Dommergue, A., Bahlmann, E., Ebinghaus, R., Ferrari, C., Boutron, C., 2007. **Laboratory simulation of Hg° emissions from a snowpack.** *Analytical and Bioanalytical Chemistry* 388, 319-327.

Snow surfaces play an important role in the biogeochemical cycle of mercury in high-latitude regions. Snowpacks act both as sources and sinks for gaseous compounds. Surprisingly, the roles of each environmental parameter that can govern the air–surface exchange over snow are not well understood owing to the lack of systematic studies. A laboratory system called the laboratory flux measurement system was used to study the emission of gaseous elemental mercury from a natural snowpack under controlled conditions. The first results from three snowpacks originating from alpine, urban and polar areas are presented. Consistent with observations in the field, we were able to reproduce gaseous mercury emissions and showed that they are mainly driven by solar radiation and especially UV-B radiation. From these laboratory experiments, we derived kinetic constants which show that divalent mercury can have a short natural lifetime of about 4–6 h in snow.

V.Masson-Delmotte et al., **A review of Antarctic surface snow isotopic composition : observations, atmospheric circulation and isotopic modelling**, J. Climate, 21, 13, 3359-3387, 2008.

A database of surface Antarctic snow isotopic composition is constructed using available measurements, with an estimate of data quality and local variability. Although more than 1000 locations are documented, the spatial coverage remains uneven with a majority of sites located in specific areas of East Antarctica. The database is used to analyze the spatial variations in snow isotopic composition with respect to geographical characteristics (elevation, distance to the coast) and climatic features (temperature, accumulation) and with a focus on deuterium excess. The capacity of theoretical isotopic, regional, and general circulation atmospheric models (including "isotopic" models) to reproduce the observed features and assess the role of moisture advection in spatial deuterium excess fluctuations is analyzed.

1-3-2 – Other references without abstracts

Bock, J., and H.-W. Jacobi, **Development of a mechanism for nitrate photochemistry in snow**, *J.Phys.Chem.A* **114**, 1790–1796, 2010.

F. Domine, M. Albert, T. Huthwelker, H.-W. Jacobi, A. A. Kokhanovsky, M. Lehning, G. Picard, and W. R. Simpson, **Snow physics as relevant to snow photochemistry,** *Atmos. Chem. Phys.*, 8, 171-208, 2008

Grannas, A.M., et al. **An overview of snow photochemistry: Evidence, mechanisms and impacts**, *Atmos.Chem.Phys.* **7**, 4329-4373, 2007.

Castebrunet, H., P. Martinerie, C. Genthon and E. Cosme, **A three-dimensional model study of methanesulphonic acid to non sea salt sulphate ratio at mid and high-southern latitudes.** Atmos. Chem. Phys., 9, 9449-9469, 2009.

Fain, X., C. P. Ferrari, A. Dommergue, M. Albert, M. Battle, L. Arnaud, J.M. Barnola, W. Cairns, C. Barbante and C. Boutron, **Mercury in the snow and firn at Summit Station, Central Greenland, and implications for the study of past atmospheric mercury levels.** Atmos. Chem. Phys., 7, 18221-18268, 2007.

Fain, X., S. Grangeon, E. Bahlmann, J. Fritsche, D. Obrist, A.Dommergue, C. Ferrari, W. Cairns, R. Ebinghaus, C. Barbante, P. Cescon and C. Boutron, **Diurnal production of gaseous mercury in the alpine snowpack before snowmelt.** Journal Geophys. Res., 10.1029/2007JD008520, 112, 2007.

Fain, X., S. Grangeon, E. Bahlmann, FritscheJ., D. Obrist, C.P. Ferrari, W. Cairns, W. Ebinghaus, C. Barbante, P. Cescon and C.Boutron, **Diurnal production of Gaseous Mercury in the alpine snowpack before snowmelt.** Journal of Geophysical Research, 10.029/2007JD008520, 112, D21311, 2007.

U.Heikkilä, Beer, J., Jouzel, J., Feitchter, J., Kubik, P., **10Be measured in a GRIP snowpit and modelled using the ECHAM5-HAM general circulation model**, Geophys. Res. lett., 35, 5, L05817, 2008.

Wang Y.T, Hou S.G, Masson-Delmotte, V. and Jouzel J. **A new spatial distribution map of d18O in Antarctic surface snow.** Geophys. Res . Lett., 36, L06501, 2009.

Y.T.Wang, S.G.Hou, V.Masson-Delmotte and J.Jouzel, **A generalized additive model for the spatial distribution of stable isotopic composition in Antarctic surface snow.** Chemical Geology, 271, 3-4, 133-141, 2010.

2 – GLACIERS

2-1 Main references with abstracts

Wagnon, P., A. Linda, Y. Arnaud, R. Kumar, P. Sharma, C. Vincent, J. Pottakal, E. Berthier, A. Ramanathan, S.I; Hasnain & P. Chevallier, **Four years of mass balance of Chhota Shigri glacier (Himachal Pradesh, India), a new benchmark glacier in western Himalaya**, *J. Glaciol., 53*(183), 603-610, 2007.

Little is known about the Himalayan glaciers although they are of particular interest in terms of future water supply, regional climate change and sea level rise. In 2002, a long-term monitoring program was started on Chhota Shigri glacier (32.2°N, 77.5°E; 15.7 km^2, 6263 to 4050 m a.s.l., 9 km long) located in Lahaul and Spiti valley, Himachal Pradesh, India. This glacier lies in the monsoon-arid transition zone (western Himalaya) which is alternatively influenced by Asian monsoon in summer and the mid-latitude westerlies in winter. Here, we present the results of 4 years of mass balance and surface velocities. Overall specific mass balances are mostly negative during the study period and vary from a minimum value of -1.4 m water equivalent (w.e.) in 2002-2003 and 2005-2006 (Equilibrium line altitude (ELA) at ~5180 m a.s.l.) to a maximum value of +0.1 m w.e. in 2004-2005 (ELA at 4855 m a.s.l.). Chhota Shigri glacier seems rather similar to mid-latitude glaciers with an ablation season limited to the summer months and a mean vertical gradient of mass balance in the ablation zone (uncovered part) of 0.7 m w.e. 100 m^{-1}, similar to those reported in the Alps. Mass balance is strongly dependent on debris cover, exposure and shading effect of surrounding steep slopes.

Vuille M., B. Francou, P. Wagnon, I. Juen, G. Kaser, B. Mark, R. Bradley, **Climate change and tropical Andean glaciers - past, present and future,** *Earth Science Review, 89*, 79-96, 2008.

Observations on glacier extent from Ecuador, Peru and Bolivia give a detailed and unequivocal account of rapid shrinkage of tropical Andean glaciers since the Little Ice Age (LIA). This retreat however, was not continuous but interrupted by several periods of stagnant or even advancing glaciers, most recently around the end of the 20th century. New data from mass balance networks established on over a dozen glaciers allows comparison of the glacier behavior in the inner and outer tropics. It appears that glacier variations are quite coherent throughout the region, despite different sensitivities to climatic forcing such as temperature, precipitation, humidity etc. In parallel with the glacier retreat, climate in the tropical Andes has changed significantly over the past 50-60 years. Temperature in the Andes has increased by approximately 0.1°C/decade, with only two of the last 20 years being below the 1961-90 average. Precipitation has slightly increased in the second half of the 20th century in the inner tropics and decreased in the outer tropics. The general pattern of moistening in the inner tropics and drying in the subtropical Andes is dynamically consistent with observed changes in the large-scale circulation, suggesting a strengthening of the tropical atmospheric circulation. Model projections of future climate change in the tropical Andes indicate a continued warming of the tropical troposphere throughout the 21st century, with a temperature increase that is enhanced at higher elevations. By the end of the 21st century, following the SRES A2 emission scenario, the tropical Andes may experience a massive warming on the order of 4.5˚-5˚C. Predicted changes in precipitation include an increase in precipitation during the

wet season and a decrease during the dry season, which would effectively enhance the seasonal hydrological cycle in the tropical Andes.
These observed and predicted changes in climate affect the tropical glacier energy balance through its sensitivity to changes in atmospheric humidity (which governs sublimation), precipitation (whose variability induces a positive feedback on albedo) and cloudiness (which controls the incoming long-wave radiation). In the inner tropics air temperature also significantly influences the energy balance, albeit not through the sensible heat flux, but indirectly through fluctuations in the rain-snow line and hence changes in albedo and net radiation receipts.
Given the projected changes in climate, based on different IPCC scenarios for 2050 and 2080, simulations with a tropical glacier-climate model indicate that glaciers will continue to retreat. Many smaller, low-lying glaciers are already completely out of equilibrium with current climate and will disappear within a few decades. But even in catchments where glaciers do not completely disappear, the change in streamflow seasonality, due to the reduction of the glacial buffer during the dry season, will significantly affect the water availability downstream. In the short-term, as glaciers retreat and lose mass, they add to a temporary increase in runoff to which downstream users will quickly adapt, thereby raising serious sustainability concerns.

Gilbert, A. P.Wagnon, C. Vincent, P. Ginot & M. Funk, **20th century temperature reconstitution in a high altitude tropical site from Illimani (6340 m a.s.l., Bolivia 16°39'S) englacial temperature,** *J. Geophys. Res.,* 115, D10109, doi:10.1029/2009JD012961, 2010.

In June 1999, a deep (138.7-meter) ice core was extracted from the summit glacier of Illimani (Bolivia, 6340 m a.s.l., 16°39'S) and an englacial temperature profile was measured in the borehole. Using on-site and regional meteorological data as well as ice core stratigraphy, past surface temperatures were reconstructed with a heat flow model. The englacial temperature measurements exhibit a profile that is far from a steady state, reflecting an increasing atmospheric temperature over several years and non-stationary climatic conditions. Englacial temperature interpretation using air temperature data, borehole temperature inversion and melting rate quantification based on ice core density shows two warming phases from 1900 to 1960 (+0.5 ± 0.3 K starting approximately in 1920-1930) and from 1985 to 1999 (+0.6 ± 0.2 K), corresponding to a mean atmospheric temperature rise of 1.1 ± 0.2 K over the 20th century. According to various climate change scenarios, the future evolution of englacial temperatures was simulated to estimate when and under what conditions this high-elevation site on the Illimani summit glacier could become temperate in the future. Results show that this glacier might remain cold for more than 90 years in the case of a +2 K rise over the 21st century, but could become temperate in the first 20 meters depth between 2050 and 2060 if warming reaches +5 K.

Berthier, E., R. Le Bris, L. Mabileau, L. Testut, and F. Rémy (2009), **Ice wastage on the Kerguelen Islands (49S, 69E) between 1963 and 2006**, *Journal of Geophysical Research*, 114, F03005, doi: 10.1029/2008JF001192.

We observed the wastage of ice masses on the Kerguelen Islands (Indian Ocean, 49°S, 69°E) using historical information and recent satellite data. Overall, the total ice-covered area on the islands declined from 703 to 552 km² between 1963 and 2001, a reduction of 21%. The area of Cook ice cap (the main ice body) decreased asymmetrically from 501 to 403 km². West-flowing glaciers lost 11% of their area while east-flowing glaciers lost 28%. After 1991, the retreat rate accelerated from 1.9

km²/yr (1963-1991) to 3.8 km²/yr (1991-2003). Between 1963 and 2000, the ice volume loss was 25-30 km^3, equivalent to an area-average ice thinning rate of 1.4-1.7 m/yr. The glacial retreat took place in the climatic context of a relatively low level of precipitation (compared to the 1950s) and a ~1°C warming that occurred between 1964 and 1982. The acceleration of the ice losses since, at least, the 1990s indicates that the state of the ice bodies on the Kerguelen Islands is still far from balanced. Together with other studies in Patagonia, South Georgia and Heard Island, our analysis is consistent with a pattern of strong and accelerated wastage of ice masses influenced by the Southern Ocean.

Berthier, E., E. Schiefer, G.K.C. Clarke, B. Menounos, and F. Rémy (2010), **Contribution of Alaskan glaciers to sea level rise derived from satellite imagery**, *Nature Geoscience,* 3(2), 92-95.

Over the last 50 years, retreating glaciers and ice caps (GIC) contributed 0.5 mm/yr to sea level rise (SLR), and one third is believed to originate from ice masses bordering the Gulf of Alaska. However, these estimates of ice wastage in Alaska are based on methods that measure a limited number of glaciers and extrapolate the results to estimate ice loss for the many thousands of others. How these methods capture the complex pattern of decadal elevation changes at the scale of individual glacier and mountain range is unclear. Here, combining a comprehensive glacier inventory with elevation changes derived from sequential digital elevation models (DEMs), we found that, between 1962 and 2006, Alaskan glaciers lost 41.9±8.6 km^3/yr water equivalent (w.e.) and contributed 0.12±0.02 mm/yr to SLR. Our ice loss is 34% lower than previous estimates. Reasons for our lower values include the higher spatial resolution of our glacier inventory and the reduction of ice thinning under debris and at the glacier margins which were not resolved in earlier work. Estimates of mass loss from GIC in other mountain regions could be subject to similar revisions.

Sicart, J. E., R. Hock, P. Ribstein and J. P. Chazarin (2010), **Sky long-wave radiation on tropical Andean glaciers: parameterization and sensitivity to atmospheric variables**, Journal of Glaciology, 56 (199), 854–860.

Abstract. In mountain environments, long-wave radiation provides large amounts of melt energy for high-albedo snow surfaces and can dominate in the energy balance of snow or glacier surfaces under cloudy skies. This study examines the atmospheric controls of sky long-wave radiation at Zongo Glacier, Bolivia (16°15'S, 5060 m asl) over an entire year to derive a parameterization suitable for melt studies. Tropical glaciers are characterized by a pronounced seasonality of long-wave radiation due to cloud emissions during the wet season that strongly enhance the small emissivity of the thin and dry clear-sky atmosphere of very high altitudes. Clear-sky radiation is well simulated as a function of air temperature and humidity but changes in humidity atmospheric profiles from daytime to nighttime entail different optimized coefficients for hourly and daily data. Cloud emission, which enhances clear-sky emissivity by up to 60% with an average of 20%, is estimated using daily atmospheric transmissivity for solar radiation. Partial correlations show that in high mountains cloud emissions control the variations of long-wave radiation, far more than clear-sky emissivity and temperature of the emitting low atmosphere. An independent test on Antizana Glacier in the humid tropics of Ecuador (0°28'S, 4860 m asl) indicates that the parameterization is robust for the Central Andes.

Sicart J. E., R. Hock, D. Six (2008), **Glacier melt, air temperature, and energy balance in different climates: The Bolivian Tropics, the French Alps, and northern Sweden,** Journal of Geophysical Research, 113, D24113, doi:10.1029/2008JD010406.

Abstract. This study investigates the physical basis of temperature-index models for three glaciers in contrasting climates: Zongo (16°S, 5050 m, Bolivian tropics), St Sorlin (45°N, 2760 m, French Alps), and Storglaciären (67°N, 1370 m, northern Sweden). The daily energy fluxes were computed during melt seasons and correlated with each other and with air temperature on and outside the glacier. The relative contribution of each flux to the correlations between temperature and melt energy was assessed. At Zongo, net short-wave radiation controls the variability of the energy balance and is poorly correlated to temperature. On tropical glaciers, temperature remains low and varies little, melt energy is poorly correlated to temperature, and degree-day models are not appropriate to simulate daily melting. At the yearly scale, the temperature is better correlated to the mass balance because it integrates the ablation and the accumulation processes over a long time period. At Sorlin, the turbulent sensible heat flux is greater because of higher temperatures, but melt variability is still controlled by short-wave radiation. Temperature correlates well with melt energy mainly through short-wave radiation, probably due to diurnal advection of warm air from the valley. At Storglaciären, high correlations between temperature and melt energy result from substantial variability and good correlations with temperature of the turbulent fluxes of sensible and latent heat, which both supply energy to the glacier. In the three climates, long-wave irradiance is the main source of energy, but its variatibility is small and poorly correlated to the temperature mainly because of cloud emissions

Pomeroy, J. W., A. Rowlands, J. Hardy, T. Link, D. Marks, R. Essery, J. E. Sicart, and C. R. Ellis (2008), **Spatial Variability of Shortwave Irradiance for Snowmelt in Forests,** Journal of Hydrometeorology, *9*(6), 1482–1490, doi: 10.1175/2008JHM86.

Abstract. The spatial variation of melt energy can influence snow cover depletion rates and in turn be influenced by the spatial variability of shortwave irradiance to snow. The spatial variability of shortwave irradiance during melt under uniform and discontinuous evergreen canopies at a U. S. Rocky Mountains site was measured, analyzed, and then compared to observations from mountain and boreal forests in Canada. All observations used arrays of pyranometers randomly spaced under evergreen canopies of varying structure and latitude. The spatial variability of irradiance for both overcast and clear conditions declined dramatically, as the sample averaging interval increased from minutes to 1 day. At daily averaging intervals, there was little influence of cloudiness on the variability of subcanopy irradiance; instead, it was dominated by stand structure. The spatial variability of irradiance on daily intervals was higher for the discontinuous canopies, but it did not scale reliably with canopy sky view. The spatial variation in irradiance resulted in a coefficient of variation of melt energy of 0.23 for the set of U. S. and Canadian stands. This variability in melt energy smoothed the snow-covered area depletion curve in a distributed melt simulation, thereby lengthening the duration of melt by 20%. This is consistent with observed natural snow cover depletion curves and shows that variations in melt energy and snow accumulation can influence snow-covered area depletion under forest canopies.

Sicart, J. E., and Y. Arnaud (2007), **Preliminary spectral characterization of snow in a high altitude tropical glacier and potential effects of impurities in snow on albedo of tropical glaciers**, Hydrological Processes, *21*(26), 3642-3644.

Abstract. This paper presents some preliminary measurements of snow spectral reflectance on the tropical Bolivian Zongo glacier. Measurements show a correct agreement with theoretical spectral albedo of pure snow in the near infrared region, but lower values in the visible region (by 10-20%) probably due to aerosols contained in snow. Impurity contents ranged from 10 to 100 ppmw in one-week-old snow collected from the Zongo glacier, but measurements are scarce. Large amounts of snowfall partly compensate the proximity of dust sources in mid-latitude glaciers, whereas on outer-tropical glaciers precipitations are not abundant and are very seasonal, and sources of aerosols are proximate.

Sicart, J. E., P. Ribstein, B. Francou, B. Pouyaud, and T. Condom (2007), **Glacier mass balance of tropical Zongo glacier, Bolivia, comparing hydrological and glaciological methods,** *Global Planetary Change, 59*(1), 27-36.

Abstract. A glaciological program has been undertaken since 1991 on Zongo glacier in Bolivia (6000-4850 m asl, 2.4 km(2), 16 degrees S). This program involves mass balance measurements, hydrological studies and energy balance investigations. On outer-tropical glaciers, melting and snow accumulation are both maximum in the wet season (austral summer), whereas the dry season (winter) is a period of low ablation. Errors on each term of the glaciological (stakes, snow-pits and integration method of the measurements) and hydrological (precipitation, discharge and runoff coefficient of free ice areas) methods are investigated to estimate the overall accuracy of the mass balance measurements. The hydrological budget is less than the glaciological one (mean difference: 60 cm w.e. per year), but both methods reproduce similar inter-annual variations. Errors in assessment of evaporation or water storage inside the glacier cannot explain the discrepancy. Errors using the glaciological method are large (around +/- 40 cm w.e. per year), but no bias can explain the departure from the hydrological balance. Errors on discharge measurements are small and the uncertainty on the runoff coefficient has a minor effect on the mass balance. We concluded that hydrological budgets are too low due to the catch deficiency of rain gauges and absence of precipitation measurements at high altitudes, emphasizing the difficulty to assess snowfall distribution in high mountainous basins.

Berthier, E., Y. Arnaud, S. Ahmad, R. Kumar, P. Wagnon, and P. Chevallier (2007), **Remote sensing estimates of glacier mass balances in the Himachal Pradesh (Western Himalaya, India)**. *Remote Sensing of the Environment, 108*(3), 327-338.

Although they correspond to an important fraction of the total area of mountain glaciers (33,000 km2 out of 546,000 km2), Himalayan glaciers and their mass balance are poorly sampled. For example, between 1977 and 1999, the average area surveyed each year on the field was 6.8 km2 only. No direct mass balance measurement is available after 1999. To contribute to fill this gap, we use remote sensing data to monitor glacier elevation changes and mass balances in the Spiti/Lahaul region (32.2°N, 77.6°E, Himachal Pradesh, Western Himalaya, India). Our measurements are obtained by comparing a 2004 digital elevation model (DEM) to the 2000 SRTM (Shuttle Radar Topographic Mission) topography. The 2004 DEM is derived from two SPOT5 satellite optical images without any ground control points. This is achieved thanks to the good onboard geolocation of SPOT5 scenes and using SRTM elevations as a reference on the ice free zones. Before comparison on glaciers, the two DEMs are analyzed on the stable areas surrounding the glaciers where no elevation change is expected. Two different biases are detected. A long wavelength bias affects the SPOT5 DEM and is correlated to an anomaly in the roll of the SPOT5 satellite. A bias is also

observed as a function of altitude and is attributed to the SRTM dataset. Both biases are modeled and removed to permit unbiased comparison of the two DEM on the 915 km2 ice-covered area digitized from an ASTER image. On most glaciers, a clear thinning is measured at low elevations, even on debris-covered tongues. Between 1999 and 2004, we obtain an overall specific mass balance of −0.7 to −0.85 m/a (water equivalent) depending on the density we use for the lost (or gained) material in the accumulation zone. This rate of ice loss is twice higher than the long-term (1977 to 1999) mass balance record for Himalaya indicating an increase in the pace of glacier wastage. To assess whether these ice losses are size-dependant, all glaciers were classified into three samples according to their areal extent. All three samples show ice loss, the loss being higher for glaciers larger than 30 km2. In the case of the benchmark Chhota Shigri glacier, a good agreement is found between our satellite observations and the mass balances measured on the field during hydrological years 2002–2003 and 2003–2004. Future studies using a similar methodology could determine whether similar ice losses have occurred in other parts of the Himalaya and may allow evaluation of the contribution of this mountain range to ongoing sea level rise.

Caballero, Y., P. Chevallier, A. Boone, J. Noilhan, and F. Habets (2007), **Calibration of the Interaction Soil Biosphere Atmosphere land-surface scheme on a small tropical high-mountain basin (Cordillera Real, Bolivia),** *Wat.Resour.Res.*, *43*(W07423).

In a continuing effort to test the behaviour of Meteo France's land-surface scheme, ISBA, under a wide range of hydro-meteorological conditions, the scheme was applied to a small tropical high mountain river basin of the Cordillera Real in Bolivia. The surface scheme simulates the key hydrological processes, such as evaporation, infiltration, surface runoff, and snow and soil ice freeze-thaw processes, which are essential for accurately simulating the hydrological behaviour of the river basin in this type of location. The 12.5 km² nonglacierized sub-basin has been divided into homogeneous surface units with irregular shapes, based on their elevation and soil surface characteristics. The ISBA scheme was applied to each unit and the water fluxes were transferred from one unit to another using a system dynamics modelling approach. The method was applied step by step, improving its efficiency based on several hypotheses. This special application of the ISBA scheme, combining the high mountain conditions and the tropical seasonality is discussed.

Lopez, P., P. Sirguey, Y. Arnaud, B. Pouyaud, and P. Chevallier (2008), **Snow cover monitoring of Northern Patagonia Icefield using MODIS satellite images (2000-2006)**, *Global & Planetary Change*, *61*, 103-116.

The snow cover of the Northern Patagonia Icefield (NPI) was monitored after applying the Normalized Difference Snow Index (NDSI) and the Red/NIR band ratio to 134 Moderate Resolution Imaging Spectroradiometer (MODIS) images captured between 2000 and 2006. The final results show that the snow cover extent of the NPI fluctuates a lot in winter, in addition to its seasonal behaviour. The minimum snow cover extent of the period (3600 km2) was observed in March 2000 and the maximum (11,623 km2) in August 2001. We found that temperature accounts for approximately 76% of the variation of the snow cover extent over the entire icefield. We also show two different regimes of winter snow cover fluctuations corresponding to the eastern and the western sides of the icefield. The seasonality of the snow cover on the western side was determined by temperature rather than precipitation, while on the east side the seasonality of the snow cover was influenced by the seasonal behaviour of both

temperature and precipitation. This difference can be explained by the two distinct climates: coastal and continental. The fluctuations in the winter snow cover extent were more pronounced and less controlled by temperature on the western side than on the eastern side of the icefield. Snow cover extent was correlated with temperature R2 = 0.75 and R2 = 0.74 for the western and eastern sides, respectively. Since limited meteorological data are available in this region, our investigation confirmed that the change in snow cover is an interesting climatic indicator over the NPI providing important insights in mass balance comprehension. Since snow and ice were distinguished snow cover fluctuations can be associated to fluctuations in the snow accumulation area of the NPI. In addition, days with minimum snow covers of summer season can be associated to the period in which Equilibrium Line Altitude (ELA) is the highest.

Lopez, P., P. Chevallier, V. Favier, B. Pouyaud, F. Ordenes, and J. Oerlemans (2010), **A regional view of fluctuations in glacier length in Southern South America,** *Global & Planetary Change*, *71*(1-2), 85-108.

Fluctuations in the length of 72 glaciers in the Northern and Southern Patagonia Icefield (NPI and SPI, respectively) and the Cordillera Darwin Icefield (CDI) were estimated between 1945 and 2005. The information obtained from historical maps based on 1945 aerial photographs was compared to ASTER and Landsat satellite images and to information found in the literature. The majority of glaciers have retreated considerably, with maximum values of 12.2 km for Marinelli Glacier in the CDI, 11.6 km for O'Higgins Glacier in the SPI and 5.7 km for San Rafael Glacier in the NPI. Among the 20 glaciers that have retreated the most relative to their size, small (less than 50 km²) and medium (between 50 and 200 km²) glaciers are the most affected. However, no direct relation between glacier retreat and size was found for the 72 glaciers studied. The highest percentage retreat in the CDI was by the CDI-03 Glacier (37.9%) and Marinelli Glacier (37.6%). In the SPI, relative retreats were heterogeneous and fluctuated between 27.2% (Amelia Glacier) and 0.4% (Viedma Glacier). In the NPI, relative retreat was very high for Strindberg and Cachet glaciers (35.9% and 27.6%, respectively) but for the remaining glaciers in this icefield it ranged between 11.8% (Piscis Glacier) and 3.6% (San Quintín Glacier). In addition to surface area, the surface slope (calculated on the basis of the DEM SRTM) was also related to the relative retreat and no straightforward relation was found. From a global point of view, we suggest that glacier retreat in the region is controlled firstly by atmospheric warming, as it has been reported in this area. Besides the general increase in temperature observed, no signal of a geographical pattern for the fluctuations in glacier length was found. Consequently, glaciers appear to initially react to local conditions most probably induced by their exposition, geometry and hypsometry. The heterogeneity of rates of retreat suggests that differences in basin geometry, glacier dynamics and response time are key features to explain fluctuations of each glacier.

Suarez, W., P. Chevallier, B. Pouyaud, and P. Lopez (2008), **Modelling the water balance in the glacierized Parón Lake basin (White Cordillera, Peru)**, *Hydrological Sciences Journal*, *53*(1), 266-277.

The White Cordillera (northern Peru), with a glacial surface of 631 km2, is the largest glacierized mountain range in the Tropics. Due to the lack of physical data from most of its sub-basins, it is difficult to build a physical model to estimate the water resource flowing from the glaciers at the present time and a fortiori for the future. The most

recent GCM simulations indicate a significant increase in the temperature and an accelerated shrinking of the glaciers. Consequently, we sought a model that would be based on the data available within instrumented sub-basins. A theoretical/conceptual water model makes it possible to quantify the local glacier contribution, which could then be applied to the other non-instrumented subbasins. A total of 43.6% of Parón Lake's instrumented sub-basin area (47.4 km2) corresponds to glacial surfaces. Within this sub-basin, a smaller watershed (8.8 km²), called Artesón, with 72.9% glacierized area, has been accurately observed over a 5-year hydrological period (September 2000–August 2005). This information allowed us to calibrate the model over the Artesón sub-basin. The parameters obtained were applied to the entire Parón basin using the same modelling approach.

Trouvé, E. et al., 2007, **Combining Airborne Photographs and Spaceborne SAR Data to Monitor Temperate Glaciers: Potentials and Limits** IEEE TRANSACTIONS ON GEOSCIENCE AND REMOTE SENSING, VOL. 45, NO. 4, APRIL 2007

Abstract—Monitoring temperate glacier activity has become more and more necessary for economical and security reasons and as an indicator of the local effects of global climate change. Remote sensing data provide useful information on such complex geophysical objects, but they require specific processing techniques to cope with the difficult context of moving and changing features in high-relief areas. This paper presents the first results of a project involving four laboratories developing and combining specific methods to extract information from optical and synthetic aperture radar (SAR) data. Two different information sources are processed, namely: 1) airborne photography and 2) spaceborne C-band SAR interferometry. The difficulties and limitations of their processing in the context of Alpine glaciers are discussed and illustrated on two glaciers located in the Mont-Blanc area. The results obtained by aerial triangulation techniques provide digital terrain models with an accuracy that is better than 30 cm,which is compatible with the computation of volume balance and useful for precise georeferencing and slope measurement updating. The results obtained by SAR differential interferometry using European Remote Sensing Satellite images show that it is possible to measure temperate glacier surface velocity fields from October to April in one-day interferograms with approximately20-m ground sampling. This allows to derive ice surface strain rate fields required to model the glacier flow. These different measurements are complementary to results obtained during the summer from satellite optical data and ground measurements that are available only in few accessible points.

Pétillot Ivan, Emmanuel Trouvé, Philippe Bolon, Andreea Julea, Yajing Yan, Michel Gay, and Jean-Michel Vanpe. **Radar-Coding and Geocoding Lookup Tables for the Fusion of GIS and SAR Data in Mountain Areas** IEEE GEOSCIENCE AND REMOTE SENSING LETTERS, VOL. 7, NO. 2, APRIL 2010

Abstract—Synthetic aperture radar (SAR) image orthorectifi- cation induces an important alteration of information due to the side-looking geometry of SAR acquisition. In high-relief areas, the difficulty is increased by the foldover effect: The images acquired with low incidence angles cannot be registered by a bijective trans- formation like polynomial transformations, as usually proposed by conventional software. In this letter, a simple and efficient method, fitted to geocoded data and SAR images, is introduced to propose a generic coregistration tool that takes SAR geometry into account without requiring the exact sensor model, specific parameters, and precise navigation data. This method is based on a simulated SAR image and on the

computation of lookup tables (LUTs) that represent the coordinate transform from one geometry to the other. Results are presented on a high-relief area in the Alps, where satellite and airborne SAR images are used for glacier evolution monitoring. A comparison to other sensor-independent approaches has been performed, showing that the proposed ap- proach performs better in mountain areas. The resulting LUTs allow merging SAR data with the georeferenced data, either in ground geometry by orthorectifying the SAR information or in radar geometry by the inverse transformation, namely, radar- coding data from a geographic information system, to improve the analysis of SAR images and the result interpretation.

Rabatel, A., V. Jomelli, B. Francou, P. Naveau, D. Grancher. 2008. **The Little Ice Age in the tropical Andes of Bolivia (16°S) and its implication for a climate reconstruction**. *Quaternary Research*, 70, 198-212, doi: 10.1016/j.yqres.2008.02.012.

Abstract: Dating moraines by lichenometry enabled us to reconstruct glacier recession in the Bolivian Andes since the Little Ice Age maximum. On the 15 proglacial margins studied, we identified a system of ten principal moraines that marks the successive positions of glaciers over the last four centuries. Moraines were dated by performing statistical analysis of lichen measurements based on the extreme values theory. Like glaciers in many mid-latitude mountain areas, Bolivian glaciers reached their maximal extent during the second half of the 17th century. This glacier maximum coincides with the Maunder minimum of solar irradiance. By reconstructing the equilibrium-line altitude and changes in mass-balance, we think the glacier maximum may be due to a 20 to 30% increase in precipitation and a 1.1 to 1.2 °C decrease in temperature compared with present conditions. In the early 18th century, glaciers started to retreat at varying rates until the late 19th to early 20th century; this trend was generally associated with decreasing accumulation rates. By contrast, glacier recession in the 20th century was mainly the consequence of an increase in temperature and humidity. These results are consistent with observations made in the study region based on other proxies.

Rabatel, **A.**, J.-P. Dedieu, E. Thibert, A. Letreguilly, C. Vincent. 2008. **Twenty-five years of equilibrium-line altitude and mass balance reconstruction on the Glacier Blanc, French Alps (1981-2005), using remote-sensing method and meteorological data.** *Journal of Glaciology*, 54 (185), 307-314.

ABSTRACT. Annual equilibrium-line altitude (ELA) and surface mass balance of Glacier Blanc, Ecrins region, French Alps, were reconstructed from a 25 year time series of satellite images (1981–2005). The remote-sensing method used was based on identification of the snowline, which is easy to discern on optical satellite images taken at the end of the ablation season. In addition, surface mass balances at the ELA were reconstructed for the same period using meteorological data from three nearby weather stations. A comparison of the two types of series reveals a correlation of r > 0.67 at the 0.01 level of significance. Furthermore, the surface mass balances obtained from remote-sensing data are consistent with those obtained from field measurements on five other French glaciers (r ¼ 0.76, p < 0.01). Also consistent for Glacier Blanc is the total mass loss (10.8mw.e.) over the studied period. However, the surface mass balances obtained with the remote-sensing method show lower interannual variability. Given that the remote-sensing method is based on changes in the ELA, this difference probably results from the lower sensitivity of the surface mass balance to climate parameters at the ELA.

2-2 – Other references without abstracts

Lejeune, Y., P. Wagnon, L. Bouilloud, P. Chevallier, P. Etchevers, E. Martin, J.E. Sicart, F. Habets, **Melting of snow cover in a tropical mountain environment: processes and melting**, *J. Hydrometeorol., 8,* 922-937, Doi: 10.1175/JHM590.1, 2007.

Blard, P.H., J. Lavé, R. Pik, P. Wagnon & D. Bourlès, **Persistence of full glacial conditions in the central Pacific until 15,000 years ago,** *Nature*, *449*, doi:10.1038/nature06142, 2007.

Favier, V., A. Coudrain, E. Cadier, B. Francou, E. Ayabacha, L. Maisinsho, E. Praderio, M. Villacis, P. Wagnon, **Evidences of underground circulations on Antizana ice covered volcano, Ecuador,** *Hydrol. Sci.J.*, *53*(1), 278-291, 2008.

Soruco, A., C. Vincent, B. Francou, P. Ribstein, T. Berger, J.E. Sicart, P. Wagnon, Y. Arnaud, V. Favier & Y. Lejeune, **Mass balance of Glaciar Zongo, Bolivia, between 1956 and 2006, using glaciological, hydrological and geodetic methods,** *Ann. Glaciol., 50,* 1-8, 2009.

Winkler, M., I. Juen, T. Mölg, P. Wagnon, J. Gómez, and G. Kaser, **Measured and modelled sublimation on the tropical Glaciar Artesonraju, Perú,** *The Cryosphere, 3,* 21-30, 2009.

Six, D., Wagnon, P., Sicart, J.E. & Vincent C., **Meteorological controls on snow and ice ablation for two contrasting months on Glacier de Saint-Sorlin, France**, *Ann. Glaciol., 50*(50), 66-72, 2009.

Gascoin, S., C. Kinnard, R. Ponce, S. Lhermitte, S. MacDonell, A. Rabatel. 2010. **Glacier contribution to streamflow in two headwaters of the Huasco River, Dry Andes of Chile**. *The Cryosphere Discussion.* 4, 2373–2413, doi:10.5194/tcd-4-2373-2010.

Rabatel, A., H. Castebrunet, V. Favier, L. Nicholson, C. Kinnard. 2010. **Glacier changes in the Pascua-Lama region, Chilean Andes (29°S): recent mass-balance and 50-year surface-area variations**. *The Cryosphere Discussion*, 4, 2307–2336, doi:10.5194/tcd-4-2307-2010.

Nicholson, L., J. Marín, D. Lopez, A. Rabatel, F. Bown, A. Rivera. 2009.**Glacier inventory of the upper Huasco valley: glacier characteristics, recent change and comparison to the upper Aconcagua valley,** Chile. *Annals of Glaciology*, 53, 111-118

Jomelli, V., V. Favier, A. Rabatel, D. Brunstein, G. Hoffmann, B. Francou. 2009. **Fluctuations of glaciers in the tropical Andes over the last millennium and paleoclimatic implications: a review.** *Palaeogeography, Palaeoclimatology, Palaeoecology*, 281, 269-282. doi:10.1016/j.palaeo.2008.10.033.

Favier, V., M. Falvey, A. Rabatel, E. Praderio, D. Lopez. 2009. **Interpreting discrepancies between discharge and precipitation 1 n in high altitude 2 area of Chile's Norte Chico region (26°S-32°S).** *Water Resources Research*, 45, W02424, doi:10.1029/2008WR006802.

Vincent, C., A. Soruco, D. Six and E. Le Meur, **Glacier thickening and decay analysis from fifty years of glaciological observations performed on Argentière glacier, Mont-Blanc area, France.** *Annals of glaciology*, **50**, 73-79, 2009.

Le Meur, E., M. Gerbaux, M. Schäfer and C. Vincent, **Disappearance of an Alpine glacier over the 21st Century simulated from modeling its future surface mass balance**. *Earth Planet. Sci. Lett.*, 10.1016/j.epsl.2007.07.022, (261) 367-374, 2007.

Schaefer, M. and E. Le Meur, **Improvements od a 2D-SIA ice flow model ; application to the Saint Sorlin glacier, France,.** *Journal of Glaciology*, **53**, (183) 713-722, 2007.

Vincent, C., E. Le Meur, D. Six, M. Funk, M. Hoelzle and S. Preunkert, **Very high-elevation Mont Blanc glaciated areas not affected by the 20th Century climate change**. *Journal of Geophysical research*, **112**, (D9) D09120, 2007.

Vincent, C., E. Le Meur, D. Six, P. Possenti, E. Lefebvre and M. Funk, **Climate warming revealed by englacial temperatures at Col du Dôme (4250 m, Mont Blanc area).** *Geophys. Res. Lett.*, 10.1029/2007GL029933, **34**, L16502, 2007.

Vincent, C., S. Auclair and E. LeMeur, **Outburst flood hazard for glacier-dammed Rochemelon lake (France),** 56. *Journal of Glaciology*, 56, (195) 91-100, 2010.

Vincent, C., S. Garambois, E. Thibert, E. Lefebvre, E. LeMeur and D. Six , **Origin of the outburst flood from Tête Rousse glacier in 1892 (Mont-Blanc area, France)**. *Journal of Glaciology*, 56, (198) 688-698, 2010.

3- SEA ICE

3-1- Main references with abstracts

Girard, L., S. Bouillon, J. Weiss, D. Amitrano, T. Fichefet, V. Legat, **A new modelling framework for sea ice ice mechanics based on elasto-brittle rheology**, *Annals Glaciol*., 52(57), 123-132, 2011

We present a new modeling framework for sea-ice mechanics based on elasto-brittle (EB) behavior. The EB framework considers sea ice as a continuous elastic plate encountering progressive damage, simulating the opening of cracks and leads. As a result of long-range elastic interactions, the stress relaxation following a damage event can induce an avalanche of damage. Damage propagates in narrow linear features, resulting in a very heterogeneous strain field. Idealized simulations of the Arctic sea-ice cover are analyzed in terms of ice strain rates and contrasted to observations and simulations performed with the classical viscous–plastic (VP) rheology. The statistical and scaling properties of ice strain rates are used as the evaluation metric. We show that EB simulations give a good representation of the shear faulting mechanism that accommodates most sea-ice deformation. The distributions of strain rates and the scaling laws of ice deformation are well captured by the EB framework, which is not the case for VP simulations. These results suggest that the properties of ice deformation emerge from elasto-brittle ice-mechanical behavior and motivate the implementation of the EB framework in a global sea-ice model.

Rampal, P., Weiss, J. and Marsan, D., **Positive trend in the mean speed and deformation rate of Arctic sea ice, 1979-2007,** *J. Geophys. Res*., 114, C05013, 2009

Using buoy data from the International Arctic buoy Program, we found that the sea ice mean speed has substantially increased over the last 29 years (+17% per decade for winter; +8.5% for summer). A strong seasonal dependence of the mean speed is also revealed, with a maximum in October and a minimum in April. The sea ice mean strain rate also increased significantly over the period (+51% per decade for winter; +52% for summer). We check that these increases in both sea ice mean speed and deformation rate are unlikely a consequence of a stronger atmospheric forcing. Instead, they suggest that sea ice kinematics plays a fundamental role in the albedo feedback loop and sea ice decline: increasing deformation means stronger fracturing, hence more lead opening and therefore a decreasing albedo. This accelerates sea ice thinning in summer and delays refreezing in early winter, therefore decreasing the mechanical strength of the cover and allowing even more fracturing and larger drifting speed and deformation, and possibly a faster export of sea ice through the Fram Strait. The September minimum sea ice extent of 2007 might be a good illustration of this interplay between sea ice deformation and sea ice shrinking, as we found that for both winter 2007 and summer 2007, exceptionally large deformation rates affected the Arctic sea ice cover.

Weiss, J., Schulson, E.M., Stern, H.L., **Sea ice rheology from in-situ, satellite and laboratory observations: Fracture and friction**, *Earth Planet. Sci. Lett*., 255, 1-8, 2007

On the basis of an analysis of in-situ ice stresses and of satellite-derived ice strain-rates, as well as of a comparison between field and laboratory behaviour, we describe

an alternative viewpoint for modelling sea ice deformation during winter. We propose that fracture and frictional sliding govern inelastic deformation over all spatial and temporal scales, even under small stresses. Consequently, winter and/or perennial sea ice does not behave as a viscous material, even at large scales, the normal flow rule is not obeyed (as observed during laboratory tests on sea ice samples harvested from the field), and stresses are highly intermittent and poorly correlated spatially.

Pierre Mathiot, Bernard Barnier, Hubert Gallée, Jean Marc Molines, Julien Le Sommer, Mélanie Juza and Thierry Penduff, **Introducing katabatic winds in global ERA40 fields to simulate their impacts on the Southern Ocean and sea-ice**, OCEAN MODELLING Volume: 35 Issue: 3 Pages: 146-160, doi:10.1016/j.ocemod.2010.07.001

A medium resolution (10–20 km around Antarctica) global ocean/sea-ice model is used to evaluate the impact of katabatic winds on sea-ice and hydrography. A correction is developed to compensate for the drastic underestimation of these katabatic winds in the ERA40 reanalysis. This correction derives from a comparison over 1980–1989 between wind stress in ERA40 and those downscaled from ERA40 by the MAR regional atmospheric model. The representation in MAR of the continental orography surrounding the ocean, like the Transantarctic Mountains, and a specific parameterisation of roughness length in the planetary boundary layer yield a major improvement in the representation of katabatic winds along the coast of Antarctica. Wind stress directions at the first ocean point are remarkably similar in ERA40 and MAR, but MAR wind stress amplitudes are much greater. From this comparison, a scale factor constant in time (i.e. no seasonal variation) but spatially varying (decreasing off-shore over a distance of about 150 km) is created for the meridional and zonal wind stress components and adapted to the wind vector. The correction thus consists of a local amplification of the amplitude of the 6-hourly ERA40 wind vector components at ocean points near the coast. The impact of katabatic wind correction is investigated in 40-year long twin simulations of a global ocean/sea-ice model. The wind stress over polynyas is increased by a factor of 2, and amplitudes of sensible and latent air–sea heat exchanges are increased by 28% and 18%, respectively. Sea-ice thickness and ice-fraction near the coast of Antarctica show a marked decrease. The amplified katabatic winds also increase the extent of coastal polynyas by 24% (i.e. the total polynya area is augmented by 60,000 km^3 around Antarctica), and the winter sea-ice production in polynyas is greater by 42%. Outside polynyas, the impact is a reduction of sea-ice production in the Southern Ocean sea-ice pack. Impacts on the ocean circulation are also marked. Katabatic wind amplification strengthens the local overturning in coastal polynyas with a more intense transformation of Antarctic Surface Waters into colder and denser shelf waters (in total over all polynyas around Antarctica, the overturning reaches 4.7 Sv in annual mean, an increase of 1.8 Sv, and peaks to 6 Sv in winter). The modification of shelf water properties and of the zonal surface winds yields an increase of the amplitude of the seasonal cycle of the Antarctic Coastal Current.

Houssais M.-N., Herbaut C., Schlichtholz P. and C. Rousset, **Arctic salinity anomalies and their link to the North Atlantic during positive phases of the Arctic Oscillation**, *Progress in Oceanogr.*, 73, 160-189, 2007

Many of the changes observed during the last two decades of the 20th century in the Arctic Ocean and adjacent seas have been linked to the concomitant abrupt decrease of the sea level pressure associated with a shift of the Arctic Oscillation (AO) to a

positive phase, which persisted throughout the mid 1990s. The present study investigates modifications in the ocean circulation and in the fresh water storage and transport by sea ice in the context of idealized ice-ocean experiments forced by atmospheric surface wind-stress or temperature anomalies representative of a positive AO index. Wind stress anomalies representative of a positive AO index generate a decrease of the fresh water content of the upper Arctic Ocean, which is mainly concentrated in the eastern Arctic. Sea ice contributes to about two-third of this salinification. The volume of ice exported through Fram Strait increases by 20% primarily due to thicker ice advected into the strait from the northern Greenland sector, the increase of ice drift velocities having comparatively less influence. The export anomaly is comparable to those observed during events of Great Salinity Anomalies and induces substantial freshening in the Greenland Sea, which in turn contributes to increasing the fresh water export to the North Atlantic via Denmark Strait. With a fresh water export anomaly of 7 mSv, the latter is the main fresh water supplier to the subpolar North Atlantic. The removal of fresh water by sea ice mainly occurs through enhanced thin ice growth in the eastern Arctic. Winter SAT anomalies have little impact on the thermodynamic sea ice response, which is rather dictated by wind driven ice deformation changes. The global sea ice mass balance of the western Arctic indicates almost no net sea ice melt due to competing seasonal thermodynamic processes. The surface freshening and likely enhanced sea ice melt observed in the western Arctic during the 1990s should therefore be attributed to extra-winter atmospheric effects, such as the noticeable recent spring–summer warming in the Canada–Alaska sector, or to other modes of atmospheric circulations than the AO, especially in relation to the North Pacific variability.

Williams, G. D., Hindell M., Houssais M.-N. , Tamura T. and I. C. Field, **Upper ocean stratification and sea ice growth rates during the summer-fall transition, as revealed by Elephant seal foraging in the Adélie Depression, East Antarctica**, *Ocean Sci. Discuss*., 7, 1–40.

Southern elephant seals (Mirounga leonina), fitted with Conductivity-Temperature-Depth sensors at Macquarie Island in January 2005 and 2010, collected unique oceanographic observations of the Adélie and George V Land continental shelf (140-148ºE) during the summer-fall transition (late February through April). This is a key region of dense shelf water formation from enhanced sea ice growth/brine-rejection in the local coastal polynyas. In 2005 two seals occupied the continental shelf break near the grounded icebergs at the northern end of the Mertz Glacier Tongue for nearly two weeks at the onset of sea ice growth. In 2010, after that years calving of the Mertz Glacier Tongue, two seals migrated to the same region but penetrated much further southwest across the Adélie Depression and occupied the Commonwealth Bay polynya from March through April. Here we present unique observations of the regional oceanography during the summer-fall transition, in particular the upper ocean stratification across the Adélie Depression, including alongside iceberg C28 that calved from the Mertz Glacier and the convective overturning of the deep remnant seasonal mixed layer in Commonwealth Bay from sea ice growth (7.5–12.5 cm s−1). Heat and freshwater budgets to 200–300m are used to estimate the ocean heat content, heat flux and sea ice growth rates. We speculate that the continuous foraging by the seals within Commonwealth Bay during the summer-fall transition was due to favorable feeding conditions resulting from the convective overturning of the deep seasonal mixed layer and chlorophyll maximum that is a reported feature of this location.

Krinner, G., A. Rinke, K. Dethloff, et I. Gorodetskaya. **Impact of prescribed Arctic sea ice thickness in simulations of the present and future climate.** *Climate Dynamics*, **35**, 619-633, 2010.

This paper describes atmospheric general circulation model climate change experiments in which the Arctic sea-ice thickness is either fixed to 3 m or somewhat more realistically parameterized in order to take into account essentially the spatial variability of Arctic sea-ice thickness, which is, to a first approximation, a function of ice type (perennial or seasonal). It is shown that, both at present and at the end of the twenty-first century (under the SRES-A1B greenhouse gas scenario), the impact of a variable sea-ice thickness compared to a uniform value is essentially limited to the cold seasons and the lower troposphere. However, because first-year ice is scarce in the Central Arctic today, but not under SRES-A1B conditions at the end of the twenty-first century, and because the impact of a sea-ice thickness reduction can be masked by changes of the open water fraction, the spatial and temporal patterns of the effect of sea-ice thinning on the atmosphere differ between the two periods considered. As a consequence, not only the climate simulated at a given period, but also the simulated Arctic climate change over the twenty-first century is affected by the way sea-ice thickness is prescribed.

3-2 - Other references:

Marsan, D., Weiss, J., Metaxian, J.P., Grangeon, J., Roux, P.F. and Haapala, J., **Low frequency bursts of horizontally-polarized waves in the Arctic sea ice cover: a signature of remote regional-scale icequakes?**, *J. Glaciol.*, in press

Rampal, P., Weiss, J., Marsan, D. and Bourgoin, M., **Arctic sea ice velocity field: general circulation and turbulent-like fluctuations,** *J. Geophys. Res.*, 114, C10014, 2009

Girard, L., Weiss, J., Molines, J.M., Barnier, B. and Bouillon, S., **Evaluation of high resolution sea ice models on the basis of statistical and scaling properties of Arctic sea ice drift and deformation**, *J. Geophys. Res.*, 114, C08015, 2009

Weiss, J. and Schulson, E.M., **Coulombic faulting from the grain scale to the geophysical scale: Lessons from ice**, *J. Phys. D: Appl. Phys*., 42, 214017, 2009

Weiss, J., Marsan, D. and Rampal, P., **Space and time scaling laws induced by the multiscale fracturing of the Arctic sea ice cover**, in *Scaling in Solid Mechanics* , IUTAM Bookseries Vol. 10, Springer (P. Borodich Ed.), 101-109, 2009

Weiss, J., **Intermittency of principal stress directions within Arctic sea ice**, *Phys. Rev. E*, 77, 056106, 2008

Rampal, P., Weiss, J., Marsan, D., Lindsay, R., Stern, H., **Scaling properties of sea ice deformation from buoy dispersion analysis**, *J. Geophys. Res.*, 113, C03002, 2008

Germe, A., Houssais M.-N., Herbaut C. and C. Cassou, **Greenland Sea sea ice variability over 1979-2007 and its link to the surface atmosphere**, *J. Geophys. Res.*, submitted, 2010.

Schlichtholz, P. and M.-N. Houssais, **Forcing of oceanic heat anomalies by air-sea interactions in the Nordic Seas area**, *J. Geophys. Res*., doi:10.1029/2009JC005944, 2010.

4- ICE SHEETS

4-1 Dynamics and modelling

4-1-1 - Main references with abstracts

Alvarez-Solas, J., S. Charbit, C. Ritz, D. Paillard, G. Ramstein and C. Dumas, **Links between ocean temperature and iceberg discharge during Heinrich events**. Nature Geoscience, 10.1038/ngeo752, 10.1038/ngeo752, (122126) 2010.

Palaeoclimate records have revealed the presence of millennial-scale climate oscillations throughout the last glacial period1. Six periods of extreme cooling in the Northern Hemisphere—known as Heinrich events—were marked by an enhanced discharge of icebergs into the North Atlantic Ocean2,3, increasing the deposition of ice-rafted debris2. Increased sliding at the base of ice sheets as a result of basal warming has been proposed to explain the iceberg pulses4–6, but recent observations7,8 suggest that iceberg discharge is related to a strong coupling between ice sheets, ice shelves and ocean conditions. Here we use a conceptual numerical model to simulate the effect of ocean temperature on ice-shelf width, as well as the impact of the resultant changes in ice-shelf geometry on ice-stream velocities. Our results demonstrate that ocean temperature oscillations affect the basal melting of the ice shelf and will generate periodic pulses of iceberg discharge in an ice sheet with a fringing shelf. We also find that the irregular occurrence of Heinrich events seen in the palaeoclimate records can be simulated by periodic ocean forcing combined with varying accumulation rates of the ice sheet. Our model simulations support a link between millennial-scale ocean temperature variability and Heinrich events during the last glacial period.

Charbit, S., C. Ritz, G. Philippon, V. Peyaud and M. Kageyama, **Numerical reconstructions of the Northern Hemisphere ice sheets through the last glacial-interglacial cycle**. Climate of the Past, 15-37, 2007.

A 3-dimensional thermo-mechanical ice-sheet model is used to simulate the evolution of the Northern Hemisphere ice sheets through the last glacial-interglacial cycle. The ice-sheet model is forced by the results from six different atmospheric general circulation models (AGCMs). The climate evolution over the period under study is reconstructed using two climate equilibrium simulations performed for the Last Glacial Maximum (LGM) and for the present-day periods and an interpolation through time between these snapshots using a glacial index calibrated against the GRIP 18O record. Since it is driven by the timing of the GRIP signal, the temporal evolution of the ice volume and the ice-covered area is approximately the same from one simulation to the other. However, both ice volume curves and spatial distributions of the ice sheets present some major differences from one AGCM forcing to the other. The origin of these differences, which are most visible in the maximum amplitude of the ice volume, is analyzed in terms of differences in climate forcing. This analysis allows for a partial evaluation of the ability of GCMs to simulate climates consistent with the reconstructions of past ice sheets. Although some models properly reproduce the advance or retreat of ice sheets in some specific areas, none of them is able to reproduce both North American or Eurasian ice complexes in full agreement with observed sea-level variations and geological data. These deviations can be attributed to shortcomings in the climate forcing and in the LGM ice-sheet reconstruction used

as a boundary condition for GCM runs, but also to missing processes in the ice-sheet model itself.

Peyaud, V., C. Ritz and G. Krinner, **Modelling the Early Weichselian Eurasian ice sheets: role of ice shelves and influence of ice-dammed lakes.** Climate of the Past, 375-386, 2007.

During the last glaciation, a marine ice sheet repeatedly appeared in Eurasia. The floating part of this ice sheet was essential to its rapid extension over the seas. During the earliest stage (90 kyr BP), large ice-dammed lakes formed south of the ice sheet. These lakes are believed to have cooled the climate at the margin of the ice. Using an ice sheet model, we investigated the role of ice shelves during the inception and the influence of ice-dammed lakes on the ice sheet evolution. Inception in Barents sea seems due to thickening of a large ice shelf. We observe a substantial impact of the lakes on the evolution of the ice sheets. Reduced summer ablation enhances ice extent and thickness, and the deglaciation is delayed by 2000 years.

Gagliardini, O., G. Durand, T. Zwinger, R. Hindmarsh and E. LeMeur, **Coupling of ice-shelf melting and buttressing is a key process in ice-sheets dynamics**. Geophys. Res. Lett., 10.1029/2010GL043334, 10.1029/2010GL043334, (L14501) 2010.

Increase in ice-shelf melting is generally presumed to have triggered recent coastal ice-sheet thinning. Using a full-Stokes finite element model which includes a proper description of the grounding line dynamics, we investigate the impact of melting below ice shelves. We argue that the influence of ice-shelf melting on the ice-sheet dynamics induces a complex response, and the first naive view that melting inevitably leads to loss of grounded ice is erroneous. We demonstrate that melting acts directly on the magnitude of the buttressing force by modifying both the area experiencing lateral resistance and the ice-shelf velocity, indicating that the decrease of back stress imposed by the ice-shelf is the prevailing cause of inland dynamical thinning. We further show that feedback from melting and buttressing forces can lead to nontrivial results, as an increase in the average melt rate may lead to inland ice thickening and grounding line advance.

Durand, G., O. Gagliardini, B. De Fleurian, T. Zwinger and E. Le Meur , **Marine Ice-Sheet Dynamics : Hysteresis and Neutral Equilibrium**. J. of Geophys. Res, 10.1029/2008JF001170, 10.1029/2008JF001170, (114) F03009, 2009.

The stability of marine ice sheets and outlet glaciers is mostly controlled by the dynamics of their grounding line, i.e., where the bottom contact of the ice changes from bedrock or till to ocean water. The last report of the Intergovernmental Panel on Climate Change has clearly underlined the poor ability of models to capture the dynamics of outlet glaciers. Here we present computations of grounding line dynamics on the basis of numerical solutions of the full Stokes equations for ice velocity, coupled with the evolution of the air ice– and sea ice–free interfaces. The grounding line position is determined by solving the contact problem between the ice and a rigid bedrock using the finite element code Elmer. Results of the simulations show that marine ice sheets are unstable on upsloping beds and undergo hysteresis under perturbation of ice viscosity, confirming conclusions from boundary layer theory. The present approach also indicates that a 2-D unconfined marine ice sheet sliding over a downsloping bedrock does not exhibit neutral equilibrium. It is shown that mesh resolution around the grounding line is a crucial issue. A very fine grid size (<100 m spacing) is needed in order to achieve consistent results.

Parrenin, F., et al. **1-D ice flow modelling at EPICA Dome C and Dome Fuji, East Antarctica.** Climate of the Past, 3, 243-259, 2007.

One-dimensional (1-D) ice flow models are used to construct the age scales at the Dome C and Dome Fuji drilling sites (East Antarctica). The poorly constrained glaciological parameters at each site are recovered by fitting independent age markers identified within each core. We reconstruct past accumulation rates, that are larger than those modelled using the classical vapour saturation pressure relationship during glacial periods by up to a factor 1.5. During the Early Holocene, changes in reconstructed accumulation are not linearly related to changes in ice isotopic composition. A simple model of past elevation changes is developed and shows an amplitude variation of 110–120m at both sites. We suggest that there is basal melting at DomeC (0.56±0.19 mm/yr). The reconstructed velocity profile is highly non-linear at both sites, which suggests complex ice flow effects. This induces a non-linear thinning function in both drilling sites, which is also characterized by bumps corresponding to variations in ice thickness with time.

Colleoni, F., G. Krinner, et M. Jakobsson. **The role of an Arctic ice shelf in the climate of the last glacial maximum of MIS 6 (140 ka).** *Quat. Sci. Res.*, **29**, 3590-3597, 2010.

During the last decade, Arctic icebreaker and nuclear submarine expeditions have revealed large-scale Pleistocene glacial erosion on the Lomonosov Ridge, Chukchi Borderland and along the Northern Alaskan margin indicating that the glacial Arctic Ocean hosted large Antarctic-style ice shelves. Dating of sediment cores indicates that the most extensive and deepest ice grounding occurred during Marine Isotope Stage (MIS) 6. The precise extents of Pleistocene ice shelves in the Arctic Ocean are unknown but seem comparable to present existing Antarctic ice shelves. How would an Antarctic-style ice shelf in the MIS 6 Arctic Ocean influence the Northern Hemisphere climate? Could it have impacted on the surface mass balance (SMB) of the MIS 6 Eurasian ice sheet and contributed to its large southward extent? We use an Atmospheric General Circulation Model (AGCM) to investigate the climatic impacts of both a limited MIS 6 ice shelf covering portions of the Canada Basin and a fully ice shelf covered Arctic Ocean. The AGCM results show that both ice shelves cause a temperature cooling of about 3 °C over the Arctic Ocean mainly due to the combined effect of ice elevation and isolation from the underlying ocean heat fluxes stopping the snow cover from melting during summer. The calculated SMB of the ice shelves are positive. The ice front horizontal velocity of the Canada Basin ice shelf is estimated to ≈ 1 km yr^{-1} which is comparable to the recent measurements of the Ross ice shelf, Antarctica. The existence of a large continuous ice shelf covering the entire Arctic Ocean would imply a mean annual velocity of icebergs of ≈12 km yr^{-1} through the Fram Strait. Our modeling results show that both ice shelf configurations could be viable under the MIS 6 climatic conditions. However, the cooling caused by these ice shelves only affects the Arctic margins of the continental ice sheets and is not strong enough to significantly influence the surface mass balance of the entire MIS 6 Eurasian ice sheet.

4-2 Surface mass-balance

4-2-1 - Main references with abstracts

O. Magand, G. Picard, L. Brucker, M. Fily, and C. Genthon **Snow melting bias in microwave mapping of Antarctic snow accumulation** *The Cryosphere*, 2, 109-115, 2008

Abstract. *Satellite records of microwave surface emission have been used to interpolate in-situ observations of Antarctic surface mass balance (SMB) and build continental-scale maps of accumulation. Using a carefully screened subset of SMB measurements in the 90°–180° E sector, we show a reasonable agreement with microwave-based accumulation map in the dry-snow regions, but large discrepancies in the coastal regions where melt occurs during summer. Using an emission microwave model, we explain the failure of microwave sensors to retrieve SMB by the presence of layers created by melt/refreeze cycles. We conclude that regions potentially affected by melting should be masked-out in microwave-based interpolation schemes.*

Urbini S., Frezzotti M., Gandolfi S., Vincent C., Scarchilli C., Vittuari L., Fily M., 2008, **Historical behaviour of Dome C and Talos Dome (East Antarctica) as investigated by snow accumulation and ice velocity measurements.**, *Global and Planetary Change, 60, 576-588*.

Ice divide–dome behaviour is used for ice sheet mass balance studies and interpretation of ice core records. In order to characterize the historical behaviour (last 400 yr) of Dome C and Talos Dome (East Antarctica), ice velocities have been measured since 1996 using a GPS system, and the palaeo-spatial variability of snow accumulation has been surveyed using snow radar and firn cores. The snow accumulation distribution of both domes indicates distributions of accumulation that are non-symmetrical in relation to dome morphology. Changes in spatial distributions have been observed over the last few centuries, with a decrease in snow accumulation gradient along the wind direction at Talos Dome and a counter-clockwise rotation of accumulation distribution in the northern part of Dome C. Observations at Dome C reveal a significant increase in accumulation since the 1950s, which could correlate to altered snow accumulation patterns due to changes in snowfall trajectory. Snow accumulation mechanisms are different at the two domes: a wind-driven snow accumulation process operates at Talos Dome, whereas snowfall trajectory direction is the main factor at Dome C. Repeated GPS measurements made at Talos Dome have highlighted changes in ice velocity, with a deceleration in the NE portion, acceleration in the SW portion and migration of dome summit, which are apparently correlated with changes in accumulation distribution. The observed behaviour in accumulation and velocity indicates that even the most remote areas of East Antarctica have changed from a decadal to secular scale.

Magand, O., C. Genthon, M. Fily, G. Krinner, G. Picard, M. Frezzotti, and A. A. Ekaykin, 2007, **An up-to-date quality-controlled surface mass balance data set for the 90 180E Antarctica sector and 1950 2005 period,** *J. Geophys. Res.*, 112, D12106, doi:10.1029/2006JD007691.

On the basis of thousands of surface mass balance (SMB) field measurements over the entire Antarctic ice sheet it is currently estimated that more than 2 Gt of ice accumulate each year at the surface of Antarctica. However, these estimates suffer from large uncertainties. Various problems affect Antarctic SMB measurements, in

particular, limited or unwarranted spatial and temporal representativeness, measurement inaccuracy, and lack of quality control. We define quality criteria on the basis of (1) an up-to-date review and quality rating of the various SMB measurement methods and (2) essential information (location, dates of measurements, time period covered by the SMB values, and primary data sources) related to each SMB data. We apply these criteria to available SMB values from Queen Mary to Victoria lands (90–180E Antarctic sector) from the early 1950s to present. This results in a new set of observed SMB values for the 1950–2005 time period with strong reduction in density and coverage but also expectedly reduced inaccuracies and uncertainties compared to other compilations. The quality-controlled SMB data set also contains new results from recent field campaigns (International Trans-Antarctic Scientific Expedition (ITASE), Russian Antarctic Expedition (RAE), and Australian National Antarctic Research Expeditions (ANARE) projects) which comply with the defined quality criteria. A comparative evaluation of climate model results against the quality-controlled updated SMB data set and other widely used ones illustrates that such Antarctic SMB studies are significantly affected by the quality of field SMB values used as reference.

Fettweis, X., E. Hanna, H. Gallée, P. Huybrechts and M. Erpicum, **Estimation of tfe Greenland ice sheet surface mass balance for the 20th and 21st centuries**. *The Cryosphere*, **2**, 117-129, 2008.

Results from a regional climate simulation (1970 2006) over the Greenland ice sheet (GrIS) reveals that more than 97% of the interannual variability of the modelled Surface Mass Balance (SMB) can be explained by the GrIS summer temperature anomaly and the GrIS annual precipitation anomaly. This multiple regression is then used to empirically estimate the GrIS SMB since 1900 from climatological time series. The projected SMB changes in the 21st century are investigated with the set of simulations performed with atmosphere-ocean general circulation models (AOGCMs) of the Fourth Assessment Report of the Intergovernmental Panel on Climate Change (IPCC AR4). These estimates show that the high surface mass loss rates of recent years are not unprecedented in the GrIS history of the last hundred years. The minimum SMB rate seems to have occurred earlier in the 1930s and corresponds to a zero SMB rate. The AOGCMs project that the SMB rate of the 1930s would be common at the end of 2100. The temperature would be higher than in the 1930s but the increase of accumulation in the 21st century would partly offset the acceleration of surface melt due to the temperature increase. However, these assumptions are based on an empirical multiple regression only validated for recent/current climatic conditions, and the accuracy and time homogeneity of the data sets and AOGCM results used in these estimations constitute a large uncertainty.

Fettweis, X., J.P. Van Ypersele, H. Gallée, F. Lefebre and W. Lefebvre, **The 1979-2005 Greenland ice sheet melt extent from passive microwave data using and improved version of the melt retrieval XPGR algorithm.** *Geophysical Research Letter*, 10.1029/2006GL028787, **34**, L05502, 2007.

Analysis of passive microwave satellite observations over the Greenland ice sheet reveals a significant increase in surface melt over the period 1979-2005. Since 1979, the total melt area was found to have increased by +1.22 x 10(7) km(2). An improved version of the cross-polarized gradient ratio (XPGR) technique is used to identify the melt from the brightness temperatures. The improvements in the melt retrieval XPGR algorithm as well as the surface melt acceleration are discussed with results from a

coupled atmosphere-snow regional climate model. From 1979 to 2005, the ablation period has been increasing everywhere over the melt zone except in the regions where the model simulates an increased summer snowfall. Indeed, more snowfall in summer decreases the liquid water content of the snowpack, raises the albedo and therefore reduces the melt. Finally, the observed melt acceleration over the Greenland ice sheet is highly correlated with both Greenland and global warming suggesting a continuing surface melt increase in the future.

Eisen, O., et al. **Snow accumulation in East Antarctica**. *Review of Geophysics*, 10.1029/2006RG000218, **46**, (46) RG2001, 2008.

The East Antarctic Ice Sheet is the largest, highest, coldest, driest, and windiest ice sheet on Earth. Understanding of the surface mass balance (SMB) of Antarctica is necessary to determine the present state of the ice sheet, to make predictions of its potential contribution to sea level rise, and to determine its past history for paleoclimatic reconstructions. However, SMB values are poorly known because of logistic constraints in extreme polar environments, and they represent one of the biggest challenges of Antarctic science. Snow accumulation is the most important parameter for the SMB of ice sheets. SMB varies on a number of scales, from small-scale features (sastrugi) to ice-sheet-scale SMB patterns determined mainly by temperature, elevation, distance from the coast, and wind-driven processes. In situ measurements of SMB are performed at single points by stakes, ultrasonic sounders, snow pits, and firn and ice cores and laterally by continuous measurements using ground-penetrating radar. SMB for large regions can only be achieved practically by using remote sensing and/or numerical climate modeling. However, these techniques rely on ground truthing to improve the resolution and accuracy. The separation of spatial and temporal variations of SMB in transient regimes is necessary for accurate interpretation of ice core records. In this review we provide an overview of the various measurement techniques, related difficulties, and limitations of data interpretation; describe spatial characteristics of East Antarctic SMB and issues related to the spatial and temporal representativity of measurements; and provide recommendations on how to perform in situ measurements

Krinner, G., B. Guicherd, K. Ox, C. Genthon and O. Magand, **Influence of oceanic boundary conditions in simulations of Antarctic climate and surface mass balance change during the coming century.** *J. of Climate*, 10.1175/2007JCLI1690.1, **21**, 938-962, 2008.

This article reports on high-resolution (60 km) atmospheric general circulation model simulations of the Antarctic climate for the periods 1981-2000 and 2081-2100. The analysis focuses on the surface mass balance change, one of the components of the total ice sheet mass balance, and its impact on global eustatic sea level. Contrary to previous simulations, in which the authors directly used sea surface boundary conditions produced by a coupled ocean-atmosphere model for the last decades of both centuries, an anomaly method was applied here in which the present-day simulations use observed sea surface conditions, while the simulations for the end of the twenty-first century use the change in sea surface conditions taken from the coupled simulations superimposed on the present-day observations. It is shown that the use of observed oceanic boundary conditions clearly improves the simulation of the present-day Antarctic climate, compared to model runs using boundary conditions from a coupled climate model. Moreover, although the spatial patterns of the simulated climate change are similar, the two methods yield significantly different

estimates of the amplitude of the future climate and surface mass balance change over the Antarctic continent. These differences are of similar magnitude as the intermodel dispersion in the current Intergovernmental Panel on Climate Change (IPCC) exercise: selecting a method for generating boundary conditions for a high-resolution model may be just as important as selecting the climate model itself. Using the anomaly method, the simulated mean surface mass balance change over the grounded ice sheet from 1981-2000 to 2081-2100 is 43-mm water equivalent per year, corresponding to a eustatic sea level decrease of 1.5 mm yr^{-1}. A further result of this work is that future continental-mean surface mass balance changes are dominated by the coastal regions, and that high-resolution models, which better resolve coastal processes, tend to predict stronger precipitation changes than models with lower spatial resolution.

Krinner, G., O. Magand, I. Simmonds, C. Genthon, and J.-L. Dufresne. **Simulated Antarctic precipitation and surface mass balance at the end of the 20th and 21st centuries.** *Clim. Dyn.*, **28**, 215-230, 2007.

The aim of this work is to assess potential future Antarctic surface mass balance changes, the underlying mechanisms, and the impact of these changes on global sea level. To this end, this paper presents simulations of the Antarctic climate for the end of the twentieth and twenty-first centuries. The simulations were carried out with a stretched-grid atmospheric general circulation model, allowing for high horizontal resolution (60 km) over Antarctica. It is found that the simulated present-day surface mass balance is skilful on continental scales. Errors on regional scales are moderate when observed sea surface conditions are used; more significant regional biases appear when sea surface conditions from a coupled model run are prescribed. The simulated Antarctic surface mass balance increases by 32 mm water equivalent per year in the next century, corresponding to a sea level decrease of 1.2 mm $year^{-1}$ by the end of the twenty-first century. This surface mass balance increase is largely due to precipitation changes, while changes in snow melt and turbulent latent surface fluxes are weak. The temperature increase leads to an increased moisture transport towards the interior of the continent because of the higher moisture holding capacity of warmer air, but changes in atmospheric dynamics, in particular off the Antarctic coast, regionally modulate this signal.

4-2-2 – Other references without abstracts

G. Picard, M. Fily, H. Gallee, **Surface melting derived from microwave radiometers: a climatic indicator in Antarctica.** *Annals of Glaciology*, vol 46, pp 29-34, 2007

Genthon, C., Magand, O., Krinner, G., Fily, M., 2009, **Do climate models underestimate snow accumulation on the Antarctic plateau? A reevalutation of / from in-situ observations in East Wilkes and – Victoria Lands,** *Annals of Glaciology*, **50,** 61-65.

Genthon, C., G. Krinner and H. Castebrunet, **Antarctic precipitation and climate change predictions : Horizontal resolution and margin vs plateau issues**. *Annals of glaciology*, **50**, 55-60, 2009.

Genthon, C., P Lardeux and G. Krinner, **The surface accumulation and ablation of a blue ice area near Cap Prudhomme, Adélie Land, Antarctica.** *J. Glaciol.*, **183**, (53) 635645, 2007.

5 - ICE CORES AND POLAR FIRN

5-1 Ice cores

5-1-1 Main references with abstracts

Jouzel J. et al, **Orbital and millenial antarctic climate variability over the last 800 000 years**, *Science*, 317, 793, 2007, DOI: 10.1126/science.1141038

Abstract: A high-resolution deuterium profile is now available along the entire European Project for Ice Coring in Antarctica Dome C ice core, extending this climate record back to marine isotope stage 20.2, ~800,000 years ago. Experiments performed with an atmospheric general circulation model including water isotopes support its temperature interpretation. We assessed the general correspondence between Dansgaard-Oeschger events and their smoothed Antarctic counterparts for this Dome C record, which reveals the presence of such features with similar amplitudes during previous glacial periods. We suggest that the interplay between obliquity and precession accounts for the variable intensity of interglacial periods in ice core records.

K.Kawamura, et al., **Northern Hemisphere forcing of climatic cycles in Antarctica over the past 360,000 years**. *Nature,* 2007

Abstract: The Milankovitch theory of climate change proposes that glacial–interglacial cycles are driven by changes in summer insolation at high northern latitudes. The timing of climate change in the Southern Hemisphere at glacial–interglacial transitions (which are known as terminations) relative to variations in summer insolation in the Northern Hemisphere is an important test of this hypothesis. So far, it has only been possible to apply this test to the most recent termination, because the dating uncertainty associated with older terminations is too large to allow phase relationships to be determined. Here we present a new chronology of Antarctic climate change over the past 360,000 years that is based on the ratio of oxygen to nitrogen molecules in air trapped in the Dome Fuji and Vostok ice cores. This ratio is a proxy for local summer insolation, and thus allows the chronology to be constructed by orbital tuning without the need to assume a lag between a climate record and an orbital parameter. The accuracy of the chronology allows us to examine the phase relationships between climate records from the ice cores and changes in insolation. Our results indicate that orbital-scale Antarctic climate change lags Northern Hemisphere insolation by a few millennia, and that the increases in Antarctic temperature and atmospheric carbon dioxide concentration during the last four terminations occurred within the rising phase of Northern Hemisphere summer insolation. These results support the Milankovitch theory that Northern Hemisphere summer insolation triggered the last four deglaciations.

Loulergue, L., Schilt, A., Spahni, R., Masson-Delmotte, V., Blunier, T., Lemieux, B., Barnola, J.-M., Raynaud, D., Stocker, T. F., and Chappellaz, J. (2008). **Orbital and millennial-scale features of atmospheric CH4 over the past 800,000 years**. Nature 453, 383-386.

Abstract : Atmospheric methane is an important greenhouse gas and a sensitive indicator of climate change and millennial-scale temperature variability1. Its concentrations over the past 650,000 years have varied between ,350 and ,800 parts

per 109 by volume (p.p.b.v.) during glacial and interglacial periods, respectively2. In comparison, present-day methane levels of ,1,770 p.p.b.v. have been reported3. Insights into the external forcing factors and internal feedbacks controlling atmospheric methane are essential for predicting the methane budget in a warmer world3. Here we present a detailed atmospheric methane record from the EPICA Dome C ice core that extends the history of this greenhouse gas to 800,000 yr before present. The average time resolution of the new data is ,380 yr and permits the identification of orbital and millennial-scale features. Spectral analyses indicate that the longterm variability in atmospheric methane levels is dominated by ,100,000 yr glacial–interglacial cycles up to ,400,000 yr ago with an increasing contribution of the precessional component during the four more recent climatic cycles. We suggest that changes in the strength of tropical methane sources and sinks (wetlands, atmospheric oxidation), possibly influenced by changes in monsoon systems and the position of the intertropical convergence zone, controlled the atmospheric methane budget, with an additional source input during major terminations as the retreat of the northern ice sheet allowed higher methane emissions from extending periglacial wetlands. Millennial-scale changes in methane levels identified in our record as being associated with Antarctic isotope maxima events1,4 are indicative of ubiquitous millennial-scale temperature variability during the past eight glacial cycles.

Lüthi, D., Le Floch M., Bereiter B., Blunier T., Barnola J.M., Siegenthaler U., Raynaud R., Jouzel J., Fischer H., Kawamura K. and Stocker T.F. (2008). **High-resolution carbon dioxide concentration record 650,000-800,000 years before present**, Nature, 453: 379-382.

Abstract: Changes in past atmospheric carbon dioxide concentrations can be determined by measuring the composition of air trapped in ice cores from Antarctica. So far, the Antarctic Vostok and EPICA Dome C ice cores have provided a composite record of atmospheric carbon dioxide levels over the past 650,000 years1–4. Here we present results of the lowest 200m of the Dome C ice core, extending the record of atmospheric carbon dioxide concentration by two complete glacial cycles to 800,000 yr before present. From previously published data1–8 and the present work, we find that atmospheric carbon dioxide is strongly correlated with Antarctic temperature throughout eight glacial cycles but with significantly lower concentrations between 650,000 and 750,000 yr before present. Carbon dioxide levels are below 180 parts per million by volume (p.p.m.v.) for a period of 3,000 yr during Marine Isotope Stage 16, possibly reflecting more pronounced oceanic carbon storage. We report the lowest carbon dioxide concentration measured in an ice core, which extends the pre-industrial range of carbon dioxide concentrations during the late Quaternary by about 10 p.p.m.v. to 172–300 p.p.m.v.

Lourantou A., Lavric J.V., Köhler P., Barnola J.M., Michel E., Paillard D., Raynaud D. and Chappellaz J. (2010). **Constraint of the CO2 rise by new atmospheric carbon isotopic measurements during the last deglaciation.** Global Biogeochemical Cycles, 24, GB2015, doi:10.1029/2009GB003545, 2010.

Abstract: The causes of the 80 ppmv increase of atmospheric carbon dioxide (CO_2) during the last glacial-interglacial climatic transition remain debated. We analyzed the parallel evolution of CO_2 and its stable carbon isotopic ratio ($\delta^{13}CO_2$) in the European Project for Ice Coring in Antarctica (EPICA) Dome C ice core to bring additional constraints. Agreeing well but largely improving the Taylor Dome ice core record of lower resolution, our $\delta^{13}CO_2$ record is characterized by a W shape, with two negative $\delta^{13}CO_2$ excursions of 0.5‰ during Heinrich 1 and Younger Dryas events, bracketing a positive $\delta^{13}CO_2$ peak during the Bølling/Allerød warm period. The comparison with marine records and the outputs of two C cycle box models

suggest that changes in Southern Ocean ventilation drove most of the CO_2 increase, with additional contributions from marine productivity changes on the initial CO_2 rise and $\delta^{13}CO_2$ decline and from rapid vegetation buildup during the CO_2 plateau of the Bølling/Allerød.

Baroni, M., M. H. Thiemens, R. J. Delmas, and J. Savarino (2007), **Mass-independent sulfur isotopic compositions in stratospheric volcanic eruptions,** *Science*, *315*(5808), 84-87.

The observed mass-independent sulfur isotopic composition (Î”33S) of volcanic sulfate from the Agung (March 1963) and Pinatubo (June 1991) eruptions recorded in the Antarctic snow provides a mechanism for documenting stratospheric events. The sign of Î”33S changes over time from an initial positive component to a negative value. Î”33S is created during photochemical oxidation of sulfur dioxide to sulfuric acid on a monthly time scale, which indicates a fast process. The reproducibility of the results reveals that Î”33S is a reliable tracer to chemically identify atmospheric processes involved during stratospheric volcanism.

Baroni, M., J. Savarino, J. Cole-Dai, V. K. Rai, and M. H. Thiemens (2008), **Anomalous sulfur isotope compositions of volcanic sulfate over the last millennium in Antarctic ice cores**, *Journal of Geophysical Research*, *113*(D20), D20112, 10.1029/2008jd010185.

The reconstruction of past volcanism from glaciological archives is based on the measurement of sulfate concentrations in ice. This method does not allow a proper evaluation of the climatic impact of an eruption owing to the uncertainty in classifying an event between stratospheric or tropospheric. This work develops a new method, using anomalous sulfur isotope composition of volcanic sulfate in order to identify stratospheric eruptions over the last millennium. The advantages and limits of this new method are established with the examination of the 10 largest volcanic signals in ice cores from Dome C and South Pole, Antarctica. Of the 10, seven are identified as stratospheric eruptions. Among them, three have been known to be stratospheric (Tambora, Kuwae, the 1259 Unknown Event) and they exhibit anomalous sulfur isotope compositions. Three unknown events (circa 1277, 1230, 1170 A.D.) and the Serua eruption have been identified as stratospheric eruptions, which suggests for the first time that they could have had significant climatic impact. However, the Kuwae and the 1259 Unknown Event stratospheric eruptions exhibit different anomalous sulfur isotope compositions between South Pole and Dome C samples. Differences in sulfate deposition and preservation patterns between the two sites can help explain these discrepancies. This study shows that the presence of an anomalous sulfur isotope composition of volcanic sulfate in ice core indicates a stratospheric eruption, but the absence of such composition does not necessarily lead to the conclusion of a tropospheric process because of differences in the sulfate deposition on the ice sheet.

Cole-Dai, J., D. Ferris, A. Lanciki, J. Savarino, M. Baroni, and M. H. Thiemens (2009), **Cold decade (AD 1810-1819) caused by Tambora (1815) and another (1809) stratospheric volcanic eruption,** *Geophysical Research Letters*, *36*(22), L22703, doi:22710.21029/22009GL040882.

Climate records indicate that the decade of AD 1810–1819 including the year without a summer (1816) is probably the coldest during the past 500 years or longer, and the cause of the climatic extreme has been attributed primarily to the 1815 cataclysmic Tambora eruption in Indonesia. But the cold temperatures in the early part of the decade and the timing of the Tambora eruption call into question the real climatic impact of volcanic eruptions. Here we present new evidence, based on sulfur

isotope anomaly (D33S), a unique indicator of volcanic sulfuric acid produced in the stratosphere and preserved in polar snow, and on the precise timing of the volcanic deposition in both polar regions, that another large eruption in 1809 of a volcano is also stratospheric and occurred in the tropics. The Tambora eruption and the undocumented 1809 eruption are together responsible for the unusually cold decade.

5-1-2 – Other references without abstracts

2007

J.Jouzel, M.Stiévenard, S.J.Johnsen, K.Fuhrer, A.Landais, V.Masson-Delmotte, A.E.Sveinbjörnsdottir, F.Vimeux , J.W.C.White. **The GRIP deuterium-excess record**, *Quat.Sci.Rev*., 26, 1-17, 2007.

Hou, S., et al. (2007) **Summer temperature trend over the past two millennia using air content in Himalayan ice.** *Climate of the Past*, **3, 1**-7

A.Landais, N.Combourieu Nebout, V.Masson-Delmotte, J.Jouzel, T.Blunier, M.Leuenberger, D.Dahl-Jensen, S.J. Johnsen et B.Luz, **Millenial scale variations of the isotopic composition of atmospheric oxygen over Marine Isotopic Stage 4**. *Earth.Planet.Sci.Lett.*, 258 (1-2): 101-113, 2007.

F. Parrenin, et al., **1-D-ice flow modelling at EPICA Dome C and Dome Fuji, East Antarctica.** *Climate of the past* 3 (2): 243-259, 2007

G.Raisbeck, F.Yiou, J.Jouzel, T.Stocker, **Direct North-South synchronisation of abrupt climate changes using Beryllium 10,** *Climate of the past*, 3, 1-7, 2007

G.Dreyfus, F.Parrenin, B.Lemieux-Dudon, G.Durand, V.Masson-Delmotte, J.Jouzel, J.M.Barnola, L.Panno, R.Spahni, A.Tisserand, U.Siegenthaler, M.Leuenberger, **Anomalous flow below 2700 m in the EPICA Dome C ice core detected using d18O of atmospheric oxygen measurements***, Climate of the Past*, Special issue (EPICA ice cores age scales), 3, 341-353, 2007.

F.Parrenin, et al., **The EDC3 chronology of the EPICA Dome C ice core,** *Climate of the Past*, Special issue (EPICA ice cores age scales), 3, 485-497, 2007.

E. Bard, Raisbeck, G., Yiou, F., Jouzel, J. **Comment on "Solar activity during the last 1000 yr inferred from radionuclide records"** by Muscheler et al. (2007), *Quat. Sci. Rev*., 26, 17 - 18, 2301 - 2304, 2007.

Raynaud, D., Lipenkov, V., Lemieux-Dudon, B., Duval, P., Loutre, M-F., and Lhomme, N. (2007) : **The local insolation signature of air content in Antarctic ice: A new step toward an absolute dating of ice records:** *Earth and Planetary Science Letters*, doi:10.1016/j.epsl.2007.06.025.

2008

C. Waelbroeck, J. Jouzel, F. Parrenin, V. Masson-Delmotte, D. Genty, **Tranferring radiometric dating of the last interglacial sea level high stand to marine and ice core records**. *Earth Planet Sci. Lett.,* 265, 183-194, 2008.

D. Luthi, Le Floch, M., Bereiter, B., Blunier, B., Barnola, J.M., Siegenthaler, U., Raynaud, D., Jouzel J., Fischer, H., Kawamura, K., Stocker F.. **Low carbon dioxyde in Dome C ice 650,000 - 800,000 years before present**. *Nature*, 453, 7193, 379 - 382, 2008.

J.P.Steffensen, et al. **High resolution ice core data show abrupt climate change happens in few years**, *Science*, 321, 5889, 680-689, 2008.

G. Dreyfus, Raisbeck, G.M., Parrenin, F., Jouzel , J, Guyodo, Y., Nomade, S., Mazaud, A. **An ice core perspective on the age of the Matuyama - Brunhes boundary**. *Earth Planet Sci. Lett.,* 274, 151 - 156, 2008.

2009

Tzedakis, P. C., Raynaud, D., McManus, J. F., Berger, A., Brovkin, V., and Kiefer, T. (2009). **Interglacial diversity.** Nature Geoscience**, 2,** 751-755.

Vinther, B. M., et al., (2009). **Significant Holocene thinning of the Greenland ice sheet**. Nature 461, 385-388

2010

A.Landais, G. Dreyfus, E. Capron, V. Masson-Delmotte, M.F. Sanchez-Goñi, S.Desprat, G.Hoffmann, J.Jouzel, M.Leuenberger, S.Johnsen. **What drives the millennial and orbital variations of $d^{18}O_{atm}$?** *Quaternary Science Review,* 29, 1-2, 235-246, 2010.

V.Masson-Delmotte, B.Stenni, K.Pol, P.Braconnot, O.Cattani, S.Falourd, J.Jouzel, A.Landais, B.Minster, J.R.Petit, S.Johnsen, R.Röthlisberger, J.Chappellaz, J.Hansen, **EPICA Dome C record of glacial and interglacial intensities,** *Quaternary Science Review,* 29, 1-2, 113-128, 2010.

G.Dreyfus, J.Jouzel, M.L.Bender, A.Landais, V. Masson - Delmotte, M. Leuenberger, **Firn processes and $\delta^{15}N$: potential for a gas-phase climate proxy,** *Quaternary Science Review*, 29, 1-2, 28-42, 2010.

B.Stenni, V.Masson-Delmotte, E.Selmo, H.Oerter, H.Meyer, R.Rothlisberger, J.Jouzel, O.Cattani, S.Falourd, H.Fischer, G.Hoffmann, P.Iacumin, S.Johnsen, B.Minster. **The deuterium excess records of EPICA Dome C and Dronning Maud Land ice cores (East Antarctica),** *Quaternary Science Review*, 29, 1-2, 146-159, 2010.

C.Risi, A.Landais, S.Bony, J.Jouzel, V.Masson-Delmotte, F.Vimeux. **Understanding the ^{17}O-excess glacial-interglacial variations in Vostok precipitation**. *J.Geophys.Res*. 115, D10112, 2010.

A.A.Ekaykin, Lipenkov, V.Ya., Petit, J.R., Johnsen, S., Jouzel, J., Masson-Delmotte, V. **Insights into hydrological regime of Lake Vostok from differential behavior of deuterium and oxygen-18 in accreted ice**. *J.Geophys.Res.,* 115, C05003, 2010.

V.Masson-Delmotte, et al., **Abrupt change of Antarctic moisture origin at the end of Termination II,** *P.N.A.S,* 107, 27,12091-12094, 2010.

K.Pol, et al., **New MIS 19 EPICA Dome C high resolution deuterium data: hints for a problematic preservation of climate variability in the "oldest ice",** *Earth Planet.Sci. Lett.*, 298, 1-2, 95-103, 2010.

E.Capron, et al., **Millennial and sub-millennial climatic variations recorded in polar ice cores over the last glacial period**. *Clim Past, 6, 345 - 365*, 2010.

J.Jouzel and V.Masson-Delmotte. **deep ice cores : the need for going back in time**. *Quaternary Science Review,* 29 Issue: 27-28 Pages: 3683-3689, *2010*

Lourantou, A., Chappellaz, J., Barnola J-M., Masson-Delmotte, V., Raynaud, D. (2010). **Changes in atmospheric CO2 and its carbon isotopic ratio during the penultimate deglaciation,** Quaternary Science Reviews, 29, 1983-1992

5-2 Polar firn

5-2-1 Main references with abstracts

Faïn, X., Ferrari, C.P., Dommergue, A., Albert, M.R., Battle, M., Severinghaus, J., Arnaud, L., Barnola, J.-M., Cairns, W., Barbante, C., Boutron, C., 2009. **Polar firn air reveals large-scale impact of anthropogenic mercury emissions during the 1970s.** *Proceedings of the National Academy of Sciences of the United States of America* 106, 16114-16119.

Mercury (Hg) is an extremely toxic pollutant, and its biogeochemical cycle has been perturbed by anthropogenic emissions during recent centuries. In the atmosphere, gaseous elemental mercury (GEM; Hg°) is the predominant form of mercury (up to 95%). Here we report the evolution of atmospheric levels of GEM in mid- to high-northern latitudes inferred from the interstitial air of firn (perennial snowpack) at Summit, Greenland. GEM concentrations increased rapidly after World War II from _1.5 ng m_3 reaching a maximum of _3 ng m-3 around 1970 and decreased until stabilizing at _1.7 ng m_3 around 1995. This reconstruction reproduces real-time measurements available from the Arctic since 1995 and exhibits the same general trend observed in Europe since 1990. Anthropogenic emissions caused a two-fold rise in boreal atmospheric GEM concentrations before the 1970s, which likely contributed to higher deposition of mercury in both industrialized and remotes areas. Once deposited, this toxin becomes available for methylation and, subsequently, the contamination of ecosystems. Implementation of air pollution regulations, however, enabled a large-scale decline in atmospheric mercury levels during the 1980s. The results shown here suggest that potential increases in emissions in the coming decades could have a similar large-scale impact on atmospheric Hg levels.

Martinerie, P., E. Nourtier-Mazauric, J. M. Barnola, W. Sturges, D. R. Worton, E. Atlas, L. Gohar, K. Shine, G. P. Brasseur, **Long-lived halocarbon trends and budgets from atmospheric chemistry modelling constrained with measurements in polar firn**. *Atmos. Chem. Phys.*, 9, 3911-3934, 2009.

Abstract : The budgets of seven halogenated gases (CFC-11, CFC-12, CFC-113, CFC-114, CFC-115, CCl_4 and SF_6) are studied by comparing measurements in polar firn air from

two Arctic and three Antarctic sites, and simulation results of two numerical models: a 2-D atmospheric chemistry model and a 1-D firn diffusion model. The first one is used to calculate atmospheric concentrations from emission trends based on industrial inventories; the calculated concentration trends are used by the second one to produce depth concentration profiles in the firn. The 2-D atmospheric model is validated in the boundary layer by comparison with atmospheric station measurements, and vertically for CFC-12 by comparison with balloon and FTIR measurements. Firn air measurements provide constraints on historical atmospheric concentrations over the last century. Age distributions in the firn are discussed using a Green function approach. Finally, our results are used as input to a radiative model in order to evaluate the radiative forcing of our target gases. Multi-species and multi-site firn air studies allow to better constrain atmospheric trends. The low concentrations of all studied gases at the bottom of the firn, and their consistency with our model results confirm that their natural sources are small. Our results indicate that the emissions, sinks and trends of CFC-11, CFC-12, CFC-113, CFC-115 and SF_6 are well constrained, whereas it is not the case for CFC-114 and CCl_4 . Significant emission-dependent changes in the lifetimes of halocarbons destroyed in the stratosphere were

obtained. Those result from the time needed for their transport from the surface where they are emitted to the stratosphere where they are destroyed. Efforts should be made to update and reduce the large uncertainties on CFC lifetimes.

5-2-2 – Other references without abstracts

Clark, I.D., L. Henderson, J. Chappellaz, D. Fisher, R. Koerner, D.E.J. Worthy, T. Kotzer, A.L. Norman, J.M. Barnola, **CO_2 isotopes as tracers of firn air diffusion and age in an Arctic ice cap with summer melting, Devon Island, Canada**. *J. Geophys. Res.*, 112, D01301, 2007.

Worton, D. R., W. Sturges, L. Gohar, K. Shine, P. Martinerie, D. Oram, S.P. Humpfrey, P. Begley, R. Gunn, J.M. Barnola, J. Schwander, R. Mulvaney, **Atmospheric trends and radiative forcings of CF_4 and C_2F_6 inferred from firn air**. *Environ. Sci. Technol.*, 31, 2184-2189, 2007.

Laube, J.C., P. Martinerie, E. Witrant, T. Blunier, J. Schwander, C.A.M. Brenninkmeijer, T.J. Schuck, M. Bolder, T. Röckmann, C. Van Der Veen, H. Bönisch, A. Engel, G.P. Mills, M.J. Newland, D.E. Oram, C.E. Reeves, WT. Sturges, **Accelerating growth of HFC-227ea (1,1,1,2,3,3,3heptafluoropropane) in the atmosphere**. *Atmos. Chem. Phys.*, 10, 5903-5910, 2010.

Witrant, E., P. Martinerie, **A Variational Approach for Optimal Diffusivity Identification in Firns**. *Proc. of the 18th IEEE Med. Conf. on Control & Automation*, 892-897, 2010.

G.Dreyfus, J.Jouzel, M.L.Bender, A.Landais, V. Masson - Delmotte, M. Leuenberger, **Firn processes and δ15N: potential for a gas-phase climate proxy,** Quaternary Science Review, 29, 1-2, 28-42, 2010.

6 - PERMAFROST

6-1- Main references with abstracts

Koven, C., P. Friedlingstein, P. Ciais, D. Khvorostiyanov, G. Krinner, et C. Tarnocai. **The effects of cryoturbation and insulation by organic matter on the formation of high-latitude soil carbon stocks in a land surface model.** *Geophys. Res. Lett.*, **36**, L21501, 2009.

We modify the soil component of the ORCHIDEE terrestrial carbon cycle model to include vertically-discretized soil carbon. With this model, we investigate the feedback of considering thermal insulation by soil carbon, which modifies the soil thermal regime by lowering the thermal conductivity and increasing the heat capacity of a carbon-rich soil, on the total carbon stocks the model builds up. In addition, we demonstrate the effects of diffusive vertical mixing of soil organic matter by cryoturbation on the total carbon stocks that the model builds up in mineral soils in equilibrium with a steady climate. We show that including these two effects together leads to up to 30% higher soil carbon stocks in the top meter of permafrost soils, as well as large stocks of carbon below 1m in the upper permafrost soil layers. The vertical profile of partitioning of carbon between different lability pools is also affected, as the slower pools are more deeply mixed; also the time to reach equilibrium lengthens considerably. These effects are largest in the coldest regions such as Eastern Siberia. The inclusion of cryoturbative mixing and insulation by soil carbon leads to better agreement with estimates of high-latitude soil carbon stocks, where substantial amounts of carbon are found in permafrost regions, to depths of three meters; however we do not include peat, Yedoma, or alluvial deposition processes here, so the total carbon stocks are still lower than observed.

Khvorostyanov, D., G. Krinner, P. Ciais, M. Heimann, and S.A. Zimov. **Vulnerability of permafrost carbon to global warming. Part I. Model description and role of heat generated by organic matter decomposition.** *Tellus*, **60**, 250-264, doi:10.1111/j.1600-0889.2007.00333.x, 2008.

We constructed a new model to study the sensitivity of permafrost carbon stocks to future climate warming. The one-dimensional model solves an equation for diffusion of heat penetrating from the overlying atmosphere and takes into account additional in situ heat production by active soil microorganisms. Decomposition of frozen soil organic matter and produced CO_2 and methane fluxes result from an interplay of soil heat conduction and phase transitions, respiration, methanogenesis and methanotrophy processes. Respiration and methanotrophy consume soil oxygen and thus can only develop in an aerated top-soil column. In contrast, methanogenesis is not limited by oxygen and can be sustained within the deep soil, releasing sufficient heat to further thaw in depth the frozen carbon-rich soil organic matter. Heat production that accompanies decomposition and methanotrophy can be an essential process providing positive feedback to atmospheric warming through self-sustaining transformation of initially frozen soil carbon into CO_2 and CH_4. This supplementary heat becomes crucial, however, only under certain climate conditions. Oxygen limitation to soil respiration slows down the process, so that the mean flux of carbon released during the phase of intense decomposition is more than two times less than without oxygen limitation. Taking into account methanogenesis increases the mean carbon flux by 20%. Part II of this study deals with mobilization of frozen carbon stock in transient climate change scenarios with more elaborated methane module,

which makes it possible to consider more general cases with various site configurations. Part I (this manuscript) studies mobilization of 400 GtC carbon stock of the Yedoma in response to a stepwise rapid warming focusing on the role of supplementary heat that is released to the soil during decomposition of organic matter.

Comité National Français de Géodésie et Géophysique

French National Committee of Geodesy and Geophysics

RAPPORT QUADRIENNAL DU CNFGG A l'UGGI

QUADRENNIAL REPORT OF CNFGG TO IUGG

ANNEXES

ANNEX

Bureau du CNFGG / Bureau of CNFGG

Jérôme Dyment (*Président* / President)
jdy@ipgp.fr
Roland Schlich (*Trésorier* / Treasurer)
roland.schlich@orange.fr
Michel Menvielle (*Secrétaire Général* / Secretary General)
michel.menvielle@latmos.ipsl.fr
Claude Boucher (*Premier Vice Président* / First Vice President)
claude-boucher@club-internet.fr
Daniel Schertzer (*Second Vice Président* / Second Vice President)
daniel.schertzer@enpc.fr

Bureau des Sections / Bureau of the Sections

Section 1: *Géodésie* / Geodesy

Richard Biancale (*Président* / President)
richard.biancale@cnes.fr
Pascal Willis (*Vice Président* / Vice President)
willis@ipgp.fr
Stéphane Durand (*Secrétaire* / Secretary)
stephane.durand@esgt.cnam.fr
Claude Boucher (*Ancien Président* / Past Président)
claude-boucher@club-internet.fr

Section 2: *Sismologie et Physique de l'Intérieur de la Terre* / Seismology and Physics of the Earth Interior

Tony Monfret (*Président* / President)
monfret@geoazur.unice.fr
Hélène Lyon-Caen (*Vice Président* / Vice President)
helene.lyon-caen@ens.fr
Mireille Laigle (*Secrétaire* / Secretary)
laigle@ipgp.fr
Anne Deschamps (*Ancien Président* / Past Président)
deschamps@geoazur.unice.fr

Section 3: *Volcanologie et Chimie de l'Intérieur de la Terre* / Volcanology and Chemistry of the Earth Interior

Patrick Allard (*Président* / President)
pallard@ipgp.fr
Pierre Briole (*Secrétaire* / Secretary)
pierre.briole@ens.fr

Section 4: *Géomagnétisme et Aéronomie* / Geomagnetism and Aeronomy
Benoit Langlais (*Président* / President)
benoit.langlais@univ-nantes.fr
Jean-Baptiste Renard (*Vice Président* / Vice President)
jbrenard@cnrs-orleans.fr
Erwan Thébault (*Secrétaire* / Secretary)
ethebault@ipgp.fr

Section 5: *Météorologie et Sciences de l'Atmosphère* / Meteorology and Atmospheric Sciences **Vacant**

Section 6: *Sciences Hydrologiques* / Hydrological Sciences
Pierrick Givone (*Président* / President)
pierrick.givone@cemagref.fr
Marc Lointier (*Secrétaire* / Secretary)
lointier@teledetection.fr
Claude Cosandey (*Ancien Président* / Past Président)
Claude.Cosandey@cnrs-bellevue.fr

Section 7: *Sciences Physiques de l'Océan* / Physical Sciences of the Ocean
Alain Colin de Verdière (*Président* / President)
acolindv@univ-brest.fr
Marie-Noëlle Houssais (*Secrétaire* / Secretary)
mnh@locean-ipsl.upmc.fr
Michel Crépon (*Ancien Président* / Past Président)
crepon@locean.jussieu.fr

Section 8: *Sciences de la Cryosphère* / Cryospheric Sciences
Michel Fily (*Président* / President)
Michel.Fily@lgge.obs.ujf-grenoble.fr

Conseil du CNFGG / Council of CNFGG

Le Conseil du CNFGG est constitué du bureau du CNFGG, des bureaux des sections, et des membres français du bureau de l'UGGI ou de l'une de ses Associations. Sont membres du Conseil à ce dernier titre :
The Council of CNFGG is made of the Bureau of CNFGG, the bureaus of the Sections, and the French members of the IUGG bureau or the bureau of one of the Associations. Are members of the Council as for the latter rule:

Pierre Hubert (*Secrétaire Général de l'AISH* / Secretary General of IAHS)
pjy.hubert@free.fr
Mioara Mandéa (*Secrétaire Général de l'AIGA* / Secretary General of IAGA)
mioara@ipgp.fr